# RENEWABLE ENERGY CONFERENCE '86

## SESCI/BIOMASS CONFERENCE

**Sunday, June 22nd to Wednesday June 25th, 1986**

**University of Manitoba, Winnipeg**

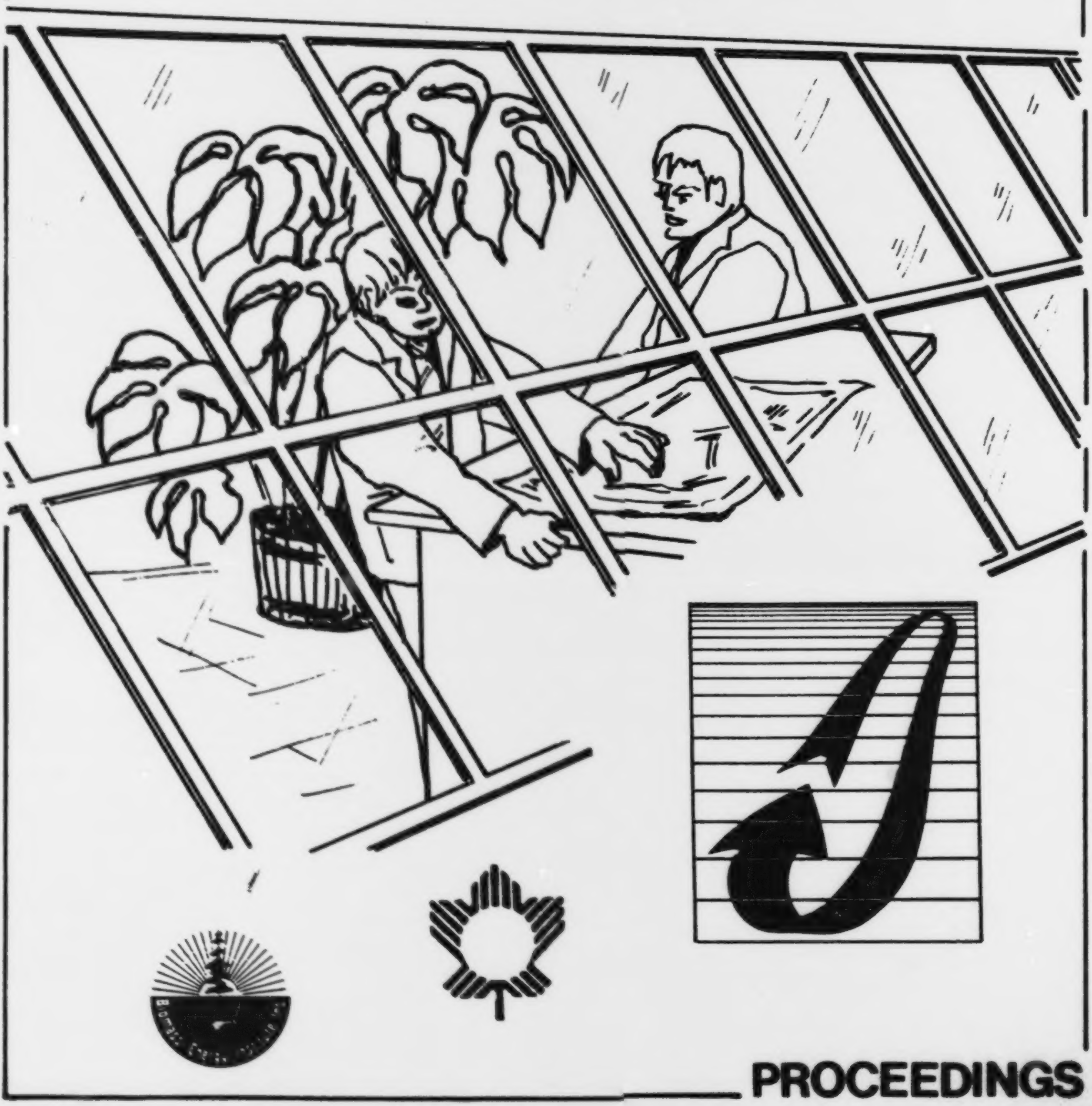

**PROCEEDINGS**

# RENEWABLE ENERGY CONFERENCE '86

June 22 – 25

University of Manitoba, Winnipeg

# PROCEEDINGS

SOLAR ENERGY SOCIETY OF CANADA INC. • THE BIOMASS ENERGY INSTITUTE, INC.

Papers appearing in these proceedings were accepted on the basis of the review of the abstract only. The Solar Energy Society of Canada Inc., therefore does not in any way warrant or guarantee the accuracy of the information contained herein.

All papers were prepared by the authors according to a predetermined format, and were reproduced from camera-ready copy supplied by the authors.

Published by:

Solar Energy Society of Canada Inc.,
Suite 206 - 135 York Street
Ottawa, Ontario
Canada,
K1N 5T4

Copyright 1986 by the Solar Energy Society of Canada Inc. These Proceedings or any part thereof, may not be reproduced for resale or stored in a retrieval system without written permission of the publisher.

# TABLE OF CONTENTS

## RENEWABLE ENERGY CONFERENCE '86

- STEERING COMMITTEE
- BOARD OF DIRECTORS
- FOREWARD
- LETTERS OF WELCOME
- ACKNOWLEDGEMENTS
- REVIEWERS

### SESSION ONE - ALTERNATIVE FUELS

1. A BIOMASS AND CHEMICAL CONVERSION SYSTEMS 1
- Jim Bolton

1. B CHARACTERIZATION DE DIFFERENTES MICCROLAQUES POUR LA VALORISATION D'EFFLUENTS POLLUNTANTS 5
- Y. Pouloit, G. Buelnaet, J. de la Nove

1. C PHOTOLYSIS AND RADIANT FLASH PYROLYSIS OF COAL DERIVATION FROM WASTE 10
- James J. Worman, Joseph J. Worman S.B. Hawthorne and R.E Sears

1. D DEMONSTRATION OF CONDENSING FLUE GAS HEAT RECOVERY 16
- T.J. Molczan, A.P. Scriven and J. Magro

### SESSION TWO - SOLAR RADIATION

2. A RECENT DEVELOPMENTS IN DIFFUSE RADIATION RESEARCH 22
- A.P.Brunger

2. B USE OF SOLAR RADIATION DATA FOR SOLAR ENERGY APPLICATIONS 26
- R.J.Morris and M.S. Geast

## SESSION TWO - SOLAR RADIATION

2. C CORRELATIONS BETWEEN THE GLOBAL AND DIFFUSE SOLAR RADIATION AND CLOUD OACITY 32
- H.F. Ma and W.T. Kierkus

2. D SOLAR RADIATION FOR SELECTED CLIMATIC ZONES IN IRAQ 33
- A.A.Krawi and I.M. Mahi

## SESSION THREE - DIRECT CONVERSION

3. A ICE CONTROL IN LAKES BY PHOTOVOLTAICS POWERED WATER CIRCULATION 41
- P.R.B. Ward, W.G. Dunford and K.I. Ashley

3. B THE USE OF BOILING MEHTANOL IN SOLAR CONCENTRATING PHOTOVOLTAIC SYSTEMS 46
- D.W.H. Fraser and D.C. Card

3. C STUDY OF SILICON PHOTOVOLTAIC MODULES RELATED TO CLIMATIC LOADING CONDITIONS 53
- R.N. Basu and L.L.Cogger

## SESSION FOUR - INDOOR AIR QUALITY

4. A INDOOR AIR QUALITY : ISSUES AND OPPORTUNITIES 54
- D.S. Walkinshaw

4. B FORMALDEHYDE ABATEMENT IN INDOOR AIR 64
- H.D. Gesser

4. C IMPROVING AIR QUALITY IN ENERGY - EFFICIENT HOUSES: AN ARCHITECTURAL APPROACH 66
- E.D. McIntyre and E.M. Sterling

4. D THE VARIATION OF THE EFFECTIVE NATURAL VENTILATION RATE WITH WEATHER CONDITIONS 70
- G.K. Yuill

## SESSION FOUR - INDOOR AIR QUALITY

4. E IMPROVING THE AIR TIGHTNESS IN EXISTING HOUSING 76
- J.A. Love

4. F DETECTION OF TOXIC MATERIALS IN WORKPLACE AND RESIDENTIAL AIR USING PASSIVE SAMPLERS COUPLED TO BIOESSAYS 82
- M. Samoiloff

## SESSION FIVE - AGRICULTURAL APPLICATIONS

5. A AGRICULTURAL APPLICATION OF SOLAR ENERGY 84
- J. Townsend

5. B AN EVALUATION OF DUAL ROLE CURTAINS FOR ENERGY CONSERVATION AND SHADE REQUIREMENTS IN COMMERCIAL GREENHOUSES 87
- E. Brundrett and V. Hassani

5. C DEVELOPMENT OF A PROGRAMMABLE CONTROLLER FOR ATTACHED SUN SPACES 93
- F.W. Chapin and H.D.Chapin

## SESSION SIX - HEAT RECOVERY

6. A TESTING AND OPERATION OF HEAT RECOVERY VENTILATORS FOR WELL SEALED HOUSES 99
- R.W. Besant, G. Schoenau and T.L. Hamlin

6. B DEVELOPMENT OF STANDARDS OF AIR TIGHTNESS AND AIR INFILTRATION 100
- G. Yuill

6. C PASSIVE SOLAR SIMULATION FOR MULTIZONE BUILDING: A FREQUENCY DOMAIN APPROACH 107
- A.K. Athienitis, H.F. Sullivan, K.G.T. Hollands

6. D MONITORED AND SIMULATED PERFORMANCES FOR A LARGE ENERGY-EFFICIENT BUILDING INCORPORATING THERMAL STORAGE 113
- B.F. Gray, G.J. Schoenau, R.W. Besant

## SESSION SEVEN - SOLAR WATER HEATING SYSTEMS

7. A DETAILED PERFORMANCE COMPARISONS BETWEEN THERMOSYPHON AND DRAINBACK SOLAR DOMESTIC HOT SYSTEMS 119
- B.E.Sibbett and T. Onno

7. B SIMPLIFIED DESIGN AND USE OF HEATERS USING CONCENTRATING SOLAR HOT WATER COLLECTORS 125
- M.E.Lux and R.W. Besant

7. C DOWNWARD TRANSFER OF HEAT, WITHOUT USING PUMPS OR CONTROLS 131
- T.A. Lawand, C.Ives and W. Wight

7. D PERFORMANCE MONITORING OF SOLAR HEATING SYSTEMS IN DND 137
- D. Hampton

7. E EFFECTS OF AMBIENT TEMPERATURE VARIATION ON THE PERFORMANCE OF AN ACTIVE SOLAR SYSTEM 142
- K.G.T. Hollands, L. D'Andrea and J.D. Morrison

## SESSION EIGHT - PASSIVE APPLICATIONS

8. A SANDSTONE VALLEY ECUMENICAL CENTRE - A SOLAR CHURCH IN CALGARY 145
- R. Sordi and T. Lee

8. B SITE-PLANNING PRINCIPLES FOR EFFECTIVE USE OF SOLAR ENERGY IN NEW HOUSING 146
- E.M. Elias

8. C THE POTENTIAL OF SECOND-GENERATION BUILDING TECHNOLOGY TO MEET THE R-2000 STANDARD 153
- S. Carpenter, G. Allen, M. Kani and M. Glover

8. D GRAPHEAT: A GRAPHICAL METHOD OF DESIGNING ENERGY-EFFICIENT BUILDINGS 159
- S. Carpenter and E. Burnett

8. E VERIFICATION OF HOTCAN 3.0 164
- C. Wray and G. Yuill

8. F STRATIFICATION ENHANCEMENT OF LIQUID STORAGE 170
- K.G.T. Hollands and M.F. Lightstone

## SESSION NINE - ENERGY STORAGE

9. A DYNAMIC RESITANCE ELEMENTS IN A TANK STRATIFIER - W.J. Spaulding and C.K. Rush 177

9. B PERFORMANCE OF SALT HYDRATE ENERGY STORAGE AND SYSTEM IN AN ATTACHED GREENHOUSE - J.C. O'C. Young and J.A. Collicut 183

9. C THE USE OF SOIL HEAT TO TEMPER AIR - T.V. Murray and M.G. Britton 186

9. D COMPUTER ANALYSIS OF SOLAR STORAGE IN THE GROUND - V.R. Tarnawski, W.H. Leong and P.K. Yuet 191

9. E A STUDY OF BASEMENT HEAT LOSSES - W.R. Richmond and R.W. Besant 195

9. F EFFECT OF EXTERIOR INSULATION PLACEMENT ON BASEMENT HEAT LOSSES - T.M. Kostyniuk and A.C. Trupp 201

## SESSION TEN - BUILDING COMPONENTS PERFORMANCE

10. A THERMAL SCANS AND ISOTHERMS OF WINDOWS AND FRAMES - I.H. Warkentin 205

10. B THE USE OF HOTCAN 3.0 TO EVALUATE THE EFFECT OF GLAZING SYSTEMS AND THERMAL CAPACITY OF RESIDENTIAL HOUSING - L.O. Feduniw 208

10. C WHAT SHALL WE DO WITH SUPER WINDOWS? - C. Carter 213

10. D EFFECTIVE U-VALUES AND SHADING COEFFICIENTS OF PRE-HEAT/SUPPLY AIR GLAZING SYSTEMS - J.L. Wright 219

10. E THERMAL EFFICIENCY OF SIX NATURAL GAS FIRED FUELLED RESIDENTIAL FURNACES - J.F. Dale, M. Ackerman and J. Kasha 225

## SUPPLEMENTARY PAPERS

CANADIAN FEDERAL BIOENERGY PROGRAMS 229
- A.J. Dolenko

VENTURE CAPITAL AND ENERGY CONSERVATION 241
- G. Chignall

BIOENERGY TECHNOLOGY DEVELOPMENTS IN ONTARIO 244
- J.R. Herberman and P. Carrie

A REVIEW OF NRC'S SOLAR ENERGY PROGRAM 251
- T. LeFeuvre and J. Rollefson

TERTIARY BIOMASS TREATMENT AND ALGEA BIOMASS PRODUCTION
- J.B. Serodes

ENVIRONMENTAL EMISSION FROM MUNICIPAL INCINERATION
- M. McKernan

NEW THERMOSYPHON DEVELOPMENTS FOR SOLAR DOMESTIC HOT WATER SYSTEMS
- R.K. Swartman

THERMAL PERFORMANCE EVALUATION OF A PASSIVE SOLAR LOW-RISE OFFICE BUILDING
- G. Yuill and M. Zahn

## SESCI BOARD OF DIRECTORS

### * EXECUTIVE OFFICERS 1985-1986

| | |
|---|---|
| PRESIDENT | Doug Lorriman |
| VICE PRES. | Jeff Passmore |
| TREASURER | Tom LeFeuvre |
| SECRETARY | Karen Beliveau |
| EXEC. DIR. | Bill Eggertson |

### * ELECTED DIRECTORS

Ron Alward
Cyril Carter
Tang Lee
John O'E. Young
Steve Carpenter
Richard Kadulski
Gil Parker

### * ASSOCIATE DIRECTORS

John Ayer
Jon Herberman
John Martin
Ryan Campbell
Douglas LaBelle
Tim Mayo

## BIOMASS BOARD OF DIRECTORS

### * EXECUTIVE OFFICERS 1985-1986

| | |
|---|---|
| CHAIRMAN | Ted Speers |
| VICE CHAIR | Fred Stock |
| TREASURER | Herb Lapp |
| EXEC. DIR. | Peter Winter |

### * DIRECTORS

Ivan Bateman
Dianne Beaven
Jack Candlish
Ray Chant
Don Dever
Fred Hamilton
Doug McRorie
Ernie Robertson

## RENEWABLE ENERGY CONFERENCE '86

| | |
|---|---|
| Chairman | George Bowman |
| Secretary | Debbie Caughlin |
| Treasurer | Jack Tarnava |
| Technical Program | Ray Chant<br>Peter Winter |
| Fund Raising Comm. | Ryan Campbell<br>Brian Gaber<br>Ernie Robertson |
| Public Sessions | Lise Dorber |
| Facilities | Florence Tokar |
| Planetarium Program | Cathy Green |
| Exhibition | Malcolm Dewar |

# FOREWORD

It is ten years since Manitoba last held a major conference of this kind. In 1976 everyone was aware of the "energy crisis". The price of oil had jumped and we were learning to expect this trend to continue. Those who had been promoting work on the development of solar energy at last found their efforts being recognised. Since then the Canadian Government has encouraged the establishment of a Canadian Solar Industry, and, with the co-operation of the provinces, has supported a wide range of solar demonstration projects. It has spent many millions of dollars on solar research and on research in other conservation-related directions, all intended to reduce Canada's dependence on oil.

While the federal government's solar programs are now under review we are, nevertheless, able to see real benefits accruing from the research expenditures. Not only has it been demonstrated that residential energy consumption can be dramatically reduced - while improving standards of comfort - by advanced building techniques, but the building industry has shown itself willing and ready to adopt those techniques. Fully-booked seminars are being held across the country to teach contractors how to apply the new and improved building methods. One such seminar was arranged in conjunction with this conference, while the latest work on Low Energy Buildings is the subject of one group of papers.

The improved building techniques, though, have raised new issues. The air-tight buildings that result give rise to indoor air quality problems. Another group of papers addresses this topic.

I have mentioned only two groups from the wide range of papers dealing with many aspects of renewable energy and the state of to-day's research and development. Ten years ago the Winnipeg conference had as its theme "Sharing the Sun". Having considered all the related work that has gone on since then our Program Chairman, Professor Ray Chant, assembled this year's program around the theme "Sharing the Environment" - assuredly a topical one.

These Proceedings are the permanent record of the conference which could not have taken place without a great deal of unstinting hard work by the members of the Conference Committee who, as the time of the conference approached, gave up more and more of their time organising the accommodation, the exhibition, the accounts, the publicity, the luncheons, the social events and, as one only knows when one has experienced it, all the other parts which go to make up the iceberg of which this document is but the tip.

George S. Bowman

George S. Bowman
Conference Chairman.

GOVERNMENT HOUSE
WINNIPEG
R3C 1S4

## MESSAGE FROM THE HONOURABLE PEARL McGONIGAL
## LIEUTENANT-GOVERNOR OF MANITOBA

I am pleased to send my warmest greetings to the delegates attending the Renewable Energy Conference '86.

The dedicated efforts with good results of the Biomass Energy Institute and the Solar Energy Society of Manitoba merit special recognition at this time. My association with the Biomass Energy Institute and the Solar Energy Society of Manitoba has been important to me in the past and I look forward to maintaining that special relationship in the future.

I wish you continued progress and success as you plan for the future. May I take this opportunity also to extend my best wishes for a successful Conference.

Pearl McGonigal

THE UNIVERSITY OF MANITOBA
OFFICE OF THE PRESIDENT
Winnipeg, Manitoba
Canada R3T 2N2

June 3, 1986

Mr. George Bowman
Chairman
Conference Committee
Renewable Energy Committee
P.O. Box 1256
Winnipeg, Manitoba
R3C 2Y4

Dear Mr. Bowman:

On behalf of all members of the University of Manitoba, I would like to welcome the Solar Energy Society of Canada to our Campus. We are proud that you have elected to hold your eleventh annual national conference here. It provides a valuable opportunity for our faculty and students to share in your activities, both as participants and as members of the audience.

The University of Manitoba has had a continuing commitment to energy research for many years, coordinated through our Energy Forum by Professors Ray Chant and John Welch. Your conference will heighten this commitment.

We hope that while you are visiting the University of Manitoba, you will have time to enjoy the facilities of the entire campus. We wish you a very warm welcome and hope that the sun shines on you and your important events.

Sincerely yours,

A. Naimark

AN/dc

# ACKNOWLEDGEMENTS

APPIN SOLAR AND ASSOCIATES INC.

BLACK AND MCDONALD LTD.

CANADIAN IMPERIAL BANK OF COMMERCE

DEPARTMENT OF ENERGY AND MINES, MANITOBA

DEPARTMENT OF ENERGY, MINES, AND RESOURCES, CANADA

E.J. FARACI AND ASSOCIATES LTD.

MANITOBA ENERGY COUNCIL

INTER-CITY GAS CORPORATION

MANITOBA SCIENCE TEACHERS ASSOCIATION

MUSEUM OF MAN AND NATURE

NATIONAL SCIENCE AND ENGINEERING RESEARCH COUNCIL

NATIONAL RESEARCH COUNCIL, CANADA

NECA/ANCE

RENEWABLE ENERGY NEWS

ROYAL BANK OF CANADA

UNIES LTD.

# REVIEWERS

SESCI/BIOMASS AND THE ORGANIZERS OF THIS CONFERENCE GRATEFULLY ACKNOWLEDGE THE ASSISTANCE OF THE FOLLOWING PEOPLE IN REVIEWING THE PAPER ABSTRACTS.

Mr. Tom Akerstream
Manitoba Department of Energy and Mines

M.E. Barabas
Saskatchewan Power Corporation

Dr. S. Barakat
National Research Council of Canada

Prof. R.W. Besant
University of Saskatchewan

Prof. R. Chant
University of Manitoba

Dr. Mark Chappell
National Research Council of Canada

Prof. W.G Colborne
University of Windsor

Dr. Bob Dumont
National Research Council of Canada

Prof. George Green
University of Saskatchewan

Dr. K.T. Hollands
University of Waterloo

Dr. Richard Perez
State University of New York at Albany

E.A. Speers
Industrial Research and Development of Winnipeg

Mr. Don Urquhart
Spectral Engineering

Dr. D. Walkinshaw
National Research Council of Canada

Prof. John Welch
University of Manitoba

Dr. Gren Yuill
G.K. Yuill and Associates Ltd.

# Biomass and Chemical Conversion Systems/ Alternative Fuels

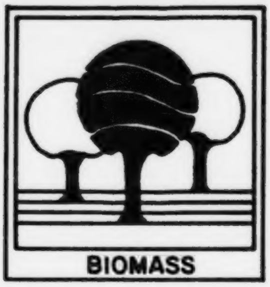

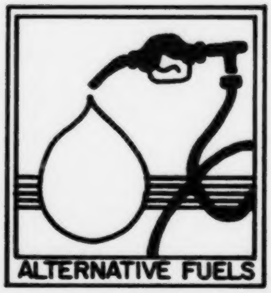
ALTERNATIVE FUELS

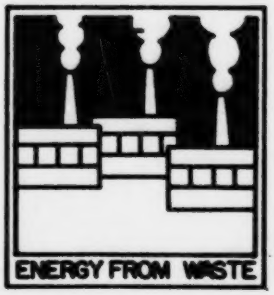
ENERGY FROM WASTE

# BIOLOGICAL AND CHEMICAL CONVERSION SYSTEMS

James R. Bolton

Photochemistry Unit
Department of Chemistry
The University of Western Ontario
London, Ontario, N6A 5B7

## ABSTRACT

Biological systems through photosynthesis convert and store more solar energy than any man-made system by a large margin. In this lecture I shall examine the process of photosynthesis from the standpoint of a solar conversion system and its efficiency. I shall then examine artificial chemical conversion systems, some of which are meant to model the natural process. Finally, I shall look to the future as to what new systems might be developed.

## 1. INTRODUCTION

The annual amount of solar energy stored by photosynthesis (green plants on land and algae in the oceans) is about 10 times the total world annual energy consumption! Thus it is vital that we understand this process particularly from the standpoint of a solar energy conversion system. Nature has had several billion years in which to develop this remarkable process, so it is unlikely that artificial photosynthesis (in totality) can be developed in the near future; however, there are some very promising developments which will be outlined in this lecture.

Chemical conversion and storage of solar energy (which includes photosynthesis) encompasses those applications in which sunlight is used to drive useful chemical reactions. The reactions may be endergonic (uphill in energy), in which case the product of the reaction could be either electricity or a fuel (e.g., hydrogen or methane), or the reaction may be exergonic and photocatalytic (downhill in energy); in which case sunlight is used to overcome an activation barrier to catalyze the synthesis of useful chemicals (e.g., Vitamin D).

Chemical conversion can be divided into two major areas:

1. *Direct processes*: those applications in which reactions are driven by the direct absorption of photons of light by dye molecules or a semiconductor. The resulting excited state then initiates useful photochemistry or photoelectrochemistry.
2. *Thermal processes*: those applications in which concentrated sunlight generates high temperatures which are then used to drive useful chemical reactions.

These two areas involve quite different approaches (and even disciplines). In this lecture I shall concentrate on the first process since photosynthesis is the principal example of a direct conversion process.

## 2. PHOTOCHEMICAL PROCESSES

The solar spectrum at the earth's surface extends from about 300 nm to over 6 μm; however, the characteristics of most dyes or semiconductors which can be employed to drive photochemical processes limit the useful range for photochemical processes to 300-1000 nm, with most limited to the UV and visible range (300-700 nm). Consequently, photochemical systems usually contain highly colored substances.

The absorption of photons of broadband solar radiation raises a sensitizer S to various upper states which then relax to the lowest excited state $S^*$ in less than 1 ps ($10^{-12}$ s). Intersystem crossing can convert $S^*$ to another excited state T (a triplet state). Photochemistry may occur from either state.

At first sight one might assume that the excitation energy $\Delta U(S^*)$ could be stored as chemical energy of the products. However, thermodynamically this is an internal energy $\Delta U$. Thermodynamic analysis of this problem shows that the maximum available energy (the Gibbs energy $\Delta G$) is about 80% of $\Delta U(S^*)$. Real systems will, in addition, exhibit non-ideal, device-dependent losses which will mean lower practical efficiencies. For example, estimates have been made that the efficiency of the solar photolysis of water to hydrogen and oxygen would be ~12-20%, depending on the complexity of the system.

## 3. PHOTOSYNTHESIS

The photosynthesis reaction is clearly the most important chemical reaction, since life could not exist without it. The overall stoichiometric reaction of photosynthesis is

$$1 \quad CO_2(g) + H_2O(\ell) \xrightarrow{\text{sunlight}} \frac{1}{6}\, C_6H_{12}O_6(s) + O_2(g)$$

where $C_6H_{12}O_6$ is D-glucose, the major energy storage product of photosynthesis from which most plant and animal biomass is derived.

Certain photosynthetic bacteria carry out another photosynthetic reaction in which substrates such as $H_2S$ or organic acids are oxidized rather than water.

It is helpful to think of the photosynthesis reaction as the sum of an oxidation half reaction (the oxidation of water to oxygen) and a reduction half reaction (the reduction of $CO_2$ to D-glucose). The latter occurs in the aqueous stroma phase of the chloroplast, whereas the former (which involves the solar energy conversion step) occurs within the thylakoid membrane structure of the chloroplast.

The primary photochemistry of photosynthesis takes place within very specialized reaction center proteins situated within the thylakoid membrane. Most (> 99%) of the chlorophyll and other pigments are present as an antenna system to gather light photons and channel them to one of two reaction centers. In effect, the antenna chlorophyll acts as a luminescent concentrator, concentrating sunlight by a factor of about 300.

Within the reaction center a very simple but remarkable photochemical reaction takes place. A special chlorophyll species becomes excited by the photon absorption process and causes an electron to be transported across the protein to an electron acceptor (e.g., plastoquinone) on the other side of the protein. This photochemical electron transfer reaction results in a separation of charge and generates an electric potential of ~1 V. In effect the plant has developed a biological solar cell to convert sunlight to electricity. Of course, there is no electric current flowing in a leaf; however, if it were possible to place wires on both sides of the reaction center protein, one could draw off electricity at an efficiency of ~16%, which is as good or better than most commercial solar cells! The plant uses the electric potential to drive the relatively slow biochemical reactions of photosynthesis. By the time the end products of photosynthesis are produced, the overall sunlight to chemical energy conversion efficiency has dropped to ~5% under the best conditions. Efficiencies in the field are at best 1-3%.

Recently an X-ray structure of one of the reaction center proteins has become available which shows a complex but highly ordered structure involving several intermediate electron acceptors. It seems that Nature has accomplished the remarkable job of "catching a sunbeam" by organizing a series of planar aromatic macrocycles which form a kind of "molecular wire" to permit the transport of the electron from the chlorophyll species to the acceptor.

## 4. BIOMIMICRY OF PHOTOSYNTHESIS

Several groups (including our own) are now trying to mimic the primary photochemistry of photosynthesis. Most of the studies involve the synthesis of porphyrins linked to quinones via a covalent linkage. One such P-Q molecule is shown below. The absorption of red light causes an electron to be transported from the porphyrin to the quinone, in much the same manner as the primary photochemical reaction of photosynthesis. We now have a better (but by no means complete) understanding of the factors which control the rate and efficiency of this between P and Q, the nature of the linkage and the surrounding solvent. These molecules may serve as the basis of a new type of solar cell (see below).

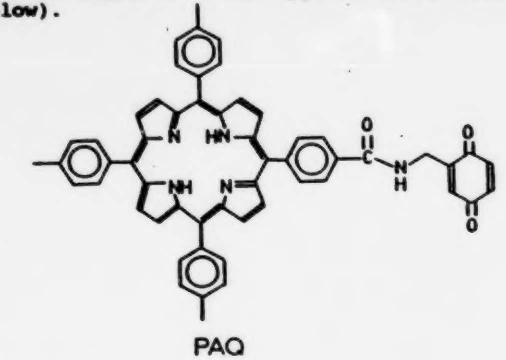

PAQ

## 5. SOLAR FUELS

The photosynthesis reaction is one example of a "photoredox" reaction in which the primary photochemical step is a one-electron transfer from a donor (D) to an acceptor (A)

$$D + A \xrightarrow{\text{sunlight}} D^+ + A^-$$

in which a substantial fraction of the excitation energy may be stored temporarily as the chemical energy of $D^+$ and $A^-$. The reaction may involve the excitation of either D or A or an ancillary sensitizer.

Since $D^+$ and $A^-$ are usually very reactive and will, in the absence of other reactions, revert quickly to D and A with the loss of their stored energy as heat, fast secondary reactions must occur to trap some of the energy in metastable products. This usually involves the use of catalysts to integrate several redox equivalents on both the oxidizing and reducing sides.

Useful redox energy storage reactions involve common reagents such as $H_2O$, $N_2$ or $CO_2$ producing a fuel such as $H_2$, $NH_3$ or $CH_4$ and molecular oxygen as a by-product. Several fuel-generation reactions have been proposed but the one which has received the most attention is the photochemical decomposition of water

$$H_2O \longrightarrow H_2 + \frac{1}{2}O_2$$

to produce hydrogen, a valuable fuel.

Since water is transparent in the UV and visible range, colored sensitizers must be used to drive this reaction with sunlight.

The water reaction, as written above, involves the transfer of two electrons per molecule of hydrogen produced. Since each photon can, at most, transfer one electron, charge accumulation catalysts such as colloidal platinum, must be employed to store charge until a hydrogen molecule can be generated. Similarly on the oxidizing side, four electrons must be removed from a catalyst such as $RuO_2$ before one molecule of oxygen can be produced.

Although research is very intensive in the study of the water reaction, no one has as yet devised a complete system for water photolysis which has a significant efficiency.

An alternative, and very promising, method to carry out the water photolysis reaction is to utilize semiconductor electrodes such as p-type indium phosphide in an aqueous electrolyte solution. Efficiencies as high as 12% have been achieved with such systems.

## 6. PHOTOCATALYTIC SYSTEMS

In photocatalytic systems, the energy of the absorbed photons is utilized to surmount the activation energy of an otherwise very slow exergonic reaction. The usefulness of these reactions lies in the value of the photoproducts as clearly no energy is stored. Recently, Jim Guillet at the University of Toronto has reported a very interesting system in which transparent cross-linked amorphous polymer beads were impregnated with the substrate for a photochemical reaction. These beads were then floated on top of a pond for several hours or days of solar irradiation. The balls were then collected and the photoproduct extracted. Using this method, he obtained high yields in the conversion of ergosterol to Vitamin D and several other promising reactions.

Another photocatalytic process of interest is the sensitized photo-oxidation of pollutants in water supplies. For example, we have shown that *p*-benzoquinone will generate hydroxyl radicals from water at a high efficiency. The hydroxyl radical is a potent oxidizing agent and will react with many common pollutants such as methylene chloride and dichloroethane. In this manner the addition of small amounts of a non-toxic sensitizer to a water system (*e.g.*, in sewage treatment) may result in the removal of large quantities of pollutants. I have calculated that it should be possible, with conservative assumptions, to remove up to ½ tonne per day of pollutants per hectare of water surface exposed to the Sun.

## 7. HIGH TEMPERATURE THERMAL CONVERTERS

In this type of converter a high-ratio concentrator (*e.g.* as provided by a parabolic dish) is required to produce the temperatures necessary to drive thermochemical reactions, which in many cases require temperatures in excess of 1000°C. This places severe materials restrictions for the high-temperature reactor. Two types of processes have been studied: direct one-step reactions and multistep processes.

The direct approach offers the advantage of simplicity, but usually at the expense of the need for very high temperatures. The thermal dissociation of $SO_3$ to $SO_2$ and oxygen has been studied extensively as a possible energy-storage system for solar thermal power stations to allow them to operate at night.

Another direct process is the high-temperature dissociation of water to hydrogen and oxygen. The thermodynamics of this process are well understood, but the major problem is the separation of the hydrogen and oxygen gases at temperatures about 2500 K.

Most of the interest in indirect processes lies around the thermochemical dissocation of water. Many cycles involving 3-6 steps have been proposed. One being developed in Japan involves four steps with a maximum temperature requirement of 700°C.

## 8. CONCLUSIONS

In this lecture I have emphasized the efficiency and beauty of the natural process of photosynthesis as carried out by green plants and algae. One can easily say that if photosynthesis is so good, we should concentrate on collecting the biomass which is the product of photosynthesis. Indeed this is a viable option and is being developed in many various applications, such as methane from the anaerobic digestion of plant and animal wastes, hydrolysis of cellulose to sugars and then to ethanol by fermentation, and, of course, the burning of wood. However, biomass often is not easily converted to the product desired. For example, to convert biomass to electricity, the biomass must first be dried, burned to generate steam which is then used to operate a turbogenerator. The end efficiency is not high and the costs are high.

It seems to me much better to devise processes which, although patterned on photosynthesis, will yield the desired end product. What can be more elegant and simple than a solar cell converting sunlight to electricity with no moving parts and with no pollution? Conventional solar cells are made from very pure silicon and are too expensive for general use. Our patented concept of a solar cell, based on the biological solar cell, could convert sunlight to electricity in an ulta-thin film deposited on a cheap plastic substrate. Unfortunately, I cannot yet show you a prototype cell, but our research is advancing and who knows what the future will bring?

In recent years Chemistry has received a bad name because of chemical disasters such as Bophal. I hope that this lecture has convinced you that Chemistry, and in particular Photochemistry, can do much good in Society. In fact, without the science of Chemistry, we would still be in the Dark Ages!

## 9. FURTHER READING

*Chemical conversion and storage of solar energy*

J.R. Bolton and M.D. Archer *Proc. INTERSOL-85* Montreal, 1985,Pergamon Press (in press)

J.R. Bolton and D.O. Hall *Annu. Rev. Energy*, 4, 353 (1979).

C. Kutal *J. Chem. Educ.* 60, 882 (1983).

*Photosynthesis*

D.O. Hall and K.K. Rao "Photosyntheis" 3rd Ed., Edward Arnold Ltd., London (1982).

E. Rabinowitch and Govindjee "Photosynthesis" John Wiley and Sons, New York (1969).

*Biomimicry of Photosynthesis*

J.R. Bolton, ACS Symposium Series No. 211, 1 (1983).

J.S. Connolly, in "Photochemical Conversion and Storage of Solar Energy, 1982" J. Rabani, Ed., The Weizmann Science Press of Israel, Israel, p. 175 (1982).

*Solar Fuels*

J. R. Bolton *Science* 202, 705 (1978).

M. Grätzel, Ed. "Energy Conversion through Photochemistry and Catalysis", Academic Press, New York (1983).

A.M. Braun, Ed. "Photochemical Conversions", Presses Polytechniques Romandes, Lausanne, Switzerland (1983).

*Photocatalytic Systems*

J.E. Guillet et al. J. *Photochem.* 25, 501 (1984).

*Ultra-thin solar cell*

J.R. Bolton, *Proc.* 17th *Photovoltaics Specialists Conf.*, IEEE, 345 E 47 St., New York, N.Y. 10017, p. 759 (1984).

# CARACTERISATION DE DIFFERENTES MICROALGUES POUR LA VALORISATION D'EFFLUENTS POLLUANTS.

Y. Pouliot[1], G. Buelna[2] et J. de la Noüe[2]

[1] BIONOV CNP INC., 454 Latourelle, #3, Québec, Qué., Canada G1R 1E2
[2] Groupe de recherche en recyclage biologique et aquiculture,
Centre de recherche en nutrition, Université Laval, Ste-Foy, Qué., Canada G1K 7P4

## RESUME

L'étude présente une synthèse des résultats obtenus depuis trois ans avec différentes espèces de microalgues utilisées pour le traitement et la valorisation des eaux usées domestiques et du lisier de porc. Ces microalgues (Spirulina maxima, Spirulina platensis, Scenedesmus sp, Phormidium sp et un groupe d'algues filamenteuses) ont été sélectionnées pour répondre aux critères d'application des systèmes de cultures à grande échelle.

La limitation de croissance observée sur milieu à base de lisier de porc ne semble pas causée par une carence en micronutriments, mais par un effet toxique. Le cuivre révèle sa toxicité à des concentrations supérieures à 0.5 mg/L. Le seuil de toxicité de l'ammoniac se situe à environ 45 mg/L pour toutes les algues étudiées à l'exception de Scenedesmus qui montre une grande résistance aux facteurs inhibiteurs. Le rapport N/P ne joue pas de rôle prépondérant dans la croissance de Spirulina maxima et de Spirulina platensis. Par ordre décroissant de résistance aux contaminations par d'autres espèces de microalgues, on trouve Scenedesmus, Phormidium et le groupe d'algues filamenteuses; Spirulina maxima se montre plus performante que Spirulina platensis sur milieu de lisier de porc.

Les eaux usées apparaissent un milieu fort favorable pour les microalgues étudiées. Le lisier de porc présente dans plusieurs cas des phénomènes d'inhibition des cultures, sauf pour Scenedesmus qui est la plus apte à croître sur ce milieu.

## ABSTRACT

This study is a summary of the results obtained during the last three years with different microalgal species used for the treatment and upgrading of domestic wastewaters ang pig manure. These microalgae (Spirulina maxima, Spirulina platensis, Scenedesmus sp., Phormidium sp. and a group of filamentous algae) were selected to meet the criteria required for their application to large-scale culture systems.

The limitations observed on the growth of algae cultivated on a medium based on pig manure do not seem to be caused by a lack of micronutrients, but are rather the result of a toxic effect. At concentrations of greater than 0.5 mg/L, copper seems to be toxic. Ammonia concentrations of about 45 mg/L are toxic for all algae except Scenedesmus. The latter proves to be very resistant to inhibiting factors. The N/P ratio is not a determining parameter for the growth of Spirulina maxima and Spirulina platensis. In decreasing order of resistance to contamination by other microalgal species are Scenedesmus, Phormidium and the group of filamentous algae. Also, Spirulina maxima is less susceptible to contaminations than Spirulina platensis within a pig manure environment.

Domestic wastewaters seem to be a very favorable culture medium for the microalgae studied. In many cases, pig manure appears to cause culture inhibition, except for Scenedesmus which is best suited to this medium.

## INTRODUCTION

Les travaux portant sur l'utilisation rationnelle des cultures de microalgues comme système de traitement des eaux usées remontent à une quarantaine d'années (1,2). Bien que le concept d'un système combiné de traitement des eaux usées et de production de biomasse d'intérêt alimentaire offre un fort potentiel d'application (3), son application reste aujourd'hui encore relativement faible.

Au cours des dernières décennies on a constaté que le développement de ces systèmes a été freiné par différents facteurs, les principaux étant l'absence de techniques efficaces et économiques pour la récolte des algues microscopiques après le traitement, la difficulté de maintenir en culture monospécifique les algues choisies, la qualité de la biomasse et les coûts d'opérations qui constituent donc autant de critères à retenir pour le choix d'un système performant.

Devant l'ampleur des problèmes environnementaux du Québec liés à la pollution des eaux par des effluents d'origine domestique ou agro-alimentaire et l'intérêt potentiel des systèmes de microalgues sous nos latitudes, et a fortiori pour les pays en voie de développement, des expériences ont été entreprises par le Centre de recherche en nutrition en 1976 (4,5); les aspects de développement relevant de Bionov CNP Inc. (6). Le présent article fait état des résultats récemment obtenus avec des algues [Spirulina maxima, Spirulina platensis, Phormidium sp, Groupe d'algues filamenteuses (non identifiées) et Scenedesmus sp. sélectionnées pour répondre aux critères ci-haut mentionnés.

## MATERIEL ET METHODES

Les expériences sont menées en laboratoire dans des erlenmeyers de 250 mL. L'éclairement est assuré par des bancs de tubes fluorescents ("Cool white" et "Grow lux") libérant une intensité lumineuse de 8000 lux à 4 cm de distance. La croissance des algues est mesurée par prélèvement d'aliquotes de culture, tamisage sur filtre "Whatman" (934 AH) pré pesé, séchage à l'étuve pendant 24 heures à 98°C, passage pendant 1 heure au dessicateur et pesée sur une balance "Mettler H-15". La densité optique (D.O.) à 560 nm sur un spectrophotomètre "LKB ULTRO SPEC II" est parfois utilisée pour évaluer la croissance des cultures de Spiruline. L'agitation et l'aération des cultures sont obtenues par bullage d'air à un débit d'environ 400 mL/min. La température des cultures est maintenue à 23°C. Les détails additionnels relatifs aux différents points traités dans cet article sont présentés dans chacune des sections.

## RESULTATS ET DISCUSSION

### Spirulina

Les Spirulines, Spirulina maxima et Spirulina platensis, sont des cyanobactéries (algues bleu-vert) croissant naturellement dans les lacs peu profonds des régions sub-tropicales. On trouve la première en Amérique centrale et la seconde en Afrique. Le grand intérêt suscité par ces microalgues découle de l'excellente qualité alimentaire de leur biomasse (7). Elles contiennent plus de 60% de protéines (poids sec) et les profils d'acides aminés répondent aux normes de la FAO (8). De plus leur teneur en vitamine B12, en pigments (carotènes et phycocyanine) et en minéraux est élevée.

Depuis trois ans, nous tentons d'acclimater S. maxima sur milieu de lisier de porc. Ces expériences ont permis d'abaisser ses exigences en NaCl et $NaHCO_3$ de 10 g/L à moins de 4 g/L (9). En deçà de cette valeur, la croissance de la culture est considérablement réduite.

Les résultats obtenus démontrent que des milieux constitués de lisier de porc (2.5%, V/V), de NaCl (4 g/L) et de $NaHCO_3$ (4 g/L) permettent une bonne croissance de Spiruline (9). Cependant, les cultures se maintiennent rarement plus de trois à quatre semaines, après quoi elles dégénèrent. Ce comportement est passé jusqu'ici inaperçu, la plupart des travaux réalisés sur la production de Spiruline avec le lisier de porc (10,11) ou les eaux usées (12) ne rapportant pas d'expérience d'une durée supérieure à quinze jours.

Des expériences liées à la toxicité du milieu, à la carence de certains éléments et à l'effet de la lumière ont été réalisées. Les facteurs qui ont retenu notre attention sont la carence en microéléments, la toxicité du cuivre ($Cu^{++}$), le rapport azote/phosphate (N/P) et l'éclairement.

### Carence en microéléments

Afin de savoir si le milieu de culture à base de lisier de porc souffre de carences en microéléments, des cultures de Spiruline maxima ont été menées avec ajout de quantités variables de lisier tous les deux jours. Le lisier a subi un traitement d'aération à un pH 9.0 obtenu par ajout de NaOH de façon à réduire sa teneur en ammoniac ($NH_3$) par effet d'entraînement gazeux ("stripping"). Ont été ainsi obtenus des lots de lisier à trois concentrations d'azote ammoniacal (1 134 mg/L; 524 mg/L; 272 mg/L), qui ont été utilisés pour faire varier les ajouts de lisier et de ses micronutriments tout en maintenant l'azote ammoniacal à une concentration de 35 mg/L, soit une valeur inférieure au seuil d'un effet potentiel de toxicité (8). Les résultats, présentés aux figures 1 et 2, montrent que l'augmentation de la quantité de micronutriments découlant d'un apport accru de lisier réduit, au lieu d'améliorer, la croissance de S. maxima et de S. platensis. L'hypothèse d'un phénomène de carence en micronutriments doit donc être abandonnée, celle de la toxicité apparaissant plus plausible.

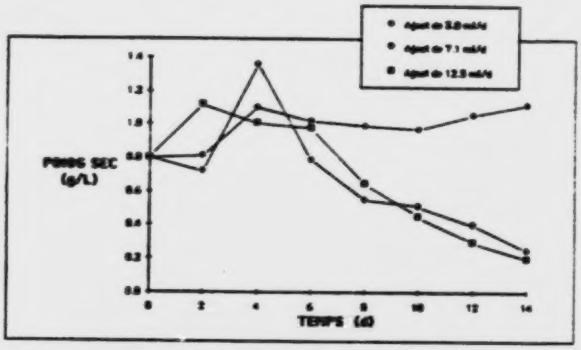

Figure 1. Effet de la quantité de lisier ajouté sur la croissance de Spirulina maxima pour une teneur constante en ammoniaque.

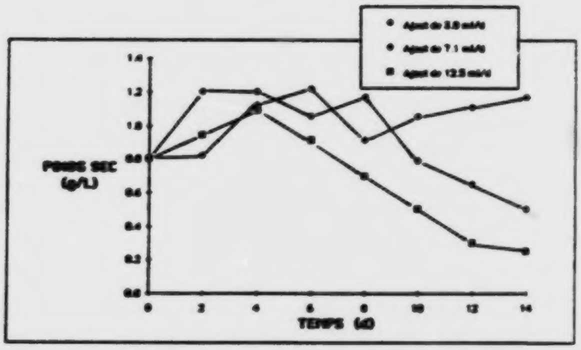

Figure 2. Effet de la quantité de lisier ajouté sur la croissance de Spirulina platensis pour une teneur constante en ammoniaque.

### Toxicité du cuivre

Nous avons évalué l'effet de différentes concentrations en cuivre ($Cu^{++}$) sur la croissance de Spirulina. Le cuivre a été choisi comme une substance potentiellement toxique, puisqu'il est considéré comme un élément inhibiteur de croissance pour le phytoplancton (13). L'expérience a été menée avec S. maxima, car cette algue présente des limitations évidentes de croissance après un certain temps sur milieu de lisier de porc (9).

Une culture de S. maxima alimentée en lisier de porc, celui-ci contenant 0.15 mg/L de cuivre sous forme de $Cu^{++}$, constituait le témoin (0.006 mg de $Cu^{++}$/L). Les cinq autres milieux de culture étaient enrichis en cuivre et contenaient initialement de 0.5 mg/L à 2.5 mg/L de $Cu^{++}$. Les résultats présentés à la figure 3 démontrent que cet élément réduit considérablement la croissance de *S. maxima*. Les résultats obtenus ne permettent toutefois pas de conclure sur la toxicité du cuivre "naturel" dans le lisier de porc, car on ne peut trouver de lisier exempt de cet élément (le cuivre est ajouté à la farine alimentaire des porcs comme agent de préservation à raison de 9.7 mg/kg d'aliment). De plus, les essais n'ont pas été effectués à des doses comprises entre 0.05 et 0.1 mg/L. Cependant, l'effet de toxicité du cuivre doit être retenu, car on sait que des concentrations de 0.1 mg/L-0.5 mg/L inhibent la croissance de microorganismes (14). Puisque l'ajout de lisier augmente la concentration de $Cu^{++}$ de 0.006 mg/L·d, la teneur en cuivre du milieu de culture augmente progressivement pour atteindre, par exemple, une valeur de 0.15 mg $Cu^{++}$/L après 25 jours, moment à partir duquel se manifeste généralement un déclin des cultures.

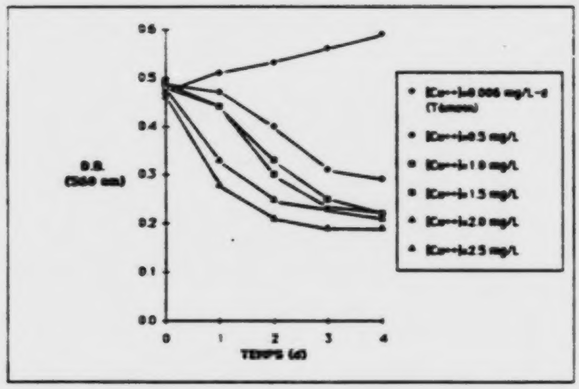

Figure 3. Effet de la concentration du cuivre ($Cu^{++}$) dans le lisier de porc sur la croissance de *Spirulina maxima*.

## Rapport N/P

Afin de vérifier l'hypothèse, proposée dans des travaux antérieurs (8) selon laquelle le rapport N/P du lisier joue un rôle important dans la cinétique de croissance de *S. maxima*, des expériences à différents rapports N/P ont été effectuées. Le lisier a été enrichi en phosphore en ajoutant du $H_3PO_4$ de telle sorte que des lots de lisier, à trois concentrations d'orthophosphate (467 mg/L, 900 mg/L, 1800 mg/L) et même concentration d'azote ammoniacal (2100 mg/L), ont été obtenus. Il a été ainsi possible de faire varier le rapport N/P du milieu de culture par ajout quotidien d'une quantité constante de lisier (2.4 mL/d) et de maintenir la concentration d'azote ammoniacal à 25 mg/L. Les résultats, présentés aux figures 4 et 5, montrent que pour *S. maxima*, le rapport N/P est sans effet. Pour *S. platensis*, un rapport N/P de 8 donne des résultats inférieurs. Le rapport N/P ne semble donc pas jouer de rôle prédominant dans la croissance de *Spiruline* et le rendement de *S. maxima* est meilleur que celui de *S. platensis*, quelque soit le rapport considéré.

## Eclairement

Afin d'établir l'effet de faibles intensités lumineuses sur la croissance de *S. maxima* en culture sur lisier de porc (inoculum de 0.5 g/L; D.O. = 0.5), des expériences à différentes intensités lumineuses ont été menées. Les résultats présentés à la figure 6 montrent une diminution de la croissance pour des éclairements de 2400 lux et moins.

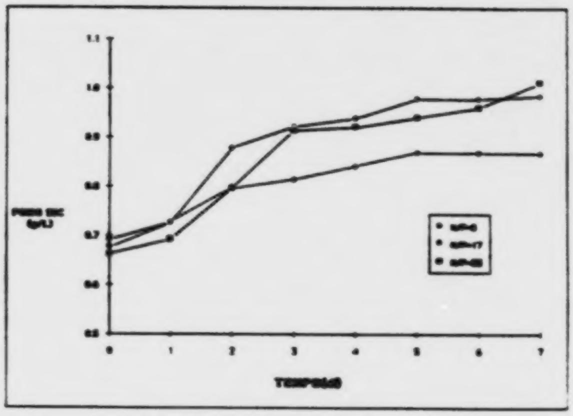

Figure 4. Effet du rapport N/P sur la croissance de *Spirulina* platensis.

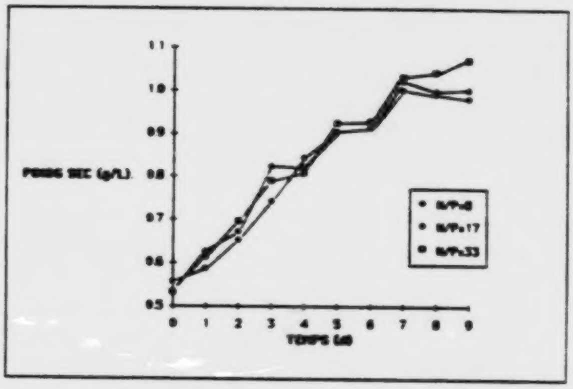

Figure 5. Effet du rapport N/P sur la croissance de *Spirulina maxima*.

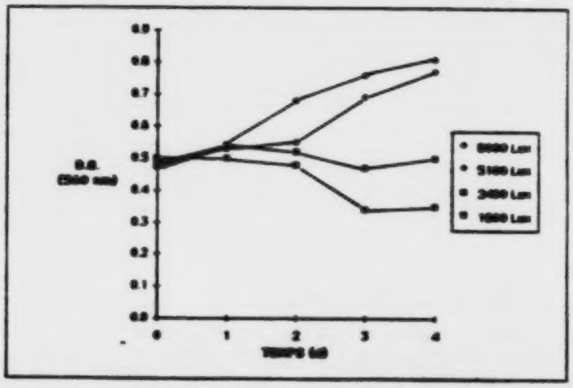

Figure 6. Effet de l'éclairement sur la croissance d'une culture de *Spirulina maxima* à une concentration initiale de 0.5 g (poids sec)/L.

## Scenedesmus

Cette microalgue est une Chlorophycée (algue verte) très répandue qui croît naturellement dans les milieux eutrophes. Sa prédilection pour les milieux pollués fait qu'elle se retrouve spontanément dans les eaux usées et qu'elle est de ce fait l'un des genres les plus utilisés dans les systèmes de cultures de microalgues (15). Son rendement est bon (16), mais sa récolte difficile et sa faible valeur alimentaire pour les non ruminants (6) nuisent à la rentabilité économique à grande échelle du système.

### Phormidium

Cette cyanobactérie est apparue spontanément dans nos cultures en laboratoire. Elle a crû pendant plusieurs semaines aussi bien sur milieu de lisier de porc que sur eaux usées. Son caractère épiphytique fait qu'elle se fixe à des particules en suspension de façon à former des flocs de 0.3 à 1.0 mm de diamètre, ce qui permet une récolte par simple filtration sur un tamis à mailles grossières (100-200 µ).

### Groupe d'algues filamenteuses

Ce mélange d'algues a été isolé des étangs d'oxydation de Saint-Apollinaire dans la banlieue de Québec. Il est composé de quatre chlorophycées filamenteuses et d'une cyanophycée filamenteuse. Ce groupe d'algues a la particularité de floculer en un laps de temps très court (2 minutes environ). La taille des flocs peut atteindre 5 mm de diamètre, ce qui permet une récolte par sédimentation ou par tamisage.

### Milieu de culture

Deux sortes d'eaux usées ont été essayées, la première ayant subi un simple traitement primaire et la seconde, un traitement primaire-secondaire. Les algues filamenteuses ont été maintenues sur eaux usées depuis près de deux ans (17) et Phormidium pendant quelques mois. On sait que les eaux usées en général supportent mieux la croissance de microalgues que les milieux synthétiques (résultats non publiés).

Tel que mentionné précédemment, le milieu de lisier de porc supporte une bonne croissance des microalgues pendant une période de deux à trois semaines, mais cause des problèmes par la suite, à l'exception de Scenedesmus. Cette dernière, reconnue pour sa résistance, a été isolée directement d'une lagune à lisier. Sa productivité et son pouvoir épurateur (assimilation de l'azote et du phosphore) se révèlent bons sur milieu de lisier de porc (18) comme sur eaux usées (19). Des expériences visant à évaluer l'effet de différents pré-traitements (digestion aérobie, floculation) ont montré que les meilleurs résultats sont obtenus avec le lisier brut (non traité) (20).

### Résistance aux contaminations

Des cultures mixtes contenant deux algues d'espèces différentes ont été préparées afin de connaître les dominances relatives. Les essais, avec les mêmes concentrations d'algue sur une base de poids sec, ont été effectués avec les mélanges suivants: Phormidium + Groupe d'algues filamenteuses; Phormidium + Scenedesmus; Groupe d'algues filamenteuses + Scenedesmus; Spirulina maxima + Spirulina platensis. Le milieu utilisé était celui à base de lisier de porc, sauf pour les Spirulines, pour lesquelles un milieu synthétique était utilisé (13). Les résultats révèlent que Phormidium remplace progressivement le Groupe d'algues filamenteuses et qu'elle se maintient en présence de Scenedesmus. Cette dernière remplace rapidement le Groupe d'algues filamenteuses. Ainsi, par ordre décroissant de résistance à la contamination par une autre espèce, on retrouve: Scenedesmus sp > Phormidium sp > Groupe d'algues filamenteuses. S. maxima et S. platensis sur milieu synthétique cohabitent sans dominance marquée, mais des expériences menées avec du lisier de porc démontrent une meilleure résistance de S. maxima sur ce milieu.

### Toxicité de l'ammoniaque

Les expériences réalisées avec Phormidium sur milieu de lisier de porc contenant différentes teneurs en ammoniaque ($NH_3$) montrent un effet de toxicité (déclin des cultures) à pH 9.0 pour des valeurs d'azote ammoniacal supérieures à 45 mg/L. Des résultats semblables ont été obtenus avec le Groupe d'algues filamenteuses.

### CONCLUSION

De plus amples recherches sont nécessaires pour élucider le phénomène de toxicité engendré par le lisier de porc. L'excellente valeur fertilisante de ce milieu s'exprime jusqu'à ce qu'un facteur inhibiteur vienne limiter la croissance des cultures. Scenedesmus constitue la microalgue la plus apte à croître sur lisier de porc. Cependant, dans la perspective où cette algue est retenue pour les systèmes de traitement de lisier de porc et de production de biomasse, un système efficace de récolte doit être développé.

Les eaux usées apparaissent un milieu favorable aux microalgues étudiées. Parmi les algues étudiées, Phormidium présente les meilleures caractéristiques pour application éventuelle. Même si sa tolérance aux fortes teneurs en ammoniaque est peu élevée, sa récolte est facile et sa résistance aux contaminations est relativement grandes. Un système en continu est actuellement à l'étude et, advenant des rendements satisfaisants, des analyses de la qualité alimentaire de cette microalgue seront effectuées.

### REFERENCES BILIOGRAPHIQUES

(1) Caldwell, D.H. Sewage oxidation ponds - performance, operation and design. Sewage Works J. 18: 433-458 (1946).

(2) Oswald, W.J. et H.B. Gotaas. Photosynthesis in sewage treatment. Trans. Am. Soc. Civ. Eng. 122(73):105 (1957).

(3) Shelef, G., R. Moraine, A. Meydan et E. Sandbank. Combined algae production - wastewater treatment and reclamation system. In: Microbial Energy Conversion, H.G. Schlegel et J. Barneau, eds, Erich Goltze Kg, Göttingen, pp. 427-442 (1978).

(4) Picard, G.A., J. de la Noüe, J.P. Piette et C. Kirouac. Utilisation de l'algue Oocystis sp. pour le traitement tertiaire des eaux usées I - Culture en vrac de cellules préalablement conditionnées en cyclostat. Water Res. 13:1203-1212 (1979).

(5) de la Noüe, J., G.A. Picard, J.P. Piette et C. Kirouac. Utilisation de l'algue Oocystis sp. pour le traitement tertiaire des eaux usées II - Effet du conditionnement préalable dés cellules en cyclostat sur leur vitesse de prise en charge

de l'azote lors d'incubation de longue durée. Water Res. 14:1125-1130 (1980).

(6) Cyr, B. et J.L. Sansregret. Etude de faisabilité sur la valorisation des surplus de lisier de porc par production de microalgues et par digestion aérobie autothermophile. Document préparé par Bionov CNP Inc. pour le Centre de valorisation de la biomasse, Ste-Foy, 94 p. janvier 1986.

(7) Cifferi, O. Spirulina, the edible microorganism. Microbiological Review, Déc. pp. 551-578 (1983).

(8) Gauthier, J., P. Talbot, G. Lessard, Y. Pouliot et J. de la Noüe. Epuration du lisier de porc et production de spiruline. Rapport de recherche, Centre de recherche en nutrition et Comp. Lallemand, Québec, 98 p. (1985).

(9) Pouliot, Y., P. Talbot et J. de la Noüe. Biotraitement du purin de porc par production de biomasse de Spirulina. Entropie (sous presse) (1986).

(10) Chiu, R.J., H.I. Liu, C.C. Chen, Y.C. Chi, H. Shao, P. Soong et P.L.C. Hao. The cultivation of Spirulina platensis on fermented swine manure. In: Animal Wastes Treatment and Utilisation. Pro. Int. Symp. on Biogaz, Microalgae and Livestock, Chang Po éd. Taïwan, pp. 435-446 (1980).

(11) Chung, Po., W.G. Pond, J.M. Kingsbury, E.F. Walker et L. Krook. Production and nutritive value of Arthrospira platensis, a spiral blue-green algae grown on swine wastes. J. Anim. Sci. 47:319-330 (1978).

(12) Kosaric, N., H.T. Nguyen et M.A. Bergougnou. Growth of Spirulina maxima in effluent of secondary wastewater treatment plants. Biotech. Bioeng. XVI:881-896 (1974).

(13) Zarrouk, C. Contribution à l'étude d'une Cyanophycée: Influence de divers facteurs physiques et chimiques sur la croissance et la photosynthèse de Spirulina maxima. Thèse, Université de Paris (1966).

(14) Bremond, R. et R. Vuichard. Paramètres de la qualité des eaux. Ministère de la Protection de la Nature et de l'Environnement. La Documentation française, Paris, 179 p. (1973).

(15) Goldman, J.C. Outdoor mass cultures. 1- Applications. Water Res. 13:1-19 (1979).

(16) Lincoln, A.P. et D.T. Hill. An integrate microalgae system. In: Algae biomass: production and use. Elsevier/North Holland, G. Shelef et C. Soeder (eds), Biomedical Press, Amsterdam, pp. 229-244 (1980).

(17) Waligora, Y. Communication personnelle, Université Laval (1986).

(18) Martin, C., J. de la Noüe et G. Picard. Intensive cultivation of freshwater microalgae on aerated pig manure. Biomass 7:245-259 (1985).

(19) Pouliot, Y. et J. de la Noüe. Mise au point d'une installation pilote de traitement tertiaire des eaux usées par microalgues. Rev. frçse Sci. Eau, 4(2-3):207-222 (1985a).

(20) Normandin, D. et J. de la Noüe. Production de Scenedesmus sp. sur lisier de porc. Communication présentée au 54ième congrès de l'ACFAS, Montréal, 12-17 mai 1986.

# PHOTOLYSIS AND RADIANT FLASH PYROLYSIS OF COAL-DERIVED WASTES

James J. Worman, Joseph J. Worman, Steven B. Hawthorne, and Rodney E. Sears
University of North Dakota Energy Research Center
Box 8213, University Station
Grand Forks, ND 58202

## ABSTRACT

It is attractive to think that coal-derived wastes could be converted to useful fuels by irradiation with solar energy. This would eliminate energy-intensive steps in the processing of coal gasification condensate water as well as provide an inexpensive alternate source of energy. Environmental concerns for the distribution of contaminants from biosludge would be minimized.

This paper demonstrates that coal gasification condensate water in the presence of photoconductors and varying wavelengths of light can produce useful fuels in addition to lowering the total organic carbon content. Biosludge obtained from the processing of the condensate water can be irriadiated in the solid state with a high-intensity xenon flash to give fuel-type products as identified by GC/MS.

## 1. INTRODUCTION

### 1.1 Photolysis of Organics in Water

In the last decade heterogeneous photocatalysis has been used to initiate many chemical conversions. The process involves the continuous excitation of a solid catalyst surface, which then converts reactants via free radical and electron transfer mechanisms to different species. Many of these conversions are of environmental interest because they can change a hazardous organic compound into a safe, biodegradable substance. Of particular interest recently has been the photocatalytic dechlorination, in the presence of $TiO_2$, of such species as chloroform (1) and trichloroethylene (2). The stoichiometries of the reactions were found to be:

$$Cl_2C{=}CHCl + H_2O + 3/2\ O_2 \xrightarrow[\text{Near UV}]{TiO_2} 2\ CO_2 + 3\ HCl$$

$$CHCl_3 + H_2O + 1/2\ O_2 \xrightarrow[\text{Near UV}]{TiO_2} CO_2 + 3\ HCl$$

Even polychlorinated biphenyls (PCBs) have been shown to react under these conditions (3).

The production of fuels from organics and water irradiated at 350 nm in the presence of $TiO_2$ began about 1978, when it was shown that methane could be generated from the irradiation of acetic acid (4).

$$CH_3\text{-}C\text{-}OH \xrightarrow[350\ nm]{H_2O,\ TiO_2/Pt} CH_4 + CO_2$$

The use of platinized $TiO_2$ in the presence of organics to give hydrogen, carbon dioxide, and ammonia has been documented (5). Irradiation of an aqueous suspension of Texas lignite (6) and solutions of phenols and catechols (7) under similar conditions give hydrogen as the only fuel gas. A mixture of photocatalysts (8) and the use of solar energy (9) as the excitation source have been studied, and the results suggest that, in general, organic compounds in water in the presence of a solid photoconductor and the correct wavelength of light will give hydrogen and carbon dioxide which can be represented by the overall reaction shown below (7).

$$R\text{-}CH_2\text{-}CH_3 + 2\ H_2O \xrightarrow[h\nu]{TiO_2} R\text{-}CH_3 + 3\ H_2 + CO_2$$

Table 1 shows the concentration of organics in the raw water and stripped gas liquor from the Great Plains Gasification Plant in Beulah, North Dakota, and from the slagging fixed-bed gasifier at the University of North Dakota Energy Research Center (UNDERC). Many of the chemicals that appear in these waters, such as catechols, phenols, alcohols, and acids, have been previously irradiated in water in the presence of $TiO_2$ catalyst to give hydrogen and carbon dioxide. There is no reason to suspect that a combination of these chemicals in the gasifier water will act any differently.

TABLE 1

CONCENTRATION OF ORGANIC COMPONENTS (PPM)
IN THE RAW WATER AND SGL FROM BOTH
GPGA AND UNDERC CONDENSATE WATERS

| Component | GPGA Raw Water | GPGA SGL | UNDERC Raw Water | UNDERC SGL |
|---|---|---|---|---|
| m-Cresol | 770 | ND | 950 | 0 |
| Methanol | 600 | 280 | 1450 | 230 |
| Ethanol | ND | ND | 5 | 0 |
| Acetone | 520 | ND | 40 | 10 |
| Catechol | -- | 30,127,280 | | |
| Acetate | 490 | 400 | | 180 |
| Formate | 160 | 110 | | 40 |
| Phenol | 2490 | 10 | 3840 | 130 |

### 1.2 Radiant Flash Pyrolysis of Coal and Coal-Derived Wastes

The first flash pyrolysis of coal (10) produced temperatures in excess of 1000°C in one or two milliseconds using a xenon flash tube. The product gases contained hydrogen, acetylene, and $CS_2$, to mention only a few. Conclusions from this work did not suggest a way to use flash irradiation as a process tool, but with the advances made in the uses of solar energy, and similartly of the xenon emission spectrum to that of the sun, make the flash irradiation application less vague. More recent investigations have concentrated on the conversion of biomass to useful fuels (11). Table 2 gives the mass percent yields of gases that resulted from the flash radiant pyrolysis of various biomass material when irradiated with a xenon flash tube at 9025 joules/pulse. The percent of the sample converted to gases ranged from 30 to 57 percent, depending on the specific sample. These studies suggest that a solar arc of identical radiant flux would produce the same results.

Little or no information exists on the radiant flash pyrolysis of biosludge. Work at Princeton is being designed to accomplish this feat on sewage sludge (12) and, in fact, may have been accomplished at this writing. Differential calorimetry and thermogravimetry have been used to examine sewage under moderate heating rates (13). This study is deemed necessary in order to develop the detailed kinetics, which could then be extrapolated to the higher heating rates that are required by flash pyrolysis.

## 2. EXPERIMENTAL PHOTOLYSIS

Stripped gas liquor (SGL) (50 ml) was placed in a large test tube leaving approximately 30 mL of headspace. To this was added 300 mg of a catalyst. The tube was stoppered with a neoprene septum and the headspace purged with nitrogen. The samples were then inserted into a homemade Srinivasan-Rayonet-type reactor which was capable of delivering light at either 254 or 350 nm. The samples were irradiated for 25 hours; a gas sample was drawn with an air-tight gas syringe and analyzed with a Hewlett Packard gas analyzer. Solar energy experiments were performed by irradiating 250 mL of SGL containing 1 gm of catalyst. Light was focused on the sample with a Fresnel lens. This provided both heat and light energy, which caused the sample to reflux. Total organic carbon analyses were done prior to and after one and three hours of irradiation. Results of the photolysis experiments are shown in Tables 3 and 4.

TABLE 2

PRODUCTS OF THE FLASH PYROLYSIS OF VARIOUS BIOMASS MATERIALS
(MASS PERCENT YIELDS OF ORIGINAL SAMPLE)

| Sample | $CO_2$ | CO | $H_2$ | $C_2H_2$ | $CH_4$ | $C_2H_4$ | Gas | Liq | Sol[a] | Total |
|---|---|---|---|---|---|---|---|---|---|---|
| Lignin | 2.1 | 31.6 | 4.0 | 3.9 | 0.2 | 0.2 | 42.0 | 13.2 | 20.0 S | 75.2 |
| Redwood | 4.2 | 42.3 | 3.3 | 5.9 | 0.6 | 0.5 | 56.8 | 15.1 | 6.7 SP | 78.6 |
| Dextrose | 3.6 | 24.8 | 1.9 | 4.1 | 0.7 | 0.0 | 35.1 | 54.2 | 10.1 U | 99.4 |
| D-cellobiose | 4.5 | 23.9 | 1.5 | 3.2 | 1.0 | 1.6 | 35.7 | 49.4 | 8.9 U | 94.0 |
| Kraft Paper | 2.4 | 22.8 | 1.3 | 1.8 | 0.7 | 0.5 | 29.6 | 10.0 | 43.1 PA | 82.7 |

[a] The form of the solid remaining in the reactor after the flash varied with the substrate. The letters to the right of the solid mass fraction yield indicate the type of solid found in the reactor cell after the experiment: P = primary char; S = secondary char; A = ash; and U = unpyrolyzed substrate.

TABLE 3

RESULTS FROM THE ANALYSIS OF GAS EVOLVED DURING IRRADIATION
OF COAL GASIFICATION CONDENSATE WATER FOR 24 HOURS

| ϒ of Excitation | Time of Irradiation | Catalyst | Normalized Air Free (Mole Percent) | | | |
|---|---|---|---|---|---|---|
| | | | $H_2S$ | $H_2$ | $CO_2$ | $C_3H_8$ |
| 350 nm | 24 hours | None | -- | 37.41 | -- | -- |
| 350 nm | 24 hours | $TiO_2$ | -- | 93.26 | -- | -- |
| 350 nm | 24 hours | $TiO_2$/Pt | -- | 99.38 | -- | -- |
| 350 nm | 24 hours | $V_2O_5$ | 1.04 | 84.47 | 0.65 | 4.31 |
| Xenon Strobe | 24 hours | $TiO_2$/Pt | -- | 75.01 | 25.00 | -- |

## TABLE 4

## RESULTS FROM THE ANALSIS OF GAS EVOLVED DURING IRRADIATION OF COAL GASIFICATION CONDENSATE WATER AT 254 nm

| $\nu$ of Excitation | Time of Irradiation (hr) | Catalyst | Normalized Air Free and Nitrogen Free Mole Percent | | | TOC mg/L |
|---|---|---|---|---|---|---|
| | | | $H_2$ | $CO_2$ | CO | |
| 254 nm | 24 | None | 14.29 | 47.62 | 33.33 | -- |
| 254 nm | 24 | $SnO_2/TiO_2$ | 100.00 | -- | -- | -- |
| 254 nm | 24 | $V_2O_5$ | 100.00 | -- | -- | -- |
| 254 nm | 24 | $TiO_2/Pt$ | 14.29 | 85.72 | -- | -- |
| Sunlight | 3 | $TiO_2$ | -- | -- | -- | 578 |
| Sunlight | 1 | $TiO_2$ | -- | -- | -- | 750 |

### 2.1 Radiant Flash Pyrolysis

Biosludge obtained from the biodegradation of SGL was in the form of an aqueous slurry and was dehydrated by heating at 110°C in a drying oven for several hours. The sample was then pulverized and sieved to give a constant particle size range from about 212 to 425 µm. The samples (0.2 to 0.5 grams) were placed in a reactor tube, then placed in the xenon flash pyrolysis cell (Figure 1). Helium gas was passed over the sample and through the cell for 15 minutes. A Tenax trap was then attached to the exit line of the pyrolysis cell. Helium was allowed to pass through the cell continuously at 120 cc/min during the entire experiment. The xenon flash was adjusted to deliver 15,000 joules/pulse in 10 milliseconds. Three consecutive pulses were delivered to the samples and the exit gases were collected on the Tenax trap. The GC/MS data was obtained by thermally desorbing (He flow) the trap at 200°C for 10 minutes into a DB-5 column held at -50°C. The column was heated rapidly to 0°C and then at 8°C/min until a maximum of 300°C was reached. The GC/MS of the coal gasification condensate water irradiated biosludge is shown in Figure 2.

## 3. RESULTS AND DISCUSSION

### 3.1 Photolysis

Irradiation of the SGL at 350 nm (Table 3) gives a small amount of hydrogen in the absence of a catalyst but is most efficient in the presence of $TiO_2$ and platinum. The percentages are reported as normalized air-free and nitrogen-free mole percent. The actual percentage of hydrogen in the headspace ranged from 1 to 6 percent. The absence of $CO_2$ must be due to the formation of carbonate in the basic gasifier water, although this has not been proven. In the presence of $V_2O_5$, hydrogen sulfide and propane form in addition to hydrogen and carbon dioxide. This may be due to the stronger oxidation power of $V_2O_5$ over $TiO_2$, but details of the mechanism are unknown. The presence of carbon dioxide when xenon strobes are used for irradiation may be due to the fact that the greater amount of visible radiation from the xenon strobe accelerates the water splitting reaction from the photoconductor, and thus the rate of oxidation of the organics, to give more carbon dioxide. As the wavelength of irradiation is decreased or the energy

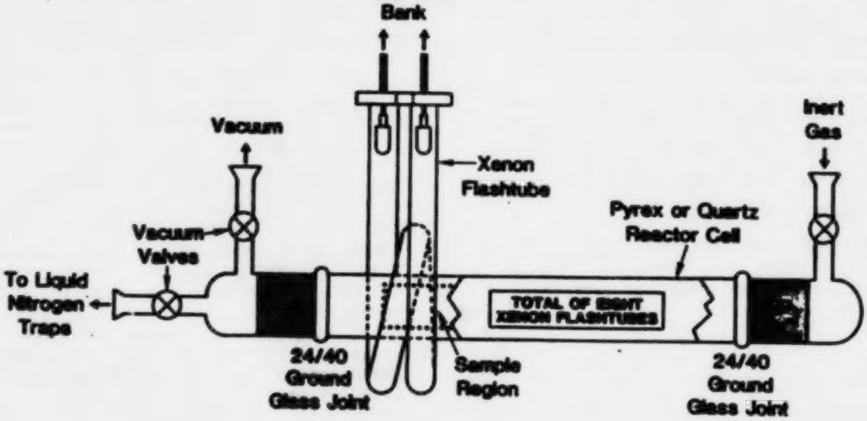

Figure 1. Sketch of xenon flash pyrolysis apparatus.

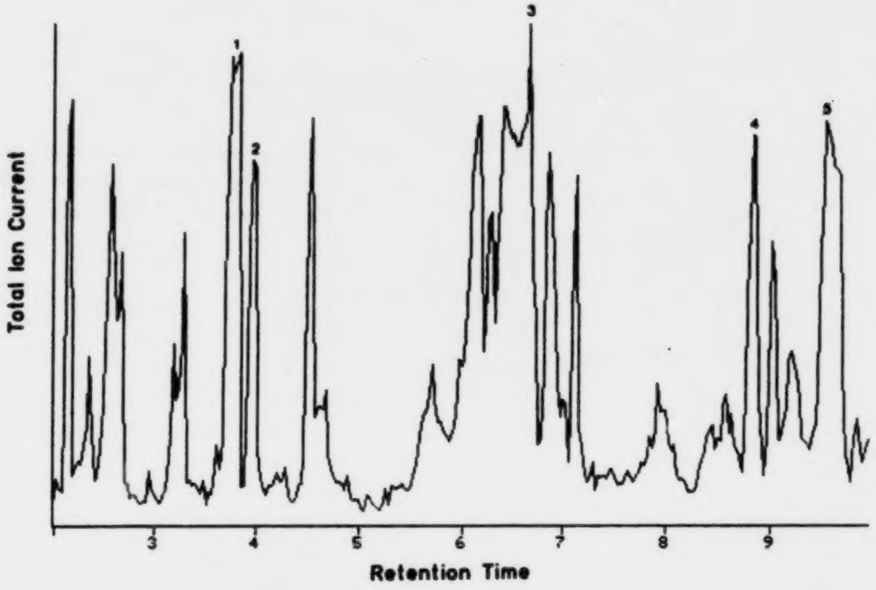

Figure 2. Partial GC/MS of compounds trapped from xenon flash pyrolysis of biosludge.

increased (Table 4), hydrogen production in the presence of $TiO_2$ is less productive. The energy is not conducive to excitation of an electron from the valence to the conduction band on the photoconductor. On the other hand, $V_2O_5$ and $SnO_2/TiO_2$ must absorb the 254 nm light and promote the water splitting reaction since hydrogen is the only gas formed. Several solar energy experiments were carried out, and after a three-hour period approximately 23 percent of the total organic carbon was reduced.

Neither estimates of energy input versus volume of fuel gas produced nor the quantitative analyses of individual organics in solution have been accomplished at this time.

A mechanism consistent with the formation of carbon dioxide and hydrogen from the organics has been proposed (7). It is reasonable to assume that a similar mechanism is taking place during photolysis of the coal gasification condensate water.

(I) formation of an alcohol and a carboxylic acid

$$H_2O + p^{\cdot +} \longrightarrow \cdot OH + H^+$$

$$H^+ + e^- \longrightarrow 1/2\ H_2$$

$$RCH_2CH_3 + 2\ \cdot OH \longrightarrow RCH_2CH_2OH + H_2O$$

$$RCH_2CH_2OH \longrightarrow RCH_2CHO + H_2$$

$$RCH_2CHO + H_2O \longrightarrow RCH_2COOH + H_2$$

$p^{\cdot +}$ = photoactivated semiconductor surface

(II) decomposition of a carboxylic acid (photo-Kolbe reaction)

$$RCH_2COOH \longrightarrow RCH_3 + CO_2$$

(III) total reaction

$$RCH_2CH_3 + 2\ H_2O \longrightarrow RCH_3 + 3\ H_2 + CO_2$$

There are no alkanes present in the water, but a significant number of alcohols, acids, and compounds from which alcohols can be made are present; thus, there is no reason to suspect that an alternate mechanism is taking place.

For practical and environmental concerns, the catalysts used were insoluble in the water. They can then be recovered approximately 100 percent by filtration, thereby eliminating contamination of the condensate water by additional toxic metals.
There is sufficient evidence to indicate that it is possible to irradiate the coal gasification water to give fuel gases and to reduce the total organic carbon. The potential for using this process to clean up the gasifier water and to utilize it as an alternate fuel source is imminent, and thus, the reason for this study. At present, Great Plains Gasification Plant (GPGP) is purifying coal gasification condensate water by solvent stripping, steam stripping, biotreatment, and carbon filtration. It will be possible from operational parameters to make an economic assessment of this process in terms of cost/gallon to process condensate water. Using solar energy as the excitation source, the Btu value of the fuel gas and the equipment cost of the photochemical process will be made and compared to the GPGP system.

### 3.2 Radiant Flash Pyrolysis of Biosludge

The results of the pyrolysis of biosludge are shown in Figure 2. This represents a plot of the intensity versus retention time as recorded by GC/MS. The individual peaks, as numbered, were identified by matching the mass spectral fragmentation patterns to those of known compounds. The peaks were: 1 - benzene, 2 - thiophene, 3 - toluene, 4 - C$_2$-benzenes and 5 - styrene. The larger amounts of toluene and benzene may make the biosludge a source of fuel additives. In addition, the many other chemicals formed may afford a source of raw materials. The unique feature of the flash pyrolysis unit is that one gets instantaneous heating and cooling, which prevents a secondary reaction from occurring. The glass surface also minimizes catalytic effects of metal surfaces that are present in normal pyrolysis units. These features should make it possible to look at primary pyrolysis products and, therefore, aid in understanding the mechanism of bond breaking in the pyrolysis of coal and coal-derived materials. Recent experiments on the pyrolysis of coals and peats show that compounds from radiant flash pyrolysis show more unsaturation than those obtained from thermal pyrolysis. The use of the xenon flash pyrolysis unit as a model for solar energy furnaces is possible in the future and, thus, would minimize costs.

## 4. CONCLUSION

Preliminary results show that coal gasification condensate water can be converted to hydrogen gas by irradiation in the presence of semiconductor catalysts. Questions remain as to the efficiency of this process, the lifetime of the catalysts, and adaptability to solar irradiation. Flash pyrolysis of coal-derived biosludge gives oils which contain large quantities of benzene and toluene among other chemicals offering a potential source of fuel additives and source of raw materials.

## 5. ACKNOWLEDGEMENTS

The advice of Dr. Warrack Willson, Manager of the Fuels Conversion and Process Chemistry Research Division, and the support from the U.S. Department of Energy Grand Forks Project Office were appreciated.

## 6. REFERENCES

1. Ollis, D.F. Environ. Sci. Tech., 19, 481, (1985).
2. Ahmed, S. and D.F. Ollis. Solar Energy, 32, 597, (1984).
3. Carey, J.H., J. Lawrence, and H.M. Tosine. Bull. Envir. Cont. and Tox., 16, 697, (1976).
4. Kraentler, B. and A.J. Bard. J. Am. Chem. Soc., 100, 2239, (1978).
5. Kawai, T. and T. Sakata. Chem. Letters, 81, (1981); and references therein.
6. Sato, S. and J.M. White. Ind. Eng. Chem. Prod. Res. Dev., 19, 542, (1980).
7. Hashimoto, K., T. Kawai, and T. Sakata. J. Phys. Chem., 88, 4083, (1984).
8. Carey, J.H. and B.G. Oliver. Water Poll. Res. J. of Canada, 15, 157, (1980).
9. Kawai, T. and T. Sakata. J. Chem. Soc. Chem. Comm., 1047, (1979).
10. Hawk, C.O., M.D. Schlesinger, and R.W. Hiteshue. United States Department of the Interior, Bureau of Mines, Report of Investigations, 6264, (1963).
11. Hopkins, M.W. and M.J. Antal, Jr. Journal of Applied Polymer Science, 29, 2163, (1984).
12. Urban, D.L. and M.J. Antal, Jr. Fuel, 61, 799, (1982).
13. Antal, M.J., Jr., L. Hofmann, and J.R. Mareira. Solar Energy, 30, 299, (1983).

DISCLAIMER

This report was prepared as an account of work sponsored by the United States Government. Neither the United States nor any agency thereof, nor any of their employees, makes any warranty, express or implied, or assumes any legal liability or responsibility for the accuracy, completeness, or usefulness of any information, apparatus, product, or process disclosed, or represents that its use would not infringe privately owned rights. Reference herein to any specific commercial product, process, or service by trade name, mark, manufacturer, or otherwise, does not necessarily constitute or imply its endorsement, recommendation, or favoring by the United States Government or any agency thereof. The views and opinions of authors expressed herein do not necessarily state or reflect those of the United States Government or any agency thereof.

# DEMONSTRATION OF CONDENSING FLUE GAS HEAT RECOVERY

T.J. Molczan, A.P. Scriven and J. Magro
Canada Packers Inc.
Toronto, Ontario

## ABSTRACT

Canada Packers Inc. has successfully demonstrated condensing flue gas heat recovery under the Federal/Provincial Conservation and Renewable Energy Demonstration Agreement.

The heat recovery system was designed and manufactured by John Thurley Ltd. and has been in operation at the Winnipeg Plant since the summer of 1982. It is capable of recovering about four times as much heat as conventional systems, such as economizers and combustion air preheaters. This is due to its ability to recover latent heat by condensing the flue gas water vapour, and to recover a greater portion of the sensible heat. As a result, the exit flue gas temperature is reduced to about 30°C. The heat recovery system is capable of heating water to about 60°C, thus it is ideally suited to operations which require large quantities of hot water. At Winnipeg the pre-heated water is used for processing, sanitation and boiler make-up.

## BACKGROUND

Until recently, the amount of heat that could be recovered from a boiler's flue gases was limited by the requirement that they not be cooled below about 150°C in order to prevent condensation of water vapour and various acidic compounds. This was done to prevent corrosion problems from occuring in the boiler's breeching and stack as well as the heat recovery equipment.

The potential fuel cost savings from recovering more of the waste heat were not sufficient to justify the extra cost for larger heat transfer surfaces and more extensive use of corrosion resistant materials.

### Conventional Flue Gas Heat Recovery Systems

Conventional flue gas heat recovery systems are either economizers or combustion air preheaters.

An economizer is an air-to-liquid heat exchanger used to preheat boiler feedwater. It usually consists of an arrangement of finned tubes located in the boiler's stack, through which the feedwater flows. In order to prevent corrosion problems due to condensation of water vapour and acids, the flue gas temperature must be maintained above 150°C. Feedwater provides a simple answer to this consideration since it normally enters the economizer at a temperature above 100°C, which is sufficient to maintain the external surface temperature of the heat exchange tubes above 150°C.

A combustion air preheater is an air-to-air heat exchanger. It saves fuel by preheating the air used to sustain combustion.

One type of air preheater is called a recuperator. It usually consists of a plate heat exchanger with the flue gas and combustion air flowing on opposite sides of the plate. Another type of preheater, called a regenerator, transfers heat by alternately exposing a thermal storage mass to the flue gas and the combustion air. A very common type of regenerator is the heat wheel. It consists of a rotating mass, half of which is in the flue gas stream while the other is in the combustion air stream.

Economizers and air preheaters have proven to be very practical devices over many years. They can improve the overall boiler combustion efficiency to as much as 85 percent.

### Condensing Heat Recovery Systems

Today's high fuel prices have prompted several companies to address the potential to economically recover more of the heat from boiler flue gases. This has resulted in the development of condensing heat recovery systems, which are capable of recovering about four times as much heat as conventional economizers and air preheaters. This vast improvement in performance has been achieved as follows. First, most of the sensible heat is recovered from the flue gases by cooling them to an exit temperature of 30°C or less. This low flue gas temperature in turn causes the water vapour to condense from the flue gas and release its latent heat of vapourization which can then also be recovered.

Table 1 shows an example of the potential improvement in performance of condensing heat recovery systems compared with conventional systems. The condensing system can recover nearly four times as much heat as the conventional system. This improves the overall combustion efficiency to 96.3 percent compared to 84.1 percent with a conventional system.

Although they can recover much more heat than conventional systems, condensing heat recovery systems are also much more costly. There are several reasons for this. Condensing systems tend to be physically larger than conventional systems in order to provide extra heat transfer surface. They also require the extensive use of corrosion resistant materials due to the condensing of acidic compounds with the water vapour. Finally, condensing systems can be more complex than conventional systems, requiring auxiliary equipment such as pumps and fans and more sophisticated controls.

Whether or not the extra cost of a condensing heat recovery system can be justified, depends largely on the price of fuel, which varies widely across Canada. Therefore each potential installation should be evaluated separately.

### Application Of Condensing Heat Recovery At The Winnipeg Packinghouse

In 1981, various flue gas heat recovery systems were considered for the three boilers at the Winnipeg packinghouse plant. Among them were condensing heat recovery systems designed to preheat water for use in processing and sanitation as well as for boiler feed. A study of the plant's daily and seasonal steam and hot water production profile confirmed that the cost of recovering the additional heat could be justified.

A condensing heat recovery system designed and manufactured by John Thurley Ltd., and called a Direct Contact Heat Recuperator was selected. Due to the technical risks associated with applying new technology, and the longer payback period for the recuperator compared to an economizer, a proposal was made to demonstrate the technology under the Manitoba/Canada Conservation and Renewable Demonstration Program. This proposal was approved in the fall of 1981.

The Direct Contact Heat Recuperator was installed during the summer of 1982. The remainder of this report documents the first six months' performance of the unit.

## DIRECT CONTACT HEAT RECUPERATOR

In the summer of 1982, a heat recuperator designed and manufactured by John Thurley Ltd., was installed at the Winnipeg Packinghouse plant. This system recovers waste heat from the flue gases of the three steam boilers.

### Principle Of Operation

The Thurley recuperator recovers heat from flue gases by bringing them into direct contact with cold water sprays. The cold sprays are essential to achieving the recuperator's high rate of heat recovery. They cause the water vapour in the flue gas to condense, thereby releasing its latent heat of vapourization to the water spray. The latent heat provides approximately half of the heat recovered by the recuperator. The remainder is due to sensible heat transfer.

The recuperator produces water at a temperature of approximately 54°C. The water is passed through a plate heat exchanger to heat potable process water. The flue gases leave the recuperator at a temperature of 38°C or less, thereby raising the overall combustion efficiency to in excess of 96 percent.

The Thurley recuperator is ideal for operations which can make use of large quantities of hot water. Many companies in the Food and Beverage sector fall into this category because of their need for hot water for processing and sanitation. The heat can also be used to preheat boiler make-up water.

TABLE 1

PERFORMANCE OF CONVENTIONAL vs. CONDENSING HEAT RECOVERY SYSTEMS

| Heat Recovery System | Exit Flue Gas Temperature | Overall Combustion Efficiency (1) | Heat Recovery Rate (2) % Fuel Input | Heat Recovery Rate (2) % Waste Heat |
|---|---|---|---|---|
| None | 238°C | 80.0% | 0.0 | 0.0 |
| Conventional | 150°C | 84.1% | 4.1 | 20.5 |
| Condensing | 30°C | 96.3% | 16.3 | 81.5 |

(1) Assuming 25 present excess air.
(2) Assuming no losses in heat recovery system.

### Description Of Recuperator

A schematic diagram of the heat recuperator is shown in Figure 1. The recuperator consists of two sections. The lower section, incorporates the flue gas inlet and quench zone and the upper section houses the demister and the flue gas outlet.

During operation, the flue gas bypasses the existing boiler stack and is forced through the recuperator by means of an induced draft fan. A recirculating water loop transfers heat from the flue gas to cold, potable water via a plate heat exchanger. This heated water (49°C) is then further heated with live steam to be used for plant processes, sanitation and as boiler make-up.

Recirculating water cooled in the plate heat exchanger is sprayed into the upper contact section of the recuperator and collected on a stainless steel baffle plate. This partially heated water is then run off to a head tank, from which it is pumped to the sprays of the lower quench section. After collection in the base of the recuperator it is then pumped back to the plate heat exchanger, which completes the loop.

Direct contact with acidic compounds in the flue gas causes the recirculating water to become acidic. Furthermore, recirculation causes the acids to concentrate, thereby continuously reducing the pH. This effect is partially countered by adding make-up water at the head tank to dilute the acid, and maintain the pH above 4. This minimizes the acidity but does not eliminate it, therefore corrosion resistant materials have been used throughout the recuperator. Stainless steel has been used in the components located in the lower section, which have the most contact with the recirculating water. The stack and flue gas outlet have been constructed of fibreglass reinforced plastic.

The recirculating water flow rate can be manually or automatically controlled in order to maintain a maximum temperature of 54°C in the base of the recuperator. To maintain efficient spray contact action and quenching, the water flow rate is maintained above a minimum allowable level. Thus, under conditions of reduced boiler load, a lower recirculating water temperature will result, but the heat recovery efficiency will, however, be maintained.

## HEAT RECUPERATOR PERFORMANCE

### Recuperator Utilization

In order to maximize the savings, it is necessary to maximize the utilization (operating hours) of the recuperator.

Each shift, the stationary engineer reads an elapsed time meter and records the number of recuperator operating hours, along with the reasons for any down-time. This information has been valuable to the project engineer in identifying and solving problems.

The utilization rate is shown in Table 2. It has been expressed in hours per week and as a percent of the maximum possible hours (168). The table shows that the utilization rate averaged 86.4 percent during the monitoring period. The utilization rate averaged a rather low 60 percent during the first seven weeks of the monitoring period. This was largely due to frozen damper air control lines (see Problem Areas and Solutions). When that problem was solved, the utilization improved to its present rate, in excess of 95 percent.

### Heat Recovery Rate

The amount of heat recovered is measured by a meter which records the heat transferred from the recuperator water to the plant water in the plate heat exchanger. This data is used to calculate the heat recovery as an hourly rate and as a percentage of the boiler fuel input, as shown in Table 2. The latter figure is a good indicator of the recuperator's heat recovery performance.

Table 2 shows that during the monitoring period, the heat recovery rate averaged 4.38 GJ/h. This is equivalent to 10.4 percent of the boiler fuel consumption. Effectively, the overall combustion efficiency has been improved by 10.4 percent, from 81.8 percent to 92.2 percent.

The heat recovery efficiency of the recuperator averages approximately 70 percent, which is considered to be good performance for any heat recovery system.

### Reduction In Steam And Fuel Use

A total of 16,489 GJ was recovered during the monitoring period, as shown in Table 2. This information was used to estimate the amount of steam and fuel saved:

1. Allowance For Storage Tank Losses - A portion of the water heated by the recuperator on the night shift and on weekends is stored in a 21,200 $m^3$ outdoor tank. It has been estimated that 10 percent of the weekly heat recovered is lost due to the heat losses in the tank. Therefore the net heat recovered has been calculated to be 90 percent of the gross:

   Net Heat Recovered = 0.9 x 16489
   = 14,800 GJ

2. Steam Savings Estimate - The net heat recovered replaces heat which would otherwise have been obtained from steam.

FIG. 1. THURLEY DIRECT CONTACT RECUPERATOR

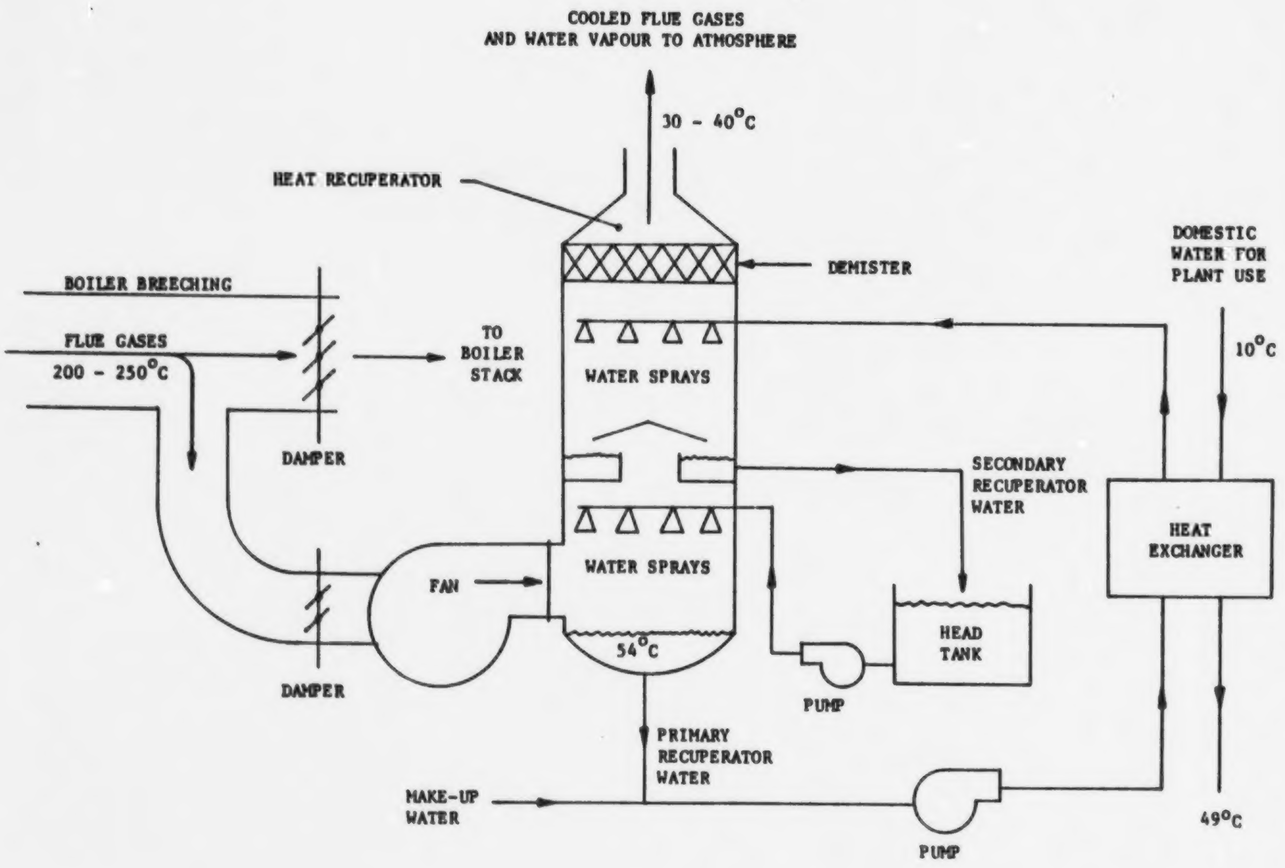
COOLED FLUE GASES
AND WATER VAPOUR TO ATMOSPHERE
30 - 40°C
HEAT RECUPERATOR
DEMISTER
DOMESTIC
WATER FOR
PLANT USE
BOILER BREECHING
FLUE GASES
200 - 250°C
TO
BOILER
STACK
WATER SPRAYS
10°C
DAMPER
SECONDARY
RECUPERATOR
WATER
HEAT
EXCHANGER
FAN
WATER SPRAYS
HEAD
TANK
54°C
DAMPER
PUMP
PRIMARY
RECUPERATOR
WATER
MAKE-UP
WATER
49°C
PUMP

## TABLE 2 RECUPERATOR PERFORMANCE

| Week Beginning | Recuperator Utilization | | Ave. Boiler Fuel Input | Heat Recovery Rate | | |
|---|---|---|---|---|---|---|
| | | | | Total | Average* | Fuel Input |
| | Hours | % | GJ/h | GJ | GJ/h | % |
| Oct. 2, 1982 | 117 | 69.6 | N/A | 559 | 4.78 | N/A |
| 9 | 37 | 22.0 | 37.7 | 156 | 4.22 | 11.2 |
| 16 | 94 | 56.0 | N/A | 373 | 3.97 | N/A |
| 23 | 144 | 85.7 | 40.0 | 705 | 4.90 | 12.2 |
| 30 | 119 | 70.8 | 44.5 | 566 | 4.76 | 10.7 |
| Nov. 6 | 120 | 71.4 | 42.2 | 502 | 4.18 | 9.9 |
| 13 | 113.5 | 67.6 | 41.0 | 550 | 4.85 | 11.8 |
| 20 | 167.5 | 99.7 | 43.2 | 778 | 4.64 | 10.8 |
| 27 | 168 | 100.0 | 41.7 | 701 | 4.17 | 10.0 |
| Dec. 4 | 150 | 89.3 | 42.4 | 647 | 4.31 | 10.2 |
| 11 | 108 | 64.3 | 49.4 | 559 | 5.18 | 10.5 |
| 18 | 150.5 | 89.6 | 42.4 | 507 | 3.37 | 7.9 |
| 25 | 145 | 86.3 | 35.3 | 468 | 3.23 | 9.1 |
| Jan. 1, 1983 | 168 | 100.0 | 41.3 | 702 | 4.18 | 10.1 |
| 8 | 140 | 83.3 | 51.9 | 535 | 3.82 | 7.4 |
| 15 | 168 | 100.0 | 47.2 | 759 | 4.52 | 9.6 |
| 22 | 168 | 100.0 | 45.7 | 838 | 4.99 | 10.9 |
| 29 | 166.5 | 99.0 | 44.3 | 858 | 5.15 | 11.6 |
| Feb. 5 | 168 | 100.0 | 42.3 | 794 | 4.73 | 11.2 |
| 12 | 160 | 95.0 | 40.3 | 836 | 5.23 | 13.0 |
| 19 | 168 | 100.0 | 40.8 | 839 | 4.99 | 12.2 |
| 26 | 168 | 100.0 | 38.0 | 727 | 4.33 | 11.4 |
| Mar. 5 | 162 | 96.4 | 41.8 | 675 | 4.17 | 10.0 |
| 12 | 168 | 100.0 | 38.6 | 655 | 3.90 | 10.1 |
| 19 | 166 | 98.8 | 40.8 | 664 | 4.00 | 9.8 |
| 26 | 168 | 100.0 | 35.7 | 536 | 3.19 | 8.9 |
| | 3,772 | 86.4 | 42.0 | 16,489 | 4.38 | 10.4 |

* Total divided by recuperator operating hours.

It has been estimated that an average of 0.5198 t (metric tons) of steam are saved for every gigajoule of heat recovered at Winnipeg. Therefore the steam saving is:

Steam Savings = 14,800 x 0.5198
= 7,700 t

3. Fuel Savings Estimate - The fuel savings depend on the steam savings and the efficiency of the boilers. The boiler efficiency was accurately accounted for by multiplying the steam savings by the boiler's fuel to steam ratio which was calculated using metered fuel and steam consumption data. During the monitoring period the fuel to steam ratio averaged 81.3 $m^3/t$ (cubic metres of natural gas per metric ton of steam). Therefore, the fuel savings were:

Fuel Savings = 7,700 x 81.3
= 626,000 $m^3$

## Energy For Auxiliary Equipment

The heat recovery system contains 82.9 kV·A of auxiliaries. The recuperator normally operates 24 hours per day, therefore the plant's peak demand for power has increased by 82.9 kV·A.

The recuperator operated for 3772 hours during the monitoring period at an estimated power factor of 90 percent. Therefore the energy consumption was:

Energy = 82.9 kV·A X 3772 h X 0.9 W/(V·A)
= 281,429 kW·h
= 1,013 GJ

## PROBLEM AREAS AND SOLUTIONS

### Freezing Of Moisture In Pneumatic Controls

Much of the down-time during the early part of the monitoring program was due to seized-up flue gas control dampers. This was caused by the freezing of moisture in the pneumatic controls during periods of cold weather. The problem was solved by installing an air dryer to remove moisture from the compressed air in the control system.

### Corrosion Of Recuperator Circulating Pumps

The water re-circulation pumps provided with the recuperator had been expected to be able to withstand acidic solutions. As it turned out, all four pumps were badly damaged by corrosion and had to be replaced after four months of operation. John Thurley Ltd. provided stainless steel pumps, which have operated for several months so far without any corrosion.

## ECONOMIC ANALYSIS

### Fuel Savings

During the six month monitoring period of October 1982 to March 1983, the fuel savings were estimated to be 626,000 $m^3$ of natural gas. It is expected that during the following six months, from April 1983 to September 1983, the savings will decrease by 25 percent to 470,000 $m^3$. This is due to the normal 25 percent seasonal variation in the plant's steam production, which will result in a corresponding decrease in the amount of heat recovered.

The annualized fuel savings is the sum of the above savings, which is 1,100,000 $m^3$ of natural gas. At the current fuel price of 0.1427 $\$/m^3$ the annual cost reduction will be $157,000. Allowing $11,700 for power to auxiliaries and $4300 for maintenance, the net operating savings will be $141,000 per year.

### Capital Cost

The capital cost of the project was as follows:

| Item | Cost |
|---|---|
| Recuperator and Controls | $225,000 |
| Installation and Auxiliaries | 175,275 |
| Total Installed Cost | $400,275 |

### CREDA Contribution

The capital cost of the heat recovery system was reduced by a $160,192 contribution from the Manitoba/Canada Conservation and Renewable Energy Demonstration Agreement (CREDA). A further $20,400 has been allocated by CREDA to cover the cost of monitoring the project and publicizing the results to industry.

### Simple Payback

Based on the capital cost of $400,275 and net annual savings of $141,000, the simple payback of the recuperator is:

400275/141000 = 2.84 years

With the CREDA grant, the simple payback was improved to:

240083/141000 = 1.70 years

## CONCLUSION

The condensing flue gas heat recovery system installed at Winnipeg has proven to be both technically and financially successful.

The decision to install a condensing system should be based on the return on investment of the additional expense over a conventional heat recovery system.

* * *

# Solar Radiation

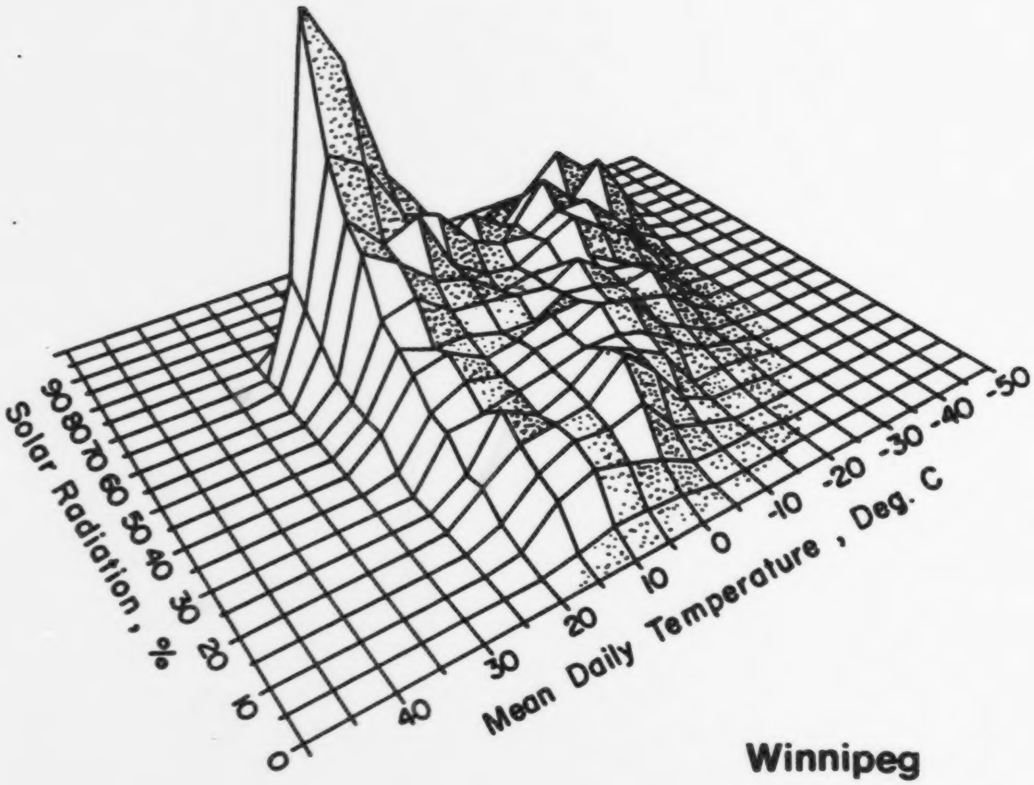

**Winnipeg**

# RECENT DEVELOPMENTS IN DIFFUSE RADIATION RESEARCH

**A. P. Brunger, P. Eng.**

**Department of Mechanical Engineering**
**University of Toronto**
**5 King's College Road**
**Canada, M5S 1A1**

## ABSTRACT

There appears to be an increasing interest in the problem of characterizing the anisotropic nature of the diffuse sky radiance for the purpose of refining estimates of the solar radiation income of sloping solar arrays. Most of the recent efforts in this area of research have been based on the approach of assuming a simple sky radiance distribution and calibrating the resulting mathematical description by comparing the calculated irradiance to irradiance measured on sloping planar surfaces. Ongoing work at the University of Toronto has taken the demanding but more straightforward approach of measuring the sky radiance directly. This paper emphasizes the advantages of the latter approach, gives some background on the significance of the diffuse component of solar radiation, and describes new quantitative information obtained from an analysis of narrow field-of-view sky radiance measurements made at Toronto.

## 1. INTRODUCTION

This paper discusses recent progress made in the investigation of the magnitude and distribution across the sky of the diffuse component of solar radiation. The diffuse component is made up of the scattered solar radiation that reaches the ground indirectly after being scattered out of the direct solar beam. The term sky radiance, with units of watts per square metre per steradian, is used in this paper to refer to the shortwave radiant energy flux per unit area per unit solid angle coming from a particular direction in the sky.

The interaction of solar radiation with Earth's atmosphere results in a depletion of the direct beam by scattering and absorption as depicted in Fig. 1. Some of the radiation that is removed from the direct beam is scattered back into space and some is absorbed by the atmosphere. The scattered radiation that reaches the ground is called the diffuse component. The direct component usually refers to the radiation measured by a pyrheliometer having a circular field of view with a 2.8 degree radius. The direct component, therefore, includes some radiation scattered through small scattering angles. The diffuse component includes the radiation reaching the ground from all other directions in the sky.

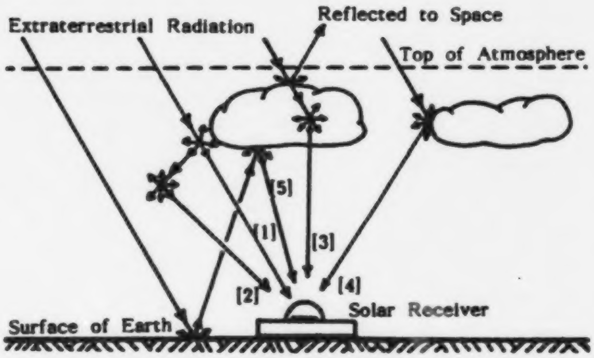

*Fig. 1. The interaction of solar radiation with the atmosphere. [1] Transmission of the depleted direct beam. [2] Single and multiple scattering by aerosols and gasses. [3] Diffuse transmission through clouds. [4] Diffuse reflection from clouds. [5] Multiple reflection between ground and clouds.*

Clouds, which are highly reflective for solar radiation, play an important role in the redirection of the incoming solar radiation and are primarily responsible for the overall planetary albedo (reflectance) of about 43 percent.(1) Rayleigh scattering from air molecules and Mie scattering from aerosols and water droplets in the atmosphere give rise to the characteristically anisotropic nature of the distribution of the diffuse component across the sky. It is this anisotropic distribution that has been the subject of recent research at the University of Toronto.

## 2. THE DIFFUSE COMPONENT: AN IMPORTANT SOURCE OF SOLAR ENERGY

Figure 2 shows the magnitude of both the diffuse component and the global solar irradiation as a function of latitude for 37 North American locations. There are at least two important observations to be made from this figure. One is that the diffuse irradiation is a significant fraction of the total solar energy, representing between 5 and 7.5 $MJ \cdot m^{-2} \cdot day^{-1}$. The other important observation is that the magnitude of the diffuse component stays relatively constant with latitude compared to the substantial decrease in global irradiation with increasing latitude. Figure 3, which shows the ratio of diffuse to global irradiation, demonstrates that the diffuse component is a large fraction of the total and that the fraction diffuse tends to increase with latitude. Indeed, the study of the characteristics of the diffuse component and of its utilization is proportionately more important in the Canadian context since the diffuse fraction is larger at the more northerly latitudes. An analysis of the data in Fig. 3 combined with data recently published by the Atmospheric Environment Service (AES) (2) reveals that, although local climate can strongly influence the diffuse fraction, on average the diffuse fraction increases one percentage point for every 270 km of northward distance.

## 3. THE VARIABILITY OF SKY RADIANCE

Diffuse solar radiation is the result of complex scattering processes that take place in the atmosphere. These processes are influenced by the variable amounts of cloud, dust, water vapour, etc. in the atmosphere, and result in an observed sky radiance distribution that is highly variable in time. It is possible to describe a single scattering event in the atmosphere if the wavelength and the direction of the incoming radiation are known and if the size and optical properties of the particle with which the radiation interacts are known. However, the atmosphere is made up of many components such as the mixed gasses, ozone, water droplets and aerosols, each with its own particle size distribution and optical properties. Furthermore, the atmosphere is in a continual state of change so that its composition at any one time cannot be known in detail. An accurate calculation of the results of scattering in a complex atmosphere has to account for multiple scattering and for the redistribution of the radiation field from one scattering event to another throughout the atmosphere. These complex calculations have been performed for a limited number of model atmospheres (3) but the calculations are very demanding of computer time. For these reasons the analytical prediction of the distribution of sky radiance under real conditions is not practicable. Therefore, the major part of research on the diffuse component has been empirically based rather than analytically based.

The naturally high variability of sky radiance, which is due in part to the constantly changing solar position, atmospheric turbidity and cloudiness, has two consequences important to the modelling of sky radiance. Firstly, good estimates of average sky radiance distributions must be based on a large number of measurements. Secondly, mean sky radiance distributions are of most value for describing long term average conditions. Mean distributions are of very little value in predicting or duplicating sky radiance patterns occurring during specific short time periods since sky radiance patterns are rarely repeated in nature. Moreover, individual narrow field-of-view sky radiance observations can be as much as twice the mean sky radiance for the same cloud amount and solar position. As a result, the direct measurement of sky radiance must involve a considerable commitment of time and resources to develop a measurement record large enough to be useful.

## 4. THE ADVANTAGES OF AN ANGULAR DISTRIBUTION MODEL

Despite the difficulty of determining the sky radiance distribution by direct measurement, there are significant advantages to having available a map of sky radiance based on actual measurements. One major advantage is the ability to accurately calculate irradiance on receivers having limited views of the sky (such as moderately concentrating solar collectors) and another is the ability to realistically account for angle of incidence effects when calculating energy absorbed at receiving surfaces having optical efficiencies that vary significantly with the angle of incidence of the incoming radiation. Inappropriate modelling of the directional nature of the diffuse component in this regard can be shown to lead to significant miscalculation of the energy performance of some types of solar arrays.(4) The simple sky radiance models currently employed in calculating irradiance on sloping

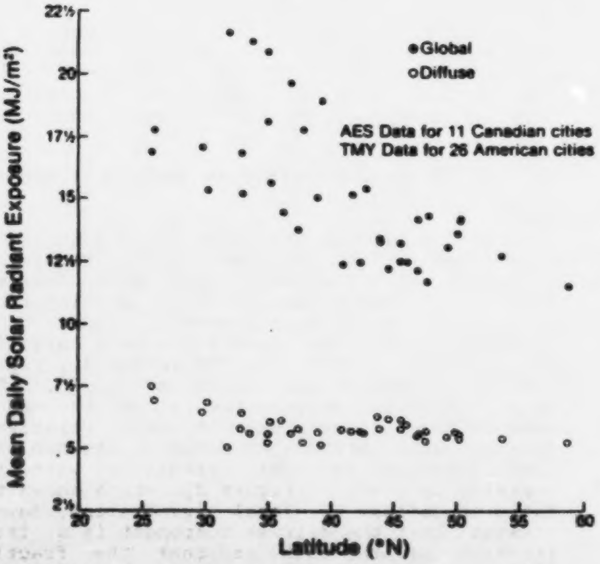

*Fig. 2. Average daily global and diffuse solar radiation at 37 North American location.*

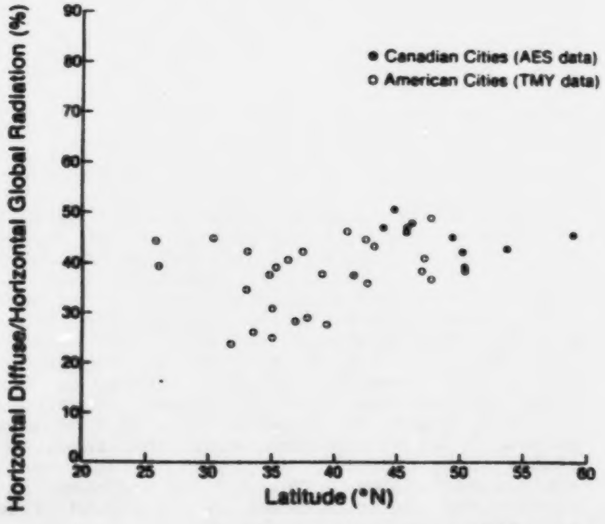

*Fig. 3. Average daily diffuse solar irradiance expressed as a percentage of the average daily global irradiance for the same locations as in Fig. 2.*

surfaces do not share such flexibility in application. It has been demonstrated that accuracy in reproducing the sky diffuse irradiance on a horizontal surface is necessary but not sufficient evidence for proving that a given model accurately describes the radiance distribution across the sky dome.(5) It follows that models such as those of Hay (6), Klucher (7), and Perez (8), which perform reasonably well for calculating diffuse irradiance on planar surfaces, are not necessarily accurate for calculations that are more sensitive to incidence angles since these models are simplistic in the way they distribute the sky radiance across the sky. The only kind of model which will allow angle of incidence effects to be accounted for accurately is one which closely describes the radiance as a function of direction in the sky. Such a model must be based on actual measurements of sky radiance. The need for sky radiance data against which to validate models, and the dearth of published sky radiance measurements, provided the motivation for the development of the sky radiance monitoring project at the University of Toronto.

## 5. SKY RADIANCE MEASUREMENT AT TORONTO

Research on the distribution of the shortwave sky radiance has been ongoing at the University of Toronto since 1977. A database of almost 94,000 individual, quality controlled, five-degree half-angle sky radiance measurements has recently been compiled.(9) The measurements were made during the thirteen months from February 1983 through February 1984, and cover the full range of sky conditions encountered at Toronto. An analysis of these measurements has yielded new quantitative information on the distribution of sky radiance across the sky. Some of this new information is presented below.

## 6. MEAN SKY RADIANCE DISTRIBUTIONS FOR TORONTO

The most important factor affecting the magnitude of the radiance of each element of sky area is its position in the sky relative to the solar position and relative to the zenith. Figures 4 and 5 show the distribution of radiance across the sky for three rather broad ranges of solar elevation angle. Each graph shows box plots for the sky radiance measured at each of 17 measurement positions in the sky. Figure 4 shows the sky radiance at ten degree intervals along sky scans made from horizon to horizon in the azimuthal plane of the sun. Figure 5 shows similar measurements along scans made in a plane perpendicular to the solar azimuth. At each measurement position, the box plot shows the interquartile range (the box) and the ninety-fifth and the fifth percentiles (the upper and lower lines) of the sky radiance measurements.

The plots of sky radiance demonstrate the naturally high variability of sky radiance noted above. Analysis of these data (10) has shown that some of the variance can be explained by the factors; cloud amount, global and diffuse irradiance on a horizontal surface, air temperature (which is highly correlated with solar declination), and variaions in solar elevation angle within each of the ranges plotted. However, even after taking into account these factors, there still remains a consider-

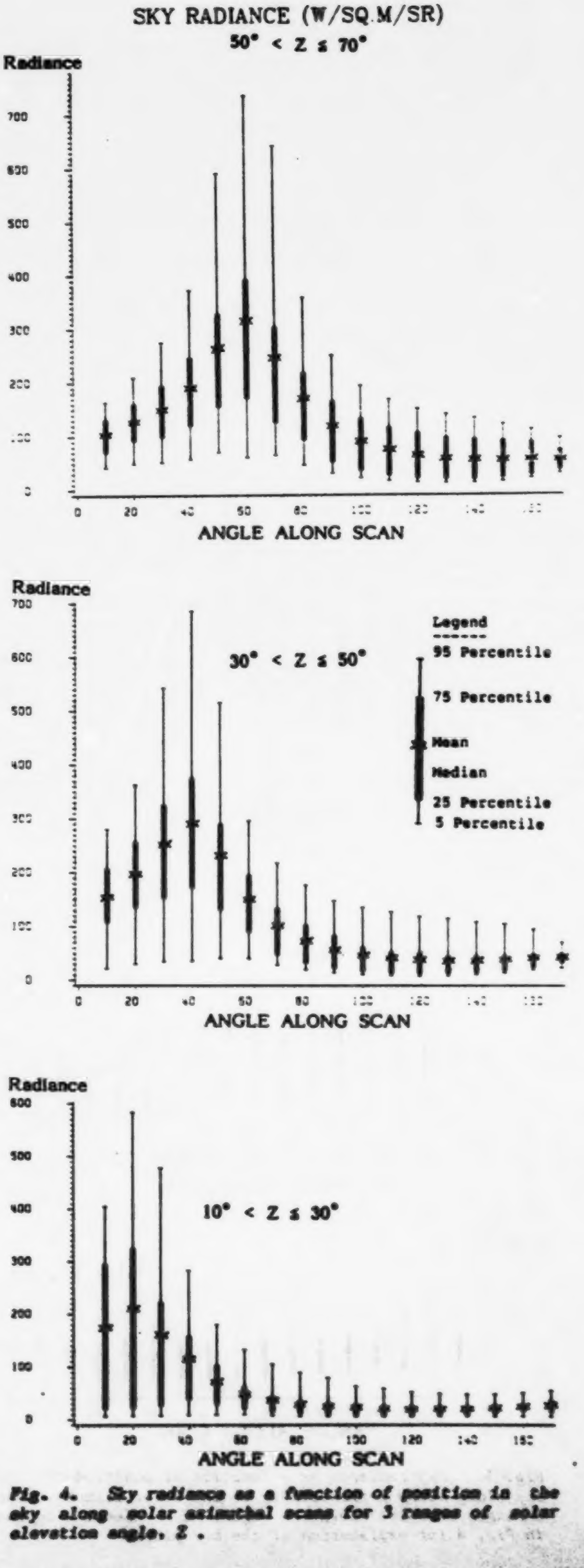

*Fig. 4. Sky radiance as a function of position in the sky along solar azimuthal scans for 3 ranges of solar elevation angle, Z .*

able variance in the sky radiation. Work now in progress will attempt to develop a model which can be used to describe these data as closely as posible. Meanwhile, the information contained in Fig's. 4 and 5 can serve to indicate the magnitude and variability of the diffuse sky radiance at Toronto.

## 7. CONCLUSIONS

The sky diffuse component has been shown to be an important part of the solar resource in Canada. The distribution over the dome of the sky of this diffuse source of solar radiation is important in the calculation of the solar energy absorbed at receiving surfaces having limited views of the sky or having optical efficiencies that vary significantly with the angle of incidence of the incoming radiation. The information in Fig's. 4 and 5 can be used to indicate the range of radiance values expected from various directions in the sky, and to estimate the relative importance of the various directions as sources of solar radiation. It would now be desirable to compare these measurements, which have been made at Toronto, with measurements made in other regions in order to evaluate the influence of climate on the distribution of sky radiance across the dome of the sky.

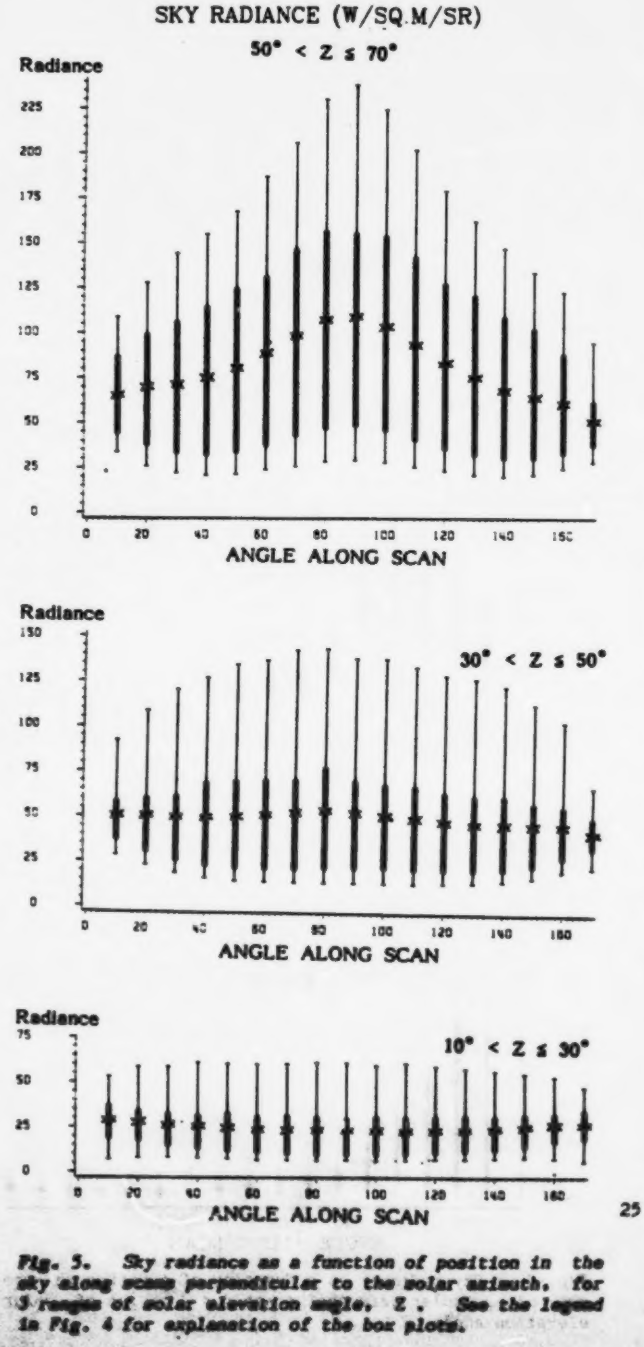

*Fig. 5. Sky radiance as a function of position in the sky along scans perpendicular to the solar azimuth, for 3 ranges of solar elevation angle, Z . See the legend in Fig. 4 for explanation of the box plots.*

## 8. ACKNOWLEDGEMENTS

The material in this paper derives from the author's doctoral research which has benefited from the contributions in guidance from Professor F. C. Hooper. Financial support from the Atmospheric Environment Service and from the Natural Sciences and Engineering Research Council is gratefully acknowledged.

## 9. REFERENCES

(1) Threlkeld, J.L., *Thermal Environmental Engineering*, p. 333. Prentice-Hall, 1970.

(2) McKay, D.C., and Morris, R.J., *Solar Radiation Data Analysis for Canada 1967-1976. Vol. 3: Ontario*, a Canadian Climate Program publication, Atmospheric Environment Service, Downsview, Ontario, 1985.

(3) Dave, J.V., Extensive datasets of the diffuse radiation in realistic atmospheric models with aerosols and common absorbing gasses, *Solar Energy*, Vol. 21, pp. 361-369, Pergamon Press, 1978.

(4) Hooper, F.C., and Brunger, A.P., Including the distribution of the diffuse component of sky radiation in solar simulator testing, *Energy Developments: New Forms, Renewables, Conservation*, F.A. Curtis editor, pp. 175-179. Pergamon Press, 1984.

(5) McArthur, L.B., and Hay, J.E., An assessment of the techniques for determining the distribution of the diffuse solar radiance for the sky hemisphere, *Solar Energy*, Vol. 25, pp. 573-574. Pergamon Press, 1980.

(6) Hay, J.E., and Davies, J.A., Calculation of the solar radiation incident on an inclined surface, *Proceedings First Canadian Solar Radiation Data Workshop*, J.E. Hay and T.K. Won editors, pp. 59-72. Supply and Services Canada, 1980.

(7) Klucher, T.M., Evaluation of models to predict insolation on tilted surfaces, *Solar Energy*, Vol. 23, pp.111-114. Pergamon Press, 1979.

(8) Perez, R.R., Stewart, R., and Arbogast, C., Climatology of an anisotropic diffuse sky radiation model for slopes, *INTERSOL 85, Proceedings of ISES*, Montreal, 1985.

(9) Brunger, A.P., Hooper, F.C., and Wardle, D.I., A comprehensive sky radiance data base,*INTERSOL 85, Proceedings of ISES*, Montreal, 1985.

(10) Hooper, F.C., and Brunger, A.P., *Analysis and Presentation of Mean Sky Radiance Data for Toronto*. Unpublished report to the Atmospheric Environment Service. DSS Contract number OSE84-00111, 1986.

# USE OF SOLAR RADIATION DATA FOR SOLAR ENERGY APPLICATIONS

R.J. Morris
Canadian Climate Centre
Atmospheric Environment Service
4905 Dufferin Street
Downsview, Ontario M3H 5T4

M.S. Gaast
Canadian Climate Centre
Atmospheric Environment Service
4905 Dufferin Street
Downsview, Ontario M3H 5T4

## ABSTRACT

A discussion of the use of solar radiation data for solar energy applications is presented along with selected analyses for four Canadian locations: Vancouver, B.C., Resolute Bay, N.W.T., Winnipeg, Man. and Fredericton, N.B.

## 1. INTRODUCTION

The heightened interest and activity in solar energy over the last ten years or so has spawned an increased requirement for climatological design information including, but not restricted to, solar radiation data. The Atmospheric Environment Service (AES) of Environment Canada has historically measured solar radiation amounts on a horizontal surface for a Canadian network of about 50 locations. This information has been made available through publications from AES (climatological normals and monthly summaries) on a long standing basis.

More recently, Hay (1977) and McKay and Morris (1985) have provided information on solar radiation amounts on various sloped surfaces for selected Canadian locations. This information resulted from the application of modelling techniques to estimate the tilted surface solar radiation amounts primarily from the horizontal surface radiation amounts. These publications serve the solar energy community as a whole in providing general solar resource information such as mean hourly or daily solar radiation amounts values by month, by location, by component (direct, sky diffuse, ground reflected and global, defined as the total of the individual components) and by surface orientation. Although the values presented are well defined physical values, for many solar energy applications the information serves as an index to indicate the relative magnitude of the solar resource amongst different locations, seasons, components and surface orientations.

Although climatological information provides basic characterization of the solar resource, it is often too general to be used as design information for specific system performance evaluation. This is not difficult to understand, considering the wide variety of possible hardware configurations. Apart from surface orientation, there are many additional considerations.

Performance of a photovoltaic or passive solar installation, which is linear with respect to solar radiation amounts, only depends on seasonal totals. Some active solar energy systems may only effectively use solar radiation amounts above threshold values. In systems incorporating storage, the persistence structure of the solar radiation time series data is a critical design consideration. For sun tracking collection systems the direct component of solar radiation amounts is important; conversely, the diffuse component is essential for natural illumination applications.

The provision of more specific climatological analyses will aid the design process. Taken to the practical limit, the use of long-term data sets of hourly radiation amounts and other meteorological elements provide the required flexibility for almost any design requirement although problems include lack of common formats and the requirement for computers and mass storage.

The objective of this paper is to promote the effective use of climatological information in the solar energy community for design, planning and system evaluation purposes. In particular new solar radiation analyses are presented and discussed for four Canadian locations: Vancouver, Resolute Bay, Winnipeg and Fredericton. Finally the reader is encouraged to contact the authors to provide input to AES long term planning of future climatological products.

## 2. EXISTING CLIMATOLOGICAL DATA AND ITS USES

The recent publication of Solar Radiation Data Analyses for Canada 1967-1976 (McKay and Morris, 1985) was the culmination of a multi-year AES project to develop and provide an hourly data base and climatological analyses of hourly solar radiation amounts for 144 Canadian locations. The publication presents, in six regional volumes, a variety of statistics for each location including, in map and tabular form, mean hourly and daily solar radiation amounts by component and by month on a horizontal surface and (for mean daily amounts only) on 19 various tilted surface orientations.

The information is voluminous because of many locations and the various surface orientations and components presented. The value of the basic statistics is recognized. However, there is much design related information that can be gleaned from the data sets of hourly values. This has prompted the analyses presented in the next section. They were intended not as a definitive treatment of Canada's solar radiation climatology, but as an illustration of more specific design data, and to stimulate the reader to apply such analyses to design work.

## 3. DISCUSSION OF DATA

### 3.1 Mean Daily Solar Radiation Amounts by Month on Various Slopes

Four AES climatological observing sites were chosen at which analyses were performed to show various features of Canadian solar radiation climatology. The locations are Vancouver UBC (49.25°N, 123.25°W), Resolute A (74.72°N, 94.98°W), Winnipeg International A (49.9°N, 97.23°W) and Fredericton A (45.92°N, 66.62°W). Long term observed records of hourly global and diffuse solar radiation amounts were available from all locations. The same AES solar simulation software package used to generate sloped surface information for *Solar Radiation Data Analyses for Canada* was used to estimate the hourly data subsequently analyzed and presented in this section. Note that the original hourly data for a large selection of locations on magnetic tape or floppy disk and analyses similar to those presented here can be provided by AES, subject to federal government cost recovery fees and policies.

Figure 1 presents graphs of mean daily global solar radiation amounts on four surface orientations for the 1967-76 period. Features to note include:

1). At the three southern sites there is a general pattern of horizontal surface values showing a peak in June and minimum in December. As the tilt increases summer values diminish and spring and fall values increase. For the vertical surface the peaks are in spring and fall. At the two colder southerly locations, Winnipeg and Fredericton, the spring peak is greater than the fall peak because of more persistent snow cover in March compared to September, contributing to higher values of albedo (surface reflectance), and hence higher contributions from the ground diffuse component. At the much more northerly Resolute location, the sloped surfaces show a strong peak in May reflecting the influence of the persistent snow cover (through the assumption used by the model) and the lower sun elevation angles. The seasonal asymmetry about June increases with colder and generally more northerly climates.

2). At Resolute there is an obvious spring and summer seasonal concentration of solar energy.

3). The increase in solar radiation amounts on a sun tracking surface compared to the fixed orientations is evident with the greatest increase in the summer. The 48 MJ/m² daily average in Resolute in May is noteworthy. This significantly high value is due in part to 24 hour sunshine and high albedo.

### 3.2 Daily Amounts from Hourly Values Exceeding Thresholds

Figure 2 presents daily mean global solar radiation on a southfacing surface (tilt = latitude) for 1967-76 incorporating only those hourly amounts exceeding the indicated threshold of equivalent hourly irradiance. The curves corresponding to a 0.0 W/m² threshold are identical to those of the same surface orientation in Figure 1. Such analyses could be used to indicate the available solar resource for collection systems which only effectively use solar radiation once a threshold irradiance level is exceeded. The considerable decrease in mean daily amounts from the 0.0 to 200 W/m² threshold indicates that much of the available solar energy is received on this surface orientation in hourly amounts equivalent to a mean hourly irradiance less than 200 W/m².

### 3.3 Frequency of Periods of Specific Daily Amounts

Figure 3 presents an analysis of the frequency of periods during the 1967-76 interval in which individual daily solar radiation amounts on a southfacing surface (tilt = latitude) were less than the indicated daily threshold amounts. For instance, inspecting the upper curve on the Winnipeg graph reveals that on average there are about 63 periods each year of one day duration or longer in which the daily solar radiation amount remains below 18.0 MJ/m², 10 periods each year corresponding to a minimum duration of 5 days, one period each year corresponding to 15 day minimum duration, and one tenth period each year (once every ten years) corresponding to a 32 day duration. Such information can be important for solar collection systems using storage, especially in remote locations where no back up is used.

A few features of these graphs are striking:

1) The minimum duration of the once in ten year event for the 18.0 MJ/m² daily threshold is 22 and 32 days for Fredericton and Winnipeg respectively compared to 78 days at Vancouver, probably reflecting mainly the cloudiness of a west coast winter coupled with low surface albedo (lack of snow on the ground).

2). The graph for Resolute is very distinctive. Compared to the three southern locations there are fewer periods per year of short duration. Also the minimum duration for the less frequent periods, especially, is much longer. The discontinuity at one period per year, reflecting the polar night, is particularly noticeable.

### 3.4 Interannual Variability

Interannual variability or the variation from year to year can be as important as the mean annual solar radiation amount. Table 1 shows the time series of yearly means of daily global solar radiation amounts on horizontal and south facing vertical surfaces for about 30 years for the four locations. At the bottom of the table are listed summary statistics including the range as a percentage defined as within one standard deviation of the mean value. This latter indicates the percentage range within which 68% of the yearly values fall, to the extent that the yearly values are normally distributed.

The absolute ranges for both surface orientations at Vancouver and Fredericton are fairly low, about 20%, and are a little higher at Resolute and lower at Winnipeg. Except at Resolute, the range defined by one standard deviation either side of the mean value was under 10%. Assuming the yearly values are distributed normally, one can therefore conclude that for 68% of the years the daily mean values will fall within 5% of the long term mean values.

## 4. SUMMARY

Climatological analyses of solar radiation have been presented for four Canadian locations with a view to better understand the basic nature of the solar resource and to promote the use of climatological information in solar collection systems design and deployment.

AES is currently planning for the provision of a comprehensive solar atlas and handbook for Canada for about 1990. In addition to the basic site-specific analyses in the *Solar Radiation Data Analyses for Canada* this atlas will provide more detailed design information such as those presented in Figures 1-3 and Table 1. The issues of spectral components and interpolation between data locations will also be addressed. With the promise of large capacity and inexpensive mass storage devices such as optical disks and increasingly powerful microcomputers, the possibility of incorporating a large design data base and analysis software for popular microcomputers will be considered. Readers with comments or ideas about such a product are invited to make their views known to the authors. The intention of the product is, after all, to serve the solar energy and related communities.

## 5. REFERENCES

Atmospheric Environment Service, 1982: Canadian Climate Normals (Vol. 1, Solar Radiation), AES, Downsview, Ontario, 1982.

Atmospheric Environment Service, monthly serial publication: Monthly Radiation Summary, AES, Downsview, Ontario.

Davies, J.A., M.Abdel-Wahab and D.C. McKay, 1984: Estimating Solar Irradiation on Horizontal Surfaces, Int. J. Solar Energy, Vol. 2, pp. 405-424.

Hay, J.E., 1977: An Analysis of Solar Radiation Data for Selected Locations in Canada. Climatological Studies No. 32., Atmospheric Environment Service, Downsview, Ontario. 1977.

Hay, J.E. and D.C. McKay, 1985: Estimating Solar Irradiance on Inclined Surfaces: A Review and Assessment of Methodologies. Int. J. Solar Energy, Vol. 3., pp.203-240.

McKay, D.C. and R.J. Morris, 1985: Solar Radiation Data Analyses for Canada 1967-1976 (six regional volumes). Atmospheric Environment Service, Downsview, Ontario, 1985.

NOTE: Atmospheric Environment Service publications are available from the Canadian Government Publishing Centre, Supply and Services Canada, Ottawa, Ontario, K1A 0S9.

TABLE 1

MEAN DAILY SOLAR RADIATION AMOUNTS (MJ/m²) BY YEAR ON HORIZONTAL AND SOUTH FACING VERTICAL SURFACES

| YEAR | VANCOUVER |  | RESOLUTE |  | WINNIPEG |  | FREDERICTON |  |
|---|---|---|---|---|---|---|---|---|
|  | SF VERTICAL | HORZ | SF VERTICAL | HORZ | SF VERTICAL | HORZ | SF VERTICAL | HORZ |
| 1953 | 11.81 | 10.82 | - | - | 15.39 | 12.83 | 14.44 | 12.39 |
| 1954 | 11.89 | 10.73 | - | - | 15.44 | 12.78 | 13.39 | 11.83 |
| 1955 | 12.19 | 10.93 | 9.91 | 7.35 | 16.68 | 13.50 | 14.99 | 12.78 |
| 1956 | 12.91 | 11.84 | 12.05 | 8.90 | 16.06 | 13.18 | 15.18 | 12.85 |
| 1957 | 13.51 | 11.56 | 10.74 | 7.97 | 16.58 | 13.41 | 15.54 | 13.19 |
| 1958 | 13.43 | 12.39 | 11.25 | 8.77 | 16.48 | 13.71 | 14.78 | 12.65 |
| 1959 | 12.35 | 11.03 | 12.20 | 8.82 | 16.49 | 13.15 | 15.19 | 12.77 |
| 1960 | 13.28 | 11.80 | 11.93 | 8.76 | 17.21 | 14.19 | 15.05 | 13.04 |
| 1961 | 13.82 | 12.59 | 12.54 | 8.90 | 17.13 | 14.07 | 14.07 | 12.02 |
| 1962 | 13.30 | 11.96 | 12.41 | 9.02 | 16.83 | 13.57 | 13.73 | 11.57 |
| 1963 | 13.57 | 12.16 | 11.52 | 8.83 | 17.73 | 13.90 | 14.29 | 12.10 |
| 1964 | 13.53 | 12.01 | 10.39 | 8.43 | 17.54 | 13.77 | 15.28 | 12.89 |
| 1965 | 14.48 | 13.00 | 11.28 | 8.96 | 16.73 | 13.58 | 16.68 | 14.09 |
| 1966 | 12.88 | 11.62 | 11.49 | 8.83 | 16.93 | 13.47 | 14.90 | 12.77 |
| 1967 | 13.79 | 12.22 | 10.92 | 8.45 | 16.87 | 13.59 | 14.77 | 12.41 |
| 1968 | 13.27 | 11.79 | 12.51 | 10.12 | 15.61 | 12.35 | 15.11 | 12.61 |
| 1969 | 13.38 | 11.77 | 11.04 | 8.40 | 16.06 | 13.00 | 14.22 | 12.11 |
| 1970 | 13.79 | 11.98 | 12.10 | 9.18 | 16.61 | 13.11 | 14.71 | 12.06 |
| 1971 | 12.35 | 10.91 | 11.98 | 9.09 | 16.34 | 13.05 | 15.16 | 12.47 |
| 1972 | 13.42 | 11.89 | 11.66 | 8.79 | 17.38 | 13.84 | 14.52 | 12.40 |
| 1973 | 13.64 | 12.29 | 10.97 | 8.34 | 16.67 | 13.25 | 14.70 | 12.42 |
| 1974 | 13.75 | 12.03 | 11.04 | 8.80 | 16.86 | 13.58 | 14.27 | 11.82 |
| 1975 | 13.80 | 12.16 | 11.79 | 8.63 | 16.45 | 13.07 | 14.12 | 11.87 |
| 1976 | 12.83 | 11.22 | 12.44 | 9.09 | 17.92 | 14.14 | 14.29 | 11.81 |
| 1977 | 14.12 | 12.45 | 11.39 | 8.56 | 16.49 | 13.28 | 14.66 | 12.12 |
| 1978 | 13.76 | 12.08 | 11.80 | 8.93 | 17.93 | 14.03 | 16.28 | 13.22 |
| 1979 | 14.31 | 12.49 | 10.76 | 7.99 | 15.80 | 12.94 | 13.89 | 11.58 |
| 1980 | 12.71 | 11.36 | 11.06 | 8.23 | 16.59 | 13.58 | 14.56 | 11.99 |
| 1981 | 13.42 | 11.56 | 11.41 | 8.84 | 15.98 | 13.03 | 13.94 | 11.88 |
| 1982 | 13.91 | 12.03 | 10.28 | 9.00 | 15.88 | 12.97 | 15.37 | 12.95 |
| 1983 | 13.84 | 11.83 | 10.06 | 8.20 | 15.32 | 13.00 | 13.82 | 11.64 |
| 1984 | 13.44 | 11.81 | 11.03 | 8.65 | 15.88 | 13.12 | 14.55 | 12.48 |
| MAX | 14.48 | 13.00 | 12.54 | 10.12 | 17.93 | 14.19 | 16.68 | 14.09 |
| MIN | 11.81 | 10.73 | 9.91 | 7.35 | 15.32 | 12.35 | 13.39 | 11.57 |
| MEAN | 13.33 | 11.82 | 11.40 | 8.69 | 16.56 | 13.38 | 14.70 | 12.40 |
| STD DV | .66 | .54 | .73 | .48 | .71 | .44 | .70 | .57 |
| RANGE | 2.67 | 2.27 | 2.63 | 2.77 | 2.61 | 1.84 | 3.29 | 2.52 |
| RANGE EXPRESSED AS A PERCENTAGE OF THE MEAN VALUE FOR THE PERIOD | 20.03 | 19.20 | 23.07 | 31.86 | 15.76 | 13.76 | 22.38 | 20.32 |
| RANGE WITHIN ONE STANDARD DEVIATION OF THE MEAN EXPRESSED AS A PERCENT | 9.95 | 9.21 | 12.75 | 11.10 | 8.52 | 6.61 | 9.56 | 9.17 |

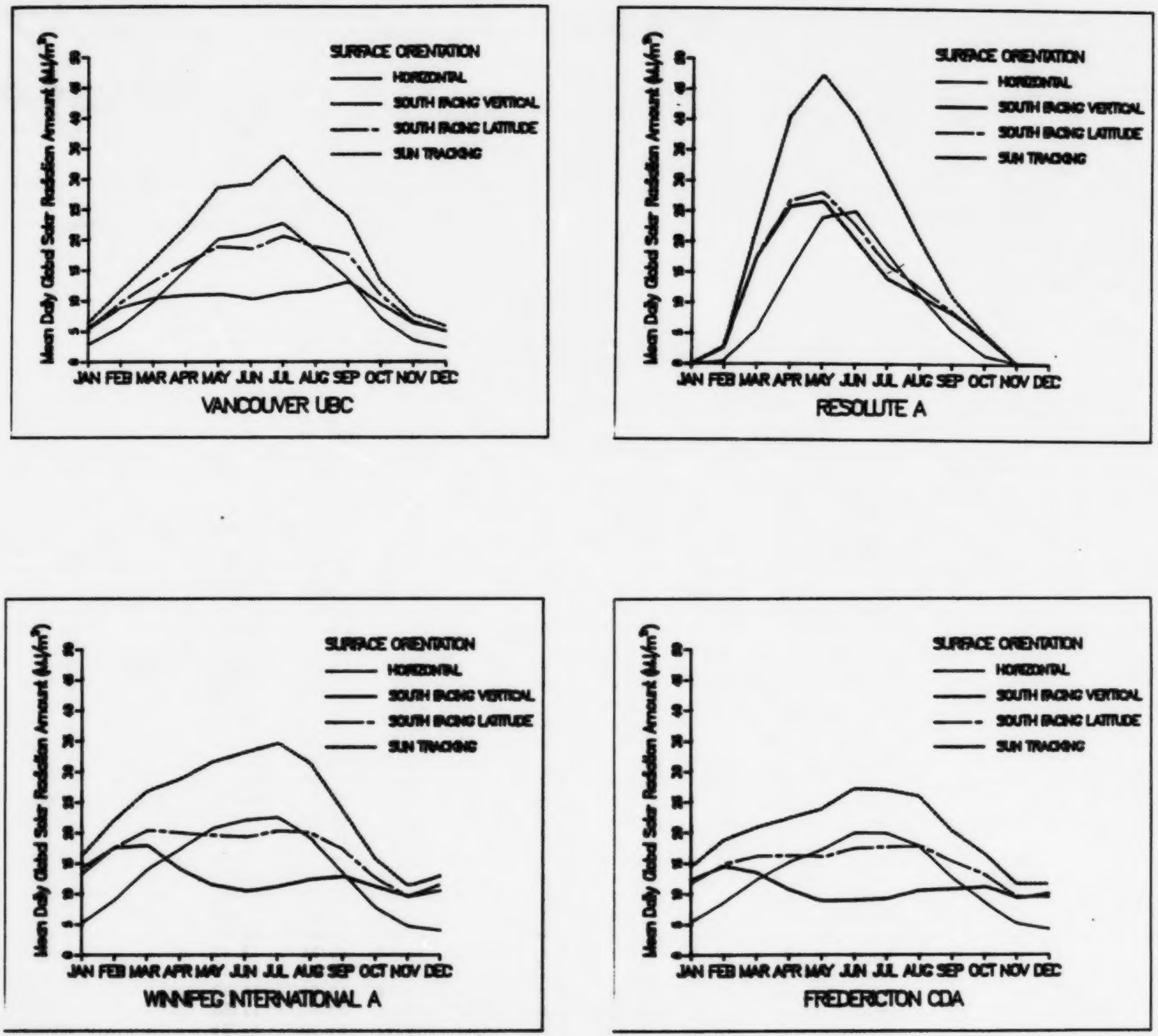

Figure 1. Mean daily global solar radiation amounts by month for various surface orientations for the period 1967-1976.

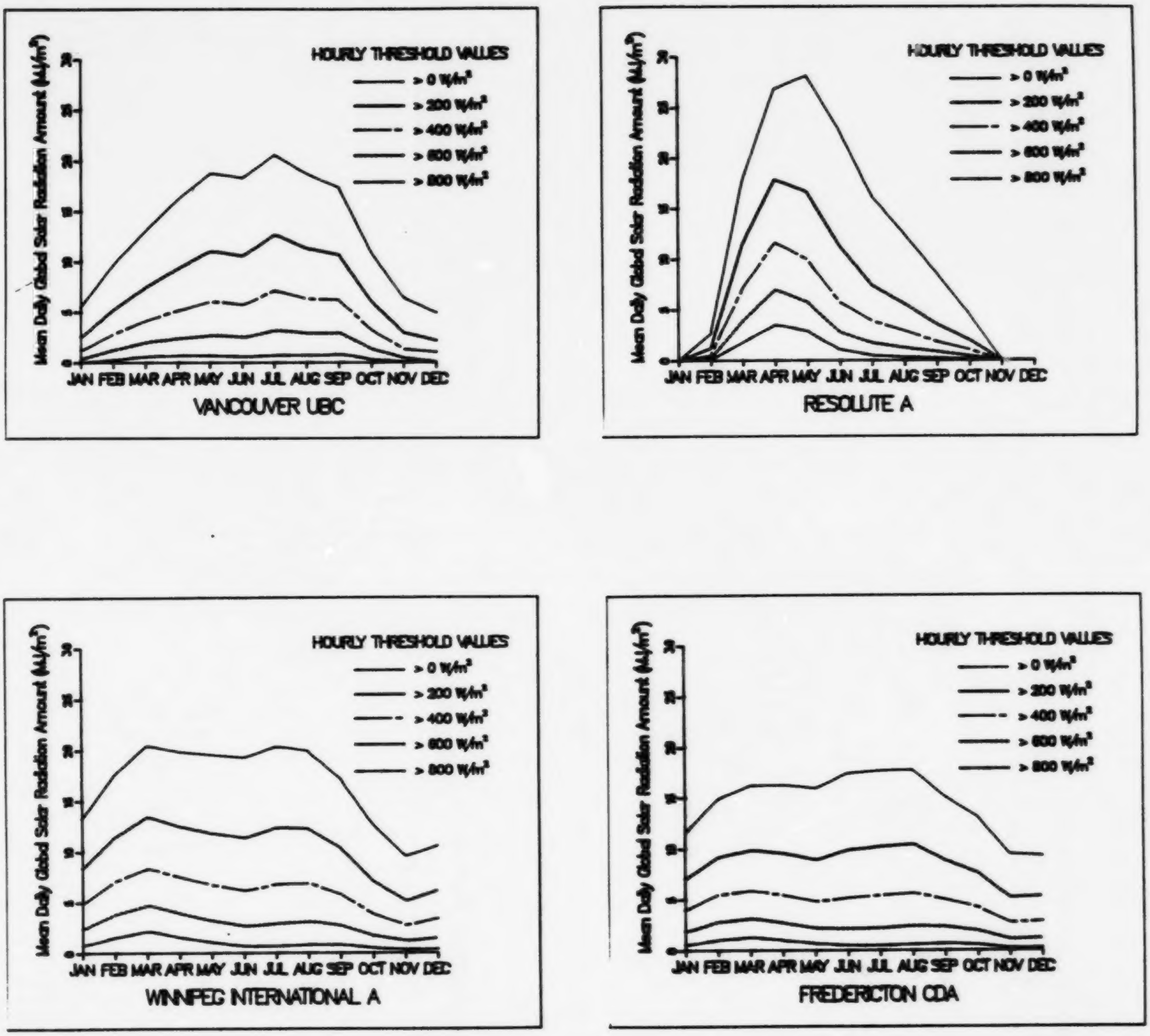

Figure 2. Mean daily global solar radiation amounts by month for a southfacing surface (tilt = latitude of the location) for the period 1967-1976 calculated using only those hourly radiation amounts exceeding the indicated equivalent irradiance threshold.

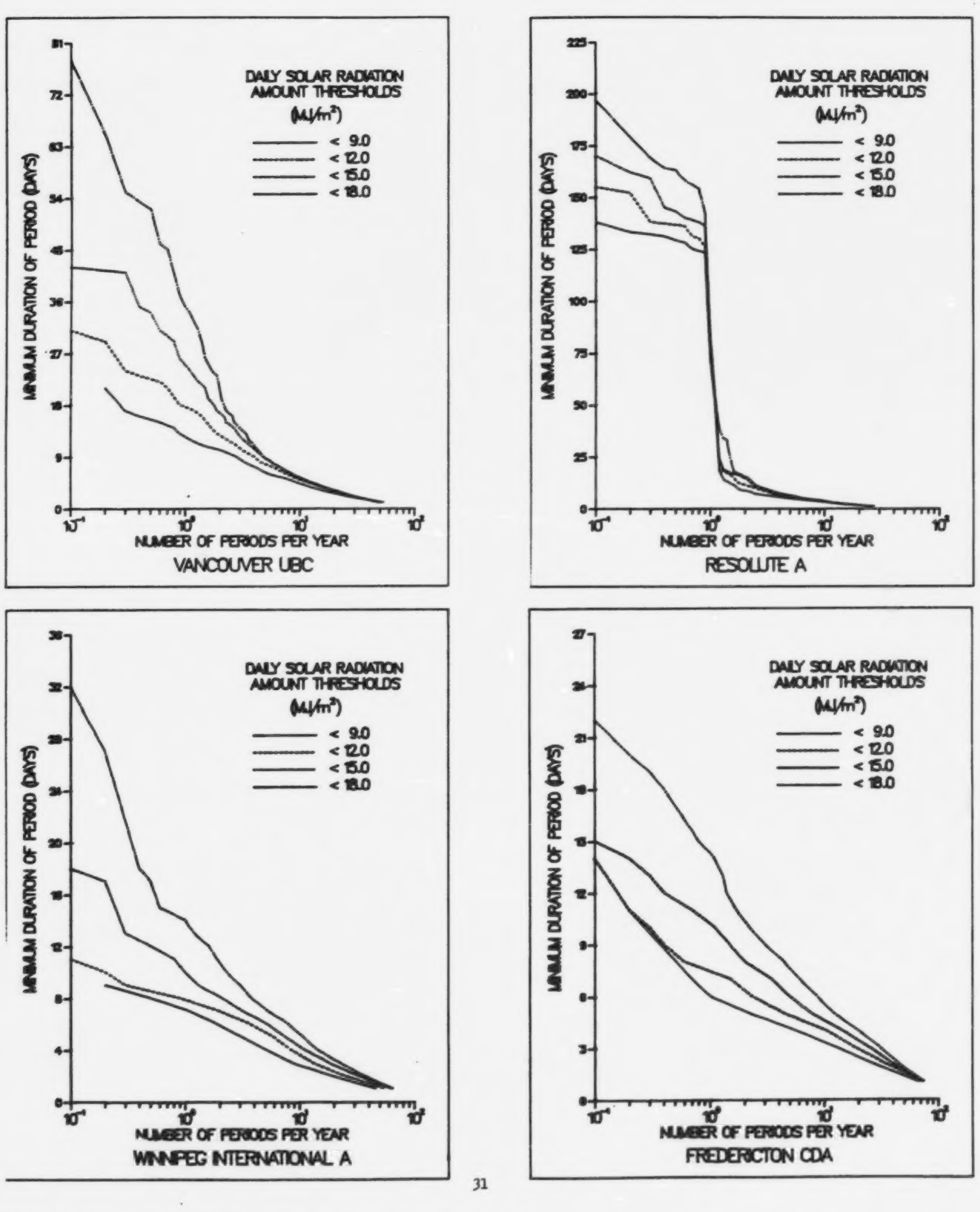

Figure 3. Frequency of periods during which the daily global solar radiation amounts on a southfacing surface (tilt = latitude of the location) remained less than the indicated threshold values for the period 1967-1976.

# CORRELATIONS BETWEEN THE GLOBAL AND DIFFUSE SOLAR RADIATION AND THE CLOUDS OPACITY (CANADIAN STUDY)

H.F. Ma and W.T. Kierkus
Building Energy Group
University of Windsor

## ABSTRACT

According to the recent data, from as many as 317 principal climatological stations operated by the Atmospheric Environment Service (AES), only 49 stations, comprising the Canadian Radiation Network, are recording regularly the global radiation and 9 of them have the diffuse radiation on an hourly basis. Therefore only 9 locations in Canada have the sufficient solar radiation data for engineering applications. These data are in different periods of recording, from 4 to 27 years (as of 1984).

The attached figure shows the locations of the 9 stations recording the global and diffuse radiation, the numbers indicate the years of recordings for global and diffuse radiation respectively at each location. Each of these stations also has a multiyear observations of the cloud formations, usually more than 30 years, recorded on an hourly basis. As it is apparent from the figure, seven stations, namely Charlottetown (PEI), Montreal (QUE), Toronto (ONT), Winnipeg (MAN), Bad Lake (SAS), Edmonton (ALB) and Port Hardy (BC) are located near the major populated centers of the country, two other stations, Goose Bay (NFL) and Resolute (NWT) are located in sparsly populated or remote parts of Canada.

In order to utilize the recorded global radiation in all 49 stations across the country, the diffuse component of global radiation have to be known as well. Using all the available data from the 9 stations named above, the explicit, verified correlation will be presented.

$$M_s = f(M_k' \ \beta)$$

where $M_s$ : the ratio of the diffuse radiation intensity received on horizontal surface to exterrestrial radiation intensity.

$M_k$ : the ratio of the global radiation intensity received on horizontal surface to exterrestrial radiation intensity.

$\beta$ : solar altitude.

An attempt also will be made to relate the $M_s$ and $M_k$ to the recorded total cloud opacity. For those locations where there is no radiation data available, global and diffuse solar radiation can be predicted from cloud opacity, using the correlations developed between them.

## BIBLIOGRAPHY

1. Iqbal, M., Prediction of hourly diffuse solar radiation from measured hourly global radiation on a horizontal surface. Solar Energy 24, 491-503 (1980).
2. Ideriah, F.J.K., On the relationship between diffuse and global solar radiation. Solar Energy 31(1), 119-124 (1983).
3. Mani, A. and Rangarajan, S., Techniques for the precise estimation of hourly values of global, diffuse and direct solar radiation. Solar Energy 31(6), 577-595 (1983).
4. Sherry, J.E. and Justus, C.G., A simple hourly all-sky solar radiation model based on meterological parameters. Solar Energy 32(2), 195-204 (1984).
5. Bird, Richard E., A Simple, solar spectral model for direct-normal and diffuse horizontal irradiance. Solar Energy 32(4), 416-471 (1984).
6. Kimura, K. and Stephenson, D.G., Solar radiation on cloudy days. ASHRAE Transaction, 227-233 (1969).

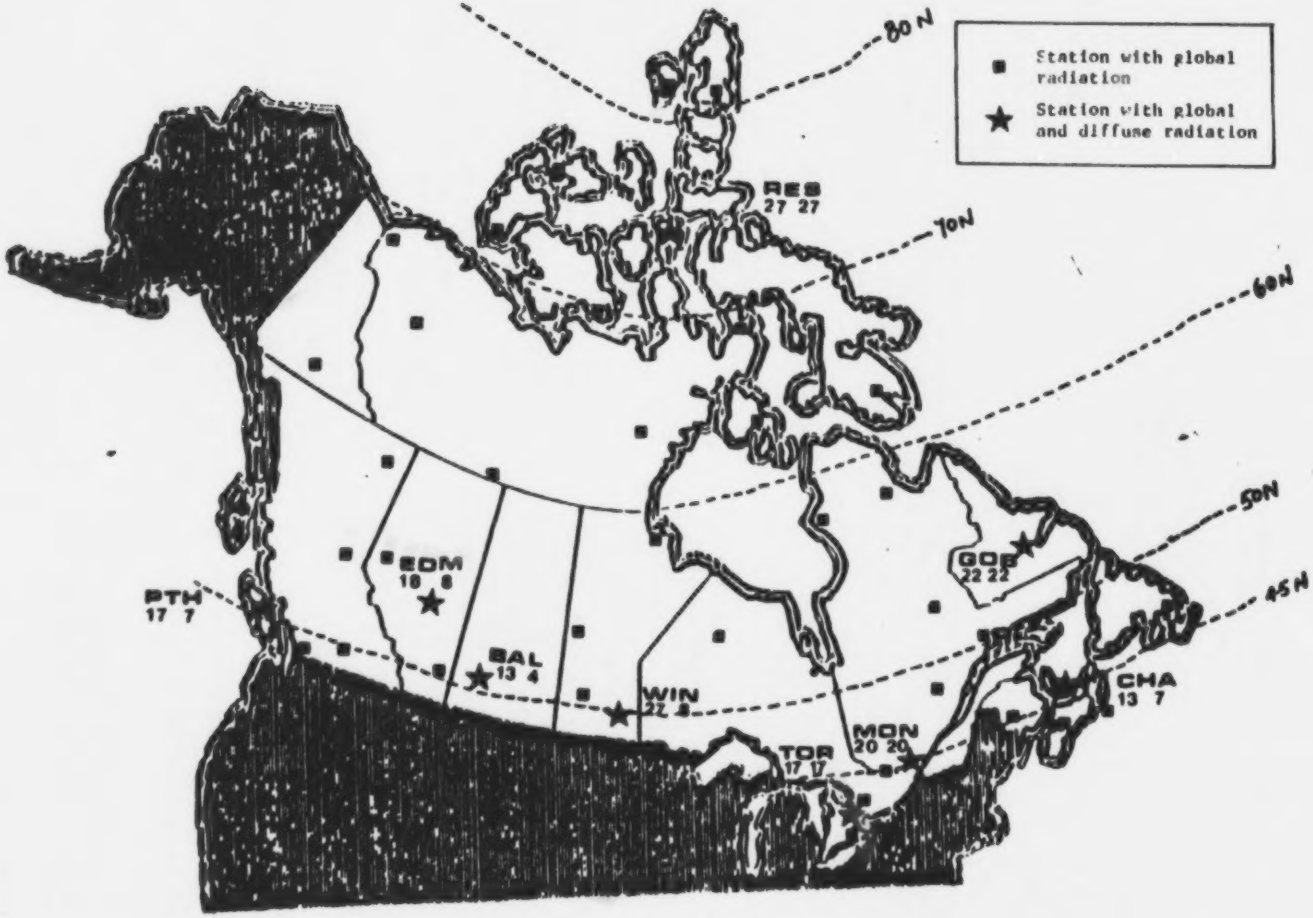
80 N
70N
60N
50N
45N
■ Station with global radiation
★ Station with global and diffuse radiation
RES
27 27
EDM
18 8
PTH
17 7
BAL
13 4
WIN
22 8
TOR
17 17
MON
20 20
GOB
22 22
CHA
13 7

Locations of Climatological stations with solar radiation data

# SOLAR RADIATION ESTIMATES FOR SELECTED CLIMATIC ZONES IN IRAQ

A. Akrawi
Solar Energy Research Centre
Scientific Research Council
P. O. Box 13026
Jadiriyah Baghdad
IRAQ

I. M. Muhi
College of Science
Baghdad University
Baghdad
IRAQ

## ABSTRACT

The estimates of global solar radiation (Q) for four principal towns in Iraq were deduced from their sunshine data using the simplest linear relationship between Q and the average daily duration of sunshine (S) as developed by Angstrom. The coefficients of this relationship were obtained by linear regression method using daily radiation and sunshine data measured at Mosul, Baghdad, Rutbah and Nasiriyia, representing the radiation climates for the Northern, Central, Southwestern and Southeastern climatic zones in Iraq.

The computations show that the highest value of the percentage deviation between the observed and the calculated values of the global solar radiation are 6.63% in Mosul in July, 4.7% in Baghdad in December, 8.5% in Rutbah in August and 9% in Al-Nasiriyia in September.

The diffused solar radiation is also estimated.

## 1. INTRODUCTION

The first study was by Kimball (1), who found a straight line could be used to express the relationship between solar radiation and average monthly values of cloudiness and sunshine duration. It was Angstrom (2), who first expressed the relationship mathematically. In his classic paper he formulated a statistical relation between the daily duration of sunshine and the daily total global solar radiation. Similar studies based on the Angstrom relationship have been carried out in America (3), India (4), Singapore (5) and Malaysia (6). The purpose of this paper is to establish relationships of the Angstrom type, applicable at different climatic zones in Iraq.

## 2. GEOGRAPHICAL FEATURES

Iraq is located in Southwestern Asia; the geographical limits of the country approximately extending from latitudes 20°N to 37.5°N and longitudes 39°E to 48.5°E. It is situated in the midst of a vast arid region with desert or semi-desert conditions. The country is flat in appearance, except in the north and northeast and in the extreme western parts of the country where the terrain is mountainous.

Most of Itaq lies within the desert and steppe climates, with cool moist winters and hot dry summers.

## 3. MEASUREMENTS OF SOLAR RADIATION AND SUNSHINE DURATION

In Iraq, the daily total incoming solar radiation is recorded at a few weather observing stations. The most authoritative data are those at Mosul, Baghdad, Rutbah and Nasiriyia where data have been recorded for long periods. The geographical data of these stations are given in Table (1).

From climatological and topographical points of view, the actinometric measurements at these stations are considered to represent the radiation climates for the Northern, Central, Southwestern and Southeastern zones in Iraq.

The recording instruments used at these stations are the biometallic actinograph of the Robitzch type. The solar radiation data are published by the Iraqi Meteorological Organization as daily totals in mWcm$^{-2}$. Duration of bright sunshine is recorded by means of a Campbell-stokes sunshine recorder, and recorded daily at all meteorological observing stations, throughout the country.

The relation connecting the solar radiation to the sunshine duration as suggested by Angstrom (2) is,

$$Q/Q_o = a + b\ (S/S_o) \qquad \ldots (1)$$

where:

$Q$ = The average daily total global radiation received per unit area on the earth's surface at a particular location.
$Q_o$ = Amount of total radiation per unit area per day on a horizontal surface available above that location but outside the earth's surface.
$S$ = Average actual daily duration of sunshine at that location.
$S_o$ = Maximum possible daily duration of sunshine at that location on the same day (i.e. the theoretical duration between sunrise and sunset).

(a) and (b) are empirical constants.

It was often inferred that on a cloudless day

$$a + b = 1,$$
$$\text{as } Q = Q_o \text{ and } S/S_o = 1.$$

The determination of 'a' is of a certain interest because it is equal to the ratio of the mean daily global radiation for a completely overcast sky ($S/S_o$ = 0) to a perfectly clear sky.

Such regression equations are based on climatological means and can not necessarily be expected to apply to extreme values for particular days.

Several workers have determined the value of 'a' for different localities and different atmospheric conditions and have found it to vary considerably, M.A. Abbas and M.K. Elnesr (7). In determining the monthly mean daily radiation at Mosul, Baghdad and Basrah Ahmed et al. (8) used the average yearly values of a and b. This assumption is inadequate, as certain applications in solar energy require more accurate data. Some values of a and b obtained by different authors for example the values obtained for a by Angstrom, Kimbal, Luneland, Mosby, Fritz for Stockholm, Madison, Helsinki, the Arctic (74°N) and eleven stations in the U.S.A. were:
0.235, 0.220, 0.268, 0.540 and 0.350 respectively. The original Angstrom formula could be presented by the regression equation:

$$Q/Q_o = 0.35 + 0.61\, S/S_o,$$

with a correlation coefficient of +0.88 between $Q/Q_o$ and $S/S_o$, $(a + b)$ in the last equation is less than one. This is expected as no recording instrument could give a full recording of sunshine on cloudless days. Black, Bonython and Prescott obtained the following overall regression equation for the stations they studied:

$$Q/Q_o = 0.23 + 0.48\, S/S_o.$$

## 4. ANALYSIS OF DATA

Daily radiation data were available at four principal towns in Iraq viz, Mosul, Baghdad, Rutbah and Nasiriyia, the period of records used is indicated in Table (1).

The monthly average total global radiation values, Q were computed on the basis of these data. The values of monthly average duration of daily sunshine (S) were also computed using sunshine data for the same periods, the average monthly maximum daily duration of sunshine were obtained from the Smithsonian Meteorological table No. 171 (9). Values of $Q_o$ were obtained using the tables of radiation outside the atmosphere for given dates at different latitudes based on the work of Milanovitch given in the Smithsonian Meteorological table No. (132)(9).

The regression equations were calculated by the method of least squares as a regression of $Q/Q_o$ on $S/S_o$. The advantage of this procedure is that all variations between different climates and latitudes appear in the regression coefficients a and b. It is then possible to explore systematically the variation from place to place. The values of a and b are computed for each calendar month for each of the four towns. These values are given in Table 2. The yearly average values of a and b were found to be 0.328 and 0.362 respectively at Mosul, 0.310 and 0.512 for Baghdad, 0.220 and 0.546 for Rutbah, 0.296 and 0.610 for Nasiriyia.

## 5. ESTIMATES OF DIFFUSED RADIATION

The regression equation (1) provides a very simple means of obtaining an estimate of the diffused solar radiation. In the complete absence of sunlight, that is, $S = 0$ equation (1) reduces to:

$$Q = a\, Q_o \qquad \ldots(2)$$

These estimates are given in Table (2). The percentage of the estimated diffused radiation to the measured mean daily total global radiation is evaluated monthly and annually. These percentages for Mosul and Baghdad appear to be rather high in comparison with other estimated values (10).

## 6. CONCLUSIONS

1. The values of Q were estimated using the deduced monthly regression equations.

   It was found that the highest percentage deviations between the measured values of Q and those obtained using the regression equations were 6.63% for Mosul, 4.7% for Baghdad, 8.5% for Rutbah, 9.0% for Nasiriyia.
2. The poorest correlation was found for the months of extreme daily sunshine durations.
3. If low percentage of possible sunshine coincides with the season of high turbidity generally in spring, the value of 'a' will be low and the value of 'b' high.
4. In places with high values of possible sunshine 'a' tends to be high and 'b' low.
5. There are few peculiarities in the climate of Iraq that affect the characteristics of the regression equations obtained, cloud characteristics and atmospheric transparency change markedly from one season to another. In winter, conditions of middle latitude disturbances prevail, cloud types are normally opaque to the direct beams and the turbidity of the atmosphere is low. The spring is characterized by the passage of small and shallow thermal disturbances, with the onset of such thermal lows, vertical visibility deteriorates progressively with increasing dust content in the lower layers of the atmosphere. Occasionally, this is accompanied by stratified cloud types that proceed from high transparent cirrus type to medium opaque alto- and nimbo-stratus clouds. After the passage of the disturbance cumuliform clouds and low turbidity prevail.
6. It should be noted that the regression formulae obtained in this paper should not be used to predict the daily values of total radiation from sunshine values, as the values were derived on the basis of climatological mean monthly values.
7. There appears to be a latitudinal effect, the values of 'a' tend to be high for higher latitudes, provided that the transmission characteristics of the atmosphere does not change over a limited range of latitudes.
8. The mean yearly average of the sum of 'a' and 'b' for the latitudes considered in this paper equals 0.766.
9. Having evaluated 'a' and 'b' for the four climatological regions of Iraq, it is possible to esitmate the monthly and yearly averages of daily radiation in other localities where the sunshine duration data are available.
10. The monthly average global radiation Q was calculated using the average monthly values of 'a' and 'b' Table (1). When comparing the value of Q obtained in this paper with those estimated by Ahmed et al. (8), it was found that Ahmed et al. (8) values under estimated Q by 5 to 10 percent for each month and in all regions. This was revealed specifically at Rutbah and Nasiriya. In order to obtain an accurate estimation of Q. It is more desirable to apply the monthly average values of 'a' and 'b' rather than the mean yearly values.

## REFERENCES

(1) H. H. Kimbal, Monthly weather review, 47, 769 (1919).

(2) A. Angstrom, Solar and terrestrial radiation. Quart. J. Roy. Met. Soc., 50, 121-126 (1924).

(3) R. K. Swartman and O. Ogunlade, Solar radiation estimates from common parameters Solar Energy 22(3/4), 170-172 (1967).

(4) A. Mani and O. Chacko, Solar radiation climate of India, Solar Energy 14, 139-156 (1973).

(5) C. L. Sien, Sunshine and solar radiation in Singapore, The Meteorological Mag. 1166, 98, 265-274 (1969).

(6) D. G. S. Chuah and S. L. Lee. Solar radiation estimmes in Malaysia, Solar Energy 26, p. 33-40 (1981).

(7) M. A. Abbas and M. K. Elnaer. Relation between Sunshine Duration and Mean Daily Solar Radiation on A Horizontal Surface in Iraq. Arab Physical Society, The Conference on the Physics of Solar Energy. University of Ghar Younis, 29 Oct. 4 Nov. (1976).

(8) I. Ahmad, N.I. Al-Hamdani and Ibrahim. Solar Radiation Maps for Iraq, Solar Energy 31, 29, (1983).

(9) Smithsonian Meteorological Tables, Sixth Revised Edition, Smithsonian Institution Press, City of Washington, Table 132, p. 418 (1949).

(10) A. A. Akrawi, H. Y. Najjar, "Calculations and Mapping of the Distribution of Global and Diffuse Solar Radiation in Iraq", to be published.

Geographical Data of Solar Radiation Observing Stations.

| Station | Climate zone | Latitude °N | Longitude °E | Elevation above M.S.L.(Metre) | Period of record |
|---|---|---|---|---|---|
| Mosul | Northern | 36 19 | 43 09 | 223 | (1971 - 1980) |
| Baghdad | Central | 33 14 | 44 14 | 34 | (1967 - 1980) |
| Rutbah | Southwestern | 33 02 | 40 17 | 615 | (1975 - 1980) |
| Nasiriyia | Southeastern | 31 05 | 46 14 | 3 | (1974 - 1980) |

Table (1-a): Data for regression equation $\frac{Q}{Q_o} = a + b\frac{S}{S_o}$

| Month | Mosul 36 °N | | | | | | | | | | |
|---|---|---|---|---|---|---|---|---|---|---|---|
| | Mean S | Mean $S_o$ | a | b | a + b | Mean $Q_o$ | Mean Q measured | Q estimated | Percentage deviation | Estimated diffused radiation | Percentage diffused radiation |
| Jan. | 5.20 | 10.00 | 0.355 | 0.311 | 0.666 | 17891.3 | 9465.2 | 9243.14 | 2.30 | 6351.2 | 67.10 |
| Feb. | 6.40 | 10.90 | 0.370 | 0.333 | 0.703 | 23003.1 | 12486.2 | 13005.76 | 4.20 | 8511.14 | 68.16 |
| March | 6.90 | 12.00 | 0.300 | 0.436 | 0.736 | 29707.1 | 16156.6 | 16357.7 | 1.20 | 8912.13 | 55.16 |
| April | 7.90 | 13.10 | 0.320 | 0.384 | 0.704 | 36075.9 | 19969.5 | 19898.31 | 0.35 | 11544.28 | 57.80 |
| May | 10.80 | 14.10 | 0.265 | 0.450 | 0.715 | 40726.8 | 25018.4 | 24829.9 | 0.75 | 10792.6 | 43.13 |
| June | 11.90 | 14.60 | 0.415 | 0.278 | 0.693 | 42402.8 | 27599.5 | 27201.4 | 1.42 | 17597.16 | 41.50 |
| July | 12.60 | 14.40 | 0.295 | 0.454 | 0.749 | 41564.8 | 26983.6 | 28772.7 | 6.63 | 12261.61 | 45.44 |
| August | 12.00 | 13.50 | 0.320 | 0.342 | 0.662 | 38003.3 | 24314.57 | 23711.2 | 2.46 | 12161.05 | 50.01 |
| Sept. | 10.60 | 12.40 | 0.320 | 0.360 | 0.680 | 32263 | 21025.4 | 20438.8 | 2.70 | 10324.16 | 49.10 |
| Oct. | 8.90 | 11.30 | 0.310 | 0.400 | 0.710 | 25433.3 | 15368.92 | 15896.8 | 3.4 | 7884.32 | 51.30 |
| Nov. | 6.90 | 10.30 | 0.290 | 0.353 | 0.643 | 19483.5 | 10965.2 | 10257.12 | 6.40 | 5650.21 | 51.52 |
| Dec. | 4.70 | 9.70 | 0.380 | 0.250 | 0.630 | 16299.1 | 7986.14 | 8166.3 | 2.20 | 6193.65 | 77.55 |
| Yearly average | 8.80 | 12.20 | 0.328 | 0.362 | 0.670 | 30235.0 | 18109.18 | 18146.8 | 2.83 | 9916.89 | 54.76 |

S = hours $\qquad Q = \frac{KJ}{(m^2.d)}$

Table (1-b): Data for regression equation $\frac{Q}{Q_o} = a + b \frac{S}{S_o}$.

S = hours

$Q = \frac{KJ}{(m^2 d)}$

| Month | Baghdad 33 °N | | | | | | | | | | |
|---|---|---|---|---|---|---|---|---|---|---|---|
| | Mean S | Mean $S_o$ | a | b | a + b | Mean $Q_o$ | Mean Q measured | Q estimated | Percentage deviation | Estimated diffused radiation | Percentage diffused radiation |
| Jan. | 6.40 | 10.20 | 0.225 | 0.640 | 0.865 | 19734.9 | 12725.0 | 12955.4 | 1.80 | 4440.56 | 34.89 |
| Feb. | 7.50 | 11.30 | 0.285 | 0.550 | 0.835 | 24595.3 | 16382.9 | 16261.3 | 0.70 | 7009.87 | 52.44 |
| March | 8.00 | 12.00 | 0.350 | 0.528 | 0.878 | 30964.1 | 21239.11 | 21741.9 | 2.30 | 10837.43 | 51.10 |
| April | 9.00 | 13.00 | 0.300 | 0.540 | 0.840 | 36830.1 | 25060.3 | 24817.3 | 0.90 | 11049.03 | 44.08 |
| May | 10.60 | 13.90 | 0.400 | 0.408 | 0.808 | 40810.6 | 28747.59 | 29024.1 | 0.98 | 16324.24 | 56.78 |
| June | 12.70 | 14.30 | 0.285 | 0.530 | 0.815 | 42193.3 | 32438.9 | 32019.9 | 1.00 | 12025.3 | 37.07 |
| July | 12.70 | 14.10 | 0.370 | 0.432 | 0.802 | 41355.3 | 31642.8 | 31420.8 | 0.69 | 15301.46 | 48.35 |
| August | 12.10 | 13.40 | 0.345 | 0.436 | 0.781 | 38380.4 | 29288.1 | 28366.3 | 3.18 | 13240.4 | 45.20 |
| Sept. | 10.70 | 12.40 | 0.280 | 0.517 | 0.797 | 33268.6 | 24775.4 | 24184.6 | 2.40 | 9315.20 | 37.59 |
| Oct. | 9.10 | 11.40 | 0.325 | 0.480 | 0.805 | 26899.8 | 19311.71 | 19131.5 | 0.57 | 6184.85 | 42.51 |
| Nov. | 7.80 | 10.50 | 0.290 | 0.530 | 0.820 | 21327.1 | 14547.6 | 14631.4 | 0.97 | 6184.85 | 42.51 |
| Dec. | 6.10 | 10.00 | 0.265 | 0.560 | 0.825 | 18226.5 | 11631.4 | 11086.7 | 4.70 | 4830.23 | 41.52 |
| Yearly Average | 9.40 | 12.20 | 0.310 | 0.512 | 0.822 | 31215.5 | 22311.7 | 22424.8 | 1.64 | 9676.80 | 49.00 |

37

Table (1-c): Data for regression equation $\frac{Q}{Q_o} = a + b \frac{S}{S_o}$.

S = hours

$Q = \frac{KJ}{(m^2 d)}$

| Month | Rutbah 33 °N | | | | | | | | | | |
|---|---|---|---|---|---|---|---|---|---|---|---|
| | Mean S | Mean $S_o$ | a | b | a + b | Mean $Q_o$ | Mean Q measured | Q estimated | Percentage deviation | Estimated diffused radiation | Percentage diffused radiation |
| Jan. | 6.23 | 10.23 | 0.185 | 0.477 | 0.662 | 21817.3 | 11023.89 | 10361.87 | 6.0 | 4036.2 | 36.61 |
| Feb. | 7.30 | 10.96 | 0.200 | 0.580 | 0.780 | 26468.2 | 15021.15 | 15515.57 | 3.3 | 5293.6 | 35.24 |
| March | 8.30 | 11.96 | 0.195 | 0.585 | 0.780 | 32304.9 | 19517.0 | 19416.46 | 0.5 | 6299.66 | 32.27 |
| April | 8.70 | 12.70 | 0.130 | 0.700 | 0.830 | 37626.2 | 23737.3 | 23057.57 | 2.9 | 4891.4 | 20.58 |
| May | 10.40 | 13.80 | 0.135 | 0.742 | 0.877 | 40894.4 | 27850.9 | 28345.3 | 2.2 | 5520.74 | 19.91 |
| June | 12.10 | 14.20 | 0.215 | 0.620 | 0.835 | 41983.8 | 30645.6 | 31081.4 | 1.4 | 9026.51 | 29.45 |
| July | 12.20 | 14.10 | 0.280 | 0.530 | 0.810 | 41313.4 | 30683.3 | 30511.5 | 0.6 | 11568.59 | 37.70 |
| August | 11.90 | 13.40 | 0.320 | 0.428 | 0.748 | 38841.3 | 28248.9 | 27235.0 | 8.5 | 12429.21 | 43.99 |
| Sept. | 10.40 | 12.40 | 0.285 | 0.480 | 0.765 | 34441.8 | 24075.74 | 23694.4 | 1.6 | 9815.91 | 46.51 |
| Oct. | 9.10 | 11.40 | 0.200 | 0.600 | 0.800 | 28617.7 | 18901.09 | 19454.17 | 3.1 | 5723.5 | 30.28 |
| Nov. | 7.90 | 10.50 | 0.210 | 0.475 | 0.685 | 23338.3 | 13542.0 | 13236.2 | 2.2 | 4901.04 | 36.19 |
| Dec. | 5.80 | 10.02 | 0.285 | 0.344 | 0.629 | 20392.7 | 9842.31 | 9884.21 | 0.3 | 5811.9 | 59.05 |
| Yearly Average | 9.20 | 12.10 | 0.220 | 0.546 | 0.766 | 32334.2 | 21079.8 | 21297.7 | 2.71 | 7113.36 | 33.74 |

S = hours

$Q = \frac{KJ}{(m^2 d)}$

Table (1-a): Data for regression equation $\frac{Q}{Q_0} = a + b \frac{S}{S_0}$.

| Month | Nasiriyiah 31 °N | | | | | | | | | |
|---|---|---|---|---|---|---|---|---|---|---|
| | Mean S | Mean $S_0$ | a | b | a + b | Mean $Q_0$ | Mean Q measured | Q estimated | Percentage deviation | Estimated diffused radiation | Percentage diffused radiation |
| Jan. | 5.90 | 10.40 | 0.265 | 0.600 | 0.865 | 21201.4 | 12088.15 | 12833.9 | 6.1 | 5618.7 | 46.48 |
| Feb. | 7.20 | 11.10 | 0.230 | 0.600 | 0.830 | 25894.2 | 16701.3 | 16030.9 | 3.8 | 5955.66 | 35.72 |
| March | 7.60 | 12.00 | 0.220 | 0.650 | 0.870 | 31885.9 | 20434.6 | 20141.3 | 1.4 | 7014.89 | 34.32 |
| April | 7.80 | 12.90 | 0.305 | 0.500 | 0.805 | 37416.7 | 23141.37 | 22726.5 | 1.8 | 11412.30 | 49.31 |
| May | 9.20 | 13.70 | 0.375 | 0.400 | 0.775 | 40852.5 | 26606.5 | 26292.2 | 1.1 | 15319.8 | 57.57 |
| June | 9.00 | 14.10 | 0.325 | 0.428 | 0.753 | 42067.6 | 25599.0 | 25165.14 | 1.5 | 13671.9 | 53.49 |
| July | 8.90 | 13.50 | 0.340 | 0.383 | 0.723 | 41355.3 | 26317.3 | 24201.4 | 8.0 | 14061.6 | 53.43 |
| August | 9.70 | 13.30 | 0.340 | 0.400 | 0.740 | 38673.7 | 25416.54 | 24431.89 | 3.8 | 13149.05 | 51.73 |
| Sept. | 9.60 | 12.40 | 0.280 | 0.428 | 0.708 | 34064.7 | 22940.25 | 20824.3 | 9.0 | 9538.11 | 41.57 |
| Oct. | 8.50 | 11.40 | 0.240 | 0.545 | 0.785 | 28073.0 | 18205.55 | 18148.7 | 0.3 | 6737.58 | 37.00 |
| Nov. | 7.50 | 10.60 | 0.265 | 0.550 | 0.815 | 22751.7 | 14560.25 | 14088.8 | 2.2 | 6028.99 | 41.40 |
| Dec. | 6.10 | 10.20 | 0.375 | 0.333 | 0.708 | 19734.9 | 11799.04 | 11333.95 | 3.9 | 7400.79 | 62.72 |
| Yearly Average | 8.10 | 12.10 | 0.296 | 0.510 | 0.806 | 31973.8 | 20312.7 | 19747.47 | 3.57 | 9470.65 | 46.62 |

S = hours

$Q = mW.\ cm^{-2}$

Table (2-a): Data for regression equation $\frac{Q}{Q_0} = a + b \frac{S}{S_0}$.

| Month | Mosul 36 °N | | | | | | | | | |
|---|---|---|---|---|---|---|---|---|---|---|
| | Mean S | Mean $S_0$ | a | b | a + b | Mean $Q_0$ | Mean Q measured | Q estimated | Percentage deviation | Estimated diffused radiation | Percentage diffused radiation |
| Jan. | 5.20 | 10.00 | 0.355 | 0.311 | 0.666 | 427 | 225.9 | 220.6 | 2.30 | 151.58 | 67.10 |
| Feb. | 6.40 | 10.90 | 0.370 | 0.333 | 0.703 | 549 | 25[illegible].0 | 310.4 | 4.20 | 203.13 | 68.16 |
| March | 6.90 | 12.00 | 0.300 | 0.436 | 0.736 | 709 | 385.6 | 390.4 | 1.20 | 212.70 | 55.16 |
| April | 7.90 | 13.10 | 0.320 | 0.384 | 0.704 | 861 | 476.6 | 474.9 | 0.35 | 275.52 | 57.80 |
| May | 10.80 | 14.10 | 0.265 | 0.450 | 0.715 | 972 | 597.1 | 592.6 | 0.75 | 257.58 | 43.13 |
| June | 11.90 | 14.60 | 0.415 | 0.278 | 0.693 | 1012 | 658.7 | 649.2 | 1.42 | 419.98 | 41.50 |
| July | 12.60 | 14.40 | 0.295 | 0.454 | 0.749 | 992 | 644.0 | 686.7 | 6.63 | 292.64 | 45.44 |
| August | 12.00 | 13.50 | 0.320 | 0.342 | 0.662 | 907 | 580.3 | 565.9 | 2.46 | 290.24 | 50.01 |
| Sept. | 10.60 | 12.40 | 0.320 | 0.360 | 0.680 | 770 | 501.8 | 487.8 | 2.70 | 246.40 | 49.10 |
| Oct. | 8.90 | 11.30 | 0.310 | 0.400 | 0.710 | 607 | 366.8 | 379.4 | 3.40 | 188.17 | 51.30 |
| Nov. | 6.90 | 10.30 | 0.290 | 0.353 | 0.643 | 465 | 261.7 | 244.8 | 6.40 | 134.85 | 51.52 |
| Dec. | 4.70 | 9.70 | 0.380 | 0.250 | 0.630 | 389 | 190.6 | 194.9 | 2.20 | 147.82 | 77.55 |
| Yearly Average | 8.80 | 12.20 | 0.328 | 0.362 | 0.670 | 721.6 | 432.2 | 433.1 | 2.83 | 236.68 | 54.76 |

Table (2-b): Data for regression equation $\frac{Q}{Q_o} = a + b \frac{S}{S_o}$.

S = hours Q = mW. cm$^{-2}$

| Month | Baghdad 33 °N | | | | | | | | | | |
|---|---|---|---|---|---|---|---|---|---|---|---|
| | Mean S | Mean $S_o$ | a | b | a + b | Mean $Q_o$ | Mean Q measured | Q estimated | Percentage deviation | Estimated diffused radiation | Percentage diffused radiation |
| Jan. | 6.40 | 10.20 | 0.225 | 0.640 | 0.865 | 471 | 303.7 | 309.2 | 1.80 | 105.98 | 34.89 |
| Feb. | 7.50 | 11.00 | 0.285 | 0.550 | 0.835 | 587 | 391.0 | 388.1 | 0.70 | 167.30 | 52.44 |
| March | 8.00 | 12.00 | 0.350 | 0.528 | 0.878 | 739 | 506.9 | 518.9 | 2.30 | 258.65 | 51.10 |
| April | 9.00 | 13.00 | 0.300 | 0.540 | 0.840 | 879 | 598.1 | 592.3 | 0.90 | 263.70 | 44.08 |
| May | 10.60 | 13.90 | 0.400 | 0.408 | 0.808 | 974 | 686.1 | 692.7 | 0.98 | 389.60 | 56.78 |
| June | 12.70 | 14.30 | 0.285 | 0.530 | 0.815 | 1007 | 774.2 | 764.2 | 1.00 | 287.00 | 37.07 |
| July | 12.70 | 14.10 | 0.370 | 0.432 | 0.802 | 987 | 755.2 | 749.9 | 0.69 | 365.19 | 48.35 |
| August | 12.10 | 13.40 | 0.345 | 0.436 | 0.781 | 916 | 699.0 | 677.0 | 3.18 | 316.00 | 45.20 |
| Sept. | 10.70 | 12.40 | 0.280 | 0.517 | 0.797 | 794 | 591.3 | 577.2 | 2.40 | 222.32 | 37.59 |
| Oct. | 9.10 | 11.40 | 0.325 | 0.480 | 0.805 | 642 | 460.9 | 456.6 | 0.57 | 147.61 | 42.51 |
| Nov. | 7.80 | 10.50 | 0.290 | 0.530 | 0.820 | 509 | 347.2 | 349.2 | 0.57 | 147.61 | 42.51 |
| Dec. | 6.10 | 10.00 | 0.265 | 0.560 | 0.825 | 435 | 277.6 | 264.6 | 4.70 | 115.28 | 41.52 |
| Yearly Average | 9.40 | 12.20 | 0.310 | 0.512 | 0.822 | 745 | 532.5 | 535.2 | 1.64 | 230.95 | 49.00 |

Table (2-c): Data for regression equation $\frac{Q}{Q_o} = a + b \frac{S}{S_o}$.

S = hours Q = mW. cm$^{-2}$

| Month | Rutbah 33 °N | | | | | | | | | | |
|---|---|---|---|---|---|---|---|---|---|---|---|
| | Mean S | Mean $S_o$ | a | b | a + b | Mean $Q_o$ | Mean Q measured | Q estimated | Percentage deviation | Estimated diffused radiation | Percentage diffused radiation |
| Jan. | 6.23 | 10.23 | 0.185 | 0.477 | 0.662 | 520.7 | 263.1 | 247.3 | 6.0 | 96.33 | 36.61 |
| Feb. | 7.30 | 10.96 | 0.200 | 0.580 | 0.780 | 631.7 | 358.5 | 370.3 | 3.3 | 126.34 | 35.24 |
| March | 8.30 | 11.96 | 0.195 | 0.585 | 0.780 | 771.0 | 469.8 | 463.4 | 0.5 | 150.35 | 32.27 |
| April | 8.70 | 12.70 | 0.130 | 0.700 | 0.830 | 898.0 | 567.0 | 550.3 | 2.9 | 116.74 | 20.58 |
| May | 10.40 | 13.80 | 0.135 | 0.742 | 0.877 | 976.0 | 661.7 | 676.5 | 2.2 | 131.76 | 19.91 |
| June | 12.10 | 14.20 | 0.215 | 0.620 | 0.835 | 1008.0 | 731.4 | 741.8 | 1.4 | 215.43 | 29.45 |
| July | 13.20 | 14.10 | 0.280 | 0.530 | 0.810 | 986 | 732.3 | 728.2 | 0.6 | 276.10 | 37.70 |
| August | 11.90 | 13.40 | 0.380 | 0.488 | 0.748 | 987 | 674.2 | 650.0 | 8.5 | 296.64 | 43.99 |
| Sept. | 10.40 | 12.40 | 0.285 | 0.480 | 0.765 | 822 | 574.6 | 565.5 | 1.6 | 234.87 | 46.51 |
| Oct. | 9.10 | 11.40 | 0.200 | 0.600 | 0.800 | 683 | 451.1 | 464.3 | 3.1 | 136.60 | 30.28 |
| Nov. | 7.90 | 10.50 | 0.210 | 0.475 | 0.685 | 557 | 323.8 | 315.9 | 2.2 | 116.97 | 36.19 |
| Dec. | 5.80 | 10.02 | 0.285 | 0.344 | 0.629 | 486.7 | 234.9 | 235.9 | 0.3 | 138.71 | 59.05 |
| Yearly Average | 9.20 | 12.10 | 0.220 | 0.546 | 0.766 | 771.7 | 503.1 | 508.3 | 2.71 | 169.77 | 33.74 |

Table (2-4); Data for regression equation $\frac{Q}{Q_0} = a + b \frac{S}{S_0}$.

| Month | Nasiriyiah 31 °N | | | | | | | | | |
|---|---|---|---|---|---|---|---|---|---|---|
| | Mean S | Mean $S_0$ | a | b | a + b | Mean $Q_0$ | Mean Q measured | Q estimated | Percentage deviation | Estimated diffused radiation | Percentage diffused radiation |
| Jan. | 5.90 | 10.40 | 0.265 | 0.600 | 0.865 | 506 | 288.50 | 306.30 | 6.1 | 134.10 | 46.48 |
| Feb. | 7.20 | 11.10 | 0.230 | 0.600 | 0.830 | 618 | 398.60 | 382.60 | 3.8 | 142.14 | 35.72 |
| March | 7.60 | 12.00 | 0.220 | 0.650 | 0.870 | 761 | 487.70 | 480.70 | 1.4 | 167.42 | 34.32 |
| April | 7.80 | 12.90 | 0.305 | 0.500 | 0.805 | 893 | 552.30 | 542.40 | 1.8 | 272.37 | 49.31 |
| May | 9.20 | 13.70 | 0.375 | 0.400 | 0.775 | 975 | 635.00 | 627.50 | 1.1 | 365.63 | 57.57 |
| June | 9.00 | 14.10 | 0.385 | 0.489 | 0.753 | 1004 | 610.00 | 600.60 | 1.5 | 326.30 | 53.49 |
| July | 8.90 | 13.90 | 0.340 | 0.383 | 0.723 | 987 | 628.10 | 577.60 | 8.0 | 335.60 | 53.43 |
| August | 9.70 | 13.30 | 0.340 | 0.400 | 0.740 | 923 | 606.60 | 583.10 | 3.8 | 313.82 | 51.73 |
| Sept. | 9.60 | 12.40 | 0.280 | 0.428 | 0.706 | 813 | 547.50 | 497.00 | 9.0 | 227.64 | 41.57 |
| Oct. | 8.50 | 11.40 | 0.240 | 0.545 | 0.785 | 670 | 434.50 | 433.00 | 0.3 | 160.80 | 37.00 |
| Nov. | 7.50 | 10.60 | 0.265 | 0.550 | 0.815 | 543 | 347.50 | 355.20 | 2.2 | 143.89 | 41.40 |
| Dec. | 6.10 | 10.20 | 0.375 | 0.333 | 0.708 | 471 | 281.60 | 270.50 | 3.9 | 176.63 | 62.72 |
| Yearly Average | 8.10 | 12.10 | 0.296 | 0.510 | 0.806 | 763.1 | 484.79 | 471.30 | 3.57 | 226.03 | 46.62 |

S = hours

Q = mW. cm$^{-2}$

# Direct Conversion Systems

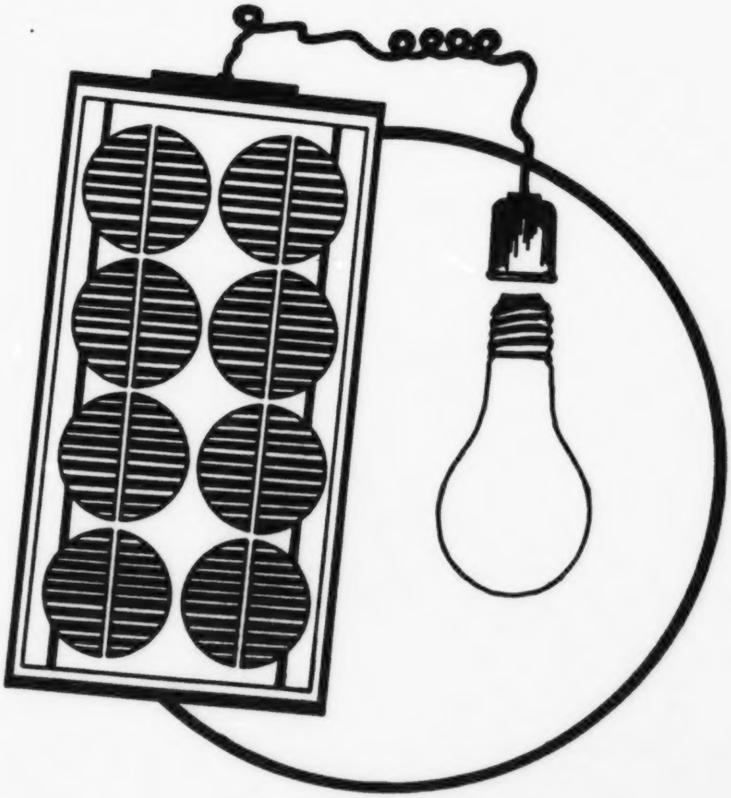

# ICE CONTROL IN LAKES BY PHOTOVOLTAICS POWERED WATER CIRCULATION

Peter R B Ward
Peter Ward & Associates Ltd
#801 - 1155 West Georgia Street
Vancouver, B.C. V6E 3H4

William G Dunford
Department of Elec Engineering
University of British Columbia
Vancouver, B.C. V6T 1W5

Ken I Ashley
Fisheries Research & Development Section
Ministry of Environment
University of British Columbia
Vancouver, BCC V6T 1W5

## ABSTRACT

A photovoltaics powered submerged water circulator, known as the Wardun "Sunstirrer" was developed and field tested. The system was used for ice control in a small, British Columbia lake (latitude 50°N), for water oxygenation (fisheries) reasons.

The system consisted of a photovoltaic array (rated at 375 watts in peak sunshine), a rechargable battery bank and a very free running, low speed, low energy consumption water circulator. Laboratory measurements showed that over the normal range of operating speeds (240 - 300 rpm) the power consumption was extremely low (23 - 38 watts) and the water flow rate was good (25 - 32 litres $sec^{-1}$).

A program of field testing was undertaken in Winter and early Spring. A data logging system monitoring field information showed that the hours of strong sunshine at the site (2.9 hours/day average) in February were more than adequate to keep the system in operation.

## 1. INTRODUCTION

Many of the most productive lakes in Canada are hostile to fish species such as trout because of the winter kill problem. During the winter an ice cover seals off the water body from oxygen exchange with the atmosphere, and the addition of new water to the lakes by river inflows is small because runoff is small. The lake becomes depleted in oxygen, and eventually the fish die from suffocation.

One procedure that has been successfully used in treating these lakes is forced water circulation using airlift pumps. These pumps contribute oxygen directly to the water body, and more important, cause a substantial ice-free patch to be created in the lake through which air exchange with the atmosphere can occur. Because of the inverted temperature gradient in lakes during the winter (0°C water near the surface, 4°C water at significant depths below surface), a pumping system may be used to bring 4°C water to the surface to melt the ice cover, (Lackey and Holmes, 1972).

The routine operation of this technique has been well established in British Columbia by Fisheries Research Section, BC Ministry of Environment, using air lift pumps powered by compressors (Ashley 1983). However finding a suitable and cost effective energy source for the compressors (rated at 1 - 7.5 kW) has been an intractable problem. The lakes of concern are usually far from the main electricity grid, and the cost of conveying and storing diesel fuel at the site is usually very large.

Although photovoltaics powered pumps have been extensively tested for medium-high head, low flow applications (Halcrow 1983, Derrick et al 1982, Ward and Dunford 1984, Pulfrey et al 1986), their application to ultra low head, large flow water circulation was novel. A modest amount of solar power from photovoltaic panels may be obtained in the Winter at latitude 50°N, and the location of many of the lakes with fish winter kill problems was in areas with relatively sunny, low precipitation climates.

The advantages of using (1) an approximately constant power system driven via rechargable storage batteries or (2) a "sunshine only" direct driven system were difficult to assess. A decision was made to construct a very low power consumption pump, and to drive it with rechargable batteries. The system designed and constructed consisted of an 8 panel (nominal 375 watt) array, a number of totally sealed lead acid batteries, a permanent magnet DC motor, and a very low friction propellor pump turning at low speed. Because of the careful electrical and mechanical design, the pump consumed only about 25 watts at its design speed, and was capable of moving a substantial flow of water.

The system was installed and operated at Menzies Lake, near Merritt, British Columbia during the winter months, and water temperatures, solar radiation, battery voltage and other operating parameters were measured. Our paper focusses on the design, laboratory testing and field evaluation aspects of the pump.

## 2. SYSTEM DESIGN

Initial calculations indicated that it would be possible to circulate 25 litres/sec of water (the design flow selected by Fisheries Research and Development Section) using about 35 - 45 watts provided the velocity was kept small. A fairly large diameter, low speed propellor was required and thus an electric motor running at low speed was needed to drive the propeller. In the interests of reliability and compactness a submersible unit was conceived, with the motor and propeller near each other in a single housing.

Information on available sunshine in the interior of southern BC in the winter showed that an average of about 2 hours of strong sunshine per day would be available in January. Using photovoltaic panels rated at 12 volts and 3 amps in optimum conditions (ARCO M75 Panel), the number of ampere hours available/day from an eight panel array, configured as 4 parallel strings of 2 panels (24 volt system) was:

$$\text{No. of ampere hours} = \text{No. of strings} \times \text{Output per panel} \times \text{No. of hours of sunshine}$$

$$= 4 \times 3.0 \times 2$$

$$\text{No. of ampere hours/day} = 24$$

With this current going into batteries and being used to operate the pump when the sun was not shining, the fractional running time for a 36 watt system was computed. The current required was 1.5 amps, that is 36 ampere-hours/day.

$$\text{Thus: Percent Time running} = \frac{\text{Power Available}}{\text{Power Required}}$$

$$= \frac{24}{36} \times 100$$

$$= 67\%$$

Plans were made to construct an electronic duty cycle switch, to allow the system to function at various fractions of the total time.

For energy storage to carry the system through a meteorological weather cycle (typical duration 4 days), the battery capacity was:

No. of ampere hours for batteries =
Amps Consumed x Required time x low temperature factor
= 1.5 x 4 x 24/0.7 = 206 Ah.

Three parallel strings of two, 12 volt Watchman II Sealed Deep Cycle Batteries, manufactured by GNB Batteries (Canada) Inc, were used, rated at about 65 Ah each for small discharge currents.

## 3. PROTOTYPE CONSTRUCTION

A Baldor DC permanent magnet motor rated at 1 hp, 180 volts and 1750 rpm was selected for driving the propeller. Operation of the 180 volt motor at 24-32 volts enabled the required low speeds to be obtained, without need for a gearbox or pulley speed reduction.

A very free running spring loaded rotary shaft seal was purchased and this seal together with two bearings formed the support for the propeller drive shaft. A rubber bushing direct drive coupling was used between the motor and propeller shaft. The Baldor motor was partially diamentled and machined down so that it would fit inside a 6 inch diameter PVC pipe. The propeller housing and the motor housing were bolted together and sealed with a large "O" ring seal. This unit, together with the 10 inch (254 mm) cast aluminium propeller, and the streamlined cover formed the prototype pump (see Figure 1).

The top cover of the pump was transparent plastic, and enabled a check to be made on the adequacy of sealing. A support hook, the electric line and an air valve were all attached to the plastic top cover. The air valve enabled the pump to be inflated to a pressure greater than the water pressure at the proposed depth of submergence of the pump. This ensured that the pressure inside the housing exceeded the pressure outside, so that no water could leak in.

The final pump design was called the Wardun WD 20 "Sunstirrer".

An electronic duty cycle controller was designed and constructed to operate the pump. The switching element was a power field effect transistor. Switches allowed timer periods of 5, 10, 20 40, 80, 160 and 320 minutes to be selected and duty cycles of 10, 20, 30, 40, 50, 60, 70, 80, 90 or 100% of total time to be selected. The Controller included built-in override circuits, so that the pump would cease operation below a preset low voltage, and go to 100% operation above a preset high voltage.

## 4. LABORATORY TESTING

A 12 inch (30.5 cm) cowling was bolted around the propeller (see Fig 1). The pump was lowered to about mid-depth in a 2½ m deep, large volume test tank in the floor of the University of British Columbia, Civil Engineering Hydraulics Laboratory. An Ott laboratory current meter was attached above the propeller in the gap between the motor housing and the cowling.

The pump was run at four values of speed, controlled by the applied voltage. The speed increased from about 180 rpm to 360 rpm as the voltage was increased. Measurements of water velocity were made, and measurements of current and voltage to the motor were recorded.

Values of power supplied, power out of motor and power imparted to water were computed as follows:

$$\text{Power out of motor} = \text{Power supplied} - \text{Power lost}$$

$$= (\text{Power supplied}) - (\text{friction loss} + i^2R)$$

$$= iV - (0.25V + 3i^2)$$

in which
V = supplied voltage
I = supplied current
R = resistance of motor windings (3 ohms)

$$\text{Power imparted to water} = \text{Power associated with dynamic head}$$

$$= 1/2\, \rho\, Q\, u^2$$

in which
$\rho$ = density of water
Q = flow rate (volume per unit time)
u = velocity of flow

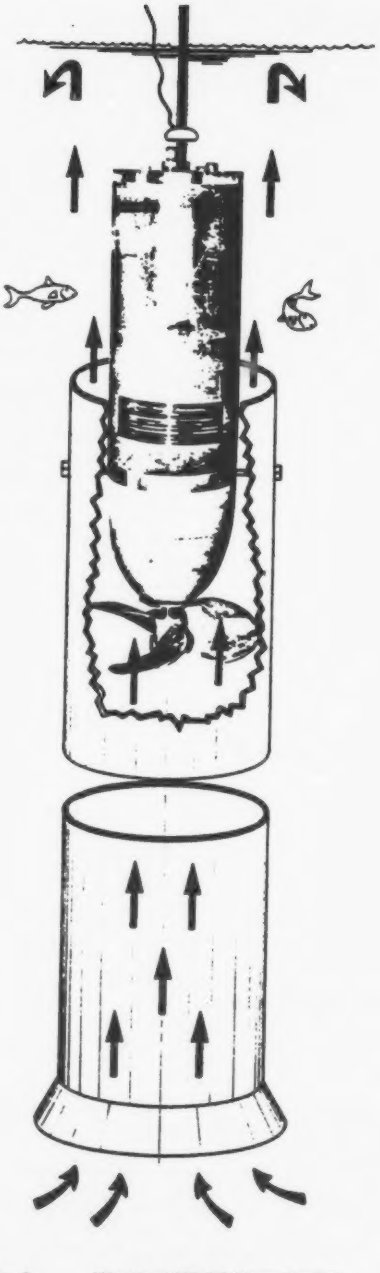

Fig. 1. Wardun WD 20 "Sunstirrer" Pump with 12 inch (305 mm) Intake Tube

Values of power were computed with these equations for each value of voltage and are listed (see Table 1). The motor efficiency is in the range 48 - 72%, a good range considering the fact that the motor was being used at only 1/70th to 1/12 of its design power. The pump efficiency was in the range 20-24% - a reasonable range considering significant losses must have occurred in the gap between the propeller tip and intake tube.

Initial problems of water leakage were overcome using the pressurization idea described in Section 3. At the planned operational voltage (25 volts) the pump drew a current of 0.91 amps and produced the design flow (approximately 25 litres/sec). Subsequent measurements in the field at low water temperatures (about 4°C) showed that the current drawn was 1.00 amps at 25 volts. This was a very satisfactory finding because the current was significantly smaller than the original design current of 1.5 amps, and meant that the pump would easily be able to exceed its design performance.

## 5. FIELD TRIALS AND RESULTS

Plans were made by BC Ministry of Environment, Fisheries Research and Development Section to carry out field testing at Menzies Lake, British Columbia (about 20 km south-east of Merritt). Menzies Lake has a surface area of 3.7 hectares, a volume of $209 \times 10^3$ $m^3$ and a maximum depth of 15 m. A 2.5 m x 2.5 m raft to carry the solar panels, pump and batteries was designed. The raft was in modular form, and could be dismantled for road transport. The battery compartment was designed to be well submerged in water, in order to ensure that the batteries were kept at a temperature no colder than the water temperature. Space in the raft was also allocated to housing the Microscout data logging system. The Microscout system is a microprocessor controlled data system that stores information in solid state memory for later retrieval. The system (manufactured in Richmond, B.C.) is versatile and will work in the field in winter conditions for periods of 3 months or more.

The Microscout was readied for field operation and a total of six data recording channels were prepared, as follows:

| | | |
|---|---|---|
| Channel 1 | Water Temperature | °C |
| Channel 2 | Water Temperature | °C |
| Channel 3 | Water Temperature | °C |
| Channel 4 | Solar radiation monitored by small PV panel | mA |
| Channel 5 | Charge current from main PV array | mA |
| Channel 6 | Battery voltage | v |

The equipment was transported to Menzies Lake by road, and assembled. A rectangular hole was cut in the ice (which was about 0.6 m thick). A 4.9 m long, 0.3 m diameter galvanised sheet-iron pipe (the intake tube) was attached below the pump, and the whole unit lowered through the opening in the ice. The rod supporting the pump was attached to the raft so that the top of the pump was about 1.4 m below the water surface. The pump intake was then about 6.5 m below the water surface, enabling relatively warm (3.7°C) water to be available at the intake for pumping.

TABLE 1 EXPERIMENTAL PERFORMANCE DATA FOR WARDUN "SUNSTIRRER" PUMP, MEASURED IN LABORATORY

| POWER SUPPLIED | | | MOTOR POWER | | POWER IMPARTED TO WATER | | | | EFFICIENCIES | |
|---|---|---|---|---|---|---|---|---|---|---|
| EMF volts | Current amps | Power watts | Power lost in motor watts | Power out watts | Current meter revs. n | Velocity m.sec-1 | Flow l.sec-1 | Final Power Delivered watts | Motor | Pump |
| 18.75 | 0.59 | 11.1 | 5.7 | 5.3 | 5.74 | 0.355 | 18.0 | 1.14 | 0.48 | 0.21 |
| 25.1 | 0.91 | 22.8 | 8.8 | 14.1 | 8.1 | 0.485 | 24.6 | 2.89 | 0.62 | 0.21 |
| 31.2 | 1.21 | 37.8 | 12.2 | 25.6 | 10.7 | 0.626 | 31.7 | 6.20 | 0.68 | 0.24 |
| 37.7 | 1.62 | 61.1 | 17.3 | 43.8 | 12.2 | 0.707 | 35.8 | 8.93 | 0.72 | 0.20 |

Electrical connections between the photovoltaic array, the batteries and the motor were made, and the system set on an 80% duty cycle, with a 40 minute period (approx. 32 mins. on, 8 mins. off). The current drawn by the motor was measured as 1.00 amps, with a battery voltage of approximately 25v. The solar powered pump was then ready for operation (see Fig. 2).

Fig. 2 Photovoltaic Powered Water Circulator (Wardun WD 20 Sunstirrer) and Support Raft

The Microscout system was set up, with temperature probe 1 placed in the exit flow from the pump, and probes 2 and 3 at submergence depths of 4.5 and 9 m respectively. Channels 4, 5 and 6 were also connected, and the system set to sample at 1 hour intervals starting at 12.15 hours, 12 February. Initial measurements of water temperature showed that the water being pumped (Channel 1) and the water at 9 m (Channel 3) was the same temperature (3.7°C), and the water at 4.5 m (Channel 2) was 3.5°C. Calibration in melting ice prior to the field trip had indicated that the accuracy of the temperature probes was good (about ± 0.1°C). After 1 day's initial operation a hole in the ice of about the same diameter as the raft (2.5 m) had been created, and the raft settled into the water and became free floating.

The system was visited after 10 days' operation, by which time a substantial ice free patch (about 6 m diameter) had been formed (see Fig. 3). During the 10 days' operation temperatures had been very cold indeed, with a four day period when night temperatures averaged -24°C and day time temperatures averaged -15°C. About 40 cm of snow fell during the period, with 19 cm falling during a single storm on

14 - 15 February. The Microscout was downloaded at 10.15 hours on February 22nd, and restarted about 1 hour later. At the date of writing (April 10) the whole system was continuing to work satisfactorily, and an ice free patch of dimensions 20 m x 25 m had been created around the pump.

Daily averages and totals for the days of sampling are shown (see Table 2). These are based upon hourly readings. An example listing for one day of operations is also presented (see Table 3).

The battery voltage after 10 days operation indicated that the batteries were still 1/3 to 1/2 charged on this date, despite a five day period when almost zero current was supplied to the batteries because of a major snow storm.

The water temperature of the water pumped (Channel 1) decreased a very small amount (from 3.7°C to 3.5°C) during the initial 10 day period. The water temperature at 9 m depth (Channel 3) decreased a negligible amount in the same period. Data from the photovoltaic monitor panel (Channel 4) indicated that a daily average of 1.91 ampere hours of electricity had been obtained during the 10 day period. With a peak monitor panel current of 0.65 amps in bright sun, the average hours of bright sun during the period are 1.09/0.65 = 2.9 hours. If further measurements at this time of year confirm the result, then there is significantly more bright sunshine available than were used in the design calculations (2 hours per day assumed).

TABLE 2 DAILY AVERAGE READINGS OF WATER TEMPERATURES (CHANNELS 1 - 3), PV PANEL OUTPUTS (CHANNEL 4 - 5) AND BATTERY VOLTAGE (CHANNEL 6)

| | DAILY AVERAGES AND TOTALS | | | | | |
|---|---|---|---|---|---|---|
| DAY | Chn# 1 deg C | Chn# 2 deg C | Chn# 3 deg C | Chn# 4 AH | Chn# 5 AH | Chn# 6 volts |
| Feb 12,86 | 3.7 | 3.5 | 3.7 | 1.0 | 11.7 | 26.0 |
| Feb 13,86 | 3.7 | 3.5 | 3.7 | 4.0 | 58.4 | 27.8 |
| Feb 14,86 | 3.6 | 3.5 | 3.7 | 2.3 | 31.6 | 27.2 |
| Feb 15,86 | 3.5 | 3.4 | 3.6 | 0.2 | 0.0 | 25.4 |
| Feb 16,86 | 3.6 | 3.4 | 3.6 | 1.1 | 0.0 | 25.1 |
| Feb 17,86 | 3.5 | 3.4 | 3.6 | 1.5 | 0.0 | 25.0 |
| Feb 18,86 | 3.6 | 3.3 | 3.6 | 1.9 | 0.8 | 24.9 |
| Feb 19,86 | 3.6 | 3.3 | 3.6 | 2.5 | 0.6 | 24.7 |
| Feb 20,86 | 3.5 | 3.2 | 3.6 | 2.4 | 18.8 | 25.2 |
| Feb 21,86 | 3.5 | 3.2 | 3.6 | 1.8 | 37.7 | 25.7 |
| Feb 22,86 | 3.4 | 3.2 | 3.6 | 0.4 | 0.0 | 25.2 |

TABLE 3 ONE DAY'S DATA SET - HOURLY READINGS OF WATER TEMPERATURES PV PANEL CURRENT AND BATTERY VOLTAGE

| | | | | | | | |
|---|---|---|---|---|---|---|---|
| Feb 13,86 | 0:15: | 3.5 deg C | 3.5 deg C | 3.7 deg C | 0.0 mAMPS | 0.0 mAMPS | 25.4 volts |
| Feb 13,86 | 1:15: | 3.8 deg C | 3.5 deg C | 3.7 deg C | 0.0 mAMPS | 0.0 mAMPS | 25.2 volts |
| Feb 13,86 | 2:15: | 2.6 deg C | 3.6 deg C | 3.7 deg C | 0.0 mAMPS | 0.0 mAMPS | 25.4 volts |
| Feb 13,86 | 3:15: | 3.8 deg C | 3.6 deg C | 3.7 deg C | 0.0 mAMPS | 0.0 mAMPS | 25.1 volts |
| Feb 13,86 | 4:15: | 3.1 deg C | 3.6 deg C | 3.7 deg C | 0.0 mAMPS | 0.0 mAMPS | 25.2 volts |
| Feb 13,86 | 5:15: | 3.9 deg C | 3.6 deg C | 3.8 deg C | 0.0 mAMPS | 0.0 mAMPS | 25.1 volts |
| Feb 13,86 | 6:15: | 3.7 deg C | 3.4 deg C | 3.8 deg C | 0.0 mAMPS | 0.0 mAMPS | 25.2 volts |
| Feb 13,86 | 7:15: | 3.9 deg C | 3.6 deg C | 3.8 deg C | 0.0 mAMPS | 0.0 mAMPS | 25.1 volts |
| Feb 13,86 | 8:15: | 3.8 deg C | 3.6 deg C | 3.8 deg C | 25.0 mAMPS | 0.0 mAMPS | 25.3 volts |
| Feb 13,86 | 9:15: | 3.9 deg C | 3.6 deg C | 3.8 deg C | 188.0 mAMPS | 2470.0 mAMPS | 27.1 volts |
| Feb 13,86 | 10:15: | 3.9 deg C | 3.6 deg C | 3.7 deg C | 527.0 mAMPS | 8060.0 mAMPS | 32.6 volts |
| Feb 13,86 | 11:15: | 3.7 deg C | 3.5 deg C | 3.7 deg C | 621.0 mAMPS | 9060.0 mAMPS | 33.3 volts |
| Feb 13,86 | 12:15: | 3.7 deg C | 3.5 deg C | 3.7 deg C | 663.0 mAMPS | 9660.0 mAMPS | 33.5 volts |
| Feb 13,86 | 13:15: | 3.7 deg C | 3.5 deg C | 3.7 deg C | 657.0 mAMPS | 9510.0 mAMPS | 33.4 volts |
| Feb 13,86 | 14:15: | 3.7 deg C | 3.5 deg C | 3.7 deg C | 591.0 mAMPS | 8500.0 mAMPS | 33.2 volts |
| Feb 13,86 | 15:15: | 3.6 deg C | 3.5 deg C | 3.7 deg C | 454.0 mAMPS | 7150.0 mAMPS | 32.9 volts |
| Feb 13,86 | 16:15: | 3.6 deg C | 3.4 deg C | 3.6 deg C | 271.0 mAMPS | 4020.0 mAMPS | 32.0 volts |
| Feb 13,86 | 17:15: | 3.6 deg C | 3.4 deg C | 3.6 deg C | 6.0 mAMPS | 0.0 mAMPS | 26.4 volts |
| Feb 13,86 | 18:15: | 3.6 deg C | 3.4 deg C | 3.7 deg C | 0.0 mAMPS | 0.0 mAMPS | 26.1 volts |
| Feb 13,86 | 19:15: | 3.6 deg C | 3.5 deg C | 3.7 deg C | 0.0 mAMPS | 0.0 mAMPS | 26.0 volts |
| Feb 13,86 | 20:15: | 3.7 deg C | 3.5 deg C | 3.8 deg C | 0.0 mAMPS | 0.0 mAMPS | 26.1 volts |
| Feb 13,86 | 21:15: | 3.7 deg C | 3.5 deg C | 3.7 deg C | 0.0 mAMPS | 0.0 mAMPS | 25.8 volts |
| Feb 13,86 | 22:15: | 3.8 deg C | 3.5 deg C | 3.7 deg C | 0.0 mAMPS | 0.0 mAMPS | 26.0 volts |
| Feb 13,86 | 23:15: | 3.8 deg C | 3.5 deg C | 3.7 deg C | 0.0 mAMPS | 0.0 mAMPS | 25.8 volts |

Fig. 3 Whole System After 10 Days Operation

## 6. CONCLUSIONS

A prototype photovoltaics powered pumping system (the Wardun WD 20 "Sunstirrer") was designed, built and field tested. The pump was built using a new, direct drive principal using a DC permanent magnet motor. This enabled an efficient power transfer from electrical energy to mechanical energy to water circulation power to be achieved, minimising the cost of the photovoltaic panels.

An open water patch 20 ft (6 m) across was created after 10 days operation at Menzies Lake (near Merritt, BC). This was a surprisingly large opening in the ice (which was 0.6 m thick) in view of extremely low temperatures during the period. Water temperatures and solar radiation data were measured. Solar radiation during February was more than had been anticipated, and the pump used less power than anticipated to circulate a flow of 25 litres sec$^{-1}$. With minor modifications the system would be capable of circulating 1½ to 2 times the present flow. In addition we believe it may be possible to dispense with the batteries and use a directly driven (sunshine only) pumping system. This would pump vigorously (at 10 -20 times the present power) in full sunshine, and shut down completely in low light conditions.

## 7. ACKNOWLEDGEMENTS

Funding for this project was kindly made available by the Habitat Conservation Fund, through the British Columbia Ministry of Environment, Fish and Wildlife Branch.

Assembly and testing of the Wardun "Sunstirrer" was carried out in the U.B.C. Civil Engineering Hydraulics Laboratory. Dr Michael C Quick, Department of Civil Engineering, U.B.C., provided ideas on propeller performance and pump design. Field work was carried out with the help of BC Ministry of Environment Regional Fisheries Biologist and Technical Staff, Kamloops Branch.

## 8. REFERENCES

1. **Ashley, K.I.,** "Hypolimnetic aeration of a naturally entrophic lake : physical and chemical effects". Can. Journal of Fisheries and Aquatic Sciences 40 (9), pp. 1343-1359, 1983.

2. **Derrick, A., McNelis, B., Starr, M.R., and Wright, D.E.,** "The state of the art of commercially available, small-scale photovoltaic pumping systems", Proc. 16th Photovoltaic Specialists Conf., pp. 194-198, IEEE: New York, 1982.

3. **Halcrow, W.** et al., Small scale solar powered pumping systems: The technology, its economics and advancement", Main report to the World Bank, UNDP Project GLO/80/003, June 1983.

4. **Leckey, R.T.,** and **Holmes, D.W.,** "Evaluation of two methods of aeration to prevent winterkill". Prog. Fish Culturist 34 (3), pp. 175-178, 1972.

5. **Pulfrey, D.L., Ward P.R.B.** and **Dunford, W.G.,** "A Photovoltaic-Powered System for Medium Head Pumping", Solar Energy (In Press), 1986.

6. **Ward, P.R.B.,** and **Dunford, W.G.,** "Solar Powered Groundwater Pumping for Medium Heads", Challenges in African Hydrology and Water Resources (Proceedings of the Harare Symposium), IAHS Publ. No. 144, pp. 249-258, 1984.

# THE USE OF BOILING METHANOL IN SOLAR CONCENTRATING PHOTOVOLTAIC SYSTEMS

D.W.H. Fraser and D.C. Card
Mechanical Engineering Deptartment
University of Manitoba
Winnipeg, Manitoba, Canada
R3T 2N2

## ABSTRACT

This paper illustrates the benefits obtainable by utilizing boiling methanol as opposed to water as a coolant in solar concentrating photovoltaic and photovoltaic/thermal systems. The system analyzed consists of four 20.32 $mm^2$ cells on a 25.4 x 25.4 mm diameter coolant channel with concentration ratios of 50 to 300. Saturated or subcooled boiling methanol was found to offer higher heat transfer rates at lower pressure drops than single-phase water. This advantage, though small at low concentration ratios, becomes large at high concentration ratios. For example, the system analyzed herein at a concentration ratio of 300 has a heat transfer coefficient of 8,100 $W/m^2$ at a pressure drop as low as 180 $N/m^2$ for saturated boiling methanol. On the other hand, single-phase water requires a much higher flow rate for the same heat transfer coefficient, resulting in a pressure drop of 1,800 $N/m^2$. Therefore, parasitic pumping power can be greatly reduced by using boiling methanol as a coolant. This trend is likely to be seen in larger systems as well. Possible two-phase flow instabilities, if present, can be readily controlled. Flow patterns expected are discussed.

## 1. INTRODUCTION

Photovoltaic concentrating systems are presently being energetically investigated and the technology is developing rapidly. In these systems, the concentrated sunlight increases the power output of the individual solar cells. The heat which develops in the cells due to concentration can be removed by passive or active cooling. If it is removed by a circulating coolant, the heat is available for thermal applications such as residential or industrial heating [1-8].

Cooling of the cells also improves their efficiency and increases their lifetime [9-13]. The use of Fresnel lens concentrators reduces the total cost by replacing the high priced cell area with the lower priced lenses [14].

The analysis herein theoretically predicts the thermal-hydraulic performance of an actively cooled solar concentrating photovoltaic or photovoltaic/thermal system of the type described in reference 1. A comparison between single-phase water and boiling methanol coolants is presented.

The principal advantages offered by a two-phase collector is the enhanced heat transfer rate associated with boiling. Large concentration ratios are possible with a correspondingly small temperature increase at the same pumping power. This results in significantly lower perisitic pumping losses compared to single-phase systems.

A review of solar energy literature reveals that two-phase solar collector research is limited primarily to the flat plate thermal collector case. For the flat plate case, Soin et al. [17] have investigated the performance of acetone and petroleum ether as working fluids. Bol and Lang [18] have worked with butane, while Downing and Walden [19] have used fluorohydrocarbon refrigerants, such as R-11 and R-114. In all of these investigations, a closed loop thermosyphon type system has been used. More recently, B. Abramson et al. [20] have investigated a flat-plate boiling thermal collector with forced convective cooling for various fluids such as water, methanol, acetone, n-pentane, diethyl ether, and R-113. As well, E.K. May and L.M. Murphy [21] investigated the performance benefits of direct generation of steam in line-focus thermal solar collectors. All of the above investigators have found that collectors containing a boiling fluid have a thermal efficiency that is greater than a single-phase collector.

The use of boiling methanol as a coolant in a concentrating photovoltaic collector has not been previously investigated. It was decided to investigate methanol because it has a high latent heat of vaporization, and its saturation temperature, (~65°C) at one atmosphere, is close to the desired operating temperature of the solar cells. Boiling methanol also has the advantage of keeping the solar cells at closer to the same temperature thus enabling them to operate at more nearly the same voltage.

Possible two-phase flow instabilities associated with a parallel flow system of channels are also addressed in this paper.

## 2. THE COLLECTOR MODEL

A typical system layout is shown in Figure 1. The single-phase coolant enters the collector at the temperature $T_i$. We will look at the case where $T_i$ is lower than the saturation temperature, $T_s$, at the working pressure, P, and also the case where $T_i = T_s$. Boiling will occur when the tube inner temperature exceeds the saturation temperature ($T_w > T_s$).

Boiling will be of the subcooled type if the average fluid temperature is lower than the saturation temperature ($T_f < T_s$). If the temperature of the fluid is at saturation ($T_f = T_s$), saturated boiling will occur.

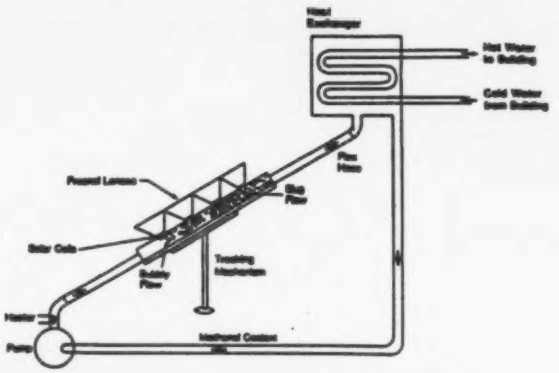

Fig. 1 Concentrator Photovoltaic/Thermal system

For the analysis presented here, pressure drop along the channel will be quite small. The effect of this in lowering the saturation temperature, $T_s$, of the fluid was therefore neglected in the present analysis.

### 2.1 Conditions for Comparison

It was decided to investigate the characteristics of a 3.175 mm thick, 25.4 mm x 25.4 mm channel incorporating four 20.32 mm x 20.32 mm square solar cells with square fresnel lenses as concentrators. The channel length had to be changed as the concentration ratio was varied. This was due to the size of the fresnel lens required in each case.

Each system of four cells/channel length was analyzed under the following conditions:

- Solar insolation of 1 kW/m$^2$;
- Concentration ratios of 50, 100, 150, 200, 250, and 300;
- Heat flux, q", varying from 24,580 W/m$^2$ (CR=50) to 147,580 W/m$^2$ (CR=300);
- Photovoltaic conversion efficiencies of 12%;
- An estimated heat transfer area beneath the cell of 1.2 times the cell area;
- Four cells/channel length;
- Channel lengths of 0.576 m, 0.813 m, 0.996 m, 1.148 m, 1.285 m, and 1.408 m, corresponding to the above mentioned concentration ratios;
- Mass flux, G, from 35 kg/m$^2$ s to as high as 350 kg/m$^2$ s for boiling methanol;
- Reynolds number greater than or equal to 3000 for turbulent water (subcooled boiling and single-phase);
- Atmospheric pressure.

The heat flux calculations were based on an energy balance similar to that by M. O'Neill [22] for a concentration ratio of 50 and a cell temperature close to what may be expected in this system. The energy balance would vary slightly according to the specified heat flux since radiation, convection, and conduction losses are temperature dependent. Therefore, the concentration ratios specified serve only as a qualitative estimate.

The average bulk temperature of the fluid along the channel for both water and methanol was set at 65°C for the saturated boiling methanol versus water case, and at 55°C for the subcooled boiling methanol versus water case.

Each channel was assumed to be perfectly insulated with heat loss occurring only at the lens assemblies.

### 2.2 Heat Transfer

Single-phase turbulent heat transfer to water was calculated via three separate correlations. Of the three, two were in close agreement with each other so that only two lines appear in Figures 2 to 5.

Experimental data for turbulent flow through a long tube or channel for fluids having a Prandtl number between 0.5 and 100 can be correlated by the well-known Dittus-Boelter equation [23]:

$$Nu_D = 0.023\ Re_D^{0.8}\ Pr_L^{1/3} \qquad \ldots\ 2.1$$

In this equation all physical properties are evaluated at the mean film temperature ($\overline{T}_f$) which is the average between the wall temperature ($T_w$) and the bulk fluid temperature ($T_{b,av}$) evaluated halfway between inlet and outlet:

$$\overline{T}_f = (T_w + T_{b,av})\ /\ 2 \qquad \ldots\ 2.2$$

$T_{b,av}$ was taken at 65°C for comparison to saturated boiling methanol and at 55°C for comparison to 10°C subcooled boiling of methanol.

In close agreement with the Dittus-Boelter equation is the relation by Colburn [24]:

$$St = .023\ Re^{-0.2}\ Pr_L^{-0.66} \qquad \ldots\ 2.3$$

Again, in this equation, fluid properties are taken at the mean film temperature ($\overline{T}_f$). Because of the close agreement to the Dittus-Boelter these two equations appear as one line in Figures 2 to 5.

For comparison, the heat transfer coefficient was also calculated by the Seider and Tate correlation [23]:

$$Nu_d = 0.027\ Re_d^{0.8}\ Pr_L^{0.33}\ (\mu_b/\mu_w)^{0.14} \qquad \ldots\ 2.4$$

Where:

$\mu_b$ = viscosity at average bulk temperature $T_{b,av}$

$\mu_w$ = viscosity at wall temperature $T_w$

This equation correlated well with data from rectangular ducts with a large temperature variation between the surface and bulk fluid temperature [25]. These results are shown in Figures 2 to 5.

Because of the variation in handling viscosity effects between the three correlations, the Seider and Tate correlation predicts a higher rate of heat transfer.

At low flow rates, the single-phase heat transfer rate to water was found to be too low, thereby creating a wall temperature above the saturation temperature of water at one atmosphere (i.e. $T_w > 100$°C). Under these conditions subcooled boiling of water will occur. The heat transfer rate was found by Chen's extension to subcooled boiling [27]:

$$q'' = h_{NCB}\ (T_w - T_{SAT}) + h_c\ (T_w - T_{f(z)}) \qquad \ldots\ 2.5$$

Subcooled boiling of methanol was also calculated by Equation (2.5).

Saturated boiling of methanol was found by Chen's [26-28] correlation for saturated boiling. Chen assumed that the contribution via the single and two-phase heat transfer mechanisms are additive. This superposition can be represented as:

$$h_{TP} = h_{NCB} + h_C \qquad \ldots\ 2.6$$

In order to determine the minimal heat transfer rate possible during non-flow situations, nucleate pool boiling heat transfer to methanol was calculated. A review of the literature revealed the correlation of Stephan and Abdelsalam [29] for the pool boiling of methanol. They produced an empirical correlation of the form:

$$h_{NCB} = C\, q''^{.670} \qquad \ldots\ 2.7$$

Where C is an experimentally derived constant found to be equal to 2.5 for boiling methanol at one atmosphere. It has been noted that various degrees of surface roughness as well as different surface-fluid combinations can affect the value of $h_{NCB}$. In deriving the above formula, a surface roughness of 1 μm, as is often encountered in technical applications, was assumed.

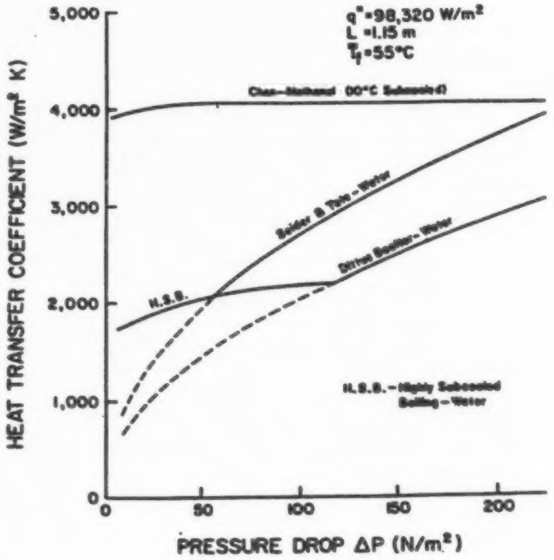

Fig. 2 Subcooled Boiling Methanol vs. Water at 200X Concentration.

## 2.3 Pressure Drop

Two-phase and single-phase pressure drops were calculated neglecting the static head term. In single-phase flow the static head term will be recoverable in the return section to the bottom of the collector (Figure 1). In two-phase flow the heat exchanger, located at the top of the collector, will condense the flow resulting in a large single-phase recoverable pressure drop in the return section as well.

Single-phase pressure drop was calculated using the usual Darcy-Weisbach [30] equation and the Moody diagram for smooth pipes.

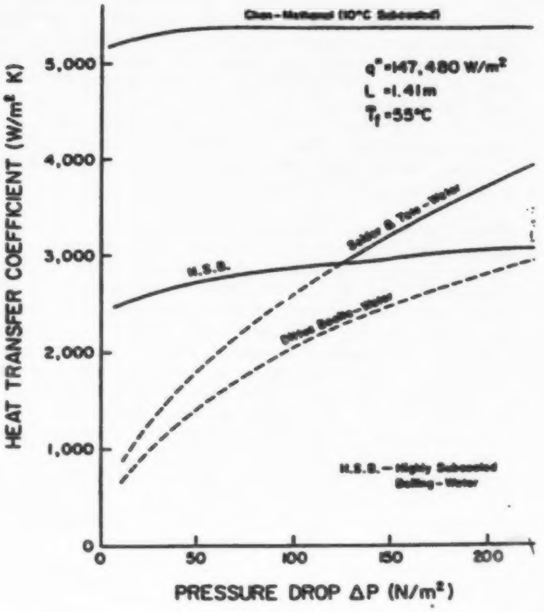

Fig. 3. Subcooled Boiling Methanol vs. Water at 300X Concentration.

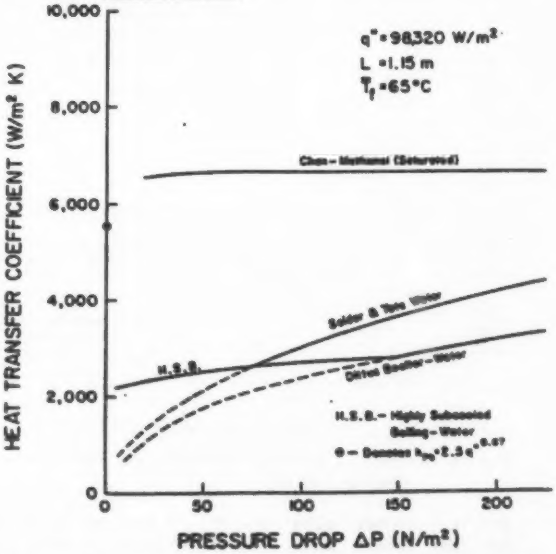

Fig. 4 Saturated Boiling Methanol vs. Water at 200X Concentration

Subcooled boiling is characterized by two regions. These are defined as the highly subcooled region and the fully developed subcooled boiling region. The highly subcooled boiling region is characterized by the growth and collapse of vapour bubbles while still attached to the heated surface. This was found to only enhance the surface roughness of the pipe. In the present analysis, this would occur at an area directly beneath the cell only. Enhanced pressure drop would thus be marginal and was neglected. Therefore, the pressure drop was calculated assuming single-phase flow.

In the fully developed subcooled boiling region, bubbles formed are found to detach from the wall leading to an increase in quality and void fraction. The method of Saha and Zuber [31] was used to determine the degree of subcooling required to initiate fully developed subcooled boiling, referred to as the point of net vapour generation. It was found that in all the cases analyzed, the subcooled boiling of methanol was in the fully developed region, whereas for water, only highly subcooled boiling would occur.

Fully developed subcooled boiling of methanol will occur only in an area directly beneath each cell. Any vapour generated there will subsequently recondense in the flow direction. In order to determine the pressure drop, the variation in void fraction with axial distance from beneath the cell would have to be determined. This is a complex process dependent particularly on bubble radius, flow velocity, and degree of subcooling. M. Akiyama and F. Tachibana [32] obtained growth and collapse data of vapour bubbles under surface boiling of water with a velocity ranging from .05 m/s to 5 m/s, with subcooling ranging from 20 to 80°C and with atmospheric pressure. Although here the main concern is for 10°C subcooled boiling methanol, the results obtained in their study can be used to approximate what may be expected in the present case.

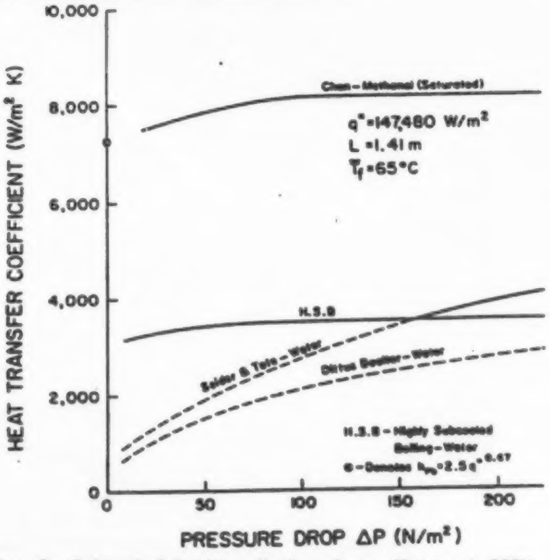

Fig. 5 Saturated Boiling Methanol vs. Water at 300X Concentration

At the lowest flow rate of .05 m/s (which corresponds to the lowest mass flux of 35 kg/m² in this case) and a subcooling of 20°C for water, Akiyama and Tachibana found that the bubbles travelled about 0.3 mm before collapsing. At higher flow rates, this distance was lessened.

With 10°C subcooled boiling methanol, the expected lifetime of the bubble would be greater. In the present case at a concentration ratio of 50, the cell interspacing is about 144 mm, while at a concentration ratio of 300 this distance becomes 362 mm. Within this large distance it is safe to assume that all of the bubbles generated will have condensed prior to encountering the next cell in the flow direction.

Fully developed subcooled boiling of methanol pressure drop was calculated using the levy [27] correlation:

$$\phi^2_{fo} = (1 - x(z))^{1.78} / (1 - \alpha)^2 \qquad \ldots\ 2.8$$

The method of Saha and Zuber [31] was used to calculate the quality x, and void fraction α, in this equation. Their analysis is too lengthy to be reproduced here and the reader is asked to refer to their paper [31]. The quality and void fraction calculated by Saha and Zuber were obtained empirically by experiments with a uniform heat flux. For the purpose of this analysis the heated part of the channel would extend to no more than 1/3 of the periphery of the channel at each cell location, therefore imparting a local quality and void fraction of about 1/3 of that predicted by Saha and Zuber's method. Therefore, these values were used in Equation 2.9.

Saturated boiling methanol pressure drop was calculated by the homogeneous flow model [27]. The total static pressure gradient is expressed as:

$$-\frac{dP}{dZ} = \frac{\left(\frac{2f_{TP}G^2v_f}{D_H}\right)\left(1 + x\frac{v_{fg}}{v_g}\right) + G^2v_f\frac{v_{fg}}{v_f}\frac{dx}{dZ} + \frac{g\sin\theta}{u_f(1 + xv_{fg}/v_f)}}{\left(1 + G^2x\frac{dv_g}{dP}\right)}$$

... 2.9

In order to interpret this equation with respect to axial length some assumptions can be made:

1) $G^2 x \frac{(d v_g)}{dP} \ll 1.$ The compressibility of the gaseous phase may be neglected. This approximation has been found valid even at high pressure and high quality flows [27].
2) $v_{fg}/v_f$ and $f_{TP}$ remain constant over the length considered ($dx/dz \neq 0$ under cell alone).
3) Each channel of four cells can be subdivided into five sections. Assuming the fluid entering as being single-phase at saturation temperatures, the first section will be single-phase. Upon encountering the first cell a sharp linear increase in quality will occur, then remain constant (assuming the channel to be perfectly insulated) until the next cell where the process repeats itself. Therefore, the acceleration pressure drop beneath the cell is added to the frictional pressure gradient in each two-phase section.
4) The static head term was neglected for reasons already discussed.
5) The effect of the linear increase in quality in the length $\Delta x$ is negligible on the frictional pressure drop.

With these assumptions, Equation 2.10 becomes, for each two-phase section:

$$\Delta P = \left(\frac{2f_{TP}G^2Lv_f}{D_H}\right)\left(1 + x\frac{v_{fg}}{v_f}\right) + G^2v_{fg}\Delta x$$

$\Delta x$ is the change in quality encountered under each cell, and L is the length of each section. The single phase pressure drop in the first section was summed with the two-phase pressure drop in each subsequent section to give the total pressure drop.

In defining the two-phase friction factor $f_{TP}$ it was found that considerably good agreement, at low to moderate flow rates, was obtained by defining the two-phase viscosity as [27]:

$$\mu_{TP} = \mu_f\ [1 + x\ (v_{fg}\ /\ v_f)] \qquad \ldots\ 2.11$$

The friction factor was found by the Blausius Equation [27]:

$$f_{TP} = .079\ [GD_H/\mu_{TP}]^{-.25} \qquad \ldots\ 2.12$$

## 2.4 Flow Pattern

Weisman and Kang's [33] general flow pattern maps for horizontal, vertical and upwardly inclined tubes were used in our analysis.Due to the low quality nature of the flow, in horizontal or upwardly inclined flow, wavy, broken slug or annular flow will not be encountered in a 4 cell channel at the low mass flow rates analysed herein. However, during horizontal flow, stratified flow will be encountered at mass flow rates less than 335 kg $m^{-2}s^{-1}$. Stratified flow would result in a dryout of the upper portion of the tube where the cells are located, leading to elevated temperatures and possible cell damage and therefore must be avoided. Operation of the entire collector in the subcooled boiling mode during horizontal flow would eliminate stratified flow at lower flow rates and is therefore recommended.

During inclined flow it has been observed [33] that the disappearance of stratified flow appears to correspond to the disappearance of a clear gas passageway at zero flow. This corresponds to the condition that

$$\sin\theta > D/L \qquad \text{... 2.13}$$

where L= length of pipeline; D=pipeline diameter; and $\theta$ = angle of inclination (upward). For a length of .576 m (CR=50) this corresponds to $\theta = 1.9°$ whereas for a length of 1.41 m (CR=300), $\theta = .8°$ for the channel considered here, ($D_H$=1.905 cm). Therefore, for each case, a slight upward tilt of the collector will eliminate stratified flow from occuring at the low flow rates considered in the analyses.

The disappearance of stratified flow at low to higher angles of inclination will be followed by intermittent (slug, plug), or bubble flow. Broken slug flow in which the water slug does not reach the top of the tube) will not be encountered, again due to the low quality nature of the flow.

## 2.5 Operating Stability

Possible system instabilities in two-phase flow could lead to temperature excursions, control problems, or mechanical vibrations causing damage to the components. Pederson and May [34] identified five modes of flow instability that could occur in a parallel flow system of a field of line-focusing solar collectors. For a parallel flow system of point-focusing collectors the principals leading to the instabilities are essentially the same. These instabilities are the ledinegg instability, acoustic, pressure-drop, density wave oscillations, and flow pattern transition. The Ledineggin stability results if conditions exist such that an increase in mass flow (G) can cause a reduction in channel pressure drop ($\Delta P$), perhaps due to a lower vapour generation rate. A necessary, but not sufficient, condition for this to occur is:

$$\partial\Delta P/\partial G < 0 \qquad \text{... 2.14}$$

In all of the cases analysed herein an increase in flow always resulted in an increase in pressure drop thereby ruling out these instabilities.

As well, the condition expressed in Equation (2.14) is a necessary, but not sufficient, condition for acoustic and pressure drop oscillations to occur, and can therefore also be ruled out.

Density-wave oscillations though, are commonly observed in parallel channel systems. These are of a dynamic nature due to the interaction of flow rate, vapour generation rate, and pressure drop. Single-phase flow fluctuations at the inlet of a channel can propagate into void-fraction fluctuations in the boiling region causing a dynamic two-phase pressure drop. A criteria for this instability that was confirmed experimentally by Saha et al. [35] is:

$$N_{pch} - N_{sub} \leq F\,(k) \qquad \text{... 2.15}$$

the term F(k) is a function of the inlet and outlet pressure restrictions, and the frictional pressure drop within the channel [34,35]. Inlet pressure restrictions are stabilizing while outlet restrictions are found to be destabilizing.

For the collector of concern here, the worst case of a density wave instability would occur at the highest heat flux (C.R. = 300), and with the fluid entering at saturation temperature ($N_{sub}$ = 0). According to the criteria in eqn. (2.15) it was found that at the lowest mass flow rate of 35 kg/$m^2$s, an inlet restriction of only 13 N/$m^2$ is required to ensure stability. This would raise the overall pressure drop negligibly. At a higher flow rate of 87 kg/$m^2$s an inlet restriction of 80 N/$m^2$s is required. On the other hand at a lower concentration ratio of 50 and mass flow rate, G=87 kg/$m^2$ s, an inlet restriction of only 15 N/$m^2$ is required to ensure stability. Therefore, this type of instability will only have a small effect on the performance of a small scale system such as a parallel arrangement of 4 cells/channel studied here. In larger systems, Pederson and May [34] found this instability negligible in their analysis of a 120 m long channel, with a high vapour generation rate.

A final type of instability, that is a possibility, is flow pattern transition instability. This has been found to occur during the transition from intermittent, or bubble flow, to annular flow. This would not occur in the collector analysed herein due to the low quality and low flow rates, but may be of concern in larger systems where annular flow is possible.

## 3. DISCUSSION AND RESULTS

The principle objective of this study was to show that by using boiling methanol instead of water as a coolant larger heat transfer rates are achievable with a lower pressure drop. The overall result of this combination is to greatly reduce parasitic pumping power yet still maintain cell temperatures at a minimum.

Figures 2 and 3 are the predictions for subcooled boiling heat transfer of methanol, and heat transfer to water, versus pressure drop. The average channel temperature for the methanol and the water was set at 55°C.

In all of the graphs the heat transfer coefficients are defined as $q''/(T_w - T_f)$. The heat transfer rate to water is either by highly subcooled boiling at low flow rates (low $\Delta P$) or by single phase at higher flow rates. The intersection of the H.S.B. (highly subcooled boiling) line and the segmented lines represents the condition such that the wall temperature is equal to the saturation temperature of water (100°C). By further increasing the flow rate ($\Delta P$), heat transfer is by single phase. This is shown as two solid lines, depending on whether equation (2.1) and/or (2.3) is used or whether equation (2.4) is used.

Figures 4 and 5 represent the heat transfer rates to saturated boiling methanol and to water versus pressure drop. Water was compared at the saturation temperature of methanol (65°C).

In all of the cases subcooled or saturated boiling methanol offers substantially higher rates of heat transfer than single-phase or subcooled boiling water at the same pressure drop. This trend is seen to increase with an increase in the heat flux (concentration ratio). Subcooled boiling of methanol has an advantage over saturated boiling of methanol in that the required thermal energy can be removed at a lower temperature. If the degree of subcooling at the channel inlet is such that the fluid temperature is lower, or near the saturation temperature at the exit, then the pressure drop through the heat exchanger will be via single-phase alone. Two-phase flow instability and stratified flow patterns are likely to not be of concern under these conditions. On the other hand, saturated boiling of methanol offers a higher temperature source for thermal applications and a greater heat transfer rate than subcooled boiling methanol.

In Figures 4 and 5 the value of the saturated nucleate pool boiling heat transfer coefficient is shown on the ordinate for zero flow rate (ΔP). This corresponds to the lowest possible heat transfer rate and provides a safety feature in the event of pump failure.

Flow patterns expected from this system are bubble and intermittent flow. A slight upward tilt is found to prevent stratified flow from occurring. Transition to broken slug or annular flow may occur with larger systems having a greater vapour generation.

TABLE 1. ΔP for Single Phase Water and Subcooled Boiling Methanol at the Same Heat Transfer Coefficient

| C.R. | 50 | 100 | 150 | 200 | 250 | 300 |
|---|---|---|---|---|---|---|
| L (m.) | 0.576 | 0.813 | 0.996 | 1.15 | 1.3 | 1.41 |
| h (W/m$^2$ K) | 2,200 | 2,450 | 3,350 | 4,050 | 4,750 | 5,380 |
| $\Delta P_{sc}$ meth. (N/m$^2$) | 30 | 30 | 50 | 50 | 50 | 70 |
| $\Delta P_f$ water (N/m$^2$) | 58 | 90 | 218 | 380 | 602 | 870 |
| $T_w$ (°C) | 72.2 | 75 | 77 | 79.3 | 80.9 | 82.4 |

TABLE 2. ΔP for Single Phase Water and Saturated Boiling Methanol at the Same Heat Transfer Coefficient

| C.R. | 50 | 100 | 150 | 200 | 250 | 300 |
|---|---|---|---|---|---|---|
| L (m.) | 0.576 | 0.813 | 0.996 | 1.15 | 1.3 | 1.41 |
| h (W/m$^2$ K) | 3,500 | 4,675 | 5,600 | 6,650 | 7,500 | 8,150 |
| $\Delta P_{so}$ meth. (N/m$^2$) | 30 | 30 | 60 | 60 | 100 | 100 |
| $\Delta P_f$ water (N/m$^2$) | 115 | 302 | 560 | 943 | 1404 | 1812 |
| $T_w$ (°C) | 71.7 | 75.2 | 77.9 | 79.5 | 80.9 | 82.8 |

A pressure drop comparison between saturated or subcooled boiling of methanol versus single-phase water (at the same temperature) was made for the same heat transfer coefficient. Tables 1 and 2 show this comparison. It can be shown that at the flow rates for single-phase water used in constructing these tables, the Dittus-Boelter and/or Colburn correlation are in close agreement with the Seider and Tate correlation. These tables show the inside channel wall temperature beneath the cell associated with each case. The ΔP variation shown in the tables for the two-phase methanol case covers the range over which no appreciable change in the heat transfer rate was predicted. Also, the wall temperature in either the subcooled or saturated case remains essentially the same. No appreciable benefit arises from the use of boiling methanol at a concentration ratio of 50, though, it may be of benefit in a thermosyphoning collector. At higher heat fluxes the benefit arising from using boiling methanol is quite apparent. As shown in Table 2, at 300X C.R., two-phase methanol ΔP is 100 N/m$^2$, whereas for single-phase water at the same temperature (65°C) the required pressure drop will be about 1800 N/m$^2$. An inlet pressure restriction of about 80 N/m$^2$ may be required to ensure stability for the channel utilizing two-phase saturated methanol bringing the overall pressure drop to 180 N/m$^2$.

All of the assumptions made in this analysis were conservative, being such as to favour water as a coolant. Even with this tendency two-phase methanol can be seen to offer a significant advantage over single-phase water as a coolant for concentrator photovoltaic systems.

## 4. CONCLUSION

For solar concentrator photovoltaic systems, two-phase saturated or subcooled boiling methanol is superior to single-phase water as a coolant, especially at high heat fluxes. Possible density wave instabilities can be overcome by including minor pressure restrictions at the channel inlet. This advantage would also be expected in other systems employing different sizes and number of cells as well as different channel geometries.

## 5. ACKNOWLEDGEMENT

The authors gratefully acknowledge the funding provided for this project by the Natural Sciences and Engineering Research Council of Canada (NSERC).

## 6. NOMENCLATURE

| | |
|---|---|
| A | Channel cross-sectional area m$^2$ |
| C.R. | Concentration ratio |
| D | Pipe diameter, m |
| $D_e$ | Equivalent hydraulic diameter, m |
| $f_{TP}$ | Two-phase friction factor |
| g | Acceleration due to gravity, m/s$^2$ |
| G | Mass velocity, kg/m$^2$s |
| $h_c$ | Convective heat transfer coefficient, W/m$^2$ °C |
| $h_{ncs}$ | Nucleate boiling heat transfer coefficient, W/m$^2$ °C |
| $h_{TP}$ | Two-phase heat transfer coefficient, W/m$^2$ °C |

| | |
|---|---|
| $L$ | Channel length, m |
| $N_{pch}$ | Equilibrium phase change number |
| $N_{sub}$ | Subcooling number |
| $Nu_D$ | Nusselt number based on $D_H$ |
| $\Delta P$ | Pressure drop, N/m$^2$ |
| $Pr_L$ | Liquid Prandtl number |
| $Q$ | Total heat addition to channel, W |
| $q''$ | Heat flux, W/m$^2$ |
| $Re_D$ | Reynolds number based on $D_H$ |
| $St$ | Stanton number |
| $T$ | Temperature, °C |
| $T_{b,av}$ | Average bulk fluid temperature in channel, °C |
| $T_f$ | Fluid film temperature, °C |
| $T_{SAT}$ | Saturation temperature, °C |
| $v$ | Specific volume, m$^3$/kg |
| $x$ | True vapour quality |
| $z$ | Axial location |

### Greek

| | |
|---|---|
| $\mu$ | Viscosity, N·s/m$^2$ |
| $\alpha$ | Void fraction |
| $\phi_{Ltt}$ | Lockhart-Martinelli factor |
| $\phi^2_{fo}$ | Two-phase frictional multiplier |
| $\theta$ | Angle of inclination from horizontal, degrees |

### Subscripts

| | |
|---|---|
| b | Bulk fluid |
| f | Fluid |
| TP | Two-phase |
| W | At the wall |
| i | Inlet |
| s | At saturation |
| g | Vapour phase |

## 7. REFERENCES

1. D.J. Mbewe. H.C. Card, D.C. Card, A Model of Silicon Solar Cells For Concentrator Photovoltaic and Photovoltaic/Thermal System Design, Solar Energy, Vol. 35, No. 3, pp. 247-258, (1985).
2. S. Broadbent, et al., Proc. 15th Photovoltaics Spec. Conf., Kissimee, Florida, p. 323, May (1981).
3. A. Kirpich, Ibid., p. 81.
4. C.M. Zittle, Ibid., p. 86.
5. S.I. Kaplan, and C.M. Benson, Ibid., p. 90.
6. M.J. O'Neill, Proc. 14th Photovoltaics Spec. Conf., San Diego, P. 125 (1980).
7. Y. Nakata, et al., Proc. 16th Photovoltaics Spec. Conf., San Diego, Paper #P3-13B-4, (1982).
8. B.Spencer, Ibid., Paper #P3-13B-2.
9. E.C. Boes, B.D. Shafer and D.G. Schueler, Solar Cells, Vol. 6, pp. 3-15 (1982).
10. B.C. Shafer, et al., Proc. 15th Photovoltaics Specialists Conference, Kissimee, Florida, p. 317, May (1981).
11. L.W. Florschuetz, Solar Energy, Vol. 22, pp. 361-366 (1979).
12. D.A. Pritchard, Proc. 15th Photovoltaics Spec. Conf., Kissimee, Florida, p. 178, May (1981).
13. C.M. Whitkaker, et al., Proc. 15th Photovoltaics Specialists, Session 16B, San Diego, Sept. (1982).
14. Y. Nakata, et al., A 30 KWP concentrating Photovoltaic/thermal Hybrid System Application, Energy Conv. Laboratories, 16th Photovoltaics Specialists Conference, San Diego, p. 993 (1982).
15. E.C. Boes, Photovoltaic Concentration Progress, 16th Photovoltaics Specialists Conference, San Diego, p. 702, (1982).
16. Y. Nakata, N. Shibuya, T. Kobe, K. Omato, A. Suzuki and T. Tsuji, Performance of Circular Fresnel Lens Photovoltaic Concentraton, Japanese Journal of Applied Physics, Supplement 19-2, pp. 75-78, Vol. 19 (1980).
17. R.S. Soin, K. Sangameswar, D.P. Rao and K.S. Rao, Performance of a Flat Plate Solar Collector with Fluid Undergoing Phase Change, Solar Energy, 23, pp. 69-73, (1979).
18. K. Bol, M. Lang, Two-Phase Working Fluid in Solar Collectors, AIAA Paper N354, p. 1, (1978).
19. R.C. Downing, V.H. Waldin, Phase Change Heat Transfer in Solar Hot Water Heating Using R-11 and R-14, Transactions ASHRAE, Vol. 86, p. 848, (1980).
20. B. Abramzon, I. Yaron, and I. Borde, An Analysis of a Flat Plate Solar Collector with Internal Boiling, Journal of Solar Energy Engineering, Vol. 105, p. 454, (1983).
21. E.K. May, L.M. Murphy, Performance Benefits of the Direct Generation of Steam in Line-Focus Solar Collectors, Journal of Solar Energy Engineering, Vol. 105, p. 126, (1983).
22. M.J. O'Neill, The 25 Kw Fresnel Lens/Photovoltaic Concentrator Application Experiment at Dallas-Fort Worth Airport, 14th Photovoltaics Specialists Conference, San Diego, Jan. 1980.
23. F. Kreith, Principles of Heat Transfer, 3rd edition, Harper and Row, New York, (1973).
24. Rohsenow and Hartnett, Handbook of Heat Transfer, McGraw-Hill (1973).
25. Kays and Crawford, Convective Heat and Mass Transfer, 2nd edition, McgGraw-Hill, (1980).
26. J.C. Chen, A Correlation for Boiling Heat Transfer to Saturated Fluids in Convective Flow, ASME Paper No. 63-HT-34, (1964).
27. J.G. Collier, Convective Boiling and Condensation, 2nd edition, McGraw-Hill, (1981).
28. J.C. Chen, D.L. Bennett, Forced Convective Boiling in Vertical Tubes for Saturated Pure Components and Binary Mixtures, AICHE Journal, Vol. 26, No. 3, (1980).
29. K. Stephan and D. Abdelsalam, Heat Transfer Correlation for Natural Convective Boiling, Int J. Heat and Mass Transfer, Vol. 23, pp. 73-87, (1980).
30. Fox and MacDonald, Introduction to Fluid Mechanics, 2nd Edition, McGraw-Hill, (1981).
31. P. Saha, N. Zuber, Point of Net Vapour Generation and Void Fraction in Subcooled Boiling, 5th International Heat Transfer Conference, Japan, Vol. 4 (1974).
32. M. Akiyama, F. Tachibana, Motion of Vapour Bubbles in Subcooled Heated Channel, Bulletin of the JSME, Vol. 17, No. 104, February (1974).
33. J. Weisman, S. Kang, Flow Pattern Transitions in Vertical and Upwardly Inclined Lines, Int. J. Multiphase Flow, Vol. 7, p. 271, (1973).
34. R.J. Pederson, E.K. May, Flow Instability During Direct Steam Generation in a Line-Focus Solar Collector System, SERI TR-632-1354, Solar Energy Research Institute, Golden, Colorado, March (1982).
35. P. Saha, M. Ishi, N. Zuber, An Experimental Investigation of the Thermally Induced Flow Oscillations in Two-Phase Systems, ASME Journal of Heat Transfer, Vol. 98, pp. 616-622, (1976).

# Indoor Air Quality

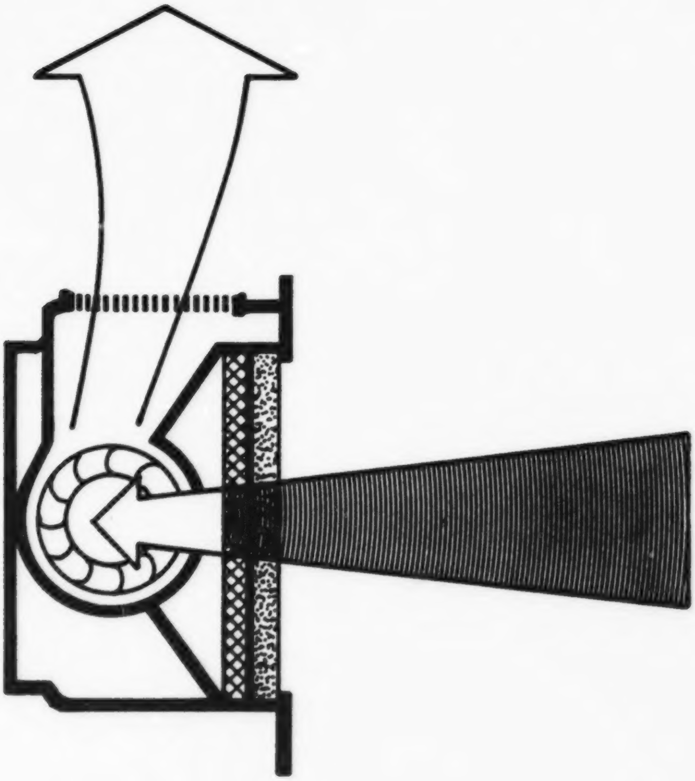

# ABSTRACT OF PAPER FOR RENEWABLE ENERGY CONFERENCE

R. N. Basu and L. L. Cogger
The University of Calgary
2500 University Drive N.W.
Calgary, Alberta T2N 1N4

## ABSTRACT

The performance of SPV modules, made in Japan, have been monitored over a period of eighteen months. During this period a continuous record has been kept of the climatic factors e.g. sunlight, wind, rain, temperature and humidity by a computerized monitoring and communication system which provides a reading of each of the parameters including the solar voltage output every ten minutes. Details included are the pyroelectric data i.e. irradiance for solar radiation, irradiance for thermal radiation, effective sky temperature, and average albedo. From these records, curves have been plotted showing the correlation between solar electricity and the different parameters. Simple empirical relationships are deduced from 'these data'. These relationships are compared with the mathematical models deduced by other researchers. From the results of loading tests, some conclusions are drawn about the expected performance of solar-powered electric devices e.g. motors, coolers etc. Methods for optimum choice of Solar PhotoVoltaic modules and ancillary equipment for a community size installation and future trends based on the current state-of-the-art are briefly reviewed.

# INDOOR AIR QUALITY: ISSUES AND OPPORTUNITIES

Douglas S. Walkinshaw

Coordinator, Indoor Air Quality, Institute for Research in Construction
National Research Council of Canada, Ottawa, Ontario

## INTRODUCTION

The quality of indoor air as it affects human health, comfort and safety, has emerged as an issue demanding public and scientific attention at a level that, for the Air Pollution Control Association, for example, parallels that being accorded to acid rain, as well as to the disposal of hazardous chemical and radioactive wastes (APCA, 1985). Twenty percent of the research budget of the American Society of Heating, Refrigeration and Air Conditioning Engineers (ASHRAE), which numbers over 50 000 members, is now targetted for indoor air quality (ASHRAE, 1985).

While the emergence of indoor air quality (IAQ) as a major health issue has coincided with the introduction of certain energy conservation measures in buildings beginning in the mid-1970s, IAQ implications extend far beyond this. For example, consideration of IAQ implications is beginning to have a new or increased influence on the design and selection of building materials and furnishings; on the design, selection, maintenance, and operation of building heating, cooling, humidification, and air handling systems; on the design and operation of cooking systems; on the acceptability of tobacco smoking indoors; and on the desirability of openable windows and tight-enclosure buildings. The broad scope of the integrated IAQ activity is shown in Figure 1.

As health authorities, building managers and scientists continue to discover new gaseous, particulate and biological pollutants indoors, often at levels exceeding those outdoors, there seem to be good reasons for the concerns being expressed. This is particularly true for the many Canadians and peoples of other cold climate regions who spend the majority of their time indoors in winter months, both in their own residences and in schools, offices, ice arenas and other facilities.

An extensive program has been underway in Canada for several years now to identify and alleviate the health impacts of urea formaldehyde foam insulation (UFFI) which had been used in many, often older residences, and was subsequently banned in 1980 (Shurb, 1985 and Broder, 1985). Other major programs are being carried out to assess and control residential radon exposures (Létourneau, 1985), and to develop mechanical ventilation techniques for tight-enclosure houses (Ficner, 1985).

In the United States and Europe, broad studies are focussing on identifying pollutants associated with "sick" buildings. They are also assessing the levels and impacts of unvented combustion pollutants, of involuntary or passive tobacco smoke inhalation, of formaldehyde exposures, particularly from pressed wood products in mobile houses, of exposure to radon in homes, and of biological pollutants, such as legionella bacteria, associated with pools of stagnant water in HVAC equipment and continuously wetted building materials.

## INDOOR POLLUTANTS AND THEIR CONTROL

### Pollutant Standards

While the U.S. Environmental Protection Agency (EPA) has set national ambient air quality standards (Table 1) (EPA), parallel standards for indoor air have not yet been promulgated. However, the World Health Organization (WHO) Working Group on IAQ has developed some guidelines, also shown in Table 1 (WHO, 1982).

The U.S. National Council on Radiation Protection and Measurements (NCRP) has recently recommended an indoor radon standard of 2 WLM/year which is equivalent to an indoor concentration of 8 pCi/l (NCRP, 1984).

The U.S. Housing and Urban Development Agency (HUD) has set a target formaldehyde level of 480 $\mu g/m^3$ (0.4 ppm) for mobile homes. It is expected that this target will not be exceeded if product emission standards for particle board and plywood as measured in large chamber tests are set at 0.3 ppm and 0.2 ppm, respectively, if the indoor temperature does not rise above 77°F, if the relative humidity is less than 50%, if the ventilation rate is at least 0.5 air changes per hour, and if there are no other major emitters of formaldehyde (HUD, 1985).

The U.S. National Institute on Occupational Safety and Health (NIOSH) has been investigating airborne particles of biological origin such as bacteria, moulds and fungi, and developing guideline levels based on the numbers of colony-forming units (CFU) present in the air. One number suggested is 1000 $CFU/m^3$ (Morey, 1984).

Finally, the level of ambient carbon dioxide due to human respiration is generally considered to be a reasonable proxy for ventilation rate and the overall level of indoor air pollutants. In Japan (NTIS, 1974), indoor carbon dioxide levels are to be less than 1.8 $g/m^3$ (0.1 percent or 1000 ppm). Where air-cleaning devices are employed or where there are non-human sources of $CO_2$, this value may not be appropriate.

Mechanisms for controlling these and other indoor pollutants include increasing indoor-outdoor air exchange rates where the outdoor air has lower concentrations, as is normally the case; improving internal air circulation; cleaning the air to remove particles and gases; and eliminating or reducing pollutants at source. Normally, control at source is the most effective mechanism. However, particular circumstances may govern the most cost-effective approach. Since many indoor pollutants cannot be eliminated at source or by air cleaning, at least some outdoor air will be required.

## Ventilation Standards

Since 1973 ASHRAE has maintained a building ventilation standard which is generally applied in North American buildings (ASHRAE, 1973). Standard 62-73 specifies minimum and recommended ventilation rates, with the recommended rates generally exceeding the minimum rates by factors of 1.5 to 2.

However, ASHRAE Standard 90, which is concerned with energy conservation in new buildings, recommends adherence to the minimum ventilation values specified in 62-73 when it was first issued in 1975 (ASHRAE, 1975) and then again in 1980 (ASHRAE, 1980). With the increased IAQ concerns, a new version of the ventilation standard eliminating this minimum and recommended value approach was issued in 1981 (ASHRAE, 1981).

ASHRAE Standard 62-81 specifies two minimum ventilation rates in non-residential buildings, one for settings with tobacco smoking and a much lower rate for settings with no smoking. In this standard, a portion of the ventilation air can be recirculated provided it is treated to meet the ambient air quality standards. In addition, Standard 62-81 specifies an alternative air quality procedure in which lower ventilation rates can be used, provided specified pollutant concentrations are not exceeded and odour levels are acceptable to 80 percent of a 20-person panel of untrained observers.

Until Standard 62-81, the ASHRAE ventilation standard had only been applied to mechanically ventilated buildings, which essentially excluded single-family residences, as these rely on infiltration and natural ventilation (windows and vents). During the review period, ASHRAE 62-81 was challenged by the Formaldehyde Institute because of the 0.1-ppm standard for formaldehyde. The Institute felt that inclusion of this new formaldehyde criterion in the standard would cause problems for residences, especially for manufactured housing with its extensive use of urea formaldehyde-bonded, pressed wood panelling, and other formaldehyde-containing materials. As a consequence, the standard was not endorsed by the American National Standards Institute. Since Standard 62-81 failed to gain general acceptance, ASHRAE is in the process of developing a revised standard (Janssen, 1985).

It seems probable that the revised ASHRAE standard will propose a single ventilation rate, likely the higher (smoking) rate of Standard 62-81 except in non-smoking settings where it could be lower, and a minimum outdoor air ventilation rate of 15 cfm/person for all settings. The IAQ procedure likely will not set a formaldehyde limit, however, it may propose a higher NCRP radon standard of 8 pCi/l, and a lower carbon dioxide limit of 1000 ppm to be used as a proxy for other pollutants that affect comfort. In addition, concerns may be expressed about biological pollutants in HVAC systems, and unvented combustion products, such as those discharged from rink cleaners used in arenas.

In Canada, the 1985 version of the National Building Code (NBC, 1985) requires new dwelling units to have mechanical ventilation systems capable of providing at least one-half an air change per hour during the heating season, based on the interior finished volume of the dwelling unit. This code also draws attention to the possible risk of carbon monoxide poisoning due to chimney backdrafting in new houses stemming from increased enclosure tightness. To help avoid this risk, fireplaces are now required to have their own supply of combustion air.

## Pollutants of Concern

There are several individual pollutants and groups of pollutants of particular current interest. Concerns about one of these, formaldehyde, a colourless gas with a pungent odour, have centered on its biological reactivity (Drucksache, 1985). Depending on individual sensitivity, formaldehyde exposure can result in irritation to the mucous membranes of the eyes, nose and throat. For example, exposure to levels ranging between 0.4 and 0.7 ppm appeared to be the reason for symptoms such as headache, nausea, dizziness, burning eyes and fatigue in a recently reported case (Marchant, 1985).

Action of formaldehyde in concentrations as low as 0.05% can cause allergic contact dermatitis. Perhaps the primary concern relative to formaldehyde is that it may be a carcinogen. However, this concern is based on nasal cancers which have been observed in tests on rats exposed to lifelong exposures at comparatively high levels. Epidemiological studies have so far failed to indicate carcinogenic effects on people (Drucksache, 1985).

Higher indoor levels of formaldehyde may result from the extensive use of: particle board without a covering layer, UFFI, or some sealing materials for parquet floors, adhesives, varnishes and lacquers, textiles, wall paper, carpets and curtains. Some of the highest non-industrial formaldehyde exposure levels have been recorded in mobile homes (Syrotynski, 1985).

Pressed wood products emit formaldehyde at rates that increase with temperature and humidity, and decrease as the ambient formaldehyde levels increase (Matthews, 1985). Long-term emission decay rates of these materials are not yet available, but emissions are known to continue for years. Studies show that particle board subflooring emissions can be reduced by a factor of two or more by covering the floor with polyethylene or vinyl linoleum (Matthews, 1985). Recent studies by NASA at the National Space Technology Laboratories in Mississippi have claimed that spider plants can cleanse indoor air of formaldehyde (Wolverton et al., 1984).

The question has been raised as to whether formaldehyde, or some other contaminant related to microbial activity, is the primary cause of UFFI-related health complaints (Samoiloff, 1985). Further, the question of the relative seriousness of the UFFI health effects is still unresolved. For example, 18 subjects, nine of whom had previously complained of non-respiratory adverse effects from UFFI, failed to show any significant pulmonary function reaction when exposed for 90 minutes to UFFI offgas (formaldehyde concentration of 1.2 ppm) in a chamber (Day, 1984). On the other hand, a study of occupants in 450 UFFI homes has tentatively indicated the possibility of some individuals suffering from irritation effects associated with the presence of UFFI, possibly due to the slightly higher formaldehyde levels which averaged 0.044 ppm vs 0.035 for 225 control homes (Broder, 1985).

Radon is a colourless, odourless, radioactive noble gas produced by the alpha decay of radium. Radium is present in trace amounts in all geologic materials. Radon decays to a series of short-lived (<30 minutes) daughters, exposure to which can eventually cause lung cancer (Walsh, 1984).

Radon gas can enter buildings from the soil through basement cracks and openings, or via untreated well water. It is also emitted by masonry materials (Bruno, 1983). Control of soil radon entering through the basement, often the major source of indoor radon, can be achieved through sealing of the subgrade cracks, such as those between foundation wall and slab, in combination with introducing sub-slab ventilation utilizing, for example, an existing sump and its lead-in water draining pipes (Nitschke, 1985). Circulating basement air seems to control radon daughter levels by causing plate-out of the host dust particles (Desrochers, 1985). Dust filters and electrostatic precipitators may also help (Hinds, 1983).

Unvented combustion products, including carbon monoxide, carbon dioxide, nitrogen dioxide, and particulates, can accumulate to levels of concern where adequate precautions are not taken. In ice arenas, for example, the hourly cleaning of the ice surface with machines powered by gasoline, propane or heating oil can raise carbon monoxide levels beyond safe limits if the building is not properly ventilated. Symptoms of carbon monoxide poisoning include headache, fatigue and nausea. In a recent survey in British Columbia, 32 of 64 arenas had CO levels above the B.C. guideline of 25 ppm, with 19 above 50 ppm. The highest recorded level was 206 ppm. While most of the arenas surveyed had ventilation fans, 73% were not being operated. Evidently many arena managers thought that the accumulation of CO from exhaust is accompanied by an odour and that only at that time need the fans be operated (Hillman, 1984).

Automobile fumes from attached and underground parking garages can be drawn indoors. Gas stoves produce nitrogen oxides, the amounts of which can be reduced through use of new burner flame inserts (DeWerth, 1985), elimination of pilot lights, and fumehood exhausting (Tamura, 1984).

With the sealing of housing enclosure leaks, the possibility of chimney backdrafting as a result of the coincident operation of furnaces and fireplaces, and bathroom and clothes dryer exhaust fans, has increased. One study of 100 Canadian homes of various styles and ages showed that 34% were at risk, with depressurization by fireplaces the major contributing factor (Moffatt, 1985).

In mechanically ventilated buildings, the fraction of exhaust air recirculated as intake air can change by a factor of five, depending on the use of rain caps, the placement of exhausts and intakes, and the ratio of exhaust to wind velocities (Wilson, 1985). This can be a real concern for buildings with multiple fumehood exhausts where up to 10 percent of the exhaust has returned through the ventilation system (Reihle, 1985).

Epidemics of Legionnaires' disease, a bacterial pneumonia, have been associated with aerosols from cooling towers and evaporative condensers and with dusts from landscaping and construction (Walsh, 1984). The recent incident of 37 deaths and 163 persons infected with the disease in a U.K. hospital has been attributed to faulty design (ENR, 1985). The problem appeared to be with the connection of a vertical drain pipe from a roof-top cooling tower to a horizontal drain pipe from a lower floor air conditioner. Evidently, at night and on weekends when the fans were off, polluted water from the cooling tower reached the air conditioner drip trays where bacteria were identified on the mastic around the trays.

Legionella bacteria can also proliferate in hot water systems to be released in showers. Control measures against this latter possibility include maintaining hot water tanks above 60°C, continuous chlorination and periodic hyperchlorination, and, possibly, avoidance of plastic shower hoses (Kallings, 1984).

In general, allergenic and pathogenic biologic organisms can replicate in HVAC system components such as water spray systems, humidifiers, air handling and drain pans, and fan-coil units

(Morey, 1984). Complaints in homes, schools and workplaces of eye, nose and throat irritation as well as fatigue can be correlated with unpleasant earthy, musty odours produced by abundant saprophytic mould growth (Samson, 1985).

A recent study has linked the presence of the fungal species, *Stachybotrys atra*, found in a house in Chicago, to recurring occupant illnesses suggestive of trichothecene toxicosis. These maladies included headaches, fatigue, dermatitis, intermittent localized hair loss, and general malaise (Croft, 1985). In this study the mould occurred in a section of a cold air return duct with a 2-cm layer of dust containing moist lint and carpet fibres, and in sections of wood fibreboard wetted by a leaking roof and plumbing. Contaminated areas had a black, sooty appearance. Evidently moist materials of high cellulose and low nitrogen content such as fibreboard, straw, dust and lint which are subjected to temperature fluctuations in the 0 to 40°C range provide ideal conditions for *S. atra* toxin production. Continuous water accumulation can result from faulty plumbing, ceiling or basement leaks, or condensation at moisture barriers.

## ISSUES

The emerging IAQ concerns just described have potentially significant implications for Canadians who, because they live in a colder climate, spend the great majority of their time indoors. In addition to potential impacts on the building and health care industries, there are economic implications for the chemical industry relative to the use of consumer products and building materials, the tobacco industry and the growing public concern over passive smoke exposures, and the energy industry in terms of IAQ impacts on building energy conservation and fuel selection. The extent of the implications will depend on three questions:

1. To what extent is IAQ now affecting human health, comfort and productivity, and what are the future trends?
2. How readily will these trends be adjusted to accommodate IAQ concerns as they become defined?
3. What role will government, industry and the public assume in seeking answers to questions 1 and 2, and in supporting regulatory standards for the indoor environment?

As indicated above, the impact of IAQ on health, comfort and productivity is very poorly understood at present. Certainly, Legionnaires' disease, a building-related illness, is known to have caused deaths in hospitals and hotels on an epidemic scale. However, the incidence of this pneumonia, particularly from residential exposures, is unknown and could be under-reported.

While formaldehyde residential exposures at levels of 0.04 ppm are widespread in Canada (Shurb, 1985), and levels above 0.1 ppm are not unusual in new, tight-enclosure homes (Dumont, 1984), the sensitivity of the population to this irritant is not statistically calibrated.

The incidence of lung cancer due to indoor radon exposures is not known and while small compared to that due to tobacco smoke (Létourneau, 1985), the implementation of low cost construction and ventilation techniques for its avoidance might still eliminate a significant number of lung cancers each year (Love, 1985).

While many people are no longer willing to tolerate the irritating effects of passive tobacco smoke inhalation, the extent of illness caused by this pollutant is still being defined with particular concern being expressed for children (Shopland, 1985).

Although there appears to be significant potential for chimney backdrafting in residences, the amount of combustion product backdrafting and related discomfort, illness and death is unknown.

A recent study of 1091 out of 5292 employees in a large Canadian office complex indicated that most employees had suffered from upper respiratory tract and eye irritation which was troublesome at work but not at home (McDonald, 1985, Bénard, 1985). Symptoms also included headaches, drowsiness, exhausting sleeplessness and irritability, and skin dryness and irritation. As is typical for such symptoms, the etiology of these problems was not established.

In 1984, IAQ investigations were carried out in 94 Canadian federal buildings (Kirkbride, 1985). NIOSH is doing similar studies. In general, in the majority of office buildings where such complaints occur, the problem is addressed through improvements to the ventilation system. This includes better air circulation, and humidity and temperature control. In only some of the cases are specific pollutants identified. The re-entry of building exhaust, the entry of motor vehicle exhaust, copy machines, tobacco smoke and newly glued carpets are among the most frequently identified sources.

Current trends in building design and operation are toward increasingly tighter-enclosure, mechanically ventilated structures. The temptation to save energy costs by reducing outdoor air intake in such buildings will be strong, particularly if the associated health risks are unquantified. Increased use of air conditioning in offices and residences reinforces the trend to lower air exchange rates with the outdoors. As a result of these trends, which will tend to increase indoor pollutant levels, standards developed by ASHRAE and the National Building Code of Canada call for increased mechanical ventilation. Whether these standards can be met in practice, and whether the result will be more or less outdoor air being circulated to occupants when compared to that previously experienced with leaky enclosures and openable windows, is not known.

With respect to one indoor pollutant, tobacco smoke, there is a move to reduce involuntary exposures in office buildings, hospitals, airplanes, hotels, and restaurants by limiting smoking to restricted, separately ventilated areas (Shopland, 1985).

Because of the off-oil emphasis of national energy policies, there is increased use of electricity, gas and wood for heating and cooling Canadian buildings (NEB, 1984). Use of unvented kerosene heaters for individual room heating has increased substantially. The full impact on IAQ of these changes in mode of heating is not yet known.

There seems to be an increased use of pressed wood products, such as particle board, in building structures as subflooring, wall finishes, and in furniture. As a result of the formaldehyde concern, particle board emission standards are now in place in Germany (ETB-Baurichtlinie, 1980).

While the use of synthetic building materials and furnishings with their associated increases in indoor levels of organic gases may well continue to rise, changing fashions such as the trend in residences to hardwood floors with centre area rugs, rather than wall-to-wall carpets, make forecasting difficult.

In general, the relative influence of building materials on the level of air pollutants versus maintenance practices and other sources of pollutants needs to be put in perspective.

With respect to human factors, the aging of the Canadian population and the trend for more women to work outside the home could both influence the incidence of IAQ problems.

The fact - that there are so many air pollutants indoors, ranging from gases and dust to bacteria and fungal spores;

- that buildings, their equipment and their occupants are the pollutant sources;
- that there are human productivity as well as health concerns; and
- that the economic impacts of regulation will be large,

makes IAQ a difficult issue for governments to address on more than a pollutant-by-pollutant basis. Nevertheless, in Canada (Walkinshaw, 1985) and the United States (Millhone, 1985), many federal agencies have become involved in developing coordinated approaches to the issue. However, as a result of recent cutbacks in energy-related research, this activity had to be reduced in Canada.

In addition to the federal government activity in Canada, a workshop of 37 persons from industry, universities, the provinces, and municipalities indicated a desire to see more IAQ research done on a cooperative basis between the building and health disciplines (Wilson, 1985). This group saw the need for a central industry/government coordinating committee and the establishment of centres of excellence.

With respect to indoor pollutant standards, a federal-provincial working group on IAQ is developing residential guideline limits for carbon monoxide, radon, nitrogen dioxide, humidity, ozone, formaldehyde, other aldehydes and carbon dioxide (Wyile, 1985).

In the United States, the gas (Billick, 1985, DeWerth, 1985), electric (Purcell, 1985), and building controls (Lane, 1985) industries, several states such as California and Minnesota, and universities such as Harvard and Princeton, are carrying out a number of studies.

In projecting those aspects of IAQ on which government attention and action are likely to focus, Douglas and Wildavsky (1982) point out that societal selection of risks to be avoided may depend more on cultural biases than on scientifically based cost-benefit projections. For example, the societal health costs resulting from typical rates of tobacco smoking most probably far exceed the costs incurred through involuntary passive smoking. However, society is moving to reduce the involuntary risk by providing additional ventilation or restricting smoking locations, rather than regulating the voluntary consumption of tobacco.

By analogy, this suggests that non-residential building environments will eventually be subject to regulations while individual home environments, where more time is spent, will not. Nevertheless, as information on the concentrations and impacts of indoor pollutants become clear, it may reasonably be expected that deepening concerns will result in changing attitudes toward individual rights and in a stiffening resolve to insist on corrective action. In this vein, the movement is growing for the designation of separate smoking areas in public places, in airplanes, in restaurants, and in hotel rooms. As a result of individual initiatives, there is already a small market for low-pollution residences (Small, 1985a). In response to case studies of children showing that their learning ability had been severely hampered by the presence of indoor pollutants in schools (Maclennan, 1985), one school board is attempting to alleviate the problem (Small, 1985b). In the United States, Bonneville Power Administration is promoting residential energy conservation measures while informing consumers about potential IAQ problems and, where radon levels exceed 5 pCi/l, subsidizing cost for ventilation with heat recovery devices (Love, 1985).

## OPPORTUNITIES

The field of IAQ presents an opportunity for industry and government to work together in several areas of mutual interest.

One of these areas would be to develop IAQ screening methods for building materials and furnishings which would help to avoid costly future crises such as those that occurred with asbestos and UFFI. This would minimize the risks to building owners, builders, manufacturers, and governments when new materials are introduced. In the case of UFFI, for example, total remedial costs and property value losses probably exceed $1 billion, yet with the lower formaldehyde levels now being recorded in houses that contain UFFI, the causes for concern remain unclear.

As IAQ standards are adopted by government health authorities for various indoor pollutants, there will be a broad market for related pollutant sensors and pollution-testing services, and government and industry should coordinate their efforts so that these can be put in place in a timely fashion. Coincidently, the demand for low-pollution residences and building materials will increase.

The era of electro-mechanically controlled indoor environments, begun in the 1960s in non-residential buildings with the introduction of air conditioning and large-scale floor plans with offices remote from windows, is now extending to Canadian residences as a result of the revolutionary adoption of polyethylene vapour barriers and flexible sealants to eliminate enclosure leaks. As a result, there is a growing demand for heat recovery ventilation devices, and sensors and controls which condition the indoor environments for energy-efficient housing.

Owing to energy conservation and health and comfort concerns, the demand for air cleaners is growing for the residential and office environments, but there is uncertainty as to the relative merits of the various technologies being employed. The cooperation of government and industry in developing more comprehensive air cleaner performance standards would provide this industry with an opportunity to market its best products and to increase its market penetration. For buildings in the Far North where energy costs are high, there is a particular opportunity for using air cleaners and recirculated air to minimize ventilation costs.

Because of the magnitude, complexity and newness of the IAQ issue, there are a number of reasons for multi-disciplinary, multi-organizational and multi-lateral cooperation. For example, large-scale scientific surveys of building environments are required to identify pollutants, their sources and building ventilation characteristics, in order to assess the gravity of the IAQ problem.

Such surveys could most certainly benefit from international cooperation so as to share test protocol development costs, and to establish and evaluate a more comprehensive and meaningful IAQ and building parameter data base. With these data on hand, building research priorities could be set, and meaningful clinical and epidemiological studies would follow.

Increased multi-disciplinary cooperation will ensure that health science and building science IAQ research efforts are focussed on common objectives, iterate quickly toward useful results, and remain complementary. Such cooperation will facilitate the study of synergistic effects of groups of contaminants, and the development of innovative IAQ measurement devices and indicators, and practicable remedial measures.

The real opportunities, of course, are for the safeguarding of public health and productivity through the avoidance of building-related illnesses and discomfort, whether these be episodic like Legionnaires' disease, or chronic like the so-called twentieth century disease of hypersensitive individuals.

## ACKNOWLEDGEMENT

The author appreciates the opportunity to present this paper at the Renewable Energy Conference '86. It was previously presented at the Fourth Canadian Building Congress and published at the Invitation of the Canadian Institute of Public Health Inspectors in the Environmental Health Review.

## REFERENCES

APCA News, 1985. Mar/Apr, Vol. 2, No. 6, p. 1. Air Pollution Control Association, Pittsburgh, PA.

ASHRAE, 1973. Standard 62-73 (ANSI B 194.1-1977), Standards for Natural and Mechanical Ventilation. American Society for Heating, Refrigeration and Air Conditioning Engineers Inc., Atlanta, GA.

ASHRAE, 1975. Standard 90-75, Energy Conservation in New Building Design. Ibid.

ASHRAE, 1980. Standard 90A-1980, Energy Conservation in New Building Design. Ibid.

ASHRAE, 1981. Standard 62-1981, Ventilation for Acceptable Indoor Air Quality. Ibid.

ASHRAE, 1985. ASHRAE Details Air Quality Efforts. ASHRAE Journal, Vol. 27, No. 7, p. 6-9, July 1985.

Bénard, J.M., T.A. McKenna, D.L. McKinnon, and J.P. Farant, 1985. Relating Health and Environmental Studies in a Tight Building Syndrome Investigation. Transactions Air Pollution Control Association Specialty Conference TR-6, Indoor Air Quality in Cold Climate: Hazards and Abatement Measures. Ottawa, 1985, D.S. Walkinshaw, Editor. 622 pages.

Billick, I., 1985. Industry-Government Cooperation and Coordination in Indoor Air Quality Research. Transactions APCA Specialty Conference, Ibid.

Broder, I., F. Corey, P. Cole, S. Mintz, M. Lipa, and J. Nethercott, 1985. Health Status of Residents in Homes Insulated With Urea Formaldehyde Foam. Transactions APCA Specialty Conference, Ibid.

Bruno, R.C., 1983. Source of Indoor Radon in Houses: A Review. APCA Journal, Vol. 33, No. 2, p. 105-107, Feb. 1983.

Croft, W.A., B.B. Jarvis and C.S. Yatawara, 1985. Airborne Outbreak of Trichothecene Toxicosis. Atmospheric Environment. To be published, 1985.

Day, J., R.E.M. Lees, R.H. Clark, and P.L. Pattee, 1984. Respiratory Response to Formaldehyde and Off-Gas of Urea Formaldehyde Foam Insulation. CMAJ, Vol. 131, No. 9, p. 1061-1065, Nov. 1984.

Desrochers, D. and A.G. Scott, 1985. Residential Ventilation Rates and Indoor Radon Levels. Transactions APCA Specialty Conference, Ibid.

DeWerth, D.W. and F.R. Kurzynske, 1985. Burner Flame Inserts for Lower $NO_X$ Emissions. Transactions APCA Specialty Conference, Ibid.

Douglas, M. and A. Wildavsky, 1982. Risk and Culture. University of California Press, Berkeley, CA, p. 14-20, 1982.

Drucksache 10/2602, 1985. Formaldehyd, Deutcher Bundestag-10 Wahlperiode, p. 96-101, 1985.

Dumont, R.S., 1984. Air Quality Measurements in Low-Leakage Houses. National Research Council of Canada, Division of Building Research, Building Research Note No. 218, 25 p., September 1984.

ENR, 1985. British Legionella - Hospital Disease Outbreak Traced to Plumbing Links. Engineering News Record, Vol. 214, No. 26, p. 15, June 27, 1985.

EPA. Environmental Protection Agency (U.S.) National Primary and Secondary Ambient Air Quality Standards, Code of Federal Regulations. Title 40, Part 50, (40 CFR 50).

ETB-Baurichtlinie, 1980. Richtline über die Verwendung von Spanplatten hinsichtlich der Vermeidung unzumutbarer Formaldehydkonzentrationen in der Raumluft. Fassung April 1980. Beuth Verlag: Berlin/Köln.

Ficner, C., M. Riley and M. Luhun, 1985. Improving Indoor Air Quality Through Energy Conservation Programs. Transactions APCA Specialty Conference, Ibid.

Hillman, K.E., 1984. The Potential for and Control of Carbon Monoxide Poisioning in British Columbia Arenas. Environmental Health Review, Vol. 28, No. 4, p. 99-108, Dec. 1984.

Hinds, W.C., S.N. Ruduick, E.F. Maher, and M.W. First, 1983. Control of Indoor Radon Decay Products by Air Treatment Device. APCA Journal, Vol. 33, No. 2. p. 134-136, Feb. 1983.

HUD, 1985. Manufactured Home Construction and Safety Standards. U.S. Code of Federal Regulations, Title 24, Section 3280.308 and 3280.309. Revised April 1, 1985. Housing and Urban Development Agency, Arlington, VA.

Janssen, J. and D. Grimsrud, 1985. Updating ASHRAE 62-81: Problems and Issues. Transactions, APCA Specialty Conference, Ibid.

Kallings, I., S. Hoffner and B. Nystrom, 1984. Eradication of Legionella Pneumophilia from Potable Water Systems. Proceedings Indoor Air Quality Conference, Stockholm, 1984. Vol. 3, p. 283-286. Swedish Council for Building Research, Stockholm.

Kirkbride, J., 1985. Private correspondence, Sept. 1985.

Lane, C.A. and J.E. Woods, 1985. Cooperative Indoor Air Quality Research Between Government and Industry--A Minnesota Case Study. Transactions APCA Specialty Conference, Ibid.

Létourneau, E.G., 1985. Development of a Radon Standard for Canada. Transactions APCA Specialty Conference, Ibid.

Love, R., 1985. Bonneville Power Administration's Risk Management Strategy For Mitigating Indoor Air Quality Effects in its Home Weatherization Program. Transactions APCA Specialty Conference, Ibid.

Maclennan, J.G., 1985. The Impact of Indoor Air Pollution on the Behaviour and Learning Ability of School Children. Transactions APCA Specialty Conference, Ibid.

Marchant, R., K. Yoshida, and D.A. Figley, 1985. Exposure to a High Concentration of Formaldehyde: A Case Study. Transactions APCA Specialty Conference, Ibid.

Matthews, T.G., W.G. Dreibelbis, C.V. Thompson, and A.R. Hawthorne, 1985. Preliminary Evaluation of Formaldehyde Mitigation Studies in Occupied Research Houses. Transactions APCA Specialty Conference, Ibid.

McDonald, J.C. et al., 1985. Building Illness in a Large Office Complex. Transactions APCA Specialty Conference, Ibid.

Millhone, J.P. and K.Y. Teichman, 1985. The U.S. Indoor Air Quality Research Strategy. Transactions APCA Specialty Conference, Ibid.

Moffatt, S. 1985. Combustion Ventilation Hazards in Housing - Failure Mechanisms, Identification Technologies, and Remedial Measures. Transactions APCA Specialty Conference, Ibid.

Morey, P.R. et al., 1984. Environmental Studies in Moldy Office Buildings: Biological Agents, Sources and Preventative Measures. Annals of the American Conference of Governmental Industrial Hygienists: Evaluating Office Environmental Problems. Vol. 10, p. 21-35, 1984.

NRC, 1985. National Building Code of Canada, NRCC No. 23174, Ottawa.

NCRP, 1984. Exposure From the Uranium Series With Emphasis on Radon and Its Daughters. National Council on Radiation Protection & Measurement, Bethesda, MD, NCRP Report 77, Chapt. 10, p. 89, 1984.

NEB, 1984. Canadian Energy Supply and Demand 1983-2005. National Energy Board Technical Report, Appendix 4, p. A63. Sept. 1984.

Nitschke, I.J., 1985. Detailed Field Tests of Radon Control Techniques in New York State Houses. Transactions APCA Specialty Conference, Ibid.

NTIS, 1974. Building Control Law and Dust Collectors (In Japanese, English Abstract), National Technical Information Service, APT 1GNO 63252, 1974.

Purcell, G., 1985. The Electric Power Research Institute Indoor Air Quality Program. Transactions APCA Specialty Conference, Ibid.

Reible, D.D., P. Yonts and F.H. Shair, 1985. The Effect of the Return of Exhausted Building Air on Indoor Air Quality. Transactions APCA Specialty Conference, Ibid.

Samoiloff, M.R., 1985. The Nematode Bioassay for Toxicity of Urea-Formaldehyde Foam Insulation from Winnipeg Homes. Transactions APCA Specialty Conference, Ibid.

Samson, R.A., 1985. Occurrence of Moulds in Modern Living and Working Environments. European Journal of Epidemiology, Vol. 1, No. 1, p. 54-61, March 1985.

Shopland, D.R., 1985. Passive Tobacco Smoking Policies Indoors in Various U.S. States. Transactions APCA Specialty Conference, Ibid.

Shurb, R.W., 1985. The Canadian UFFI Assistance Program. Transactions APCA Specialty Conference, Ibid.

Small, B.M., 1985a. Low-Pollution Building Design and Construction. Transactions APCA Specialty Conference, Ibid.

Small, B.M., 1985b. Recommendations for Action on Pollution and Education in Toronto: A Report Prepared for the Board of Education for the City of Toronto, May 1985.

Syrotynski, S., 1985. Prevalence of Formaldehyde Concentrations in Residential Settings. Transactions APCA Specialty Conference, Ibid.

Tamura, G.T., 1984. Measurement of Combustion Products From a Gas Cooking Stove in a Two-Storey House. Proceedings of 77th Annual Meeting of APCA, June 1984.

Walkinshaw, D.S., 1985. Indoor Air Quality Research in Canada. Proceedings, Indoor Air Quality Seminar, "Implications for Electric Utility Conservation Programs", Atlanta, GA and Denver, CO, EA/EM-3824, Section 13, p. 13.1-13.19, Jan. 1985.

Walsh, P.J., C.S. Dudney and E.D. Capenhaver, 1984. Indoor Air Quality, CRC Press, Inc. p. 8 and p. 93.

WHO, 1982. Indoor Air Pollutants: Exposure and Health Effects Assessments. EURO Reports and Studies 78, World Health Organization, Copenhagen, 1982.

Wilson, A.G. and J.P. Farant, 1985. Workshop on Indoor Air Quality: Canadian Issues and Opportunities, Consumer and Corporate Affairs Canada, Ottawa, 1985.

Wilson, D.J., 1985. Contamination of Ventilation Intake Air by Nearby Exhausts. Transactions APCA Specialty Conference, Ibid.

Wolverton, B.C., R.C. McDonald and E.A. Watkins Jr., 1984. Foliage Plants for Removing Indoor Air Pollutants from Energy Efficient Homes. Economic Botany, Vol. 38, No. 2, p. 224-228, 1984.

Wyile, W.H. and V. Armstrong, 1985. Guidelines for Indoor Air Quality. Transactions APCA Specialty Conference, Ibid.

---

This paper is a contribution from the Institute for Research in Construction, National Research Council of Canada.

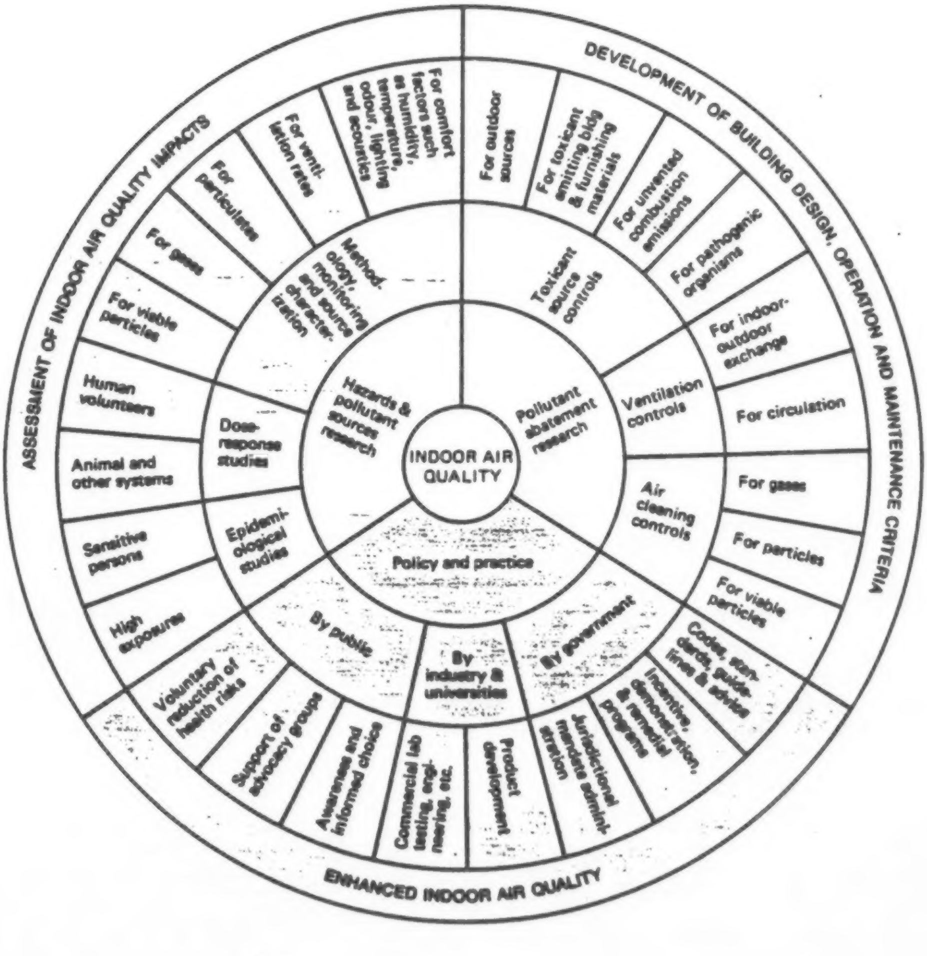
INDOOR AIR QUALITY
Hazards & pollutant sources research
Pollutant abatement research
Policy and practice
Method-ology, monitoring and source character-ization
Dose-response studies
Epidemi-ological studies
Toxicant source controls
Ventilation controls
Air cleaning controls
By public
By industry & universities
By government
For comfort factors such as humidity, temperature, odour, lighting and acoustics
For venti-lation rates
For particulates
For gases
For viable particles
Human volunteers
Animal and other systems
Sensitive persons
High exposures
For outdoor sources
For toxicant emitting bldg & furnishing materials
For unvented combustion emissions
For pathogenic organisms
For indoor-outdoor exchange
For circulation
For gases
For particles
For viable particles
Codes, stan-dards, guide-lines & advice
Incentive, demonstration, & remedial programs
Jurisdictional mandate admini-stration
Product development
Commercial lab testing, engi-neering, etc.
Awareness and informed choice
Support of advocacy groups
Voluntary reduction of health risks
ASSESSMENT OF INDOOR AIR QUALITY IMPACTS
DEVELOPMENT OF BUILDING DESIGN, OPERATION AND MAINTENANCE CRITERIA
ENHANCED INDOOR AIR QUALITY

Fig. 1 Scope of the Indoor Air Quality Activities

TABLE 1. Some Air Quality Contaminant Concentration Criteria*

| | EPA Ambient Air Standards | | WHO Indoor Air Guidelines | |
|---|---|---|---|---|
| Contaminant | Time | Level | Concentration of Limited or No Concern | Concentration of Concern |
| Carbon monoxide | 1 h | 40 000 (35 ppm) | | |
| | 8 h | 10 000 (9 ppm) | 11 000<br>(9.6 ppm) | 30 000<br>(26 ppm) |
| Carbon dioxide | | | 4.5 g/m$^3$<br>(2500 ppm) | 12 g/m$^3$<br>(6700 ppm) |
| Lead | 3 mo | 1.5 | | |
| Nitrogen dioxide | 1 yr | 100 (0.055 ppm) | 190<br>(0.1 ppm) | 320<br>(0.17 ppm) |
| Ozone | 1 h | 235 (0.12 ppm) | 120<br>(0.06 ppm) | 150<br>(0.08 ppm) |
| Sulphur dioxide | 24 h | 365 (0.14 ppm) | 500<br>(0.2 ppm) | 1350<br>(0.5 ppm) |
| | 1 yr | 80 (0.03 ppm) | | |
| Formaldehyde | | | 60<br>(0.05 ppm) | 120<br>(0.1 ppm) |
| Particulates | 24 h | 260 | | |
| | 1 yr | 75 | | |
| Asbestos | | | 0 | 0.1 fibre/cm$^3$ |
| Radon | | | 0 | 70 Bq/m$^3$<br>(2 pCi/l) |

*Units are µg/m$^3$ unless noted otherwise.
EPA — Environmental Protection Agency (U.S.)
WHO — World Health Organization (UN)

# FORMALDEHYDE ABATEMENT IN INDOOR AIR

H. D. Gesser,
Department of Chemistry,
University of Manitoba,
Winnipeg, Manitoba,
Canada R3T 2N2.

## ABSTRACT

Formaldehyde can be removed from air by passing the contaminated air through a filter coated with a polymeric organic amine or hydrazene. The only volatile product is water. By plasticizing the coating, it is possible to extend the useful life of the coating to over one month when a fiber glass furnace filter is used in the home and the furnace fan is run continuously.

## 1. INTRODUCTION

The problem of formaldehyde as an indoor air pollutant in homes insulated with Urea Formaldehyde Foam Insulation (UFFI) has been well documented (1)(2). Formaldehyde also originates from other sources (3)(4), in particular, from particle board and plywood which use urea formaldehyde adhesive resins.

Starting in the fall of 1981, we investigated the use of ammonia gas as an inhibitor for the release of formaldehyde from UFFI. We also began to test the effectiveness of coatings for fiberglass furnace filters for the removal of indoor formaldehyde gas by recirculating the indoor air by means of the furnace fan. The results were reported (5) and the coatings patented in the U.S.A. (6). A problem remained since the coatings were quickly exhausted and their usefulness limited to a week or two. It soon became apparent that the coatings were too hard and only the surface of the coated layer reacted with formaldehyde. Diffusion was too slow and, though the unreacted coating was still present, it was inaccessible to the gas phase for further reaction with formaldehyde vapor. The solution to this problem is now reported.

## 2. EXPERIMENTAL

The procedure used to coat filters and to test their effectiveness has been previously described (5). The most common coating used — polyethylenimine (PEI) — was commercially available as a 50% solution in water (Eastman Chemical). It was used as a 5% aqueous solution sprayed on to the filter (approx. 100 mL) to give a dry coating density of about 0.3 g/dm$^2$.

Formaldehyde was analysed by the modified pararosaniline method (5).

## 3. RESULTS AND DISCUSSION

Commercial polyethylenimine contains primary and secondary amines which may be represented as $R\text{-}CH_2NH_2$ and $R_1R_2NH$, respectively, where R represents a long chain. The reaction of these polymeric amines with formaldehyde ($H_2CO$) is as follows:

$$R{-}CH_2{-}NH_2 + H_2CO \longrightarrow R{-}CH_2N{=}CH_2 + H_2O \qquad (1)$$

$$R_1R_2NH + H_2CO \longrightarrow R_1R_2N{-}CH_2OH \qquad (2)$$

The dry polymer is hard or very viscous depending on the source. Hence diffusion within the coated layer is slow and not sufficient to renew the surface. This limits the amount of amine capable of reacting with formaldehyde. One method of increasing the available polymeric amine is to increase the surface area of the supporting filter. This is usually accompanied by an increase in air resistance if the nominal area of the filter is kept constant. Hence, it was decided to increase the fluidity of the coating by adding an inert plasticizer. Though several high boiling water soluble liquids were tested, only glycerol was medically acceptable.

A one storey bungalow (with basement) which had urea formaldehyde foam insulation was tested for formaldehyde. The levels were determined to range from 0.085 to 0.120 ppm. When a fiber glass filter 40.6 cm x 50.8 cm x 2.5 cm (16" x 20" x 1") was treated with polyethylenimine, 150 mL of 5% PEI in water (6.2 g dry PEI on the filter) the level of formaldehyde dropped to 0.015 ppm within a week but after an additional 10 days the formaldehyde concentration in the house rose to 0.095 ppm.

When a similar filter was treated with 150 mL of a 5% polyethylenimine solution of glycerol/water, 30/70 by volume, the level of formaldehyde remained below 0.040 ppm for one month. The actual life of the coated filter was not determined.

The coating can be applied to other supports such as open cell reticulated polyurethane foam sponge. Fans fitted with coated filters can be effective in small rooms.

Since the coating is basic it is most likely also effective in removing acidic gases from air, such as carbon dioxide, hydrogen sulphide, hydrogen chloride and hydrogen fluoride.

## 4. CONCLUSION

It is possible to chemically design a polymeric solution to be applied to a support which can specifically react with a particular pollutant. By mixing solutions or by stacking such coated filters it should be possible to remove more than one type of indoor gaseous contaminant. This system has been successfully applied to the removal of formaldehyde from indoor air.

## 5. ACKNOWLEDGEMENT

Grateful acknowledgement is made to Career Start '84 for the support of student assistants.

## 6. REFERENCES

(1) Tataryn, L. Formaldehyde on Trial, J. Lorimar & Co., Toronto (1983).

(2) Van der Wal, J. F. Formaldehyde Measurements in Dutch Houses, Schools and Offices in the Years 1977-1980, Atmos. Environ., 16, 2471 (1982).

(3) National Academy of Sciences. Formaldehyde and Other Aldehydes, National Academy Press, Washington, D.C. (1981).

(4) National Research Council. Indoor Pollutants, National Academy Press, Washington, D.C. (1981).

(5) Gesser, H. D. The Reduction of Indoor Formaldehyde Gas and that Emanating from Urea Formaldehyde Foam Insulation (UFFI), Environ. Intern., 10, 305 (1984).

(6) Gesser, H. D. Abatement of Indoor Pollutants, U.S. Patent #4,547,350, Issued, Oct. 15, 1985.

# IMPROVING AIR QUALITY IN ENERGY EFFICIENT HOUSES: AN ARCHITECTURAL APPROACH

E.D. McIntyre and E.M. Sterling
Theodor D. Sterling Ltd.
#70 - 1507 W. 12th Avenue
Vancouver, B.C.
V6J 2E2

## ABSTRACT

Two energy efficient townhomes were designed and constructed in an experiment of improvement of indoor air quality by:

1. Limiting infiltration of outdoor radon gas.
2. Reducing indoor levels of formaldehyde off-gassed by construction and finishing materials and combustion gases generated by appliances.

To reduce indoor concentrations of formaldehyde generated by finishing and construction materials, chemically stable materials were used wherever possible and limited use made of glues, sealants, interior grade plywood and particle board. Indoor sources of combustion gases were eliminated from both units by use of electric appliances. To minimize radon gas infiltration, the houses were constructed on ventilated crawlspaces and an air vapour barrier installed between the main floors of the townhomes and the crawlspaces. Air quality in the two experimental units and in other control buildings was monitored to evaluate the effectiveness of the designs for improvement of indoor air quality.

## 1. INTRODUCTION

Two energy efficient airtight townhomes were designed and constructed to evaluate the effectiveness of an architectural approach for providing acceptable indoor air quality in energy efficient, airtight buildings. An architectural approach implies a design and construction process defined not only by aesthetic, technological and financial considerations, but also by the impact on indoor air quality of the components and configuration of buildings.

The most significant advantage of an architectural approach to provision of acceptable indoor air quality is energy efficiency. Acceptable air quality is provided through manipulation of the architectural component of a building. The form and structure of the building work, without consuming any energy resources, is to provide acceptable indoor air quality.

In the context of the townhome project, architectural solutions for improving air quality by limiting radon gas infiltration and limiting indoor sources of formaldehyde were explored. After construction of the townhomes, the effectiveness of an architectural approach in reducing indoor radon and formaldehyde levels was evaluated through air quality monitoring. Radon and formaldehyde, and also xylene and toluene concentrations in each of the two experimental townhomes were recorded.

## 2. PROJECT DESIGN

To meet local building code regulations, the townhomes were designed as two storey, 1800 square feet, side by side units sharing a party wall (Figure 1).

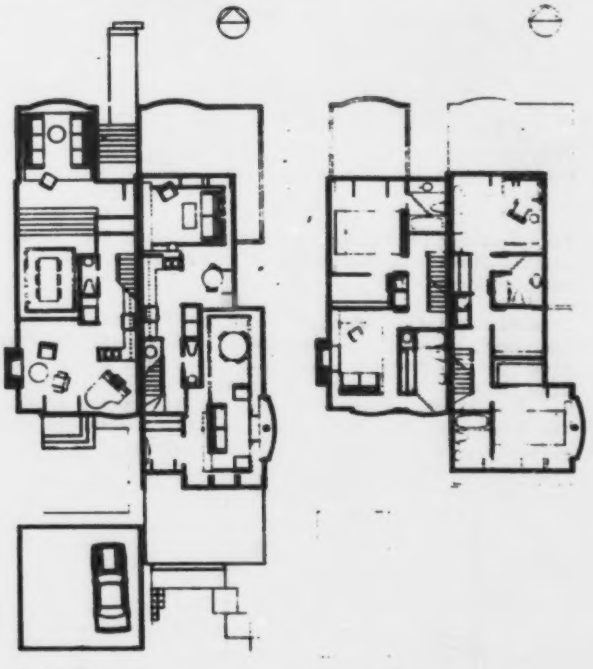

Fig. 1. Main and Second Floor Plans of Experimental Townhomes

Energy efficient construction technology developed by the Canada Mortgage and Housing Corporation Energy Efficient Housing Program was specified and used in the construction of the townhomes (1). Exterior walls were constructed with 2" x 6" lumber, and 2" x 10" wood joists were used in the roof construction. R20 fibreglass insulation was installed in the exterior walls and R28 fibreglass insulation installed in the exterior ceilings. Airtight air/vapour barriers were installed at the interior surface of exterior walls to prevent heat loss through, and moisture damage to the building structure. After construction, airtightness testing found Unit 1 to have an airtightness rating of 3.7 air changes per hour and Unit 2 a rating of 3.6 air changes per hour.

### 2.1 Limiting Infiltration of Radon Gas

In standard energy efficient residential construction, the basement or crawlspace beneath a home is not separated from the living areas by an air vapour barrier (1). As a result, radon gas may infiltrate into (Figure 2) and accumulate in the living areas of a home (2) (3).

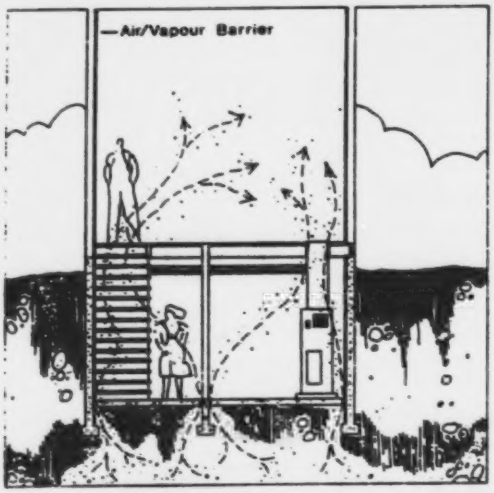

Fig. 2. Standard Basement/Crawlspace/Living Area Configuration Showing Infiltration of Radon Gas into the Occupied Area

To minimize infiltration of radon gas from the ground into the living areas of the experimental townhomes, the main floors of the townhomes were separated from the ground by crawlspaces. Vents were installed in the crawlspace walls to allow natural cross ventilation. The living areas of the homes were then separated from the crawlspaces by a plywood air vapour barrier subfloor installed between the crawlspaces and main floor (Figure 3).

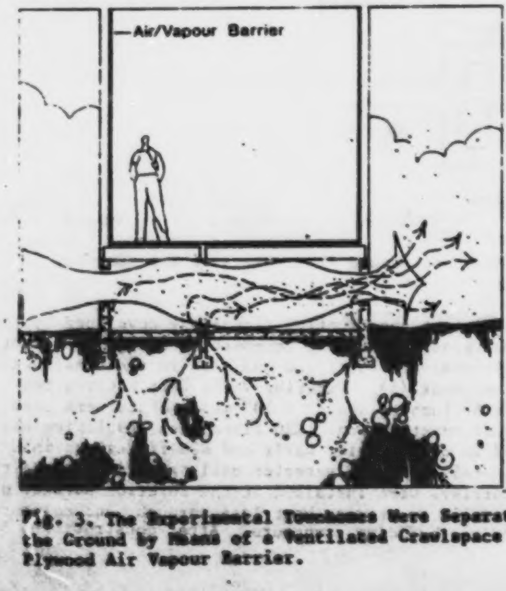

Fig. 3. The Experimental Townhomes Were Separated from the Ground by Means of a Ventilated Crawlspace and Plywood Air Vapour Barrier.

### 2.2 Limiting Indoor Sources of Formaldehyde

Commonly used household equipment and construction and finishing materials which represent a potential source of formaldehyde were identified. Alternates were substituted where possible.

For example, interior grade plywood, which is bonded by urea formaldehyde based glue, is normally used for construction of subfloors. In the experimental townhomes, interior grade plywood was replaced with exterior grade plywood. The plys of exterior grade plywood are bonded together by phenol formaldehyde based glue which off-gasses at a lower rate than interior grade plywood (3). Hardwood flooring and ceramic tile were substituted for carpeting and vinyl flooring as interior floor finishes. Installation of hardwood and ceramic tile minimized the possiblity of formaldehyde off-gassing from glues and synthetic carpet fibres. It should also be noted that the substitution of hardwood for carpeting also avoided bacterial, shampoo residue and fibre problems which may be associated with carpets (4) (5).

Electric hot water tanks, heating systems and appliances were used in the townhomes. Electric appliances eliminate problems associated with indoor combustion of fossil fuels such as creation of formaldehyde, CO, $CO_2$ and $NO_x$ (6) (7).

Further review of construction technology and finishing materials for possible sources of formaldehyde identified acoustical sealant as a possible source of xylene and toluene. Acoustical sealant is used in energy efficient homes to seal the sheets of polyethylene used to construct an air vapour barrier into a continuous membrane (Figure 4).

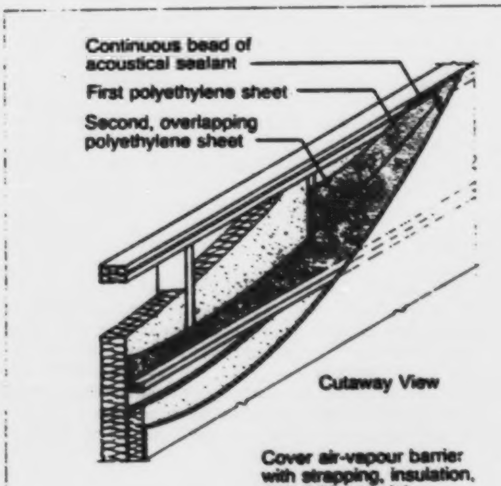
Continuous bead of acoustical sealant
First polyethylene sheet
Second, overlapping polyethylene sheet
Cutaway View
Cover air-vapour barrier with strapping, insulation, and rigid material (plasterboard, wallboard, etc.)

Fig. 4. Standard Polyethylene/Acoustical Sealant Air Vapour Barrier

An alternative vapour barrier technology, known as the Airtight Drywall Approach or ADA has been developed (8). The ADA (Figure 5) approach eliminates the use of polyethylene and requires only minimal use of acoustical sealant. The drywall, in conjunction with foam gaskets and a vapour proof paint is used to seal the building. In order to quantify the effect of acoustical sealant on indoor air quality, one of the townhomes was constructed with an ADA air vapour barrier, and the other townhome was constructed with a polyethylene air vapour barrier.

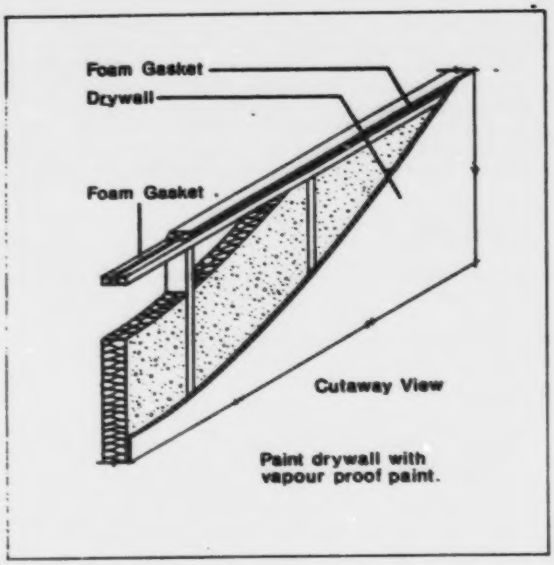

Fig. 5. Drywall/Gasket/Vapour Proof Paint Air Vapour Barrier

## 3. EVALUATION

After completion of the homes, and prior to occupancy, radon and formaldehyde, and xylene and toluene concentrations were monitored.

### 3.1 Radon Testing

The effectiveness of direct outdoor ventilation of the crawlspace in reducing occupant exposure to radon contamination was evaluated by comparing indoor radon levels in one of the experimental townhomes and two immediately adjacent residences during October to December 1985:

House A: Experimental townhome, Unit 2

House B: A 67-year old unoccupied house with a basement.

House C: A 50-year old occupied house with a basement.

All three houses are two-storey wood frame homes and are located adjacent to each other.

Terradex Trac Etch Type SF Radon Detectors were placed in the basement/crawlspaces and living areas of House A and C for 88 days and of House B for 75 days. In all locations, the Trac Etch Detectors were pinned to interior vertical partition walls a minimum of 9 feet away from exterior windows and midway between the floor and ceiling.

A concentration of .82 pCi/L (picocurie per litre, measurement of concentration of radon) was recorded in the living area of House A (Unit 2 of the experimental townhomes) compared with 2.04 pCi/L and 1.57 pCi/L in Houses B and C respectively (Table 1). The average radon level measured in a sample of Canada R2000 energy efficient houses was 3.55 pCi/L (9). The ventilated crawlspace and living areas separated by an air vapour barrier in the experimental townhome (Unit 2), resulted in reduction of indoor radon levels approximately 65% as compared to Houses B and C. In addition, the .82 pCi/L measurement recorded in the experimental townhomes is 77% lower than the average concentration reported in energy efficient R2000 homes and 59% lower than the 2 pCi/L concentration defined by the American Society of Heating, Refrigeration and Air Conditioning Engineers 62-1981 Ventilation Standard as acceptable (10).

TABLE 1

RESULTS OF RADON MEASUREMENTS IN THREE HOUSES IN VANCOUVER

| | | | Yearly WLM[2] |
|---|---|---|---|
| | pCi/L | | WL[1] |
| House A (Test House) | Crawlspace | 0.07 | |
| | First Floor | 0.82 | 0.0041 |
| House B (Unoccupied Control) | Basement | 0.38 | |
| | First Floor | 2.04 | 0.0102 |
| House C (Unoccupied Control) | Basement | 0.82 | |
| | First Floor | 1.57 | 0.0079 |

[1] 1 WL=200 pCi/L, assuming an equilbrium between radon and its daughters of 0.5. U.S. EPA recommend remedial action if WL>0.015.

[2] 1 WLM=680 hours of exposure to 1 WL.

### 3.2 Formaldehyde Testing

The effectiveness of the use of exterior grade plywood, hardwood and ceramic tile flooring and electric appliances in reducing indoor levels of formaldehyde was evaluated by monitoring formaldehyde concentrations in the two townhomes. Air Quality Research Inc. International PF-1 Passive Formaldehyde Paired Monitors were installed for approximately 118 hours in the two townhomes. The monitors were installed at waist level in the centre of the test spaces. Sampling results (Table 2) indicated levels of formaldehyde in both residences between .015 ppm (parts per million) and .032 ppm. The .015 - .032 range is 46 - 71% lower than the average formaldehyde level of .059 ppm recorded in a R2000 program survey of airtight energy efficient Canadian homes (9).

TABLE 2

RESULTS OF FORMALDEHYDE MEASUREMENTS IN TWO EXPERIMENTAL TOWNHOMES IN VANCOUVER[1]

| | Unit 2 | Unit 1 | Outdoor |
|---|---|---|---|
| Sampling Time (Hours) | 118.2 | 118.2 | 118.4 |
| Sample 1 | .021 | .031 | .038 |
| Sample 2 | .015 | .032 | .037 |

[1] All measurements in parts per million (ppm).

Both the formaldehyde levels measured in the two experimental townhomes and the average level reported in the R2000 sponsored survey are well below the Canadian Department of Health and Welfare guidelines of .1 ppm (9). However, the energy efficient R2000 home survey average formaldehyde concentration exceeds the 105 ppm objective adopted to define acceptable formaldehyde levels in UFFI insulated homes by the Canadian Government Urea Formaldehyde Remedial Program (9). The recorded formaldehyde concentrations in the experimental townhomes are 35 - 65% lower than the 105 ppm objective.

It should be noted that the formaldehyde measurement levels of .021 ppm and .015 ppm recorded in Unit 2 were significantly lower than the .031 and .032 measurements recorded in Unit 1. While no specific cause for this difference has been identified, it may be due to the different air vapour barrier technologies used in the two Units. Fibreglass insulation is a source of formaldehyde (3). The polyethylene air vapour used in Unit 2 may be a more effective barrier against infiltration of formaldehyde off-gassed from the fibreglass insulation than the drywall air vapour barrier used in Unit 1.

### 3.3 Xylene and Toluene Testing

The improvement in indoor air quality associated with use of a drywall air vapour barrier, and the impact on air quality of acoustical sealant in conjunction with polyethylene air vapour barriers was evaluated by monitoring xylene and toluene concentration in the experimental townhomes using Dupont AA Passive Air Monitoring Devices. The monitor devices were hung at the mid point of the test spaces and at an outdoor location on the townhome site. Sampling times ranged between 523 minutes and 535 minutes. Measurement range of .015 - .026 ppm was recorded for xylene and .012 - .068 ppm for toluene in the experimental townhomes (Tables 3, 4). The outdoor concentration of xylene was recorded as .012 and .080 ppm. The outdoor concentrations were .011 and .012 ppm.

TABLE 3

RESULTS OF XYLENE MEASUREMENTS IN TWO EXPERIMENTAL TOWNHOMES IN VANCOUVER[1]

| | Unit 2 | Unit 1 | Outdoor |
|---|---|---|---|
| Sampling Time (Minutes) | 535 | 530 | 523 |
| Sample 1 | .015 | .026 | .080 |
| Sample 2 | .017 | .013 | .012 |

[1] All measurements in parts per million (ppm).

TABLE 4

RESULTS OF TOLUENE MEASUREMENTS IN TWO EXPERIMENTAL TOWNHOMES IN VANCOUVER[1]

| | Unit 2 | Unit 1 | Outdoor |
|---|---|---|---|
| Sampling Time (Minutes) | 535 | 530 | 523 |
| Sample 1 | .023 | .068 | .012 |
| Sample 2 | .012 | .030 | .011 |

[1] All measurements in parts per million (ppm).

Comparison of indoor and outdoor xylene and toluene concentrations indicate that acoustical sealant used to create a polyethylene air vapour barrier does not have significant impact on air quality in an energy efficient, airtight building. However, comparison of recorded toluene measurements in Units 1 and 2 indicate that some component of the drywall air vapour barrier system, most likely the vapour proof paint, is off-gassing approximately 50% more toluene than the components of polyethylene air vapour barrier system.

## 4. CONCLUSION

An architectural approach to improving air quality can be an effective and energy efficient means of improving air quality in buildings. Separation of the living area from the ground by a crawlspace and installation of an air vapour barrier between the crawlspace and living areas of the townhomes resulted in radon concentrations 65% lower than those recorded in adjacent homes. Radon concentrations in the experimental townhomes were also 77% lower than the average concentration reported in a survey of Canadian energy efficient homes. Use of exterior grade plywood, hardwood and ceramic tile flooring and electric appliances was effective in reducing formaldehyde concentrations in the experimental townhomes as compared with the average concentration reported in the energy efficient home survey. Acoustical sealant does not appear to have any significant impact on air quality in buildings constructed with a polyethylene air vapour barrier. However, toluene concentrations in homes constructed with a drywall air vapour barrier system may be significantly higher.

## 5. NOMENCLATURE

pCi/L - picocurie per litre, measurement of concentration of radon

ppm - measurement in parts per million

## 6. REFERENCES

(1) CMHC, (Canada Mortgage and Housing Corporation), Energy Efficient Housing Construction, CMHC, Ottawa, 1982

(2) LaFavore, M., The Radon Report, Rodales New Shelter, January, 1986

(3) Meyer, B., Indoor Air Quality, Addison-Wesley Pub-

(4) Kreiss, K. et al. Respiratory Irritation Due to Carpet Shampoo: Two Outbreaks. Environment International 8: 337-342, 1982.

(5) Morey, P.R., Hodgson, M.J., Sorenson, W.G., Kullman, G.J., Rhodes, W.W., Visvesuara, G.S., Environmental Studies in Molding Office Buildings: Biological Agents Sources and Preventive Measures, Annals of the American Conference of Governmental Industrial Hygienists, Volume 10:21-35, 1984.

(6) Sterling T.D. and Sterling E.M., Carbon Monoxide Levels in Kitchens and Homes with Gas Cookers, Journal of the Air Pollution Control Association, March, 1979.

(7) Traynor, et al., Effects of Ventilation of Indoor Air Pollution from a Gas-Fired Stove: Test Results from a Single Family Dwelling, Conference Proceedings, International Symposium on Industrial Prevention Health and Energy Conservation, University of Massachusetts, 1981.

(8) Latiborek, Lischoff, A New Approach to Affordable Low Energy House Construction, Alberta Department of Housing, 1984.

(9) Dumont, R., A Few Comments on the Air Quality Monitoring Activities in the R2000 Program, Canada Mortgage and Housing Corporation, File No. C29803, January, 1986.

(10) ASHRAE, American Society of Heating, Refrigeration and Air Conditioning Engineers Standard 62-1981: Ventilation for Acceptable Indoor Air Quality, Atlanta, Georgia, 1981.

# THE VARIATION OF THE EFFECTIVE NATURAL VENTILATION RATE WITH WEATHER CONDITIONS

G. K. Yuill
G. K. Yuill and Associates Ltd.
1441 Pembina Highway
Winnipeg, Manitoba
R3T 2C4

## ABSTRACT

The recent increased public awareness of indoor air quality has caused more interest in the ventilation of residential dwellings. The ASHRAE Standard 62-81 "Ventilation for Acceptable Air Quality" gives guidelines as to the minimum ventilation rates that should exist in buildings in order to keep the concentration of indoor pollutants below dangerous levels.

However, the ventilation rate in a house which is ventilated by natural infiltration varies continuously with changing weather conditions. The object of the work reported here was to provide a link between house properties and weather data for a particular house in a particular location, and the ventilation which the house experiences throughout the year.

Dr. Max Sherman of Lawrence Berkeley Laboratories has developed a simple model (the LBL model) which relates the instantaneous infiltration rate to house properties, ambient temperature and wind velocity. This model predicts that the ventilation rate will occasionally be zero, when the indoor-outdoor temperature difference and the wind velocity are both zero. However, the pollutant concentration obviously will not rise to infinity, because of the capacity of the air in the house to absorb it. To deal with this effect the concept of the equivalent steady state ventilation rate has been introduced.

If this ventilation rate, Q, is constant and the source strength S is constant, the pollutant concentration is given by

$$C = S/Q$$

When the infiltration rate is varying, the concentration will also vary, and will not be given by the above equation. However, we can define an equivalent steady state flow rate

$$Q_s = S/C$$

which depends on the instantaneous value of the concentration, C.

A differential equation can be written for $Q_s$ as a function of house volume and leakage rate. Using the LBL model this equation can be solved numerically to compute the time variation of $Q_s$ throughout the year. It would be expensive to solve this equation for every house of interest. To avoid this, the equation has been recast as a relationship between three dimensionless numbers, only one of which contains weather related terms. This has made it possible to solve for the weather variation only once for each location, and to present the results in the form of a graph. Thus the equivalent state ventilation rate $Q_s$, can be found from this graph for any house whose physical characteristics are known. If $Q_s$ satisfies the requirements of ASHRAE Standard 62-81, then the house may be considered to be adequately ventilated by natural infiltration.

A significant finding of this work is that there appear to be no air quality disasters due to periods of very low infiltration driving force. The analysis of ten years of data in seven Canadian cities showed that such periods are short and that the damping effect of house volume suppresses any transients in pollutant concentration.

## 1.0 INTRODUCTION

The object of the work reported here was to develop a relationship describing the variation of equivalent steady state ventilation rate in a house as a function of source strength, weather conditions and house characteristics. This work was carried out to support the development of a Standard specifying how tight a house may be sealed, in a retrofit project to reduce infiltration, before artificial ventilation need be provided.

In most locations there will be times during the year when the wind velocity is zero and the indoor-outdoor temperature difference is zero. However, if such periods are short, the levels of indoor pollutants may not rise to intolerable levels, because of the capacity of air in the house. This project was directed towards examining the performance of houses in the weather conditions of several Canadian locations to discover how pollutant concentrations would vary with weather. The model used to predict infiltration as a function of weather conditions was that developed by Sherman et al (Ref. 1) at Lawrence Berkeley Laboratory. This was combined with a simple single zone pollutant concentration model in a computer program which would analyse hourly weather data to predict variations in concentration throughout the year.

Canadian houses have a wide range of physical properties. To model enough houses to characterise the entire housing stock would be a prohibitively time-consuming job. Therefore, a set of dimensionless numbers was developed to make it possible to find more general solutions to the problem. One of these, the instantaneous tracer concentration index, CI, is a dimensionless index of pollutant concentration. CI is a function of two other variables, the relative leakage, LR, which is a dimensionless number characterising house properties and the equivalent steady state tracer concentration index, CSS, which is a dimensionless index of weather conditions. Thus for a given city and a given LR, the variation of CI throughout the year can be calculated.

## 2. THEORY

### 2.1 Infiltration Rate

According to Sherman et al (Ref. 1), the infiltration rate is given by:

$$Q = L\,(P_s \Delta T + P_w U^2)^{1/2} \;.\;.\;.\;.\;.\;.\; (1)$$

where L is the effective leakage area at 4 Pa [$m^2$]
P is the stack effect parameter [$m^2/°C\ S^2$]
T is the indoor-outdoor temperature difference (°C)
P is the wind effect parameter [dimensionless]
U is the wind velocity [m/s]

$P_s$ and $P_w$ can be estimated by the method outlined in Ref. 4. The equivalent leakage area (ELA) measured by the method of CGSB Standard CAN2-149.10-M84 (Ref. 2) is related to L by the expression:

$$ELA/L = 2.5^{(n-0.5)}/0.611 \;.\;.\;.\;.\;.\; (2)$$

where n is the exponent in the expression $Q = C\Delta P^n$ relating leakage flow, Q, to pressure difference, $\Delta P$
2.5 is the ratio between the pressure (10 Pa) at which time the ELA is calculated and the pressure (4 Pa) at which L is calculated
0.611 is the orifice coefficient which is used in calculating ELA, but ignored in calculating L.

The average value of n for 200 Canadian houses in which ELA measurements were made was 0.68. At this value of n, ELA/L = 1.930.

### 2.1.2 Pollutant Concentration

If a house of volume V [$m^3$] contains a pollutant source of strength S [parts/sec], the rate of change of pollutant concentration C is given by:

$$dC/dt = S/V - QC/V$$

where t = time

or:

$$dC/(S-QC) = dt/V$$

If Q is constant between time 0 and time t, this expression can be integrated over this period to yield the final concentration:

$$C = [S + (QC_0 - S)e^{-Qt/V}]/Q \;.\;.\;.\;.\;.\; (2)$$

where $C_0$ is the concentration at the beginning of the time period.

### 2.2 Dimensional Analysis

The physical process described by equation (2) can be represented by three dimensionless numbers. These are:

#### a) The Instantaneous Tracer Concentration Index

$$CI = (C\,L\,r_0\,(P_s/P_{so})^{1/2})/S \;.\;.\;.\;.\;.\; (3)$$

where $r_o$ is a normalising constant equal to 0.75 m/s ($r_0$ is the average value over North America of the term $(P_s \Delta T + P_w U^2)^{1/2}$ from Equation (1). This term represents the air velocity in the leaks in the house.)

$P_{so}$ is a normalising constant equal to 0.015 $m^2/s^2$ °C. (This is a typical value of the stack effect coefficient $P_s$ from the same equation.)

CI is an index of tracer concentration in a house. The top half of the term is the rate at which the tracer leaves the house if the air velocity through the leaks is $r_0$, the North American average value. The bottom half is the rate at which the tracer is generated in the house. Thus, the average value of CI over the year and over North America will be 1.

#### b) The Relative Leakage

$$LR = (Lr_0\,(P_s/P_{so})^{1/2}\,t)/V \;.\;.\;.\;.\; (4)$$

where t is the time period of interest and the other variables are as previously defined.

LR is the total number of air changes in the period of interest, if the house in question were experiencing average North American weather in an area with average wind shielding. Letting the time period for LR be one hour, its value is equal to the air changes per hour in such conditions.

#### c) The Equivalent Steady State Tracer Concentration Index

$$CSS = r_0\,/(P_{so}\,\Delta T + P_{so}\,(P_w/P_s)U^2)^{1/2}$$

CSS is the ratio of the North American average air velocity in house leaks to the actual instantaneous velocity.

The three dimensionless numbers chosen were selected because they are useful in reducing the computations required to a minimum. There are only two independent variables other than local weather conditions. These are LR and $P_w/P_s$. Thus in any location CI is a function only of these two variables and time.

Some may find it easier to grasp the physical significance of the dimensionless numbers by considering their inverses. The inverse of CSS is the instantaneous infiltration rate, normalised so that its average value over the year and over North America is 1. The inverse of CI is the equivalent steady state infiltration rate, normalised so that its average value is also 1. (The equivalent steady state infiltration rate is the infiltration rate which, if it remained steady at that value, would produce a particular tracer concentration in a house. It is different from the instantaneous infiltration rate because of the capacity of the air in the house to absorb the tracer.)

The actual value of the instantaneous infiltration rate, in air changes per hour is given by the ratio LR/CSS, and the actual value of the equivalent steady state flow rate, in the same units is given by the ratio LR/CI.

If the outdoor temperature and the wind velocity are constant, the pollutant concentration is given by:

$$C = S/Q \;.\;.\;.\;.\;.\;.\;.\;.\;.\;.\; (6)$$

This equation can be rearranged in dimensionless form by the introduction of CI and CSS values, as

$$CI = CSS \;.\;.\;.\;.\;.\;.\;.\;.\;.\;.\; (7)$$

as would be expected for this particular case, with wind velocity and outdoor temperature constant.

If the outdoor temperature and wind velocity change, Equation (2) must be used. Substituting into it the equations for CI, CSS and LR yields:

$$CI = CSS + [CI(0) - CSS]e^{-LR/CSS} \quad . . . \; (8)$$

This equation applies to a period during which wind velocity and temperature are constant, but are different from their value in the previous time period.

The first term, CSS, is the equilibrium value of CI at the new conditions. The term [CI(0) - CSS] is the difference between the previous value of CI and the new equilibrium value. The exponential term indicates how this difference has decayed away during the period of interest. The exponent LR/CSS is the number of air changes which have occurred during the period of interest.

This equation may also be written in the form:

$$CI = CI(0)e^{-LR/CSS} + CSS(1 - e^{-LR/CSS})$$

This form makes it clear that the exponential term is a weighting factor which determines the fractional influence on CI of two terms, the previous value of CI (=CI(0)) and the new equilibrium value of CI (=CSS). As LR/CSS decreases and the exponential term approaches 1, the fluctuation of CI becomes more heavily damped against fluctuations in CSS.

Note that if $\Delta T$ and U are equal to zero, then the infiltration rate Q given by equation (1) is equal to zero. This implies that CSS approaches infinity as Q approaches zero and, with $\Delta T$ and U equal to zero, CSS is undefined. Thus, the rate of change of pollutant concentration is given by:

$$dC/dt = S/V$$

This expression can be integrated over the period time 0 to time t to yield:

$$C = C_0 + St/V \quad . . . . . . . . \; (9)$$

Equation (9) can be represented in dimensionless form by the use of CI and LR values, as:

$$CI = CI(0) + LR \quad . . . . . . . . (10)$$

This dimensional analysis allows for a much simplified approach to predicting equivalent steady state ventilation rates in houses across Canada. It is no longer necessary to analyse each individual house type in each location. Now CI can be calculated as a function of only two variables, LR and $P_W/P_S$, in each location, since the latter term, along with the local weather data, specifies CSS.

## 3. RESULTS

A computer program has been developed to compute hourly CI and CSS values throughout the year, using hourly weather data. Results were obtained for seven Canadian cities, for three $P_W/P_S$ ratios and for five LR values. Since it is not certain what period should be used to designate the maximum allowable pollutant concentration, several different CI peaks have been calculated. In each month the maximum values of CI averaged over a one-hour period, a four-hour period, an eight-hour period and a day have been found. In addition the monthly and annual average values have been found. The values considered in this study were 0.1, 0.2, 0.4, 0.7 and 1.0. The locations studied were Frobisher Bay, Montreal, Ottawa, St. John's, Toronto, Vancouver and Winnipeg. Figures 1 to 4 show samples of these results.

To make these results more useful, they have been plotted in the form shown in Figures 5 to 8. The user can now calculate the equivalent steady state flow rate for any house in a particular location by a simple manual calculation. First $P_W/P_S$ are evaluated as functions of local terrain and wind shielding, using the method of Ref. 1. Then LR is calculated as a function of leakage area and house volume, using Equation 4. From the graph (such as Figs. 5 to 8) CI can then be found. Then inverting Equation 3, the equivalent steady state ventilation rate can be calculated by:

$$Q_S = S/C = Lr_0 \, (P_S/P_{SO})^{1/2}/CI \quad . . . . .(11)$$

If Figure 8 (for example) had been used to find CI, then the value of $Q_S$ found would be the average value on the worst day of the heating season in Winnipeg.

Note that $Q_S$ is not an actual flow rate. It is the hypothetical steady state flow rate which would produce the same pollutant concentration as actually occurs in a transient situation. Since ASHRAE Standard 62-81 "Ventilation for Acceptable Air Quality" specifies minimum allowable steady state ventilation flow rates, this equivalent steady state flow rate can be compared with the Standard's requirement, to determine if it is satisfied by the house under consideration.

## 4. CONCLUSIONS

1. A model has been developed which allows the calculation of time-varying pollutant concentrations and equivalent steady state infiltration rates in real houses in particular locations.
2. The indoor air pollution crises which have been postulated to occur in mild windless weather when infiltration is relied on for ventilation does not happen. This is because periods of zero wind and zero temperature difference are fairly short, and the house volume is sufficient to damp out the sharp rises in pollutant concentration that would occur during these periods.

## 5. ACKNOWLEDGEMENTS

The work presented here was supported by the Building Energy Technology Transfer Program of Energy Mines and Resources Canada through a subcontract from the Saskatchewan Research Council. John Lovatt and Grant Wilson of B.E.T.T. provided helpful guidance and advice during the project.

The assistance of Dr. David Wilson of the University of Alberta is also very much appreciated. He provided both useful data and valuable comments and suggestions.

## 6. REFERENCES

(1) Grimsrud, D. T., Sherman, M. H., Sonderegger, R. C., Infiltration Measurements in Audit and Retrofit Programs, Energy & Environment Division, Lawrence Berkeley Laboratory, University of California, Report No. LBL-12221, April, 1981.
(2) Canadian General Standards Board, Determination of the Equivalent Leakage Area of Buildings by the Fan Depressurization Method, CAN-149.10-M84, Eighth Draft, October, 1984.
(3) The American Society of Heating, Refrigeration, and Air-Conditioning Engineers Inc., Ventilation for Acceptable Indoor Air Quality, ASHRAE Standard 62-81, 1981.
(4) Levin, P.A., Modera, M.P., Sherman, M.H., A Detailed Examination of the LBL Infiltration Model using the Mobile Infiltration Test Unit, ASHRAE Transactions 1983, Vol. 89, Parts 2A & B.

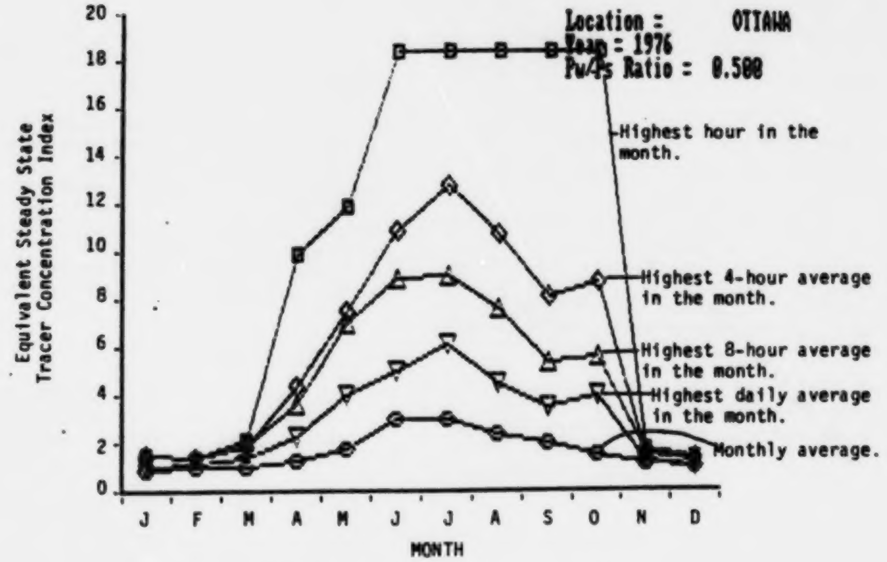

Fig. 1 Variation of Equivalent Steady State Tracer Concentration Index with Time of Year

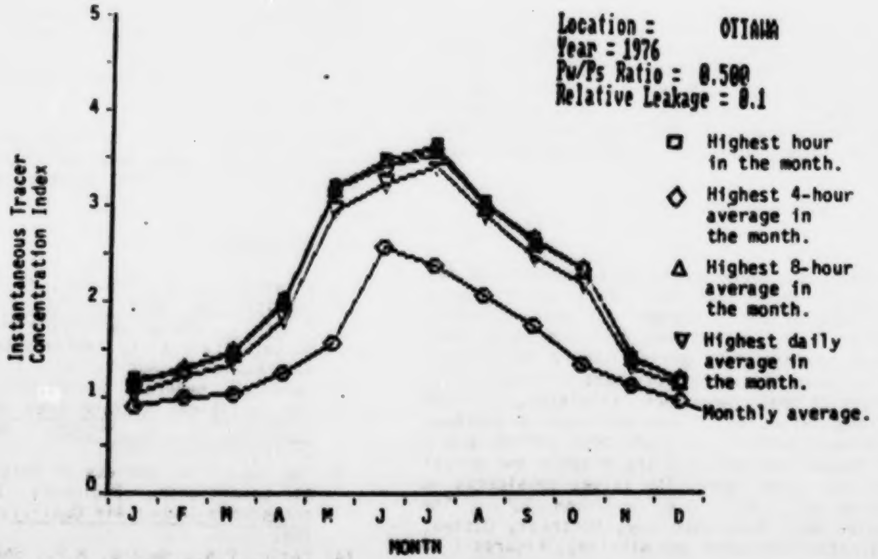

Fig. 2 Variation of Instantaneous Tracer Concentration Index with Time of Year

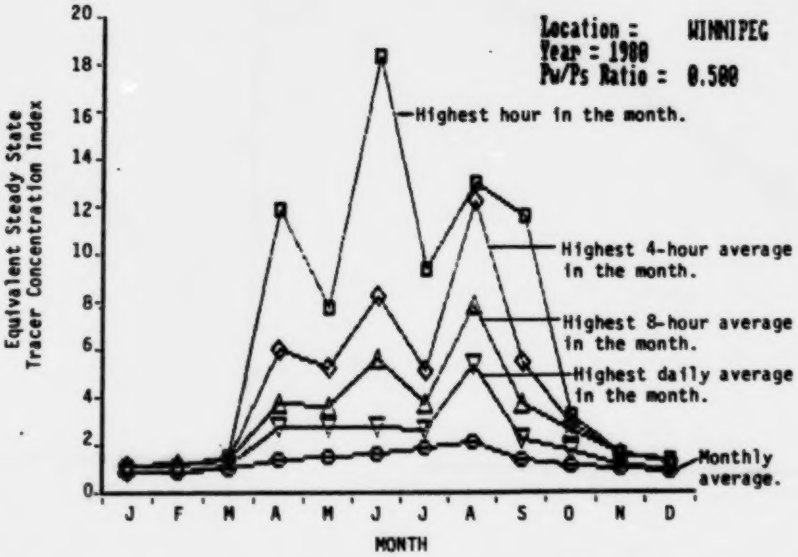

Fig. 3 Variation of Equivalent Steady State Tracer Concentration Index with Time of Year

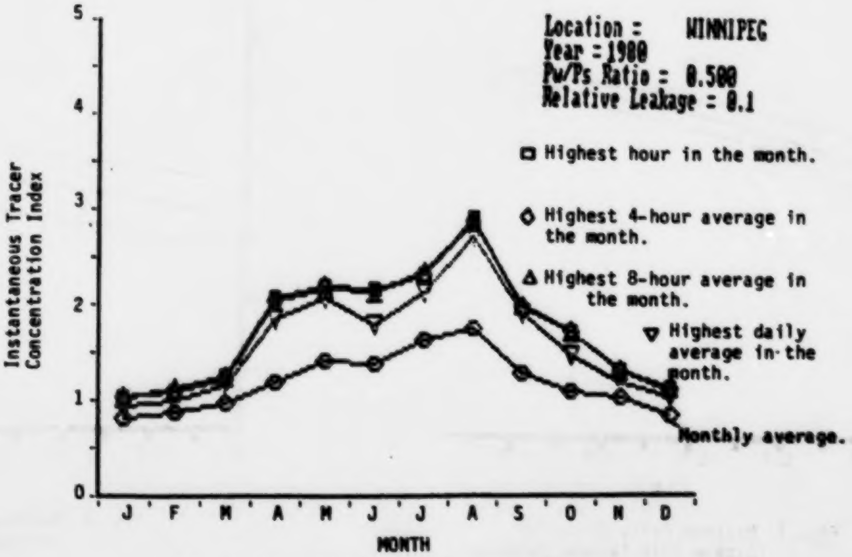

Fig. 4 Variation of Instantaneous Tracer Concentration Index with Time of Year

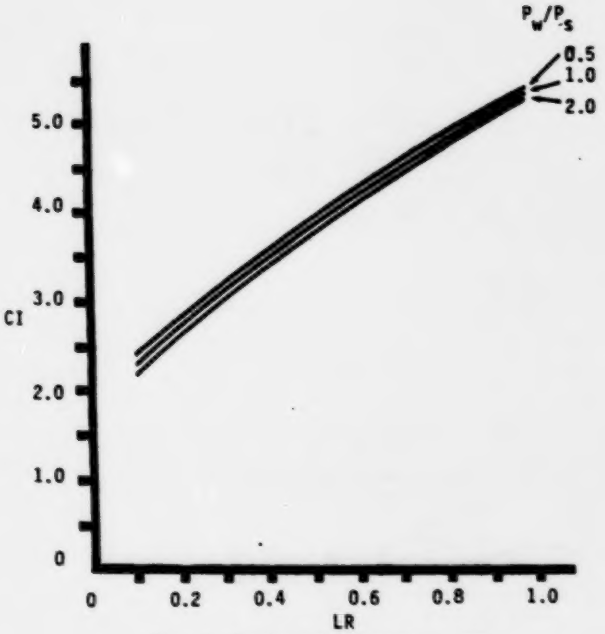

Fig. 5 Maximum Hourly CI vs. LR
Ottawa 1976 (Winter Season)

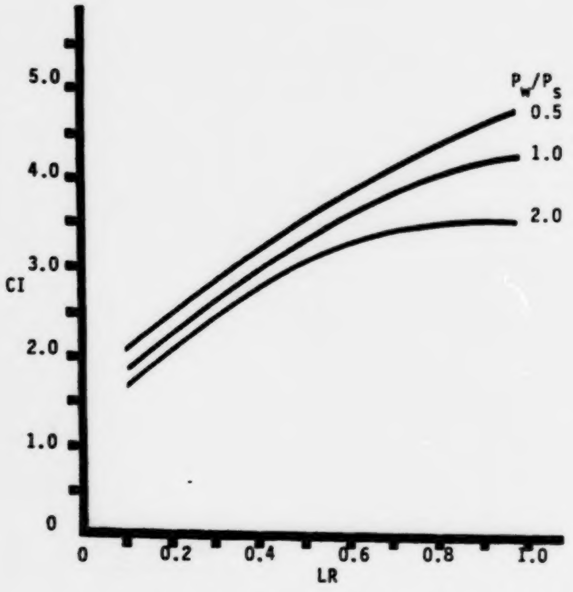

Fig. 6 Maximum Hourly CI vs. LR
Winnipeg 1980 (Winter Season)

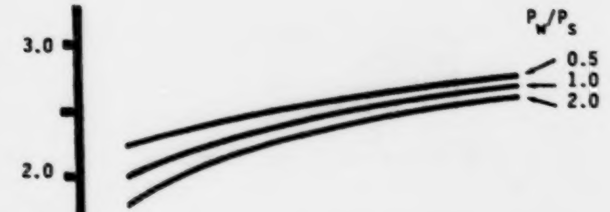

Fig. 7 Maximum Daily CI vs. LR
Ottawa 1976 (Winter Season)

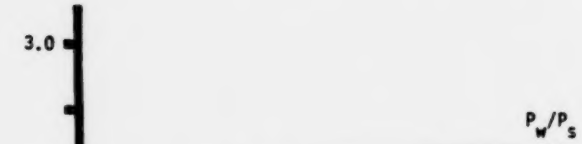

Fig. 8 Maximum Daily CI vs. LR
Winnipeg 1980 (Winter Season)

# IMPROVING THE AIR-TIGHTNESS OF THE EXISTING HOUSING STOCK

J.A. Love
Faculty of Environmental Design
The University of Calgary
Calgary, Alberta
T2N 1N4

## ABSTRACT

This paper addresses the problems of reducing air leakage in existing Canadian housing. Air infiltration has been recognized for some time as one of the major heating loads in Canadian housing. Field research indicates that many gaps exist in our understanding of housing performance and conservation measures. Some recent work is reviewed with regard to relative effectiveness and economy of measures. Methods of assessing and predicting infiltration are discussed. Air-tightness of the existing housing stock is considered in terms of standards for the provision of fresh air. The problem of occupant behaviour in housing performance research is outlined. The need for field research on full-scale unoccupied housing is discussed.

## 1. INTRODUCTION

Infiltration has been recognized for some time as a major contributor to residential space heating costs and as a cause of occupant discomfort. Several hundred housing units built in Canada in the past few years have demonstrated that space heating requirements can be reduced to levels much lower than have been common in typical post-war housing. Substantial reductions have been achieved by increasing insulation levels and envelope air-tightness, and by using more efficient heating and ventilation systems. The breakthroughs in housing technology were a result of a comprehensive and systematic analysis of the detached house as a set of systems.

Less progress has been made in understanding performance effects of physical modifications to the existing housing stock. It has been demonstrated that dramatic improvements, of the order of magnitude of those achieved in new superinsulated air-tight housing, can be achieved by applying "super-retrofit packages" to older housing (1). The efficacy and "side effects" of single and combinational conservation measures have been less completely identified. A recent Swedish study of combined wall and attic insulation upgrades found actual savings were about half the theoretically predicted savings. It notes that

> "No definite conclusions can be drawn
> to explain why the combination of wall
> and attic insulation did not produce
> the anticipated savings. Further studies
> are required (2)".

This finding is in agreement with a major review of retrofit activity in the United States (3). Other studies of insulation upgrades have found measured savings to be substantially greater than predicted (4,5). Such findings indicate the need for more field research to resolve discrepancies. This is equally essential in the case of uncontrolled air flow, which is a very complex problem and has implications for indoor air quality.

Improvement of the energy efficiency of existing dwellings will most effectively be achieved by treating the dwelling as a set of subsystems subjected to particular climatic conditions and occupant interventions and developed according to particular cost factors.

## 2. MEASURES TO REDUCE INFILTRATION

Air flow through building envelopes is an intricate process due to the complexity of the driving forces and leakage paths. Wind and stack effect generate continually varying pressure differentials which, in turn, induce infiltration and exfiltration (6). Air moves through a myriad of apertures in any envelope. If either pressure differentials or gaps are reduced, uncontrolled air flow will be reduced.

Experiments with a number of small test buildings at the Alberta Home Heating Test Facility have indicated that elimination of the furnace flue would reduce air infiltration by about 50 percent (7). It has been suggested by a member of the research team that installing a condensing gas furnace and sealing the unused furnace flue would result in reductions of a similar magnitude in existing housing (8). Of course, in full-scale housing one would have to deal with the domestic water heater flue and consider the effects of fireplace chimneys. As well, the investigators have pointed out that savings in full-scale housing may be different due to lower surface area to volume ratios.

The author attempted to demonstrate savings through flue leakage reduction by building sealed mechanical rooms around gas-fired combustion appliances in two Calgary row houses (9). Combustion air was ducted to the mechanical rooms. Temperature-corrected energy use reductions amounted to 21% and 6%, a very wide range. Further studies would be required to determine the reasons for the range, since the test houses differed in a number of features. Unless carried out as part of a general basement redevelopment, construction of a mechanical room is a relatively costly conservation measure (about $160 for materials alone). Sealing of all apertures for ducts and pipes is a particularly demanding task.

A number of other field studies have been undertaken to identify performance improvements from increased air-tightness of housing. Scanada Consultants undertook step-by-step sealing and pressure testing of 15 houses in Ontario (10). An effort was made to determine whether sealing basement or attic leaks was more effective and what contribution each made to leakage reduction. The testing was carried out concurrently with work by a sealing contractor which prevented the researchers from following a regular procedure in sealing and hence nothing useful was "learned about the effectiveness of individual steps in the process". The average reduction for 10 of the houses which were determined to be "non-anomalous" was 22 per cent. The difficulties encountered in this study indicate the complexity of air-tightness studies in existing housing.

A more recent study assessed sealing measures on a step-by-step basis for 21 houses in Calgary (11). The components of the envelope sealed were:

- band-joist
- window & door frames, attic hatch, light fixtures
- window gasket (upgrade)
- plumbing stacks & chimney chases
- wall penetrations, electrical plugs and switches
- exterior baseboard

The first four measures each increased tightness by about 5 per cent, the latter two by about 2 per cent. The total increase in tightness was 26 per cent. Standard deviation for each tightness increase was less than 5 per cent.

Pre- and post-sealing testing was conducted for a larger sample of houses in the Calgary study. Some homes were sealed by owners, others by a contractor equipped with pressure testing equipment. The homeowners achieved a substantially greater average improvement in air-tightness than did the contractor.

The overall air-tightness improvement achieved that obtained at the Alberta Home Heating Test Facility for the single measure of eliminating the furnace flue, yet the average contractor price per dwelling in both cases was $800. Typically, cost-effectiveness of condensing furnaces has been based solely on reduced fuel use, but comparisons with sealing work indicate that this could lead to substantial underestimates of investment returns.

Energy Mines and Resources Canada funded two studies of the effects of adding loose fill insulation to empty stud wall cavities in older wood frame houses (12,13). Apart from direct thermal effects, air-tightness of 6 Winnipeg houses was increased by an average of 22 percent. The same average increase was obtained for 8 Ottawa houses. This is another example of a conservation measure not aimed at air-tightness improvement, but having that effect. Both indoor air quality and cost-effectiveness of adding insulation would be affected by the air-tightness changes.

The results of a number of studies suggest that most leakage paths are well-distributed over the envelopes of houses rather than concentrated in a few major, easily sealed points (14,15). This contrast with the findings of one of the seminal studies of air leakage in housing, undertaken by Princeton University in the 70's which focussed on one townhouse project in New Jersey (16).

## 3. ASSESSING TIGHTNESS AND PREDICTING INFILTRATION

Both infiltration and the space heating requirements generated by infiltration are of interest in studies of housing performance. Only assessment of infiltration will be considered here. Prediction of infiltration is necessary to determine:

(i) potential for performance improvement,

(ii) adequacy of fresh air supply, and

(iii) effectiveness of measures to improve air-tightness.

Tracer gas methods can be effective in identifying instantaneous infiltration rates, but extrapolation of individual measurements to predict infiltration for an entire heating season is not a well-defined procedure (14).

Pressure testing of housing has become the most commonly used test of air-tightness, since it offers a rapid and repeatable measure of performance (15). Some standardized measures of tightness have been adopted, notably the air change rate with a 50 pascal pressure differential induced across the building envelope (AC50). Another is the equivalent leakage area (ELA), which assumes that all openings may be represented by a single square edged orifice whose area is determined by (17):

$$\text{ELA} = 0.001157\ \text{Oo}\ K\ 10^{n-0.5} \qquad (1)$$

where ELA is equivalent leakage area ($m^2$)
Oo is the local density of air ($kg\ m^{-3}$)
K is the flow constant determined by measurement ($m^3\ s^{-1}\ Pa^{-n}$)
n is the flow exponent determined by measurement

Since the entire envelope is tested with flow induced entirely inward or entirely outward, questions have arisen regarding the validity of pressure testing as a means of assessing infiltration.

Empirical evidence suggests that the magnitude of average natural infiltration may be found by dividing the air change rate at a pressure differential of 50 pascals across the building envelope by a factor of 10 to 12 (10). A more precise mathematical characterization relating air-tightness measured under pressure test to normal infiltration has been developed and validated by comparison of predicted and measured infiltration in more than 300 houses located throughout North America (14). This procedure, developed at Lawrence Berkeley Laboratory (LBL), relates wind and stack induced flow to a value called effective leakage area (not to be confused with equivalent leakage area as defined above), defined by the formula:

$$L_o = Q_4\ (2{\wedge}P/p)^{-1} \quad \text{and} \qquad (2)$$

$$Q_4 = K\ ({\wedge}P)^n \qquad (3)$$

where

$L_o$ is the effective leakage area ($m^2$)
$Q_4$ is the flow at 4 Pa determined by extrapolation from flows at higher induced pressure differentials ($m^3\ s^{-1}$)
^P is the pressure causing this flow (4 Pa)
p is the density of air ($1.2\ kg\ m^{-3}$)

$$Q_{stack} = L_o\ f_s\ ({\wedge}T)^{0.5} \quad \text{and} \qquad (4)$$

$$Q_{wind} = L_o\ f_w\ v \qquad (5)$$

^T is the indoor-outdoor temperature difference ($^oK$)
v is the measured wind speed ($m\ s^{-1}$)
$f_s$ is the stack parameter ($m\ s^{-1}\ {}^oK^{0.5}$)
$f_w$ is the wind parameter

Two additional expressions are used in this method:

$$R = (L_c + L_f)\ L_o^{-1} \qquad (6)$$

$$X = (L_c - L_f)\ L_o^{-1} \qquad (7)$$

where

$L_f$ is the floor leakage area ($m^2$)
$L_c$ is the ceiling leakage area ($m^2$)

then

$$f_s = 0.33(1+0.5R)[1-(X^2(2-R)^{-2})]^{1.5}(gH_hT^{-1}) \qquad (8)$$

and

$$f_w = C'(1-R)^{0.33}[(d_h(0.1H_h)^y\ )(d_m(0.1H_m)^y\ )^{-1}$$

where

C' is the shielding coefficient for the house site
R and X are as defined in (6) and (7)
$d_h$ and $y_h$ are terrain constants for the house
$H_h$ is the height of the house from grade to the top of the living space (m)
$d_m$ and $y_m$ are terrain constants for the wind measurement site
$H_m$ is the height of the wind measurement site (m)

Total infiltration is then given by:

$$Q = \sqrt{Q^2_{stack} + Q^2_{wind}} \qquad (10)$$

which may also be expressed as

$$Q = L_o \sqrt{f_s^{\,2}{\wedge}T} + \sqrt{f_w^{\,2}v^2} \qquad (11)$$

where Q is the infiltration ($m^3\ s^{-1}$)

While values for Lo were found to range from 0.0100 to 0.2000 $m^2$ for the houses used in the validation study, typical values were found to be 0.0600 to 0.0700 $m^2$.

## 4. AIR-TIGHTNESS OF THE EXISTING HOUSING STOCK

A couple of major air-tightness studies have been carried out in Canada, and data included in the published results were used to calculate effective leakage areas as shown in Tables 1 and 2. A couple of patterns are evident from the above surveys. There is a wide range in tightness of recently built Canadian housing. Secondly, newer housing in some provinces is not as air-tight as housing built in the 60's and 70's in Saskatchewan. On the whole Canadian housing is as tight as, or substantially tighter than, other housing in North America.

## 5. ADEQUACY OF FRESH AIR SUPPLY

Grimsrud, Sherman and Sonderegger suggest that an air-tightness standard, reflecting house design and regional climate, could be developed by ensuring that infiltration, as predicted by the LBL calculation procedure and supplemented by mechanical ventilation, exceeds fresh air requirements stipulated in ASHRAE Standard 62-81 (20). However, they proposed basing the standard on wind and temperature averages over the entire heating season. The more critical case would be in moderate weather when stack effect is reduced but windows might be closed.

The ASHRAE ventilation standard specifies target ventilation values for new residences of 4.67 x10-3 $m^3 s^{-1}$ (10 cfm) per room. For a typical 3 bedroom bungalow with kitchen, dining room, living room and bathroom, the required minimum supply rate for fresh air would be 32 $m^3 s^{-1}$ or about 0.3 ach without considering additional intermittent ventilation required in the kitchen and bathroom.

New Brunswick houses described in Sulatisky's report would appear to make the best test case for adequacy of fresh air supply. They are much more air-tight than the Canadian average and descriptive data would suggest that a substantial number are not mechanically ventilated.

The information to compute factors R and X is typically not available in published air tightness surveys. Leakage distributions R=0.5 and X=0.0 are used for reference analyses by Grimsrud (lower level leakage equals upper level leakage). These values would appear to be satisfactory approximations for general analysis where more specific information is not available since 50% variations in either R or X produce variations of 25% or less in projected air flow rates. For houses in terrain class III and shielding class III (rural area, moderate shielding),

$$f_s = 0.120 \text{ m } {}^{o}K^{0.5} \text{ s}^{-1} \text{ and } f_v = 0.128$$

Assuming a wind speed of 2.8 $m s^{-1}$ (10 $km h^{-1}$) and an indoor-outdoor temperature differential of 5 $^{o}K$, the infiltration flow would be 17 $m^3 s^{-1}$. This is half the ASHRAE recommended rate.

A forced air furnace, of the size that would be found in a 60's bungalow would introduce about 0.14 $m^3 s^{-1}$ of fresh air into the return air plenum when in operation (21). Thus, even if operating full time, it would not adequately supplement infiltration in this case. On the other hand, given the average $L_o$ for housing surveyed by Sulatisky, under the same conditions the infiltration flow would be 26 $m^3 s^{-1}$ which would be close to the ASHRAE standard.

This analysis indicates that some existing housing may already be close to or below minimum fresh air requirements and that infiltration should not be further reduced unless adequate mechanical ventilation is provided. It certainly indicates a need for further field studies of the LBL procedure and housing performance. Note that, given findings about condensing combustion appliances, a homeowner installing new equipment could inadvertently reduce fresh air supply below an acceptable rate.

## 6. OCCUPANT BEHAVIOUR AS A CONFOUNDING FACTOR

Human behaviour has a major yet unpredictable influence on housing performance. The author found, in a historical review of temperature corrected energy use in 22 row house units with the same floor plan, that energy use could vary by more than 100% with a change in tenants. This is consistent with results obtained by Sonderegger (22). Quarterly energy use by the same tenants also showed substantial variations from year to year. These were rental units which received no retrofit treatment over the period studied. It is not known what combination of temperature settings, window opening patterns, and domestic hot water use generated particular variations.

A study of projected and actual retrofit-generated energy savings for 264 occupied dwellings was conducted by the Bonneville Power Administration (23). The ratio of actual-to-expected savings varied substantially from dwelling to dwelling; actual energy use increased for more than 10% of the dwellings, while actual savings were more than double the audit estimates in more than 10% of the houses. There was no basis for ascertaining the extent to which performance was affected by occupant behaviour, but it seems likely that such widespread increases in use could only be explained by this factor.

If useful results on physical modifications are to be obtained from field studies, it is evident that occupant behaviour must be controlled for or eliminated. Extensive monitoring would be required to keep track of all potential effects of occupant behaviour on space heating - thermostat settings, hot water usage, and door and window opening patterns. Even if known, the latter can be particularly difficult to correct for in measured results. It is assumed in studies of measures applied to large numbers of housing units that vagaries of occupant behaviour will even out, on average. The problem with this assumption is that systematic error may be introduced by broad societal responses to changes in energy prices or to perceptions of energy resource abundance or shortage.

Occupant behaviour may be eliminated as a variable by using test procedures that are so short term that behavioural effects are minimized, or by experimenting with unoccupied housing. Pressure testing is one procedure that falls into the former category, but yields results which are not clouded by questions of occupant behaviour. The Alberta Home Heating Test Facility has been a leader in this sort of work, but there is a need to test conservation measures in full scale housing free of occupant intervention.

## 7. ACKNOWLEDGEMENTS

The author wishes to acknowledge the financial support of the Alberta/Canada Energy Resources Research Fund and of the Alberta Department of Housing for field work which contributed to the development of this paper.

## 8. REFERENCES

1. Marshall, B. and Argue, R., The Superinsulated Retrofit Book, Renewable Energy in Canada, Toronto, 1981, 141-144.

2. Elmroth, A., Forslund, J. and Rolen, C., "Measured energy savings in Swedish homes", Energy and Buildings, Vol. 6, No. 1, Jan. 1984, 39-54.

3. Goldman, C.A., "Measured Energy Savings from Residential Retrofits: Updated Results from the BECA-B Project", Energy and Buildings, Vol. 8 No. 2, May 1985, 137-155.

4. Wolfgram, K.J., "The Experimentally Determined Effectiveness of Insulation Added to the Exterior of Residential Foundations", Thermal Performance of the Exterior Envelopes of Buildings II, Proceedings of the ASHRAE/DOE Conference, December 6-9 1982, ASHRAE, Atlanta, 1983, 527-547.

5 Tsongas, G.A., "Retrofitted Wall Insulation Added to The Exterior of Residential Foundations, Thermal Performance of the Exterior Envelopes of Buildings II, Proceedings of the ASHRAE/DOE Conference, December 6-9 1982, ASHRAE, Atlanta, 1983, 548-570.

6. ASHRAE, Handbook of Fundamentals, American Society of Heating Refrigerating and Air-conditioning Engineers, Atlanta, 1981.

7. Ackerman, M.Y., Dale, J.D., Forest, T.W., Sadler, G.W., Wilson, D.J. and Zaheeruddin, M., Final Report on the Alberta Home Heating Research Facility, Departmental Report No. 34, Department of Mechanical Engineering, University of Alberta, February 1983, p.65.

8. "Basement Heat Loss",Dale, R.D., quoted in "En-Form, Issue No. 6, March 1986, Energy Information Society, Edmonton, P.9.

9. Love, J.A., Townhouse Retrofit Demonstration Project 1983-85: Final Report, prepared for Alberta Energy and Natural Resources, tightness Testing of Sealing Operations on Fifteen Houses", unpublished working draft, December 1983, 28 pages.

11. Bill Johnson Architect Ltd., "Calgary Air Leakage Control Study", prepared for Alberta Energy and Natural Resources, Calgary, November 1985, 22 pages.

12. Unies Ltd., Some Effects of Re-insulation on Some Houses in Winnipeg, Energy Mines and Resources Canada, Ottawa, September 1982.

13. Moffatt, S., The Effects of Re-insulation on 8 Houses in Ottawa, Energy Mines and Resources Canada, Ottawa, October 1982.

14. Grimsrud, D.T., Sherman, M.H. and Sonderegger, R.C., "Calculating Infiltration: Implications for a Construction Quality Standard", Thermal Performance of the Exterior Envelopes of Buildings II, Proceedings of the ASHRAE/DOE Conference, December 6-9 1982, ASHRAE, Atlanta, 1983, 422-452.

15. Love, J.A. and Passmore, R.S., Air Leakage in Existing Townhouses, Alberta Department of Housing, Edmonton, March 1986.

16. Socolow, R.H., "The Twin Rivers program on energy conservation in housing: Highlights and conclusions", Energy and Buildings, Vol. 1 No. 3, April 1978, 207-242.

17. Canadian General Standards Board, Determination of Air-tightness of Buildings by the Fan Pressurization Method, draft, Ottawa, September 1983.

18. Dumont, R.S., Orr, H.W. and Figley, D.A., Air Tightness Measurements of Detached Houses In the Saskatoon Area, Division of Building Research, National Research Council of Canada, Ottawa, November 1981.

19. Sulatisky, M. Airtightness Tests on 200 New Houses Across Canada: Summary of Results, Energy Mines and Resources Canada, Ottawa, January 1984.

20. ASHRAE, ASHRAE Standard 62-81: Ventilation for Acceptable Indoor Air Quality, American Society of Heating Refrigerating and Air-conditioning Engineers, Atlanta, 1981.

21. Lennox Industries, Calgary, Alberta, April 14, 1986, personal communication.

22. Sonderegger, R.C., "Movers and stayers: The resident's contribution to variation across houses in energy consumption for space heating", Energy and Buildings, Vol. 1 No. 3, April 1978, 313-324.

23. Hirst, E., White, D., Goeltz, R., and ings, Vol. 8 No. 2, May 1985, 83-91.

TABLE 1. INFORMATION ON AIR-TIGHTNESS OF 136 HOUSES TESTED IN SASKATOON DERIVED FROM DUMONT AT AL. (18).

| Period When House Was Built | Number of Houses Tested | Average AC50 (ach) | Effective Leakage Area ($m^2$) |
|---|---|---|---|
| 1961-80 | 97 | 3.6 | 0.0320 |
| 1946-60 | 20 | 4.5 | 0.0370 |
| pre 46 | 19 | 10.4 | 0.0600 |

TABLE 2. INFORMATION ON AIR-TIGHTNESS OF 182 HOUSES TESTED ACROSS CANADA DERIVED FORM SULATISKY (19).

| Province | Number of Houses Tested | Average AC50 (ach) | Equivalent Leakage Area ($m^2$) | Effective Leakage Area ($m^2$) |
|---|---|---|---|---|
| B.C. | 20 | 9.3 | 0.157 | 0.0822 |
| Alberta | 14 | 5.3 | 0.119 | 0.0616 |
| Saskatchewan | 20 | 3.2 | 0.055 | 0.0283 |
| Manitoba | 20 | 2.1 | 0.038 | 0.0190 |
| Ontario | 40 | 5.0 | 0.110 | 0.0615 |
| Quebec | 40 | 4.7 | 0.080 | 0.0399 |
| New Brunswick | 7 | 3.6 | 0.073 | 0.0388 |
| Nova Scotia | 3 | 5.2 | 0.129 | 0.0713 |
| PEI | 8 | 4.1 | 0.101 | 0.0662 |
| Newfoundland | 10 | 5.3 | 0.132 | 0.0678 |
| Average (for 182 houses) |  | 4.8 | 0.099 | 0.0536 |

# Detection of Toxic Materials in Workplace and Residential Air using Passive Samplers Coupled to Bioassays

Martin Samoiloff, Ph.D.
Bioquest International, Inc.
204 - 2989 Pembina Highway
Winnipeg, Manitoba
R3T 2H5

## Abstract

Measurement of contaminants in indoor air was performed using two passive samplers, an absorbant sampler to capture organic vapors and another to trap particles. Materials trapped by these samplers were tested for biological effects using a simple bioassay. The absorbant samplers were placed at 639 workplace sites, and detected toxic effects in 127 of these. Stimulatory effects, indicating excessive microbial growth were found at 90 of the tested workplace sites. Particle samplers were placed at 397 workplace sites, and detected 128 toxic locations and 31 stimulatory sites. In residences, of 99 sites tested with the absorbant samplers, 22 showed toxic effects and 14 showed stimulatory effects. Particle samplers were used in 46 residential locations, and these detected toxic particles at 17 locations and stimulatory particles at 6 locations.

## 1. Introduction

A sampler system for detection of toxic materials in indoor air has been developed and field tested. The system consists of two separate samplers, one containing activated molecular sieve 13X to trap organic vapors, and the other containing a buffer solution to trap viable and non-viable particles in air. The samplers are placed at various locations in the tested indoor environment for a 7 day exposure period. The samplers are then sealed and returned to the laboratory where they are extracted and tested for toxicity using the *Panagrellus redivivus* bioassay.

The bioassay detects a series of biological endpoints and provides a quantitative measure of the overall biological effect of the materials trapped in the samplers. As well as detecting direct toxic effects, the biological test also can determine stimulatory conditions, where increased levels of bacterial and fungal growth are found.

## 2. Results and Discussion

Initial tests were performed using the absorbant sampler. A total of 206 workplace locations in 9 different buildings and 46 locations in 7 homes were examined. As shown in Table I, 23.8% of the workplace sites tested showed toxic effects, and a further 10.2% of these sites showed significant stimulation of growth. Interviews of employees at these sites revealed a high level (82%) of complaints about workplace air quality, while interviews of employees at sites where toxic or stimulatory effects were not found revealed a lower level (63%) of air quality-related complaints. Tests on homes using only the absorbant sampler showed 15.2% of the sites to have significant toxic effects, and 6.5% of the sites to produce stimulatory effects.

Larger scale tests using both absorbant and particle samplers were performed at 433 workplace sites in 18 buildings. In 36 of these tests, spillage or evaporation caused the loss of the particle sampler. The absorbant sampler detected toxic effects in 18.0% of the tested sites, while the particle sampler detected toxic effects in 32.4% of the sites. The absorbant sampler detected stimulatory effects in 15.9% of the tested sites, while the particle sampler found stimulatory materials in only 7.8% of the tested sites. There appears to be two distinct classes of contaminants in that each sampler appears to detect different types of contaminant. The particle sampler seems most efficient in smoking areas, near dry process copiers, welding and machine shops, and in areas where high levels of dust occur. The absorbant sampler appeared most efficient in areas where high levels of solvents were present, such as print shops, paint shops, in fume vents, and near liquid-process copiers.

Tests using both absorbant and particle samplers were also applied to 53 sites in 8 different homes. Seven particle samplers were lost due to spillage or evaporation. The absorbant sampler found toxic effects in 28.3% of the tested sites, and detected stimulation in 20.8% of the tested sites. The particle sampler found toxic effects in 37% of the tested sites, and found stimulation in 16.7% of the tested sites. Typically the absorbant sampler found toxic effects in high sites in basements, kitchens and bedrooms, and stimulatory effects in living rooms. The particle sampler found toxic and stimulatory effects primarily in basements and living rooms.

The passive sampler/bioassay system provides a cost-effective method to detect the primary location of material in air that are sources of health complaints.

Table I. Preliminary tests on workplaces and homes using the absorbent sampler only.
T indicates detected toxic effects.
S indicates detected growth stimulation.
- indicates no detected effect.

| | - | T | S | Total |
|---|---|---|---|---|
| Buildings | 136 | 49 | 21 | 206 |
| Homes | 36 | 7 | 3 | 46 |

Table II. Tests on workplaces using the absorbent and particle sampler. The columns indicate the number of particle samplers detecting a particular effect, while the rows indicate the number of absorbent samplers detecting a particular effect.
T indicates detected toxic effects.
S indicates detected growth stimulation.
- indicates no detected effect.
? indicates particle sampler lost.

| Gas/Particle | - | ? | T | S | Total |
|---|---|---|---|---|---|
| - | 175 | 25 | 67 | 19 | 286 |
| T | 48 | 6 | 19 | 5 | 78 |
| S | 41 | 5 | 20 | 3 | 69 |
| ALL | 321 | 36 | 129 | 31 | 433 |

Table III. Tests on residences using the absorbent and particle sampler. The columns indicate the number of particle samplers detecting a particular effect, while the rows indicate the number of absorbent samplers detecting a particular effect.
T indicates detected toxic effects.
S indicates detected growth stimulation.
- indicates no detected effect.
? indicates particle sampler lost.

| Gas/Particle | - | ? | T | S | Total |
|---|---|---|---|---|---|
| - | 14 | 5 | 7 | 1 | 27 |
| T | 8 | 2 | 4 | 1 | 15 |
| S | 8 | 0 | 2 | 1 | 11 |
| ALL | 40 | 7 | 17 | 6 | 53 |

# Agricultural Applications

# AGRICULTURAL APPLICATIONS OF SOLAR ENERGY

James S. Townsend
Agricultural Engineering
University of Manitoba
Winnipeg, Manitoba
CANADA   R2M 0T9

## ABSTRACT

Agriculture has been using solar energy for a very, very long time since the photosynthetic process is powered by solar energy. The dual needs of more food production and energy conservation can be met by the proper application of solar energy in agriculture. Solar energy for process heat and space heating can be used widely in the drying of crops and the heating of animal housing units. Much of the technical information for the application of solar energy is available today but there is still room for innovation. The major problem of cost effectiveness in the application of solar energy to most agricultural applications has not been solved.

## 1. INTRODUCTION

Since the time of Malthus there have been periods of pessimisism due to shortages of food followed by periods of optimism when food supplies seemed to be dependable. In most regions increases in food production have kept up to continually growing populations with the notable exception of Africa. Some agricultural scientists have estimated that the current world food production could be increased about 30 times with maximum inputs of modern high technology (6, 14). But these high inputs would probably be impractical and uneconomical.

A sustainable world population of 10 billion people has been predicted for the year 2200. Other estimates state that the current world population of about 4.5 billion people is already 14 percent too high. Both of these two scenarios imply the same thing. World food production must be increased. If the 10 billion people are to be fed at current levels then food production will need to be increased about 220 percent in the next 214 years.

Much of the needed increase in food production must come from increased yields through better varieties and more fertilizer rather than increased area since most of the prime agricultural land is already in production. More inputs mean that more energy will be needed. Solar energy will be increasingly called upon to supply the additional energy. The really successful agricultural applications of solar energy today will indicate the areas where research effort will be most profitable.

## 2. DISCUSSION

It can be convincingly argued that the best application of solar energy in agriculture is through the natural phenomenon of photosynthesis (9). Life, as it is known on Earth, had its beginning in photosynthesis and has been sustained by photosynthesis (2). Solar energy drives the process of combining carbon dioxide and water into living plant material or biomass. Plant materials, including the fossil fuels, are used by the world's population for food, feed and fiber.

The sun through the solar energy that reaches the biosphere controls agriculture by the type of climate that exists (7). Climate and the effects of weather are the dominant factors in determining the crops that can be successfully grown in any location. Climates are slowly changing and modern agriculture must be able to cope with the changing climate (1).

In some locations agriculture may be determined by a single weather factor. But in most cases the local combination of several weather factors or the sequence of several weather events decide the scale and type of agricultural production. For field-scale agricultural production systems the important weather considerations are as follows: 1. the length of day or night, 2. the temperature of the air and the soil, 3. the solar energy input and growing space heat balance, 4. the rainfall and overall soil-water balance, 5. the evaporation and transpiration of water, 6. the relative humidity, 7. the wind, and 8. any weather hazards such as frost, hail, snow, floods and others.

The sun and solar energy are directly connected with most of the above factors and indirectly connected with the rest. Yields are strongly influenced by the total amount of solar energy received. Solar energy in most cropping systems is not the limiting factor in the determination of total production. Some plants reach the saturation point for solar energy utilization even on moderately cloudy days.

The photosynthetic reaction operates at very low overall efficiency (5). The world average for natural ecosystems is about 0.1 percent. The theoretical maximum efficiency for photosynthesis has been quoted as 23 percent. Under ideal field conditions it is possible to convert about five percent of the incident solar radiation into dry matter. One percent efficiency is possible with many field crops. Sugar cane has been recorded as producing up to 112 tonnes(dry matter)/hectare. This yield would indicate an average efficiency of about 2.5 percent.

The effect of the amount of solar energy absorbed on yields of spring wheat has been illustrated on the Glenlea Research Station at the University of Manitoba. The surface albedo for five different tillage systems was measured over the growing season (13). Albedo, the reflection of incoming short-wave radiation, is an indirect measure of the amount of solar energy absorbed in the growing space. Thus, low albedo values should result in higher yields as illustrated in Table 1. The albedos ranged from a low of 6 percent for the intensive tillage treatment to a high of 16 percent for the zero tillage treatment early in the growing season. At the harvest time all treatments had albedos of 17 percent which was the albedo value for the standing crop.

TABLE 1 AVERAGE WHEAT YIELDS AND MINIMUM AVERAGE ALBEDOS FOR FIVE TILLAGE SYSTEMS (13).

| Type of Tillage System | Average Yield (t/ha) | Minimum Average Monthly Albedo (%) |
|---|---|---|
| Intensive | 2.3 | 6 |
| Deep | 2.0 | 7 |
| Conventional | 1.8 | 9 |
| Minimum | 1.8 | 9 |
| Zero | 1.5 | 15 |

The balance of this paper will deal with agricultural applications of solar energy in areas other than plant growth and photosynthesis. The use of solar energy in greenhouses will not be covered. Most of the information presented here has been selected for its applicability to the agricultural conditions of the Canadian Prairies. In this context short growing seasons with average yearly incident solar energy inputs of approximately 13 MJ/square meter are normal (4, 8).

A current research project in Agricultural Engineering at the University of Manitoba involves the operation of a buried-pipe air-tempering system (11). In reality the system is solar powered with the soil used as a heat sink or source depending on the time of year. Tempered air moving through the buried pipes could be utilized for heating or cooling farm buildings.

A simplified finite-element model was developed to describe the operating characteristics of the system. The model incorporates many system variables including pipe length and diameter, air velocity, soil texture, soil thermal properties, convective-heat-transfer coefficients, inlet air temperature and undisturbed soil temperature. The model also considers ice formation in the soil, condensation inside the pipe and soil moisture migration.

For the specific site conditions at the Glenlea Research Station the model predicts the following steady-state results. A system with a pipe of 0.5 m diameter, 30 m long, and air velocity of 3 m/s would have a heat capacity of 5 kW when air inlet temperature was -20 degrees Celsius. The efficiency would be 20 percent with a temperature gain of 5 degrees Celsius. Efficiency was defined as the actual temperature difference achieved compared to the maximum possible temperature difference. The undisturbed deep soil temperature was 5.8 degrees Celsius.

The efficiency of the system could be improved to about 70 percent by reducing the pipe diameter to 0.15 m. But the system thermal capacity would fall to 1 kW while the temperature difference would rise to 17 degrees Celsius. A generalization to be drawn from this research is that heat capacity varies directly with pipe diameter while efficiency and temperature differential vary inversely with pipe diameter. Longer pipes result in greater heat capacity and greater temperature differentials.

Dimensionless curves were developed that should prove very useful in the preliminary design of buried-pipe air-tempering systems. The curves cover the cases of winter heating of the inlet air and summer cooling of the inlet air. The assumed input variables are manipulated until the desired system efficiency is obtained at which time the variables become the system design parameters.

Solar energy collection for process heat and space heating has many direct applications in agriculture. The applications are in drying processes and in space heating for livestock buildings (10,15). Active solar energy utilization has the characteristics of high cost and low output. Passive solar energy has more promise but the current economics of many applications are not favorable. For instance, high speed grain drying with solar energy is not economical and even solar assisted aeration is not promising if economics are considered.

In spite of the current uneconomical applications of solar energy in agricultural applications much research has been done and is being done. Solar energy powered irrigation pumps in small scale applications have good potential since the need for water coincides with the hours of sunshine so that storage of energy can be avoided. Wind energy could also be of use in some situations where the total demand is not too high.

Crop storage and preservation through cooling and drying or dehydration can be assisted with the application of solar energy. Unfortunately, the cooling requirement for food preservation is usually a 24 hour job every day but solar energy availability, without energy storage, is at peak performance only about 8 hours per day even on clear days. Energy storage in rock beds or similar devices usually increases the cost a prohibitive amount.

Integrated energy systems where solar energy supplements the energy from crop residues for anaerobic digester heating for the production of methane gas are possible. The energy produced in such systems is storable and can be used for space heating in swine nurseries or for tempering ventilation air for animal housing units.

Solar energy utilization in most agriculture production systems still needs a great deal of innovation to produce profitable results. Three examples of creative applications of solar energy are the use of liquid desiccants for grain drying with regeneration of the desiccant by solar energy over a 10 month period in preparation for the next 2 month drying period (3), the possible production of hydrogen directly from biological sources (12) and the use of solar distillation to produce fresh water from saline water for irrigation in arid regions.

## 3. CONCLUSIONS

The problems of food production for the whole world include occasional food surpluses coexisting with long-lasting food deficiencies. For some people it is a question of survival while for others the choice of luxury foods is a matter of the quality of life. Solar energy has always been an essential factor in food production. Basic research in increasing the efficiency of photosythesis could solve food supply problems for a stablized world population for all time.

Much solar technology that has wide application in agricultural production systems has been proven to be technically feasible. There is still much scope for the refinement of these technologies so that they can be profitably applied to agricultural production systems.

## 4. BIBLIOGRAPHY

(1) ____________. 1985. Agricultural Compendium for Rural Development in the Tropics and Subtropics. Elsevier Science Publishing Company Inc., New York.

(2) __________. 1970. The Biosphere. A Scientific American Book, W.H. Freeman and Company, San Francisco.

(3) ____________. 1981. Agricultural Energy Vol. 1 - Solar Energy: Livestock Production. Selected papers and abstracts from the 1980 ASAE National Energy Symposium,

American Society of Agricultural Engineers, St. Joseph, Michigan.

(4) __________. 1981. An Assessment of the Potential of Solar Energy in Manitoba. Prepared for the Manitoba Department of Energy and Mines by UNIES Ltd., Winnipeg, Manitoba.

(5) __________. 1976. Solar Energy in Agriculture. Joint Conference between The University of Reading and the UK Section of ISES, University of Reading, UK.

(6) __________. 1979. A Series of Papers on World Food Issues. Center for the Analysis of World Food Issues, Cornell University, Ithaca, NY 14853

(7) Croxall, H.E. and L.P. Smith. 1984. The Fight for Food - Factors Limiting Agricultural Production. George Allen and Unwin, London.

(8) Duffie, J.A. and W.A. Beckman. 1974. Solar Energy Thermal Processes. John Wiley and Sons, New York.

(9) Fogg, G.E. 1972. Photosynthesis. The English Language Book Society and Hodder and Stoughton, Mill Road, Dunton Green, Sevenoaks, Kent, UK.

(10) Hall, D.O. and J. Morton, Eds. 1982. Solar World Forum - Solar Technology in the Eighties. Proceedings of the International Solar Energy Society Congress, Brighton, UK. Pergamon Press, Willowdale, Ontario.

(11) Lei, Q., M.G. Britton and J.S. Townsend. 1985. Modeling Air Tempering with a Soil-Heat Sink/Source. Paper No. 85-4016 presented at the 1985 Summer Meeting of the American Society of Agricultural Engineers, St. Joseph, MI 49085

(12) Lewis, A. 1983. A Solar Cell Based on a Biological System. Engineering: Cornell Quarterly, 17(4), Spring 1983.

(13) Townsend, J.S. and P. Migchels. 1981. Albedo of Wheat Fields Under Five Tillage Systems in Manitoba. Paper No. 81-1014 presented at the 1981 Summer Meeting of the American Society of Agricultural Engineers, St. Joseph, MI 49085

(14) Townsend, J.S. 1983. Potential Use of Hydrogen in Agricultural Production on the Canadian Prairies. A paper presented at the First Canadian Hydrogen Workshop, Vancouver, B.C., 83 05 09-10.

(15) Vogt, F., Ed. 1981. Energy Conservation and Use of Renewable Energies in the Bio-Industries. Proceedings of the International Seminar on Energy Conservation and the Use of Solar and Other Renewable Energies in Agriculture, Horticulture and Fishculture. Pergamon Press, Willowdale, Ontario.

# AN EVALUATION OF DUAL ROLE CURTAINS FOR ENERGY CONSERVATION AND SHADE REQUIREMENTS IN COMMERCIAL GREENHOUSES

Ewart Brundrett
Dept. of Mechanical Engineering
University of Waterloo
Waterloo, Ontario, Canada

Vahab Hassani
Dept. of Mechanical Engineering
University of Waterloo
Waterloo, Ontario, Canada

## ABSTRACT

The application of energy conserving curtains is examined in commercial greenhouses. The study is extended to include dual role curtains, that provide summer solar shading, as well as energy conservation, since they provide an added economic advantage. A highly insulative thick curtain, and a semi-opaque thick curtain have been extensively tested in the laboratory and in commercial applications. A new highly reflective polyester and aluminum curtain is examined.

## 1. INTRODUCTION

Energy conserving curtains have played a significant role in commercial greenhouses for more than a decade. In fact houses operated during the months of December to February usually require 50% of the total heat demand of the year, in Southern Ontario, due to the low light levels and low temperatures, (1). Many greenhouse operators have avoided growing during these energy intensive months, to reduce operating costs. However, their vegetable crops often arrive at the market at the same time as southern field crops, thereby obtaining a lower price. The installation of energy curtains is an obvious alternative that permits growing during the winter months at significantly reduced energy levels. However, the curtains must be economically feasible. The resulting energy savings must be at least as great as the annual cost of the curtain installation and operation, as well as any loss of productivity resulting from light blockage by the stored curtains.

Simpkins, et.al. (2), conducted an early study of thin film materials in single glass greenhouses. He concluded that energy savings at night could be as high as 59% for well sealed curtains, but was often reduced to 46% or lower by air leakage between the curtain and the glazing.

Winspear et.al. (3), (4), have shown that energy curtains can appreciably reduce heat demands during high winds, for single glazed greenhouses, if the curtains were well sealed when deployed. Evidently air that infiltrated between the laps of the glass did not come into direct contact with the heated crop growing zone positioned below the curtains. Instead it would appear that the air that infiltrated through the windward roof laps was exhausted through the downwind roof laps.

A parallel development has been the increasing percentage of greenhouse construction that is partially or totally double glazed. Double glazing is applied to all side walls in most new houses, as well as to an increasing number of the roofs. There is a marked reduction in air leakage, since the many lapped joints of glass construction is overcome, in fact air leakage rates of as low as .5 air changes per hour have been suggested by Winspear et.al. (3), (4). Two layers of polyethylene separated by air pressure has been widely applied for roofs, since it can be deflated during snow buildup to enhance the melting rate, however, the material has to be replaced every two to three years. Nevertheless the material has received wide acceptance due to the low initial cost and relative ease of replacement. In short it provides a very good economic solution to energy conservation.

A rigid double walled acrylic or polycarbonate sheet have been used as well. These materials are typically of 1.2 m width, and of varying lengths of up tp 10 m. The two surfaces are separated by an air gap of 6 to 16 mm. Spacing is achieved by regularly spaced flutes that connect perpendicularly to the two surfaces. The flutes reduce the thermal resistance of the sheet, but provide significant structural rigidity. The sheets if properly installed can be nearly as effective in infiltration reduction, as is double layer polyethylene. A 6 mm double walled polycarbonate sheet was chosen for the following experimental and model studies.

Finally, it has been shown by Brundrett et.al. (5), (6), that dual purpose energy and shade curtains have the best promise of rapid economic repayment for greenhouse applications in southern Ontario. Often, in fact, horticultural considerations will require the use of shade curtains in the summertime. The additional use of the curtains for energy conservation in the winter is an important but often secondary consideration.

## 2. CURTAIN MATERIALS AND INSTALLATIONS

### 2.1 Gutter to Gutter Installations

A typical gutter to gutter curtain installation can be seen in figure 1.

Gutter to gutter curtains were an early favourite of greenhouse operators, particularly to retrofit existing houses. The curtains were installed below overhead heating lines, ventilation tubes, and rack and pinion drives of overhead vents. The arrangement is acceptable provided that the gutter height permits sufficient head room after the curtains are installed. Often, however, the limited headroom and overhead clutter has prevented the installation of curtains by any means in older houses.

Disadvantages of gutter to gutter curtain systems include the isolation of overhead ventilation tubes heating lines, and lights, during the night time.

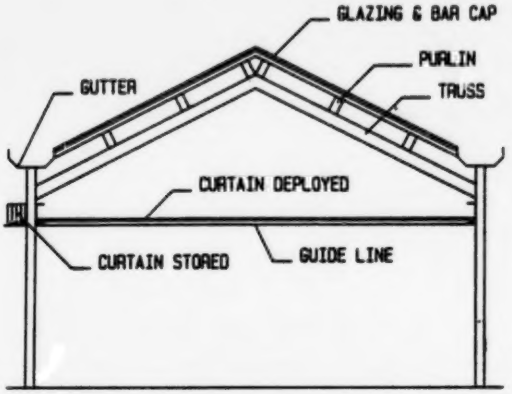

Figure 1. A typical gutter to gutter curtain installation. Showing stored and deployed positions.

In addition light blockage of the curtains is concentrated at the gutter location. Brundrett et.al. (6), have shown that a thick curtain installed in a rose greenhouse significantly increased light blockage. The horizontal gutter shadow was increased from a value of approximately 1 m to a value of 2 m with curtains installed. Even though significant energy conservation was achieved, it was outweighed by the loss of productivity associated with the increased light blockage. This effect is most pronounced for greenhouses situated such that the gutters run in an east-west direction.

In addition, gutter to gutter curtains trap a great deal of cold air in the curtain-glazing zone. Care must be exercised when opening curtains on cold mornings to ensure that the crop is not chilled. The problem has been largely overcome by either turning on heating lines in the cold zone prior to opening the curtain, or by only opening the curtain a small amount, until the cold zone is warmed.

## 2.2 Truss to Truss Installations

A typical truss to truss curtain system can be seen in figure 2.

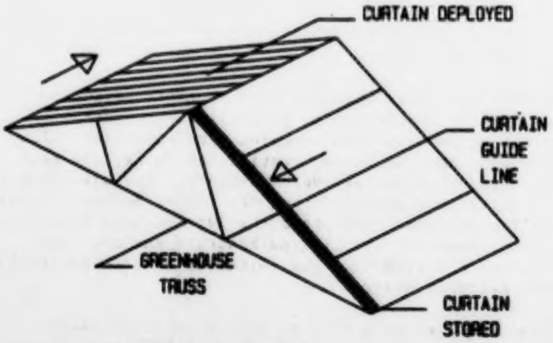

Figure 2. A typical truss to truss curtain installation, showing stored and deployed positions.

Truss to truss curtain systems are being increasingly favoured by builders and growers. The curtains are often provided with a separate sub-truss that supports the curtain hardware and guide lines. If necessary the curtains can be placed well below the glazing, to clear vent hardware. Curtains of one truss can be attached to those of a second truss below the gutter; provided that the gutter posts are located at the trusses. The resulting curtains installations can be made quite air tight by using sealing strips on the leading edge of the travelling boom, as shown in figure 3.

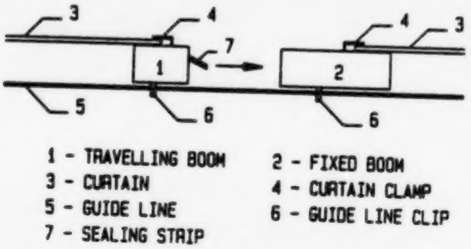

Figure 3. Details of typical truss to truss curtain hardware. Drive motor and mechanisms are not shown.

Good closure is achieved by the sealing strip when it is brought into firm contact with the fixed boom by the gear motor and rope wrap or rack and pinion drive. This has been an increasingly evident feature of installations and hardware that has been observed in Canada, and more particularly, in Great Britain and the Netherlands, (7).

Truss to truss curtains overcome many of the disadvantages of gutter to gutter arrangements. Overhead lights, ventilation tubes and heating lines are not isolated at night. The volume of air between the curtain and glazing is significantly reduced. There is no loss of headroom. And, finally, the additional light blockage of the stored curtains is more distributed than for gutter to gutter applications. In fact, the geometry of the system results in fewer unfavourable greenhouse orientations, with due north-south being the only undesirable direction above 50 degrees north latitude.

A further refinement of the boom arrangement of figure 3 has been the replacement of the box sections by "C" sections that permit storage of the curtain within the booms during the daytime, (7). The further reduction in light blockage is significant, and the curtain material is shielded from solar degradation and dust accumulation.

## 2.3 Curtain Materials

The advent of double glazed materials for greenhouses, has placed increasing emphasis on energy curtains that possess improved thermal resistance. Two curtain materials have been extensively tested that can best be described as thick curtains. They may be seen with reference to figure 4.

Curtain 4b was developed in 1979 by Brundrett and Brundrett (8), and has been in operation in their greenhouse since that time. The three layers are sewn together at the edges of the curtains, and at pleats which are formed on alternate sides, at spacings of 225 mm. The material has proven to have excellent wear and solar resistance, but is bulky when stored in the daytime. The significant daytime solar blockage and high initial cost are disadvantages of this material. The material is completely opaque, and thus may be used for solar blackout in the summer, but not for solar shading. Nevertheless, the material has made practical the growing of Nigerian orchids throughout the year in southern Ontario, since 1979.

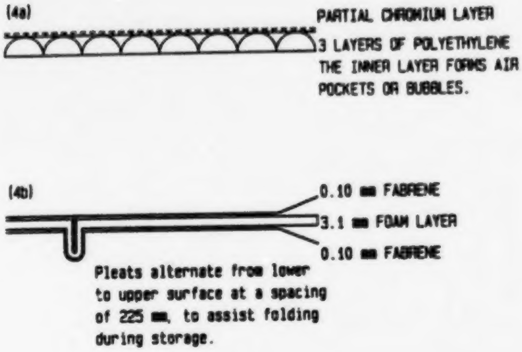

Figure 4. Two thick curtain materials. 4a is a polyethylene bubble film material. 4b is fabricated from two layers of fabrene and a layer of polyethylene foam.

Curtain 4a is recent design. The partial chromium layer on the top surface provides some reflectivity while permitting approximately 40% solar transmission. The material is fabricated into curtains of custom size by heat welding. The curtain must be suspended from the guide lines, by plastic hooks, since it has low wear resistance. The material has proven to have a rather high level of solar shading, is prone to rapid wear and tearing, and is quite bulky when stored, (5). Significant energy conservation was achieved using this curtain material, however, the bulk of the curtains created a significant reduction in light transmission and in productivity, (6), for winter rose crops. It was concluded that the material presented too many disadvantages to be readily accepted by commercial growers.

A curtain recently developed in Sweden, figure 5, was considered next.

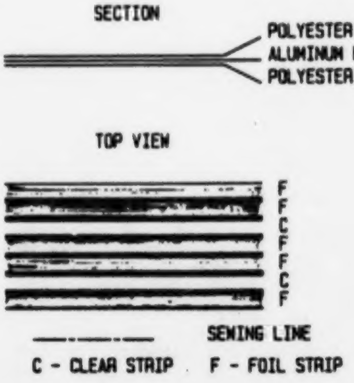

Figure 5. A thin composite curtain with a pattern of two strips of aluminum foil, and a clear strip. This curtain has a 66% solar shading coefficient.

This curtain is fabricated by placing 5 mm strips of .05 mm aluminum foil between two .1 mm layers of polyester film. The layers are held together by sewing along each edge of the aluminum foil. Gaps can be left between the strips of aluminum foil by selective removal, to create a lattice type of shade curtain. The resulting thermal properties are still quite attractive, with respect to energy conservation. In addition, the curtain provides solar shading during the summer. The dual role has been shown to be an economic advantage, (6).

The commercial material has specified code names, such that LS 10 refers to a completely clear curtain, i.e., there are no aluminum strips; LS 11 is a completely opaque curtain, i.e., there are no gaps between the aluminum strips; and LS 16 is the 66% solar shading curtain shown in figure 5.

The thermal radiation properties of the five curtain materials and 6 mm double walled polycarbonate glazing are presented in table 1. The properties were experimentally determined using a Gier-Dunkle DB-100 reflectometer. Hemispherical emissivity corrections were made per figure 4-6 of Siegel and Howell, (9).

TABLE 1

RADIATIVE PROPERTIES OF CURTAINS AND GLAZING

| Item | Emmis. upper | Reflt. upper | Trans. upper | Emmis. lower | Reflt. lower | Trans. lower |
|---|---|---|---|---|---|---|
| Fabrene Fig. 4b | 0.07 | 0.30 | 0.00 | 0.70 | 0.30 | 0.00 |
| Bubble film | 0.68 | 0.12 | 0.20 | 0.65 | 0.15 | 0.20 |
| Glazing 6 mm | 0.50 | 0.10 | 0.40 | 0.50 | 0.10 | 0.40 |
| LS 10 clear | 0.41 | 0.14 | 0.45 | 0.41 | 0.14 | 0.45 |
| LS 11 opaque | 0.25 | 0.75 | 0.00 | 0.65 | 0.35 | 0.00 |
| LS 16 66% shade | 0.30 | 0.55 | 0.15 | 0.57 | 0.28 | 0.15 |

LS 16 properties are 1/3 LS 10 and 2/3 LS 11.

## 3. EXPERIMENTAL AND ANALYTICAL CURTAIN EVALUATIONS

### 3.1 Experimental Tests

A thermal rig was constructed to test combinations of the 6 mm glazing material with and without curtains. The rig was instrumented and calibrated in a laboratory, and was transported to the roof of the laboratory to obtain authentic winter night sky conditions. The rig accommodated a standard 1.22 m by 2.44 m sheet of glazing. The bubble film and fabrene curtain materials of figure 4 were tested, at a distance of 75 mm below the glazing. The rig was operated in a horizontal position to obtain a unity sky view factor. The side and bottom walls of the rig were insulated with 150 mm of SM styrofoam, which reduced heat loss through these surfaces to 6% of the total loss, the remainder being through the glzed surface. The side and bottom surface heat loss was subtracted from the calibrated electrical heat input to obtain the glazed surface heat loss.

The test rig was instrumented to provide the house, curtain, air gap, inner glazing,outer glazing, and outside air temperatures. Sky radiation temperature was calculated from the correlation of Paltridge and Platt,

$$\sigma T_{sky}^{4} = 5.31x10^{-13} T_{a}^{6} + 60CC$$

$T_a$ is the ambient air temperature, and CC is the cloud cover, CC = 1 for fully cloudy conditions, and = 0 for clear sky conditions.

Test results for the glazing alone, and with either of the two curtain materials are given in the following figure 6. Full details of the test rig are given by Hassani (10).

### 3.2 Analytical Model

Heat loss through a glazed surface with and without a curtain was investigated analytically by Hassani (10). The model permits the curtain material to be transparent, semi-opaque, or opaque. Double glazing is incorporated, with semi transparent thermal properties, as noted in table 1. The model uses a 15 by 15 matrix to describe the various radiative, convective and conductive heat transfer paths. Air leakage between the curtain and the glazing is accommodated by a leakage parameter. Heat loss through the curtain-glazing system is examined for given house and ambient air temperatures, and for a specified cloud cover. The heat loss rate is adjusted by the matrix solver routines, until a match of experimental and analytical temperatures is achieved for the curtain, air gap, inner glazing and outer glazing components. The resulting analytical heat loss is then compared to the experimental value. Results of the analysis can be seen in figure 6. Agreement between the analytical and experimental results is to within 5% in all cases that were examined.

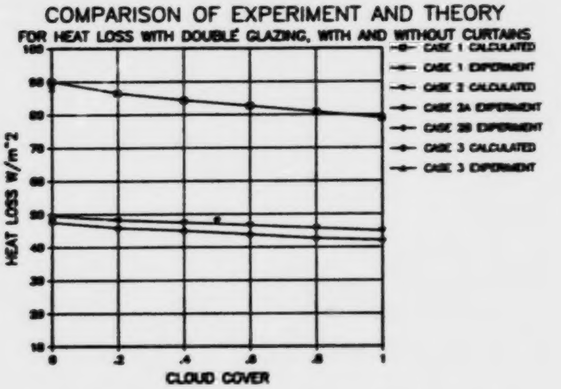

Figure 6. Case 1, no curtain. Case 2, Fabrene curtain. Case 3, Bubble film curtain.

### 3.3 Thermal Resistance Values

The thermal resistance of the various glazing and curtain materials was obtained based upon the relationship

$$\text{Heat loss} = (\text{T house} - \text{T ambient})/\text{Thermal Resistance} \quad (2)$$

The results have been extended analytically to include the LS 10, 11, and 16 curtains, using the properties given in table 1. The results can be seen in figure 7.

It is very interesting to note that the LS 11 curtain provides the best thermal resistance, due to its reflective properties. Of equal interest is the fact that the clear LS 10 curtain has a thermal resistance that is 80% of the LS 11 value. The thermal resistance of the LS 16 curtain has been obtained by direct ratio of the LS 10 and 11 values, in the proportions of 2/3 LS 11, and 1/3 LS 10.

The thermal resistance values may be equated adequately by the correlation,

$$\text{Thermal resistance} = R1 + R2 \times CC \quad (K\text{-}m^2)/W \qquad (3)$$

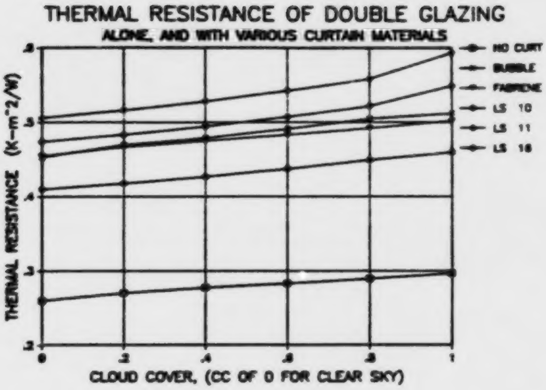

Figure 7. Thermal resistance for combinations of glazing and curtains.

The coefficients for the various combinations are given in table 2.

TABLE 2

THERMAL RESISTANCE OF 6 mm POLYCARBONATE GLAZING ALONE AND WITH SPECIFIED CURTAINS FOR WINTER SKY CONDITIONS IN S. ONTARIO

| | Glazing Alone | Glazing + Fabr- & Foam | Glazing + Bubb. Film | Glazing + LS 10 Clear | Glazing + LS 11 100% Al | Glazing + LS 16 66% Al |
|---|---|---|---|---|---|---|
| R1 | 0.260 | 0.455 | 0.453 | 0.410 | 0.506 | 0.474 |
| R2 | 0.037 | 0.047 | 0.059 | 0.050 | 0.066 | 0.061 |

### 3.4 Temperature Profiles

The analytical model solves for the heat loss through a specified combination of glazing and energy curtain by matching experimental and computed temperatures at the intermediate temperature nodes, and by computing the sky radiation temperature. The intermediate nodes are: T curtain, T air gap, T glaze 1, and T glaze 2. Solution for the temperature at these intermediate nodes was confirmed by comparing the experimental and analytical values for overall heat loss through the glazed surface. Once confidence in the process was established, it was possible to extend the analytical method to new conditions, such as variations of sky cloud cover (CC), and new curtain properties.

The analytical method has been used to examine the temperature profiles of the LS 10, 11, and 16 curtain materials, specified in tables 1 and 2. Results are presented graphically for the Fabrene and Foam (curtain 4B of figure 4), in figure 8.

The values of T house and T air out were those of the experiment noted as case 2A in figure 6. The line CC = 0 is a very close match of the experimental and analytical values (to within 3%). The additional curves were obtained via the analytical method.

It is interesting to note that both the experimental and analytical data present values of T glaze 2 that are lower than T air out. This was expected, since direct radiation transfer from the house to the glazing is blocked by the opaque curtain. It is also interesting to note the very high values of curtain temperature that are maintained. This in turn must have a beneficial effect upon the leaf canopy within the greenhouse.

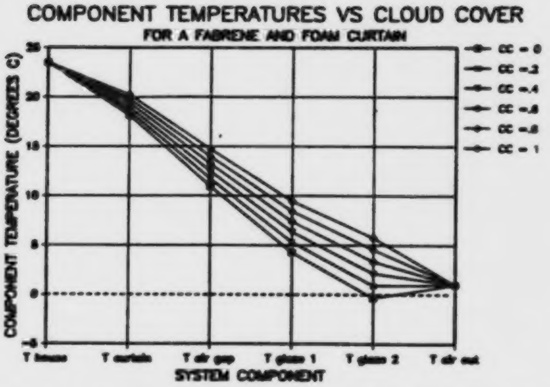

Figure 8. Component temperatures for the Fabrene and Foam curtain of figure 4b, by experiment and analytical method.

The analytical method is extended to the 100% aluminum foil and polyester curtain (LS 11), in figure 9.

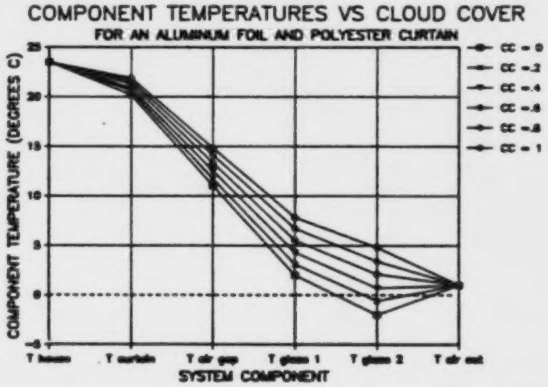

Figure 9. Component temperatures for the LS 11 aluminum and polyester curtain by the analytical method.

Again, it is interesting to note that T glaze 2 is less than T air out. In fact, the highly reflective outer surface of this thin curtain provides superior performance to that of the Fabrene and Foam curtain. Note also the superior LS 11 curtain temperatures.

Finally, the temperature profiles are plotted for the clear polyester curtain LS 10, in figure 10. Radiation transfer through the curtain to the glazing is evident, when the curtain and glazing temperatures are examined. Nevertheless, the performance of this clear thin curtain is encouraging. In fact, some growers leave the LS 10 curtain deployed during the daytime in very cold or windy weather, thereby significantly enhancing the total day and night energy conservation (7).

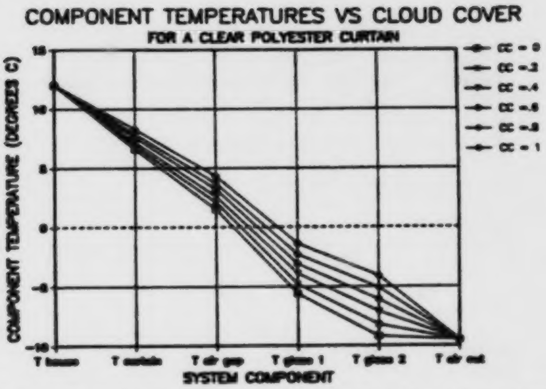

Figure 10. Component temperatures for the clear polyester LS 10 curtain, by the analytical method.

## 4. CONCLUSION

The application of energy conserving curtains was examined in commercial greenhouses. The study was extended to include dual role curtains, that provide summer solar shading, as well as energy conservation, since they provided an added economic advantage. A highly insulative thick curtain, and a semi-opaque thick curtain have been extensively tested in the laboratory and in commercial applications. A new highly reflective polyester and aluminum curtain was examined.

It was found that the properties of the two thick curtains could be quite successfully defined using a combined radiative and convective model. A heat transfer test rig was constructed to test the materials under winter night time conditions. Very good agreement has been obtained between the model and experimental results, by using an existing correlation of night sky radiation temperature vs. cloud cover, and by including an air leakage parameter.

It was found that the new highly reflective curtain provided slightly superior thermal resistance, for a double glazed structure, when compared to the two thick curtains. The thin curtain can be stored in a much smaller volume during the daytime, thereby significantly reducing light blockage, during winter months. The removal of selected strips of aluminum from the curtain provides a lattice like arrangement for summer shading. A curtain was examined that has one third of the strips removed, thereby providing two thirds solar shading. It was found that the resulting thermal resistance was still quite significant.

## 5. ACKNOWLEDGEMENTS

The authors wish to express their appreciation for the continuing operating grant support of NSERC.

The senior author expresses his appreciation for a sabbatical research grant and sabbatical time provided by the University of Waterloo. The grant and sabbatical permitted an extensive examination of the greenhouse industry in several European countries.

## 6. REFERENCES

(1) Brundrett, E. "Solar Greenhouse Design Considerations for Cold Climates", Solar Energy Conversion: An Introductory Course, edited by Dixon, A.E. and Leslie, J.D., University of Waterloo, Waterloo, Ontario, Pergamon Press, 1978.

(2) Simpkins, J.C., Mears, D.R. and Roberts, W.J. "Reducing Heat Loss in Polyethylene Greenhouses:, Trans. ASAE, Vol. 19, 714-16, 1976.

(3) Winspear, K., "Thermal Screens for Glasshouse Fuel Saving", National Inst. for Ag. Eng. (NIAE) England, Subject Day Nov. 1976, paper no.7.

(4) Winspear, K., and Bailey, B., "Thermal Screens for Greenhouse Energy Effectiveness", NIAE Subject Day Aug. 1978.

(5) Brundrett, E., Brundrett, L., and Quist, B., "Evaluation of Energy Conservation Techniques for Greenhouse, Vol. 3, Part 1, Design, Construction, and Installation of Thermal Curtains", Dept. of Mech. Eng., University of Waterloo, For Ag. Can., report no. 23SV. 1916-1-EC31, Dec. 1984.

(6) Brundrett, E., Dam, D., Klepp, M. and Brundrett, K., per (5), "Vol. 3, Part 2, Influence of Thermal Curtains on Energy Demand, Light Levels and Plant Productivity", Dept. of Mech. Eng., University of Waterloo, for Ag.Can., report no. 23SV.1916-1-EC31, Dec. 1984.

(7) Brundrett, E., "Greenhouse Energy Conservation Technology and Protected Growing Practices in Selected European Countries" Dept. of Mech. Eng., report no. GR-SB85, University of Waterloo, Sept. 1985.

(8) Brundrett, E., and Brundrett, G., "A Canadian Energy-Efficient Solar Greenhouse", Journal of the Royal Horticultural Society, Vol. 109, part 12, 499-503, Dec. 1984.

(9) Siegel, R., and Howell, J.R., Thermal Radiation Heat Transfer , McGraw-Hill Book Company, 1972, pg. 104.

(10) Hassani, A., "The Effect of Insulating Curtains on Heat Loss from Glazed Structures", M.A. Sc. Thesis, Department of Mechanical Engineering, University of Waterloo, 1983.

# DEVELOPMENT OF A PROGRAMMABLE CONTROLLER FOR ATTACHED SUNSPACES

F. W. Chapin
H. D. Chapin
ABL Technologies Ltd.
Box 5550, Station B
Victoria, B.C. V8R6S4

## ABSTRACT

A programmable controller was designed to control temperatures in buildings with an attached sunspace. The controller senses temperatures in the sunspace, house and outside the building and also controls fans and other electric devices such as cooling vents in the sunspace and house, air to air heat exchangers and domestic hot water heaters. The design is based on a microcontroller integrated circuit and includes a real time clock, analog to digital circuitry, memory, and a serial interface port. A truth table is used to implement the desired control algorithms. The table can be modified by the user to implement alternative control strategies or to customize the controller for particular buildings. The controller design provides a degree of flexibility facilitating control of integrated systems which is not available in temperature controls currently on the market.

## 1. INTRODUCTION

Sunspaces, which collect solar heat and provide sunny living space, are both effective passive solar heating systems and a desirable architectural feature [1]. Sunspaces have become an increasingly popular design feature in new buildings and retrofits, but control systems have not kept pace. The research which this paper is based on suggests that there is a need for advanced control of integrated systems designed specifically to optimize temperature control in buildings with attached sunspaces through utilization of microprocessor capabilities [2].

To adequately control a building with an attached sunspace by using conventional controls requires a number of sensors and relays. This arrangement usually leads to a redundancy of discrete components. If the control logic is at all complicated it can be difficult or impossible to implement with conventional control devices.

The introduction of the microcontroller chip with a number of input and output ports has made it possible to implement sensing, control, and control logic with a minimum of components. Use of a microcontroller system for control implementation also provides additional benefits over using discrete components. In the sunspace controller design presented here a digital display indicates the time and temperature at different locations. A real time clock provides the time of day, allows 7 day programming, and provides for control of appliances on time schedules such as the hot water heater. Data such as high and low set points, the minimum/maximum temperature, or a weeks worth of temperatures can be stored by adding memory. The math capabilities of a microcontroller allow for the use of inexpensive non-linear sensing devices such as thermistors. In addition, advanced algorithms for the control of buildings can be implemented as they are developed since the microcontroller circuit is programmable and can do mathematical manipulation.

Although there are a number of programmable controllers available there are none which are specifically designed for use in attached sunspaces. The generic "programmable" building controllers on the market are mostly for simple buildings (one zone) and provide little flexibility. The controller described in this paper includes features of some existing controllers, however it is designed specifically to optimize temperature control in attached sunspaces.

## 2. DESIGN & CONTROL OF SUNSPACES

Designs for sunspaces are as numerous as the number of sunspace designers and builders. Usually sunspaces are added on or designed into a building in a particular climate with particular occupants in mind. This makes them very personal and resistant to generic control schemes and controllers.

### 2.1 Sunspace Use

Sunspace use can be categorized by function: heat production, plant production, and additional living space [3],[4]. Once designed the sunspace is apt to reflect a mixture of the three design types, e.g. some plants, some use as a living space. Although it appears that there are three distinct types, in actuality the use of the sunspace may result in a blending of types which complicates the temperature control strategy requirements.

According to a survey of sunspace designers the main reason people build attached sunspaces is to increase their living space [2]. Energy savings and improving the aesthetics of the house are secondary considerations. Plant growing is not a primary motivation for construction of sunspaces, yet the majority of sunspaces are used for growing some plants according to the survey.

### 2.2 Control Problems

The problem with sunspace control based on the perspective of the designer survey is primarily one of maximizing heat gain, the solar collector function, while providing a comfortable addition to the occupant's living space. It appears that the end result or design goal of the sunspace designer is not always compatible with the functional use of the space by the occupant. It is therefore important to be able to change control algorithms once the building is constructed and lived in (or added on to).

The basic problems of sunspace control according to this survey and other research on passive solar buildings are discomfort due to temperature fluctuations and sun damage to objects in the sunspace [5,6]. The majority of buildings monitored in studies by SERI and NRC used fans and other mechanical devices to control temperature [7,8,9]. This method of temperature control does not appear to be highly satisfactory; studies indicate that a significant proportion of solar home occupants, over thirty percent in one survey, are uncomfortable due to excessive temperature swings [6]. This indicates the need for an effective sunspace controller. Given the range of sunspace designs and goals, a programmable controller has a major advantage in sunspace control because of its flexibility. This design allows for advanced control algorithms to be implemented and for changes to be made in the function of the controller after it is installed in a building.

In a paper on "Control Applications and Limitations" [10], the author suggests the following requirements for new controllers: marginal cost-effective (justified by life-cycle costing), time variant (to meet changing environment), adaptive (adjust for changing input/output loads), predictor (anticipate heating and cooling loads), versatile, standardized, flexible, reprogrammable, conservation directed. Simple and thorough checkout procedures need to be developed. New controllers should have self testing of all modes once hooked up. Research should emphasize the development of algorithms [10]. Other reports on controls for solar energy systems [9,11] suggests a number of similar items for new controller design. The use of microprocessors will enable more complex and flexible designs using advanced algorithms to be implemented in future controllers. The technology is such that these future devices will also be smaller and use less expensive components. Within the next ten years buildings that now use a variety of fractional horsepower motors will undoubtedly contain as many or more microprocessor devices. Occupants will become more accustomed to "programming" devices and a computerized thermostat will be as common as a microwave with programmable features.

### 2.3 Control Methods

The temperature control of attached sunspaces and adjoining building can be accomplished by three basic control methods: 1. appropriate building design, 2. manual controls, 3. automatic controls.

One of the main problems for designers appears to be reconciliation of the design goal of a Type 1 heat producer sunspace with the actual use of the solarium as a Type 3 living space. Occupants want both free solar heat and a comfortable place to sit and many want to grow plants as well. Control strategy should therefore minimize energy, but optimize for comfort as defined by the occupants.

Appropriate building design involves configuration of the attached sunspace to satisfy the needs of the occupant by the use of overhangs, thermal storage, convective heat transfer, etc. to minimize temperature swings in the living space(s) and still have the sunspace provide useful heat. Since the design of sunspaces is still evolving, good sunspace design is still part art and a sunspace expert in one climate may not anticipate the climatic conditions correctly somewhere else. Even if the building is a "perfect" design there is no telling what the occupant might do, such as add rugs, plants, animals, or space heaters.

Manual controls rely on the occupant to be present in the building and to operate things like movable insulation, sliding glass doors, windows, and vents. Manual controls are effective as long as the occupants have the commitment, time, or knowledge to operate a sunspace in an optimal way.

Automatic controls are typically wired with low voltage (24 vac) control wiring. Temperature is sensed by the use of vapour filled tubes actuating a mechanical switch closure. By using a number of different devices, transformers, and relays simple control schemes can be implemented. More recently differential thermostats have been used which sense the temperatures at two different points and turn on/off a device (e.g. fan) based on the temperature difference and hysterisis set points. On/off and differential thermostats work for simple requirements but usually involve duplication of sensing elements and control logic to implement even the simplest control logic. Advanced algorithms cannot be implemented and there is little in the way of diagnostics or error checking. Additionally the wiring of the relays, thermostats, and transformers requires control expertise to implement a particular strategy using relay logic.

A programmable controller is well suited for use in sunspaces because it has the technical sophistication to deal with complex control requirements and also has the flexibility to be used in a broad range of sunspace designs and to suit requirements for individual circumstances [10,9].

## 3. SUNSPACE CONTROLLER DESIGN

The objective of the research was to design an advanced sunspace controller that is easy for the end-user to operate, can be programmed to suit specific climates and lifestyles, provides for error checking, optionally provides for system diagnosis, satisfies local code requirements, and is cost effective by life cycle costing methods.

### 3.1 Hardware Design

A block diagram of the controller design is presented in Figure 1. The main integrated circuit is IC17 the MCU (microcontroller unit). Communication with the MCU is provided by 4 ports labeled P0-P3. Ports 0 and 1 are used for data and address lines. Port 2 is an output port used for control of the output signal lines. Port 3 is configured for both input/output. Lines 0 and 7 from port 3 go to a serial input/output line (RS-232C type). Lines 1 and 2 are held high (+5vdc) with a pull-up resistor and go to 2 momentary single pole single throw contact switches on the front panel for user input. Lines 4, 5 and 6 drive the 4 digit LED display circuit on the front panel (for display of temperature, time, etc.).

### 3.2 Memory

The controller was designed with ROM for permanent program storage and RAM for storage of variables. Default values for the variables are programmed in the ROM for quick installation set-up and start-up in case of power failure. For expansion a 8k by 8 bit ROM was chosen. This provides plenty of room for program and data table storage (e.g. a preliminary program to control a sunspace used about 3k of the 8k available). An EEPROM, electrically erasable ROM, is being considered in future designs.

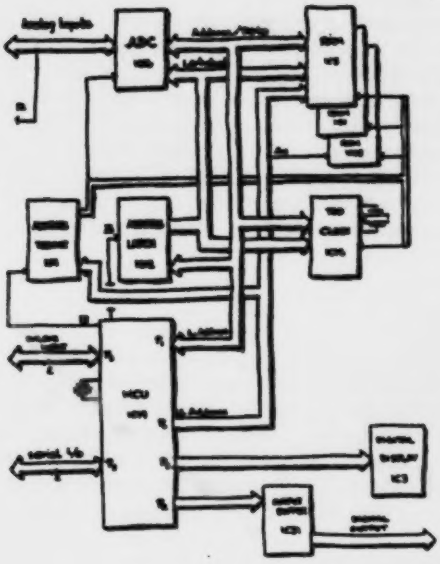

Fig. 1 System Block Diagram

### 3.3 Signal Input (Analog to Digital Conversion)

The controller is configured for thermistors by software. The specifications or type of sensor used can be easily changed. Standard logrithmic scale 10 kilo-ohm at 25 deg C thermistors were used. The analog to digital converter IC (ADC) is operated in radiometric mode (the same reference voltage for the ADC as the supply voltage for the thermistors). The ADC converts the direct current thermistor reading to an 8 bit value (0-255). A software conversion routine converts the thermistor signal to degrees C for internal variable storage and for the LED display. The conversion procedure provides a resolution of about a half a degree C up to about 30 degrees C and about 1 degree above 40 deg C. Optional sensors (for measurement of humidity, solar radiation, wind, barometric pressure) can also be implemented by changing the voltage divider resistors used for the thermistors and/or making changes in software.

### 3.4 Signal Output

Low voltage direct current (5 vdc) is used for output signals. Signal outputs are controlled through software by assigning a byte value to port 2. For example, if line number 1 is to be turned on (out of 0 through 7) then the number 2H (hexadecimal or 0000 0010 in binary) is assigned to port 2. If lines 2 and 3 need to be on simultaneously port 2 is set equal to 6H (0000 0110 binary). The signal output from the microcontroller chip drives a buffer, IC21, which in turn is used to drive a standard TTL type (5 volt dc input) triggered Solid State Relay (SSR) to control high voltage AC. Solid state relays include optical isolation and zero cross over detection which provide signal isolation and decrease line noise. As an option, a domestic hot water heater can also be controlled on a time schedule. Another option is wiring two or more of the outputs to a multiple speed fan to implement proportional control algorithms.

### 3.5 Display and Clock

A serially driven 4 digit LED is used for the controller display. The display is driven by a circuit which decodes a serial 32-bit signal. The four digits are individually software programmable providing useful display of symbols in addition to numbers 0-9, e.g. "-","H","L." The display driver routine is programmed in ROM with the character decode table.

The time of day is kept by a real time clock integrated circuit, IC15. The clock IC has internal RAM which is used to store the wake up and sleep set times for the controller. Times are stored in BCD format in the clock IC memory. The clock keeps track of the day of the week, day of month, and month for seven day timer implementation. IC15 also has a power down mode which will keep the memory alert for as little as 20 microamperes if powered by a small battery of 3 vdc.

### 3.6 Software Design

An initial analysis of the controller operation was examined, requirements written, and a flow chart developed. A number of different programs were written to test various components and meet the operational requirements.

A control program initializes all variables, drives the display, reads the input devices (thermistors, dial and front panel buttons), allows for changes, and provides signal outputs dependent upon the control logic in the truth table.

### 3.7 Control Implementation

Use of the controller is illustrated in an example of an hypothetical attached sunspace. Figure 2 shows the measured temperatures, t1 (outside), t2 (sunspace), t3 (inside temperature of attached building) and control points c1, c2, c3, and c4 for a building with attached sunspace. Where c1 = control of a vent fan in the sunspace, c2 = fan between the sunspace and attached building, c3 = furnace in the attached building, and c4 = vent fan or air conditioner for attached building. The control points represent control signals not physical devices and any control device could be wired to any of the control points, e.g. to turn on and off motorized dampers, lights, motors, fans, heaters, and humidifiers.

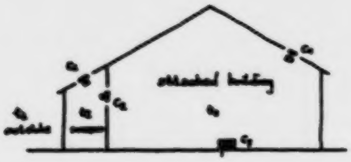

Fig 2 A Generic Attached Sunspace

The following simple control strategy was chosen as an example to illustrate how the sunspace controller operates.

a. If the house temperature is greater than the ambient temperature, t1, and exceeds the maximum set point for the house then turn on the vent fan in the house (cool the house).

if $t3 > t3max > t1$ then c4

b. If the sunspace temperature is greater than the ambient temperature and exceeds the maximum set point for the sunspace then turn on the vent fan in the roof of the sunspace.

if $t2 > t2max > t1$ then c1

c. If the sunspace temperature falls below the minimum set point temperature for the sunspace then turn on the fan in the sunspace wall to heat the sunspace from the house.

if $t2 < t2min$ then c2

d. If the house temperature falls below the minimum set point then turn on the furnace.

if $t3 < t3min$ then c3

e. If the sunspace temperature exceeds the house temperature by temperature difference, dt, then turn on the fan in the sunspace wall.

if $t2 > (t3 + dt)$ then c2

Each conditional statement is tested, a control flag is set, and is ORed (Boolean OR) with the next conditional statement in a cascading manner. This method is simple to implement but ignores errors and does not consider all possible conditions. For example, what if the user sets the high point for the house below the low set-point for the house ($t3max < t3min$). Then conditional statements a. and d. are not bounded allowing c4 to operate at the same time (simultaneous heating and cooling; not something you would ordinarily want to have happen).

To provide for error checking and to make sure all possible input states were considered a truth table was used. The truth table is derived by considering all possible input states and equating an output state for each input state. This was implemented by using a look-up table in computer memory. The control strategies (a. through e.) were used to establish the input table of all possible combinations for the five states. A desired output state was then chosen for each of the possible inputs. Undesired combinations were avoided by returning control to the previous state. The user is informed of an input error by a code on the display and an audible signal from a piezo electric crystal.

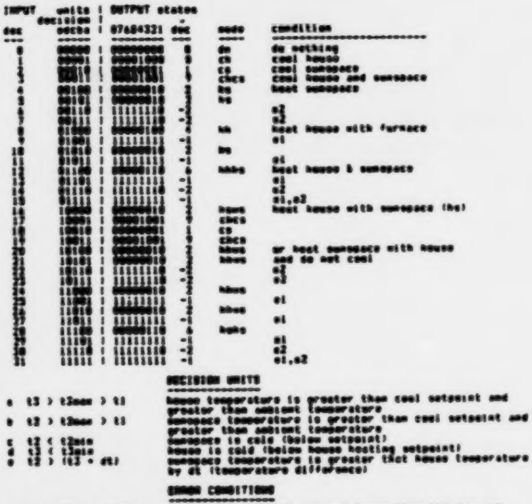

Fig 3 Control Truth Table

An example of a completed truth table to implement the conditional control statements (a–e) is presented in Figure 3. The five conditional statements (called decision units in this table) produce 32 possible combinations and are listed in the left in Figure 4 from 0–31 decimal (00000 to 11111 in binary). A zero indicates FALSE and a 1 indicates the decision unit is TRUE. For each possible input state there is a corresponding output state. From an analysis of the input states seven possible output modes were chosen in this example (0,1,2,4,6,8, and 9). Also, there are two error modes -1, and -2 (255 and 254 in 2's complement arithmetic).

The control truth table is implemented by defining the output states for each input state in ROM as a look-up table. For 32 decision units this method only uses 32 bytes. The table is written to RAM and the user is able to direct the computer's attention to either the ROM or the RAM look-up table. The RAM table can be changed by the user by entering a different output state for a particular input state. This method allows the user to implement analytically derived control strategies or choose control parameters by trial and error if desired.

Cycling is controlled in two ways. Hysterisis is provided for decision unit e. by using standard delta-T on delta-T off control. Additionally there is a "sticky" variable during the control cycle. which regulates the frequency of control implementation by controlling access to the control implementation routines. The value of "sticky" depends on the type of device being controlled. Time delay can be added for two stage thermostat type control. For example, solar heat would be given a certain amount of time to raise the temperature of the house after which time the furnace would be permitted to turn on.

### 3.8 Use for Data Acquisition

The sunspace controller can also function as a low cost data logger. Data was taken with the controller running a modified program to send the date, time and 5 readings to the serial output port. Using an interrupt feature of the real time clock, data was recorded every minute over a two hour period to study the operation of the controller connected to a typical forced air furnace. Data was stored on a battery operated microcomputer and plotted on a dot-matrix printer. Hourly or daily values could easily be transmitted and stored. Another possibility is to store data in RAM on the controller. By using an attached modem the controller can be called up by another computer to access the data, provide diagnostic analysis, or update the control program if needed.

## 4 CONCLUSIONS

Attached sunspaces present a special problem for temperature control. A review of previous research and solar design suggests that many conventional control systems presently used are inadequate because they do not provide the flexibility necessary for integrated control. The unique aspect of the controller discussed in this paper compared to other programmable controllers is the degree of flexibility. This is made possible by the use of a microcontroller integrated circuit. The controller can be completely reprogrammed to tailor it for climate conditions and individual requirements. The installer or user can modify set points, set back and wake up times and can implement a completely different control strategy by changing values in the truth table. The controller can be reprogrammed to utilize more advanced control algorithms as they become available. The flexibility of the controller is enhanced by error checking and diagnostic features.

A truth table to match input and output states was shown to be a satisfactory way to implement an attached sunspace control strategy. A truth table approach provides for error checking. The truth table stored in ROM can be written to RAM to allow user programming. This flexibility is unusual in a microprocessor thermostat.

The need for an advanced sunspace controller is clearly demonstrated in research on existing solar applications. As the field of sunspace design evolves a flexible microprocessor controller such as the one described here will be capable of keeping pace with consequent changes in temperature control of buildings.

## 5. ACKNOWLEDGEMENT

The work presented here was funded by the National Research Council Solar Energy Programs and the authors gratefully acknowledge their support.

## 6. REFERENCES

(1) Jones, Robert W. and Robert D. McFarland, "The Last Word in Sunspace Design," Solar Age, 7p, June 1984.

(2) Chapin, H.D. and F.W. Chapin, "Programmable Controller for Attached Sunspace," NRC Contract #05X83-00218, March 1985.

(3) National Research Council of Canada & Hawes, Lawand, Le Normand, Skelton,"The Solarium Workbook," National Research Council of Canada, Solar Energy Project, Ottawa, Ontario,May, 1981.

(4) Ritschard,R.L., Hang,Y.J., "Energy Savings Potential for Attached Sunspaces in Different Climates," Progress in Passive Solar Energy Systems, 1983.

(5) Scanada Consultants Ltd., "Low Energy Passive Solar House with Attached Sunspace: A Quick Appraisal," National Research Council, 37p, August 1983.

(6) NAHB Research Foundation Inc., "Assessment of Solar Technology in the Home Building Industry," U.S. Department of Energy, 1983.

(7) Balcomb,Douglas,"Designing Passive Solar Buildings to Reduce Temperature Swings," Los Alamos Labs, Los Alamos, NM 87545, #LA-UR-78-1316, 1978.

(8) Swisher, Joel and T. Cowing, "Passive Solar Performance: Summary of 1981-1982 Class B Results," Solar Energy Research Institute, U.S. Department of Energy, 1983.

(9) Systegral Engineering Limited, Toronto, Ontario,"A Study of Solar System Control Strategies and Control Systems," NRC contract # 15 SQ-31155-8-2650, Mar. 1980.

(10) Kent, Thomas B. and John E. Anderson, "Control Applications and Limitations," Proceedings of the First Workshop on The Control of Solar Energy Systems for Heating and Cooling," edited by E.F. Clark and F. de Winter, 4p, 1978.

(11) Kent, Thomas B. and Martha J. McGavin, "Assessment of Needs for New Controllers," U.S. Department of Energy/CS/31596-T1, 25p, July 1980.

# Heat Recovery

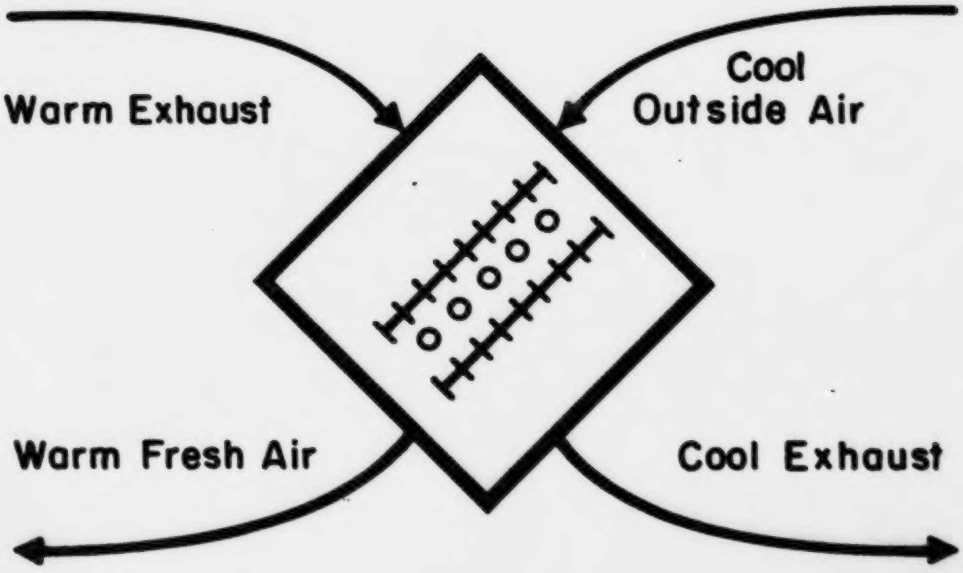
Warm Exhaust
Cool
Outside Air
Warm Fresh Air
Cool Exhaust

# TESTING AND OPERATION OF HEAT RECOVERY VENTILATORS FOR WELL SEALED HOUSES

R. W. Besant, G. J. Schoenau
University of Saskatchewan

T.L. Hamlin
Shelter Research Inc.

## ABSTRACT

This paper deals with the question of what is required of a heat recovery ventilator, its performance, operation, testing and installation. The device must not only satisfy reasonable cost and performance criteria but also it must be very reliable and especially safe. In this study, the question of heat recovery ventilator performance, and reliability was investigated through the laboratory testing of a number of commercially available units and the development of plans for an owner-built unit which was tested in the same manner. A total of three Canadian-built commercially available units were tested to CSA preliminary standard C439M while another five were subjected to somewhat less exhaustive tests.

In addition to the above laboratory test findings, the question of actual house operation has been briefly investigated. It was found that satisfactory house air quality could be maintained in houses with tight air-vapour barriers and seals when the heat recovery air ventilator was operated only 16 hours per day with a single 8-hour overnight shut off period provided that natural air flow through the air ventilator is more than sufficient to satisfy any hot water heat and furnace air requirements without any possible back draft. Under this circumstance, no defrost scheme would be required for any unit of sufficient size or capacity to preclude frost blockage in one day's operation. Defrost could take place at night and the air ventilator unit could be run on a simple timer or manual switch. It is implied by this result that perhaps the least cost and most reliable high performance unit is one that does not have an elaborate defrost scheme as implied in the CSA standard but rather is designed to have a high daily frost storage capacity and is shut off by timer over a sufficient period to ensure a complete defrost. This attractive mode of operation deserves further investigation from the point of view of safety and reliability under a wider range of operation conditions.

The general findings on heat recovery ventilators are as follows:

(1) The house air exchange provided by the heat recovery air ventilators is considered to be its prime function. This air exchange must be reliable but not necessarily continuous and under no circumstances should its operation result in a serious safety hazard. A second function of these units is to recover thermal energy. A large part of the cost of these units must provide an economic payback if they are to be cost effective.

(2) The appropriate size or flow rate capacity, the temperature range of reliable operation, the performance including air leakage and heat recovery efficiency depend on the application or house, the climate and weather, and the various costs of the heat recovery air ventilator as well as the energy supply. It is difficult to say that one design installation and operation would be most cost effective and reliable for all regions of the country. Even within a climatic region, various houses will have different needs.

(3) Of the eight heat recovery air ventilators tested in the lab, a number of performance results are notable. These are:
  (i) The airflow rates varied between 20 and 100 L/s. It is not expected that the lower values would satisfy the needs of some houses while perhaps other houses, with larger natural air infiltration rates, would not need the higher airflow rates.
  (ii) A number of airflow rate failures were recorded with various units. These were:
    (a) In one regenerative wheel unit excessive internal cross flow of up to 50% and complete freeze up failure of this same unit at -20°C fresh air inlet and +20°C stale air exhaust at 40% RH.
    (b) Frost up and air flow blockage of two units within a few hours operation at -20°C fresh air inlet and +20°C stale air exhaust at 40% RH. One of these units was a very small plate type heat exchange while the other was a regenerative wheel.
    (c) Failure of the defrost cycle in one plate type unit at -35°C fresh air intake and +20°C stale air exhaust at 40% RH. This unit did not show this same failure during other tests.
  (iii) Of the successful units (i.e., excluding (a) and (b) above) the supply air heat recovery efficiency for sensible heat ranged between 50 to 80% over a range of operating temperatures from 0°C to -35°C fresh air supply temperature. These units generally had no moving parts other than the fans and perhaps a defrost mechanism.

# THE DEVELOPMENT OF STANDARDS ON AIR TIGHTNESS AND AIR INFILTRATION

G. K. Yuill
G. K. Yuill and Associates Ltd.
1441 Pembina Highway
Winnipeg, Manitoba
R3T 2C4

## ABSTRACT

Several standards are under development at the present time on the subject of air infiltration and air leakage of houses. This paper reviews these Standards, the technical developments on which they are based, and some of the issues which had to be decided as the Standards evolved to their present forms.

The four Standards discussed are ASTM Standard E779-86, "Standard Test Method for Determining Air Leakage Rate by Fan Depressurization", ASHRAE Standard 119P, "Air Leakage Performance for Residential Buildings", CGSB Standard 149-GP-10M, "Standard for Determination of Airtightness of Buildings by the Fan Depressurization Method", and CGSB Standard CAN2-51.70-M, "A Method for Determining Compliance with Ventilations Requirements for Detached Dwellings After Retrofit Sealing". The discussion is based on the author's experiences as secretary of the ASHRAE Standard Committee and as Chairman of the two CGSB Standard Committees.

None of these Standards has yet received final approval. It is likely that ASTM E779-86 and CGSB 149-GP-10M will be finalised before June, 1986, but the other two will still be open for public comment. It is hoped that the presentation of this paper will elicit input on these latter two Standards which may influence their final form.

The two Standards on fan depressurization differ in several respects. One difference is the ASTM Standard's requirement of pressurization and depressurization tests, while the CGSB Standard requires only depressurization. A second is the CGSB Standard's requirement to seal intentional openings such as chimneys. A third is the CGSB Standard's use of "$Q^2$ weighting" in the statistical analysis of the measured data. Finally, the two Standards use different orifice coefficients and different pressures in the determination of leakage area.

The central principle of ASHRAE Standard 119P "Air Leakage Performance for Residential Buildings" is the concept of "infiltration degree days". These are degree days calculated on an hour-by-hour basis, weighted by the specific infiltration for that hour. The specific infiltration is a velocity which depends on the driving forces for wind-driven and buoyancy-driven infiltration. This Standard specifies the relationship between the maximum allowable leakage area of a house and the infiltration degree days for its location.

The last of these Standards, "A Method for Determining Compliance With Ventilation Requirements for Detached Dwellings After Retrofit Air Sealing", provides a link between the ventilation requirements specified by ASHRAE Standard 62-81 "Ventilation for Acceptable Indoor Air Quality", and the measured leakage area of a house. This link is based on a dynamic analysis of the pollutant concentration in a house throughout the year as a function of the real weather conditions at its location.

## 1. INTRODUCTION

The subject of air tightness and air infiltration have received a great deal of interest in the past ten years, as house designers have attempted to balance the drive to conserve energy with the need to maintain indoor air quality. The same dilemma has been faced by owners of existing houses as they caulked and sealed them to save energy.

These concerns have resulted in a demand for Standards. How tight should a house be? How can the tightness of a house be measured? How much ventilation does a house need? How can it be determined if infiltration is providing adequate ventilation? These are some of the questions which are difficult for the householder or the housebuilder to answer for themselves, so they have turned to Standard writing bodies for help.

Among the Standards which have been written or are presently being developed to answer these questions are:

1. ASHRAE 62-81 "Ventilation for Acceptable Indoor Air Quality"
2. ASTM E779-86 "Standard Test Method for Determining Air Leakage Rate by Fan Pressurization"
3. ASHRAE 119P "Air Leakage Performance of Residential Buildings"
4. CGSB CAN2-149.10M "Standard for Determination of Airtightness of Buildings by the Fan Depressurization Method"
5. CGSB CAN2-51.70-M "A Method for Determining Compliance with Ventilation Requirements for Detached Dwellings After Retrofit Sealing"

The first of these Standards has been in place for five years and is well known to those who must concern themselves with building ventilation. It is under revision and a new version will probably be published in late 1986 or in 1987. The other four Standards are less well known and some are still in preparation. These are the topic of this paper.

Standards are prepared by a number of Standard-writing agencies, of which there are five in Canada and many in the U.S. These agencies are accredited by the American National Standards Institute (ANSI) and the Standards

Council of Canada. Some of these agencies, such as the American Society of Heating Refrigeration and Air Conditioning Engineers (ASHRAE) or the Canadian Standards Association (CSA) are controlled by their members. Others, like the Canadian General Standards Board (CGSB) are government agencies. Whether the Standard writing agency is private or government controlled, the Standard committee is a committee of volunteers, chosen to represent all the classes of people who will have an interest in the Standard. This, of course, includes producers of the equipment to be covered, users, and the general public. The development of a Standard involves a great deal of voluntary effort on the part of the committee members. It is not uncommon for a committee to meet a dozen times over three or four years, and in addition the members must write segments of the Standard and review what others have written, between meetings.

A great deal of attention is paid to ensuring that Standard committee membership is not biased, that all members have their chances to influence the Standard, and that it is truly a consensus document. After the Draft Standard is produced, it is advertised and widely circulated so that the public has a chance to comment. Every comment or criticism, whether from the public or from a committee member, must be dealt with before a Standard can be published.

The Standard writing bodies have no legal authority to enforce their Standards. Compliance is entirely voluntary, unless a buyer and seller agree to rely on a Standard, or unless a Government passes a law adopting a particular Standard as a legal requirement. However, many voluntary Standards become so widely recognised as representing the state of the art that failure to comply with them is considered negligent by the courts.

In the following chapters, the technical background and critical issues of the four Standards covered in this paper will be addressed.

## 2. THE AIRTIGHTNESS TESTING STANDARDS

Two Standards published in 1986 prescribe methods of testing the airtightness of houses. These are CGSB CAN2-149.10-M "Determination of the Airtightness of Buildings by the Fan Depressurization Method" (149.10) and ASTM E779-86 "Standard Test Method for Determining Air Leakage Rates by Fan Pressurization" (E779). E779 and 149.10 deal with the same basic test, in which a fan draws air through a calibrated flow meter in a panel fitted into the door of a house. This creates a pressure difference across the house envelope and draws air through the leaks. It has been found that the leakage rate can be correlated to pressure difference by the expression:

$$Q = C \Delta P^n$$

where $Q$ = the flow rate
$C$ = a coefficient
$\Delta P$ = the pressure difference
$n$ = an exponent, between 0.5 and 1.0

If a series of sets of $Q$ and $\Delta P$ are measured, the values of $C$ and $n$ can be determined by statistical analysis. The procedure is to take the logarithms of both sides of the equation.

$$\ln(Q) = \ln(C) + n \ln(\Delta P)$$

Substituting $\ln(Q)$ and $\ln(\Delta P)$ $\ln(C)$ and $n$ can be found by linear regression.

The flow through an orifice is given by:

$$Q = C_D A \left(\frac{2 \Delta P}{\rho}\right)^{1/2}$$

where $C_D$ = a discharge coefficient
$A$ = the area of the opening
$\rho$ = density

Thus it is possible to find an equivalent leakage area (ELA) for an orifice which will pass the same amount of air as the leaks in the walls of the house, at some particular pressure difference. This is the basis of both E779 and 149.10.

In spite of this fundamental similarity, the two Standards differ in several important respects. These are:

1. the base pressure for calculating the ELA;
2. the orifice coefficient for calculating the ELA;
3. the use of depressurization or pressurization and depressurization;
4. the treatment of intentional openings; and
5. the statistical analysis.

The first two of these items, and the fifth, are concerned only with calculation procedures. After a 149.10 test is completed the raw data can be analysed according to E779 as well as according to 149.10. Items 3 and 4 are part of the measurement procedure however, and prevent direct comparison of the results of the two kinds of tests.

In E779, the base pressure for calculating the ELA is 4 Pa, while in 149.10 it is 10 Pa. The lower number was chosen by the E779 committee because it is in the range of pressure differences experienced by the walls of real houses. The higher number was chosen by the 149.10 committee because we wanted to avoid extrapolating outside the range of pressures at which measurements were taken. However, we later raised the pressure of the lowest reading from 10 Pa to 15 Pa, so that this argument became irrelevant.

If the exponent $n$ had the value 0.5, the pressure chosen to evaluate the ELA would be irrelevant, since the flow through the leaks and through the equivalent orifice would vary in the same way. Because $n$ is greater than 0.5, the 149.10 ELA is bigger than the E779 ELA by a factor of

$$F = (10/4)^{n-0.5}$$

This ratio will be different for each house tested, depending on $n$.

A real orifice is not perfectly efficient. In fact, the discharge coefficient is 0.611. This value was used by the 149.10 committee in defining the ELA. On the other hand, the E779 committee assumed an ideal orifice with a discharge coefficient of 1. Thus the 149.10 ELA must be bigger to pass the same flow. The ratio between the 149.10 ELA and the E779 ELA is then

$$R = (2.5^{n-.5})/.611$$

An average value of $n$ is 0.68, which gives a ratio of 1.93.

The E779 Standard requires the testing of a house by pressurization and depressurization. This decision was based on measurements which showed that the ELAs measured by pressurization and by depressurization were frequently different, but either could be higher than the other. Thus it was felt that both tests were required to determine a meaningful value for the leakiness of a house. The 149.10 committee felt, on the other hand, that the extra cost of running a second test could not be justified by the improvement in accuracy.

The view of the E779 committee was that the objective of their Standard was to obtain a number which would indicate the amount of infiltration a house would experience. Therefore they specified that the intentional openings such as flues and exhaust and supply fan openings should be left in their normal positions. The 149.10 committee felt that the objective of the test was to determine the quality of the house envelope; that is, to determine how airtight the parts of the house which are not supposed to leak have been made. Therefore we specified that all intentional openings should be sealed during the test.

The final significant difference between the two Standards is the use of "$Q^2$ weighting" in the statistical analysis specified in the 149.10 Standard. When an equation of the form

$$y = a + bx$$

is fitted to a set of x and y values by linear regression analysis, an assumption is made that the probability of errors is the same for each set of measurements. Engineers and scientists have, for many years, fitted data to equations of the form

$$y = ax^b$$

by taking logarithms of both sides to obtain

$$\ln(y) = \ln(a) + b\ \ln(x)$$

and then using linear regression to correlate ln(y) and ln(x). Unfortunately, if all values of x have the same probability of errors, all values of ln(x) do not. Therefore linear regression analysis is invalid. To correct for this, the 149.10 committee introduced "$Q^2$ weighting", a slightly modified regression analysis. This analysis gives greater weight to the measurements at higher pressure.

As it turns out, this complication makes very little difference to the results obtained. The effect of "$Q^2$ weighting" is only significant if the data to be fitted is relatively inaccurate. This is not the case with a test which conforms to the other requirements of 149.10, so that the results obtained by using "$Q^2$ weighting" are not significantly different from those which would be obtained if this refinement were ignored. On the other hand, there is no extra effort involved in using "$Q^2$ weighting" when using a previously prepared computer program to do the analysis.

It is impossible to say which of these two Standards is better. Each has its advantages. It is unfortunate that Canada and the USA could not use the same Standard for testing the airtightness of houses, but the problem is not serious except when data from the two countries is to be compared.

## 3. THE AIR LEAKAGE PERFORMANCE STANDARD

ASHRAE Standard 119 "Air Leakage Performance for Residential Buildings" is nearing completion and is unlikely to change much. However, it has not been finally approved, so its published form may not be precisely as discussed here. Anyone who wishes to comment on this Standard should contact ASHRAE and request a review copy.

This Standard has been developed to set limits on the amount of energy lost due to air infiltration in residential buildings. It specifies the maximum allowable envelope leakage of a building. It does not deal with the issue of indoor air quality except to point out that it is the designer's responsibility to assure that adequate ventilation air is available through mechanical ventilation if it is not made available through infiltration.

Standard 119 contains a classification scheme which groups buildings into categories depending on their normalised leakage. Normalised leakage depends on leakage area, floor area and building height. It is defined as

$$L_n = 1000(L/A)(H/H_o)^{0.3}$$

where $L$ = the leakage area of the space as measured by E779
$A$ = the floor area of the space
$H$ = the building height
$H_o$ = the height of a single storey (8 ft) (2.5 m)

The normalised leakage of a house is approximately equal to its annual average air change rate.

The leakage classes are defined as shown in Table 1. It should be noted that the ratio of the lower boundary to the upper boundary to each class is the square root of 2, so that the tighter classes cover a narrower range of values of normalised leakage.

TABLE 1

CLASSIFICATION OF LEAKAGE

| Normalized Leakage Range | Leakage Class |
|---|---|
| $L_n < 0.10$ | A |
| $0.10 \leq L_n < 0.14$ | B |
| $0.14 \leq L_n < 0.20$ | C |
| $0.20 \leq L_n < 0.28$ | D |
| $0.28 \leq L_n < 0.40$ | E |
| $0.40 \leq L_n < 0.57$ | F |
| $0.57 \leq L_n < 0.80$ | G |
| $0.80 \leq L_n < 1.13$ | H |
| $1.13 \leq L_n < 1.60$ | I |
| $1.60 \leq L_n$ | J |

To determine what leakage classes would be acceptable at various locations in North America, a new weather parameter, infiltration degree days (IDD) was developed. IDD is a measure of the energy consumption caused by infiltration. It includes both heating IDD and cooling IDD.

Heating IDD are defined as

$$IDD_h = \sum (S/S_o)(T_{bh} - T)/24$$

where $S$ = the specific infiltration
$S_o$ = the typical specific infiltration (=0.71 m/s)
$T_{bh}$ = the heating base temperature (= 18.3°C)
$T$ = the hourly dry bulb temperature

and the sum is over all hours for which $T$ is less than $T_{bh}$.

The specific infiltration is calculated using

$$S = ({f_w}^2 U^2 + {f_s}^2 \left|T_{in} - T\right|)^{1/2}$$

where $U$ = wind speed at 6 m
$T_{in}$ = indoor temperature
$f_w$ = 0.132 (dimensionless)
$f_s$ = 0.120 m/(s $K^{1/2}$)

Cooling IDD are defined as

$$IDD_c = \sum(S/S_o)(H - H_b)/(24Cp)$$

where $H$ = enthalpy of ambient air

$H_b$ = base enthalpy (= 65 kJ/kg)

$C_p$ = specific heat of air (= 1.024 kJ/(kg °C))

and the sum is over all hours when $H$ is greater than $H_b$ and the temperature is above 25.6°C.

Table 2 shows the IDD for 24 Canadian cities. This number is useful because it shows the variation in the energy cost of infiltration from location to location. The energy cost of infiltration for a particular house can be estimated by

$$Q = L * S_o * IDD * \rho * Cp$$

where $\rho$ = density of air

$L$ = the equivalent leakage are of the house in question, measured according to E779

The major issue facing the ASHRAE 119 committee was where to set the requirements for $L_n$ relative to IDD. Some argued that $L_n$ should be a constant very low figure. That is, all houses everywhere should be built very tight and ventilated as required. This view was rejected because it would impose an unnecessary burden on housebuilders in very mild climates, where air-vapor barriers are not used. A second view was that $L_n$ should decrease in inverse proportion to $(IDD)^{1/2}$. This was argued to be the economic optimum. It would allow houses in severe climates to use more energy for infiltration than houses in milder climates. The third view was that the product of $L_n$ and IDD should be a constant. This would impose an equal infiltration energy load in all climates. This was argued to be uneconomic since it would cost more to save the same amount of energy in more severe climates.

TABLE 2
LOCATIONS DATA

| CITY, PROVINCE | INFILTRATION DEGREE-DAYS IDD/°F-days/ | IDD/°C-days/ | DATA SOURCE |
|---|---|---|---|
| Calgary, ALB | 11269 | 6260 | 10 Year |
| Edmonton, ALB | 13109 | 7282 | WYEC |
| Fort St. John, BC | 12921 | 7178 | 10 Year |
| Prince Rupert, BC | 7668 | 4260 | 10 Year |
| Vancouver, BC | 5405 | 3002 | WYEC |
| Victoria, BC | 4922 | 2734 | 10 Year |
| Williams Lake, BC | 10016 | 5564 | 10 Year |
| Thompson, MAN | 16350 | 9083 | 10 Year |
| Winnipeg, MAN | 14758 | 8198 | WYEC |
| Saint John, NB | 10949 | 6082 | 10 Year |
| St. John's, NF | 13544 | 7524 | 10 Year |
| Stephenville, NF | 12118 | 6732 | 10 Year |
| Frobisher Bay, NWT | 25705 | 14280 | 10 Year |
| Kapuskasing, ONT | 13968 | 7760 | 10 Year |
| Ottawa, ONT | 10216 | 5675 | 10 Year |
| Sault Ste Marie, ONT | 11295 | 6275 | 10 Year |
| Thunder Bay, ONT | 11835 | 6575 | 10 Year |
| Toronto, ONT | 9246 | 5136 | WYEC |
| Windsor, ONT | 8965 | 4981 | 10 Year |
| Charlottetown, PEI | 11429 | 6349 | 10 Year |
| Montreal, QUE | 10496 | 5831 | WYEC |
| Quebec, QUE | 11697 | 6498 | 10 Year |
| Regina, SAS | 14752 | 8195 | 10 Year |
| Saskatoon, SAS | 13605 | 7558 | 10 Year |

To decide between the latter two views, a study was made of the $L_n$ values of 200 Canadian houses whose ELA had been measured previously (Ref 1). Figure 1 shows the results of this study. This graph shows that the actual $L_n$ of houses varies according to the expression

$$L_n * IDD = \text{Constant}$$

This is because houses are built tighter in cold climates to make them more comfortable and to avoid structural damage caused by condensation, not to save energy.

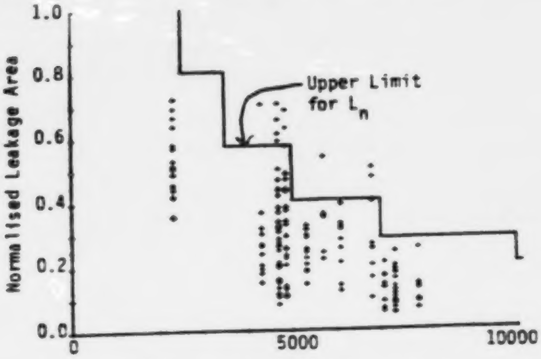

Fig. 1 Infiltration Degree Days

The limit on $L_n$ was set at the line shown in Figure 1, so that the Standard would put some pressure on the worst builders to improve, but would not require radical changes in technique. Table 3 lists the acceptable leakage classes for 24 Canadian cities. Figure 2 is a map showing the acceptable leakage classes for North America.

The R-2000 airtightness requirement of 1.5 a.c.h. at 50 Pa is the equivalent of $L_n$ = 0.09 for a 110 $m^2$ two-storey house with a basement. This is less than one third of the leakage which would be allowed by ASHRAE 119 on the Canadian prairies, and little more than 10% of that which would be allowed in Vancouver. Builders frequently beat the airtightness requirements of the R-2000 program by a wide margin, so Canadian builders should have no trouble in meeting the requirements of ASHRAE 119.

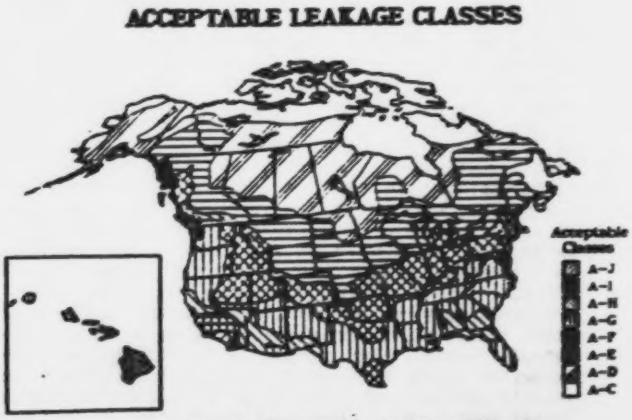

Fig. 2 Acceptable Leakage Classes

## 4. THE VENTILATION REQUIREMENTS STANDARD

A CGSB committee is presently developing Standard CAN2-51.70-M, "A Method of Determining Compliance with Ventilation Requirements for Detached Dwellings After Retrofit Sealing". The purpose of this Standard is to provide a means of determining whether or not the ventilation rate required by ASHRAE Standard 62-81 can be supplied by natural infiltration after a detached dwelling has been caulked and sealed. Several drafts of this Standard have been produced, but there is still disagreement among the committee members about the precise form the Standard should take. It is unlikely that the committee will approve a final draft before the end of the year.

TABLE 3

LOCATIONS TABLE

| PROVINCE | CITY | ACCEPTABLE CLASSES |
|---|---|---|
| ALBERTA | Calgary | A - E |
| | Edmonton | A - D |
| BRITISH COLUMBIA | Fort St. John | A - D |
| | Prince Rupert | A - F |
| | Vancouver | A - G |
| | Victoria | A - G |
| MANITOBA | Thompson | A - D |
| | Winnipeg | A - D |
| NEW BRUNSWICK | Saint John | A - E |
| NEWFOUNDLAND | St. John's | A - D |
| | Stephenville | A - E |
| NORTHWEST TERRITORIES | Frobisher Bay | A - C |
| ONTARIO | Kapuskasing | A - D |
| | Ottawa | A - E |
| | Sault Ste Marie | A - E |
| | Thunder Bay | A - E |
| | Toronto | A - E |
| | Windsor | A - F |
| PRINCE EDWARD ISLAND | Charlottetown | A - E |
| QUEBEC | Montreal | A - E |
| | Quebec | A - E |
| SASKATCHEWAN | Regina | A - D |
| | Saskatoon | A - D |

At first it might seem that there is a contradiction between the requirements of CGSB 51.70 and those of ASHRAE 119. The former prescribes a minimum allowable air infiltration while the latter prescribes a maximum allowable air infiltration. An analysis of a particular house may well show that the maximum infiltration allowed by ASHRAE 119 is less than the minimum required by CGSB 51.70. However, there is really no contradiction between these requirements. ASHRAE 119 is directed towards new construction. In this situation air tightness can be achieved at low cost, and it makes sense to build a tight house and provide fresh air through controllable mechanical ventilation. Any house which meets the requirements of ASHRAE 119 in the colder Canadian climates will certainly be too tight to rely on infiltration alone for ventilation. CGSB 51.70, on the other hand, applies to existing houses which are to be retrofit sealed. Its purpose is to distinguish between houses which are loose enough that it is possible to make them tighter without creating an air quality problem and houses which are so tight that any further sealing would make the addition of mechanical ventilation necessary.

There are many houses in the former category, and there are many homeowners who are willing to pay to make them tighter, in spite of the fact that it costs more to tighten an existing house than a house under construction. However, many homeowners are concerned with the possible air quality problems which may arise if their houses are made too tight. The objective of CGSB 51.70 is to avoid this danger.

CGSB 51.70 could be used to specify the amount of mechanical ventilation which is required to supplement infiltration in a house which has been sealed past the point of being adequately ventilated. However, it is not likely to be used this way. It would be difficult for an air sealing contractor to persuade a homeowner to pay to have his house sealed, then pay more to have mechanical ventilation added. It is more likely that air sealing contractors will use this Standard to ensure that they seal houses just to the point where infiltration provides the minimum ventilation required, and no further.

The above comments should not be taken to mean that it is never sensible to seal a house tight and then mechanically ventilate it, only that it would be hard for a contractor to persuade a customer to pay him to do so. If this work can be done cheap enough, it will be worthwhile doing it. The reason for this is that infiltration is highly variable because of the changes in outdoor temperature and wind velocity. If a house is leaky enough that infiltration provides adequate ventilation on the worst day of the heating season, the annual average value will be three or four times too high. Thus mechanical ventilation can maintain the same upper limits on pollutant concentrations at one-third to one-quarter the energy cost of infiltration.

CGSB 51.70 is based on an analysis of infiltration rates and pollutant concentrations which is described in detail in a companion paper (Ref. 2). This work will only be summarised briefly here.

The overall objective of CGSB 51.70 is not to establish ventilation requirements. It is to ensure that the ventilation requirements which have already been established by ASHRAE 62-81 are satisfied. A major problem in doing this is that ASHRAE 62-81 specifies ventilation rates which are assumed to be constant, but infiltration is not constant.

To deal with this problem, the concept of the equivalent steady state ventilation rate has been introduced. If the pollutant source strength, S, and the ventilation rate, Q, are constant, then the concentration, C, will also be constant and

$$Q = S/C \qquad (4.1)$$

If the flow rate varies, the concentration will also vary, and the above equation will no longer apply. However, we can define an equivalent steady state flow rate

$$Q_S = S/C_i \qquad (4.2)$$

based on the instantaneous pollutant concentration $C_i$.

The flow rate requirements of ASHRAE 62-81 were developed so that, if the pollutant source strength, S, were some particular value which the committee felt might occur, the pollutant concentration would not rise above some value $C_L$ which the committee accepted as an upper limit. If the equivalent steady state flow rate, $Q_S$, meets the requirement of ASHRAE 62-81, the instantaneous pollutant concentration $C_L$ will not rise above the limiting value $C_L$ which was the basis of the ASHRAE Standard. This is true even when the ventilation flow rate fluctuates widely as it does when infiltration is providing the ventilation air.

In a varying flow such as this, $Q_S$ will not fluctuate as widely as the actual flow rate. The actual flow rate will fall to zero on occasion, while $Q_S$ will not fall to less than one third of its long-term average value. If this lowest value still meets the ASHRAE 62-81 requirement, then there will be no indoor air quality disaster, because the pollutant level will rise only by a factor of three, corresponding to the fall in $Q_S$, not to the fall in the actual flow rate. A ventilation flow rate which falls to zero for a short time does not imply an extreme rise in pollutant concentration.

To calculate the fluctuations in pollutant concentration and in $Q_S$ requires a complex hour-by-hour analysis of weather data. The analysis on which CGSB 51.70 is based uses the Lawrence Berkeley Laboratory (LBL) model to predict instantaneous infiltration rate as a function of wind velocity, indoor-outdoor temperature difference, equivalent leakage area, house height, terrain and wind shielding. This model has been combined with the conservation of mass equation to predict the pollutant concentration in a house as a function of time.

The resulting equation has been rearranged in a dimensionless form so that the hour-by-hour analysis of the weather data was separated from the analysis of house properties. Thus this hour-by-hour analysis need be done only once for each weather station. The results of each analysis of a year of weather data results in a graph (Fig. 3) which relates the effective ventilation rate to the measurable properties of the house.

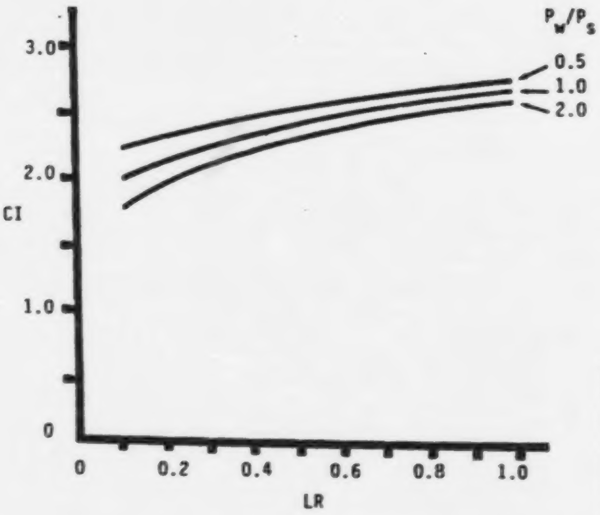

Fig. 3 Maximum Daily CI vs. LR
Ottawa 1976 (Winter Season)

The calculations required of the user of the Standard are as follows:

a. Determine the values of γ and α from Table 5 and the value of C' from Table 6. Calculate the value of the wind parameter for the dwelling, $P_w$, using the expression:

$$P_w = (A \times C' \times \alpha \times (H/10)^{\gamma})^2 \; . \; . \; . \; . \; . \quad (1)$$

where: H = the height of the highest ceiling in the dwelling above the top of the foundation.
A = a coefficient, from Table 4.

b. Calculate the value of the stack parameter for the dwelling, $P_s$, using the expression:

$$P_s = B \times H \; . \; . \; . \; . \; . \; . \; . \; . \; . \; . \quad (2)$$

where: B = a coefficient, from Table 4.

TABLE 4

Values of the Coefficients in Equations 1 and 2

| Dwelling Type | Coefficients A | B |
|---|---|---|
| Single Storey | .68 | .00665 |
| Multi-Storey | .81 | .00560 |

TABLE 5

TERRAIN PARAMETERS FOR STANDARD TERRAIN CLASSES

| Class | γ | α | Description |
|---|---|---|---|
| I | 0.10 | 1.30 | Ocean or other body water with at least 5 km of unrestricted expanse |
| II | 0.15 | 1.00 | Flat terrain with some isolated obstacles (e.g., buildings, or trees well separated from each other) |
| III | 0.20 | 0.85 | Rural areas with low buildings, trees, etc. |
| IV | 0.25 | 0.67 | Urban, industrial or forest areas |
| V | 0.35 | 0.47 | Center of large city |

c. Calculate the Orr Number, $N_O$, for the dwelling using the equation:

$$N_O = 11423 \sqrt{P_s} \; (ELA/V) \; . \; . \; . \; . \; . \quad (3)$$

where: ELA = the equivalent leakage area $[m^2]$
and V = the volume of the dwelling $[m^3]$

d. Calculate the ratio $P_w/P_s$

e. Using the values of $N_O$ and $P_w/P_s$, find the value of the Grant Number, $N_G$, from the graph in (Figure 3) which applies to your location. (Other locations are graphed in the Standard).

f. Calculate the equivalent steady state fresh air flow rate, $Q_S$, using the equation:

$$Q_s = 3173 \sqrt{P_s} \; (ELA)/N_G \; . \; . \; . \; . \; . \; . \quad (4)$$

This value shall be compared with the requirements of ASHRAE Standard 62-81 to determine whether or not the dwelling is adequately ventilated by natural infiltration.

These calculations would take a few minutes to do by hand, but it would not be difficult to develop a program for a programmable calculator to carry them out automatically. An air-sealing contractor who uses a blower door to measure airtightness will have such a calculator anyway, so his effort to comply with this Standard will not be great.

Several issues still face the CGSB 51.70 Standard committee. One is the question of how to deal with the supply of combustion air. The present approach of the committee is that this topic should be dealt with in a separate Standard, but this may change before the CGSB

TABLE 6

GENERALIZED SHIELDING COEFFICIENT VS. LOCAL SHIELDING

| Shielding Class | C' | Description |
|---|---|---|
| I | 0.324 | No obstructions (trees, fences, nearby houses) whatsoever |
| II | 0.285 | Light local shielding with few obstructions |
| III | 0.240 | Some obstructions within two house heights |
| IV | 0.185 | Obstructions around most of perimeter |
| V | 0.102 | Large obstruction surrounding perimeter within two house heights |

51.70 is finalised. A second issue is how to deal with local concentrations of pollutants within a house. This has been dealt with by increasing the minimum ventilation rate by 50% in houses which do not have warm air furnaces or other provision for internal circulation of air.

Perhaps the most difficult issue facing the CGSB 51.70 Standard committee is the choice of the appropriate period over which to analyse pollutant concentration. If the pollutant of greatest concern were an instantaneous poison such as CO, then the minimum ventilation requirement would have to be met at the worst instant of the year. If, on the other hand, the pollutant of greatest concern were a substance whose only effect is cumulative, such as radon, then it would be logical to ignore short-term peaks and require only that the annual average ventilation rate meet the specified requirement. The committee has chosen to require that the daily average ventilation rate on the worst day of the year meet the specified ventilation requirement. This choice should be validated by further research.

Although some questions remain to be answered about the accuracy of the technical background to this Standard, it is clearly an improvement over the present approach, which is to ignore the problem and assume that any house can be sealed to any level of airtightness without creating an indoor air quality problem.

## 5. CONCLUSIONS

Several Standards have been prepared recently or are now in preparation which provide guidance on the subject of air infiltration in houses. None of these have been adopted into law anywhere in Canada. However, competent professionals working on this topic should be aware of their requirements and of their technical bases.

Public input to the Standard development process is welcomed. Those who have contributions to make should contact the Standard-writing organizations to request that copies be sent to them when the public review begins.

## 6. ACKNOWLEDGEMENTS

The work behind this paper has been carried out by the many volunteers serving on the committees which produced the Standards it describes. These Standards will save energy and protect health. The people who worked to create them deserve our appreciation.

## 7. REFERENCES

1. Sulatisky, M., "Airtightness Tests on 200 New Houses Across Canada: Summary of Results", BETT Publication No. 124, January 1984.

2. Yuill, G. K., "The Variation of the Effective Natural Ventilation Rate with Weather Conditions", SESCI Conference, Winnipeg 1986.

# PASSIVE SOLAR SIMULATION FOR MULTIZONE BUILDINGS: A FREQUENCY DOMAIN APPROACH

A.K. Athienitis,

Killam Postdoctoral Fellow
Mechanical Engg Dept
The University of Alberta
Edmonton, Alberta, T6G 2G8

H.F. Sullivan, K.G.T. Hollands

Professors
Mechanical Engg Dept
University of Waterloo
Waterloo, Ont., N2L 3G1

## ABSTRACT

An efficient methodology for simulation of auxiliary heating load requirements in multizone passive solar buildings is presented. The methodology is based on a frequency domain network model, and discrete Fourier series are employed in modelling the inputs, thereby providing flexibilty in weather data requirements; if hourly weather data are available, detailed simulations may be performed by using many harmonics (e.g. 18 harmonics for a two-week period) or, if only average monthly data are given, the average performance may be determined by using a few harmonics. Predicted results are compared with measured data from the NRCC Division of Building Research Passive Solar Facility and close agreement is obtained.

## 1. INTRODUCTION

Simulation of building energy transfer on the computer is becoming an increasingly popular tool in passive solar analysis and design. Implementation of passive solar concepts such as the direct gain room with large south-facing windows and night insulation increases the importance of radiant exchanges and necessitates more modelling detail than for conventional buildings. Fortunately, new powerful microcomputers are increasingly being used in design. However, for small residential buildings, high design costs are not justified, so fast and efficient thermal design is essential. Frequency domain models appear to be promising in achieving these objectives because they take advantage of the inherent periodicity in the weather data (ambient temperature and solar radiation) which are inputs to a simulation; also, when linear network theory is employed in modelling, distributed elements (storage mass) may be represented and most network nodes can be eliminated, thereby resulting in a minimum number of equations.

Recently, there has been a significant amount of work in modelling weather data by discrete Fourier series (Hittle, [1]; Anderson et al, [2]; Smart et al, [3]. However, the main purpose of these workers was to reproduce synthetic weather data using a minimum number of harmonics and not to use these Fourier series for a frequency domain thermal solution. They obtained the most important harmonics by employing discrete Fourier transforms. Then, by using only these few harmonics they were generally able to produce synthetic data within time domain programs for hourly simulations. Fourier series representations of weather data using a small number of harmonics (less than 10) have been shown to give accurate results when used for producing synthetic hourly data to be used with time domain detailed simulation models (Hittle, [1]; Smart et al [3]). Hittle, in comparing the auxiliary energy loads calculated using BLAST[1] with actual hourly data and with synthetic data generated using up to 9 harmonics for a whole year, obtained agreement within 6%. As Hittle points out, it would have been far more efficient to determine a periodic solution (a detailed frequency domain program would be needed in such a case); his time domain simulation using BLAST was also essentially a periodic solution because the inputs were periodic. Further, in building energy analysis a completely transient analysis is rarely performed because the most reasonable assumption for the conditions before the first day of a simulation period is to assume that the previous days were identical to this day. Finally, as pointed out by Anderson [2], with frequency domain methods peak events like direct gain room overheating on sunny days can be analysed without necessitating simulation of performance over an entire year.

The purpose of the present paper is to present an efficient and flexible methodology for simulation of multizone passive solar buildings which employs network theory and models the weather data by discrete Fourier series. Further, a comparison between predicted and measured building performance for three two-room units of the NRCC Division of Building Research Passive Solar Facility [4] will be given. The basic modelling approach (Athienitis [5]) as applied to passive analysis (no auxilary heating or cooling) is described elsewhere by Athienitis et al [6,7]. This paper extends the same methodology to auxiliary load calculations using real weather data (e.g. hourly solar radiation and ambient temperature) as inputs. The methodology described by Athienitis et al [5,6,7] employs network theory and Fourier series techniques for detailed and efficient modelling of multizone buildings on the computer. It eliminates the necessity of many modelling approximations commonly made for computational efficiency: it accounts for thermal coupling between rooms, room interior radiant exchanges are modelled accurately, and discretization of the thermal mass (a distributed element) is not required.

## 2. METHODOLOGY

The frequency domain formulation consists of two basic steps. First, the conductances representing longwave radiant exchanges or convection are calculated and each wall is represented as a two-port network element; subsequently, the wall is represented by its Norton equivalent network and this leaves only K nodes (in the simplified network) corresponding to room air and interior surfaces (see ref. [5] for more detail). Then, a nodal heat balance [6] is performed for each frequency of interest, and is given by

$$[Y]_{KxK}\,[T]_K = [Q]_K \qquad (1)$$

where $[Y]_{KxK}$ is the admittance matrix (size KxK) which is a function of geometry and thermal properties of the building components, [T] is the temperature vector and [Q] is the source vector; [Q] consists of actual heat sources (such as solar radiation absorbed by a room surface) and equivalent sources due to application of the Norton theorem (equal to a transfer admittance multiplied by a specified temperature such as ambient temperature). Both [Y] and [Q] are automatically formulated by inspection [5,6]. The solution for [T] is obtained by multiplying [Q] by the inverse of [Y], namely the nodal impedance matrix [Z] (i.e. $[Z]=[Y]^{-1}$). The auxiliary source in each room is modelled by a proportional control heat source, the heat flow through it $q_{aux}$ being given by

$$q_{aux} = g(T_{sp} - T_{ai}) \tag{2}$$

where g is the source constant, $T_{sp}$ is the thermostat set-point (or set-profile) temperature and $T_{ai}$ is the actual room air temperature. When $q_{aux}$ is positive it represents heating power requirements, while when negative it represents cooling power. The auxiliary source is compactly accommodated in the nodal formulation (eqn. [1]) by modifying entries Y(1,1) and Q(1) (node 1 represents room air) as follows:

$$Y(1,1)_{new} = Y(1,1)_{old} + g \tag{3a}$$

$$Q(1)_{new} = Q(1)_{old} + gT_{sp} \tag{3b}$$

Thus, after determining the temperature $T_{ai}$ ($T_{ai} = T(1)$;) we may substitute in (2) and obtain $q_{aux}$ for each frequency. Note that, once the inverses $[Y]^{-1}$ are determined for all important frequencies, they can be stored (or just the first row if we are only interested in $q_{aux}$) and $T_{ai}$ and $q_{aux}$ may be computed for [Q] vectors representing different sets of weather inputs. By choosing suitable values for the source constant g, different types of analysis may be performed; if g is set equal to zero, the program may be used to study the building passive behavior, while by increasing g to a high value it will simulate a specified temperature; the room temperature will closely follow the desired (set) profile $T_{sp}(t)$, the order of magnitude of its swing about $T_{sp}$ being 0.1°C. It is shown in [5] that if g is greater than about $20*Y(1,1)_{g=0}$ (value of Y(1,1) with $g=0$) the above condition is satisfied.

The important frequencies are determined by performing discrete Fourier analysis (or discrete Fourier transform - see Director [8]) of the ambient temperature and of solar radiation and selecting the harmonics with significant magnitudes. For example, if hourly values of a source M(t) are given, we may represent it by a discrete Fourier series as follows:

$$M(t) = \sum_{n=-N}^{N} m_n(j\omega_n) \exp(j\omega_n t) \tag{4}$$

where $m_n(j\omega_n)$ is a phasor corresponding to the nth harmonic. The phasors may be evaluated numerically by

$$m_n(j\omega_n) = [\sum_{k=1}^{I} M(t_k) \exp(-j\omega_n t_k]/P \tag{5}$$

where P is the simulation period (e.g. a day, a week etc.), $M(t_k)$ is the value of M at time $t_k$ and the total number of hourly values of M is I. The maximum number of harmonics N in equation (4) is I/2. However, in practice, the actual number of harmonics that we need to use is significantly lower than I/2 because the magnitudes of $m_n$ may be small as compared to the value of the mean ($n=0$) or the first harmonic ($n=1$). In general, if a harmonic has a magnitude less than 1% of the magnitude of the harmonic with frequency one cycle/day, it is set to zero in the simulation. Note that $m_{-n}$ is equal to the complex conjucate of $m_n$. Thus, if $Z_n(1,j)$ is an entry of the impedance matrix in row 1 and column j, and $m_n(j)$ is the nth harmonic of an input at node j, the room temperature is then given by

$$T_{ai}(t) = \sum_{j=1}^{K} [Z_0(1,j)\, m_n + \sum_{n} \mathrm{Re}[2Z_n(1,j)\, m_n \exp(j\omega_n t)]] \tag{6}$$

where n (positive) corresponds to a harmonic such that $|m_n|/|m_1|>0.01$. Note that a summation over all nodes (K) and harmonics is performed.

The method employs the decomposition technique described in [6] for determining the nodal impedance matrix [Z] for a multizone building and is thus computationally efficient; it runs on an IBM-PC with 256KB RAM (written in FORTRAN).

## 3. APPLICATION AND COMPARISON WITH MEASURED DATA

The most important energy quantities to be obtained for a simulation period in the heating season are the mean and maximum auxiliary heating power. The mean heating power, when multiplied by the time period, gives the total auxiliary heating load. The maximum heating power needed is a good indicator of the building dynamic performance and is important in sizing heating equipment. These quantities were determined with the methodology described and are compared with measured data. Energy dumped (cooling) in the heating season is significant only if the direct gain room is nonmassive; overheating is primarily a comfort problem, and temperature swings may be estimated by setting g (eqn 2) equal to zero.

Simulations were performed for three two-room units which are part of the NRC-Division of Building Research (DBR) passive solar test facility [4]; on-site collected weather data, as well as room temperature and auxiliary power measurements were provided by S.A. Barakat [9]. The three direct gain units are briefly described below, followed by an explanation of the simulation procedure and comparison of measured and predicted auxiliary power.

### 3.1 The DBR Direct Gain Two-zone Units

The DBR passive solar test facility is located in Ottawa (latitude 45.32N). Data are obtained from the facility for studying the dynamic characteristics of buildings with different amounts of mass, as well as for verification of detailed hourly simulation programs. The facility is made up of three huts which include the three units (1,2,3) of interest. Each hut is made up of one two-room unit, a corridor, two more rooms and a basement. A floor plan of the hut which contains unit 3 is shown in Figure 1 (units 1 and 2 have about the same dimensions). Each unit consists of a south and a north room, each room having double-glazed windows with areas $2.6m^2$ and $1m^2$ respectively. All floors are carpeted. The wall construction and their effective thermal resistance values are given in Table 1. The three units only differ in the type and amount of mass present in the room interior. Unit 1 (light construction) is of conventional insulated wood-frame construction with an interior finish consisting of a single layer of 12.7mm gypsum board. Unit 2 (medium construction) contains four layers of gypsum board on vertical walls and two layers on the ceilings. In unit 3 (heavy construction), a single layer of 100mm thick cement bricks is present on vertical walls. The pertinent storage mass physical properties are given in Table 2. The total thermal capacities of units 1,2, and 3 are 1.43, 4.13, and 11.55 MJ/K respectively.

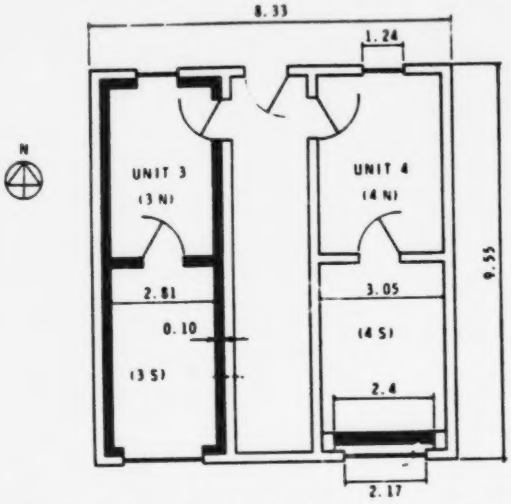

Fig. 1: Floor plan of hut which includes unit 3 (from [4]). The door between south and north rooms has an area of 1.65m$^2$, and the door between corridor and north room has an area of 1.9m$^2$.

Table 1: Wall resistance values (from [9])

| ELEMENT TYPE | CONSTRUCTION | THERMAL RESISTANCE (m$^2$K/W) |
|---|---|---|
| Wall, Light (Unit 1) | Gypsum board, Insulation Particle board | 1.97 |
| Wall, Medium (Unit 2) | Gypsum board (5 cm), Insulation, Particle board | 2.18 |
| Wall, Heavy (Unit 3) | Cement bricks, Gypsum board Insulation, Particle board | 2.04 |
| Internal Partition, Light | Gypsum board, air space, Gypsum board | 0.36 |
| Internal Partition, Medium | Gypsum board (5 cm), airspace Gypsum board (5 cm) | 0.78 |
| Internal Partition, Heavy | 10 cm Brick | 0.06 |
| Window, Double glazed | Glass, Air space, Glass | 0.2 |
| Metal Insulated Door | | 1.03 |
| Wooden Partition Door | | 0.2 |
| Ceiling (Unit 1 & 3) | Gypsum board, Insulation | 3.33 |
| Ceiling (Unit2) | Gypsum board (2.5 cm), Insulation | 3.42 |
| Floor | Carpet and underlay, Wood Insulation, Gypsum board | 7.34 |
| Outdoor air film, Walls | | 0.03 |
| Outdoor air film, Ceiling/attic | | 0.09 |

Table 2: Storage mass properties (from [9])

| Property | Gypsum board | Cement Bricks | Carpet & Underpad |
|---|---|---|---|
| Density kg/m$^3$ | 800 | 2114 | 650 |
| Specific heat J/(KgK) | 837 | 837 | 1380 |
| Thermal Conductivity W/(m·K) | 0.16 | 1.5 | 0.06 |
| Solar absorptance (measured) | 0.26 | 0.66 | 0.92 |
| Normal emittance (measured) | 0.88 | 0.91 | 0.84 |

The operation of the units will now be briefly described [10]. All units were pressurized with corridor air to eliminate infiltration. Basements were heated and kept at 21C (note that floors are well insulated -see Table 1) The corridor temperature was kept constant at approximately 20C. Each room was heated to 20C (low set-point) with an electric baseboard heater and the south rooms were equipped with an exhaust fan to cool the room with outside air when the room air temperature exceeded 27C. The units were operated in two modes: in Mode 1 the door between the two rooms was closed and thus the rooms were only conductively coupled; in mode 2 the door was open and air was circulated between the two rooms using a small fan located above the door.

3.2 The Simulation Procedure

Measured hourly weather data for the site, as well as room air temperature and auxiliary power records were provided by Barakat [9] for two time periods as follows:

1. The first period ($P_a$) was 13 days long and included the days 16Dec.(1980)-28Dec.(1980). During this time the units were operated in mode 1 (door closed).
2. The second time period ($P_b$) was 14 days long and included the days 29Dec.(1980)-11Jan.(1981). During this time the units were operated in mode 2 (door open and fan on).

Simulations were performed for both time periods for the three units. The simulation procedure consisted of two steps:

1. First, discrete Fourier analysis of the important weather data was performed, and up to 18 harmonics with the highest magnitudes were selected to represent each source by a discrete Fourier series.

2. The nodal impedance matrix was then determined and the room air temperature was calculated with eqn (6); the auxiliary power profile was then determined with eqn (2).

The room mean air temperature was estimated from the mean room temperature swing as 21C for unit 3 and 20.5C for units 1 and 2. It was subsequently found that if the low set-point (20C) was assumed to be the mean room temperature, an error of at most 1.5% was introduced.

The mean weather data for the two time periods are given in Table 3. The two most important weather inputs are the solar irradiation transmitted into the direct gain room and the ambient temperature. The complex Fourier coefficients were determined numerically (eqn (5)) with P equal to $P_a$ for period a and $P_b$ for period b. The number of hourly spaced points used to calculate the coefficients corresponding to period $P_a$ was 312 (13days x 24hours), while for period $P_b$ it was 336 (14 days). The maximum number of harmonics that may be used to represent each series is equal to half the number of points; however, it is highly inefficient to use such a high number of harmonics, and unnecessary as may be concluded from observation of the amplitude spectrum diagrams shown

Table 3. Mean weather data for the two periods

Period a is 16Dec.-28Dec.1980,
Period b is 29Dec.1980-11Jan1981.

| Period | Ambient temp.(C) | Attic temp.(C) in unit 1 | 2 | 3 | Daily clearness index |
|---|---|---|---|---|---|
| a | -16.2 | -15.7 | -13.9 | -14.1 | 0.560 |
| b | -17.6 | -17.0 | -14.8 | -15.0 | 0.605 |

in Figures 2 and 3. Figure 2 shows the amplitude line spectrum for solar radiation transmitted through the window for the two periods, while Figure 3 is the corresponding diagram for the ambient temperature. The spectra for period b showed a similar pattern. Harmonics higher than the ones corresponding to 3 cycles per day (n=39 for period a and n=42 for period b) were found to be insignificant both for solar radiation and temperature. Examination of Figure 2 reveals that the most important harmonics (apart from the mean) of the solar radiation are those corresponding to one cycle, two cycles and three cycles per day. For period a, these harmonics are the 13th, the 26th and the 39th, while for period b they are the 14th, the 28th and the 42th. Ambient temperature harmonics generally decrease in amplitude with frequency increase.

The procedure followed in selecting harmonics for representation of the sources was to choose at least the mean and the 3 important harmonics of the solar radiation, and up to about 15 more harmonics of both ambient temperature and radiation. The solar irradiation harmonics were multiplied by the window area and the room effective absorptance (equal to about 0.95, see [11]), and were also increased by the appropriate factor to account for the amount absorbed in the glazings. The resulting values are the harmonics for the total solar radiation absorbed in the room. These values were then divided among the room interior surfaces in proportion to the total radiation absorbed by each surface on a relatively clear day (determined using the model presented in [11]). The harmonics of solar radiation absorbed on exterior surfaces have a negligible effect because of the very low ambient temperature and the high exterior heat loss coefficient ($33.3W/m^2/K$). Thus, the solar radiation absorbed by each exterior surface was represented by its mean term. Also, the diffuse solar radiation absorbed through the north-facing window of the back room was modelled by its mean.

The walls coupled with the corridor, the basement and the attic, were treated in a manner similar to an exterior wall; their Norton equivalent was determined, with the temperature source acting at the back surface being the temperature in the adjacent space.

### 3.3 Results and comparison with measured data

The main objective of the simulations was to correctly calculate mean auxiliary heating requirements and to get a representative picture of the building dynamic behavior as reflected in diurnal variations of heating requirements and their maximum value. Thus, measured and computed values of the mean and maximum auxiliary heating power are compared for each mode of operation of the three units.

Significant cooling (dumping of energy) was necessary only for the south room of unit 1 (in mode 1), which contained insignificant storage mass while receiving the same amount of solar radiation as other south rooms. Thus, cooling load results are also given for this room.

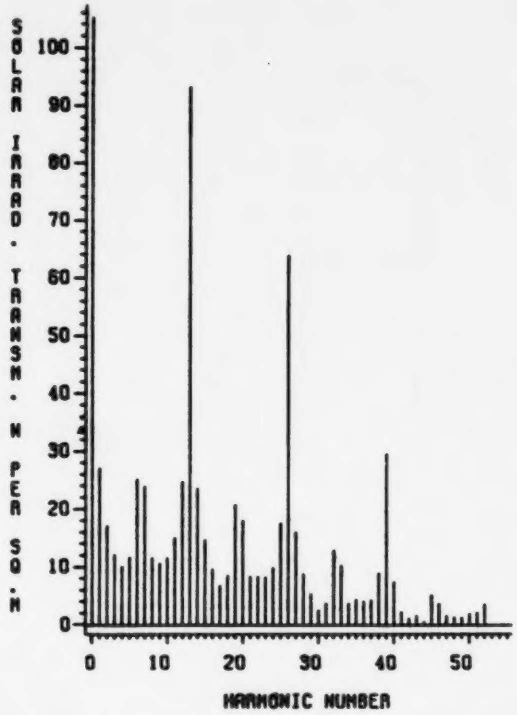

Fig. 2: Amplitude spectrum for transmitted solar irradiation (Period a) Lines indicate magnitude of complex Fourier coefficients, Period=13 days.

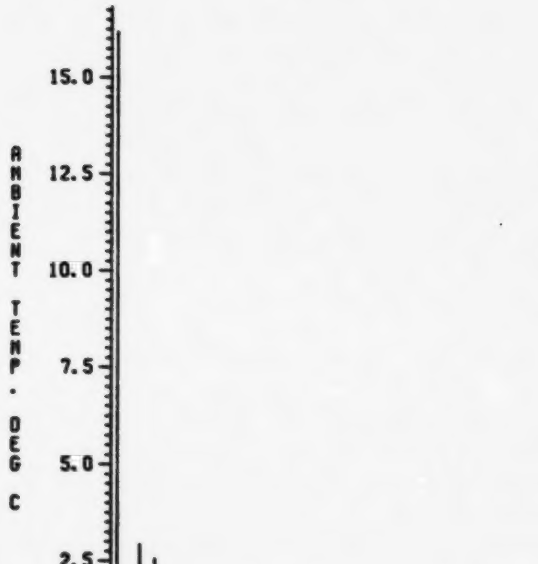

Fig. 3: Amplitude spectrum for ambient temperature (Period a) Lines indicate magnitude of complex Fourier coefficients, Period=13 days.

### Mode 1 (door closed)

The auxiliary heating power profile for each of the three units, determined with 18 harmonics, is plotted in Figure 4. As may be observed from the figure, increasing the amount of mass gives a smoother auxiliary load profile, with lower peak heating requirements. Simulated and measured results are compared in Tables 4-6. In all cases, 18 harmonics and g values of 5000W/K (slightly larger than 20Y(1,1)) were used for the auxiliary source in each room.

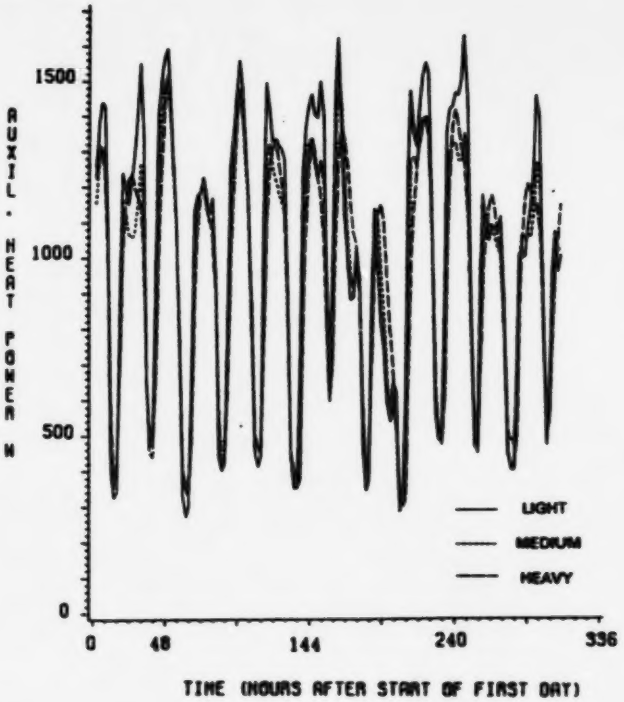

Fig. 4: Auxiliary heating power for the three units (mode 1).

Table 4. Comparison of auxiliary power(W) for unit 1 (mode 1-door closed)

| Quantity | Value | Measured | Calculated | % Difference |
|---|---|---|---|---|
| Heating (S room) | Max. | 1068 | 1034 | -1.4 |
| | Mean | 524 | 511 | -2.7 |
| Cooling (S room) | Mean | -62 | -48 | -22.5 |
| Heating (N room) | Max. | 811 | 695 | -14.3 |
| | Mean | 499 | 505 | 1.2 |
| Heating (TOTAL) | Max. | 1851 | 1628 | -12.0 |
| | Mean | 1023 | 1014 | -0.9 |

Table 5. Comparison of auxiliary power(W) for unit 2 (mode 1-door closed)

| Quantity | Value | Measured | Calculated | % Difference |
|---|---|---|---|---|
| Heating (S room) | Max. | 979 | 1006 | +2.8 |
| | Mean | 474 | 466 | -1.7 |
| Heating (N room) | Max. | 637 | 610 | -4.2 |
| | Mean | 433 | 482 | +11.3 |
| Heating (TOTAL) | Max. | 1614 | 1543 | -4.4 |
| | Mean | 907 | 947 | +4.4 |

Table 6. Comparison of auxiliary power(W) for unit 3 (mode 1-door closed)

| Quantity | Value | Measured | Calculated | % Difference |
|---|---|---|---|---|
| Heating (S room) | Max. | 905 | 899 | -0.7 |
| | Mean | 455 | 448 | -1.5 |
| Heating (N room) | Max. | 700 | 612 | -12.6 |
| | Mean | 507 | 490 | -3.4 |
| Heating (TOTAL) | Max. | 1605 | 1492 | -7.0 |
| | Mean | 962 | 938 | -2.5 |

Considering the experimental uncertainties [10], agreement within about 5% between measured and predicted values is considered to be very good. As can be observed, the mean auxiliary heating power predictions are within 5% of the measured values (the only exception is the north room of unit 2). The predictions for the maximum auxiliary power are usually lower than the measured values because high frequency fluctuations in the ambient temperature or the attic temperature may be missed. However, the results are satisfactory and clearly distinguish the relative dynamic thermal behavior of the units. An interesting observation from Table 4 is that, although the room temperature was not allowed to float significantly about its mean (21C) value, the cooling load was determined within the right order of magnitude and, considering its low absolute value, this is satisfactory. Due to the fact that the amount of storage mass present is very small, most of the solar energy not immediately used is dumped.

The effect of using fewer harmonics is shown in Table 7. As can be seen, the number of harmonics used significantly affects the accuracy of maximum heating calculations. However, its effect on average heating requirements is less important, particularly for massive rooms. Nine terms are adequate for determining the mean auxiliary heating power in the south room. For the north room, since there is no overheating, the mean is adequate for determing mean heating power (since there is no cooling involved).

Table 7: Effect of number of Fourier terms on auxiliary heating power (W) (for south rooms of units only)

| Unit | Quantity | Number of terms (N+1) 1(mean) | 9 | 18 |
|---|---|---|---|---|
| 1 | Max. heating power | N/A | 891 | 1034 |
| 1 | Mean heating power | 462 | 496 | 511 |
| 2 | Max. heating power | N/A | 810 | 1006 |
| 2 | Mean heating power | 411 | 457 | 466 |
| 3 | Max. heating power | N/A | 802 | 899 |
| 3 | Mean heating power | 427 | 444 | 448 |

### Mode 2 (door open)

For this mode of operation, only total power for each unit was recorded at the DBR facility. When the door is open and the small fan is on, forced or natural convection may dominate. To calculate a forced convection coefficient accurately we would need velocity measurements at the doorway, which are not available. The forced convection coefficient could thus be estimated by assuming hot air flowing through the top half of the doorway and cold air through the bottom half and using the fan capacity to determine the air velocity. This gave an estimate of $40W/K/m^2$ which is lower than the natural convection coefficient estimated with a correlation developed by Weber[12] (about $75W/K/m^2$); the latter value was used in the simulations. However, the auxiliary heating power was found to be relatively insensitive to changes of the interzone coefficient betwen these two values. Reducing the coefficient from $100W/K/m^2$ to zero for this period, resulted in about 2% increase in the heating load for unit 1 and about 1% for unit 3.

In order for heat transfer to be permitted between the zones, a high g value (5000W/K) was used for the north room source and a low g value (1000W/K) for the south room. Calculated and measured values are compared in Table 8 which shows satisfactory agreement.

Table 8: Comparison of auxiliary heating power(W) for mode 2 (door open; 19 terms used)

| Unit | Value | Measured | Calculated | % Difference |
|---|---|---|---|---|
| 1 | Max. | 1911 | 1858 | -2.8 |
|  | Mean | 1014 | 999 | -1.5 |
| 2 | Max. | 1689 | 1567 | -7.2 |
|  | Mean | 896 | 916 | +2.2 |
| 3 | Max. | 1701 | 1532 | -9.9 |
|  | Mean | 957 | 953 | -0.4 |

## 4. CONCLUSION

A frequency domain methodology for simulation of auxiliary heating load requirements in multizone buildings was presesnted. It was shown that, by using a small number of harmonics (about 10) to represent real weather inputs by discrete Fourier series, satisfactory accuracy may be obtained for design purposes. The method was employed in predicting the performance of three two-zone units containing different amounts of thermal mass. The satisfactory agreement between measured and predicted results provided confidence in use of the method for practical passive solar analysis. The accuracy of the method may be improved by modelling on/off controlled auxiliary heating more accurately by means of iterative techniques such as the one developed by Athienitis [13].

## ACKNOWLEDGEMENTS

We would like to express our sincere thanks to Dr. S.A. Barakat and the NRCC-Division of Building Research for providing us with measured data for this work.

## REFERENCES

1. Hittle D.C., "A Comparison of Building Energy Use Calculated with Actual and with Synthesized Weather Data", ASHRAE Trans. Vol.85, Pt.2, paper No.2538, (1979).

2. Anderson J.V. and Subbarao K., "Spectral Analysis of Ambient Weather Patterns", ASME Solar Energy Div. 3rd Ann. Conf.,Reno Nevada, (April 1981).

3. Smart M.G. and Ballinger J.A., "Fourier-Synthesized Weather Data for Building Energy Use Estimation", Building and Env., Vol.19,No.1,pp. 41-48,(1984).

4. Barakat S.A., "NRCC Passive Solar Test Facility: Passive Solar Studies at the Division of Building Research", Building Research Note 188, Div. of Build. Research, NRCC, Ottawa, (May 1982).

5. Athienitis A.K., "Application of Network Methods to Thermal Analysis of Passive Solar Buildings in the Frequency Domain", Ph.D. Thesis, Dept. of Mechanical Engineering, Univ. of Waterloo, Canada, (Apr.1985).

6. Athienitis A.K., Chandrashekar M. and Sullivan H.F., "Modelling and Analysis of Thermal Networks Through Subnetworks for Multizone Passive Solar Buildings", Journal of Applied Mathematical Modelling, Vol.9, No.2. pp.109-116, (1985).

7. Athienitis A.K. and Sullivan H.F., "Optimum Method and Algorithm for a Representative Room Temperature and its Swings", Proc. of ASME/ASES Solar Energy Conf., Knoxville Tenn. USA, pp.18-25, (March 1985)

8. Director S.W., "Circuit Theory, a Computational Approach", J.Wiley &Sons, (1975).

9. Barakat S.A., Personal Communication, (6 Dec.1984).

10. Barakat S.A., "NRCC Passive Solar Test Facility: Description and Data Reduction", Building Research Note 214, Div. of Build. Research, NRCC, Ottawa, (May 1984).

11. Athienitis A.K. and Sullivan H.F., "Efficient Method for Determination of Solar Radiation Absorbed by Each Room Interior Surface", Proc. of ISES (International Solar Energy Society) International Solar Energy Conference, Montreal, (June 1985).

12. Weber, D. and Kearny R.J., 'Natural Convective Heat Transfer Through an Aperture in Passive Solar Heated Buildings', Proc. of AS/ISES 5th Passive Solar Conf., Amherst, pp.1037-1041, (Oct.1980).

13. Athienitis A.K., "Frequency Domain Modelling and Simulation of Heat Transfer in Passive Solar Buildings", Proc. IASTED Int. Conf. on Applied Modelling and Simulation, Vancouver, June 1986, (in press).

# MONITORED AND SIMULATED PERFORMANCE OF A LARGE ENERGY EFFICIENT BUILDING INCORPORATING THERMAL STORAGE

Brian F. Gray
Greg J. Schoenau
Robert W. Besant
George H. Green †

Department of Mechanical Engineering
University of Saskatchewan
Saskatoon, Saskatchewan
S7N 0W0 Canada

## ABSTRACT

This paper presents thermal performance data and computer simulation results for a large, energy efficient building. Building performance data, for a period beginning in July 1984 and ending in June 1985, were obtained by means of an automatic data acquisition system. Thermal simulations were conducted using DOE2.1B [1]. The simulations, once verified for the existing system, were used to evaluate the performance enhancement due to the installation of thermal storage and recovery (TSR) systems. Although monitored results indicate that storage efficiency is significantly lower than originally anticipated, the addition of TSR systems reduced annual utility costs by approximately $11000.00 when compared to the optimized conventional alternative. Building performance was evaluated for electrical demand charges of $5.95/KVA, electrical consumption charges of $.017/KWhr, and steam utility costs of $7.20/MMBtu ($6.83/GJ).

## 1. INTRODUCTION

Of 11.5 billion dollars worth of energy consumed annually in Canada by non-industrial buildings, approximately 25 percent is used to provide climate conditioning in commercial and institutional buildings. With the implementation of retrofit and conservation strategies, this consumption could be reduced by as much as 50 percent.

The engineering building at the University of Saskatchewan acts as a showpiece for evolving energy technology and incorporates several innovative systems developed for the purpose of reducing building operating costs. In order to quantify the energy performance of the building and the operational enhancement due to the installation of TSR systems, an extensive automatic data acquisition system was developed and installed, and detailed thermal simulations performed using DOE2.1B. Simulations were verified by means of comparison to monitored results and subsequently used to evaluate energy performance for various primary system configurations.

The building has 240000 ft.$^2$ (23000 m$^2$) of floor area distributed over three levels and is comprised largely of laboratory, classroom and office space. A large library is located at the centre of the building and extensive computer facilities are also provided. Although varying somewhat in construction, exterior walls are all approximately R-25 (RSI 3.5) and roofs R-40 (RSI 5.0). To further reduce transmission losses, all windows are triple pane sealed glazings. South oriented glazings are treated with low transmissivity coatings to reduce solar thermal gains. Effort was made to limit free infiltration by use of vestibule entrances, sealed glazings, and an air tight vapour barrier incorporated into exterior walls. Although these efforts have reduced infiltration rates below those typical of similar buildings, infiltration remains a significant portion of winter heating loads. Conditioned air is supplied to the building by means of four, variable air volume (VAV) secondary systems. One system is dedicated to interior spaces, two to exterior building zones, and one to the area housing computer facilities.

Chilled and heated system water is provided from a heating and cooling plant located in the basement of the building. A 240 ton (3.03 GJ/hr) centrifugal chiller is equipped with dual condenser bundles, one of which is coupled to the cooling tower circuit and the other to the building's low temperature perimeter radiation system. Cooling loads associated with central computing hardware are met by packaged room cooling units cooled by domestic water supply. Recovery of available heat from these units is not, at present, economically justified.

The heating system is equipped with a steam/water shell and tube heat exchanger used to meet heating demands in excess of those met by chiller heat recovery. Steam utility requirements are met from the campus steam plant which uses natural gas fired boilers to meet the heating demands of various campus buildings.

Hot and chilled water thermal storage is provided by five 30000 gal. (136000 L) storage tanks located in the building sub-basement. Figure 1 shows a cut-away view of

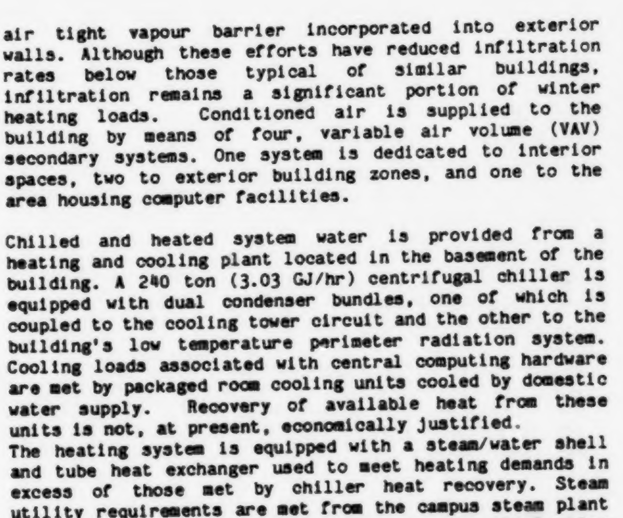
HWS
or
CHS
STORAGE TANK 30,000 gallons
(16 ft., diameter x 28 ft., long)
HWR
or
CHR
TANK MEMBRANE

Fig. 1 Membrane Isolated Thermal Storage Tanks

one of the five externally insulated steel tanks. Isolation of supply and return storage water is achieved by a flexible membrane mounted inside of the tank at the middle circumference.

Thermal storage can be used for chilled or heated storage or a combination of the two. The allocation of tanks for heated or chilled storage is controlled by physical plant staff and is dependent upon the season of operation.

All building conditioning is controlled by a computer programmed to control the operation of the conservation devices located within the Engineering Building. This system is linked to an extensive Central Control and Monitoring System (CCMS) which provides control of all buildings located on the University campus.

For large commercial users, electrical utility charges are generally a composite of demand and consumption charges. Consumption charges are combined with peak demand charges, or time of use charges implemented by utilities to encourage use of electrical energy during off-peak periods. Although alterations to building use and design can contribute to the reduction of peak electrical loads, the addition of thermal storage permits the production of cooling energy during periods of minimum electrical rates thus transferring electrical loads to periods of lower utility cost.

It is typical of large buildings that interior portions require year-round cooling while exterior portions require heating and cooling. The implementation of central refrigeration equipment provided with dual condensers, provides the opportunity for heat reclaim. The addition of heated thermal storage provides off-peak production of heated storage, and recovery of heat during non-coincident heating and cooling loads.

Because peak capacity requirements for chilled storage and heat recovery occur at different times during the year, these two operational modes do not conflict and in the Canadian climate, can both be implemented without adding to required storage capacity.

## 2. BUILDING THERMAL SIMULATION PROCEDURE

Simulation results were verified by comparing them to monitored building performance for the same period. Comparisons of monthly electrical consumption, thermal transient behavior, and diurnal cooling loads for primary and secondary systems are presented in the following section.

Manual measurements of electrical and steam consumption, strip chart records of some specific electrical demands and a computer controlled datalogging system were used to monitor the ongoing performance of specific equipment and loads associated with conditioning the building's interior. The combination of automatically monitored channels and utility measurements provided comprehensive information as to the building's performance.

Simulation input was prepared independently of monitored data and was determined from a detailed survey of building blueprints, mechanical specifications, and equipment and occupancy data. All simulations were performed on a VAX 11/780 minicomputer.

Although owners of TSR enhanced buildings generally express satisfaction with installed systems [2], data is rarely available that identifies performance enhancement due to the installation of thermal storage systems. Simulations were performed for four variations on the installed primary systems identifying peak electrical demand and total utility consumption for each. The four cases evaluated were:

1. The presently installed system utilizing chilled thermal storage for peak demand reduction and direct and indirect heat recovery using the recovery chiller and heated thermal storage.
2. A double condenser centrifugal chiller rated at peak cooling load capacity and controlled conventionally. Direct heat recovery was specified for conditions of coincident heating and cooling loads. Recoverable heat in excess of that required for perimeter heating was rejected through fresh air economizer load shedding or the cooling tower. Thermal storage was not included in this analysis.
3. Neither storage nor heat recovery systems were implemented in this case. The system utilized a conventional centrifugal chiller and economizer load shedding to meet cooling loads. Perimeter heating was provided by direct steam and hydronic perimeter radiation units. This case represented an optimized conventional system and served as the basis of comparison for thermally enhanced systems.
4. A chilled storage system utilizing equipment with identical capacities to existing equipment. No primary heat recovery equipment was simulated.

Evaluation of these four system variations provided a means of quantifying the performance enhancement due to the installation of TSR systems.

## 3. SIMULATION AND THERMAL PERFORMANCE MEASUREMENTS

Figure 2 presents monthly simulated and monitored electrical consumption indicating the accuracy with which the simulation determines electrical consumption throughout all seasons.

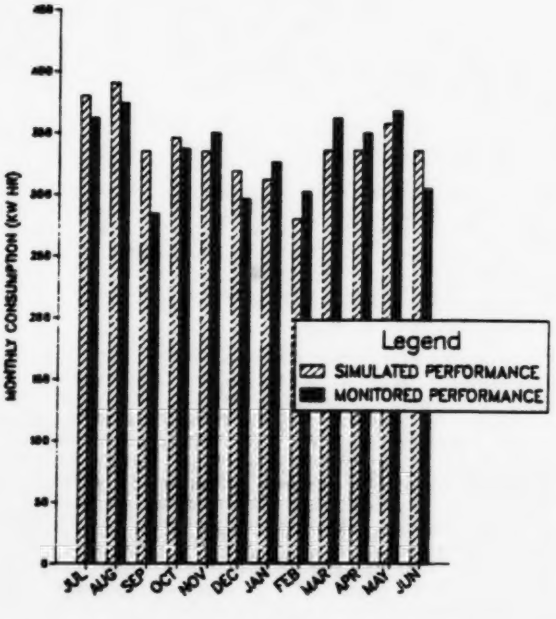

Fig. 2 Monitored and Simulated Monthly Electrical Consumption

Figure 3 presents a profile of hourly cooling loads as experienced by the primary system for conditions corresponding closely to those prescribed by the ASHRAE Fundamentals Volume [3] for summer design conditions.

Actual peak ambient conditions were 83.4°Fdb/61.0°Fwb with a diurnal temperature variation of 33°Fdb. These results indicate that primary loads are modelled with

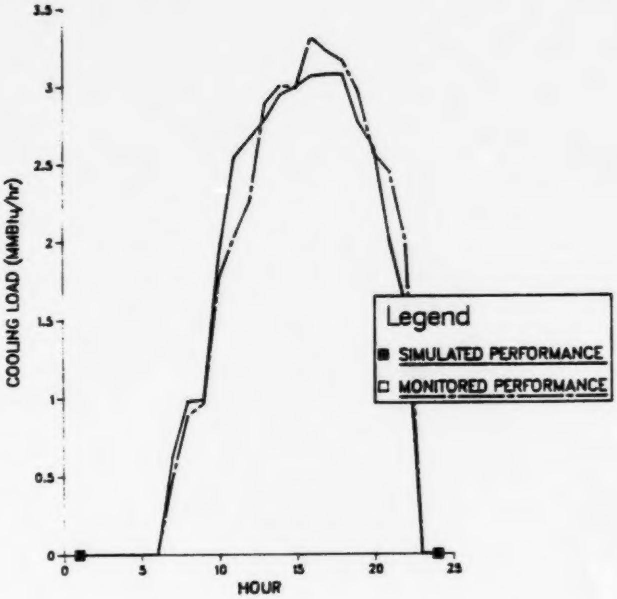

Fig.3 Simulated and Monitored Diurnal Primary Cooling Load Profile (83.4°Fdb/61.0°Fwb)

considerable accuracy. Further inspection revealed secondary system profiles were not as accurately represented as the total indicates. Table 1 contains data regarding peak and daily total cooling loads for each of the three secondary systems.

TABLE 1. PEAK AND DIURNAL COOLING LOADS (MMBtu)

| | System-1 | | System-2 | | System-3 | | Total | |
|---|---|---|---|---|---|---|---|---|
| | Peak | Daily | Peak | Daily | Peak | Daily | Peak | Daily |
| Simulation | 1.6 | 20.1 | .75 | 9.2 | .73 | 8.8 | 3.08 | 38.0 |
| Monitored | 1.96 | 22.5 | .63 | 6.2 | .73 | 7.9 | 3.31 | 36.9 |

Total demand and peak cooling loads were overestimated for exterior zones and underestimated for the interior zone. These inaccuracies tend to compensate for each other to result in reasonably accurate primary loads. The uncertainty associated with monitored data is approximately 10 percent. Results indicate that caution must be exercised if simulation results are to be used for the purpose of developing design specifications.

Thermal transient tests were performed and duplicated by the simulation to verify the dynamic accuracy of the simulation. Tests were conducted for a period of 9 hours at an average ambient temperature of -33°F. Nocturnal testing eliminated solar and ventilation energy variables from the test and minimized occupant discomfort. Internal building zones that have no exterior surfaces experience less severe transient behavior than exterior rooms that experience direct conduction and infiltration losses. Because of the differing behavior of interior and exterior zones, their results are presented separately in Table 2.

TABLE 2. THERMAL TRANSIENT TEMPERATURE CHANGES (°F)

| | Interior | Exterior | Total |
|---|---|---|---|
| Simulation | 1.4 | 3.6 | 2.1 |
| Measured | 1.3 | 3.4 | 2.0 |

Comparison of measured and simulated results indicate the accuracy with which DOE2.1B models building dynamic behavior. The limited temperature changes that occurred even under such severe ambient conditions, is indicative of the integrity of the building envelope and the considerable thermal mass inherent to the structure. Although temperature changes indicate limited heating load reductions are possible by implementation of night temperature set-back, considerable potential exists for the utilization of thermal mass for peak cooling load reduction by means of night cooling cycles and diurnal floating zone temperatures.

Monitored thermal storage efficiency revealed that chilled thermal storage experiences daily efficiencies ranging from 60 to 70 percent. This is significantly below efficiencies predicted for similar configurations by Truman and Wildin [4]. The adjacent configuration of the installed system results in substantially higher internal losses than the thermally stable configuration tested by Truman and Wildin. The existing system is not only configured in a thermally unstable manner but the membrane design results in a heat transfer area equal to half on the surface area of the tank. Proper configuration would reduce this area to the cross-section of the tank.

Buildings of all sizes have a characteristic break-even temperature that represents the ambient temperature at which internal energy gains are capable of offsetting building energy losses. Evaluation of building heating and cooling loads for various ambient conditions indicated a break-even temperature as low as 10°F (-12°C).

Simulated annual energy consumption during the monitoring period was 18780 MMBtu/yr (1.98 x $10^4$ GJ/yr) composed of electrical and steam consumption. Figure 4 shows the relative contribution of various components to total building energy demand.

Although recovered energy is not a component of utility demand, it is shown to illustrate its relevance with regard to annual energy consumption. Electrical energy related to its production is included in the categories of H.V.A.C. auxiliary equipment and the chiller demand. Figure 5 shows the breakdown of total heating load into its main components.

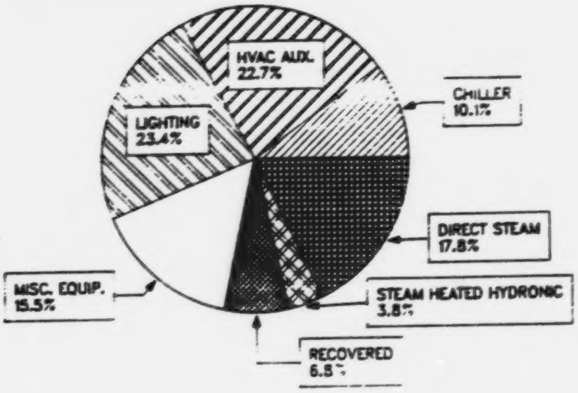

Fig. 4 Simulated Annual Energy Components

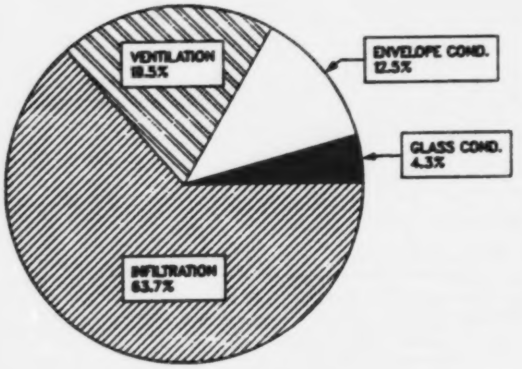

Fig. 5 Simulated Annual Heating Load Components

Although considerable effort was made to reduce infiltration loads by tight construction techniques, infiltration remains the largest single contributor to building heating loads. The majority of infiltration losses occur through building entrances on the main floor.

Figure 6 shows the average contribution of various components to building cooling loads for the peak cooling season. Lighting, fenestration, and equipment all contribute substantially to total cooling load but in spite of the installation of V.A.V. air handling systems, fan energy remains the largest single component.

The relative contribution of various demands to building peak electrical demand is shown in Figure 7. The addition of thermal storage has reduced electrical peak loads on primary cooling equipment by 110 KVA. This saving represents a reduction of approximately 15 percent for design conditions. Figure 8 shows diurnal electrical demand for the installed system as compared to a conventional system.

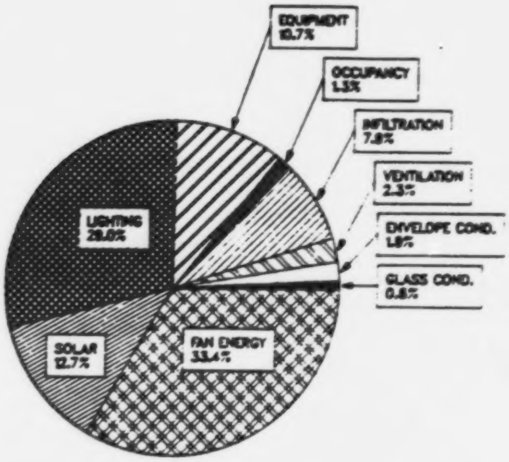

Fig. 6 Simulated Annual Cooling Load Components

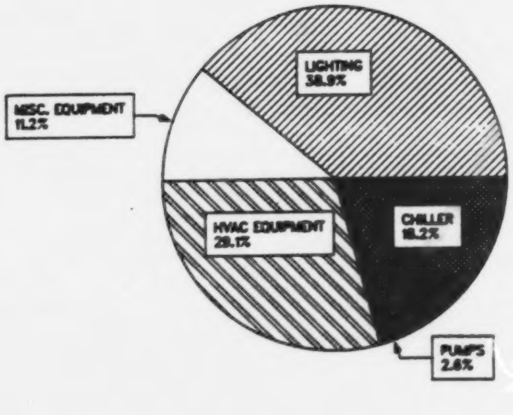

Fig. 7 Simulated Peak Electrical Load Components

The conventional system and two variations upon thermal storage and recovery systems were modelled in addition to the existing system. Annual demand and consumption, and their related charges under the existing utility price structure is presented in Table 3.

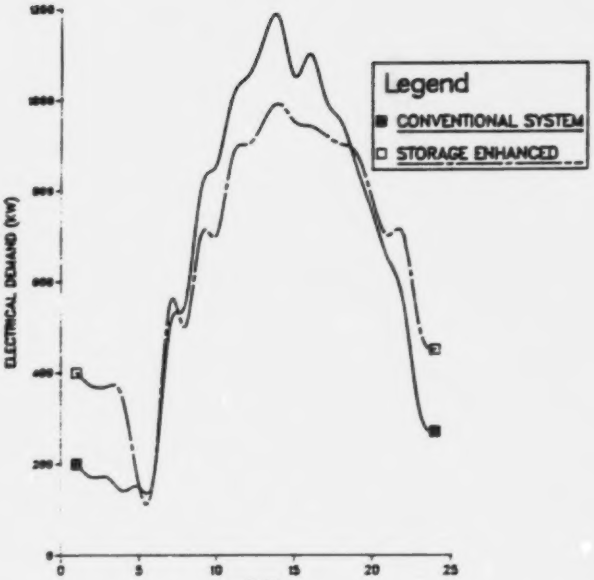

Fig. 8 Simulated Diurnal Electrical Demand for Conventional and TSR Enhanced Systems

TABLE 3. UTILITY COMPONENTS AND COSTS FOR VARIOUS OPERATIONAL STRATEGIES

| | NS/NR | NS/R | CS/NR | Existing |
|---|---|---|---|---|
| Elec. Dmd.(KVA) | 10683 | 11603 | 9824 | 10376 |
| Steam (MMBtu) | 6090 | 5167 | 6090 | 4552 |
| (GJ) | 6419 | 5446 | 6419 | 4798 |
| Elect. (MMBtu) | 13912 | 14121 | 14072 | 14318 |
| (GJ). | 14663 | 14884 | 14832 | 15091 |
| Total Cons.(MMBtu) | 20002 | 19228 | 20162 | 18870 |
| (GJ) | 21082 | 20266 | 21251 | 19889 |
| Cost Data (1985 dollars) | | | | |
| Steam | 43605 | 37200 | 43605 | 32774 |
| Elec. Cons. | 71354 | 72426 | 72175 | 73436 |
| Elec. Dmd. | 63564 | 69038 | 58452 | 61737 |
| Tot. Ut. Cost. | 178523 | 178664 | 174232 | 167947 |

NS/NR - no storage or recovery systems (conventional)
NS/R - no storage, heat recovery
CS/NR - chilled storage, no heat recovery
Existing - presently installed system

## 4. DISCUSSION AND CONCLUSIONS

Building energy performance was determined from monitored and simulated results. Data presented details the ability of DOE2.1B to accurately portray the operation and performance of TSR systems and their application to a large commercial building. Also quantified, is the affect of a TSR system upon total building utility costs for a particular utility rate structure. Results presented in Table 3 indicate that for the existing building, the addition of direct heat recovery systems would have actually resulted in increased annual utility costs due to increased peak demand charges. Conclusions as to the economic merit of installation of TSR systems can be made only after detailed analysis of annual building performance. The accurate portrayal of building and equipment characteristics, and the anticipated utility rate structure is essential if results are to be meaningful.

Storage efficiency is critical to peak demand reduction. Evaluation of the affect of storage efficiency on peak electrical demand indicates that tank thermal degradation results in 20 percent greater loads on the chiller during peak load conditions than those that exist for storage with 90 percent efficiency.

The agreement between measured and simulated thermal response indicates the model accurately portrayed thermal mass affects within the building. Calculations indicate that useful building thermal mass is equivalent to the energy stored in the chilled thermal storage tanks. Although further analysis is required, utilization of inherent thermal mass by night temperature setback cooling cycles or floating diurnal set-points may contribute to significantly reduce peak cooling loads.

Results of monitored data and simulated results have indicated that TSR systems installed have made a significant impact on total utility costs. Their impact is a composite of total energy consumption reduction facilitated through heat recovery, and peak electrical demand charge reduction facilitated through chilled thermal storage.

Simulation of a conventional primary system coupled to the existing building and secondary systems resulted in annual utility costs of $178523 for the simulated period. Motivation for the installation of chilled thermal storage systems arise from reduced peak electrical demand and associated charges. Additional capital cost of storage installation is partially offset by reduction of required chiller capacity. Operational cost reductions arising from peak load reduction are partially offset by increased electrical consumption required to offset thermal storage losses. Chilled thermal storage systems have no effect on building heating loads.

Increased capital and operating costs would result from the installation of conventionally sized refrigeration equipment with direct heat recovery capability. Because of extended chiller operation, electrical demand charges and consumption are both greater than for the conventional system and negate benefits associated with recovered energy.

The installed system consumed 77.8 KBtu/ft.$^2$ yr as compared to 83.0 KBtu/ft$^2$yr for a conventional system. Although this figure is indicative of savings arising from heat recovery, as Table 3 indicates, it fails to fairly represent savings due to peak load reduction strategies. Normalized energy consumption is but one indicator of building performance, and because the addition of chilled thermal storage actually contribute to higher energy consumption, is not representative of impact that TSR systems have on building operating costs. Installation of the existing system has for the period in question, resulted in reduction in operational costs of approximately $11000.00 when compared to the conventional alternative. Peak load reduction and heat recovery techniques are each responsible for approximately half of this total.

The following conclusions may be drawn from results obtained during this study:

1. DOE2.1B is capable of accurately simulating the thermal performance of TSR enhanced systems for northern climates. The recent development of DOE2.1B for microcomputers has substantially increased its viability as a design tool. Considerable engineering costs arising from use of the program must be justified from economic or energy conservation standpoints.
2. Installed TSR systems substantially improve system performance. Coupled heat recovery and chilled storage systems offer significant conservation improvements over either system operating separately. The installation of heat recovery or thermal storage is not in itself an assurance of reduced operating costs. Careful analysis of the interaction of utility consumption and peak demand charges is essential when installations of this nature are contemplated.
3. Monitored storage efficiency is substantially below that predicted by available literature. Low storage efficiency adds both to total electrical consumption and demand charges. Different tank configurations and insulation levels should be considered for future sites.
4. Fan energy constitutes a large portion of total building cooling loads in spite of the installation of VAV secondary systems. Careful attention must be paid in future installations to the role that fan energy has in contributing to electrical consumption, peak demand and cooling loads. Systems incorporating variable pitch vane-axial fans or variable speed fan drives perform more efficiently under partial loads than do variable outlet or inlet designs.
5. Building conduction does not constitute a large portion of either cooling or heating loads. If infiltration integrity can be maintained and building costs lowered significantly, reconsideration of insulation levels and exterior wall construction techniques is recommended for future structures.

## 5. ACKNOWLEDGEMENTS

The authors would like to express their gratitude to D. Child and H. Salisbury of the University of Saskatchewan Physical Plant for their assistance in the acquisition of material necessary for the completion of this document. This research would not have been possible without the financial support of the National Science and Engineering Research Council, the University Physical Plant, and the Canadian Mortgage and Housing Corporation.

## 6. REFERENCES

1. DOE-2 Reference Manual, Lawrence Berkeley Laboratory, Berkeley, California.

2. Franklin Research Centre, "Survey of Thermal Storage Installations in the United States and Canada", ASHRAE (1984).

3. ASHRAE Handbook, 1985 Fundamentals Chapter 23 (1985).

4. Wildin, M.W., Truman, C.R., "A Summary of Experience with Stratified Chilled Water Tanks", ASHRAE Transactions, Vol. 91, Pt. 1B, (1985).

---

† It is noted that Professor George Green died on March 15, 1986, before this paper could be completed.

# Solar
# Water Heating
# Systems

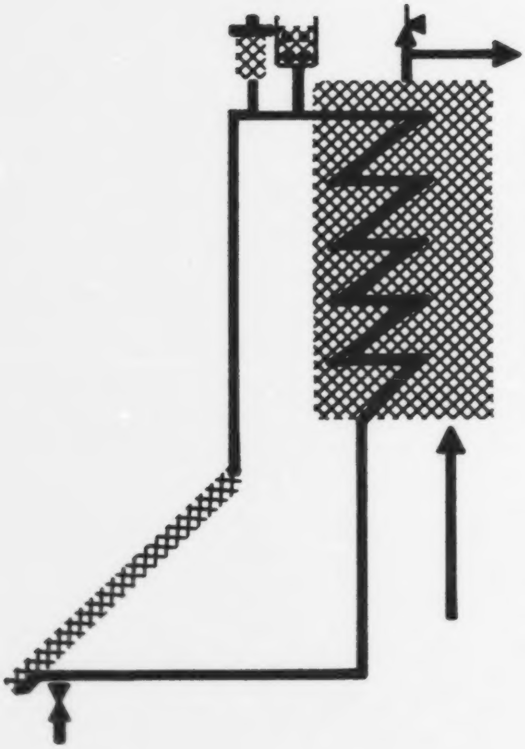

# DETAILED PERFORMANCE COMPARISONS BETWEEN THERMOSYPHON AND DRAINBACK SOLAR DOMESTIC HOT WATER SYSTEMS

Bruce E. Sibbitt
Ontario Research Foundation
Sheridan Park
Mississauga, Ontario L5K 1B3

Thomas Onno
National Research Council
Ottawa, Ontario K1A 0R6

Both formerly with the Div. of Energy, N.R.C.

## ABSTRACT

A thermosyphon solar domestic hot water system and an essentially identical pumped drainback system, operating under the same conditions, were monitored in detail for two months. Days with representative performance have been selected and analyzed to improve the understanding of the operation of these systems. Important differences between the two systems exist in collector loop control and thermal capacitance , energy delivery profile and stratification of storage.

## 1. INTRODUCTION

Initial tests in the NRC Solar Domestic Hot Water Test Facility emphasized commercially available Canadian systems, partially in support of the EMR demonstration program. In parallel with this activity, a limited research effort on thermosyphon systems was initiated.

A freeze-protected system was assembled, (1), using a storage tank having a tank-in-tank potable water heat exchanger with a glycol heat exchanger wrapped around the inner tank. This system would appear to have a number of significant performance disadvantages in comparison to an equivalent pumped drainback system: An additional heat exchanger is required to contain the glycol in the collector loop; A non-draining collector loop has increased thermal mass relative to a drainback loop and glycol mixtures have higher viscosity and lower heat capacity than water.

In spite of these considerations, the NRC thermosyphon system consistently outperformed all the commercial Canadian systems in terms of total energy delivered to load on a yearly basis. As previously reported, (2), (3), during a two year period its net energy delivered was 15% greater than the second place system. Since the thermosyphon system was considerably more reliable than the pumped systems, the above figure includes some estimation of data interpolated across periods of malfunction. Fig. 1 shows that during this test period the thermosyphon had a greater advantage in delivered energy during the summer and a smaller advantage in the winter.

During the two year period relatively low level monitoring, based primarily on integrated energy quantities, was used. Consequently, it was not possible to quantitatively evaluate the causes of the performance difference. It was assumed that the major factors were the enhanced stratification of the storage due to low collector flow rates and the inherently more accurate control of flow initiation and shutdown as a result of the themosyphon action.

As part of the documentation process associated with the phasing out of the Division of Energy, a short period of intensive monitoring was undertaken on two systems which had nominally identical collectors and storage systems. One was similar to the original themosyphon system, (except that the glycol heat exchanger was not used). The other was a drainback similar to the original second placed system.

The objectives of this testing were:

1) To gather information that would improve the understanding of the more subtle and complex phenomena that occur in these systems;

2) To develop experimental methods that would complement computer simulations of thermosyphon and drainback systems, particularly regarding transient analysis.

3) To motivate design of new system configurations and control strategies incorporating the best features of systems now in use.

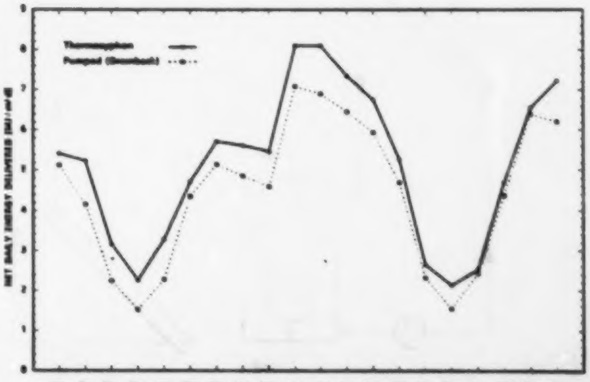

Fig. 1. Long-term Performance Comparison

## 2. APPROACH

### 2.1 Solar Systems

Fig. 2 shows the layout of the two solar systems which were operated side by side, with the same load, during the monitoring period. Table 2 lists the principal operating parameter differences between the two systems.

### 2.2 Experimental Methodology

The instrumentation layout is shown in Fig. 3. A total of 51 data channels were measured at one minute intervals. Emphasis was placed on the accurate measurement of energy flow into and out of storage. Precisely calibrated and matched platinum RTD's were used. The thermosyphon loop flow rate was measured with an Intek self-heated flow transducer. Valmet meters were used for all other flow measurements. To make detailed performance comparisons between the systems it was necessary to calculate small energy differences to high precision. Crosschecks and frequent recalibrations were used to minimize the effect of drift on these fundamental mesurements.

Since the control of the two systems was believed to be a significant factor in their performance difference, the pumped system was operated with two different settings of the critical turn-off ($\Delta$T) parameter; high accuracy, 0.2 C, and low accuracy, 2.0 C, (compared to a typical value of about 1.5 C). Turn-on $\Delta$T was close to the commonly used value of 10 C.

Estimates were done on the effect of small differences that exist between the collector arrays and the tank-in-tank heat exchangers. On Sept. 23, 1985 both systems were operated under pumped mode with essentially the same operating temperatures. Fig. 4 shows the collector performance, together with data for two other days that will be discussed later. Corrections based on this data were used to adjust system performance so that nominally identical collector arrays could be assumed. To normalize heat exchanger performance, the ratio of energy delivered to load divided by collected energy was calculated. The result is shown in Table 1.

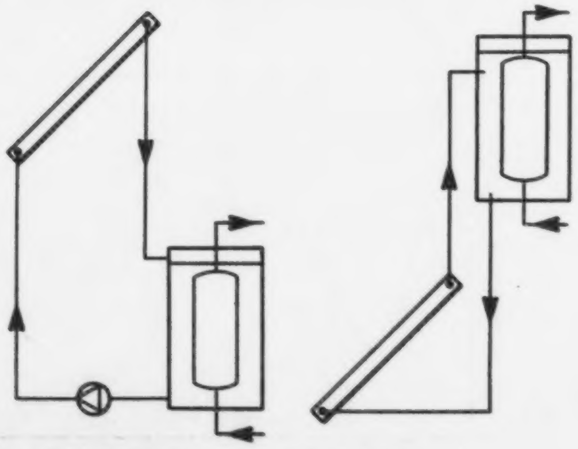
Drainback

Thermosyphon

Fig. 2 Solar System Schematics

TABLE 1 OPERATING PARAMETERS OF SYSTEMS

| | PUMPED SYSTEM | THERMOSYPHON |
|---|---|---|
| FLOW RATES | 8.2 L/min. | Variable<br>Max. 2.0 L/min<br>Max. 1.4 L/min * |
| CONTROLLER SETPOINTS | 10 C on<br>2.0 C off<br>0.2 C off ** | |
| PIPE DIAM. (COLL. LOOP) | 19 mm | 25 mm |
| TANK HEAT LOSS FACTOR | 2.28 W/C | 2.61 W/C |
| RELATIVE HEAT DELIVERY EFFECTIVENESS | 1.0 | 1.04 |

* After 85-10-01

** After 85-11-08

This data was used to make corrections to the values of solar energy delivered.

## 3. SYSTEM OPERATION COMPARISON

This section is devoted to an overview of the operation of the two systems, with quantitative results to follow in Section 4.0.

System operation has been divided into four primary periods:

a) Morning startup transient period.

b) Steady operation through the day.

c) Intermittent cloud cover through the operating period.

d) End of day shutdown transient period.

### 3.1 Typical Summer Day

A typical warm, clear summer-like day will be examined first, as it is under these conditions that the thermosyphon is known to have its best performance advantage. A good example is illustrated in Figs. 5-6. As the previous day was also clear, energy stored then resulted in relatively high operating temperatures.

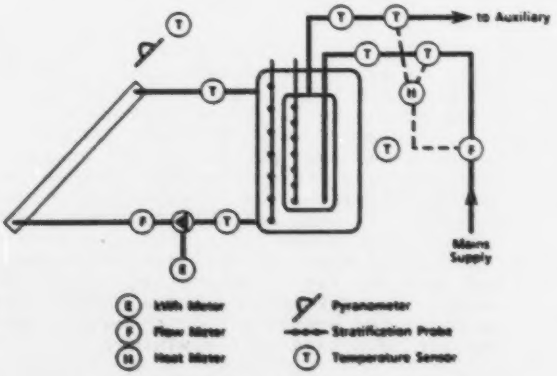

Fig. 3 Monitoring Schematic

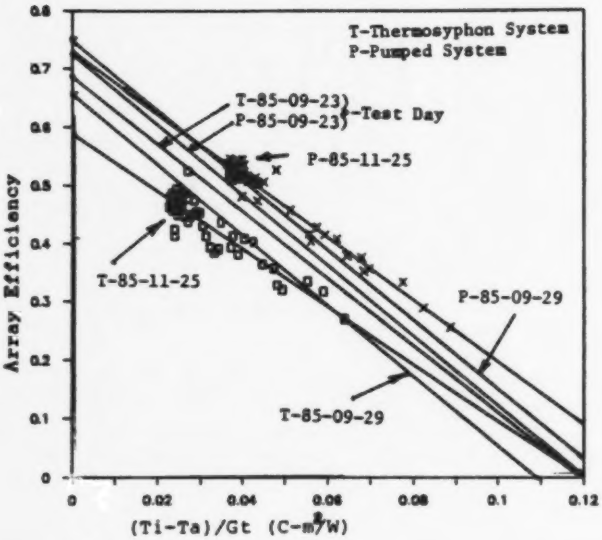

Fig. 4 Measured Collector Array Performance

Morning Startup - The thermosyphon started collecting energy about 20 minutes before the pumped system. The temperatures at the bottom of both storage tanks were within 1 C, so stratification did not significantly affect collector efficiency at that time. The location of the controller sensor clamped to the outside of the return line about 10 cm. from the collector was probably the major factor in the delay. The connecting pipe had to reach the turn-on temperature before the controller switched on. The 10 C setpoint also contributed to the delay. Almost immediately after startup the pump turned off. This is not unusual in systems that do not incorporate a time delay before turn off, especially if there is considerable thermal mass in the supply line which has been cooled to a low temperature overnight. Since the turn-off setting in this system is somewhat high, the tendency to pump switching instability is slightly exaggerated.

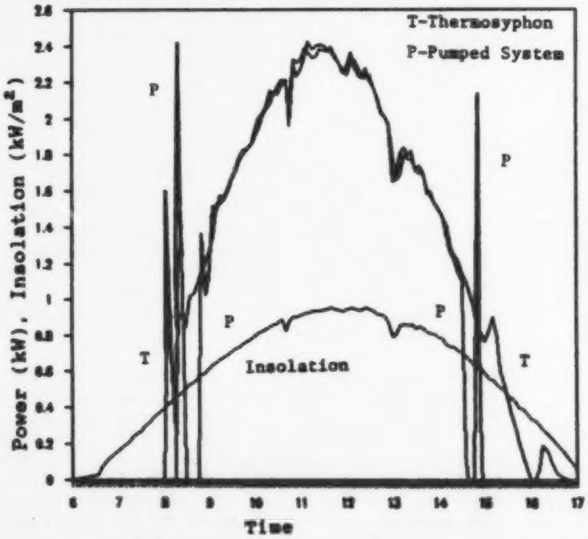

Fig. 5 Power Into Storage - 1985-09-29

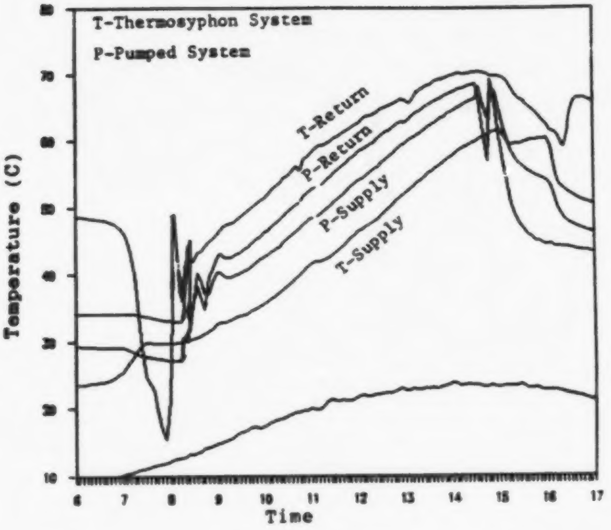

Fig. 6 Collector Loop Temperatures - 1985 9-29

The storage inlet/outlet temperatures in Fig. 6 show that the thermosyphon began to circulate water at a very low rate about an hour before energy delivery is indicated. The return temperature dipped very low, approaching the early morning ambient temperature of 9 C. The Intek flow meter has a cutoff value of 0.16 L/min, and therefore this apparent flow of negative energy into the storage was not recorded. The performance penalty associated with the non-draining thermosyphon loop is estimated from a knowledge of the thermal mass of the heat transfer fluid and the piping.

Immediately after flow was established at a level close to nominal value a significant overshoot occurred, at the same time as the return line temperature measurement peaked. The dominant cause is most likely the inertia of the fluid in the collector loop (in addition, a limited temperature rise is required to produce

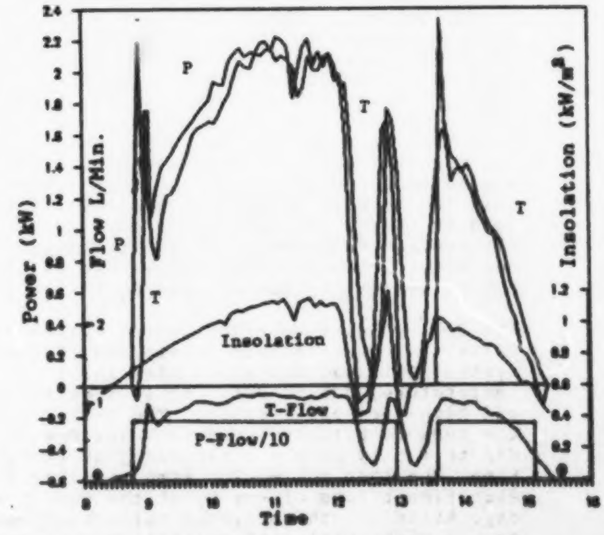

Fig. 7 Power Into Storage - 1985-11-25
And Collector Loop Flow

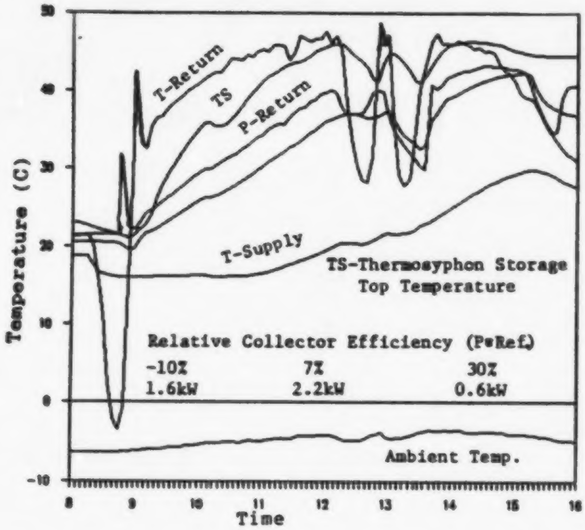

Fig. 8 Collector Loop Temperatures - 1985-11-25 and Top of Thermosyphon Storage

the flow driving bouyancy force). Since a finite time is required for the flow to accelerate, the collector can reach a higher temperature than would occur during steady-state operation under the same ambient conditions. The peak was followed by a dip in the values of flow, return temperature, and collected energy as the cold supply fluid moved through the collector at the high velocity caused by the temperature overshoot.

At startup both collector arrays experienced losses when the absorber temperatures peaked above normal operating levels. The fluid-filled thermosyphon absorber temperature rose more slowly that that of the empty drainback absorber. Some of the energy that was stored in the collectors was recovered when flow started, but part was lost to the surroundings.

Steady Operation Through The Day - The thermosyphon system collector loop had a much larger temperature rise, due to the low flow rate. Its average collector temperature was close to that of the pumped system, and the rate of energy collection appears from the graphs to have been quite close. The significant point is that the thermosyphon system produced energy at a higher temperature. This led to more energy being delivered to the load in the early part of the day. Consequently the average temperature of the thermosyphon collector gradually fell below that of the pumped system, as can be seen in Fig. 6.

End Of Day Shutdown - The pumped system stopped collection over an hour before the thermosyphon system. This was caused by high inlet temperature, due to very little stratification, and high turn-off setpoint. The latter caused the pump to quickly cycle back on. However, it did this only once and ran for just a short time. The lost collection time resulted in a significant loss of energy at the end of the day. After the thermosyphon collection went to zero, a short period of collection occurred. This was due to collector flow going to near zero and allowing the absorber to build up in temperature, much like it did before the morning startup.

## 3.2 Typical Cool Weather Operation

Figures 7 and 8 show operation corresponding to late Fall or early Spring, with sub-zero overnight temperatures. Many of the phenomena previously noted are now strongly accentuated.

Morning Startup - The thermosyphon system startup was delayed by the collector loop thermal capacitance effects so that initial energy collection lagged behind that in the pumped system.

Steady Operation - Flow in the thermosyphon system was throttled back to a peak level of 1.4 L/min. As a result, the temperature rise was over 25 C through most of the day. This was an excessive rise for the operating conditions shown in Fig. 8. The collector return temperature at 9:30 was 39 C, while the top of storage was at 27 C. The high temperature collector fluid was being diluted at a time when the collector was operating at low efficiency. Since the solar fraction will generally be fairly low during this season, there is limited benefit in trying to deliver high temperatures to load. During this time the average absorber temperature was somewhat higher than in the pumped system. The relative level of average collector temperature of the two systems changed more radically through the day than on 85-09-29, and the effect of this on efficiency is illustrated by the relative collection efficiency data at the bottom of Fig. 8. The collector performance data of Fig. 4 shows that the efficiency of the thermosyphon array is significantly reduced as a result of the low flow operation.

Since the pump controller was set to a turn-off value of 0.2 C on this day, there was no indication of pump cycling.

Intermittent Cloud Cover - Between 12:00 and 14:00 there were two periods of heavy cloud cover. These provide a clear indication of the benefits of stratification. During the first period the thermosyphon collector inlet fluid was about 16 C colder than that in the pumped system. As a result the average collector temperature was able to adjust itself to a level about 12 C colder than the pumped system, which allowed it to operate at significantly higher efficiency. In the second period the pumped system turned off and stayed off for almost an hour while the thermosyphon was able to collect a small amount of energy. The thermosyphon system tank top temperature indicates a small loss of stratification during these transients. This is probably an acceptable penalty in order to continue collection of energy.

End Of Day Shutdown - The pumped system stayed on almost as long as the thermosyphon system did. This was mainly due to the abnormally low turn-off setpoint of 0.2 C. The curves of collector loop power, Figs. 5 and 7, have the pumping power subtracted from the power delivered to storage, and the relative efficiency of the pumped system is seen to drop steadily as the turn-off point is approached. A setpoint this low is not practical, due to the specialized and expensive control hardware required.

## 4. PERFORMANCE RESULTS

### 4.1 Accuracy Considerations

An attempt was made to do overall energy balance crosschecks on the systems. Calculations were done with the measured energy into and out of the solar tank, together with calculations of stored energy based on the stratification probes. Even after a number of sources of error had been identified and corrected for, the stored energy calculation produced typical errors of more than 5% of stored energy change. It is believed that seven temperatures measured points in each tank provided insufficient resolution for accurate energy content calculation when steep and mobile temperature gradients are present. Since this prevented the energy balance from closing within the target 2-3% of collected energy, emphasis was placed on careful selection of days for detailed evaluation. These were close to calibration dates and there had to be good relative agreement between data from the two systems in terms of input/output energy flow. It is estimated that energy measurements have been corrected to about 2-4%, absolute accuracy, and that short-term incremental variations in relative collection efficiency can be established to about 1-2%.

### 4.2 Analysis Procedures

The actual and potential relative performance of the two systems was evaluated in three stages:

-Correction of energy measurements and comparisons during periods when both systems were operating.

-Calculation of losses during transient periods such as startup. These losses were estimated from the computed temperature of the stagnating collectors during the startup period.

-Estimates of additional energy that could be collected by feasible optimization of the control system.

### 4.3 Results and Discussion

During a typical summer day the thermosyphon system had a collected energy advantage of 7.4 MJ or 18% relative to the pumped drainback system. It collected about 40 MJ. Both collector loops were very close in efficiency through the middle part of the day. The main difference was at the end of the day (7.4%), due to the much colder inlet temperature of the thermosyphon system, and the poor accuracy of the control system. In the morning the advantage was considerably smaller, (4%), since the previous evening's loads had reduced the difference in tank bottom temperatures to within about 2 Deg. C. Both morning and evening energy penalties could be reduced by a significant amount with more accurate control.

During the typical Fall/Spring day the collected energies were considerably lower, at about 32 MJ. The overnight temperature was quite cold, -6 C. This had a major impact on the startup of the thermosyphon system. It required 1.5 MJ. of collection above the potentially useful threshold to bring the thermosyphon into positive energy collection. The pumped system has similar threshold loss problems due to the delay on startup, but these were much smaller at 0.3 MJ.

Through the day there was a steady change in the relative collection efficiency due to stratification effects. At 9:30 the pumped system had its best advantage (10%), due to low average operating temperature. By 12:00 the collector operating points had switched sufficiently so that the thermosyphon system had an advantage of 7%. By the end of the day (14:00-15:15) the thermosyphon had an advantage of 30%. However, by this time the collection rate was lower (0.6 kW), in comparison to the 1.5 to 2kW of the morning and mid- day cases.

During the first mid-day transient (12:00-12:50) the thermosyphon collected 2.9 MJ while the pumped system collected 2.4 MJ. The pumped system was off during the second transient. while the thermosyphon collected 1.5MJ. From the start of this transient to when steady operation was regained, the net energy difference was 1.7 MJ.

A sizable loss occured in the thermosyphon collector loop due to thermal capacitance effects, since any energy stored in the collector loop fluid at the end of the day was lost overnight. The installation used 25 mm piping, with 14 m of length. On 85-09-29 the temperature went from 11 C to 66 C during the day, resulting in a loss of 4.8 MJ. On 85-11-25 the corresponding figures were -6 to 35 C and 3.3 MJ. This indicates the importance of locating thermosyphon systems as close as possible to the building. The commonly recommended oversize pipe diameter that was used probably was not necessary in this installation, since flow was intentionally reduced during the test. Careful calculations should be done as part of any installation to establish whether a smaller pipe size is feasible for the specific collector-to-storage elevation difference.

Table 2 presents a breakdown of the energy components measured and calculated for the two days.

## 5. CONCLUSIONS

The thermal performance advantages of low and variable collector flow have been evaluated experimentally, and the following conclusions were reached:

Control - The near-optimum control of flow in the thermosyphon system indicates the potential for improved performance in pumped systems with more sophisticated control strategies.

Flow Rate - There is probably a seasonal solar fraction related optimum peak flow rate for thermosyphon systems.

Stratification - High levels of storage stratification have major advantages, both in the ability to deliver useful energy early in the day, and to extend the operation later into the afternoon. In order to avoid loss of stratification at the end of the day the application of diffusers should be studied.

Pumping Energy - A significant amount of energy is required to circulate the collector fluid in a typical pumped system. Low flow systems would reduce this.

Loop Capacitance Penalty - The disadvantages of non-draining antifreeze-filled collector loop have been demonstrated. If all else were equal, the drainback system would have had the higher performance, especially in cold weather.

Experimental Methods - In future studies, several collector absorber temperatures should be monitored to allow accurate calculation of energy loss during transients and to provide information for control optimization. It is very difficult to obtain sufficient measurement accuracy to establish small performance advantages to high absolute accuracy. In order to achieve this, redundant instrumentation and extensive overall crosschecking are essential. Alternative methods of measuring collector flow in thermosyphon systems need to be explored.

## 6. ACKNOWLEDGEMENTS

The authors would like to acknowledge the financial support of Solar Energy Program, Division of Energy, NRC, and the advice and encouragement of Dr. Tom LeFeuvre who also reviewed the manuscript. The experimental work was done by Dave Bordignon of TES Ltd. Charley DeSchiffart of DMR Associates supplied assistance in computing.

## 7. REFERENCES

(1) K. Cooper, Engineering evaluation of Two Thermosyphon DHW Packages, DSS # 0-2710, for SEP, NRC, March, 1981.

(2) E.C. Shewen, Analysis of SDHW System performance (Project Digest) DSS # 2-2790, for SEP, NRC, April 1985.

(3) S.B. Beale and B.E. Sibbitt, Monitoring of SDHW Systems at the NRCC, Proceedings of the I.S.E.S Congress, Montreal, June, 1985.

TABLE 2

PERFORMANCE SUMMARY

| Identifier | Pumped System Collected Energy | | Thermosyphon Collected Energy | | Pumped System Penalty | | Pumped Optimum Control | Net Delivered Energy | | |
|---|---|---|---|---|---|---|---|---|---|---|
| | Measured (MJ) | Calculated (MJ) | Measured (MJ) | Calculated (MJ) | Energy (MJ) | % of total (%) | (MJ) | Pumped (MJ) | Thermosyphon (MJ) | Difference (%) |
| 85-09-29 | | | | | | | | | | |
| AM Loop Capacitance | | - .26 | | -1.6 | -1.3 | -3.2 | 1.29 | | | |
| Temperature * Overshoot | | -1.0 | | -0.06 | 0.94 | 2.3 | .06 | | | |
| AM Pump Cycle | 1.2 | | 2.8 | | 1.6 | 4.0 | 2.8 | | | |
| Steady Operation | 39.0 | | 41.7 | | 2.7 | 6.6 | 41.7 | 12.1 | 14.5 | 20 |
| PM Pump Cycle | 0.07 | | 0.69 | | 0.62 | 1.5 | 0.69 | | | |
| End of Day | 0.37 | | 2.9 | | 2.5 | 6.2 | 2.9 | 23.1 | 25.2 | 10 |
| PM Loop Capacitance | | -0.55 | | -3.3 | -2.8 | -6.8 | 2.8 | | | |
| Pump Energy ** | (-2.9) | | | | (2.89) | (7.1) | | | | |
| TOTAL | 40.65 | -1.8 | 48.1 | -4.91 | 4.37 | 10.8 | 52.2 | 35.1 | 39.7 | 13 |
| 85-11-25 | | | | | | | | | | |
| AM Loop Capacitance | | -0.33 | | -1.5 | -1.2 | -4.1 | 1.2 | | | |
| Temperature * Overshoot | | -0.54 | | -0.05 | 0.48 | 1.6 | 0.05 | | | |
| Steady Operation | 21.8 | | 21.0 | | -0.73 | -2.5 | 21.0 | 5.14 | 7.38 | 44 |
| First Transient | 2.4 | | 2.9 | | 0.53 | 1.8 | 2.94 | | | |
| Second Transient | 2.8 | | 4.5 | | 1.7 | 5.6 | 4.5 | | | |
| End of Day | 2.8 | | 3.6 | | 0.85 | 2.9 | 3.6 | 13.4 | 15.8 | 18 |
| PM Loop Capacitance | | -0.31 | | -1.8 | -1.4 | -4.8 | 1.43 | | | |
| Pump Energy ** | (-2.7) | | | | (2.7) | (9.2) | | | | |
| TOTAL | 29.8 | -1.2 | 32.1 | -3.4 | 0.18 | 0.6 | 34.8 | 18.6 | 23.2 | 25 |

* For comparative use only

** Pump energy entering collector has been subtracted from other tabulated quantities

# SIMPLIFIED DESIGN AND USE OF HEATERS USING CONCENTRATING SOLAR HOT WATER COLLECTORS

M.E. Lux and R.W. Besant

Department of Mechanical Engineering
University of Saskatchewan
Saskatoon, S7N 0W0

## ABSTRACT

Solar collector systems for domestic hot water heating have found few applications on the Canadian prairies due to their high capital costs. These systems normally utilize flat plate, fixed geometry collectors. Alternative schemes such as simplified concentrating solar collectors may be less expensive, resulting in improved economics. The complexity of a solar collection system may also be reduced by restricting operating periods to spring, summer and fall months, when the possibility of damage due to freezing can be disregarded. This may again reduce costs and improve the economics of the system. A test of several different collector types and simulations of their performance was done to estimate the utilizability and economic potential of concentrating collectors on the prairies.

## 1. INTRODUCTION

The application of concentrating solar hot water collectors in the Canadian prairies will be dependant on their reliability, their appearance, their economics, on the degree of owner-operator dependancy in their operation, and on the ease with which they can be installed or adapted to existing hot water heating systems. The technology to accomplish most of these aims is now in place. The economics of the collector are dependant on the initial cost of the system and the yearly savings that can be realized in its performance. The dependancy of the concentrating collector on operator input is most prevalent in the area of focussing or aiming of the collector, so that the receiver/water tube is warmed by the sun over a sufficient period of time. The ease of installation is most dependant on the collector system itself. Because of the nature and timing of the demand for domestic hot water, some auxiliary source of water heating must be available for application during periods when the solar collection system cannot meet the demand. This would most likely be a standard water heater fuelled by electricity or natural gas, and would be used in new installations as well as retrofit situations. The plumbing arrangements for hot water heaters are standard for the vast majority of the prairie housing stock and the collector must operate with this type of system.

## 2. COLLECTOR PERFORMANCE

To initiate the study of concentrating collectors two collectors were constructed using wood for the base, aluminum angle sections for the reflector frame and aluminum sheet as the mirror base. Both collectors used circular copper tubes as the receiver with a selective surface applied directly to the copper. Both collectors were 2.46 metres in length and less then 600 mm in width. One collector was of the simple parabolic trough type and the other was of a type known as Semi-non-parabolic or SNP. The SNP collector approaches the ideal concentration ratio and has a very wide acceptance angle. These collectors were instrumented and tested for their energy delivery under ambient conditions, that is with varying inlet water temperatures, ambient temperatures, wind velocities, and the available solar radiation. Tests were conducted with and without a protective transparent cover. A computer program (SOLAR) was designed to model the collectors' outlet temperature and energy delivery. The results from the program SOLAR were also compared to results from the program f-Chart(1), which is a common tool used in the design of active solar heating systems.

A typical test result from the collector tests is shown in Figure 1, with points from the physical test results and from SOLAR simulations using the actual input data corresponding to the physical tests. The parameters used to graph the results are the collector efficiency as the dependant variable, and a parameter Y as the independant variable. The parameter Y is defined as the outlet temperature minus the ambient temperature, over the incoming radiation. The efficiencies measured on both collectors was typically in the range of 40 to 60%. The wind condition played an active role in determining the efficiency, paricularly for the SNP collector which had an odd geometry leading to eddy currents about the receiver. Temperatures at the collector outlet reached more than 55 °C.

## 3. UTILIZATION

Some design parameters of the hot water heating system can be assumed and will be equivalent for any system. Primary among these are the daily consumption of domestic hot water and its distribution during the day, the available solar radiation, the water inlet temperatures, the ambient outdoor temperatures, the wind speed and of course, the desired set point temperature for the supplied hot water.

Several design decisions have to be made at this stage for any builder. These are based on how complex (expensive) the hot water heating system may be within the builder's capability and budget. The distribution of the available solar radiation is important over the day and, on a broader scale, over the year. The daily time distribution of available solar energy must be weighed against the time distribution of water usage, to determine the amount of storage of the energy. The yearly time distribution of available solar energy must be weighed against the increased complexity required for cold weather operation.

The most important factor in determining operator input in the daily operation of the collector is the angle of acceptance of the collector. If the collector is to be mounted vertically the angle of acceptanc determines the half day operation period, assuming the collector has an azimuth of zero, that is facing south. It may also be tilted back to face the sun more directly. This set up would collect solar energy year round within the time slot each day, and would require no adjustment to maintain focus. The disadvantage is that the time slot will most likely be very small and the energy available outside the time slot in the summer months may amount to a large portion of the yearly total. The most common set up is to have the collector mounted horizontally, again with an azimuth of zero. The tilt of the collector will now be adjusted so that the south-projected solar altitude is within the collector's angle of acceptance over a sufficient period of time for a number of days. The collector may need to be periodically adjusted to maintain its access to solar radiation. Note that an adjustment interval in the order of several months could allow the collector to operate independent of re-aiming or adjustment over the summer months, when most of the yearly solar radiation is available.

The most promising geometry for a concentrating collector is a longitudinal trough collector, probably of the compound parabolic type as described by Hinterburger and Winston(2). This type of collector is one of the family known as the ideal concentrators, because the concentration ratio, defined as the ratio of the reflector area to receiver area, is equal to the inverse of the sine of the angle of acceptance. This is the maximum concentration ratio that can be achieved by a concentrating collector. The best choice for a reflector is a CPC with a half angle of acceptance of 15 to 20 degrees. The tilt of the collector during the summer would then be equal to the latitude at the site plus the half angle of acceptance. During the winter the tilt would be equal to the latitude minus the half angle of acceptance. The absorber used in a CPC could be of any cross section, including a circular tube, flattened tube or plate.

The cost of a CPC trough collector will depend not only on its size but also on the ease with which it can be constructed, both by a manufacturer and by a competent home handyman. Using a unit collector size two metres long by one metre across as an easily handled size, a commercially constructed collector could cost the consumer upwards of $600, using fibreglass as the most likely material for the reflector structure. The home constructed collector would most likely use a different construction technique, requiring less speciallized skill but more overall labour. A collector using wood for the frame and aluminum or some other metal for the mirror base, bent around a curve of the desired cross section, could cost about $150 for the materials only, assuming a ready supply of the reflective material.

Once the collector has been constructed, it may be utilized in a number of different ways. The most important consideration for its utilization is the seasons over which it is to be operated. The inclusion of winter time operation in freezing conditions necessitates the use of some scheme of freeze protection for the collector. This may be done by using an intermediate heat transfer fluid such as glycol, with a freeze point well below the minimum outdoor design temperature. The glycol would circulate in the collector and would heat the domestic hot water by means of a heat exchanger coil either in a separate water tank or installed in the domestic hot water heater. This system could suffer an efficiency penalty as the effectiveness of the heat exchanger coil will reduce the heat transfer to thehot water. The system also requires more complex plumbing and the supply of glycol.

An alternative to using glycol and a heat exchanger is to employ shut-off and drain valves in the water circulation route to the collector. These would have to be controlled by temperature, so that as the water approached the freezing point, the shut-off valves would close and the collector would drain.

The simplest system is one which has the collectors normally shut-off and drained every time the collector might freeze. This, of course, requiresa large amount of operator input when manual control is used in place of a control system for automatic drain down. However, the idea has great validity when applied on a seasonal basis. The largest portion of the yearly solar radiation is incident over the late spring, summer and early fall. The temperatures in this period are also generally above freezing. The collectors could be restricted to operation in this season only and could be manually shut off for any infrequent freezing occurences. The penalty that must be paid is the loss of energy collection over the cold weather season. Figure 2 is a time average distribution of water usage independent of the amount of consumption. This is about 100 litres per day per person or about 400 litres per day of domestic hot water for an average family of four. Figure 2 gives the percentage of daily water usage in any given hour, which would be equal to the hourly percentage of hot water consumption as well. If an average high hourly consumption can be taken as 7 percent of the daily consumption then the design hourly hot water supply from the solar collector would be 28 litres per hour. The peak hourly consumption is approximately 12 percent of the daily consumption, or 48 litres per hour, occuring between 19:00 and 20:00 hours.

The 1 metre by 2 metre example collector will be utilized in the following example by connecting 2 collectors in series mounted along a horizontal axis and facing south. Circulation from the water tank to the collector would be forced using a pump to allow flexibility of placement of the collector. The collector is fed from a tap at the cold water inlet to the water tank/heater. The return to the water tank from the collector is easiest to make at the hot water outlet at the top of the tank. This could provide acceptibly hot water at the outlet during the summer months in the central portion of the day, but at other times it may not be hot enough. An alternative is to use a two tank system, using a simple insulated tank to store the collector water. The outlet of this tank would feed the inlet of the standard hot water tank; this would now have to provide only the balance of the heating requirements, and would ensure that the water temperature at the tap was above a minimum temperature. An extension of this idea could place the second tank slightly above the collector and allow circulation between the collector and this tank by natural convection means. The storage tank could be approximately half the size of the standard hot water tank and heater, and could be insulated for freeze protection or it could be exposed to solar radiation. No pump or mechanical parts are required, meaning reduced maintenance and there may be about a ten percent rise in performance over a day, because the amount of circulation through the collector is correlated to the amount of available solar radiation.

## 4. SYSTEM PERFORMANCE

The program SOLAR was used to generate the energy delivery of the collector system and also the outlet water temperatures, using the typical day for each month. The analyses were duplicated using f-Chart to check the simulations, giving very similar results.

Table 1 summarizes the energy delivery and collector outlet water temperatures for each month for the system at 8:00, 10:00, 12:00, 14:00 and 16:00 hours as estimated by the program SOLAR. The system is assumed to operate at a flow rate of 28 litres per hour. The inlet water temperature is assumed to remain stable at the monthly water mains temperature . This gives a conservative estimate of the collector temperature as the inlet temperature may be higher during periods when the consumption of hot water is below 28 litres per hour and the storage system is returning previously-heated water to the collector inlet. The ambient temperatures are assumed to vary over the day, between plus or minus one standard deviation from the monthly mean. The daily solar radiation and the wind speed are assumed to be at the monthly mean levels. It is assumed freeze-protection equipment in the form of shut-off and dump valves is operational in the winter so that the water is never allowed to freeze. The amount of auxiliary energy required to supply domestic hot water with, and without, the solar collection system is summarized in Table 2. The third column gives the average monthly savings for each month, which is the energy delivered by the solar collector. The required domestic hot water supply temperature is 55 Celsius. At the bottom of the Table is an annual summation of the costs and savings.

The annual savings that can be attained from the use of the collector as just described amount to $133 using electricity as the backup fuel and Saskatchewan rates for the consumption. The energy output of the collector is approximately 10.9 GJ. Again this is a conservative estimate as the system is sized for a flow rate of 28 litres per hour to match the average high hourly consumption of hot water, not the average hourly consumption. The contribution of the collector output from the summer months is 53 percent of the annual output or 5.7 GJ for a savings of $70. If the auxiliary fuel used was natural gas, the costs for hot water from the heater and the savings from the solar collector are both reduced. Assuming current Saskatchewan costs of $0.1289 per cubic metre of natural gas and an average seasonal efficiency for the gas hot water heater of 55 percent, the savings from year round operation of the collector amount to $69. If operation is restricted to the summer, the savings amount to $36.

The cost for the solar collector system will depend on its complexity, whether the system is home constructed or purchased commercially and whether or not the system is professionally installed. These three determinants are not independant of one another. A complex system is more likely to be purchased commercially and installed professionally at an additional cost to the consumer. A commercial collector system using two collectors and the simplest arrangement would cost in the range of $1200. Installation could be done by the homeowner. If these collectors and the system were home-built the cost could be $300, again with self-installation. Inclusion of a second tank may increase costs by $100 regardless of system manufacture,and may also increase the complexity of installation and thus require an additional cost to have this professionally done. Any of these systems would be restricted to operation during the summer period only.

Using the summer performance only, the simplest commercial collector system without freeze protection would have a simple payback period of more than seventeen years. This is assuming electricity as the auxiliary fuel, no cost for installation and single tank operation. Using natural gas, the payback period is more than thirty-three years. The addition of a second tank would add two to three years to the payback period of either system. If an automatic control for freeze protection were used, this would allow year round operation, and increase the costs of the collector system by approximately $200 at the manufacturer's level. These costs are somewhat unknown as performance and reliablilty are high priorities and demand a price. In addition, costs for professional installation would have to be included and may amount to more than $1000. The simple payback period for electricity for this system is now eighteen years, and the system is highly operator independant for fail-safe operation. Using natural gas the payback period is thirty-five years. Note that with year-round operation seasonal adjustment may be required for re-aiming of the collector for optimum efficiency.

Using the simplest home-built collector system and summer performance only, the simple payback period for this system is almost four and a half years. Again this is assuming electricity as the base fuel and a single tank system. Using natural gas, the payback period is eight to nine years. Adding a second tank adds one to two years to an electricity based system and two to three years to a natural gas system. The operation of a system without freeze protection is much more involved than one which has automatic freeze protection, but certainly the economics are better. The addition of an automatic valve system would greatly increase costs as these are not commonly available to the average consumer. Using the payback period of four and a half years and the incremental savings of $53 for electricity, the maximum economic cost for the freeze protection system for increased economic benefit is about $290.

Similiar analysis can be done using alternate schemes of freeze protection. In all cases, the simple payback period can be used together with the incremental cost and incremental savings to obtain the maximum benefit within a given payback period. This period should only be exceeded as a response to outside factors, such as increased convenience, greater needs for fail-safe operation or personal preferences for "solar status".

## 5. CONCLUSION

In general, both the parabolic and SNP collectors performed very well in their testing. The parabolic trough collector required much more periodic adjustment of its slope to remain in focus. The maximum time that the collector would continue to function was slightly longer than two weeks, and even then performance could deteriorate toward the end of the period. The SNP collector was much less sensitive requiring adjustment only for improved accuracy of measurement. The effect of the wind was to generally decrease the efficiency at higher values of Y. The separation of the data into wind catagories still left quite a bit of scatter, however. It is felt that eddy currents played a strong part in varying the attenuation of the efficiency at higher values of Y, or enhancing it at negative values of Y. The results for the SNP collector showed particular scatter as the odd geometry twisted the wind currents more.

Covering of a concentrating collector of the types and construction tested appeared to have two effects. One was to attenuate convection losses from the surface of the receiver. However, the other effect was to attenuatethe total radiation striking the collector, and possibly scatter the beam component of the radiation. From the test data gathered, it appears that the attenuation of convection losses outweigh the radiation reduction. This would be more prevalent in colder conditions, when convection losses can be much greater. However, the effect is reversed when the ambient temperatures exceeds the average receiver surface temperature.

Solar collector systems are now becoming more popular for the heating of water either for domestic use or perhaps for the backyard swimming pool. Most of these are commercial units using flat plate collectors and cost upwards of $3000, with a third of this cost for installation. It appears that the solar industry at large has a preconception of concentrating solar collectors as touchy appliances requiring frequent cleaning and maintenance, and most importantly, complicated and frequent adjustment of the concentrating apparatus. Even using the simple parabolic trough it was shown that this is not the case. More importantly, there are designs available which would require no adjustment or maintenance over the course of a hot-water-heating season, say for a pool. These systems require much less plumbing than flat plate systems, and the fabrication of the mirrored surfaces can be done by any careful do-it-yourself homeowner.

For domestic application, from the economic analyses that were done, it can be concluded that a commerical concentrating collector of the type described is not at this time economical. The shortest payback period that was calculated was seventeen years. For a simple commercial system and a marginal payback period of five years, the cost of electricity would have to increase to 11.4 cents per kilowatt-hour from the current level of 4.4 cents per kilowatt-hour. Using natural gas, for a five year payback period, the cost of fuel would have to increase five times to 65 cents per cubic metre. Both of these calculations assume the lowest possible cost for the collector system and installation by the homeowner.

Home-constructed systems have much better economic potential under the present pricing structure for fuel on the Canadian prairies. If the auxiliary fuel is electricity, the payback period for the simplest system for summer operation is already under the marginal period of five years, if that is the criteria to the homeowner. If the base fuel is natural gas, the price for the fuel would have to increase to more than 21 cents per cubic metre. This is not likely for the near term but the homeowner may also wish to consider economics up to the nine year period using natural gas. Benefits also include the availability of an alternative fuel supply (solar).

From the study of the application of solar technology, it can be concluded that there are ample possibilities for commercial manufacture of simple concentrating collectors. This industry would be best suited as an expansion to an existing plastics manufacturer. The major concern, however, would be pricing and marketing of the completed product. The marketing strategy would have to create a need for the solar collectors beyond their economic need. This unfortunately, has not been easily accomplished by the existing solar manufacturing industry, partly because of the distance between the existing collector's cost and economic benefit to the consumer. Thus, the acceptance of solar collectors for domestic application hinges first upon a lower cost than currently prevalent. After this is achieved it is still uncertain whether the remaining gap between economic cost and benefit can be bridged by benefits in other areas, such as ecological awareness, or the status of owning a solar system. These ideas may also hold true for industrial application, but normally the overriding concern to business is economic.

## 6. REFERENCES

(1) W.A. Beckman, S.A. Klein, J.A. Duffie, "Solar Heating Design by the f-Chart Method". McGraw-Hill, New york, 1978.

(2) H. Hinterburger and R. Winston, "Efficient light coupler for threshold Cerenkov counters". Review of Scientific Instrumentation No. 37, 1966.

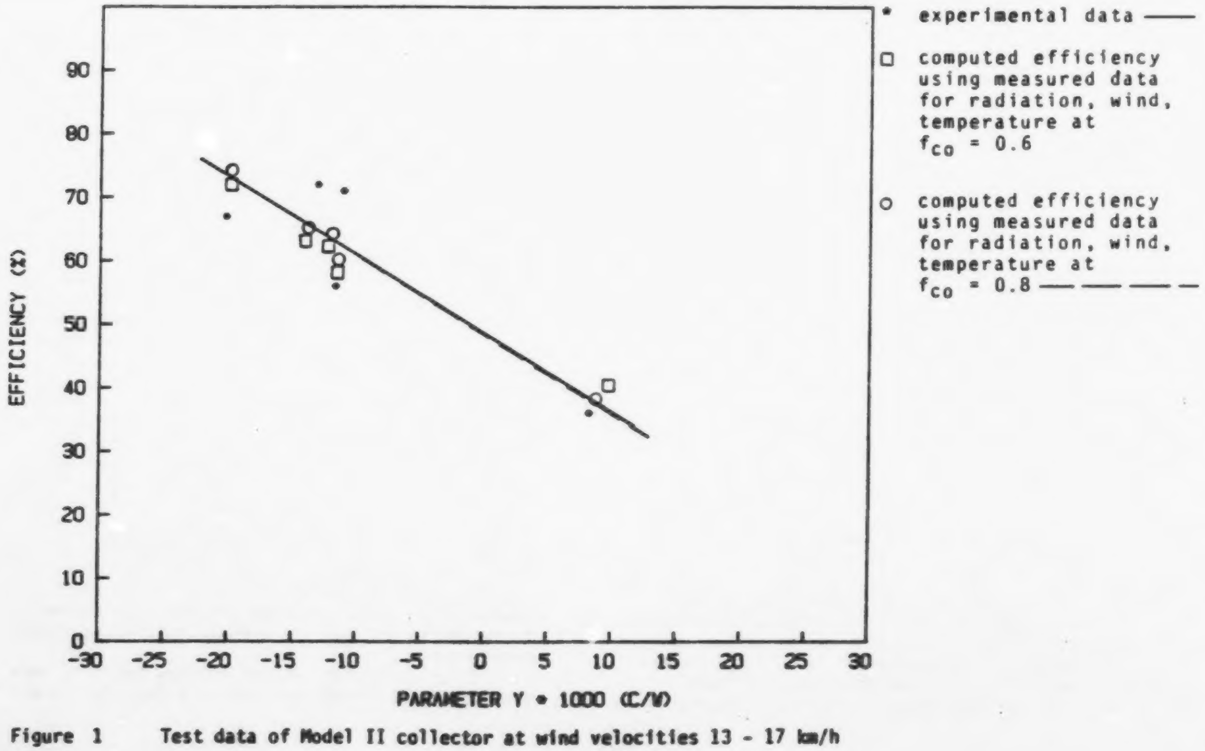

Figure 1 Test data of Model II collector at wind velocities 13 - 17 km/h

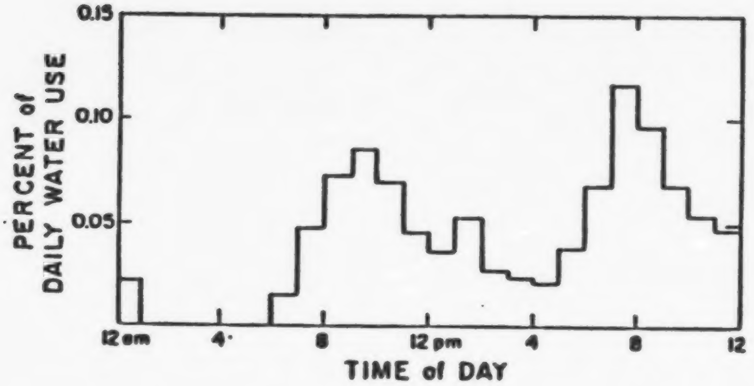

Figure 2 Average time distribution of water usage

| MONTH | | TIME | | | | |
|---|---|---|---|---|---|---|
| | | 08:00 | 10:00 | 12:00 | 14:00 | 16:00 |
| Jan | Energy (W) | 0 | 861 | 1184 | 880 | 0 |
| | Temp (°C) | 0 | 26.6 | 36.5 | 27.2 | 0 |
| Feb | Energy (W) | 11 | 1274 | 1650 | 1290 | 42 |
| | Temp (°C) | 0.3 | 39.3 | 50.9 | 39.8 | 1.3 |
| March | Energy (W) | 43 | 1460 | 1837 | 1474 | 67 |
| | Temp (°C) | 2.4 | 46.2 | 57.8 | 46.6 | 3.2 |
| April | Energy (W) | 556 | 1160 | 1432 | 1174 | 579 |
| | Temp (°C) | 19.9 | 38.6 | 47 | 39 | 20.6 |
| May | Energy (W) | 656 | 1196 | 1430 | 1207 | 674 |
| | Temp (°C) | 26.3 | 43 | 50.2 | 43.4 | 26.9 |
| June | Energy (W) | 681 | 1176 | 1386 | 1186 | 698 |
| | Temp (°C) | 31.6 | 46.8 | 53.3 | 47.1 | 32.1 |
| July | Energy (W) | 796 | 1388 | 1639 | 1398 | 809 |
| | Temp (°C) | 37.9 | 56.2 | 63.9 | 56.5 | 38.3 |
| Aug | Energy (W) | 641 | 1256 | 1524 | 1266 | 660 |
| | Temp (°C) | 35.4 | 54.3 | 62.6 | 54.6 | 35.9 |
| Sept | Energy (W) | 439 | 1029 | 1303 | 1042 | 461 |
| | Temp (°C) | 28 | 46.2 | 54.6 | 46.6 | 28.7 |
| Oct | Energy (W) | 10 | 853 | 1131 | 868 | 35 |
| | Temp (°C) | 11.4 | 37.4 | 46 | 37.9 | 12.2 |
| Nov | Energy (W) | 0 | 540 | 786 | 556 | 0 |
| | Temp (°C) | 7.22 | 23.9 | 31.5 | 24.4 | 7.22 |
| Dec | Energy (W) | 0 | 535 | 796 | 554 | 0 |
| | Temp (°C) | 1.11 | 17.6 | 25.7 | 18.2 | 1.11 |

**Table 1 Energy Delivery and Outlet Temperature from Example Collector**

| MONTH | Auxiliary Hot Water Energy Without Solar Heater MJ/month | Auxiliary Hot Water Energy With Solar Heater MJ/month | Savings From Solar Heater MJ/month |
|---|---|---|---|
| Jan | 2858 | 2205 | 653 |
| Feb | 2581 | 1721 | 860 |
| March | 2800 | 1711 | 1089 |
| April | 2626 | 1567 | 1059 |
| May | 2540 | 1388 | 1152 |
| June | 2234 | 1127 | 1107 |
| July | 2165 | 819 | 1346 |
| Aug | 2049 | 856 | 1193 |
| Sept | 2039 | 1116 | 923 |
| Oct | 2280 | 1633 | 647 |
| Nov | 2402 | 1995 | 407 |
| Dec | 2858 | 2437 | 421 |
| YEAR | 29,432 MJ | 18,575 MJ | 10,857 MJ |

Yearly electricity savings from solar heater (at 4.4¢/kWh) = $133
Seasonal (May to Sept.) electricity savings from solar heater = $70

Yearly natural gas savings from solar heater (at 12.89¢/m$^3$) = $69
Seasonal (May to Sept.) natural gas savings from solar heater = $36

Table 2 Monthly Energy Savings from 4 m x 1 m Collector

# DOWNWARD TRANSFER OF HEAT, WITHOUT USING PUMPS OR CONTROLS

## ( AS APPLIED TO A SOLAR HOT WATER HEATER )

T. Lawand
Brace Research Institute
Macdonald College of
McGill University
Ste. Anne de Bellevue,
Quebec, Canada.

C. Ives, W. Wight
Hawes & Wight Limited.
Pointe Claire,
Quebec, Canada.

## ABSTRACT

This report proceeds from laboratory model tests of a downward heat pipe to field tests of a heat pipe solar domestic hot water system at the Brace Research Institute of McGill University.

This system uses a new principle of self pumping of heat from a higher to a lower level which relies on the difference in vapour pressure of a heat transfer fluid leaving the solar collector/boiler as hot vapour; and the colder liquid leaving the heat exchanger (in the hot water storage tank), which ensures the circulation of the heat transfer working fluid in the system.

No pumps or electronic controls are required, except for an electric solenoid valve controlled by reed switches (development of a passive mechanical valve is planned at a later stage to eliminate reliance on electric power). The system is otherwise independent of external power and automatically self regulating, governed by the differences in temperature throughout the system.

Unlike thermosyphon type systems, the heat storage reservoir can be located at a level much lower than the solar collectors and, thanks to the use of a suitable refrigerant working fluid, the system does not require any protection measures against freezing.

The heat exchanger coil (in the storage reservoir) condenses vapour and can therefore be much smaller than conventional sensible heat exchangers which normally require non-standard storage tanks. This coil replaces the bottom element of a standard electric storage water heater, thereby permitting two installation options a) use of existing DHW heater only, b) addition of a standard tank to increase solar heat storage capacity.

## INTRODUCTION

This paper covers an R & D project directed by Hawes & Wight Limited in collaboration with Brace Research Institute, the purpose of developing and testing a new type of downward heat pipe which when attached to a solar water heater allows the system to operate independently of external power and electronic controls. Thus this system has the advantages of the thermosyphon without the disadvantages: the hot water storage reservoir can be placed at any elevation above or below the solar collectors and, thanks to an appropriate refrigerant working fluid, this system does not require any protection against freezing.

## CONCEPT PHASE

Before the present project, the operation of the downward heat pipe system had been evaluated in Italy with the aid of several instrumented test rigs. The results obtained enable comparison with conventional systems with electric circulating pumps. These tests showed that for a system, where the height difference between the solar collectors and the DHW storage tank was approximately 13 metres, that efficient transport of heat was feasible for a low temperature penalty.

A Proof-of-Concept project was carried out successfully in 1983 by Hawes & Wight Limited.

## LABORATORY PHASE

### Optimize Downward Heat Pipe (and Interfaces)
### (with electric simulation of solar heat input)

This Phase consisted mainly of the development of a laboratory model downward heat pipe (together with the collector interface and the Domestic Hot Water tank interface) to study Downward Heat Pipe operation. It was demonstrated that the Downward Heat Pipe functions with its source heat only and does not require external power source. Also, data was obtained to assess the technical and economic feasibility of a Domestic Hot Water solar system based on the Downward Heat Pipe. Our starting point was the proof of concept and market definition phase conducted during 1983 by Hawes & Wight Limited, which constructed and tested a laboratory proof of concept model of a downward heat pipe system based on an existing European design (by G. deBeni of Ispra, Euratom, Milan, Italy) which actually has been patented in the United Kingdom. Note that a pre-production prototype system has been constructed in Europe and has successfully undergone a full season of demonstration field testing. However, the quantity of Freon working fluid is some 8 times greater than the Hawes & Wight system developed and tested earlier. The design of a similar European system is considered to be too expensive for Canadian and North American market needs.

The market constraints for Canadian solar Domestic Hot Water systems indicate that a low cost modular sealed system would be most suitable (possibly also suitable for the Do-It-Yourself market) in order to reduce production overheads and inventory cost markups.

## PROTOTYPE PHASE

This phase included design, fabrication and testing of a working prototype Domestic Hot Water system (full operating conditions with solar heat input)

This phase consisted of modifying and refining the laboratory prototype components according to the test results obtained. It was therefore necessary to optimize and integrate the components of the system. It was also necessary to model the desired performance of the system and to compare theoretical desired results against those obtained by field testing of the working laboratory system under actual solar conditions.

## OBJECTIVES

Technical Objectives:

The technical objectives of the project were to develop a downward heat pipe system suitable for integration with a heat pipe solar collector and a conventional storage type electric water heater using a minimum of special components which would meet the following requirements:

1) which would be designed to meet an average daily combined hot water load of 150, 300, 600 litres/day, and be capable of use throughout the year, and withstand winter freezing conditions
2) where the durability of the components would provide a solar hot water heater with 20 year life, and provide energy at a net solar capacity cost of less than $300/annual GigaJoule produced
3) the systems design would be able to provide 3 alternative configurations
   a) low head systems for single storey buildings
   b) high head systems for multiple storey buildings
   c) batch systems for buildings with attic storage
4) that its modular design and fabrication would allow high quality standards and easy installation

## RESULTS OF LABORATORY PHASE

This phase of the project comprised construction and testing of the heat pipe together with integration and testing of the collector and storage tank interfaces (using electric simulation of solar heat).

The results obtained from this Phase enabled an improved laboratory DHW prototype system to be constructed.

FIGURE 1 : HEAT PIPE SOLAR HOT WATER SYSTEM - CUTAWAY DIAGRAM

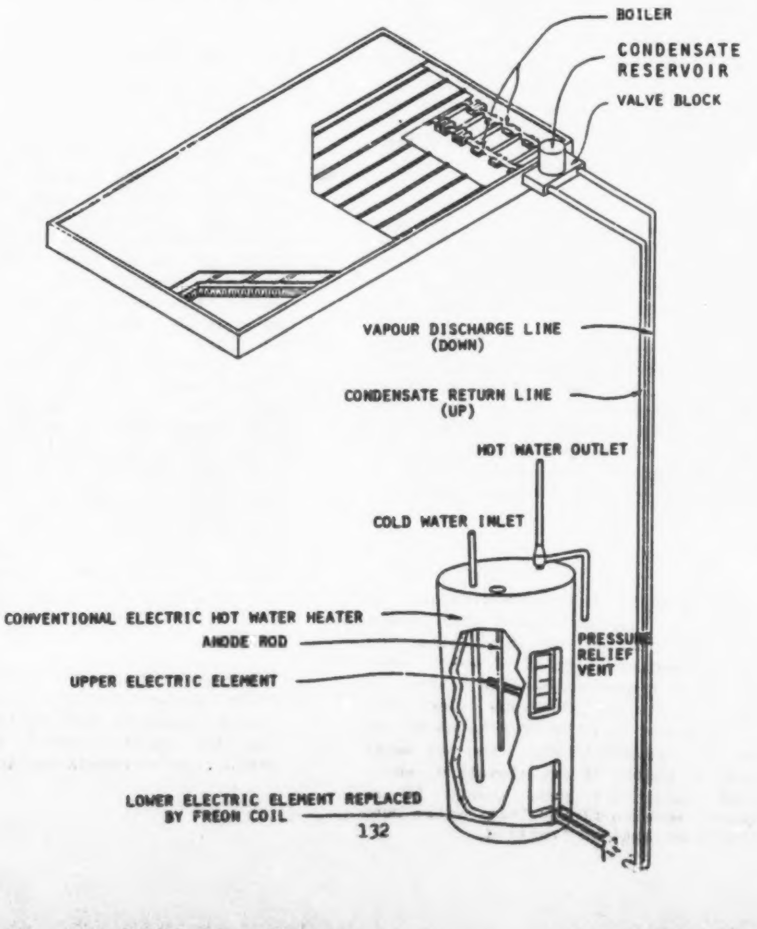
BOILER
CONDENSATE RESERVOIR
VALVE BLOCK
VAPOUR DISCHARGE LINE (DOWN)
CONDENSATE RETURN LINE (UP)
HOT WATER OUTLET
COLD WATER INLET
CONVENTIONAL ELECTRIC HOT WATER HEATER
ANODE ROD
PRESSURE RELIEF VENT
UPPER ELECTRIC ELEMENT
LOWER ELECTRIC ELEMENT REPLACED BY FREON COIL

## RESULTS OF PROTOTYPE PHASE

### Engineering of System Components:

As part of the engineering design of the systems components, several design features of the recharge cycle and the reservoir and valve components were put to the test before construction of a unique reservoir float combination. This solution used a solenoid powered snap action valve with a pilot assist (a standard refrigeration component which permits the use of a large valve orifice). This allowed an adequate vapour path for pressure equalization between the boiler and the reservoir to ensure a rapid recharge cycle.

### Actual Testing under Field Conditions with Solar Input:

The arrangement developed in the Laboratory Phase was modified to include these new components and the revised system design. (See Figure 1.)

Field testing of the system was made under different levels of natural sunshine over a period of some six weeks in order to study system response over a range of different operating conditions.

### Description of Operating Principle:

This novel system is based on adapting the vapour/liquid heat transfer system originally designed by G.de Beni which transfers heat from an elevated solar collector to a condenser/storage reservoir at a lower level. The only moving parts in this system are one or two check valves plus a float valve or a float actuated solenoid valve. This process based on a self-pumping cycle of a heat transfer liquid allows the solar DHW system to operate automatically independent of external electric power. Figure 2 - Schematic of Operating Principle - shows that the installation of a solar DHW system using a downward heat pipe differs little from a standard solar DHW system with the exception that no circulating pump or differential temperature control are required. The lower DHW storage reservoir contains a condenser coil which replaces or compliments the lower electric element. The system forms a closed sealed circuit filled with a refrigerant working fluid except for the upper condensate holding reservoir which is empty at the commencement of operation. A typical pumping cycle can be described as follows:

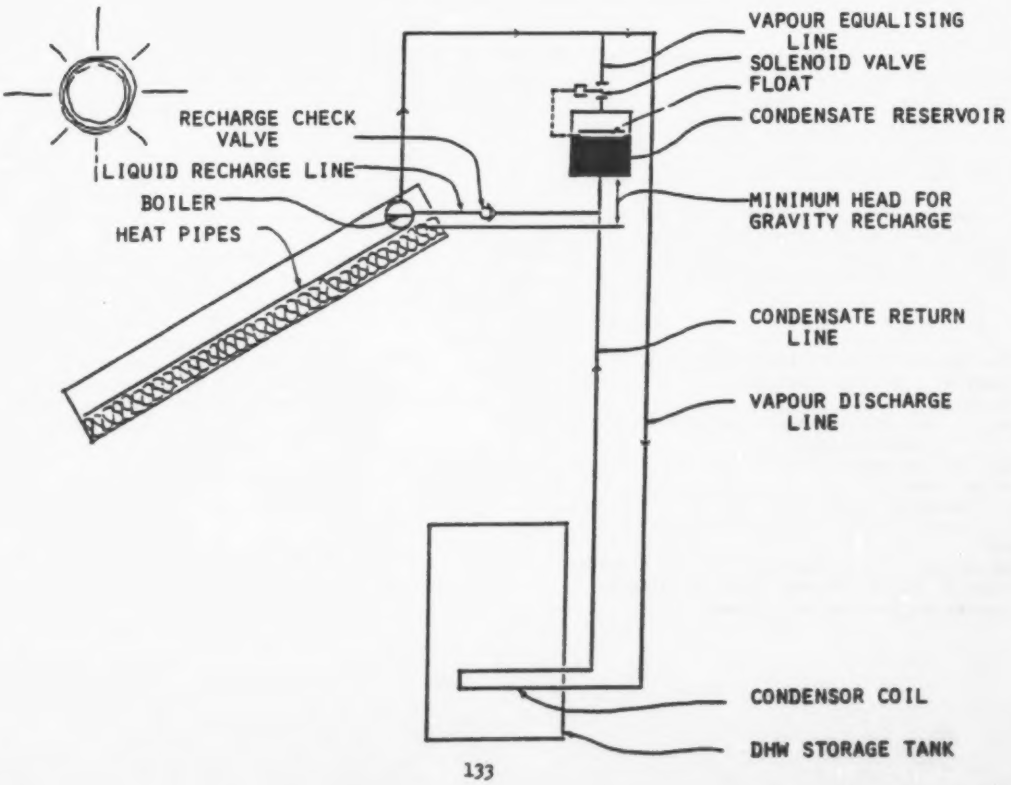

FIGURE 2 : SCHEMATIC OF OPERATING PRINCIPLE

SELF PUMPING ACTION OF DOWNWARD HEAT PIPE

From a cold start, the boiler is nearly full and the reservoir is completely empty as is all the remaining piping of the system including the condenser mounted in the DHW storage tank. This situation exists because the boiler is the coldest point during night-time conditions. Heat transport from the solar collector boiler into the Freon working fluid vaporizes the working fluid and increases the working pressure of the system to the saturation vapour pressure of the condensed working fluid in the DHW storage tank coil. The liquid condensate is pushed vertically upwards into the condensate holding reservoir (the pressure required to do this is sometimes referred to in terms of a temperature penalty required to drive the system - otherwise known as self-pumping temperature penalty, typically this lies between 5 to 10°C). Temperature penalty refers to the difference in temperature compared to conventional systems for the operating temperatures of the solar collectors. It is essential that leakage of hot vapour into the cold reservoir does not occur except of course during the brief recharge cycle described below.

- When the condensate holding reservoir (mounted immediately above the solar collector boiler) is filled with cold condensate to a pre-determined level, the action of the internal float opens a vapour pressure equalizing valve connecting the hot boiler with the cold reservoir and the liquid which fills the reservoir, is therefore able to flow by gravity through the check valve into the boiler thereby recharging the system for another heat transfer cycle.

Depending on the heat applied to the solar collector boiler, this discharge/recharge cycle repeats itself at intervals of approximately 3 to 5 minutes for each discharge cycle followed by a very short recharge cycle of approximately 2 seconds in duration.

As with a conventional system, the rate of pumping is proportional to the power input to the solar collectors. The system thus functions without any controls or start and stop mechanisms.

Details of the Test Facility:

The downward heat pipe was installed at the Experimental Station of the Brace Research Institute in Ste. Anne de Bellevue. The collector was a Brace heat pipe unit of dimensions 0.9 m. by 2.0 m. using six heat pipes total area 1.55 sq.m. Details of the installation are as follows:

1. Total surface area of the collector 1.55 sq.m.
2. Diameter of the collector heat pipes 16 mm external.
3. Length of the vapour supply/condensate return piping 12 metres total
   Downline diameter 11.4 mm. bore. Upline diameter 4.8 mm. bore
4. Heat exchanger surface area 0.11 sq.m.
   (coil heat exchanger in bottom of D.H.W.storage tank)
   (replacing 4 1/2 kW bottom electric element)
5. Volume of D.H.W. storage tank 182 litres
6. Instrumentation was as follows:

a) Exit temperature at discharge from collector boiler
b) Absorber temperature at top/centre/bottom of solar collector
c) Entry temperature to heat exchanger coil
d) Exit temperature from heat exchanger coil
e) Bottom temperature of storage tank (water)
f) Top temperature of storage tank (water)
g) Pressure at exit from collector boiler
h) Pressure at entry to heat exchanger coil
i) Pressure at top of condensate holding reservoir
j) Time duration and frequency of condensate recharge cycle

Analysis of Test Results:

Test data on system performance was obtained for several different extremes of system operation.

1) cold start at beginning of day
2) hot start at beginning of day
3) cold start at mid-day
4) hot start at mid-day

Temperature readings were taken at 3 minute intervals using a KAYE Mark III, Digistrip Recorder. Maximum tank temperature was 50°C. Minimum tank temperature was 10°C.

Recordings were also made of system overnight performance to determine shut down heat losses (these proved to be actually negligible).

Under typical operating conditions of bright sun light, system initialization (time to warm up and achieve first recharge cycle), was approximately 15 minutes at 08:00 hours and 5 minutes at 12:00 hours.

Detailed Operating Characteristics (Dynamic and Thermal):

The operation of the system can be easily depicted by plotting the temperature of the following system components.

a) collector temperature (bottom absorber/heat pipes)
b) collector temperature (top absorber/heat pipes)
c) collector boiler temperature
d) condenser coil inlet temperature
e) condenser coil exit temperature
f) D.H.W. storage tank, top and bottom temperatures
g) condensate holding reservoir temperature
h) ambient temperatures (indoor/outdoor)

Table 1 gives details of the test which gave optimum results.

TABLE 1:

OPTIMUM TEST RESULTS TABLE - WORKING PROTOTYPE
35% Overall system efficiency - one day's operation

DOWNWARD HEAT PIPE EXPERIMENT

1) Date of Test August 1985
2) Starting Time of Test 10:06 HRS.
3) Finishing Time of Test 16:47 HRS.
4) Meteorological Conditions Sunny and Clear
5) Amount of Incident Solar Radiation - Kilowatt Hours / $m^2$ 5.12
6) Solar Collector Area ($m^2$) 1.55
7) Tank Average Increase in Temperature - Celsius 12.5
8) Storage Energy - Watt Hours / °C 220/°C
9) Total Storage Energy - Watt Hours 2750
10) Overall Efficiency 35%

< Sample Calculation: $\frac{2750}{1.55 \times 5120} \times 100$ >

System operating temperatures show several distinct characteristics. The first is the rise in temperature of the collector/boiler to steady state operating conditions. The second is the initial pumping and recharge cycle. The third is characterized by a heat transfer problem between the collector heat pipes and the collector boiler shown by an unnecessarily large temperature difference between these components. The fourth is the steady rise of the top temperature of the D.H.W. storage reservoir (note that the bottom of the storage tank remains cold due to minimum mixing, thereby resulting in more efficient system operation). The fifth is the cooling down of the collector boiler at the end of the day, with eventual condensation of all the Freon working fluid in the collector boiler (note that the only overnight heat loss from the storage tank via the downward heat pipe to the cold night sky is that required to vapourize the liquid Freon contents of the condenser heat exchanger coil.

The actual heat transfer capability of the downward heat pipe is directly proportional to the frequency of the condensate recharge cycle. Under normal operation in peak sunny conditions with a recharge cycle every three to five minutes, the rate of heat transfer is about 1.5 kW for the system under test. However, in the case of a power failure which affects operation of the electric solenoid valve controlling the recharge cycle the system will stagnate. This occured accidently during testing and it was observed that rapid recovery was achieved by recharge cycling at some 20 times the normal recharge frequency. This corresponds to heat removal capability of some 20 X 1.5 kW. (i.e. 30Kw)

Provided that efficient operation of the downward heat pipe can be ensured under such rapid cycling (i.e. an acceptable ratio of recharge time/heat transfer time), it is obvious that downsizing of system components is both feasible and worthwhile. We believe that minor design modifications to the condensate holding reservoir will further improve the condensate recharge cycle.

The temperature penalty required for self-pumping decreases as the storage reservoir temperature increases. Typically for a system head of 14 metres, the temperature penalty is initially 5 to 10° C., and eventually at the end of the day reduced to 2 - 5° C., depending on actual temperatures of the storage tank. Based on test results for conventional solar D.H.W. systems (work by Los Alamos National Laboratory under D.O.E. contract) an increase in collector operating temperature of 10°C., will result in a decrease in annual collection efficiency from 50% to 45%. This penalty can not be accurately assessed until the overheating problem between the collector heat pipes and the collector boiler has been resolved. We believe that certain minor modifications to the capillary mesh wick of the collector heat pipes and to the clamps holding the collector heat pipes to the collector boiler will be able to improve this situation.

## TECHNICAL DIFFICULTIES STILL TO BE RESOLVED

As previously mentioned, the collector temperature in the system tested is unnecessarily high.

The problem appears to be in the condenser section of the collector heat pipes (not the downward heat pipe, although improvements are planned in the boiler clamps) and may be due to out-of-tolerance positioning of the brass mesh wick. Use of an alternative working fluid (e.g. Freon) would also reduce condenser temperatures. We therefore expect that our solar collectors will then operate at close to the DHP boiler temperature, which is "locked" at about 5-10°Celsius above the temperature of the DHW storage water tank.

The downward heat transport capacity of our DHP design is sufficient to rapidly stabilise system operation after a simulated power failure in strong sunlight (for example 15 second vapour discharge cycles were observed, instead of the normal 3-5 minutes cycle).

Effective capacity probably exceeds 15 kW as explained above, and downsizing of the system is extremelylikely, when the design and the key components evolve during the production prototype stages. Benefits would include smaller boiler and reservoircomponents requiring less Freon working fluid. A more compact reservoir will allow a faster recharge cycle, which in turn permits a shorter condensation (or heat transfer) cycle.

## CONCLUSIONS

Automatic and consistent downward transport of heat is feasible, without pumps or controls, using solar or other heat input to the boiler of the downward heat pipe system. Hot water in a standard DHW storage tank can be obtained for the following conditions:

- Over vertical heights of at least 7 metres for extended periods of time.
- There is no risk of frost or corrosion damage.
- With reliable operating performance and excellent downward heat pipe thermal and pumping efficiencies.
- At power levels and temperatures compatible with requirements for solar DHW heating systems.

A concept schematic for typical residential installations is shown in Figure 3.

FIGURE 3 : LINE DIAGRAM FOR DIFFERENT SYSTEM OPTIONS

(FACTORY OR FIELD ASSEMBLED KITS)

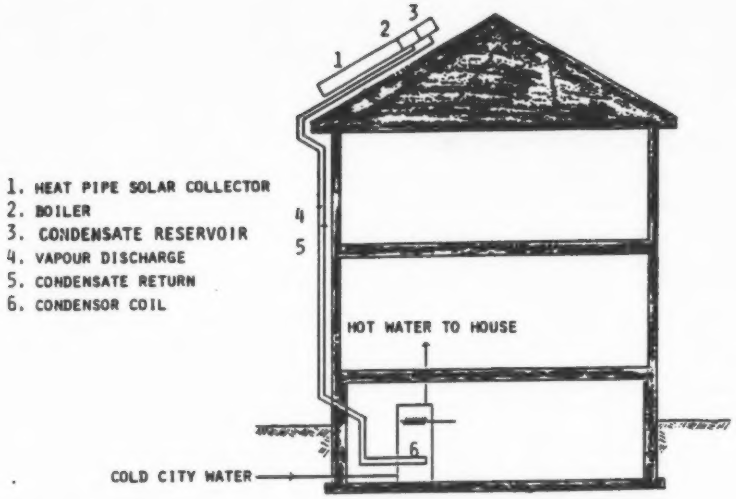

OPTION 1 - MODIFIED CONVENTIONAL ELECTRIC WATER HEATER

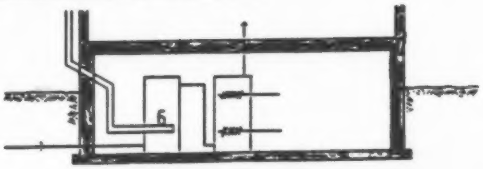

OPTION 2 - PREHEAT WATER TANK WITH CONVENTIONAL ELECTRIC WATER HEATER

## REFERENCES

de Beni, G., Friesen, R., "Passive Downward Heat Transport: Experimental Results of a Technical Unit", Commission of the European Communities Joint Research Centre, ISPRA, Italy. 1984.

de Beni, G., Friesen, R., "Passive Downward Transport of Solar Heat From a Collector to a Heat Storage Medium: Experimental Results of a Prototype", Commission of the European Communities Joint Research Centre, ISPRA, Italy. (6 pages), 5th Solar Forum, Berlin. September 1984.

Hewes & Wight Limited, "Development of Heat Pipe Solar D.H.W. Systems" - Final Report Phase 1, Pointe Claire, Quebec. Submitted to Division of Energy Research and Development, National Research Council of Canada: File 02SX.31155-2-2748. October 1983.

Hewes & Wight Limited, "Development of Heat Pipe Solar D.H.W. Systems" - Final Report Phase 2 & 3, Pointe Claire, Quebec. Submitted to Division of Energy Research and Development, National Research Council of Canada: File 04SR.31926-4-3007. November 1985.

LeNormand, J. "Short Guide for Simple Heat Pipe Design", Brace Research Institute, Faculty of Engineering, Macdonald College of McGill University, Ste. Anne de Bellevue, Quebec, Canada. Report No. T-135. April 1982.

LeNormand, J., Coffin, W., Lawand, T.A. "Development and Testing of Low Cost Heat Pipe Solar Collectors for Process and Domestic Hot Water Applications", Report submitted to Science Procurement Branch, Supply & Services Canada, DSS File No. 02SX.31155-0-2690. Brace Research Institute Report No. I-183. July 1982.

# PERFORMANCE MONITORING OF SOLAR HEATING SYSTEMS IN DND

Don Hampton
Solar Specialist
Public Works Canada
Riverside Drive,
OTTAWA KIA 0M2

## ABSTRACT

Solar heating systems on DND property is been monitored using a multitude of devices, including energy monitoring systems, and a combination of load and performance indicators. The information is being used to determine the relevance of operating these systems by estimating the value of energy being collected.

The most important criterion for maintaining these solar heating systems is the fundamental question of load, once this has been established, the next question is: how long does the solar heating system contribute energy to the load, compared with the solar available.

## 1 BACKGROUND

The design criteria for the solar heating systems for DND was established by the Solar Program Office (SPO). These standards encouraged inovative designs resulting in a proliferation of designs. Back-up to the system operators has been taken up by the Canadian Forces Military Engineering School at CFB Chilliwack. In addition O&M courses have been provided for some of the bases to provide succinct instructions for the operators on their systems. During these courses the operation of the systems was reviewed and arrangements made to upgrade them.

Most of the systems installed uder PUSH have been shut down. These include the units on the Married Quarters, but in addition, some of the larger systems have been removed. The most common problem has been the cost of maintenance, another major problem has been the high cost of bringing the systems to an acceptable condition. An underlying problem is the size of the systems relative to the loads. Unless the load is substantial it is obviously pointless to continue to operate these systems.

## 2 LOAD CRITERIA

The basic criteria for continuing to operate solar heating systems in DND is based on energy conservation. Unless the energy saved by the system exceeds the cost of O&M the systems will be abandoned. The criteria is based on the assumption that the solar heat is too precious to waste, i.e. all the heat collected by the solar heating system must be used.

### 2.1 Heat to DHW

The solar contribution to DHW should be used to preheat the water to a maximum of 40°C, thus for cold water supplied at 12°C the load should be:

$$\frac{2.5 * 10^9 \text{ J/a**}}{4189 \text{ J/(L.°C)} * (40\text{°C} - 12\text{°C}) * 0.6} = 34\,500 \text{ L.a}^{-1}$$

i.e. 97.33 $\text{L.m}^{-2}.\text{d}^{-1}$, say 100 $\text{L.m}^{-2}.\text{d}^{-1}$;

this is based on the presumption that if more than 60% of the heat is provided by the solar heating system the temperature of the water supplied from the solar heating system will exceed 40°C on a hot summer day.

### 2.2 Heat to Indoor Pool

The heat required to replace the loss due to evaporation is approximately 4250 $\text{J.m}^{-2}.\text{d}^{-1}$, based on the pool area. Thus the load for the year will be 1.55 $\text{GJ.m}^{-2}.\text{a}^{-1}$. This load may be less during the summer as the dew point of the air above the pool may be greater, i.e. on hot humid days the air conditions above the pool may be warmer than desired, and the heat required by the pool less than in winter.

The maximum solar contribution must be limited to the above, i.e. the unit solar area will be:
1.55 $\text{GJ.a}^{-1}$/2.5 $\text{GJ.m}^{-2}.\text{a}^{-1}$ = 0.62 $\text{m}^2$; or
the solar area should be a maximum of 60% of the pool area.

### 2.3 Combination Systems

For systems serving DHW and pool water heating the load provided is to be compared with the capacity, i.e. the collector area provided.

i.e. Collector area required for the DHW

= Daily water use ($\text{L.d}^{-1}$) divided by 100 [1]

Collector area required for the Pool

= Pool Area * 0.60 [2]

** Note: This section presumes that the solar collectors have the capacity to contribute 2.5 $\text{GJ.m}^{-2}.\text{a}^{-1}$ to the load. This optimistic output, for flat plate collectors, is based on low temperature operation.

### 2.4 Criterion for Acceptance

The above criteria will be included when the future of solar heating systems is considered in DND. As noted above, most of the solar heating systems have been shut down. This was based on the cost of refitting these systems, compared with the value of the estimated energy saving: e.g. it was estimated that the cost of refitting the solar heating system on the Junior Ranks Mess CFB Winnipeg was $40,000; the estimated energy savings was $5,000 per year - the payback period of eight years, ignoring O&M costs, was not attractive and the system will be removed.

The remaining systems are to be kept operating until the need for repairs is identified. The considerations available to the Base, its Command Group, and NDHQ will include:

the repair cost
the size of the system, and
the load/capacity ratio.

The latter criteria will be used to estimate the value of the energy that could be saved with the system. This will be compared with the cost of repairing the system. Systems that are not viable will be removed.

## 3 PERFORMANCE CRITERIA

The most desirable performance measurement is the amount of energy being collected. Energy meters have been provided on many systems; however, energy readings have proved relatively elusive. The failure rate of the water volume meter sections of the integrating meters being used has been high; this is due, mainly, to the excessive water volume being forced through these unics, i.e. poor design. In addition, the operating staff have some difficulty relating to the performance of the systems in terms of gigajoules; especially when the expected energy performance is not given.

Arrangements have been made to have the operating performance monitored using timers and trip indicators. These devices are simple, low cost and are simple to install, they may be connected to the pumps or controls. The other advantage conceived is that the operating staff should be able to relate to these.

### 3.1 Operating Time Criteria

A comparison has been made between the operating time for the solar heating system and the "hours of bright sunshine" in the area. The latter is recorded by the Department of Environment. The readings are made on the "Burning Glass" instrument which is calibrated to read the bright sun time in tenths of an hour, these are added to provide the "hours of bright sunshine" per day, averaged for the month, etc., from weather records from The Department Environment.

For systems with sufficient load, see #2, the operating time for the system should be about 80% of the bright sunshine time. The general level for "hours of bright sunshine" is around 2000 $h.a^{-1}$; i.e. the solar pump should operate for at least 1600 $h.a^{-1}$.

### 3.2 Cycling Rate Criteria

One of the surprises of the solar program was the failure rate of the pumps. This is in contrast to the reliability of these units in most mechanical heating systems; it has been presumed that the high failure rate is due to the high cycling rate of the earlier systems.

The general guideline provided for the bases is that the cycling rate should not exceed 6 $Hz.d^{-1}$.

## 4 PERFORMANCE OF THE SOLAR HEATING SYSTEM ON GENERAL GRANT HALL, CFB SHILO

This system provides heat for the DHW and for the pool water. The performance of the system has been monitored since the system was commissioned in May 1984. Readings of the operating time, the cycling and the energy provided to the pool water were available from September 1984.

During the first seventeen months the contribution to the pool water heating was negligible and the solar pump was cycling too much. This was due to the operation of the three way control valve serving the secondary tank set, see Figure 1. This limited the effective storage to approximately half the effective volume available and directed the solar heat to the primary tank set.

The pool heating control depended on the thermostat in the secondary tank set. As this was isolated from the solar heat the temperature of these tanks was too low to bring on the solar heating pump. With the low storage volume the incoming cold water tripped the controller as soon as water was drawn from the primary tank set.

4 Performance of the SHS at CFB Shilo (cont'd)

The operation of the three way valve was corrected during an O&M Workshop in October 1985. Since then the trip rate has been reduced to three cycles per day for the solar pump, and a maximum of five trips per day for the solar pump.

### 4.1 Results from CFB Shilo System

The operating time for the solar pump was consistantly high, around 80% of the brigh sun time. The only exception was during June when the operating time was less than 50% of the "bright sunshine hours". This was consistant as the pool was closed for cleaning during this month, see also Graph 1. It is gratifying to note that the comparative operating time has been greater since the system was adjusted last October.

The cycling rate for the solar pump was excessive, with up to thirty cycles per day, see also Graph 2. This reduced to an acceptable level after October 1985.

The load on this system, without the pool heating load, has been too low. The average load during the first seventeen months of operation was 5240 $L.d^{-1}$. The readings taken during the last winter indicate that the load during the summer is generally higher.

The energy contribution to the pool heating system has been higher than the energy provided to the DHW, since October 1985. The former is being read from the energy meter serving this section. The latter is being estimated from the water usage and the temperature readings provided.

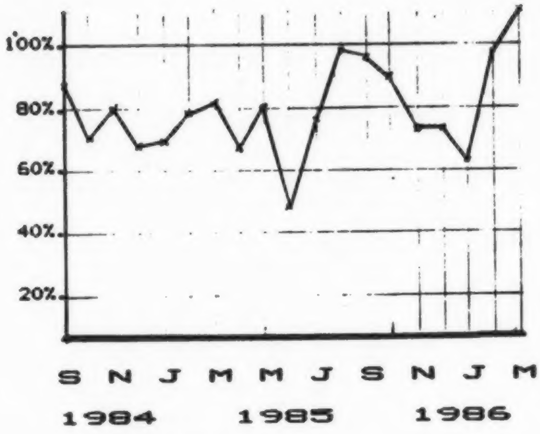

GRAPH 1

RATIO OF OPERATING TIME & HOURS OF BRIGHT SUNSHINE FOR THE SOLAR HEATING SYSTEM, CFB SHILO

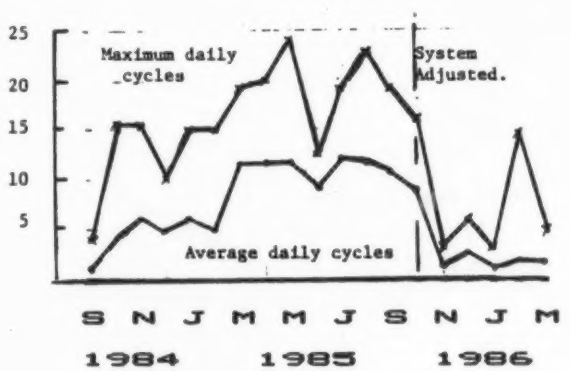

GRAPH 2

CYCLING RATE OF THE SOLAR CIRCULATOR ON THE SOLAR HEATING SYSTEM, CFB SHILO

**The system operating time was apparently acceptable before the O&M Workshop; however the cycling, both the average and the maximum cycles per day, was unacceptable.**

**The improvement in the operating time is marginal, but may be significant. The reduced cycling rate is a relief.**

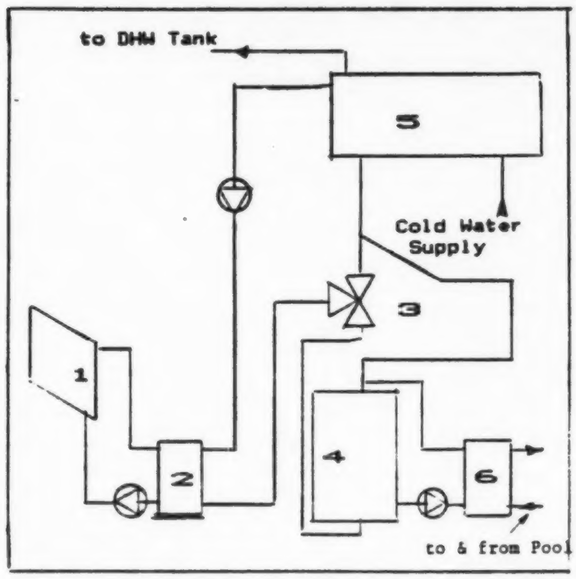

| | |
|---|---|
| 1 | PANELS |
| 2 | MAIN HX |
| 3 | CONTROL VALVE |
| 4 | 2ND TANKS |
| 5 | MAIN TANKS |
| 6 | POOL HX |

FIGURE 1

SCHEMATIC OF SOLAR HEATING SYSTEM

CFB SHILO

## 5 LOAD CHECK ON SOLAR HEATING SYSTEM, GENERAL GRANT HALL, CFB SHILO

The DHW load is averaging at 5240 $L.d^{-1}$; the minimum collector area for this load is:

from [1] 5240/100 = 52.4 $m^2$

The pool in this building is 15 m x 25 m; the minimum collector are for this load is:

from [2] 25 * 15 * 0.6 = 225 $m^2$

Total Maximum area = 277.4 $m^2$

The collector area installed for this system is approx. 200 $m^2$, i.e. the load:capacity ratio is 1.38:1, i.e. greater than the minimum 0.6:1 set.

## 6 COMPARING PERFORMANCE OF SYSTEM ON GENERAL GRANT HALL WITH F-CHART ESTIMATES

The performance of the solar heating system can be estimated from the readings of the water flow and the temperature readings of the Cold Water and the water supplied from the Solar Heating System. This is in addition to the energy readings for the pool. These readings are available for December 1985, January, February and March 1986 only.

The energy collected has been plotted with the F-Chart estimate for the same period, see Graph 3. The simulation accounts for the pool and DHW load; however, the energy provided is less than expected. Unfortunately, it has not been possible to adjust the weather conditions to account for the weather during this period.

## 7 COMPARING WEATHER DATA

The weather records for the area are limited and cannot be used for the simulation; however, some idea of the comparative conditions can be gleaned from the average temperature and bright sunshine levels for the months under consideration, and comparing these with the thirty year averages for the same months.

The average temperature, see Graph 4, was a little higher than the thirty year average; but the change is not particularly significant.

The average "hours of bright sunshine" are significantly lower, see Graph 5, about 20% below the thirty year average. This drop will affect the performance, for this time of the year, i.e. with very low ambient temperatures it could reduce the operating time and the energy collected by a similar amount.

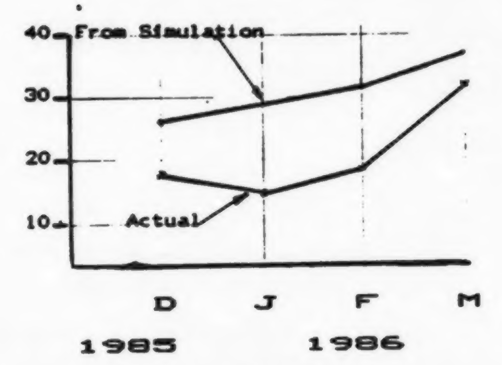

GRAPH 3

PERFORMANCE OF SOLAR HEATING SYSTEM COMPARED WITH THE PREDICTED ENERGY

SCALE SHOWS GJ/MONTH

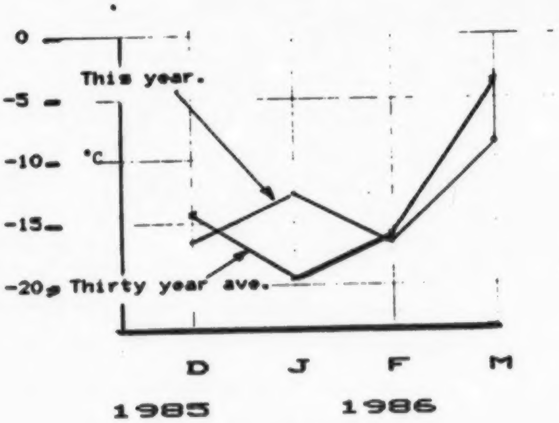

GRAPH 4

AVERAGE TEMPERATURES

A) THIRTY YEAR AVE.

B) RECENT MONTHS

The performance in January and February is poor; however, the higher gain during March may, if the operating time is a good indicator, foretell better performance during summer.

It should be noted that the annual energy quotent determined from the F-Chart simulation is 1.72 GJ/(m .a); much lower than the norm.

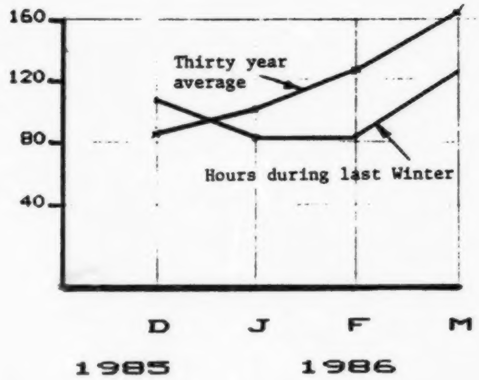

GRAPH 5

HOURS OF BRIGHT SUNSHINE, RECORDED AT BRANDON AIRPORT

A) THIRTY YEAR AVE.

B) RECORD FROM DEC 1985

I.E HOURS PER MONTH

## 8 CONCLUSION

The method used by DND to decide the usefulness of solar heating systems on their buildings is based on the cost effectiveness of operating those systems. Unless the value of energy saved is greater than the O&M costs the systems will be removed.

The difficulty of obtaining energy readings has hampered decisions, energy meters will provide direct information on the energy provided; however, the system operators need more information on their systems than the energy meters can provide. The cost of providing energy meters cannot be justified; however, basic operating monitoring equipment can be added, i.e. timers, trip indicators and water meters. The latter equipment will provide more information for the operators and the DND engineering staff; if a correlation can be established between the operating time and the energy being collected.

The most economical solar heating system for DND is a large system with a large load. The former criterion will mean that the operator is dealing with a system capable of collecting enough energy to compensate for the cost of the operator, and any minor repair costs. The latter will ensure that **all the solar energy collected is used.**

The load on a solar heating system can be estimated from the DHW load, i.e. from the volume of water being used. For systems serving indoor pools this can be related to the pool surface area.

Once the load has been established, the operating time of the solar system is required. This is something that the operator can relate to, and a comparison can be made between the operating time and the "hours of bright sunshine" readings.

A symptom of a poor solar heating system is a high cycling rate. Providing a trip indicator is a simple method of quantifying the cycling rate.

The solar heating system installed on General Grant Hall, CFB Shilo meets the criterion for the well-loaded solar heating system i.e with a solar fraction of less than 60%.

The operating time of the solar heating system is averaging about 75% during the first year. Since the system was adjusted in October last year the operating time has increased, suggesting that a system with high loads will operate longer. The evidence available to back this thesis is minimal, hopefully the results during the rest of the year will provide further support.

The cycling rate has been brought to acceptable limits; the cycling rates for the initial operating period were much too high, due to poor storage use.

The energy provided by the system, after the system was commissioned has been close to the predicted level. Further readings are needed to prove that the system is fully effective.

# EFFECT OF RANDOM FLUCTUATIONS IN AMBIENT AIR TEMPERATURE ON SOLAR SYSTEM PERFORMANCE

K.G.T. Hollands, L.J. D'Andrea, and I.D. Morrison,
Professor Research Engineer, Research Assistant,
Departments of Mechanical Engineering and Systems Design,
University of Waterloo
Waterloo, Ontario, N2L 3G1 Canada.

## ABSTRACT

This paper tests the hypothesis that ignoring the random component in the fluctuations in ambient temperature produces acceptably low errors (~1%) when simulating domestic, commercial and industrial process heat systems. The hypothesis was confirmed under a very wide range of settings in system parameters, indeed under all of the 18 settings tested using the WATSUN program. This result improves the viability of using synthetic weather data in simulating solar systems.

## 1. INTRODUCTION

Graham et al (1) have described a method for synthetically generating hourly values of solar radiation having the same statistical and stochastic character as real, measured values. The only quantities needed as input to this method are the values of $\overline{K}_T$ (mean monthly clearness index) for each month for the location in question. As explained by these authors, using this synthetic data as the input to solar simulation design programs such as WATSUN has several advantages over using the record of past data, which is the approach currently used. First, it permits simulations for locations, for example in the third world, for which past records of hourly radiation data are not available. Second, it permits savings in computer time (it eliminates read statements). Third, it reduces the computer storage requirements—particularly important for microcomputer applications.

Solar conversion devices, however, usually respond to ambient temperature as well as solar radiation, so a similar method for generating synthetic ambient temperature data is required before the method can be truly useful. The present paper addresses the generation of synthetic ambient temperature data.

Variations in a fluctuating quantity X(t), such as solar radiation or ambient temperature, can be broken down into two components: a deterministic component $\overline{X}(t)$ and a random component X'(t). The deterministic component is arrived at by taking, for each hourly time of day (eg. 9 AM to 10 AM), the average of the values of X observed in that hour over the whole month and for several years. The random component is the difference between X(t) and $\overline{X}(t)$: $X'(t) = \overline{X}(t) - X(t)$

It is well-known that the random component of solar radiation fluctuations has a pronounced effect on the performance of solar collectors. This effect is a result of the non-linear nature in their response and is brought on by the action of the pump controller. It is, for example, the reason why a single average day of solar radiation cannot be used to represent a whole month (2).

On the other hand, the effect of ambient temperature fluctuations has been far less studied, and indeed, what studies are available indicate that the effect is quite minor. Thus Klein in his (1976) thesis (3) observed that ignoring both the deterministic and the random components results in small error. Moreover, ignoring the random fluctuations is implicit in the popular utilizability method of solar design.

This paper examines the hypothesis that the random component in ambient temperature fluctuations is unimportant in the simulation of solar domestic, commercial and industrial process heat systems. If this hypothesis is valid, considerable simplication will be permitted in simulating solar systems: hourly records of past ambient temperature observations will not be needed, nor will there be a need for synthetic generation of their random component.

## 2. METHOD

The hypothesis was tested using the WATSUN program (5) to simulate one of the WATSUN's modular systems (DHWS) suitable for a wide class of domestic, commercial, and industrial heat process applications. The simulations were carried out twice: once using the observed ambient temperatures in the typical meteorological year (TMY) (see Siurna et al (6)), and the other using the ambient temperature predicted at any hour in a given month by using an equation for the determinstic component of the ambient temperature fluctuation (see later). Both simulations used identical solar radiation data as input. The two simulation results were then compared. Agreement to within tolerable accuracy, say 1%
hypothesis.

The deterministic component $\overline{T}_a(t)$ was estimated using the equation developed by Erbs et al (4), from observations at nine US cities:

$$\overline{T}_a(t) = \langle T_a \rangle + A \sum_{n=1}^{4} c_n \, (\cos n \, \theta - \theta_n) \qquad (1)$$

where $\langle T_a \rangle$ is the monthly mean ambient temperatures, $c_n$ and $\theta_n$ are universal constants (see their paper) and $\theta = 2\pi \, (t-1)/24$, where t is the number of hours from midnight. The quantity A is a measure of the amplitude of the diurnal swing and is location dependent. Erbs et al found that A (in degrees C) could be correlated against the $\overline{K}_T$ for the month; they found

$$A = (25.8\ \overline{K}_T - 5.21) \qquad (2)$$

It should be noted that this equation accounts for only part of the variation in A; departures of up to 50% must be expected.

The layout for the system simulated by WATSUN DHWS is sketched in Figure 1. This module assumes a perfectly-stratified storage tank. Since the volume of the tank containing the auxiliary heater was not, expected to be important, it was set to zero. Both heat exchangers were given an effectiveness of 75%.

The results of a simulation depend of course on a large number of system parameters—eg. collector characteristics, load pattern, etc. To cover as broad a range of parameters as possible, a base case, having specified values of each parameter, was first established and simulated, then each parameter (or group of parameters) was changed, the remainder remaining constant, and the simulations were repeated. Table 1 gives the values of parameters in the base case, and Table 2 lists how each was changed and numbers the simulations accordingly.

## 3. RESULTS

Table 3 summarizes the results by giving the annual solar fraction $f_{TMY}$ for the simulations using the TMY data, the annual solar fraction $f_D$ for the simulations using the deterministic model, and the % difference defined by

$$\%\ \text{diff} = \frac{f_D - f_{TMY}}{f_{TMY}} \times 100\ \% \qquad (3)$$

The % difference may be (loosely) interpreted as the error associated with neglecting the random variations in ambient temperature, although some of the differences may be associated with the use of equation (2), which is only an estimate of the deterministic component. The error appears to be acceptably low: over the simulations performed, the root mean square error was 0.8% and the maximum error was 1.1%. Such an error is ordinarily considered acceptable for engineering design.

For interest, a separate set of simulations was performed in which both the random and deterministic components were ignored, ie., A was set equal to zero. This gave much higher % difference, with an rms difference of 2% and a maximum difference (occuring in case 17) of 5%, which is unacceptably high.

## 4. CONCLUSIONS

1. Neglecting the random component in the ambient temperature fluctuation produces errors in simulation of the order of 1%, which is considered acceptably low.
2. Neglecting both the random and deterministic components in the ambient temperature (ie. taking it as constant) produces errors as high as 5%.
3. Conclusions (1) and (2) are restricted to standard designs of domestic, commercial and industrial process heat systems. They may, for example not be valid in passive systems, in which there is a strong correlation between ambient temperature and load.

Table 1

Values of System Parameters for Base Case

Collector area=100m$^2$; $F_R(\tau\alpha)_e$=0.75; $F_RU_L$=5.0 W/m$^2$ K; collector flow rate per unit collector area=0.01 kg/s m$^2$; collector slope=45°; collector bearing=south facing; controller differential=5°C, storage volume/collector area ratio=0.05 m$^3$/m$^2$; storage model=stratified tank, delivery temperature to load=60°C, load draw-off rate=5000 L per day; load draw-off profile=standard DHW profile; location=Toronto.

Table 2

Summary of Simulations Performed

| Simulation Number | Parameter Changed From Base Case | New Value of Parameter |
|---|---|---|
| 1 (base case) | no change | no change |
| 2 | $F_RU_L$ | 7.5 W/m$^2$K |
| 3 | load draw off rate | 20,000 L/day |
| 4 | load draw off rate | 2,000 L/day |
| 5 | Demand Profile | constant over day |
| 6 | Demand Profile | demand occurs only between 9PM and 3AM |
| 7 | Demand Profile | demand occurs only between 9AM and 3PM |
| 8 | Controller Differential | 15°C |
| 9 | Delivery Temperature to load | 45°C |
| 10 | Delivery Temperature to load | 30°C |
| 11 | Storage Volume/Collector area ratio | 0.1 m$^3$/m$^2$ |
| 12 | Storage Volume/Collector area ratio | 0.5 m$^3$/m$^2$ |
| 13 | Location | Calgary, Alta. |
| 14 | Location | Vancouver, B.C. |
| 15 | Location and,<br>$F_RU_L$ | Calgary, Alta.<br>7.5 W/m$^2$K |
| 16 | Collector Flow Rate per unit Collector area | 0.0033 kg/s m$^2$ |
| 17 | Collector Flow Rate per unit Collector area | 0.03 kg/s m$^2$ |
| 18 | Location and,<br>$F_RU_L$, and<br>Load draw-off rate, and<br>controller differential, and<br>storage volume | Calgary, Alta.<br>7.5 W/m$^2$K<br>20,000 L/day<br>15°C<br>0.5 m$^3$/m$^2$ |

Table 3

Results of Simulation

| Simulation No. | $f_{TMY}$ | $f_D$ | % diff. |
|---|---|---|---|
| 1 | 55.13 | 55.64 | 0.93 |
| 2 | 45.62 | 46.11 | 1.07 |
| 3 | 19.56 | 19.76 | 1.02 |
| 4 | 76.71 | 77.26 | 0.72 |
| 5 | 50.62 | 50.98 | 0.71 |
| 6 | 57.25 | 57.82 | 1.0 |
| 7 | 54.16 | 54.57 | 0.76 |
| 8 | 54.65 | 55.09 | 0.81 |
| 9 | 73.07 | 73.90 | 1.1 |
| 10 | 88.87 | 89.58 | 0.8 |
| 11 | 56.49 | 57.02 | 0.94 |
| 12 | 53.75 | 54.03 | 0.52 |
| 13 | 62.17 | 62.60 | 0.69 |
| 14 | 53.96 | 54.20 | 0.44 |
| 15 | 50.61 | 50.78 | 0.34 |
| 16 | 54.73 | 55.29 | 1.02 |
| 17 | 64.61 | 65.14 | 0.82 |
| 18 | 21.58 | 21.59 | 0.05 |

## 5. ACKNOWLEDGEMENTS

The authors acknowledge with thanks the financial support of the Department of Energy Mines and Resources, and the encouragement of M. Chandrashekar.

## 6. REFERENCES

(1) Graham, V.A., Hollands, K.G.T., Unny, T.E., "Stochastic Modeling of the Daily Solar Atmospheric Transmittance $K_T$", Proceedings INTERSOL 85, Biennial Congress of the International Solar Energy Society, Montreal, June 1985, Pergamon Press, (1986).

(2) Duffie, J.A., Beckman, W.A., Solar Engineering of Solar Processes, Wiley, New York, Page 602, (1980).

(3) Klein, S.A., "A Design Procedure for Solar Heating Systems", Ph.D. Thesis, Department of Chemical Engineering, University of Wisconsin, Madison, Wisconsin (1976).

(4) Erbs, D.G., Klein, S.A., Beckman, W.A., "Estimation of Degree-Days and Ambient Temperature Bin Data from Monthly Average Temperatures, ASHRAE Journal, pp. 60-65, June, 1983.

(5) D'Andrea, L.J., Chandrashekar, M., Hollands, K.G.T., "WATSUN User's Manual and Program Documentation Version 8.0/85.86", University of Waterloo WATSUN Centre, Waterloo, Canada, N2L 3G1, (1985).

(6) Siurna, D.L., D'Andrea, L.J., Hollands, K.G.T., "A Canadian Representation Meteorological Year for Solar System Simulation", Proceedings 1984 Annual Meeting of SESCI, pp. 85-88, SESCI, Ottawa, Canada, (1984).

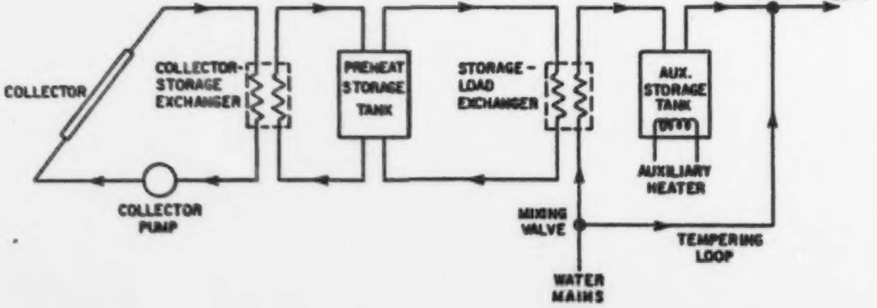
MIXING VALVE
LOAD
COLLECTOR
COLLECTOR-STORAGE EXCHANGER
PREHEAT STORAGE TANK
STORAGE-LOAD EXCHANGER
AUX. STORAGE TANK
AUXILIARY HEATER
COLLECTOR PUMP
MIXING VALVE
TEMPERING LOOP
WATER MAINS

Fig. 1 Schematic of WATSUN DHWS Systems Used in Simulations

# Passive
# Solar
# Performance

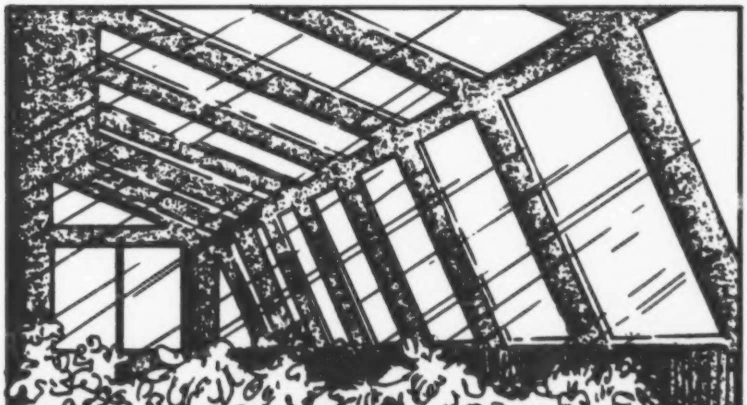

# SANDSTONE VALLEY ECUMENICAL CENTER - A SOLAR CHURCH FOR CALGARY

Richard Sordi
Tang G. Lee Architect
20 Dalbrook Bay N.W.
Calgary, Alberta T3A 2G9

ABSTRACT

An ecumenical church is being designed and scheduled for spring 1986 construction. The two congregations will have their own sanctuary space and share a large lobby, administration, library, classrooms, lounge, gymnasium hall, recreation and service space. The total area is 3,000 square meters.

The design incorporates the use of natural daylighting while still maintaining energy conserving features. The front facade is both an important architectural feature and acts as a solar air collector. Some one hundred square meters of glazing with a selective surface backing constitutes the collectors. The heat will be delivered to the general return air system in order to reduce the heating load. Rather than providing a separate storage system, the building itself acts as the storage.

A hydronic heating system will be used for space heating. Because of ventilation requirements a run-around heat recovery system is being designed. Air-to-air heat exchanger are not specified because of limited available space.

It is our intention that over the next several years the building will be monitored for energy conservation and compared to other similar buildings.

# SITE PLANNING PRINCIPLES FOR EFFECTIVE USE OF SOLAR ENERGY IN NEW HOUSING

Emad M. Elias
1477 Mississauga Valley Blvd.
#601, Mississauga, Ont.
L5A 3Y4 Canada

## ABSTRACT:

Utilizing the benefits of solar energy in site planning has become one of the most important considerations in today's energy-conscious urban design practice. There is a gap between the need for and the availability of suitable information which can be attributed to two factors. First, many city planners are not fully aware with solar access techniques - second relevant solar access techniques is not available in a format simple enough to meet building designers practical needs. This paper deals with the site planning principles and related solar energy design issues with particular reference to new housing developments.

## 1. INTRODUCTION

If solar energy principles are to be used and become a part of the normal site planning and design practice, two basic steps have to be taken:

(1) Guidelines listing site planning and design principles have to be developed and applied.

(2) Specific design objectives have to be set.

Steps have to be taken to make the housing industry and the public aware of the advantages of and savings from planning for solar energy gain.

## 2. BACKGROUND - ENVIRONMENTAL FORCES AND LAND FORM

### 2. a Land Form Description

Understanding the interaction between environmental forces and land form is an important stage in arriving to a comprehensive set of design guidelines for the construction of manmade forms. Topography, either in a natural undisturbed state or as manipulated by man, has the ability to modify ameliorate climatic variations in a wide range of ways.

Topographical maps are often found in planning agencies and should be examined to identify the environmental forces and features. City of Hamilton Ref. 2 came up with a unique type of chart called "the Ecochart". The poster-sized chart shows the ecological description for a specific area.

### 2. b Sun/Shadow - Mechanics

The intensity of solar radiation striking the earth's surface varies with latitude, season and time of day because of their effect on the angle at which the sun's rays pass through the atmosphere. The location of the sun at any time relative to a point on the earth is defined by its altitude and its azimuth. Altitude is the vertical angle above the horizon and azimuth is the clockwise angle from due north.

The times of day and year in which the sun will be available within a particular site can be determined by drawing the existing objects on the site on a sun path diagram. Sun path diagrams show the path of the sun in the sky dome as projected on to a horizontal surface. The heavy lines running from east to west represent the path of the sun on the 21st day of each month of the year.

The heavy lines running perpendicular to the sun lines indicate hours of the day. The light lines radiating from the center of the diagram indicate the sun's azimuth. The concentric light lines indicate the sun's altitude. (See fig. 1) (Ref. 1).

### 2. c Factors Effecting Solar Access Vegetation/Wind

Adopting provisions concerning solar access and properly siting vegetation such as trees, shrubs and grass have a beneficial effect on the energy requirements of a swelling. Controlling trees may seem like a new or unsuitable area for local government involvement, but it is not as unusual as it may first appear. Many communities plant and maintain vegetation in parks and along streets. Planting vegetation on private property may also be regulated. Private trees may be trimmed if they obstruct lines and trees may be removed if the roots block sewer lines.

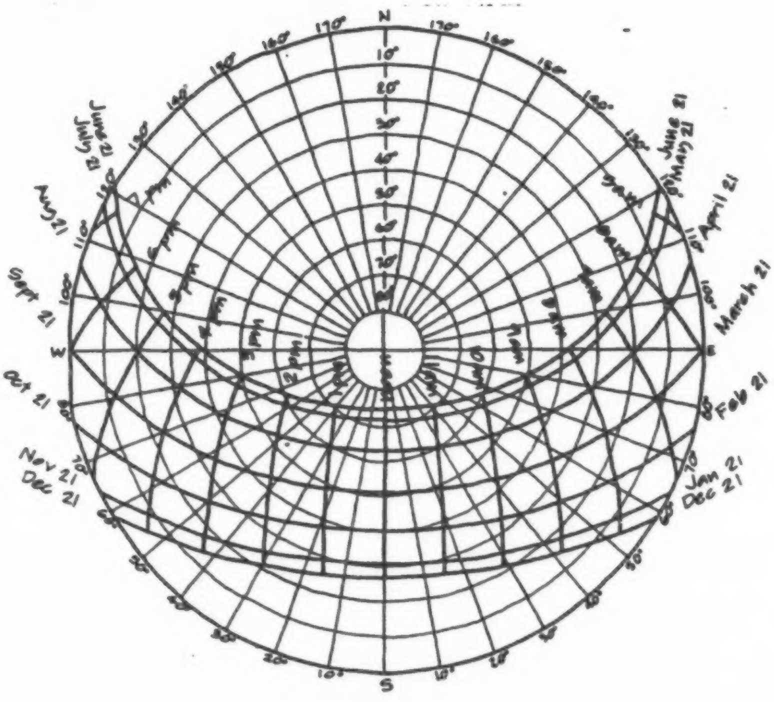

Fig. 1 . Sun Path Diagram 40°N Latitude.

(Sources: Brown, G.Z., "Sun, Wind and Light", 1985).

Spruce trees are often planted along or near property lines to provide a windbreak. However, windbreaks of coniferous trees would not cause solar access conflicts because of their likely location and do not grow very tall. Deciduous trees can create solar access problems even though their leaves fall. Problems can occur for two reasons: The timing of the leaf season and density of winter twigs and branches. (See fig. 2)

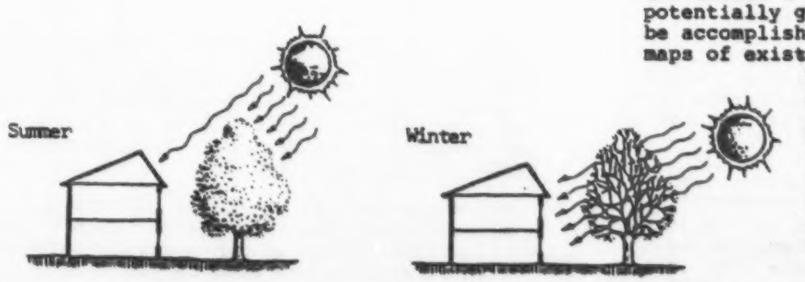

Fig. 2 Deciduous Trees Provide Summer Protection from and Winter Access for Sun.

(Source: Ontario Ministry of Municipal Affairs and Housing - "Handbook for Energy Efficient Residential Subdivision Planning", 1981.)

## 3. SITE ANALYSIS PROCEDURES

### 3. a Data Collection

It is of utmost importance that this be done accurately and methodically. A site plan data collection checklist, which can help the planner to identify the site problems and uncover the missing planning information will include information on the following: (Ref. 3)

1. Primary function of the site.
2. Regional and local climates.
3. Type of topographical characteristics.
4. Site planning maps which can be obtained from municipality agencies.
5. Site landmarks and existing features, both natural and man-made need to be perceived.
6. Area surroundings and main transportation exits related to the site under review.
7. Expected type of housing development.
8. Type and purpose of the solar energy systems that might be used in the new buildings.
9. Any existing local zoning restrictions.

### 3. b Site Analysis Evaluation

Site analysis must identify the land most suitable for construction of different building forms as well as natural and man-made features which may become a part of the project's planning and design. Understanding of both the positive and negative effects of siting and site development on the utilization of solar radiation and energy conservation is essential.

The planner or building designer must establish and follow a basic work plan to determine the potentially good land uses. (Ref. 3) This can be accomplished by using different coloured maps of existing site analysis information, which can be placed over the base map in single layers or in groups to help the planner to come up with final site planning pictures while assessing and evaluating the suitability or unsuitability of such land use for solar access; such maps can be described as follows:

1. The base map which includes site topographical characteristics (See Fig. 3)
   - A. Location and type of existing trees and vegetation.
   - B. Indication of different slopes and flat areas.
   - C. Location of historic sites, existing buildings, significant natural features and parks.
   - D. Indication of the various site elevations and contours.
2. First overlay map for all potential solar access obstructions
   - A. Estimation of height and location of tall objects on the site or on adjoining property that can cast shadows.
   - B. Indication of fog pockets or north slopes or other areas with poor solar access.
   - C. Indication of shadow patterns of peculiar tall obstructions.
3. Second overlay map for all energy conserving factors of the site
   - A. Type of ground surfaces such as reflective surfaces as sand, water or concrete.
   - B. Indication of seasonal wind directions.

At this point, site analysis procedures, with the assistance of computer analysis, would be complete, and available for the planner or building designer for further developments. (See Fig. 4)

## 4. SITE PLANNING CONSIDERATIONS

### 4. a General Solar Access Review Checklist

Completing a general solar access review checklist by the building designer or planner for a specific site will be helpful to get a sense of a community's solar access situation. In addition, completing this review of solar access will increase general awareness of solar access availability and of the obstacles that create shading. The general review considers nine important characteristics: street orientation, street width, typical lot sizes, typical building height, typical building orientation, relationship of different zoning districts, location of parks and natural features, vegetation and topography.

### 4. b Proposed Street and Lot Orientation

To best provide for solar access to the lots, streets should be oriented in a general east-west direction. For those streets that cannot be as arranged, it may be possible to modify the lot configuration or the dwelling design to provide solar access. (See Fig. 5) (Ref. 5)

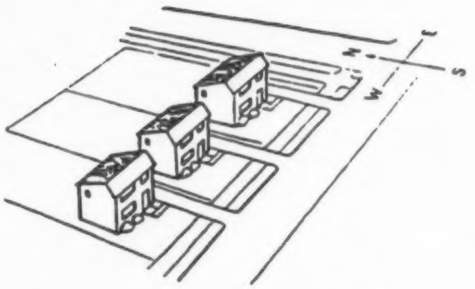

Fig. 5 East-West Street Pattern is Most Appropriate for Purposes of Passive Solar Heating.

(Sources: Ontario Ministry of Municipal Affairs and Housing - "Handbook for Energy Residential Subdivision Planning", 1981.)

### 4. c Proposed Street Layout

Usually subdivision regulations and established engineering standards form the street layout. Municipalities normally require that streets be oriented to line up with existing streets outside of the development site, or that streets must be oriented to follow topography to reduce erosion and grading problems in the development. Because street layout provisions are very general, and in many cases absent from subdivision regulations, it is necessary that new types of provisions be considered by communities wishing to protect solar access which takes into account proper road, lot, and building orientations within the development. While many subdivision regulations do not specifically address the layout of streets, there are some time provisions that do have an effect on it. Many regulations call for alignment or new streets with existing streets.

In urban redevelopment situations, street plan may be very difficult to achieve, if not undesirable. If so, other measures to assure proper orientation can be taken, instead of forcing an east-west street plan on the parcel. Clustering, innovative yard and setback approaches, can be used in lieu of the street plan to achieve good orientation.

Also, if a community chooses to require a certain minimum percentage of east-west street orientation in its subdivision regulations, it may be necessary to provide some guidelines for granting approvals to what could be an unreasonable and inflexible requirement. Typical guidelines might cover the following:

- Allow flexibility to follow topography.
- Allow flexibility to preserve natural features.
- Allow flexibility if other design techniques like clustering are used to get good orientation and access.

Fig. 3 . Base Map with all Topographical Characteristics

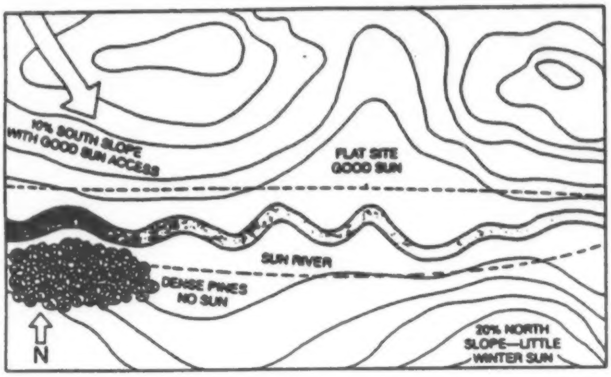
10% SOUTH SLOPE WITH GOOD SUN ACCESS
FLAT SITE GOOD SUN
SUN RIVER
DENSE PINES NO SUN
N
20% NORTH SLOPE—LITTLE WINTER SUN

Fig. 4 . Land Use as Allocated on the Site

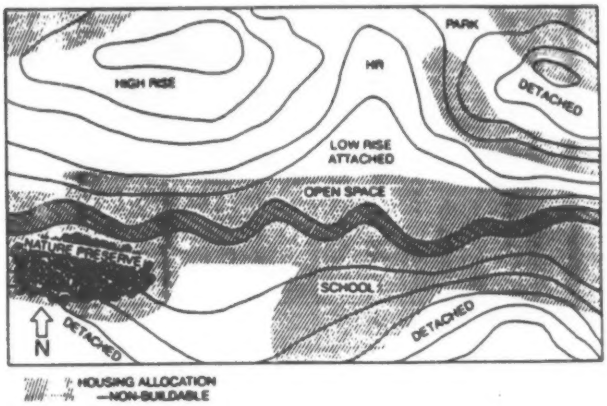

(Sources: Martin, Jaffe and Duncan, Erley; "Site Planning for Solar Access", 1979)

The implication of the design and layout of street systems in new housing subdivisions for solar access have to be considered in subdivision planning regulations. If the orientation and layout of the street system is geared to providing the greatest possible solar access, many problems can be avoided as the development proceeds. (Ref. 4)

4. d Proposed Building Orientation

Ideally, a building is designed for the specific site, location and climate. Occasionally, however, the same building design may be replicated with only minor changes on different sites and in different climates. Site planning solutions are difficult to replicate, because each site has a unique geography, geology and ecology. The correct way to integrate a building with its site requires careful site analysis, and siting the building with a minimum of disruption and the greatest recognition and acceptance of the site's distinctive features. It is possible, however, to provide general techniques for integrating buildings with their sites.

In solar access planning, a building elongated along the east-west axis exposes the longer south side of the building to maximum heat gain during the winter months, while exposing the shorter east and west sides to maximum heat gain in the summer, when the sun is not wanted. (Ref. 6)

In all northern latitudes (32° to 56°), the south side of the building receives nearly 3 times as much solar radiation in the winter than the east and west sides of the building. During the summer, the situation is reversed and the south side receives much less radiation in comparison to the roof and east and west sides of the building. Both in summer and winter the north side of the building receives very little radiation. Besides being an efficient shape, the large southern exposure is ideal for the collection of solar radiation. Major collecting areas of rings or collectors of the building oriented to the south will intercept the maximum amount of solar radiation available during the winter months.

The number of degrees which can be shifted depends on the climate of the area. More moderate climates allow a greater degree of variation from the due east-west orientation than more extreme climates. Long axis east-west orientation is an ideal, however, which may not be achievable for all types of housing. High density urban developments, where houses are located close together or townhouses, where interior dwellings may not even have wall or roof areas exposed to the south, clearly requires different orientation guidelines from moderate or low-density detached housing. In these development situations, the best orientation would be to have the long axis of a structure oriented north and south. North-south orientation of the long axes of these buildings would assure each dwelling unit of south-facing solar access along the unit's narrow side, and windows or greenhouses on these shorter sides that can appreciably assist winter heat gain to the interior of the building. An orientation as suggested here for dense development would be valid for most types of solar energy systems in most latitudes. (See Figs. 6, 7)

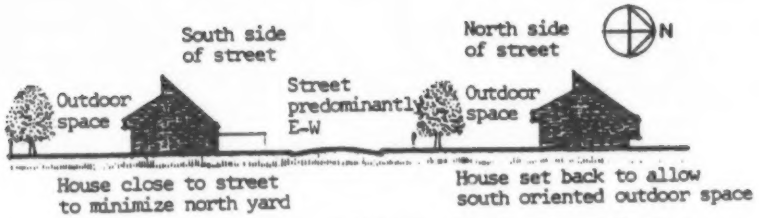
South side
of street
North side
of street
N
Outdoor
space
Street
predominantly
E-W
Outdoor
space
House close to street
to minimize north yard
House set back to allow
south oriented outdoor space

Fig.6 . Section Through Two Dwelling Locations on Level Sites to Obtain Optimum Solar Potential.

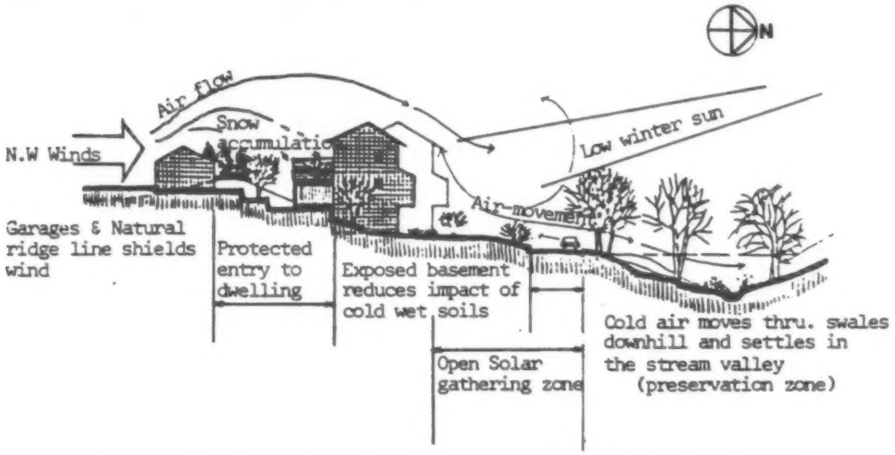
N
Air flow
Snow
accumulation
N.W Winds
Low winter sun
Air-movement
Garages & Natural
ridge line shields
wind
Protected
entry to
dwelling
Exposed basement
reduces impact of
cold wet soils
Cold air moves thru. swales
downhill and settles in
the stream valley
(preservation zone)
Open Solar
gathering zone

Fig.7 Section Through Dwelling Location on a Slope to Provide a Clear South Horizon.

(Source: For both figures, Colton, Norman, "Solar Heated Houses", 1978.)

## 5. RECOMMENDED CHANGES TO ZONING REGULATIONS

### 5.1 Municipalities Typical Control Measures

### 5.1 a Heights

While most residential zones have a building height limitation of 11 meters or 2½ stories, relatively few new homes are built to this height. One method to provide the proper solar access is to establish a building height limit that is more consistent with the actually expected building heights. This would help assure a more uniform building height in the area and improve solar access to all homes. Reducing the height limit of buildings has the effect of reducing shadow lengths and providing greater flexibility in siting neighboring buildings. (Ref. 4)

### 5.2 b Frontage

Increased lot depth is a useful technique to increase the solar access when streets are oriented along an east-west axis. Increasing the lot depth creates a greater distance between homes from north to south and can help provide solar access without any overshadowing. Increases allowed in lot depths should be accompanied by reductions in frontage requirements to ensure that the total size of the lot remains the same but its shape is narrower and deeper. This in turn means a greater distance between buildings from north to south, and better solar access. This technique is most practical only for critical latitudes and slopes and for larger lots because side yards and setbacks are more likely to remain adequate.

For lots located on streets that are oriented in directions other than east/west (e.g. north/south), improving solar access would require that the frontage be increased in width. Since lot width is typically the smaller dimension of the lot, such an increase would result in radically different lot shapes. Short lots with large frontages would increase the length of streets, cost of utilities, and would reduce the yard privacy of individual houses. (Ref. 4)

### 5.2 c Setbacks

In zoning districts where buildings are sited in the traditional way with front, side and rear yard requirements, solar access may be better for some buildings than others. For lots and buildings on east/west streets, adding the street right of way to the setback distances of buildings can mean a greater building separation distance between building fronts than between their backs. The precise change in setback depends on the length of shadows cast under local latitude and the topography of the zoning district, as well as on the structure's orientation.

Builders and developers retain the right to locate the building anywhere on the lot within the minimum setback lines.

Uniform setback requirements can provide more solar access for two reasons. First, the setback would be established to provide for optimal spacing to provide solar access. Second, staggered buildings can cause significant shading in the morning and afternoon and such shading would be reduced if all homes were set back uniformly.

## 6. Conclusions

1. The general acceptance of site planning for solar access approach will depend on our ability to make a comprehensible and easy guide to follow for all the building designers, planners, developers, and above all, the community as a whole. Such guidelines can be presented in sequence in the following manner:

a) Program and Information Collection

A comprehensive information collection should be well prepared and organized in a program document. Such information should cover the site land form description, environmental natural forces as temperatures, wind, sun, shadow and humidity. Also, the study of the existing zoning regulations, market demand and prospective developers most needs, should be considered at this stage by the planner or building designer. (Refer to Section 3a for further details.)

b) Site Analysis/Evaluation

A basic form of work plan technique which can help the planner to evaluate and analyze the final layout land uses. Planners at this stage should also consider the tradition values of people and community as a whole (Refer to Section 3b for details.)

c) Site Planning Design Consideration

The architectural designer or planner, at this point, can start to record his findings from the site analysis evaluation and site observation information on the general solar access review checklist assessment for the site under study. With other site planning considerations the planner will be able to identify his objectives and the best possible solutions for site planning design for solar access (Refer to Section 4 for further details.)

d) Removing Site Barriers and Controlling Vegetation

Removing possible barriers to the sun of solar energy is an important step for improving the site and making whatever additions or revisions to zoning ordinances that are necessary to enable the installation of solar equipment, and to facilitate solar access availability (Refer to Section 2c for details.)

e) Zoning Regulations

Usually municipalities' zoning regulations and standards are prescribed procedures that will define the range of allowable discretions (such as height provisions, frontage and setback requirements, solar envelope and performance standard definitions) which must be made clear in the ordinances (Refer to Section 5 for further information.)

f) Site Planning Design Development

The architectural designer or planner, at this point, can start to exercise his design thoughts and talents in developing the site plan to accommodate the new housing layout planning in different settings and shapes consistent with the site planning considerations and the municipal zoning regulations for solar access (Refer to the site planning organizational chart, Fig. 8, for showing the sequence of principle tasks and considerations that planners or designers can use as a guideline to follow.)

2. The planner or building designer should understand fully the site analysis, planning and design process. This process should be made visible and clear to insure its useage to fully understand the problem, the site, barriers, constraints and potential interest in the project. The available decision-making options should be communicated at each stage in the process and these should be used to assist in evaluating the costs of various alternatives at each stage in the process.

3. Site planning design guidelines here are intended to guide rather than to set fixed requirements. They are not formulated so as to be incorporated in part or in whole as formal municipal requirements, although they may be of some assistance in the formation of municipal planning policies and by-laws. Their main purpose is to assist architectural designers and planners in the assessment of major site planning principles for solar access in new housing developments.

Finally, we need to believe there is something to be gained from a comprehensive site planning design for solar access approach, to create an appreciation for the potential benefits by the general public; and then provide the building designer and planner with the tools for implementation. If we do not, building designers, planners, and public agencies will continue to frequently accept development proposals which work against their own community's best interests.

FIG 8 SITE PLANNING ORGANIZATIONAL CHART

(Sequence of principle tasks and considerations)

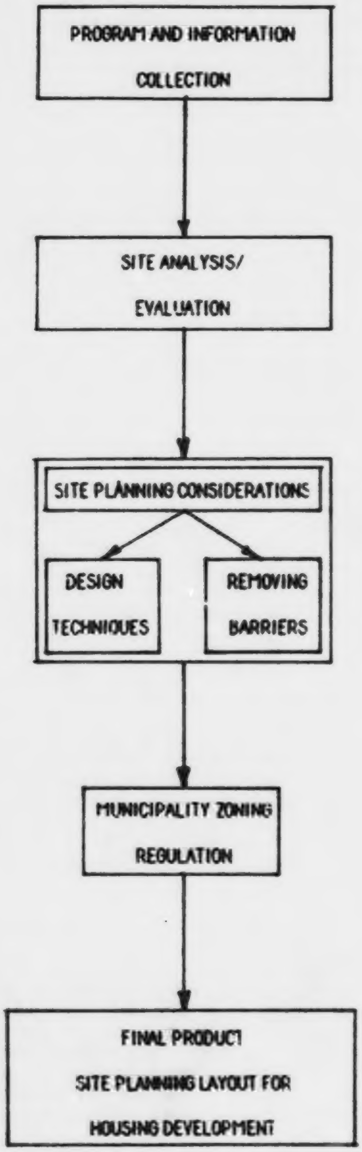
PROGRAM AND INFORMATION COLLECTION
SITE ANALYSIS/ EVALUATION
SITE PLANNING CONSIDERATIONS
DESIGN TECHNIQUES
REMOVING BARRIERS
MUNICIPALITY ZONING REGULATION
FINAL PRODUCT SITE PLANNING LAYOUT FOR HOUSING DEVELOPMENT

## 7. References

1. Brown, G.Z., "Sun, Wind, and Light", John Wiley & Sons, 1985.

2. City of Hamilton, "Design Criteria for Energy Efficient Neighbourhood Planning" September, 1982.

3. Duncan, Erley and Martin, Jaffe for the American Planning Association, "Site Planning for Solar Access", 1979.

4. Duncan, Erley and Martin, Jaffe for the American Planning Association, "Protecting Solar Access for Residential Development", February 1980.

5. Ontario Ministry of Municipal Affairs and Housing, "Handbook for Energy Efficient Residential Subdivision Planning", Part 1, 1981.

6. Olgyay, Victor, "Design with Climate", Princeton University Press, 1963.

# THE POTENTIAL OF SECOND GENERATION BUILDING TECHNOLOGY TO MEET THE R2000 STANDARD

Stephen Carpenter
Enermodal Engineering Limited
368 Phillip Street, Unit 2
Waterloo, Ontario
N2L 5J1

Greg Allen, Mario Kani
Allen Associates
33 Madison Avenue
Toronto, Ontario
M5R 2S2

Michael Glover[1]
Tensions Fabricating
Ottawa, Ontario

## 1. INTRODUCTION

First generation R2000 building technology typically involves high levels of building envelope insulation in combination with an airtight air/vapour barrier and an air-to-air heat exchanger. This paper examines the potential of the emerging second generation technologies for meeting the R2000 performance standard at a significantly lower cost. In contrast to first generation technology, second generation systems are more technically sophisticated involving improved component technology specifically for windows and heat recovery devices. These systems can be easily retrofitted to houses and used to reduce electricity consumption during periods of peak electrical demand.

## 2. THE STUDY

### 2.1 The Reference House

In order to examine the thermal performance of second generation technology, a typical 200 m² house located in Ottawa was analysed using the detailed computer program, ENERPASS [1]. The house is pictured in Figure 1. The house was assumed to be insulated to the 1983 Measures for Energy Conservation standard [2]. The house was assumed to have a natural air change rate of 0.4 ACH with RSI 3.6 above-grade walls, RSI 2.2 below-grade walls, RSI 5.6 ceiling, no basement floor insulation and double glazed windows. The ratio of net window area to floor area is 11.5%, with the majority of the windows located on the south side. Given the flat energy savings curve and low incremental cost for double glazed windows, it is unlikely that the cost or energy consumption of the house would change much with a larger or smaller window area. There was no air heat recovery and heating was achieved by a forced air electric furnace and an electric water heater.

With these insulation levels and a conventional heating system, the house had a predicted annual energy consumption for space and water heating of 109.2 GJ. To meet the R2000 standard, the energy consumption would have to be reduced by 42.4% or 46.3 GJ.

### 2.2 The Conventional R2000 House

The conventional or first generation means of reducing the energy consumption to meet the R2000 performance standard is to use an airtight air/vapour barrier in combination with an air-to-air heat exchanger, upgraded

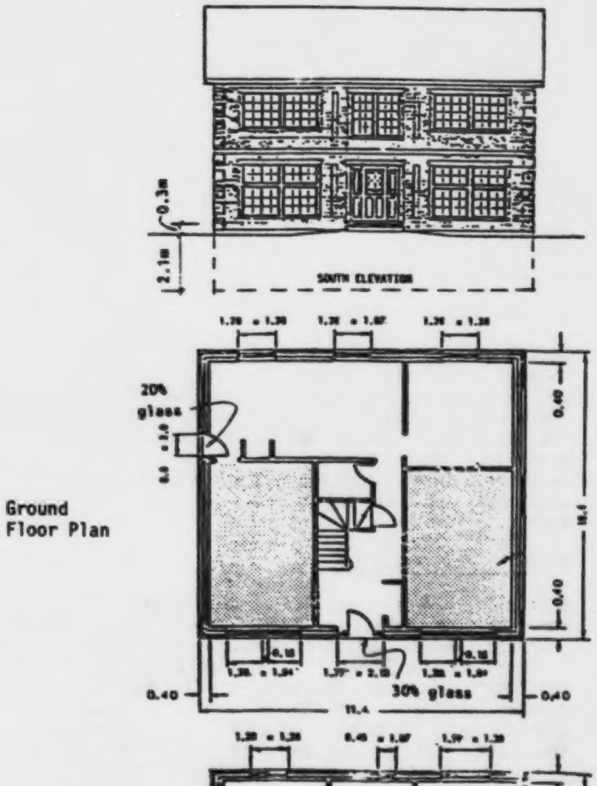

Fig. 1. House Used In Analysis

---

[1] Formerly of Solar Energy Program, National Research Council of Canada.

insulation and slightly better insulating windows. The insulation levels in the reference house were increased to RSI 5.6 walls, RSI 9.0 ceilings, RSI 1.8 basement floor, RSI 3.5 above grade basement walls. The air/vapour barrier was made airtight and an air-to-air heat exchanger with 0.7 heat recovery effectiveness was added to maintain adequate supply of fresh air (0.4 ACH). North, east and west windows were upgraded from double to triple glazed. This house had an annual energy consumption of 62.9 GJ (as predicted by ENERPASS), just meeting the R2000 performance standard.[1] The energy savings is made up of 54% for air-to-air heat exchanger, 38% for improved insulation and 8% for triple glazing.

The cost of upgrading the reference house to the R2000 standard is estimated to be approximately $6400, (see Appendix for calculation). The cost figures were obtained from references 3 and 4 and adjusted to 1986 dollars using the consumer price index. The simple payback on this investment is 10.8 years (assuming electric heating at 4.6 ¢/kWhr). On a component basis, the paybacks are 6.6 years for the air tightness/heat exchanger, 11.7 years for triple glazing and 16.7 years for the insulation. The poor payback for improved insulation is a result of the asymptotic performance curve of increasing insulation; the insulation levels have to be almost doubled to achieve the R2000 performance standard. The remainder of this report will examine how, rather than investing $3800 in increased insulation, the same energy savings can potentially be achieved at a lower cost by use of second generation technology.

### 2.3 Second Generation Technologies

Second generation technologies generally improve building energy efficiency through improved window technology and advanced heat recovery and mechanical systems. These products are or soon will be commercially available and by proper sizing and selection, can be used to meet the R2000 performance standard. This section describes three improved window systems, two methods of increasing net solar heat gain and four advanced mechanical systems.

#### Super Window Technology

Recently, several improved double glazed windows have come on the market. Through use of low emissivity coatings and/or plastic inner glazings, (e.g. Heat Mirror®) manufacturers have been able to produce windows with RSI values of up to 0.7. The National Research Council initiated the Super Window program in 1982 with the goal of developing an RSI 1.0 window. Products that are expected to be initially commercialized as a result of this program include improved triple (RSI 1.06) and super quad (RSI 1.6) [5] (See Table 1).

The improvements to window technology can be grouped into those relating to the glazing system, and those relating to edge seal and frame. For the glazing system, the main improvement is the development of low-emissivity coatings which reduce radiation heat loss. The effectiveness of low-e coatings is enhanced if used in combination with inert gas fill (e.g. argon) to reduce convective heat loss. Low-e coatings and argon gas are very low in material cost. With new low-cost manufacturing techniques under development, the cost of producing high R value glazings should be small when mass produced. New window frame designs overlap the wall and are manufactured from new low conductivity plastics that significantly reduce heat loss. With a conventional window, approximately 25% of the glazing area is frame with an average RSI value of 0.35. A significant part of this heat loss is due to the metallic spacer at the perimeter which interconnects the two panes of glass. An insulated spacer can reduce frame losses by an estimated 30% [6].

Table 1. Window Costs and Performance Characteristics

| WINDOW TYPE | RSI OF GLAZING | RSI OF FRAME[1] | SHADING COEFF. | COST OF GLAZING SYSTEM | COST OF FRAME PER M2 | COST OF WINDOW PER M2* |
|---|---|---|---|---|---|---|
| 1. Conventional Double | RSI 0.35 | 0.35 | 0.88 | $20. | $180. | $200. |
| 2. Conventional Triple | RSI 0.50 | 0.50 | 0.80 | $35. | $210. | $245. |
| 3. Best Commercially Available<br>- double glazed with low-e plastic inner glazing and conventional frame | RSI 0.70 | 0.70 | 0.72 | $60. | $190. | $250. |
| 4. Improved Double<br>- low iron glass<br>- low-e coating<br>- argon gas fill<br>- plastic spacer & frame<br>- overlap frame design | RSI 0.60 | 1.47 | 0.72 | $30. | $180. | $210. |
| 5. Improved Triple<br>- low iron glass<br>- low-e coating on flexible film<br>- argon gas fill<br>- plastic spacer & frame<br>- overlap frame design | RSI 0.90 | 2.27 | 0.72 | $40. | $195. | $235. |
| 6. Super Quad<br>- two low-e coatings on two flexible films<br>- argon gas fill<br>- plastic spacer & frame<br>- overlap frame design | RSI 1.60 | 2.51 | 0.55 | $50. | $210. | $260. |
| 7. Preheat Triple<br>- with low-e coating | RSI 1.02 | 1.02 | 0.48 | $30. | $245. | $275. |

* The cost assumptions for windows 4 - 7 assume quantity production and a mature market.
1 Because of the complex heat transfer in the window frames 4 - 7 these values are only estimates of the best attainable.

In addition to the above window designs, there are two other means of increasing the net solar heat gain to the buildings: preheat windows and sunspaces.

By bringing building ventilation air through the interior of a window, the window convective heat loss can be captured and blown back into the house. If a low emissivity coating is used on one of the glazing surfaces, the radiative heat loss can be significantly reduced. By means of computer simulation it was determined that a triple glazed preheat window would have a thermal resistance of RSI 1.02 at a premium of only $75/m² over double glazing. This type of window is well-suited to a building with an exhaust air heat pump because the heat pump can provide the building negative pressure to draw air in through the window.

Many new homeowners are having sunspaces built as part of their houses. If operated properly with appropriate mechanical systems, the sunspace can significantly reduce the heating requirement of the main house. While the energy savings alone cannot justify the construction cost of the sunspace, to many homeowners it is an aesthetic feature that will pay for itself on house resale. As such, the construction cost of sunspace has not been included in the analysis. The cost, however, of any mechanical equipment to make use of the sunspace heat is included. The sunspace is assumed to be one storey high attached to the full width of the south side of the house and insulated to the 1983 Measures, with vertical double glazed windows. No heating or cooling system is used in the sunspace; its temperature is allowed to float with the weather conditions. Two methods of using the heat generated in the sunspace are examined: preheating of ventilation air as it is brought through the sunspace into the house and heating domestic water by using an indoor air heat pump (see description below).

---

[1] For this house to meet the R2000 performance standard, it's energy consumption must be under 59 GJ as predicted by HOTCAN. This house, when simulated using HOTCAN Version 3.0, had an annual energy consumption of 58.1 GJ. The 4.8 GJ difference between HOTCAN and ENERPASS is thought to be due to differences in weather data, value of ventilation air density (1.1 kg/m³ for HOTCAN, 1.2 kg/m³ for ENERPASS) and the method of handling basement-above grade thermal coupling. For the purposes of this report it has been assumed that any house that has an annual energy consumption under 63 GJ as predicted by ENERPASS would meet the R2000 performance standard.

## Advanced Mechanical Systems

The main improvement in second generation mechanical systems is the use of heat pump technology. In general, second generation heat pump systems have four advantages over conventional heating systems. First, heat pumps allow for more efficient use of energy, since several heating and cooling requirements can be serviced by a single system. These systems can use exhaust air, passive solar gains or waste water to meet the majority of the DHW load. Second, systems that incorporate a storage system can easily be designed to take advantage of off-peak electrical power and to reduce winter peak load demand. Third, heat pumps that extract heat from exhaust air have the advantage of causing a constant supply of fresh air to be pulled into the house rather than being dependent on wind for adequate ventilation. Fourth, some systems can supply all or part of the summer cooling requirement. Although important features, in this analysis no cost benefit has been included for these last three advantages. Three heat pump systems are discussed below and their costs are summarized in Table 2 along with the cost of a conventional heating system [7].

### - Exhaust Air Heat Pump (EAHP)

As an alternative to air-to-air heat exchangers, an exhaust air heat pump can be used to recover heat from exhaust air. Several different models are presently being commercialized. The difference between units is where the recovered heat is used, either for heating space, water, ventilation air or combinations of these. For this report, only the combined space and water heating EAHP was analysed. One advantage of exhaust air heat recovery systems is that it is not necessary to have a very tight air/vapour barrier. For a typical house, the cost saving is estimated to be $600., although the key advantage is that it simplifies on-site quality control for the contractor. The performance of the EAHP is effectively constant and is assumed to be 2.05 kW heat recovered and a COP of 2.87 at a flow rate of 68 l/s [4]. At present this imported product sells for $3000 [8] plus an additional $900 for installation. When the market for this product matures and it is produced in Canada, it's costs should fall in-line with those of other heat pumps. Young and Lange [9] have estimated the installed cost of residential heat pumps in 1986 dollars as $1200 plus $1200 per Ton. This is also consistent with the cost of heat pumps presented in Reference 7. Using this formula the installed cost of EAHP could fall to $2300. plus the cost of the DHW system.

### - Indoor Air Heat Pump (IAHP)

An indoor air heat pump heats water by cooling the air around it. From an energy standpoint, this heat pump is of most benefit when it is located in a space that doesn't need to be heated (e.g. basement or sunspace). A commercially available unit has a range of C.O.P.'s from 2.4 to 3.5, and a heat output from 2.6 kW to 4.6 kW and an installed cost of approximately $1500 [10].

Table 2. Mechanical Equipment Costs

| | Equipment | Installation | Total | Incremental |
|---|---|---|---|---|
| 1. Conventional System | | | | |
| a. Cost of DHW system | $200. | $200. | $400. | - |
| b. Cost of Electrical Space Heating System | 700. | 900. | 1600. | - |
| c. Conventional Metal Ducts | - | 1300. | 1300. | - |
| 2. Exhaust Air Heat Pump | | | | |
| at present | 3000. | 900. | 3900. | 3500. (less 1a) |
| mature market | 1800. | 900. | 2700. | 2300. (less 1a) |
| 3. Indoor Air Heat Pump | 1300. | 200. | 1500. | 1500. |
| 4. Integrated System | 4000. | 1000. | 5000. | 3000. (less 1a,1b) |
| 5. Radiant Heating | - | 2250. | 2250. | 950. (less 1c) |

### - Integrated Mechanical System (IMS)

Cost reductions in mechanical systems can be achieved by integrating the different pieces of mechanical equipment into a single piece of equipment. An integrated mechanical system has been proposed [11] that combines the functions of space heating, DHW heating, ventilation air recovery, summer cooling, grey water heat recovery and even food refrigeration with only one piece of equipment and one heat pump unit. This product, although still at the prototype stage, is expected to be installed at a cost of $5000. or $3000. above the cost of an electric furnace and water heater. The integrated mechanical system can provide full summer air-conditioning, however, in this analysis no cost benefit has been attributed to this feature. The combined functions and storage features of this unit are of benefit to utilities in that the whole house would use very little electricity during periods of peak electric demand.

### - Radiant Heating

In addition to the heat pump systems described above, hydronic radiant heating offers potential for reduced building energy usage over forced air systems. Product research on active solar technology has reduced the cost of hydronic radiant panels, so that radiant systems can potentially be competitive with metallic duct work systems. If the building is heated by radiant panels instead of forced air, it is possible to lower the indoor air temperature to achieve the same comfort level. For a typical residential setting the air temperature can be lowered 0.8 C° for every 1 C° increase in mean radiant temperature [12]. To meet the house heat load by radiant heating the mean radiant temperature would have to be 23.5 °C. Thus the air temperature could be reduced 2 C° to 19 °C.

## 2.4 Combining Second Generation Strategies

While there are numerous ways in which the windows and mechanical systems can be combined, only seven of the more cost-effective strategies are presented. Many of the other combinations either do not meet the R2000 performance standard, have longer payback periods or do not make physical sense. Because south-facing windows receive significantly more solar radiation than north-facing windows, they should have a higher solar transmission. Thus, to optimize cost effectiveness, the south-facing windows will be different from the north, east and west windows. The seven strategies studied are listed in Table 3 and are divided into two main groups. The first group, consisting of five strategies, is based on commercially available technology whereas the remaining group of two strategies uses products that are expected to be on the market within the next few years. For the first group, two costs are given. The first is the present incremental installed cost and the second is the expected cost (in 1986 dollars) assuming reasonable market penetration and production automation. The costing on the second group is based on a mature market. The calculation of the costs is summarized in the Appendix.

The performance of houses using the seven strategies are given in Table 3. The energy savings and incremental capital cost are as compared to the reference house (see Section 2.1). For comparison purposes, the conventional R2000 house is also listed in Table 3. All seven strategies met the R2000 performance standard, used less energy, cost less and were more cost-effective than conventional R2000 practice. In some cases strategies had significantly shorter payback times (Systems 4, 5) and in other cases had significantly lower energy usage (3, 4, 6). The important point, however, is that it is not necessary to use high insulation levels and an air-to-air heat exchanger to achieve the R2000 performance standard.

Since all the strategies easily achieved the R2000 performance standard, the next question that arises is: How far below the R2000 performance standard can houses go if they use high insulation levels, super-windows and advanced mechanical systems? An eighth strategy, a house using the insulation levels of conventional R2000 homes and the windows and mechanical systems of Strategy 2 was simulated. Its annual energy consumption was 37.4 GJ, or 40% below the R2000 performance standard. Use of some of the other systems could result in even lower energy usage. An important result from Strategy Eight is that it is more cost effective than conventional R2000 practice despite the much lower energy consumption. This result shows that it is not always necessary to accept longer payback periods to save more energy.

## 3. CONCLUSIONS

This report has presented seven combinations of improved windows and advanced mechanical systems that can be used in a moderately well-insulated house to meet the R2000 energy standard.

1. All of the second generation systems examined used less energy and were less expensive than the conventional R2000 practice of super-insulating walls, ceiling and floor and installing an air-to-air heat exchanger.

2. At present, using the best commercially available windows and an exhaust air heat pump appears to be the most cost effective means of achieving the R2000 performance standard.

3. With a mature market, most of the strategies had paybacks of under five years.

4. Using second generation technology and high insulation levels it is possible to design homes that use 40% less energy than the R2000 performance standard and are more cost effective than conventional R2000 practice.

Table 3. Results of Analysis

| SYSTEM | SOUTH WINDOWS | NORTH WINDOWS | BUILDING ENVELOPE | MECHANICAL SYSTEM | ENERGY CONSUMPTION | ENERGY SAVED | INCREMENTAL COST* | PAYBACK* |
|---|---|---|---|---|---|---|---|---|
| Measures | Conventional Double | Conventional Double | Measures | Conventional | 109.2 | - | - | - |
| R2000 | Conventional Double | Conventional Triple | Super insulation<br>Airtight barrier | Air-to-air heat exchanger | 62.9 | 46.3 | 6413 | 10.8 |
| Second Generation | | | | | | | | |
| Strategy 1 | Improved Double | Improved Double | Measures | EAHP | 57.5 | 51.7 | 5056<br>(2611) | 7.7<br>(4.0) |
| Strategy 2 | Improved Double | Preheat Triple | Mesaures<br>Airtight barrier | EAHP | 55.9 | 53.3 | 5984<br>(4002) | 8.8<br>(5.9) |
| Strategy 3 | Improved Double | Improved Double | Measures | EAHP<br>+ Radiant heating | 47.6 | 61.6 | 6006<br>(3561) | 7.6<br>(4.6) |
| Strategy 4 | Improved Double<br>Preheat Sunspace | Improved Double | Measures<br>Airtight barrier | EAHP | 48.5 | 60.7 | 5220<br>(3155) | 6.7<br>(4.1) |
| Strategy 5 | Improved Double<br>Sunspace | Improved Double | Measures<br>Airtight barrier | Air-to-air Heat Exchanger<br>IAHP in Sunspace | 54.3 | 54.9 | 4680<br>(3818) | 6.7<br>(5.4) |
| Strategy 6 | Improved Triple | Super Quad | Measures | EAHP | 50.6 | 58.6 | (3678) | (4.9) |
| Strategy 7 | Improved Double | Preheat Window | Measures | Integrated Mechanical System | 53.6 | 55.6 | (4063) | (5.7) |
| Strategy 8 | Improved Double | Improved Double | Super insulation | EAHP | 37.4 | 71.6 | 8850<br>(6405) | 9.7<br>(7.0) |

* bracketed quantities are estimates of mature market cost and payback

5. Unlike first generation technologies, most second generation technologies can be easily retrofitted to houses.

## 4. REFERENCES

1. Enermodal Engineering Limited, ENERPASS, Version 2.0.1 User's Manual, Waterloo, Ontario, 1985.
2. Measures for Energy Conservation in New Buildings 1983, National Research Council of Canada.
3. Dumont, R.S. and H.W. Orr, Cost of Energy Conservation Measures for New Housing, National Research Council Building Research Note 176, Ottawa, Sept. 1981.
4. Hawken, P.J., A Comparison of Ventilation Strategies for Tightly Constructed Houses in Cold Climates, National Research Council Technical Report No. 24082.
5. Glover, M., personal communication, February, 1986.
6. Heat Transfer through Windows during hours of darkness with the Effect of Infiltration Ignored, Bertil Jonsson, Swedish Council for Building Research, D13-1985, Stockholm, Sweden.
7. Ferguson, J.E. and H.F. Sullivan, Analysis of Residential Space Heating Systems In Canada, prepared by Spider Engineering Associates (Waterloo), Inc. for Division of Building Research, National Research Council of Canada, March, 1984.
8. Miller, Larry, Fibreglass Canada, personal communication, April, 1986.
9. Young, D.J. and H.F. Lange, Optimization and Evaluation of a Northern Climate Residential Air-Source Heat Pump, prepared by Ontario Hydro Research Division for Canadian Electrical Association, October, 1980.
10. E-Tech Product Literature, available from Watershed Energy Systems Limited, Toronto, Ontario.
11. Allen, G., M. Kani and S. Carpenter, Mechanically Enhanced Passive Solar Thermal Storage, 1984 SESCI Conference, Calgary, Alberta, August, 1984, pg. 72-78.
12. Wray, W.O., Solar Energy, Vol. 25, pg. 327-333, "A Simple Procedure for Assessing Thermal Comfort in Passive Solar Heated Buildings".

## 5. ACKNOWLEDGEMENTS

The report on which this paper is based was funded by the Solar Energy Program of the National Research Council. Their assistance is gratefully appreciated.

## APPENDIX

COSTING ANALYSIS FOR REFERENCE TO R2000 HOUSE

| REFERENCE | R2000 | COST [$/m2] | AREA [m2] | TOTAL [$] |
|---|---|---|---|---|
| Ceiling<br>RSI = 5.6 | RSI = 9.0 | 4.78 | 103.50 | 494.70 |
| Wall<br>single stud<br>RSI = 3.5 | double stud<br>RSI = 6.4 | 15.76 | 182.50 | 2875.79 |
| Basement (above grade)<br>interior insulation<br>RSI = 2.2 | interior insulation<br>RSI = 3.5 | 1.99 | 41.00 | 81.74 |
| Basement (below grade)<br>interior insulation<br>RSI = 2.2 | interior insulation<br>RSI = 2.2 | 0.00 | 84.50 | 0.00 |
| Basement Floor<br>no insulation<br>RSI = 0.2 | below fl insulation<br>RSI = 1.8 | 3.30 | 103.50 | 341.26 |
| South Windows<br>double | double | 0.00 | 19.55 | 0.00 |
| Other Windows<br>double | triple | 45.00 | 11.57 | 520.65 |
| Ventilation/Mechanical<br>electric furnace | HRV installed | | | 1460.00 |
| vapour barrier<br>0.4 ACH | upgraded vapour<br>barrier - 0.15 ACH | | | 639.00 |
| | | | TOTAL | 6413.14 |

COSTING ANALYSIS FOR STRATEGY ONE

| | | COST [$/m2] | AREA [m2] | TOTAL [$] |
|---|---|---|---|---|
| South Windows<br>double | best commercially available | 50.00 | 19.55 | 977.50 |
| Other Windows<br>double | best commercially available | 50.00 | 11.57 | 578.50 |
| Ventilation/Mechanical<br>electric furnace | EAHP installed | | | 3,500.00 |
| | | | TOTAL | 5,056.00 |

COSTING ANALYSIS FOR STRATEGY TWO

| | | COST [$/m2] | AREA [m2] | TOTAL [$] |
|---|---|---|---|---|
| South Windows<br>double | best commercially available | 50.00 | 19.55 | 977.50 |
| Other Windows<br>double | cheapest triple | 75.00 | 11.57 | 867.75 |
| Ventilation/Mechanical<br>electric furnace | EAHP installed | | | 3,500.00 |
| | airtight vapour barrier | | | 439.00 |
| | | | TOTAL | 5,784.25 |

COSTING ANALYSIS FOR STRATEGY THREE

| | | COST [$/m2] | AREA [m2] | TOTAL [$] |
|---|---|---|---|---|
| South Windows<br>double | best commercially available | 50.00 | 19.55 | 977.50 |
| Other Windows<br>double | best commercially available | 50.00 | 11.57 | 578.50 |
| Ventilation/Mechanical<br>electric furnace | EAHP plus radiant heating | | | 4,450.00 |
| | | | TOTAL | 6,006.00 |

COSTING ANALYSIS FOR STRATEGY FOUR

| | | COST [$/m2] | AREA [m2] | TOTAL [$] |
|---|---|---|---|---|
| South Windows<br>double | best commercially available | 50.00 | 10.05 | 502.50 |
| Other Windows<br>double | best commercially available | 50.00 | 11.57 | 578.50 |
| Sunspace<br>--- | double | | | 0.00 |
| Ventilation/Mechanical<br>electric furnace | EAHP installed | | | 3,500.00 |
| | airtight vapour barrier | | | 639.00 |
| | | | TOTAL | 5,220.00 |

COSTING ANALYSIS FOR STRATEGY FIVE

| | | COST [$/m2] | AREA [m2] | TOTAL [$] |
|---|---|---|---|---|
| South Windows<br>double | best commercially available | 50.00 | 10.05 | 502.50 |
| Other Windows<br>double | best commercially available | 50.00 | 11.57 | 578.50 |
| Sunspace<br>--- | double | | | 0.00 |
| Ventilation/Mechanical<br>electric furnace | HRV installed plus IAHP in sunspace | | | 2,960.00 |
| | airtight vapour barrier | | | 639.00 |
| | | | TOTAL | 4,680.00 |

## COSTING ANALYSIS FOR STRATEGY SIX

| | | COST [$/m2] | AREA [m2] | TOTAL [$] |
|---|---|---|---|---|
| South Windows<br>double | improved triple | 35.00 | 19.55 | 684.25 |
| Other Windows<br>double | super quad | 60.00 | 11.57 | 694.20 |
| Ventilation/Mechanical<br>electric furnace | EAHP installed | | | 2,300.00 |
| | | | TOTAL | 3,678.45 |

## COSTING ANALYSIS FOR STRATEGY SEVEN

| | | COST [$/m2] | AREA [m2] | TOTAL [$] |
|---|---|---|---|---|
| South Windows<br>double | improved double | 10.00 | 19.55 | 195.50 |
| Other Windows<br>double | preheat triple | 75.00 | 11.57 | 867.75 |
| Ventilation/Mechanical<br>electric furnace | IMS installed | | | 3,000.00 |
| | | | TOTAL | 4,063.25 |

## COSTING ANALYSIS FOR STRATEGY EIGHT

| | | COST [$/m2] | AREA [m2] | TOTAL [$] |
|---|---|---|---|---|
| Ceiling<br>RSI = 5.6 | RSI = 9.0 | 4.78 | 103.50 | 494.70 |
| Wall<br>single stud<br>RSI = 3.5 | double stud<br>RSI = 6.4 | 15.76 | 182.50 | 2875.79 |
| Basement (above grade)<br>interior insulation<br>RSI = 2.2 | interior insulation<br>RSI = 3.5 | 1.99 | 41.00 | 81.74 |
| Basement (below grade)<br>interior insulation<br>RSI = 2.2 | interior insulation<br>RSI = 2.2 | 0.00 | 84.50 | 0.00 |
| Basement Floor<br>no insulation<br>RSI = 0.2 | below fl insulation<br>RSI = 1.8 | 3.30 | 103.50 | 341.26 |
| South Windows<br>double | best commercially<br>available | 50.00 | 19.55 | 977.50 |
| Other Windows<br>double | best commercially<br>available | 50.00 | 11.57 | 578.50 |
| Ventilation/Mechanical<br>electric furnace | EAHP installed | | | 3500.00 |
| | | | TOTAL | 8849.49 |

# GRAPHEAT: A GRAPHICAL METHOD FOR DESIGNING ENERGY-EFFICIENT RESIDENTIAL BUILDINGS

Mr. Stephen Carpenter
Enermodal Engineering Limited
368 Phillip Street, Unit 2
Waterloo, Ontario
N2L 5J1

Dr. Eric Burnett
Building Engineering Group
Department of Civil Engineering
University of Waterloo
Waterloo, Ontario
N2L 3G1

## 1. INTRODUCTION

This paper presents a graphical method, GRAPHEAT, for use in the design of energy-efficient buildings. The full method with weather data for 23 Canadian cities and blank worksheets is available from Canada Mortgage and Housing Corporation [1]. The method enables designers of low-energy, passive-solar residential buildings to:

- estimate annual space-heating energy consumption, and
- assess thermal comfort.

The graphical method is based on work by Okins, Leipciger, Cuplinskas, Kaminker and Associates for Canada Mortgage and Housing Corporation (CMHC). GRAPHEAT, an extension and redraft of the original work, was prepared by Building Engineering Group and Enermodal Engineering Limited under CMHC sponsorship.

Architects, builders and non-professionals can use the method to quantify the thermal performance of detached, semi-detached or row houses. The method presumes that the house is relatively well-designed, i.e., the enclosure is well-insulated and air-tight and glazing is intelligently sized and located. A unique feature is that the method enables the designer to estimate the solar-induced air temperature swing without tedious engineering calculations. The temperature swing is one of the indicators of thermal comfort and is of fundamental importance in the design of low-energy, passive solar buildings. The method also provides a quick and graphic means of estimating annual space-heating energy costs. GRAPHEAT is of particular interest to those designers who do not have access to computer simulation tools.

## 2. THE GRAPHEAT METHOD

A flow chart depicting the overall approach is presented in Figure 1. GRAPHEAT makes use of four distinct parts to evaluate the:

- above-grade heat loss coefficient,
- maximum indoor temperature swing,
- below-grade heat loss, and
- annual energy consumption.

As shown in Figure 1, for a comprehensive analysis, all four parts of the method must be completed. For subsequent design variations it may be possible to skip Parts 1, 2 or 3 depending on what changes are made to the building. Eleven sheets are involved--on some, data is recorded (datasheets), on some, calculations are carried out (worksheets) and on the others, nomograms or graphs are provided.

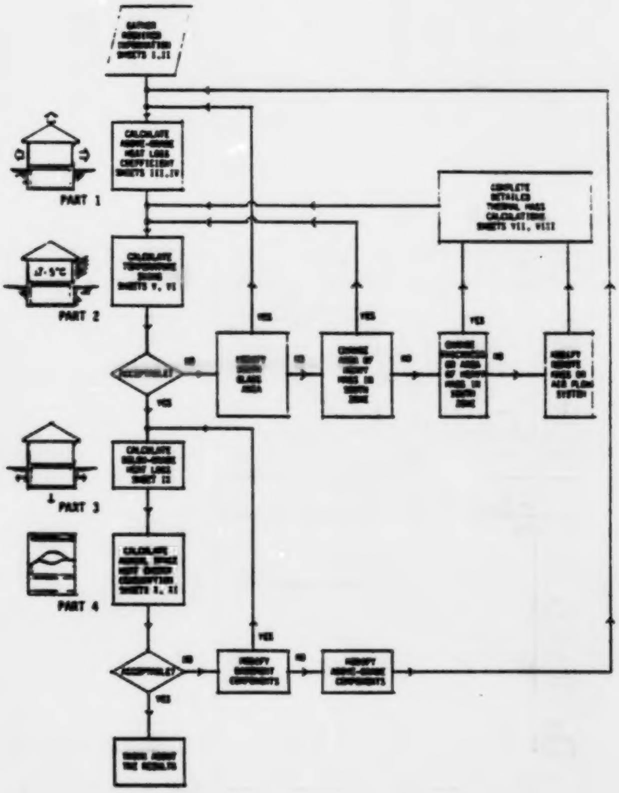
PART 1
PART 2
PART 3
PART 4
COMPLETE DETAILED THERMAL MASS CALCULATIONS SHEETS VII, VIII
CALCULATE TEMPERATURE SWING SHEETS V, VI
YES
NO

Figure 1

Only 26 simple, readily available pieces of information about the building are required. Approximately ten to fifteen minutes would be required to complete the method for a typical house. The method has been shown to give energy usage predictions on average 5% above those from HOTCAN with a standard deviation of 8% [2].

## Part 1: Above-grade Heat Loss Coefficient

The above-grade heat loss coefficient must be calculated in order to determine both the annual space-heating energy consumption and the temperature swing. This coefficient indicates the rate of heat loss, (i.e. watts per degree celsius per unit area) from the above-grade portion of the building for each degree of temperature difference between the indoors and outdoors. As such it is a useful thermal index of the likely performance of the above grade portion of any house.

The above-grade heat loss coefficient is determined by completing the nomogram in Figure 2. Each box is representative of the heat loss from main walls (Box A), above-grade basement walls (B), roof (C), infiltration (D), windows (F) and the total (E). The magnitude of the heat loss from each component can be determined by merely scaling off the appropriate distance on the nomogram. A complete set of instructions on completing this and the other nomograms is given in reference 1. The reader is cautioned not to use the copies of the nomograms in this paper since photo-reduction has altered the scale.

## Part 2: Indoor Temperature Swing

One measure of the level of thermal comfort in a building is the daily variation or swing in the indoor temperature as a result of solar heat gain. Energy-conserving homes can overheat on cold, sunny days unless measures are taken to control or store solar energy. A temperature swing of 5C° is an appropriate design target, although this may be unacceptable to some occupants. A large temperature swing (above 7C°) will cause discomfort and unnecessary heat loss. GRAPHEAT enables the user to estimate the likely temperature swing and assess the effect of varying the south glass area and other design variables.

The indoor temperature swing is determined using the nomogram in Figure 3. This procedure is based on a representative clear, sunny day in January. Solar gains minus heat loss constitutes the amount of solar heat to be stored (i.e., the net gain). If the temperature swing is acceptable, then the user should proceed onto Part 3. If, however, this calculation indicates that the temperature swing is too large, the temperature swing can be reduced by decreasing the net solar gain (less south glazing), increasing the south zone mass, or changing the air-flow system to better utilize any existing mass. The nomogram in Figure 4 contains a procedure for accounting for thermal mass or sizing either a forced-air system or a rock bin unit to control the temperature swing.

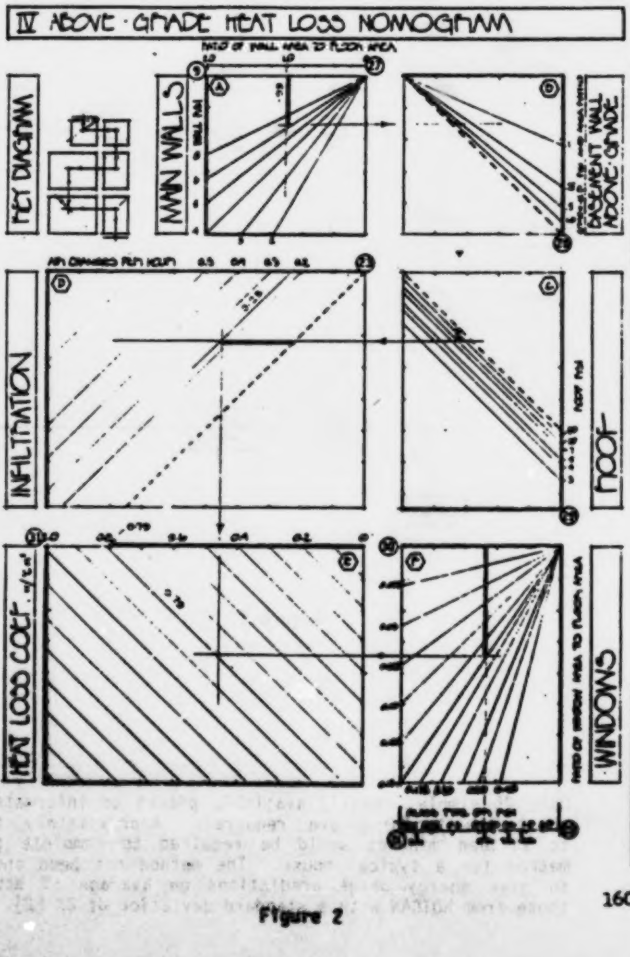
IV ABOVE-GRADE HEAT LOSS NOMOGRAM
KEY DIAGRAM
MAIN WALLS
RATIO OF WALL AREA TO FLOOR AREA
A
B
BASEMENT WALL ABOVE GRADE
AIR CHANGES PER HOUR
0.5
0.4
0.3
0.2
D
INFILTRATION
C
ROOF
0.79
E
HEAT LOSS COEF.
F
WINDOWS
RATIO OF WINDOW AREA TO FLOOR AREA

Figure 2

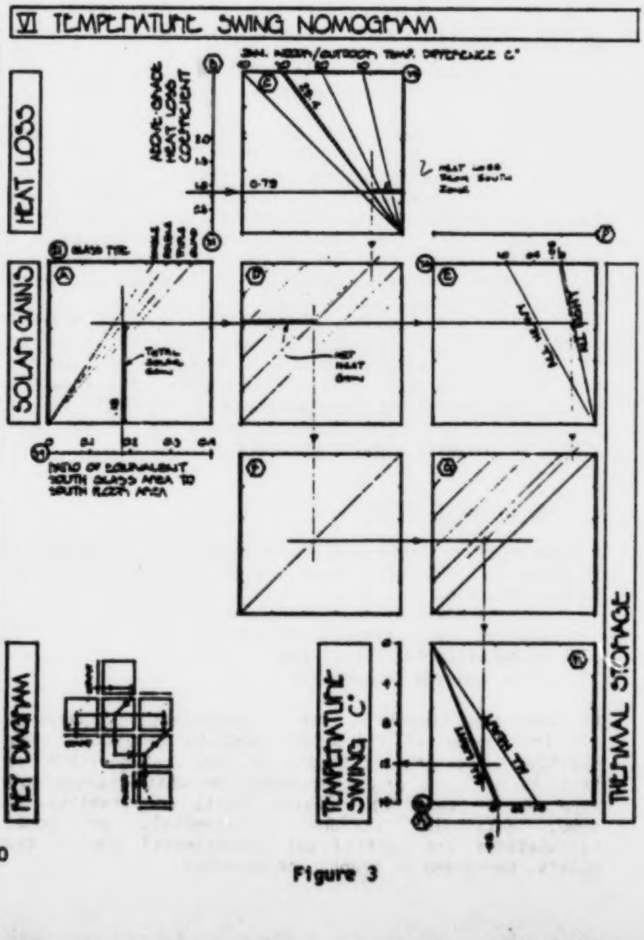
VI TEMPERATURE SWING NOMOGRAM
JAN. INDOOR/OUTDOOR TEMP. DIFFERENCE C°
ABOVE-GRADE HEAT LOSS COEFFICIENT
HEAT LOSS
0.79
HEAT LOSS FROM SOUTH ZONE
C
SOLAR GAINS
GLASS TYPE
A
TOTAL SOLAR GAIN
B
NET HEAT GAIN
E
RATIO OF EQUIVALENT SOUTH GLASS AREA TO SOUTH FLOOR AREA
0
0.1
0.2
0.3
0.4
F
G
H
KEY DIAGRAM
TEMPERATURE SWING C°
THERMAL STORAGE

Figure 3

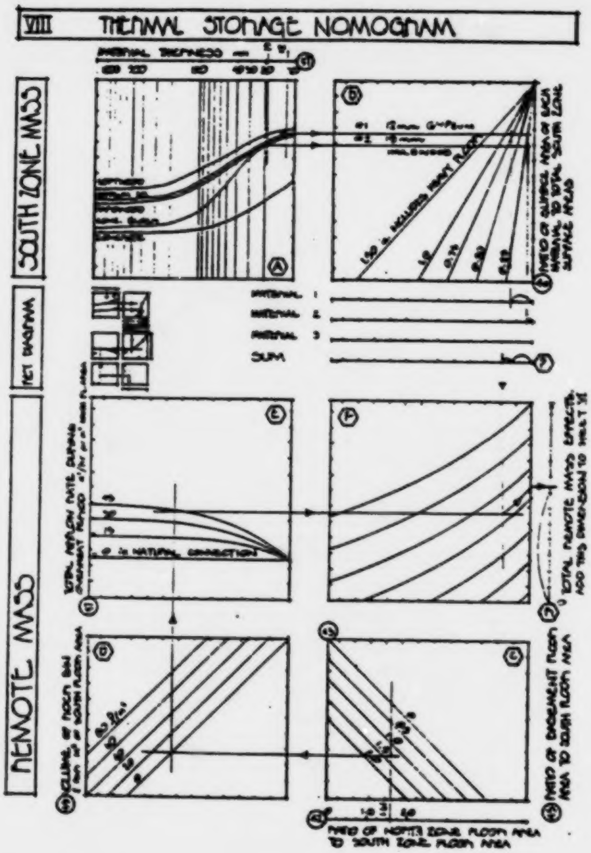
VIII
THERMAL STORAGE NOMOGRAM
SOUTH ZONE MASS
NET DIAGRAM
REMOTE MASS
MATERIAL 1
MATERIAL 2
MATERIAL 3
SUM
A
B
D
E
F
G
RATIO OF NORTH ZONE FLOOR AREA TO SOUTH ZONE FLOOR AREA

Figure 4

## Part 3: Below-grade Heat Loss

The nature of heat transfer through the below-grade basement walls and floor is very different from that of above-grade. Because of the large thermal mass of the ground, the ground temperature will lag behind the ambient above-ground temperature by several months. Subgrade heat loss is greatest in late winter and early spring.

GRAPHEAT estimates the average monthly below-grade heat loss over a seven-month periodheating season (i.e., the period over which heating is required). In Part 4, the actual length of the heating season is evaluated and if the actual heating season is greater than or less than seven months a correction factor is provided.

Using the worksheet in Figure 5 the below-grade heat loss is calculated in two stages, i.e., the floor is first considered and then the below-grade foundation walls. Note that if the calculations indicate that the below-grade heat loss is a major contributor to annual energy consumption, then a more accurate analysis procedure is recommended.

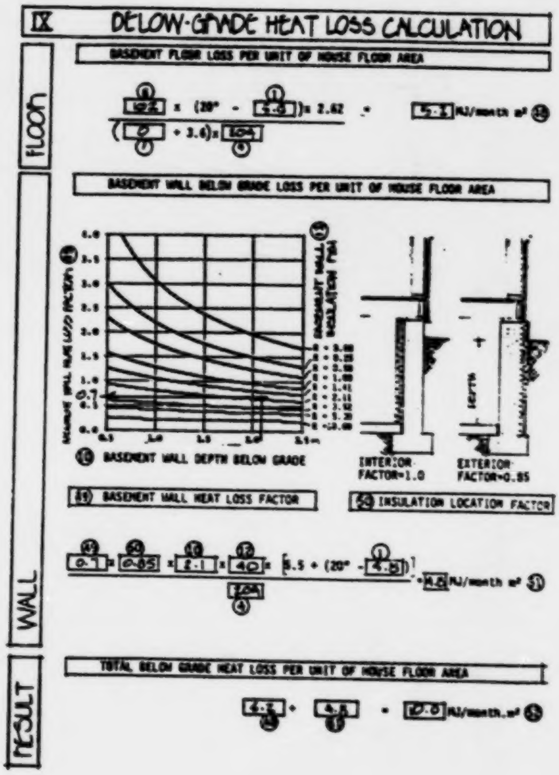
IX
BELOW-GRADE HEAT LOSS CALCULATION
FLOOR
BASEMENT FLOOR LOSS PER UNIT OF HOUSE FLOOR AREA
MJ/month m²
WALL
BASEMENT WALL BELOW GRADE LOSS PER UNIT OF HOUSE FLOOR AREA
BASEMENT WALL DEPTH BELOW GRADE
BASEMENT WALL INSULATION
INTERIOR FACTOR=1.0
EXTERIOR FACTOR=0.85
BASEMENT WALL HEAT LOSS FACTOR
INSULATION LOCATION FACTOR
RESULT
TOTAL BELOW GRADE HEAT LOSS PER UNIT OF HOUSE FLOOR AREA
MJ/month.m²

Figure 5

## Part 4: Annual Energy Consumption

This graphical method for calculating annual energy consumption is an adaptation of the degree-day method. In this section the previously calculated above-grade heat loss coefficients and the below-grade heat loss are used to evaluate transmission and infiltration heat loss. Solar and internal heat gains are then evaluated. The annual energy consumption and cost are then determined.

For 23 graphical locations heating energy graphs are provided (Figure 6). They are plots of monthly degree-day multiplied by a series of above-grade heat loss coefficients compatible with low-energy housing. The graphs are plotted to a vertical scale of one millimetre to one MJ per square metre per month, i.e., each millimetre along each vertical "month" line represents one MJ of heat loss per square metre of above-grade floor area. Each graph covers a nine month period, starting with September and ending with May. The above-grade heat loss coefficient identifies which curve on the Heating Energy Graph is to be used. The area under the Heating Energy Graph curve is equivalent to a nine month heat requirement, before any allowance is made for basement losses, internal gains and solar gains. The basement heat loss and internal heat gains are accounted for by graphical addition and subtraction respectively.

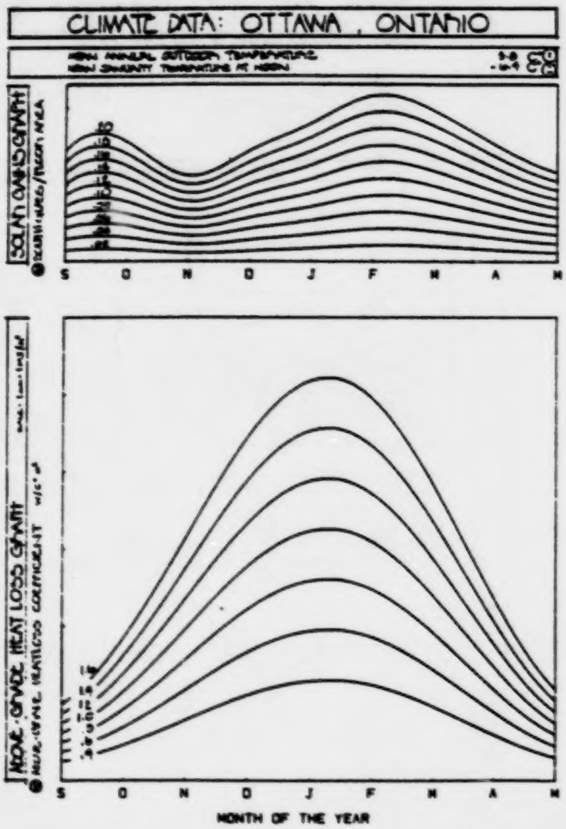

Figure 6

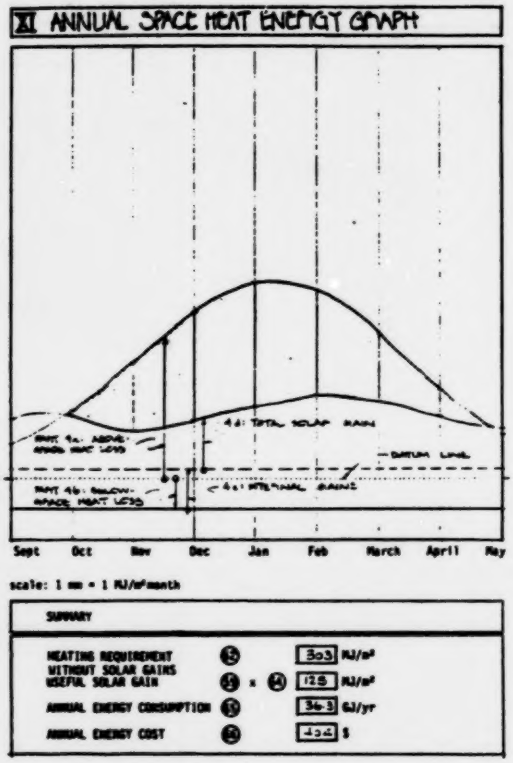

Figure 7

To account for solar gains, a graph has been prepared for each of the twenty-three locations (Figure 6). Each solar gains graph represents the solar gains through south-oriented double-glazing, multiplied by a range of likely ratios of glass area to above-grade floor area.

A completed sample graph is shown in Figure 7 illustrating the monthly contributions of the above and below-grade heat losses and the internal and solar heat gains. This graphical representation of the monthly contribution of both gains and losses is a valuable aid in understanding the nature of space-heating energy demand over the duration of the heating season. Adding up the monthly line lengths in the shaded region gives the user the total annual energy consumption.

## 3. DEALING WITH THE RESULTS

The final graph (Figure 7) and the above-grade heat loss component parts are the main guides for the designer. The annual space heat energy graph clearly shows the relative significance of the above-grade and below-grade heat loss, and the internal and solar gains over the heating season. If energy consumption is considered to be too high, either the losses can be reduced or the solar gain can be increased.

The heat loss may be reduced by changing the below-grade components or the above-grade heat loss coefficient. If the above-grade components are altered, especially the south glass area, the temperature swing should be recalculated. A change in the effective south glass area will also change the solar gains. The flow chart, Figure 1, indicates which parts of the method need to be repeated for various design modifications. Since testing various alternatives can be done relatively quickly, it is recommended that several design alternatives be checked. Their results should be compared to ensure that the design does yield the minimum annual energy consumption and that the temperature swing is not excessive.

## 4. COMMENTARY

GRAPHEAT, a graphical method for assessing the thermal performance of low-energy/passive housing, offers some decided advantages. It is quick and relatively simple to use. It permits a visual as well as a quantitative understanding of the issues involved. It can become a constructive design tool in that a "feel" for the influence of different variables or effects can readily be developed. GRAPHEAT is not meant to take the place of computer simulation, but rather to be a useful tool to those who do not have access to or feel comfortable with computers.

As with any predictive technique, the results obtained using GRAPHEAT are estimates. With a graphical procedure in addition to the numerous assumptions and approximations, both visual judgement and drafting skill influence the accuracy of any numerical result. In general, relative differences will be more accurate than absolute values, i.e., the difference in performance between designs is likely to be more accurate than specific values for either design. The primary value of GRAPHEAT is, therefore, as a design aid, i.e., to assess design changes.

## 5. REFERENCES

1. GRAPHEAT: GRAphical Passive Housing Energy Analysis Technique, A Design Aid for Estimating the Annual Space-Heating Energy Consumption and Thermal Comfort in Low-Energy/Passive Solar Residential Buildings, CMHC Report No. NHA5878 (or LHN5879 for French Version), 1986. Available from CMHC Publications Office, Montreal Road, Ottawa. $8.00

2. Burnett, F.P. and R. Nafziger, A Comparative Assessment of the Results from HOTCAN 3.0 and GRAPHEAT, Report prepared for CMHC, October, 1985.

## 6. POSTSCRIPT

An extension to GRAPHEAT is currently being prepared for CMHC. When completed the revised method will be able to predict indoor temperature swing for any month of the year, annual space cooling costs and the effects of shading on heating and cooling costs.

# VERIFICATION OF HOTCAN 3.0

Craig Wray
Gren Yuill
G. K. Yuill and Associates Ltd.
1441 Pembina Highway
Winnipeg, Manitoba
R3T 2C4

## ABSTRACT

The object of the project reported here was to verify the simulation accuracy of HOTCAN 3.0, a simple residential energy analysis computer program which performs one energy balance per month. The verification was conducted in two phases using a series of simple house models and sets of weather data to test each element of the program separately.

In the first phase, HOTCAN 3.0 predictions of above grade energy consumption were compared with results obtained using BLAST 3.0. There was good agreement between the predictions of the total heat loss and also between the predictions of the net heating load. However, the latter agreement was good partly because of the cancellation of differences in the predictions of some heat gains. Deficiencies in the thermal models were reported to the program authors.

HOTCAN 3.0 predictions of energy consumption due to infiltration were compared with hand-calculated results obtained using the Shaw and LBL infiltration models. The Shaw and LBL model results did not show perfect agreement with the HOTCAN 3.0 predictions but the differences were of the magnitude expected considering the current state of knowledge in ventilation modelling.

In the second phase, HOTCAN 3.0 predictions of energy consumption for full-depth basements and slabs-on-grade were compared with results obtained using a finite difference computer program and an analytical method. For the basement walls, there was good agreement between the heat loss predictions made by the three different methods. There was also good agreement between the basement and slab-on-grade floor heat loss predictions of HOTCAN 3.0 and the analytical method. Agreement between the HOTCAN 3.0 and finite difference computer program predictions of the basement and slab-on-grade floor heat loss was not as good.

In conclusion, HOTCAN 3.0 can be expected to perform at least as well in most real applications as it did in these studies. The below grade and infiltration heat loss model predictions of HOTCAN 3.0 are in as close agreement with other calculations as the state-of-the-art in these fields will permit.

## 1.0 INTRODUCTION

HOTCAN 3.0 is an updated version of the HOTCAN 2.0 residential energy analysis computer program. As in the verification of other simple energy analysis programs, the overall energy consumption predictions of HOTCAN 2.0 have been compared with those of well verified more detailed programs and with measured values (Ref. 1,2,3). This method can cover up program bugs and weaknesses in the thermal models used. Good agreement between the overall energy predictions can easily result from a cancellation of errors in the program being verified, or in the work being used for comparison.

Since HOTCAN 3.0 will be used to evaluate retrofits of existing residences and as a design aid in new energy efficient construction, it is important that it be known to provide accurate monthly component energy loss predictions. Due to this requirement and the updated models in HOTCAN 3.0, it was necessary to extend the previous verification work to this version of the program using a different verification approach.

The approach taken was to use a series of simple building geometries and weather conditions to exercise each model element in the program separately. The verification was conducted in two phases.

In the first phase, the simulation accuracy of the above grade elements of HOTCAN 3.0 was verified using BLAST 3.0. BLAST 3.0 is a well-verified public domain program which uses hour-by-hour analysis and is based on the fundamental equations of heat transfer. Hand calculations were used to check that the infiltration routine had been properly implemented.

In the second phase, the verification used the finite difference computer program ESHD (Ref. 4) and the analytical method ITPE (Ref. 5, 6) for comparison. Hand calculations were also used to check that the basement and slab-on-grade heat loss calculations had been properly implemented. Both ESHD and ITPE have shown good agreement with results obtained using a variety of methods for different basement and slab-on-grade foundations.

## 2. TEST CASES

### 2.1 Phase 1

The verification of the above grade elements in HOTCAN 3.0 emphasized checking the calculation of internal and solar gain utilization and the calculation of admitted solar radiation through glazings. Twenty-seven cases were investigated.

The Division of Building Research, National Research Council of Canada passive solar test facility in Ottawa, Ontario (Ref. 7) was used as the basis in developing the Phase 1 base case house description. These buildings were chosen because they closely approximate the HOTCAN 3.0 thermal mass descriptions. The buildings were also chosen because data that could be used in a future experimental verification are already available.

The base case model house was 9.27 m wide on east and west inside faces and 8.05 m wide on north and south inside faces. The transmission heat loss coefficient was 79 W/°C. The basement of the actual building was not modelled. The floor of the model house at ground level was made adiabatic.

In each of the other cases examined, the set of parameters describing the base case was changed. The changes involved were:

1. Ceiling and wall thermal resistance.
2. Wall solar absorptivity.
3. Window orientation and shading coefficient.
4. Overhang location.
5. Allowable indoor temperature rise.
6. House heat storage capacity.
7. Available internal gains.
8. Weather.

These cases altered the heat gain/heat loss ratio and the thermal mass/heat gain ratio so that the gain utilization predictions of HOTCAN 3.0 could be evaluated. The exterior surface solar heating effect was studied as a function of wall insulation level and solar absorptivity to determine the impact of the neglect of this effect in HOTCAN 3.0. The cases allowed the heat losses and gains to be analysed separately and in combination.

Five weather files were created for use in HOTCAN 3.0 and BLAST 3.0 based on hour-by-hour weather data recorded by the Atmospheric Environment Service of Canada (AES) for Ottawa in 1976. The weather files were modified to simplify the analyses by changing temperatures, humidity ratios, wind speeds and precipitation indices. Solar radiation was set to zero in two of the weather files to allow examination of the exterior surface solar heating. The changes to the weather files eliminated the random nature of daily fluctuations to make interpretation of results easier, and allowed emphasis to be placed on temperatures near the break even temperature of houses.

The separate check of the HOTCAN 3.0 infiltration predictions involved twenty-nine cases. These cases exercised each of the infiltration input combinations available in HOTCAN 3.0. Three different types of information about air tightness are accepted in HOTCAN 3.0. These are age; average natural infiltration air change rate; or equivalent leakage area and air change rate at 50 Pa. The 1961 - 1980 house age range was chosen as a baseline to check that equivalent input data of each type produced the same results. The first six infiltration cases provided reference monthly average heat losses without infiltration for each of the infiltration weather files. The general house description was the same as for the base case in the above grade studies. Internal and solar gains were excluded from the infiltration studies.

The HOTCAN 3.0 infiltration model considers three regimes:

1. Stack effect dominated.
2. Wind pressure dominated.
3. Combined stack effect and wind pressure induced.

Six steady state HOTCAN 3.0 weather files were developed for the infiltration studies. The temperature and wind speed values were typical of Canadian climates in which each of these regimes predominate.

### 2.2 Phase 2

The verification of the below grade heat loss calculations in HOTCAN 3.0 emphasized checking the effect of insulation on the foundation heat loss predictions. Six full-depth basement and slab-on-grade cases were investigated.

To test the effect of insulation location on foundation heat loss predictions of HOTCAN 3.0, two 15 m square full-depth basement models were developed. The models differed only in insulation location. One model had RSI 3.5 full-height wall insulation located inside. This model was used in the Phase 2 base case. The other model had the same insulation located outside. Neither model had floor insulation. Both models had an above grade section which was included to permit investigation of foundation wall vertical heat flow effects.

To investigate the effect of partial insulation on the foundation heat loss predictions of HOTCAN 3.0, two 15 m square slab-on-grade models were developed. The two models differed only in their partial insulation strategies. One model had RSI 3.2 edge and perimeter insulation outside the slab. The other model had only edge insulation. Neither model had insulation on the floor center section.

All of the foundations in Phase 2 were modelled without occupants and without internal or solar gains. The above grade surfaces that were not part of the foundations were considered to be adiabatic.

The HOTCAN 3.0 foundation heat loss model considers three types of soil. These soils are characterized by:

1. Dry sand, loam, clay, low water table.
2. Moist soil, high water table.
3. Permafrost.

For each type, a different soil conductivity is assigned above and below the basement floor level. Slabs-on-grade use only the lower level soil conductivity.

The first two soil types were used in the basement studies to investigate the effects of soil conductivity on the basement heat loss predictions of HOTCAN 3.0. Only the second soil type was used in the slab-on-grade studies. The soil density and specific heat capacity were those reported by Mitalas (Ref. 8) for Ottawa.

Long term normal weather data recorded by AES for Ottawa were used in the simulations. The monthly average outdoor dry-bulb temperatures were modified to duplicate the temperatures assumed by ESHD. Earth surface conditions and ground temperatures were developed by the University of Minnesota Underground Space Center for ESHD, HOTCAN 3.0 and ITPE on the basis of the AES weather data.

## 3. RESULTS AND ANALYSIS

### 3.1 Phase 1

BLAST 3.0 does not directly report either utilized internal or solar gains. Several of the cases were used as references to determine the effects of the changes in weather and house description on these parameters. HOTCAN 3.0 does report utilized gains. However, HOTCAN 3.0 does not report solar radiation admitted through glazings whereas BLAST 3.0 does. Program lines were added to HOTCAN 3.0 to output these intermediate values.

As Figure 1 shows, the agreement was excellent between the HOTCAN 3.0 and BLAST 3.0 predictions of monthly average total heat losses with a root mean square difference of 21 W. Discrepancies were a result of minor differences in component overall thermal resistances and of the use of realistic attic temperatures in BLAST 3.0. These attic temperatures were often quite different from the ambient temperature but they did not have a significant effect in reducing the monthly average total heat loss.

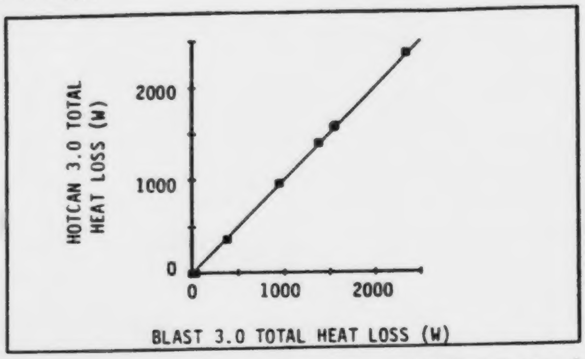

Fig. 1. Comparison of HOTCAN 3.0 and BLAST 3.0 monthly average total heat losses (without internal gains or solar radiation).

It is important to note that HOTCAN 3.0 underestimated the lower monthly average total heat losses. This resulted in extremely high percentage differences. The observed effect is to be expected of a simulation based on monthly average temperatures. HOTCAN 3.0 predicted zero total heat losses for months in which the monthly average outdoor temperature was higher than the indoor temperature. These months had periods in which heating was required when the outdoor temperature dropped below the indoor temperature. BLAST 3.0 reported these heating requirements.

HOTCAN 3.0 tended to underestimate the monthly average utilized internal gains, as shown in Figure 2. The differences were reduced as the allowable temperature rise and thermal mass increased. These differences were due to the form of the internal gain utilization model and to the exclusion of the exterior surface solar heating effect in HOTCAN 3.0.

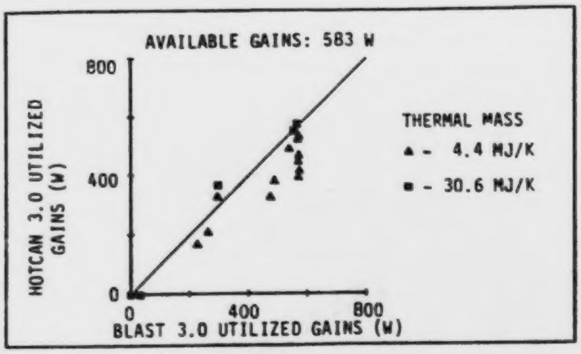

Fig. 2. Comparison of HOTCAN 3.0 and BLAST 3.0 monthly average utilized internal gains.

As Figure 2 shows, HOTCAN 3.0 predicted significant changes in utilized internal gains even when BLAST 3.0 predicted negligible changes. These differences were due to the use of the solar gain utilization model (Ref. 9) to determine internal gain utilization. HOTCAN 3.0 assumed a constant internal gain availability so there was no need for thermal storage effects to transfer gains to periods of unavailability, as required for solar gains. A better internal gain utilization model is available which will improve the agreement between HOTCAN 3.0 and BLAST 3.0 (Ref. 10).

Exterior surface solar heating had a significant effect in reducing the BLAST 3.0 monthly average total heat loss predictions with a range of 85 W to 142 W during the heating season for January through April. The reduction in BLAST 3.0 total heat losses increased the internal gain-heat loss ratios and decreased the internal gain utilization. The reduction in total heat loss was most pronounced for cases with high exterior wall solar absorptivity and low exterior wall thermal resistance. Inclusion of exterior surface solar heating in HOTCAN 3.0 would result in increased program complexity but would improve the accuracy of predictions.

HOTCAN 3.0 consistently overestimated the utilized solar gains through windows as illustrated in Figure 3. Differences were partly due to HOTCAN 3.0 overestimates of the monthly average solar radiation admitted through south facing windows. HOTCAN 3.0 underestimated the solar radiation admitted through east windows, but even in this case the net solar gain was overestimated by HOTCAN 3.0.

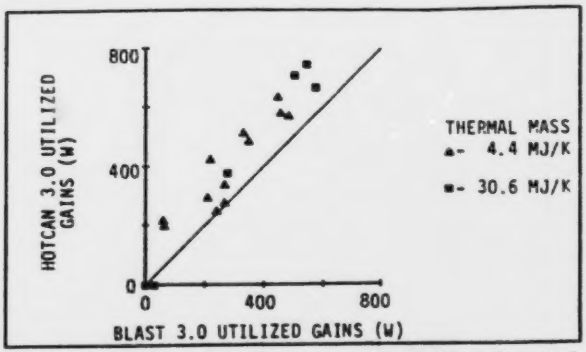

Fig. 3. Comparison of HOTCAN 3.0 and BLAST 3.0 monthly average utilized solar gains admitted through windows.

As Figure 4 shows, HOTCAN 3.0 underestimated the diffuse fraction of the monthly average total horizontal solar radiation during the heating season by as much as 46%. The errors appear to follow a sinusoidal pattern which is indicative of a systematic error in the HOTCAN 3.0 model that determines the diffuse component of the total horizontal radiation. The underestimate of the diffuse fraction caused the beam component to be overestimated and the diffuse component to be underestimated. Improvement of the model or inclusion of the diffuse radiation component in the weather file would rectify these differences.

Exterior surface solar heating was also responsible for part of the utilized solar radiation errors since it increased the solar gain-heat loss ratio in BLAST 3.0.

The HOTCAN 3.0 and BLAST 3.0 predicted monthly average net heating loads exhibit excellent agreement as shown in Figure 5 with a root mean square difference of 28 W. However, the agreement was good partly because of the cancellation of differences in the prediction of some heat gains. The overestimates of utilized solar gains through windows offset the underestimates of utilized internal gains and the exclusion of exterior surface solar heating in HOTCAN 3.0.

There was good agreement between the HOTCAN 3.0 and Shaw model (Ref. 11, 12) predictions. Differences were due to the use of a constant flow exponent in the stack effect regime equations of HOTCAN 3.0 and the use of different factors dependent on the flow coefficient in the combined stack effect and wind pressure regime equations in HOTCAN 3.0. The Shaw equations for natural ventilation are identical to the HOTCAN 3.0 equations except for these

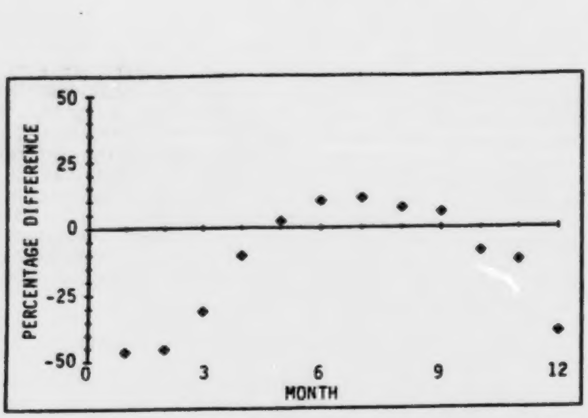

Fig. 4. Comparison of HOTCAN 3.0 and BLAST 3.0 diffuse fractions of monthly average total horizontal solar radiation. (Reference: BLAST 3.0).

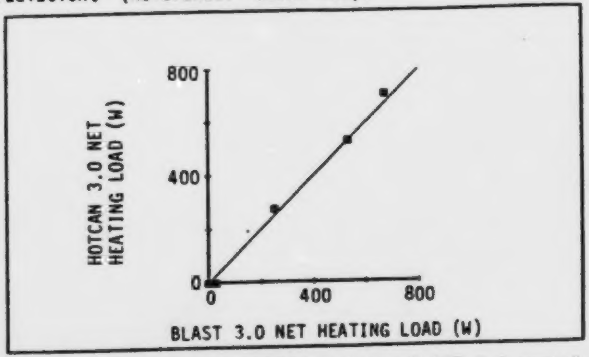

Fig. 5. Comparison of HOTCAN 3.0 and BLAST 3.0 monthly average net heating loads (with internal gains and solar radiation).

differences. However, the Shaw equations for combined natural and forced ventilation are completely different from the HOTCAN 3.0 equations. The Shaw model results for balanced forced ventilation showed a maximum deviation of 14% from the HOTCAN 3.0 results. The Shaw equations for an unbalanced system could not be applied to the comparisons.

Figure 6 illustrates that the LBL model (Ref. 13, 14, 15) results did not show perfect agreement with the HOTCAN 3.0 predictions but the differences were of the magnitude expected considering the current state of ventilation modelling.

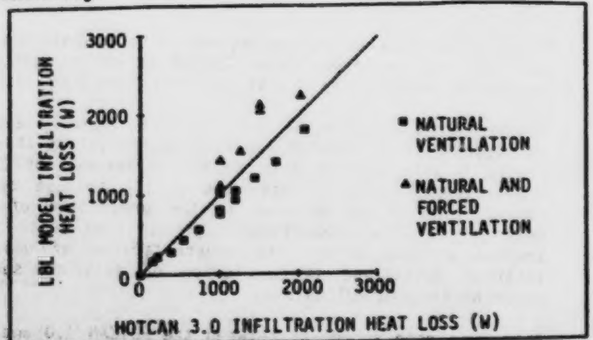

Fig. 6. Comparison of HOTCAN 3.0 and LBL model monthly average infiltration heat losses.

### 3.2 Phase 2

HOTCAN 3.0 was modified to report all sectional monthly average foundation heat losses. However, the results presented here consider only the monthly average grouped and total below grade heat losses because ITPE cannot report the sectional heat losses. The monthly average grouped heat losses were comprised of combined floor or combined below grade wall heat losses. The total monthly average heat losses were comprised of combined floor and below grade wall heat losses.

As Figure 7 shows, the agreement was good between the HOTCAN 3.0 and ITPE predictions of total monthly average basement heat loss. The root mean square difference of the annual heat loss predictions was 22 W. However, the agreement was good partly because of the cancellation of differences in the floor and below grade wall heat loss predictions.

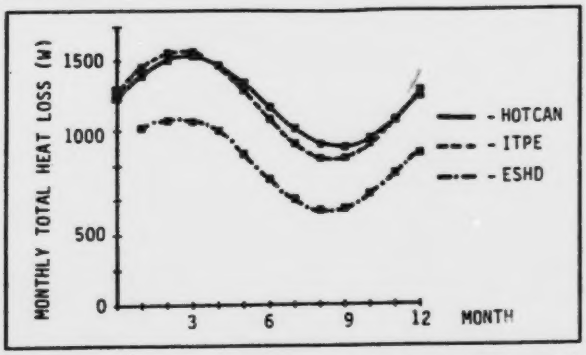

Fig. 7. Comparison of HOTCAN 3.0, ITPE and ESHD monthly average total below grade heat losses for the basement with insulation located inside.

Figure 8 shows that HOTCAN 3.0 estimated the monthly average floor heat loss to be higher than that estimated by ITPE for basements with insulation located on the inside surface of the wall. The estimates by HOTCAN 3.0 of this loss were lower than the ITPE estimates for insulation located on the outside surface of the wall as shown in Figure 9. Figures 8 and 9 also show that the converse was true for the below grade wall heat losses. HOTCAN 3.0 consistently estimated the annual below grade wall heat loss to be 64 W less than the ITPE estimate when insulation was located inside.

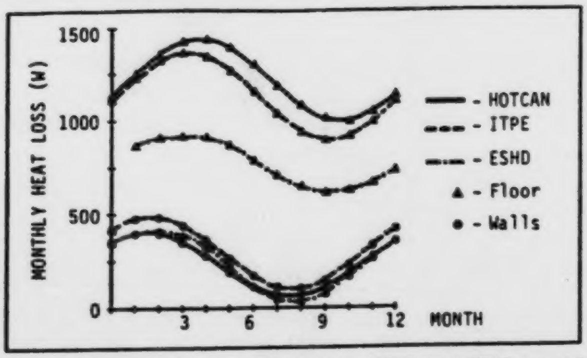

Fig. 8. Comparison of HOTCAN 3.0, ITPE and ESHD monthly average floor and below grade wall heat losses for the basement with insulation located inside.

The differences between the HOTCAN 3.0 and ITPE floor heat loss predictions were reduced with lower soil conductivity.

Comparison of Figures 8 and 9 shows that the ITPE heat loss predictions did not change significantly. However, HOTCAN 3.0 predicted significant decreases in floor heat loss and significant increases in below grade wall heat loss. The difference between the effects predicted by these two programs was due to the implicit inclusion of basement wall vertical heat flow in the HOTCAN 3.0 heat loss analysis. ITPE does not consider this effect. As expected, wall heat flow was predicted by HOTCAN 3.0 to increase due to increased losses through the footing when insulation was located outside.

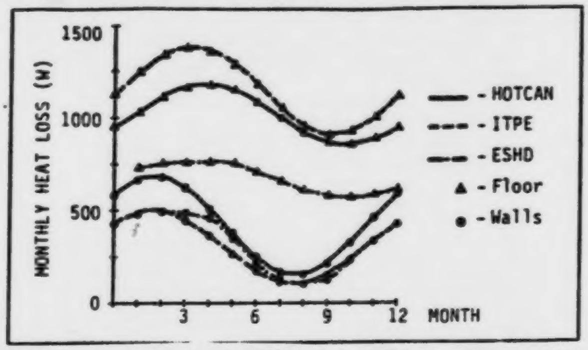

Fig. 9. Comparison of HOTCAN 3.0, ITPE and ESHD monthly average floor and below grade wall heat losses for the basement with insulation located outside.

It is important to note that ITPE was developed for basements with insulation located inside. The method treats concrete thermal resistance as a one-dimensional resistance without heat capacity. The use of this method for basements with insulation located outside has not been verified. Therefore, the validity of the ITPE results presented in Figure 9 has not yet been established.

Figure 7 also shows that the phase shift and amplitude predictions of HOTCAN 3.0 and ESHD agreed well. However, HOTCAN 3.0 estimated the annual heat loss to be higher than the estimate by ESHD with a root mean square difference of 386 W. As Figures 8 and 9 show, the HOTCAN 3.0 and ESHD predictions of below grade wall heat loss agreed well. The root mean square difference between the HOTCAN 3.0 and ESHD predictions of the annual below grade wall heat losses was 52 W. The difference between the HOTCAN 3.0 and ESHD total heat loss predictions was therefore largely due to the higher estimations by HOTCAN 3.0 of the floor heat loss. The root mean square difference between the HOTCAN 3.0 and ESHD annual floor heat loss predictions was 51% of the ESHD prediction.

Some of the deviations in the predictions between HOTCAN 3.0 and ESHD can be attributed to the different simulation techniques used in the two programs. HOTCAN 3.0 used the Mitalas method which is based on finite element simulations whereas ESHD used finite difference simulations to analyze the basement heat losses. While both techniques are similar, the Mitalas method analysis of basement exterior corner heat losses is based on three-dimensional modelling. ESHD only used two-dimensional modelling.

Reference 8 indicates that Mitalas introduced a correction factor to the mean annual floor heat loss shape factors. He multiplied these factors by 1.5 to improve the agreement between the factors he produced by finite element analysis and those he measured. This increase in the shape factors explains the discrepancy observed between the HOTCAN 3.0 and ESHD predictions. Hand calculations using the Mitalas method to predict the basement heat losses produced results identical to the HOTCAN 3.0 results. Whether the differences in floor heat loss predictions were due to an error in the Mitalas method or in ESHD is not clear. However, given the current state of foundation heat loss modelling, the deviations were of the magnitude expected.

The annual heat loss predictions of HOTCAN 3.0 and ITPE agreed well for the slab-on-grade foundation with no perimeter insulation. Differences between the HOTCAN 3.0 and ESHD predictions for the same slab-on-grade foundation were of lesser magnitude than those noted in the basement studies. A two month leading phase shift error was apparent in the HOTCAN 3.0 slab-on-grade heat loss predictions. This error was reported to the program authors.

HOTCAN 3.0 correctly predicted the effect of the partial insulation scheme. The HOTCAN 3.0 and ESHD predictions of slab-on-grade heat loss decreased with the addition of only perimeter insulation. No results could be obtained using ITPE for this case because ITPE cannot analyze partial insulation schemes.

## 4.0 CONCLUSION

The verification of HOTCAN 3.0 was carried out using a series of simple house models and sets of weather data to test each element of the program separately. This approach successfully pinpointed several program bugs which were then corrected. It also located four faults in the HOTCAN 3.0 thermal models which could not have been found by an overall verification, since they tended to cancel one another in typical houses in real climates. These faults were:

1. an overestimation of the monthly total solar radiation falling on a vertical surface;
2. the neglect of the effect of radiation falling on an opaque surface on the heat loss through that surface;
3. an underestimation of the utilisability of internal gains in reducing the net heating load; and
4. a two-month leading phase shift in the estimation of slab-on-grade monthly heat loss.

These four deficiencies were reported to the program authors.

Even with these faults in the thermal models, the overall agreement was good between HOTCAN 3.0 and the computer programs and analytical methods used for comparison. Correction of these faults will ensure that the program continues to perform well even when used for unusual house types or unusual weather conditions.

## 5. ACKNOWLEDGEMENTS

This work was supported under a contract administered by the Bureau of Management Consulting for the R-2000 Program of Energy, Mines and Resources Canada. The guidance of Mark Riley, the R-2000 Program Coordinator is greatly appreciated. We received assistance and co-operation from the staff of the R-2000 program and of Anderson Techno-Products Ltd.

The authors gratefully acknowledge the many hours contributed by Dr. George Meixel and Mr. Lester Shen of the University of Minnesota Underground Space Center. Their extensive help in the input development, ESHD computer analysis and review of results is very much appreciated.

Appreciation is also extended to Mr. David Claridge and Mr. Moncef Krarti of the University of Colorado, Boulder for their assistance in discussing the details of their ITPE method and in reviewing our results.

Consultations with Mr. Michael Lux and Mr. Gint Mitalas of the Division of Building Research, National Research

Council of Canada, contributed to the success of this project.

## 6. REFERENCES

1. R. S. Dumont, M. E. Lux, and H. W. Orr, "Comparison of Energy Consumption Calculations using HOTCAN with Measured Values from Unoccupied Test Huts", Proceedings, Solar Energy Society of Canada, Inc., Annual Meeting, Windsor, Ontario, August 1983.
2. G. K. Yuill, "Evaluation of Low-Rise Residential Energy Analysis Computer Programs and Auditing Procedures, Phase II, Verification of ECAP, HOTCAN and the Degree-Day Method", Report of G. K. Yuill and Associates Ltd. to Saskatchewan Research Council, September 8, 1983.
3. W. G. Colborne, J. D. Hall, and N. W. Wilson, "A Critical Comparison of Two Building Energy Simulation Programs", Proceedings, Solar Energy Society of Canada, Inc., Annual Meeting, Windsor, Ontario, August 1983.
4. G. D. Meixel and T. P. Bligh, "Earth Contact Systems - Final Report", prepared for the U.S. Department of Energy, Contract DE-AC03-80SF11508, Underground Space Center, University of Minnesota and Massachusetts Institute of Technology, Department of Mechanical Engineering, November 1983.
5. M. Krarti, D. E. Claridge and J. F. Kreider, "Interzone Temperature Profile Estimation, Below Grade Basement Heat Transfer Results", Department of Civil, Environmental and Architectural Engineering, University of Colorado, Boulder, Submitted to the ASME National Heat Transfer Conference, August 1985.
6. M. Krarti, D. E. Claridge and J. F. Kreider, "Interzone Temperature Profile Estimation, Slab-on-Grade Heat Transfer Results", Department of Civil, Environmental and Architectural Engineering, University of Colorado, Boulder, Submitted to the ASME National Heat Transfer Conference, August 1985.
7. S. A. Barakat, "Passive Solar Heating Studies at the Division of Building Research", Division of Building Research, National Research Council of Canada, Building Research Note No. 188, Ottawa, May 1982.
8. G. P. Mitalas, "Basement Heat Loss Studies at DBR/NRC", DBR Paper No. 1045, Division of Building Research, National Research Council of Canada, Ottawa, September 1982.
9. D. M. Sander and S. A. Barakat, "Mass and Glass", ASHRAE Journal, Vol. 26, No. 11, pp. 26-32, November 1984.
10. S. A. Barakat, Personal Communication, August 2, 1985.
11. C. Y. Shaw, "A Correlation Between Air Infiltration and Air Tightness in a Developed Residential Area", ASHRAE Transactions, Vol. 87, Part 2, 1981.
12. C. Y. Shaw, "The Effect of Mechanical Ventilation on the Air Leakage Characteristic of a Two-Storey Detached House", Division of Building Research, National Research Council of Canada, Building Research Note No. 204, Ottawa, 1983.
13. D. T. Grimsrud, R. C. Sonderegger, and M. H. Sherman, "Infiltration Measurements in Audit and Retrofit Programs", Energy and Environment Division, Lawrence Berkeley Laboratory, University of California, Report No. LBL-12221, April 1981.
14. M. H. Sherman and D. T. Grimsrud, "A Comparison of Alternate Ventilation Strategies", Energy and Environment Division, Lawrence Berkeley Laboratory, University of California, Report No. LBL-13678, July 1982.
15. ASHRAE, "ASHRAE Handbook 1981 Fundamentals", Ch. 22, American Society of Heating, Refrigerating and Air-Conditioning Engineers, Inc., Atlanta, 1981.

# LOW-FLOW, STRATIFIED-TANK SOLAR WATER HEATING SYSTEMS

K.G.T. Hollands and M.F. Lightstone
Professor Research Assistant
Department of Mechanical Engineering
University of Waterloo
Waterloo, Ontario, N2L 3G1 Canada.

## ABSTRACT

Researchers have discovered that by using collector flow rates roughly one-seventh of those currently-used and by taking special care to ensure the water in the storage tank remains unmixed (stratified), designers can increase the energy delivered by a solar system by as much as 38%. In addition, the lower collector flow rates permit substantial savings in system cost, mainly through dramatic savings in plumbing. This paper reviews the state-of-the-art in this highly-promising change in approach. Particular emphasis is given to the physical reasons for the predicted performance improvement, the savings in system cost, the current knowledge in tank stratification, and methods of analyzing and computer-simulating these systems.

## 1. INTRODUCTION

A revolution is occurring in solar water heating design. Its key words are low-flow and stratified-tank. Researchers have discovered that by using collector flow rates roughly one-seventh those currently used (low-flow), and by taking special care to ensure the water in the storage tank remains unmixed (stratified-tank), designers can increase system performance (energy delivered) by as much as 38%. (The exact improvement is difficult to quantify.)

The new concept applies to systems designed to heat water for domestic, commercial and industrial purposes. The water may be used directly, as in domestic hot water and hot water for car washing plants, bottling plants, and the like. Or it may be used to preheat (through a heat exchanger) other fluids - for example for preheating the oil going into a potato chip cooker. Despite advances in phase change storage, the best thermal storage medium for these systems is still tanks of liquid water. Figure 1 shows a typical system layout.

The gain in energy delivery obtained in going to low-flow-stratified-tank systems is certainly interesting, but it is only part of the breakthrough. What also makes the revolution interesting is the potential for reductions in initial-system-cost made possible by going to low flow: major reductions in piping, pumping, plumbing, and heat exchanger materials are possible.

Currently in its preliminary stages, the changeover to the new approach will benefit from research and development efforts. Introducing the low flow aspects presents no particular difficulty; the crucial thing is to maximize the cost reductions through imaginative design. The stratified tank, on the other hand, is not completely understood. Most of the factors causing mixing (or destratification) are known, but research is required to clarify salient points and to develop and thoroughly test devices that minimize the effects of destratification factors.

This paper will review the state-of-the-art of these new developments. It starts with an explanation of the performance advantages, then goes on to overview the cost reductions it makes possible. Next it discusses the various factors which cause mixing in tanks of water, and ways to overcome them. Finally it discusses models for water storage tanks.

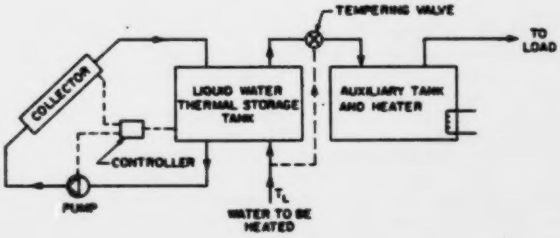

Fig. 1. Schematic of typical solar hot water system (heat exchangers not shown).

## 2. PERFORMANCE ADVANTAGES OF LOW-FLOW, STRATIFIED TANK SYSTEMS

The literature on this approach appears to date from Tabor's 1969 recommendation for low flow in thermosyphon systems (1). But this recommendation appears to have been forgotten by those working with pumped systems. Van Koppen et al (2) rediscovered the idea for pumped systems in 1979. Subsequently Cole and Bellinger (1982) (3), Collares-Pereira et al (1984) (4) independently proposed the idea. Briggs and Ferguson (1984) (5) performed an analysis. Wuestling et al (1985) (6) have recently reported the most complete analysis and Lunde (7) has given a thorough discussion of the physical reasons for the improved performance.

All of these workers have emphasized the performance benefits of low-flow stratified tank systems, but the work of Wuestling et al has made the most clear-cut case.

Figure 2 (adopted from their paper) shows a plot of yearly solar fraction (fraction of total energy demand supplied by solar energy) as a function of flow rate. The upper curve is for a system having an ideally-stratified tank in which no mixing takes place. The lower curve is for a system having a fully-mixed tank. Conventional systems of the immediate past have used a flow rate of about 15 g/s per $m^2$ of collector area and have been modeled as having fully-mixed tanks. Thus they have been thought to operate at the point A on the figure. The operating point (point B) for the new generation of systems will have a flow rate of 2. g/s $m^2$ (Note: this optimum rate is not universal) and will be designed to approach the ideally stratified tank as closely as possible. Since the solar fraction for point B is 53.4% and that for point A is 38.7%, the potential improvement in solar energy delivered is (53.4-38.7)/38.7 or 37%. (This result is of course for the exact system and location simulated by Wuestling et al - see their paper for details. Other systems in other locations should, however, show roughly the same gains.)

But these calculations have probably overestimated the gain: the conventional systems have, in fact, experienced some degree of stratification. Thus their performance should lie somewhere between that for the ideally-stratified tank and the fully-mixed tank. Since it is difficult to assess their true performance, it is difficult to exactly quantify the gain in using the new concept. On the other hand the performance of the conventional systems has almost always been estimated on the basis that their tanks are fully-mixed, since the widely-used design simulation programs (e.g. f-chart) have assumed fully-mixed tanks. Thus the optimistic (e.g. 37%) gain is an accurate measure of the calculated performance.

In order to discuss the reasons for this gain it is necessary to first review the model for the ideally-stratified tank whose performance is depicted in Figure 2. To take a simple example, we consider the "step-change charge", in which a tank initially at uniform temperature is suddenly charged from one end (the top end if the charging water is hotter than the initial tank water; for illustration we assume this to be the case). According to the model a thermal front will move down the tank from the top, the water temperature above the front being uniformly at the inlet temperature and that below the front being uniformly at the intial tank temperature. When the flow is reversed (charging from the bottom) the front moves in the opposite direction.

As explained by Lunde (7), the improved performance is due to the action of the controller and nature of the night time draw-off to the load. (Phillips and Dave (8) showed that if there is no controller and if the tank water is completely delivered to the load in one draw at night, then the fully-mixed and perfectly-stratified system perform identically, and the performance is independent of flow rate.)

The effect of the controller is a simple one: in late afternoon, the controller shuts off the pump earlier for a high flow system than for a low flow system. The controller is set to shut off the pump whenever the collector plate temperature falls below the temperature at the bottom of the tank (plus a "deadband"). (This ensures (conservatively) that the collector never loses heat.) With the low-flow, stratified-tank system, the tank bottom temperature remains at the temperature of the water to be heated ($T_L$ in Fig. 1) until the thermal front has reached the bottom of the tank. With a well-designed combination of tank volume and collector flow rate, this will not happen until the very end of the afternoon--say just before sunset. For the fully-mixed tank, on the other hand, the whole tank temperature (including the bottom) rises uniformly over the day, so that in the afternoon, with the tank temperature rising and the plate temperature falling, its pump shuts off earlier, than for the low-flow system, roughly two hours earlier according to Lunde. Because it misses the available energy in the later part of the afternoon, the conventional system collects less energy.

The effect of a less than complete night time draw-off to load can also be explained. Suppose the total night-time drawoff is equal to one tank volume and that it occurs in two separate equal draw-offs. The tank is assumed to have been uniformly heated to a high temperature $T_h$ during the daylight hours. After the first draw-off the bottom half will be at $T_L$ and the top at $T_h$. In the fully-mixed model these will be mixed to produce a tank uniformly at $(T_h + T_L)/2$. This process repeats after the second draw-off, so that after the mixing following that draw-off the tank will be uniformly at $(T_h + 3\ T_L)/4$, which is hotter than the temperature of the stratified tank temperature, now uniformly at $T_L$, the thermal wave having reached the top of its tank. At the start of the next day, then, the conventional system will be sending water at a higher temperature to the collectors, and, since collector efficiency falls off with increasing temperature, the conventional system will deliver less energy.

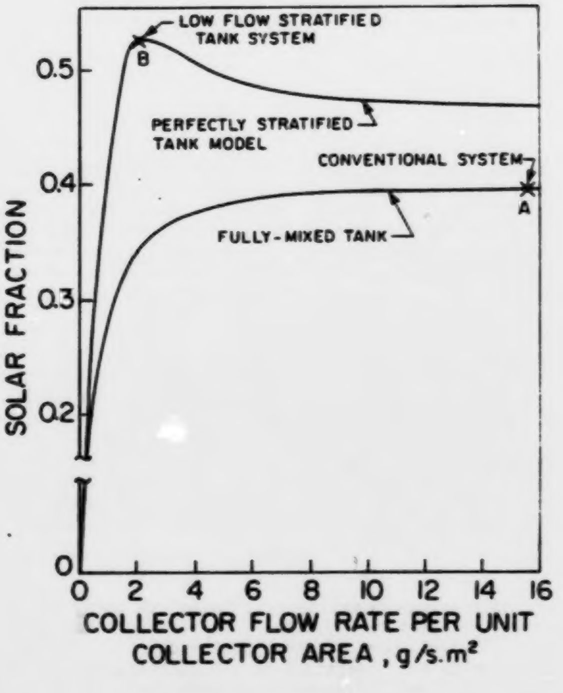

Fig. 2. Annual fraction solar vs collector flow rate adopted from Weustling et al (6). For details of system simulated, see Weustling et al (6).

## 3. COST REDUCTIONS PERMITTED BY LOW-FLOW STRATIFIED TANK SYSTEMS

Hollands et al (9) have shown how real savings in installed system cost can accrue by adopting the low flow strategy in domestic hot water systems. .(These savings are in addition to the savings associated with increased system performance.)

They note that in the past, conventional cold-climate domestic systems have contained roughly 30m of insulated, often unsightly, 13 mm OD copper pipe connecting the tank (in basement) to collector (on roof). In the (preferred) drainback mode of freeze-protection, each leg of piping has had to have a continuous downslope starting from a vented high point. A heat exchanger must be used between the collector fluid and the tank water, and because of the very low temperature differences associated with the high flow systems, thermosyphon is not possible in the loop on the tank side of the heat exchanger. Thus the systems generally have two pumps.

Hollands et al show that creative re-engineering for low flow brings major savings. Not only can the tank-side pump be eliminated by thermosyphon; collector costs are also reduced, and most importantly, the piping and plumbing costs are greatly reduced. The latter is important: one estimate put the cost of plumbing (labour and materials) at about 30% of the total installed cost of a conventional system (10). Hollands et al showed how, with low flow, the expensive copper piping can be replaced by inexpensive, easily-installed, flexible 4 mm ID nylon tubing, with low surface area (much reduced insulation cost) and low visibility. The tubes inside the collector can be serpentined tubing of the same 4 mm diameter (a savings in collector cost: the headers are eliminated), and the collectors can be connected in series, rather than parallel, reducing by two the number of connections at the collector. The draining (for freeze protection) of the tubing can now be achieved by "miniscus action", (made possible by the extremely fine tubes) so that continuous slopes and a vent are no longer required.

Similar savings for commercial and industrial systems should be possible; see Collares-Pereira et al (4).

## 4. TANK STRATIFICATION

Inspection of Fig. 2 shows that the performance penalties associated with tank-mixing at low-flow are much greater than those at high flow. Clearly designers must be very careful in designing their systems for low flow to avoid mixing and maintain stratification. To appreciate the problems involved, one must be familiar with the physics of tank stratification. This section will review our knowledge of this topic

Numerous laboratory and field experiments (11-21) and computer experiments (22-6) have been reported on stratification in liquid storage tanks.

The evidence is conclusive that under the right conditions, a tank of water will achieve a very high degree of stratification. For example, Fig. 3 shows measurements by Sliwinski et al (11) of a step-change charge in which the initial tank temperature was 42°C and the charging water temperature was 72°C. The temperature profiles shown are for successive times from start of charging. The front described earlier is clearly visible at every time (except very early times, see later). In an ideally-stratified tank, each temperature profile would be a horizontal line, and certainly deviations from this ideal are clearly visible. But from a system performance perspective, these deviations may well be unimportant.

In practice or under improper conditions, however, certain "destratification factors" can cause substantial deviations from the ideal-stratification. These are
(i) inlet jet mixing,
(ii) plume (or viscous) entrainment,
(iii) heat conduction
(iv) tank wall effects

### 4.1 Inlet Jet Mixing

The jet momentum of the water entering the tank produces a mixing that is usually localized to a small horizontal region near the inlet port, but under certain conditions this region may extend to include much of the tank. Such a mixing region can be identified over the (de-dimensionalized) height denoted by $L^*/L$ in Fig. 3. Figure 4 shows the flow in the mixing region observed by Baines et al (12). Sliwinski et al (11) found the height $L^*$ of the mixing region, when de-dimensionalized by division by the tank height L, to be a unique function of the Richardson number, defined by

$$Ri = g\beta\Delta TL/v^2$$

where g is the acceleration of gravity, $\beta$ is the thermal expansion coefficient of water, $\Delta T$ is the temperature difference between the inlet water and the initial tank temperature, and v is the water velocity at the inlet port. Figure 4, adapted from Sliwinski et al (10) shows the relation between $L^*/L$ and Ri. It indicates that $L^*/L$ is less than 0.05 if $Ri > 0.5$, but for smaller values of Ri, $L^*/L$ rises sharply. Thus designers should keep $Ri > 0.5$ to keep the mixing layer small. Designers can usually accomplish this by making the inlet port sufficiently large in cross-section. Some evidence exists (Cole and Bellinger (3)) that conventional systems have suffered from substantial jet mixing.

### 4.2 Plume Entrainment

The discussion so far has been limited to a step change charge in which either hot water entered from the top or cold water entered from the bottom. In the reverse of either of these cases (e.g. hot enteres from bottom), a thermal plume (Fig.6) is observed, identical in

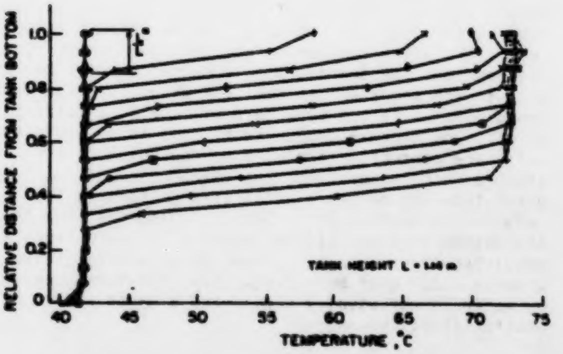

Fig. 3. Measurements of Sliwinski et al (11) of the response of a water storage tank to a step-change charge, showing temperature profiles at successive times after start of charge.

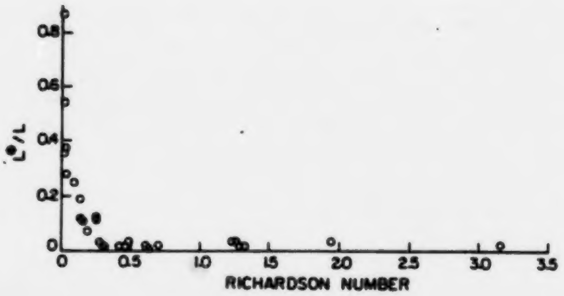

Fig. 5. Plot of L*/L vs Richardson number, measured by Sliwinski (11).

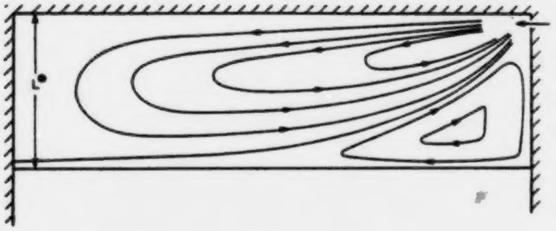

Fig. 4. Flow in the jet mixing region, adapted from Baines (12).

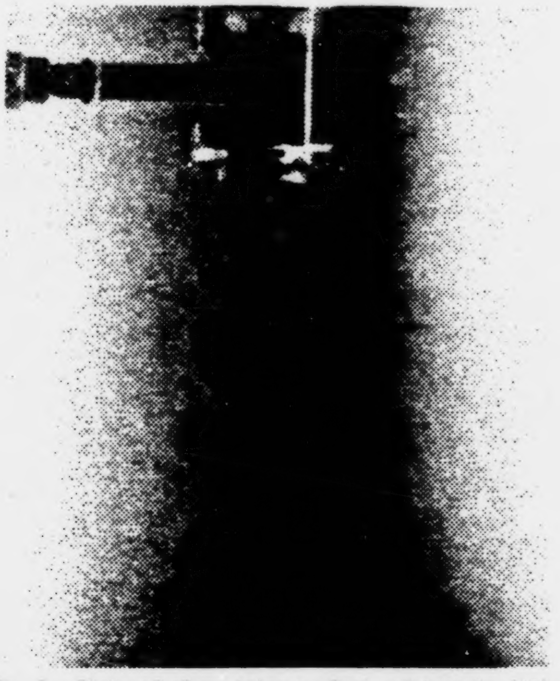

Fig. 6. Photo of plume taken by Gari and Loehrhe (12).

essence to the plumes from smoke stacks. The plume entrains the tank liquid, growing in size in the process. This entrainment clearly mixes the water, destroying ideal-stratification. Clearly designers can avoid this mixing by putting the collector return port at the tank top and the port for the water to be heated at the tank bottom.

But this step in itself will not completely eliminate plume entrainment, because in practice the tank is not at uniform temperature when charging starts. A relevant occurrence will often arise in low-flow systems about the middle of the afternoon, when the hot water returns from the collector at a lower temperature than the water at the tank top, which was heated to a higher temperature when the solar energy was more available around noon. According to an ideal-stratification model (the model assumed in Fig. 2) this return water from the collector would fall, without mixing or change in temperature, to a lower region containing water at its own temperature. But because of plume entrainment, mixing will take place en route, thus detracting from ideal stratification. As an example, Phillips and Pate (14), who were the first to note the plume entrainment effect (they called it viscous entrainment), observed that over a distance of only one-third the tank height, a plume entrained a mass of water equal to seven times its own mass, and in the process changed its temperature by 35°C.

### 4.3 Heat Conduction

If the tank is allowed to idle for some time without subsequent charging or discharging, the steep temperature profiles (like those in Fig. 3) will degrade in time, ultimately leading to a tank of uniform temperature. The water remains essentially stationary over this period; the degradation is caused by heat conduction in the water and in the tank walls. If the tank containing walls are very thin of made of a material of very low thermal conductivity, and if in addition the walls are perfectly insulated on the outside, then, given a starting profile, the calculation of the subsequent temperature profiles is straightforward (see Jaluria and Gupta (16)). Such calculations show that the degradation process is, in this instance, very slow, requiring several days. Since charge and discharge usually occur much more frequently than this, conduction by water is not usually considered a major source of destratification.

If, on the other hand, the containing walls are thick and made of a material which is a good heat conductor, this degradation process can be accelerated considerably. As shown by Jaluria and Gupta (16), the horizontal gradients are quickly removed by natural convection, so heat transfer in an idling tank can be closely modeled as one-dimensional conduction. This means that, to a reasonable approximation, one can calculate the degradation process in the same way as for the tank with thin, non-conductive walls, but using in place of the water's thermal conductivity, an effective conductivity which is a (cross-sectional area) weighted average of the conductivity of water and that of the containing walls. Using this model and experiments, Sherman et al (15) showed that wall conduction can accelerate the degradation process by a factor ranging from 1.5 for a stainless steel wall of 1.07 mm thickness to 4 for a copper wall of 0.86 mm thickness. The latter case would represent an unacceptably high conductive degradation. Designers must therefore design their tank containing walls of thin and/or low conductivity walls to avoid this important source of de-stratification.

### 4.4 Wall Effects

Up to now this discussion has assumed that the tank is perfectly insulated in the region outside the tank containing walls, so that there are no heat losses into the space in which the tank resides. Jaluria and Gupta (16) discuss the effect of finite heat loss, which is particularly important for small tasks. Designers can minimize this effect by using very high levels of insulation on the tank.

Cole and Billinger (3) noted that as the thermal front passes down or up the tank, the walls, because of their stationary position and finite thermal mass, must lag behind the front. Thus there will be for a period of time a temperature difference between the water and the wall, causing heat transfer and ultimately, a smearing of the front, destroying ideal-stratification. Designers should avoid thick, massive walls, particularly in small tanks.

### 4.5 Methods to Minimize Plume Entrainment

Through proper sizing of the inlet ports and through proper choice of tank walls and insulation, designers can minimize the effects of each destratification factor except one: plume entrainment. Three methods have been put forward to eliminate this--the most difficult factor for the designer to contend with. Firstly, Von Koppen et al (2 ) suggest a light flexible hose be connected to the tank inlet. Due to buoyancy forces, the outlet of the hose should automatically float to the correct depth, without entraining fluid as the plume does. Second Gari and Loehrke (13) suggest that a vertical porous distribution manifold be connected to the inlet port. By proper design of the hydraulic resistance inside the manifold, the water can be made to travel directly to the correct point of entry, and then travel out the porous walls. Figure 7 shows one of their manifold designs in action. Finally, Cole and Bellinger ( 3 ) suggest a device completely outside the tank: a thermostatic valve in the collector return controls the flow of the pumped water to return to a tank at a fixed temperature. The tank is thereby subjected to only two temperatures: the collector return, which enters at the top, and the temperature $T_L$ of the water to be heated, which enters at the bottom; thus thermal plumes should not arise. Wuestling et al (6) show that this latter strategy reduces collector performance by as much as 5%, so it appears that this third method is less satisfactory than the other two.

## 5. MATHEMATICAL MODELS

Until very recently perfectly-stratified tanks have been modeled (27) by dividing the tank (by horizontal planes) into N sectors, or nodes, each of which is assumed to be well-mixed. In the limit of large N, the performance of this tank was expected to approach that of the perfectly stratified-tank. Early attempts (e.g. Close (28), Guitierez et al (29)) used as few as three nodes, but Veltkamp (30) showed that if the collector flow rate is low, up to 60 nodes may be required to approach the highly stratified tank. Thus Wuestling et al (6) suggested the variable inlet plug flow model. (This model was independently developed at the University of Waterloo (31), called there the bumping model, and is incorporated into the WATSUN program. Also Kuhn, Von Fuchs and Zob (32) describe a similar model used in the SOLSYS Program.) This model is far less-consuming of computer time and gives a complete representation of the ideally-stratified tank. In this case the (uniform temperature) sectors are of variable size and are arranged in ascending order with temperature, such that the sector temperatures monotonically increase with (upward) vertical distance. After each time step (usually one hour) in the charging process, the volume of water entering in that

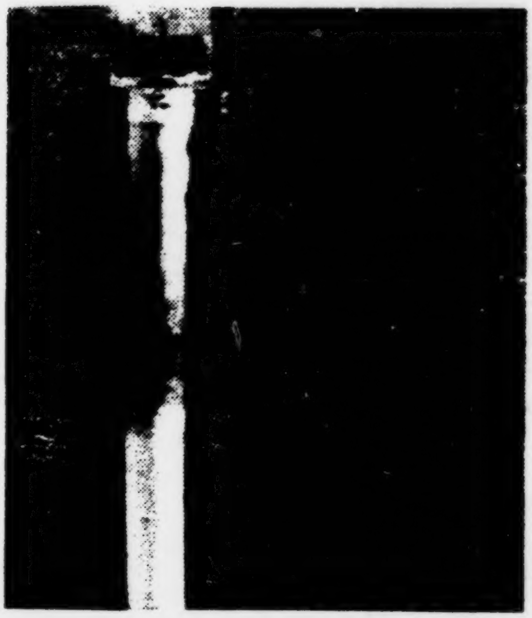

Fig. 7. Photo, due to Gari and Loehrke (13) of the action of one of their special manifolds. The tank is stratified with a roughly linear temperature gradient, and the inlet fluid, indicated by a dye, has fallen down the manifold until reaching the level appropriate to its temperature.

time step is calculated, and this volume, complete with its temperature, is inserted at its appropriate level between two sectors in the sector array, becoming in the process a new sector. The appropriate level is, of course, chosen so as to maintain the monotonic increase of sector temperature with vertical distance. The introduction of the new sector causes the other sectors to shift (or bump) along. If the charging is from the top, only the sectors below the new sector shift, in this case downward. If charging is from the bottom, only the sectors above the new sector shift, in this case upward. The sections (and fractions thereof) which are bumped out of the tank are mixed, and there temperatures calculated. They constitute the outlet of the tank over the time step.

It is clear from Section 4 that real tanks, even if well-designed, will not achieve this ideally-stratified tank behaviour. Thus models are needed for real tanks. The effect of tank heat losses is readily approximated by calculating, independently, the heat losses and temperature change of each sector over the time step ( 6 ). Phillips and Pate (14) and Han and Wu (23) describe a model to incorporate plume entrainment, which perhaps could be adopted to the plug flow, variable inlet model. Cole and Bellinger ( 3 ) describe an approximate method for incorporating wall thermal mass effects, but unfortunately, it is restricted to step-change charge situations. Full scale computer programs (22-26), that simulate the basic differential equations involving continuity of mass, momentum, and energy, can mathematically model real tanks. But, useful as they are, they are so demanding of computer time that they must be considered single tests - like experiments - and are not suitable for routine design. (Moreover, because of the extreme complexity of the flow, results of these programs should be verified by experiment, at least over part of their range.)

## 6. CONCLUSIONS

1. Low flow, stratified tank systems can increase the calculated energy delivered by solar water heating systems by up to 37%.
2. This innovation can also substantially reduce system first costs, principally through reductions in plumbing costs, but also by cost reductions in collector, pump, pipe insulating, and other sundry costs.
3. To achieve the maximum gain in performance of these systems, designers must ensure that the tanks achieve a very high level of stratification; jet-mixing, plume-entrainment, and wall effects must be minimized. This will almost definitely require the use of special devices to eliminate plume entrainment. Such devices should be further devloped and researched.
4. The new "variable inlet plug flow" or "bumping" mathematical model for water storage tanks displaces the old nodal model and gives excellent simulation of the ideally-stratified tanks with little computational effort. However developing simple models for real tanks should be given high priority. This will require further experiments of both a laboratory and numerical kind.

## 7. ACKNOWLEDGEMENTS

We wish to thank Professor G.D. Raithby for helpful discussions, the National Sciences and Engineering Research Council of Canada for a scholarship to one of the authors (MFL), and Jo-Anne Brooks for her prompt and careful typing of the manuscript.

## 8. REFERENCES

1. Tabor, H., "A Note on the Thermosyphon Solar Hot Water Heater", COMPLEX, Vol. 33, No. 17, 1969.

2. Van Koppen, C.W.J., Thomas, J.P.S., Veltkamp, W.B., The Actual Benefits of Thermally Stratified Storage in a Small and Medium Size Solar System", Sun II, Proceedings ISES Biennial Meeting, Atlanta, Ga., Vol. 2, pp. 576-580, Pergamon Press, (1979).

3. Cole, B.L., Bellinger, F.O., "Natural Thermal Stratification in Tanks", Phase I Final Report, Argonne National Laboratory, Argonne, Illinois, (1982).

4. Collares-Pereira, M., Gordon, J.M., Rabl, A., and Zarmi, Y., "Design and Optimization of Solar Industrial Hot Water Systems with Storage", Solar Energy, Vol. 32, 1984, pp. 121-133.

5. Briggs, R.J., Ferguson, J.E., "Effect of Stratification Enhancement on Performance of a Solar DHW System", Proceedings for SESCI '84 Calgary Conference, pp. 63-66, 1984.

6. Wuestling, M.D., Klein, S.A., Duffie, J.A., "Promising Control Alternatives for Solar Water Heating Systems", Journal of Solar Energy Engineering, Vol. 107, pp. 215-221, (1985).

7. Lunde, P.J., "How to Improve DHW Performance", Solar Age, August, 1985, pp. 37-38, Solar Vision-Inc., 7 Church Hill, Harrisville, NH, USA.

8. Phillips, W.F., Dave, R.N., "Effects of Stratification on the Performance of Liquid-Based Solar Heating Systems", Solar Energy, (1981), Vol. 29, No. 2, pp. 189-197.

9. Hollands, K.G.T., Richmond, D.A., Mandelstam, D.R., "Re-engineering Domestic Hot Water Systems for Low-Flow", Proceedings, Intersol '85, Pergamon Press, 1986

10. Hollands, K.G.T., "Development of the Microflow Concept", pp. 19-20, Proceedings of the Third NRC Workshop on Solar Domestic Hot Water Heating, Ottawa, Nov. 14, 1984, J.P. Rollefson, J.E. Hill, Editors, National Research Council of Canada, Ottawa, Canada, 1984.

11. Sliwinski, B.J., Mech, A.R., Shih, T.S., "Stratification in Thermal Storage During Charging", 6th International Heat Transfer Conference", Toronto, Vol. 4, pp. 149-154 (1978).

12. Baines, W.D., Martin, W.W., Smith, D.M., "Development of Stratification in a Rectangular Tank by a Horizontal Inflow", Journal of Fluids Engineering, March 1983 Vol. 105, pp. 59-64.

13. Gari, H.N., Loehrke, R.I., "A Controlled Buoyant Jet for Enhancing Stratification in a Liquid Storage Tank", Journal of Fluids Engineering, (1982), December, Vol. 104, pp. 475-481.

14. Phillips, W.F., Pate, R.A., "Mass and Energy Transfer in a Hot Liquid Energy Storage System", Proceedings of American Section of International Solar Energy Society, Orlando, Florida, (1977), pp. 17.6-17.10.

15. Sherman, C., Wood, B.D., Mason, J., "Effect of Vertical Wall Conduction on Temperature Relaxation in Thermally Stratified Liquid Thermal Storage Tanks", Sun II, Proceedings of the International Solar Energy Society Silver Jubilee Congress, May 1979, Atlanta, pp. 591-595, Pergamon Press, (1979).

16. Jaluria, Y., Gupta, S.K., "Decay of Thermal Stratification in a Water Body for Solar Energy Storage", Solar Energy, Vol. 28, No. 2, pp. 137-143, (1982).

17. Lavan, Z., Thompson, J., "Experimental Study of Thermally Stratified Hot Water Storage Tanks, Solar Energy, Vol. 19, pp. 519-524, (1977).

18. Davis, E.S., Bartera, R., "Stratification in Solar Water Heater Storage Tanks", Proceedings of Workshop on Solar Energy Storage Subsystems for Heating and Cooling of Buildings, Charlottesville, Vo., April 1975, pp. 38-42, published by ASHRAE, 1975.

19. Koldhekar, S.M., "Temperature Stratification in Hot Water Solar Thermal Storage Tanks", AIAA 19th Aerospace Sciences Meeting, Jan. 12-15, 1981, St. Louis, Missouri.

20. Gupta, S.K., Jaluria, Y., "Transient Thermal Effects in an Enclosed Water Body Due to Heated Water Discharge for Heat Rejection and Solar Energy Storage", Energy Conversion and Management, (1981), Vol. 21, pp. 3-8.

21. Rush, C.K., "Stratified Storage Tanks for Solar Water Heaters", Proceedings of the Annual Meeting of The Solar Energy Society of Canada, Inc., Calgary, Alberta, Canada, SESCI, Ottawa, Canada, 1984.

22. Cabelli, A., "Storage Tanks - A Numerical Experiment", Solar Energy, (1977), Vol. 19, pp. 45-54.

23. Wu, S.T., Han, S.M., "A Liquid Solar Energy Storage Tank Model 1. Formulation of a Mathematical Model", in Modelling, Simulation, Testing, and Measurement for Solar Energy Systems, ASME, New York, 1978.

24. Han, S.M., Wu, S.T., "Computer Simulation of a Solar Energy System with a Viscous Entrainment Liquid Storage Tank Model", Proceedings of the 3rd Southeastern Conference On Application of Solar Energy, Huntsville Alabama, April 1978.

25. Guo, K.L., Wu, S.T., "Numerical Study of Flow and Temperature Stratifications in a Liquid Thermal Storage Tank", Journal of Solar Energy Engineering, (1985), February, Vol. 107, pp. 15-20.

26. Sha, W.T., Lin, E.I.H., "Three Dimensional Mathematical Model of Flow Stratification in Thermocline Storage Tanks", Proceedings of the 3rd Southeastern Conference on Application of Solar Energy, Huntsville, Alabama, April, 1978.

27. Duffie, J.A. and Beckman, W.A., Solar Engineering of Thermal Processes, Wiley Interscience, 1980, pp. 329-331.

28. Close, D.J., "A Design Approach for Solar Processes," Solar Energy, Vol. 11, 1967, pp. 112-122.

29. Guitierez, G., Hincapie, F., Duffie, J.A., and Beckman, W.A., "Simulation of Forced Circulation Water Heaters: Effects of Auxiliary Energy Supply, Load Type and Storage Capacity", Solar Energy, (1974), Vol. 15, pp. 287-298.

30. Vellkamp, W.B., "Thermal Stratification in Heat Storage" in C. den Ouden, Thermal Storage of Solar Energy, Martenes Nijnoff, The Hague, Vol. 2, No. 6, 1980.

31. D'Andrea, L.J., Chandrashekar, M., Hollands, K.G.T., WATSUN User's Manual and Program Documentation Version 8.0/85-86, University of Waterloo WATSUN Centre, Waterloo, Canada, pp. 6.3.9-6.3.13, (1985).

32. Kuhn, J.K., von Fuchs, G.F., Zob, A.P., Developing and upgrading of solar system thermal energy storage simulation models, Boeing Computer Services, Seattle (1980).

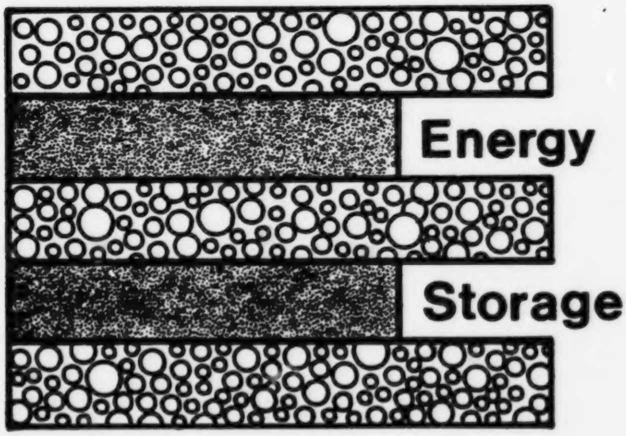
Energy
Storage

# DYNAMIC RESISTANCE ELEMENTS IN A TANK STRATIFIER

W.J. Spaulding and C.K. Rush
Queen's University, Kingston, Ontario

## ABSTRACT

This paper details an investigation into the effect of different control strategies on the operation of a hot water storage tank temperature stratifier used in a solar application. Both computer simulation results and experimental work are presented. The tank stratifier was constructed from a 2.54 cm (1 inch) diameter plastic tube, with holes along its length, extending from the top to near the bottom of the tank and included many flow resistance elements. Heated water entered the stratifier tube from the top and flowed down, then out into the tank when the incoming water's density and the tank's local water density matched. Four control strategies were simulated; fixed resistance elements, dynamic resistance elements designed to compensate for flowrate variations, dynamic resistance elements designed to compensate for density (temperature) difference variations and, fixed resistance elements with flowrate control based on density (temperature) difference variations. The simulation showed that the latter two approaches are most promising.

## 1. INTRODUCTION

The storage of hot water obtained from a variable temperature source, such as a solar collector, presents an interesting problem in maximizing the stored available energy. There are many different ways that hot water can be brought into a tank or removed from it. It must be decided whether an attempt should be made to maintain temperature straitifcation within the tank or to live with the well mixed alternative. If, for example, water is drawn off the bottom of a storage tank, filled with cold water, passes through the solar collector, is warmed to a higher temperature and is then returned to the top of the tank, the hot water will remain where it is delivered, at the top of the tank. This is because hot water is less dense than cold and will float like oil on water. As the day goes on the water in the tank may become hot. If some of the hot water is drawn from the tank there will be a quantity of cold water at the bottom of the tank. When this water is warmed by the collector it may enter the tank at a lower temperature than the water already there. As this cooler returning water enters the tank it will start to fall through the hot upper portion of the tank. It does this because cold water is more dense than hot water and sinks like a stone. As the cooler water falls it will draw some of the hotter water down into the cold bottom of the tank and force some of the cold bottom water up into the hot upper layers. Thus mixing takes place. Very shortly after the mixing process has begun the entire tank will be at an almost uniform temperature and the advantages of stratified storage are lost. There are several good reasons to try to maintain temperature stratification. By always drawing the coldest water off the bottom of the tank for use in the solar collectors, the collection efficiency is increased compared to that obtained with warmer water from a well mixed storage tank. Also, with stratification, the hottest possible water is at the tank's top and is ready for what ever purpose the user has in mind, compared to the less useful cooler water that would be available to the user in a well mixed tank. The two effects can combine to improve the solar fraction by as much as 16% [1] over a well mixed storage arrangement. Another good reason to try and maintain stratification, as compred to well-mixed storage, is that lower flowrates through the collector curcuit can be used without degrading the system performance [1]. A five fold decrease in the time required to bring the entire contents of the storage tank up to a useful temperature can be achieved [5] since the hot water enters the tank's top in a piston like fashion pushing out the cold water from the bottom.

## 2. TANK STRATIFIER

How can temperature stratification be maintained within a hot water storage tank in a solar application? This is a problem that led H.N. Gari and R.I. Loehrke at Colorado State University in the late 70's to develop a tank stratifier [2,3,4]. It consisted of a 10 cm diameter plastic pipe suspended in an open topped storage tank and extending from near the top to the bottom. This pipe, called the outer pipe, was open at both ends and had many holes along its length. Water was drawn off the bottom of the tank, heated, then returned into the tank from the top through a small diameter tube centred within the outer pipe and called an inner tube. The inner tube had many holes arranged in a way that water entered the outer pipe horizontally at low speed. If the incoming water was hotter than the tank top temperature then the incoming water rose within the outer

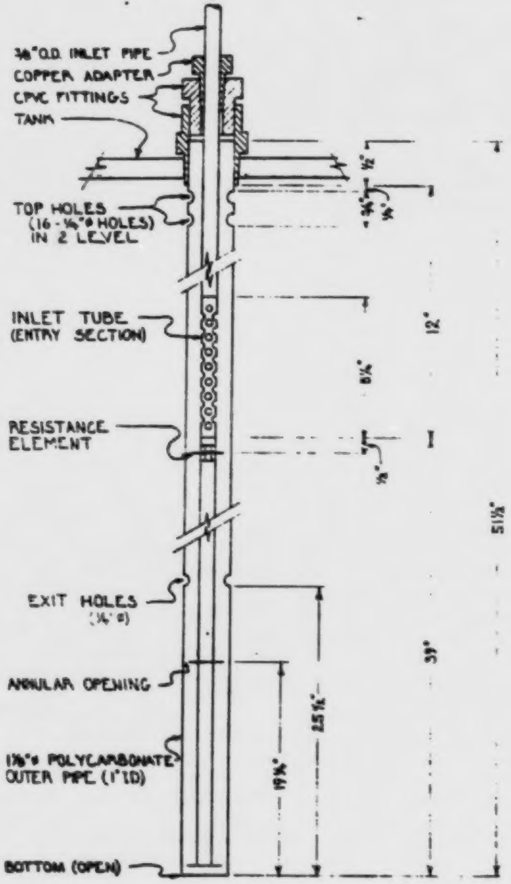
3/8" O.D. INLET PIPE
COPPER ADAPTER
CPVC FITTINGS
TANK
TOP HOLES (16 - 1/4"⌀ HOLES) IN 2 LEVEL
INLET TUBE (ENTRY SECTION)
RESISTANCE ELEMENT
EXIT HOLES (1/4"⌀)
ANNULAR OPENING
1 3/8"⌀ POLYCARBONATE OUTER PIPE (1" ID)
BOTTOM (OPEN)
12"
51 1/2"
39"

Fig. 1: Stratifier with Inner Tube and Fixed Resistance Elements.

pipe and came out the open upper end. If, on the other hand, the incoming water was cooler than the tank top temperature the incoming water fell down through the outer pipe and flowed from the outer pipe into the tank through holes located along the outer pipe's length. This is exactly the same as what incoming water would do if the outer pipe had not been in place except that in this case the mixing of the incoming and tank waters was prevented by the outer pipe until the incoming water had reached its exit level. With correct design the incoming water could be made to enter the tank at the tank level where the densities of the incoming and tank water match and the result was a temperature stratified tank.

To examine their work more closely a similar tank stratifier was built in 1983 at the Queen's Solar Laboratory [6]. The outer pipe was sized to fit through a 1 inch pipe thread hole and was made from a 28.6 mm (1 1/2 inch) O.D. clear polycarbonate tube and the inner tube was made from a 9.5 mm (3/8 inch) O.D. copper pipe with many 1.6 mm (1/16 inch) diameter holes drilled in it near its upper end to allow incoming water to enter the outer pipe from the inner tube in a horizontal direction (Fig. 1). It was found that this device worked well as long as the incoming water was hotter than that at the top of the tank. In this case water entered the outer pipe from the inner tube and turned upward, flowing out the holes located at the top of the outer pipe. When the entering water was colder than at the top of the tank several different scenarios could be followed depending on the amount of flow resistance developed by resistance elements centered along the length of the outer pipe. If the flow resistance was a little too great then most of the incoming water turned downwards and, at some level, flowed out into the tank. Some of the inlet stream, however, was forced upwards and came out of the outer pipe at the top and degraded the hot water located there. When the flow resistance of the resistance elements was a little too small the incoming water turned downwards, as before, but hot tank water was also sucked in at the top of the outer pipe and became mixed with the cooler inlet water, warming it up and flowing down and out into the tank. As a consequence of the hot

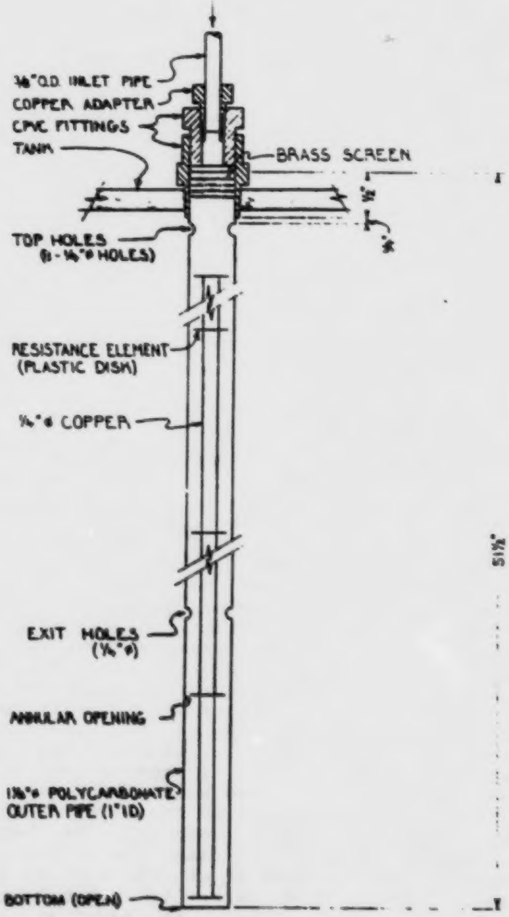
3/8" O.D. INLET PIPE
COPPER ADAPTER
CPVC FITTINGS
TANK
BRASS SCREEN
TOP HOLES (8 - 1/4"⌀ HOLES)
RESISTANCE ELEMENT (PLASTIC DISK)
1/4"⌀ COPPER
EXIT HOLES (1/4"⌀)
ANNULAR OPENING
1 3/8"⌀ POLYCARBONATE OUTER PIPE (1" ID)
BOTTOM (OPEN)
51 1/2"

Fig. 2: Stratifier without Inner Tube and Fixed or Dynamic Resistance Elements.

water being sucked in at the top of the outer pipe the thermocline within the tank rose until all the hot water had been circulated around the tank with mixing of the tank's contents. The sought after condition was that of a "perfect" flow resistance where all the cooler incoming water turned downwards and no tank water was sucked in or pushed out of the top of the outer pipe. Under these conditions temperature stratification could be maintained within the tank for an indefinite operating period.

Recently a new tank stratifier has been built (Fig. 2) with the inner pipe removed and an outer pipe of the same dimensions as used in the previous stratifier. To ensure good flow distribution within the outer pipe, several layers of brass screen were used at its upper end. Extensive testing has been done on this device and it functions in the same way as the older model. As with the old, the new model exhibits sensitivity to flow resistance in that if it is too great fluid is expelled from the top holes and if it is too small fluid is sucked in. In both the old and the new stratifiers, flow resistance was provided by many disks suspended in the center of the outer pipe at intervals along its length. Water was able to flow around these disks through an annular opening between the outer pipe and the edges of the disks. To vary the flow resistance the diameter of the disks was altered, changing the annular area available for the passage of water.

## 3. THEORY

In an effort to understand the nature of this type of flow device it was necessary to realize that the reason water was expelled or sucked into the stratifier was that a pressure difference existed between the tank and the inside of the stratifier. If the pressure within the stratifier was greater than that of the tank, at some tank height, water was expelled and if the tank pressure was greater than the pressure in the stratifier water was entrained (sucked in).

This pressure differential arises as a result of three main factors; the density difference between the inlet and tank waters, the relationship between mass flowrate of water and the friction of the resistance elements inside the stratifier and the change of mass flow rate from place to place within the stratifier due to entrainment or expulsion. Equation 1 describes how these three factors influence the pressure difference between the water in the tank and the water in the stratifier at any height in the tank.

$$\frac{d(P-P_t(z))}{dz} = g(\rho_t(z)-\rho) + \frac{2f\,\dot{m}^2}{DA^2\,\rho} + \frac{1}{A^2}\frac{d}{dz}\left(\frac{\dot{m}_e}{\rho}\right) \qquad (1)$$

**Pressure Difference** | **Density Difference** | **Flow Friction** | **entrainment expulsion**

Under ideal conditions there will be no entrainment or expulsion, in other words $\dot{m}_e = 0$. What this means is that, ideally, the pressure difference between tank and stratifier is zero, or $P-P_t(z) = 0$. Using these two "ideal" operating conditions an equation that describes the relationship between friction factor, mass flowrate, and tank and stratifier density difference can be found. This relationship is presented in Equation 2. As can be seen from this equation, for any given density difference and mass flowrate, there is an "ideal" friction factor that can be used to give "perfect" operation of the tank stratifier. The factor that most strongly influences the "ideal" state is the mass flow rate because this term is squared.

$$f = \frac{\pi^2}{32}\,\frac{gD^5\rho(\rho-\rho_t(z))}{\dot{m}^2} \qquad (2)$$

## 4. CONTROL STRATEGIES

Several possible strategies for obtaining a balance between friction factor, flowrate and temperature difference, as described in Equation 2 are available and will now be presented. Perhaps the simplest approach is to fix the value of the friction factor within the stratifier so that it represents the most common tank inlet condition and simply accept that entrainment and expulsion of water at the incorrect levels as part of the devices normal operation. Another approach is to have the friction factor vary with mass flowrate in such a way that for a given density difference the satisfaction of Equation 2 is guaranteed no matter what the flowrate. A third possibility is to work out some way of varying the friction factor with the density difference (or temperature difference) between the stratifier and the tank and set the mass flowrate to be constant. Many other possibilities exist but one likely one is to set the friction factor to a constant level and vary the mass flowrate coming into the stratifier in proportion to the density (or temperature) difference between the incoming stream and the top-of-tank temperature. This strategy will lead to "perfect" stratifier operation only at the top of the tank but will prevent the hottest temperatures in the tank from being cooled by mixing with lower levels.

## 5. COMPUTER SIMULATION

To test these four strategies a computer model of a tank stratifier similar to the one shown in Figure 2 was developed. The computer model based its predictions of actual operation on the assumption that there were one hundred sets of exit holes and one hundred sets of friction inducing devices present along the length of the stratifier. In addition, the contribution of the stratifier pipe to the total friction factor was neglected since it was found to be an order of magnitude less than the friction factor of the resistance elements. In the actual stratifier there were far fewer exit holes and friction elements present. But the total friction factor per meter of length of stratifier could be adjusted to correspond with what ever the computer simulation predicted. As a standard for comparison an inlet volume flowrate of 2 ℓ/min, an inlet water temperature of 30°C and a tank with a uniform temperature of 50°C and an infinite storage volume, was chosen. This gives a standard temperature difference between inlet and tank ΔT of 20°C. To the the model judge how well a particular strategy performed was set up to give "perfect" operation at the standard inlet conditions. "Perfect" operation was defined as when all of the incoming water was able to flow down the stratifier and flow out its open bottom end, indicating that there was no expulsion or entrainment ($\dot{m}_e = 0$). The results of the simulation are plotted in Figures 3 through 6 and will be discussed in turn. Generally, however, to test each scenario one parameter at a time was altered keeping the others fixed. The percent change away from the standard inlet conditions was found and the percent entrainment/expulsion was determined based on the percent difference between the inlet and outgoing flow at the bottom end of the stratifier. When all the inlet flow came out the bottom end % $\dot{m}_e$ was equal to zero and the stratifier was working "perfectly". If there was entrainment somewhere along the length of the stratifier then the flow coming out the bottom was greater than the flow at the inlet and led to a positive value of % $\dot{m}_e$, and as a consequence the hot water entering from the tank warmed the water in the stratifier as it flowed downward. On the other hand if there was expulsion somewhere along the length of the stratifier then the exiting flow rate at the bottom end was reduced compared to the inlet flow rate and the % $\dot{m}_e$ was a negative value. In the same way if the inlet temperature rose then the temperature difference between the inlet and tank (ΔT) was compared to the standard temperature difference and thus a negative % ΔT was observed. If the inlet temperature was lowered then the inlet/tank temperature difference (ΔT) was raised compared to the standard and the % ΔT was positive. The same situation was true for inlet flowrate. An increase in the inlet flow rate above the standard of 2 ℓ/min produced a positive % $\Delta\dot{m}$ and a reduction in inlet flowrate below the standard produced a decrease in %$\Delta\dot{m}$.

## 6. RESULTS

Figure 3 shows the results of the first simulation in which the friction factor was set at a constant value (the effect of Reynolds number on the friction factor was neglected) for any inlet temperature, flowrate or tank temperature. The line marked % ΔT, $\dot{V}$ = 2 ℓ/min shows how the flow rate out of the stratifier's bottom end varied with inlet temperature while keeping the inlet flowrate constant. As the temperature difference between the inlet and tank (ΔT) was increased the "driving potential", which caused the inlet water to "fall" down through the stratifier, was increased. This caused a pressure drop within the stratifier and some tank water was sucked in, producing an increase in the flowrate out the bottom end of the stratifier. Conversely, a rise in inlet temperature caused a decrease in ΔT and a corresponding decrease in the "driving potential". A pressure rise occurred in the stratifier as a result, and subsequently water expulsion occurred, decreasing the flowrate out of the bottom end of the stratifier. In the same way the line marked %$\Delta\dot{m}$, ΔT = 20°C shows how the flow rate out the stratifier bottom varied with inlet flow rate while keeping the "driving potential", ΔT, constant. If the inlet flowrate was increased then there was a pressure rise within the stratifier which caused expulsion and a drop in the water flowrate out the stratifier's bottom end. For a decrease in flowrate there was a drop in pressure within the stratifier which caused entrainment and led to an increase in flow out the bottom end. When tank water was sucked into the stratifier the water temperature within the stratifier changed due to mixing and subsequently effected the stratifier's operation. Using this strategy it was possible to obtain "perfect" stratifier operation at only one point. Operating errors, as shown by the values of % $\dot{m}_e$, are most sensitive to the inlet flowrate and much less sensitive to changes of inlet temperature.

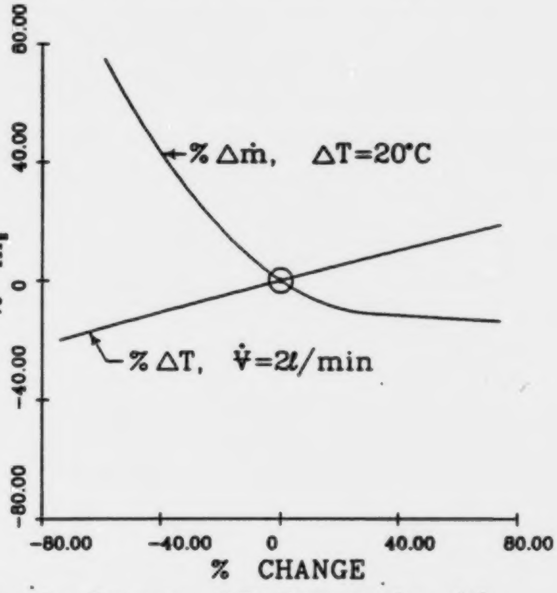

Fig. 3: Response of No Compensation with Fixed Resistance Elements.

The effect of inlet flowrate variation was eliminated by introducing a dynamic resistance element. This resistance element was to change its resistance with flowrate in such a way as to follow the "ideal" friction factor characteristic set out by Equation 2. Such a dynamic friction element was produced by cutting a disk of thin (0.0254 mm or 1 mil) plastic radially to form leaves that, when placed in the flow of the stratifier, would bend down and produce an annular opening between the disk and the inside of the stratifier wall. As the flowrate was increased, the bend in the leaves increased and produced a larger annular area which decreased the friction factor as desired. With a decreased flowrate the leaves bent a smaller amount and the annular area decreased and the friction factor increased. Extensive testing was done using these dynamic elements but few consistent results were obtained.

Simulations done later pointed out a good reason why this strategy of eliminating the effect of inlet flowrate with dynamic resistance elements was not a good idea. Figure 4 shows the results of this simulation. At the standard ΔT of 20°C there was no entrainment or expulsion in response to variation of inlet flowrate; the effect of flowrate had been eliminated. The variation of ΔT at constant inlet flowrate, however, caused massive entrainment or expulsion. When ΔT was increased the pressure, inside the stratifier, decreased and caused entrainment and an increase in the flowrate of water down through the stratifier. This caused the flow rate sensitive friction factor to become smaller just as it did in response to an increased inlet flowrate. This reduction in friction factor caused the pressure to go even lower and more entrainment took place. The variation of ΔT created a positive feedback loop within the stratifier that led to uncontrolled entrainment. In the same way a decrease in ΔT (even as small a decrease as 0.1°C) caused a pressure rise within the stratifier and expulsion was the result. The stratifier flow rate decreased, which led to an increase in the friction factor, which caused an increase in the pressure, thus increasing expulsion and soon all the water had been expelled from the stratifier and no flow was left to come out the bottom end of the stratifier. It is clear that this strategy has some serious problems and is quite unsuitable as a solution to this control problem.

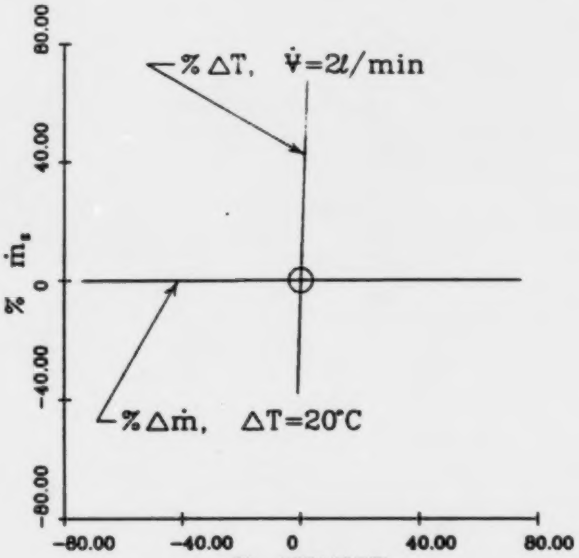

Fig. 4: Response of Flowrate Compensation with Dynamic Resistance Elements.

Another strategy examined was that of fixing the inlet flowrate to a constant value and developing a resistance element that would change its resistance to the flow of water in response to the temperature (or density) difference between the tank and the inside of the stratifier. Figure 5 shows the results of this simulation. With the inlet flowrate set to 2 ℓ/min the inlet temperature was varied and changed ΔT. As can be seen from Figure 5 "perfect" stratifier operation was always obtained, that is, all the incoming water exited the stratifier at the desired level with no entrainment or expulsion of water anywhere else. The curve marked % $\Delta\dot{m}_{error}$ demonstrates this strategie's ability to overcome deviations or errors in the setting of the inlet flowrate. It can be clearly seen that where expulsion of water took place ($\dot{m}_e < 0$) the friction factor of the resistance elements did not change and matched the % $\Delta\dot{m}$ curve of Figure 3. When entrainment of hot tank water into the cooler stratifier water took place (% $\dot{m}_e > 0$) the water temperature within the stratifier rose due to mixing, decreased ΔT and decreased the friction factor, thus increasing entrainment. As a result the entrainment due to a decrease of inlet flowrate is greater for this strategy than for the first strategy where the friction factor is set at a constant. Flowrate control is not a substantial problem, however, and in a practical application it would be possible to achieve. To this date a dynamic resistance element that responds to density or temperature difference in the way required has not been developed.

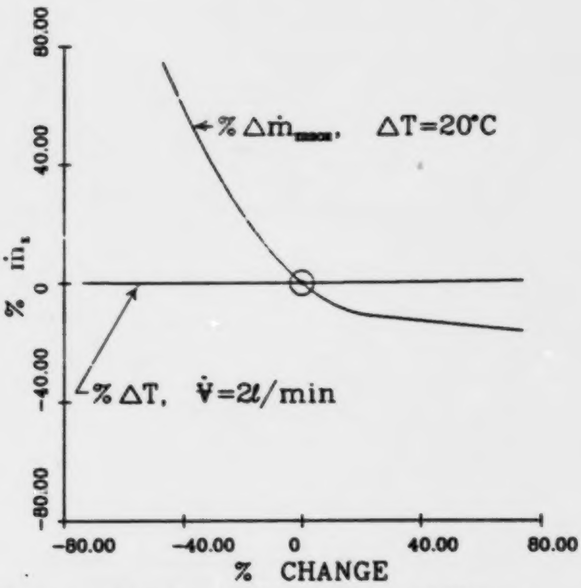

Fig. 5: Response of Temperature Difference Compensation with Dynamic Resistance Elements.

The final approach to be looked at here is that of setting the resistance elements to a fixed configuration and adjusting the inlet flowrate in response to the temperature (or density) difference between the inlet flow and the top-of-tank. Figure 6 shows the results of this simulation. The line marked % ΔT, %$\Delta\dot{m}$, 0% error demonstrates that all the water entering the stratifier left by way of the stratifier's bottom end with no entrainment or expulsion, when a variety of inlet temperatures were tried. Of course, a change in inlet temperature (or ΔT) also lead to a change in the inlet flow rate so that the pressure difference between the stratifier and the tank was always balanced. If the method of controlling the flowrate was not perfect and an error of some fixed value was present so that the flowrate still changed in response to T but in an imperfect way, some entrainment and expulsion was observed. The line marked % $\Delta\dot{m}_{error}$, ΔT = 20°C shows the expected % change in flowrate with a constant ΔT and a variety of flowrate control errors. The errors in this situation are the same as in the case of no flowrate control and fixed friction factor shown in Figure 3. At best this strategy represents a compromise in that it cannot respond to conditions within the tank other than those found at the top. If, as in this simulation, the tank temperature was constant then this approach would work well. If, however, the tank was continuously stratified or had several layers of water at differing temperatures then 'perfect' operation of the stratifier could only be expected in the top layer. Once the water passes by lower layers imperfections would occur, which must ultimately lead to mixing of the water stored in the lower layers of the tank.

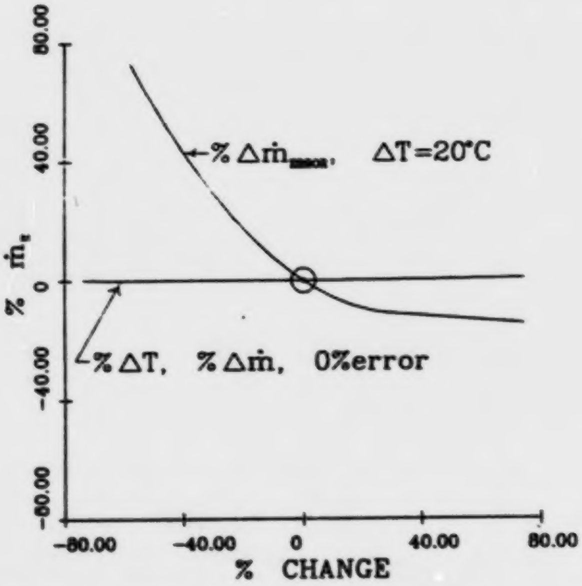

Fig. 6: Response of Inlet/Top-of-Tank Temperature Difference Compensation with Fixed Resistance Elements.

## 7. CONCLUSION

Computer simulation has been a very useful way of modelling a tank stratifier's operating characteristics and pointing out areas of oversight and showing new ways to solve problems. It is clear that in order to achieve the goal of a workable tank stratifier some sort of dynamic control over the friction factor or the flowrate in response to the temperature difference between the water in the tank and water in the stratifier is required. This simulation showed that successful control strategies are possible when the inlet flowrate is fixed at a constant level and the friction factor is varied in response to the temperature difference between tank and stratifier, and also when the friction factor is fixed and the inlet flowrate is controlled in response to the temperature difference between the top-of-tank and the incoming water.

## 8. NOMENCLATURE

$\dot{m}$ - mass flowrate into stratifier
$\dot{m}_e$ - mass flowrate of entrainment/expulsion
P - pressure within stratifier
$P_t(z)$ - pressure within tank at level z
$\rho$ - water density within stratifier
$\rho_t(z)$ - water density within tank at level z
f - friction factor
z - depth or level within tank
D - stratifier inside diameter
A - stratifier inside cross-sectional area
g - gravitational constant
$\dot{V}$ - volume flowrate into stratifier
ΔT - temperature difference
% $\Delta\dot{m}$ - % change of mass flowrate
% $\dot{m}_e$ - % entrainment/expulsion
% CHANGE - % change of test condition

## 9. REFERENCES

1. Sharp, M.K. and Loehrke, R.I., "Stratified Thermal Storage in Residential Solar Energy Applications," Journal of Energy, Vol. 3, No. 2, 1979, p. 106.

2. Loehrke, R.I., et al., "Stratification Enhancement in Liquid Thermal Storage Tanks," Journal of Energy, Vol. 3, No. 3, 1979, p. 129.

3. Gari, H.N. and Loehrke, R.I., "A Controlled Buoyant Jet for Enhancing Stratification in a Liquid Storage Tank," Journal of Fluids Engineering, Vol. 104, December 1982, p.475.

4. Loehrke, R.I., Gari, H.N. and Holzer, J.C., "Thermal Stratification Enhancement for Solar Energy Applications," Mechanical Engineering Dept., Colorado State University, Fort Collins, Colorado, Technical Report HT-TS 792, June 1979.

5. Sliwinski, B.J., Mech, A.R., and Shih, T.A., "Stratification in Thermal Storage During Charging," 6th International Heat Transfer Conference, Toronto, Vol. 4, 1978, p. 149-154.

6. Rush, C.K., "Technical Report on the Development of a Low Flow Solar Collector for Domestic Hot Water," Mechanical Engineering Dept., Queen's University, Kingston, Ontario, September, 1983.

# PERFORMANCE OF A SALT HYDRATE ENERGY STORAGE SYSTEM IN AN ATTACHED GREENHOUSE

John C. O'C. Young
Department of Chemistry
Saint Mary's University
Halifax, Nova Scotia
Canada B3H 3C3

James A. Collicutt
Department of Chemistry
Saint Mary's University
Halifax, Nova Scotia
Canada B3H 3C3

## ABSTRACT

Following the development and laboratory evaluation of a novel latent heat energy storage system based on the use of calcium chloride hexahydrate (1), a small pilot test unit was installed in an attached solar greenhouse and subjected to a performance evaluation which was initiated in July, 1985 and is continuing at the present time. Preliminary results and conclusions are presented.

## 1. INTRODUCTION

The use of latent heat storage in a greenhouse has been described by Jaffrin and Cadier (2). To achieve adequate rates of heat transfer between the storage medium and a forced circulating air flow, the stabilized calcium chloride hexahydrate salt used was diluted with sufficient water to reduce its melting point from 28°C to 15-25°C and the diluted salt was partitioned into small plastic packages to increase the interfacial heat transfer area.

As an alternative to these undesirable measures of dilution and division, our group is exploring the direct collection of solar energy in place of the extraction of sensible heat from air and recovery of stored heat through a large-area heat exchanger immersed in a continuous salt phase. The 28°C storage temperature of the undiluted salt is not excessive for use with an unglazed hydronic solar collector, and is high enough to permit this solar collector to double as space heater within the greenhouse.

An essentially "passive" system is envisaged in which a constant water flow is continuously pumped through a closed loop between the collector and the storage unit heat exchanger. Whenever solar energy absorption exceeds convective heat delivery from the collector to the greenhouse, the temperature of the circulating water flow will rise as it passes through the collector and then fall back to the collector inlet temperature level following heat delivery to the storage unit. The collector will also act as a space heater for the greenhouse whenever the surrounding air temperature drops below the salt storage temperature.

## 2. EXPERIMENTAL

A laboratory simulation of a system with these features was made using the arrangement shown in Figure 1, in which a regulated heating and cooling unit was used in place of the solar collector and space heater.

Cooling was provided by a 3-kW vapor compression refrigeration unit (RFU), which was made to run continuously at capacity rather than in its on-off control mode which induced undesirable temperature fluctuations in the water temperature at inlet to the storage unit. The output of a rheostat-controlled 6-kW electric resistance heater (VRH) was then set as necessary to provide an inlet temperature somewhat below the desired operating value. The heat input necessary to achieve and maintain this temperature was provided by a sensitive automatically-controlled 1-kW electric resistance heater (TCH) which gave temperature control within 0.1-0.2°C of the set-point. To retain this control in face of the progressive decline in the rate of heat transfer from storage which occurred throughout the delivery cycle, an occasional manual upward adjustment of the output of the larger. electric heater was made as necessary to maintain temperature control by the smaller heater. With the refrigeration unit turned off, both heaters or the smaller heater alone were used to provide controlled temperature conditions during studies of the reverse process of heat delivery to storage.

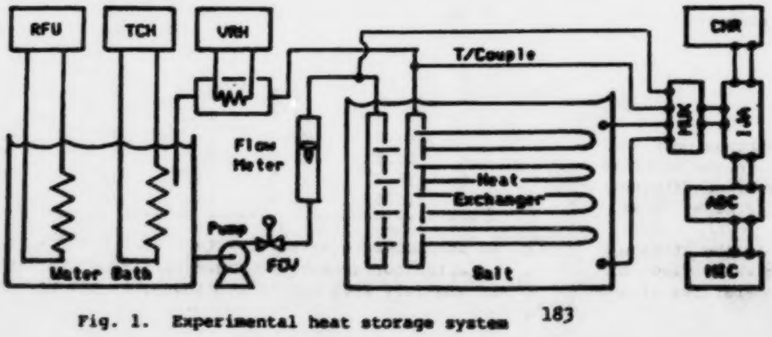

KEY

RFU - refrigeration system
VRH - voltage regulated heater
TCH - temperature-controlled heater
FCV - manual flow-control valve
MUX - variable dwell multiplexer
IJA - ice junction/step amplifier
ADC - analog/digital converter
MIC - Apple IIe microcomputer

Fig. 1. Experimental heat storage system

The circulating water flow was set by means of a manual flow-control valve (FCV) and monitored with a rotameter. Temperatures throughout the system were measured with a series of copper-constantan thermocouples. Thermocouple signals were fed through a variable dwell, 10-channel multiplexer (MUX) and a combined step-range aplifier and electronic reference function unit (IJA) to a dual channel chart recorder (CHR), and to a 12-bit A/D data logger (ADC) connected to an Apple IIe microcomputer (MIC).

An impure commercial grade of anhydrous calcium chloride (RIM "Ice Melter": Revere Products Corporation) was formulated with water to the hexahydrate composition and used without nucleating additives as the experimental heat storage medium.

The storage unit was constructed from a rectangular plastic tank, in which the salt hydrate melt was placed and covered with a thin surface film of oil to inhibit moisture exchange with the atmosphere. The heat exchanger was fabricated from a commercial EDPM extrusion consisting of parallel, web-connected tubes ("SolaRoll": BESI Corp.), which was wound into a serpentine coil to provide total heat transfer area of 2.4 $m^2$ in a salt volume of 0.040 $m^3$.

Following the completion of laboratory studies, this storage tank was detached from the heating and cooling unit and installed in a small attached greenhouse (Figure 2) where it was connected to an unglazed hydronic solar collector mounted vertically on the rear, south-facing wall of the greenhouse. This solar collector and space heater was also fabricated from the "SolaRoll" elastomeric mat material and sized to provide a projected solar energy collection area of 2.0 $m^2$, and a solarimeter was mounted vertically in the greenhouse adjacent to the collector to monitor the solar energy flux at the collector surface.

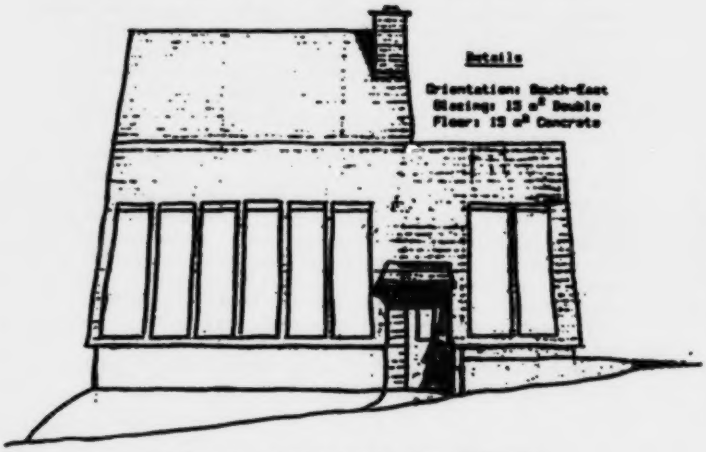

Fig. 2. Attached solar greenhouse

## 3. RESULTS AND DISCUSSION

### 3.1 Laboratory Investigation

Preliminary trials, conducted for comparison purposes using water as the heat storage medium in the experimental system, produced volumetric heat transfer coefficients ranging from 2.8 $kW/m^3$ °C at 15°C to 3.3 $kW/m^2$ °C at 30°C.

Tests on calcium chloride hexahydrate as the storage medium were carried out at circulating water flows of 0.8 - 2.1 $dm^3/m^3$ s and water inlet temperatures of 5-23°C. Data from a representative test run conducted at a water flow of 1.6 $dm^3/m^3$ s and an inlet temperature of 15°C are shown in Figure 3. Under these operating conditions, the salt temperature profile shows transient supercooling of ca. 3°C followed by a near isothermal plateau through the illustrated operating period of 120 minutes, during which the total heat recovery amounted to ca. 50% of the total energy storage capacity of the system (10 megajoules). This performance is in line with our tentative design criterion of a six-hour total discharge period at a water inlet temperature of 15°C.

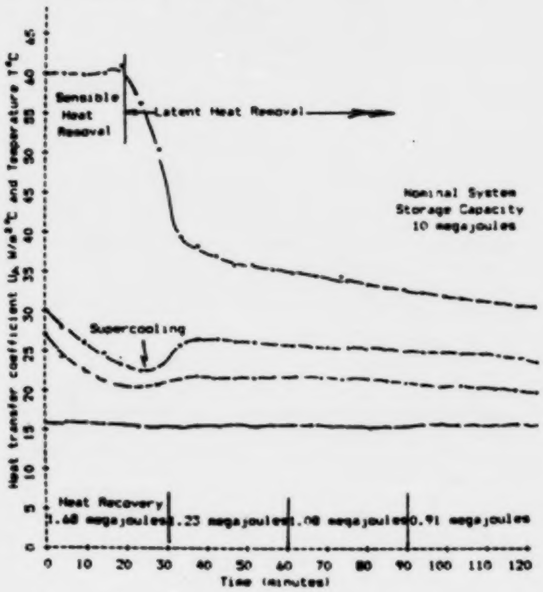

Fig. 3. Heat transfer and temperature profiles.

During the initial period of sensible heat removal and supercooling, the overall heat transfer coefficient remained essentially constant at 60 $W/m^2$ °C (3.5 $kW/m^3$ °C) and then fell progressively to 30 $W/m^2$ °C (1.7 $kW/m^3$ °C) as hydrate solids built up on exchange surfaces.

Data obtained at lower rates of heat recovery are shown in Table 1. Using the same inlet temperature of 15°C with a lower water flow rate of 0.8 $dm^3/m^3$ s, total heat recovery amounted to 75% of capacity over a 6-hour period.

TABLE 1. HEAT TRANSFER TEST DATA

| Run Time t hr | Water Inlet $T_i$ C | Water Outlet $T_o$ C | Salt Zone $T_s$ °C | Overall H.T.C. $kW/m^3$ °C | Heat Flow $kW/m^2$ |
|---|---|---|---|---|---|
| 0 | 16.1 | 25.9 | 27.4 | 1.89 | 10.6 |
| 1 | 16.3 | 25.2 | 28.1 | 1.52 | 9.7 |
| 2 | 16.3 | 24.4 | 28.6 | 1.16 | 8.8 |
| 3 | 16.0 | 22.7 | 27.9 | 0.90 | 7.3 |
| 4 | 15.7 | 21.5 | 27.0 | 0.78 | 6.3 |
| 5 | 15.7 | 20.7 | 25.7 | 0.76 | 5.4 |
| 6 | 15.9 | 20.0 | 23.8 | 0.77 | 4.5 |

An intermediate water flow rate of 1.0 $dm^3/m^3$ s was selected for greenhouse field testing which was initiated in mid-July 1985 and is continuing at the present time.

### 3.2 Greenhouse Investigation

The heat storage unit was installed in a small well-constructed, double-glazed attached greenhouse with a floor area of 15 $m^2$.

Data gathered from various sources indicate heat loss coefficients of 2-5 W/°C per square meter of floor area for double-glazed attached and free-standing greenhouses.

Assuming a heat loss coefficient at the lower end of this range, corresponding to a heat loss rate of 30 W/°C for a 15 $m^2$ floor area, to maintain the greenhouse at 20°C above ambient over a 24-hour period would call for a storage capacity of 50 megajoules or 14 kWh. Based on the nominal thermal storage capacity of 280 megajoules/$m^3$ for calcium chloride hexahydrate between 20 and 30°C, a storage volume of 180 $dm^3$ would be required as compared with 1200 $dm^3$ for thermal storage in water under the same conditions. These data suggest 10-20 $dm^3$ of salt storage per $m^2$ of floor area to be a reasonable assumption for preliminary system sizing and costing.

By this criterion, the test unit storage volume of 40 $dm^3$ (2.7 $dm^3/m^2$ of floor area) was too small to provide a significant contribution to heating and cooling of the greenhouse. However it was large enough to provide useful design data and to check out the long-term energy storage performance and chemical stability of the salt medium.

To facilitate this analysis, a computer program was written to determine mean hourly values of the heat delivery rate from the salt hydrate heat storage system to the greenhouse (q), the solar energy collection efficiency (E) of the wall-mounted absorber/space heater and the overall heat transfer coefficients of the absorber (Uh), the storage system heat exchanger (Us) and the greenhouse (Ug) from the relationships.

$$\begin{aligned} q &= m * Cp * (To - Ti) = I * (A)h * E \\ &= (U * A)h * ((To + Ti)/2 - Tg) \\ &= (U * A)s * (Ts - (Ti + To)/2) \\ &= (U * A)g * (Tg - Ta) \end{aligned}$$

based on measurements the solar radiation flux (I) incident on the projected vertical surface area of the absorber (Ah), the water circulation rate between this absorber and the tube side of the heat storage system heat exchanger (m), the ambient air temperature (Ta), the greenhouse air temperature (Tg), the salt temperature in the storage unit (Ts), and the water temperatures at the storage system outlet (i.e. the absorber/heater inlet) (To) and storage system inlet (Ti).

Testing of the experimental system is still in progress and analysis of the resulting data is far from complete. However, preliminary analyses have been made over selected test periods, including the week of July 24-30, 1985 for which the overall daily heating and cooling deliveries and spot salt temperatures shown in Table 2 were obtained.

TABLE 2. GREENHOUSE HEATING AND COOLING DATA

| Test Date | Nighttime Heating(mJ) | Daytime Cooling(mJ) | Delivery to Storage(mJ) | Salt Temp(°C) 0600hrs | Salt Temp(°C) 1800hrs |
|---|---|---|---|---|---|
| 07/24 | 3.7 | 8.2 | +4.5 | 28.5 | 36.5 |
| 07/25 | 4.2 | 5.0 | +0.8 | 28.9 | 39.0 |
| 07/26 | 3.1 | 2.3 | -0.8 | 27.6 | 28.6 |
| 07/27 | 2.9 | 1.1 | -1.8 | 27.2 | 28.5 |
| 07/28 | 3.3 | 4.2 | +0.9 | 27.2 | 32.0 |
| 07/29 | 3.0 | 3.0 | +0.0 | 28.7 | 32.2 |
| 07/30 | 2.1 | 3.2 | +1.1 | 29.8 | 32.9 |
| 24/30 | 22.3 | 27.0 | +4.7 | 28.3 | 32.8 |

Reflecting the limited storage capacity of the test unit, these data show that heat stored in the salt medium during daytime was largely returned to the greenhouse during the following night, providing approximately equal daily amounts of heating and cooling to the greenhouse. Over the 7-day observation period, total heating provided amounted to more than twice the nominal storage capacity of the unit (10 megajoules) and total cooling approached three times this capacity. The exceptionally high delivery to storage on July 24 caused the salt temperature to reach as high as 45°C. Between 0700 hrs. and 1500 hrs. on July 24, the mean normal solar flux at the absorber surface was 235 $W/m^2$ and the corresponding mean heat delivery rate to storage was equivalent to 187 $W/m^2$, indicating a mean absorber collection efficiency of approximately 80%.

A spot check of the storage capacity and heat transfer performance of the test unit was made on February 4, 1986, after somewhat more than six months of operation. The heating rate data listed in Table 3 indicate that the system absorbed 4.2 megajoules between 1000 hrs. and 1400 hrs. and then delivered more than 5.6 megajoules or approaching 60% of its nominal capacity between 1400 hrs. and 2400 hrs. This delivery was achieved following a heat absorption period in which the salt temperature, measured near the top of the tank, rose no higher than 31.7°C (Table 3). Under these conditions it is likely that melting of the salt was incomplete before the start of heat recovery. A conclusive assessment of the stability of the salt medium in service must await a system shutdown for calorimetric evaluation in the laboratory. In the meantime, the heat recovery observed on February 4 suggests that the salt hydrate has not deteriorated significantly over the first six months of operation.

TABLE 3. TEMPERATURE DATA AND HEAT FLOW RATES TO STORAGE

| Hour | Ambient Temp(°C) | Greenhouse Temp(°C) | Salt Temp(°C) | Absorber/Heater Inlet | Absorber/Heater Outlet | Heating Rate(W) |
|---|---|---|---|---|---|---|
| 1000 | -6.5 | 20.5 | 23.6 | 23.7 | 25.2 | +245 |
| 1100 | +1.7 | 24.0 | 28.0 | 28.9 | 31.2 | +375 |
| 1200 | +4.0 | 32.0 | 31.0 | 32.4 | 34.7 | +375 |
| 1300 | +6.5 | 28.5 | 31.7 | 33.1 | 34.2 | +180 |
| 1400 | +10.2 | 21.5 | 30.1 | 32.0 | 31.3 | -115 |
| 1500 | +11.2 | 20.3 | 30.1 | 30.4 | 29.4 | -165 |
| 1600 | +11.5 | 19.1 | 29.5 | 29.1 | 27.9 | -195 |
| 1700 | +5.7 | 17.5 | 28.2 | 28.0 | 26.4 | -260 |
| 1800 | -7.5 | 14.8 | 25.9 | 26.3 | 24.5 | -230 |
| 1900 | -8.5 | 13.3 | 23.3 | 22.9 | 21.8 | -180 |
| 2000 | -9.0 | 12.3 | 20.5 | 20.2 | 19.3 | -130 |
| 2100 | -9.7 | 11.5 | 18.0 | 17.8 | 17.1 | -115 |
| 2200 | -10.2 | 10.5 | 16.1 | 15.9 | 15.4 | -80 |
| 2300 | -9.5 | 10.1 | 14.5 | 14.7 | 14.2 | -50 |
| 2400 | -8.7 | 9.7 | 13.5 | 13.4 | 13.2 | -30 |

Over the heat recovery period, overall heat transfer coefficients ranged between 90 and 60 $W/m^2$ °C for the storage unit heat exchanger and 15 to 7.5 $W/m^2$ °C for the greenhouse air heater. Over the preceding heat delivery period, the solar energy collection efficiency of the absorber was ca. 80%.

The foregoing observations provide encouraging preliminary evidence of the value of salt hydrate energy storage units in attached greenhouse heating systems.

### 4. REFERENCES

(1) Young, J.C.O'C., et al., "Recovery of Stored Heat from Salt Hydrate Energy Storage Media," Proc. ISES Biennial Congress "Intersol '85," Montreal, 1985.

(2) Jaffrin, A., and P. Cadier, "Latent Heat Storage Applied to Horticulture," Solar Energy, 28(4), 313 (1982).

# USE OF SOIL HEAT TO TEMPER VENTILATING AIR

T.V. Murray and M.G. Britton
Department of Agricultural Engineering
University of Manitoba
Winnipeg, Manitoba, Canada
R3T 2N2

## ABSTRACT

A full scale experimental system to study the potential effects of buried pipe air tempering is described. Data from the first year of operation are considered and trends noted. Relationships between soil temperatures, ambient air temperatures, air velocity and pipe size are observed.

## 1. INTRODUCTION

In agriculture, as in any industry, there is a desire to increase productivity without increasing costs. Adequate ventilation and a thermally controlled environment will increase the productivity of livestock shelters and greenhouses but the costs required to achieve optimum conditions can become quite signficant. On the Canadian Prairies extreme summer and winter temperatures require outside air to be tempered before it is useful for ventilation. The use of soil heat to precondition ventilation air is a timely solution to this problem. This paper will describe an experimental air tempering system at the University of Manitoba. The project was undertaken to examine the applications and limitations of such a system in agriculture. The effect of airflow, pipe diameter and pipe lengths will be discussed.

## 2. LITERATURE REVIEW

A barn in Iowa was air-conditioned during the summer months in 1878 by using an underground passage as a heat exchanger duct (Scott et al. 1965). Scott also cites a poultry house in North New Jersey, 1940, which was cooled when a centrifugal suction fan was connected to a 150 mm (6 in) collecting main of an existing herring bone tile drain system. Scott et al. (1965) investigated these and other systems and found that there was a lack of information relevant to their operation. To rectify this, these Cornell researchers set out to determine the capability and efficiency of earth-air heat exchangers, to develop design criteria for such systems and to evaluate the economic feasibility of the process.

The system which was studied consisted of 134.1 m (440 ft) of 460 mm (18 in) diameter pipe buried at an average depth of 2.4 m (8 ft). Air temperatures were measured at the inlet and at 30.5 m (100 ft) intervals along the pipe length. The system operated under both continuous and intermittent conditions with varied airflows. Favourable tempering was observed at airflow rates of 36.7, 67.1 and 82.1 kg/s (81, 148 and 181 lb/min). Average temperature differences of 9ºC to 17ºC (16ºF to 30ºF) were measured during summer operation. Results showed that 80-90% of this temperature difference was realized during the first 91.4 m (300 ft) of pipe length. At the completion of the project, it was concluded that for the conditions prevailing, there was doubtful economic gain in using this system for animal shelter cooling. However, with increases in energy costs and the resulting trend toward energy efficient methods, this idea once again warrants investigation.

In 1976, Walker et al., reported on the temperature and humidity in a greenhouse ventilated with air from a deep coal mine. The air temperature varied from 11.1ºC to 15.6ºC throughout the year and was nearly saturated with moisture at all times. The study showed that air change rates of 1/2 to 1 change per minute provided a suitable environment for many plants. Walker and Buxton (1977) found that a small greenhouse could be heated to 10ºC using air circulated through 30.5 m of 450 mm diameter pipe buried 3.0 m in the ground if the installation was located in the southern part of the United States. The same system could effectively cool a greenhouse anywhere in the United States. Ewen et al. (1980) found that a greenhouse ventilated with ground conditioned air had an energy requirement 1/7 that of a conventional greenhouse.

Goetsch et al. (1983) describes the effects of soil type and pipe length on the temperature performance of an earth tempered ventilation system for swine-farrow nursery housing. Baud et al. (1983) reported that vertical closed-loop heat exchangers can create an electrical energy saving of 21%. Experimenting with horizontal earth heat exchanger revealed only about 3/4 of the capacity of the vertical system but lower installation costs make them competitive.

Lei (1985) developed a finite element model to simulate a buried pipe air tempering system. Variables which were incorporated into this model included pipe diameter, pipe length, air velocity, soil texture, soil thermal properties, convective heat transfer coefficient and undisturbed soil temperature. The model was found to compare favourable with other models and gave reasonable predictions of the initial performance of the earth-air heat exchanger system discussed in this paper.

## 3. SYSTEM DESIGN

The objectives of this research project, as stated in the contract proposal, were:

a. to study the performance characteristics of an earth-air heat exchanger under western Canadian climatic conditions,

b. to monitor soil properties such as specific heat, thermal conductivity, and bulk density, and

c. to develop design criteria which could be used in designing future systems.

To accommodate these objectives, a system consisting of four polyvinyl chloride pipes was chosen. Each pipe was 30.0 m long and was buried at an average depth of 3.0 m. Pipes 2 and 4 had a diameter of 150 mm while pipes 1 and 3 had a diameter of 250 mm. The pipes were spaced 5.0 m apart to ensure isolation and were sloped toward the outlet end. All four pipes emerged from the ground into a common plywood header. The air inlets were located at 1.0 m above the ground. A 1.1 kW fan was attached to the header to draw air through the four pipes simultaneously. A series of baffles inside the header allowed for individual control of the airflow in each pipe. An instrument shed was constructed at the outlet end to house the data acquisition unit.

The data collection system consisted of 330 thermocouples connected to an Optilog data logger which was in turn connected to a Corona PC microcomputer. The thermocouples were used to monitor soil and air temperatures throughout the system. Soil and air temperatures were measured at 1.0, 5.0, 10.0, 15.0 20.0 and 29.0 m from the pipe inlet with the majority of the monitoring occurring near the surface of the pipe at the inlet end. Here the greatest temperature gradient should exist and therefore this is where most of the heat transfer should occur. Air temperatures were measured at the center of the pipe while soil temperatures were measured to radii of up to 1.0 m in three directions from the pipe surface. In addition, two isolated, undisturbed soil profiles were monitored. Each profile consisted of eight thermocouples spaced 500 mm apart from 500 mm below grade to 4.0 m below grade.

The system was programmed to read all thermocouples automatically at 01 00 h, 04 00 h, 07 00 h, 10 00 h, 13 00 h, 16 00 h, 19 00 h and 22 00 h. During data collecting each point was sampled four times and individual readings compared to detect nonfunctioning thermocouples. A difference of 2°C was arbitrarily selected to define "bad" data. Temperatures were averaged and stored on disk using the Corona PC. "Bad" data were placed in a separate file for later manual inspection. All readings were compared to adjacent thermocouples, in both time and space, to detect errors that were not identified by inconsistency over sampling time.

The airflow in each pipe was balanced so that one 250 mm diameter pipe and one 150 mm diameter pipe had a volume flow rate of 0.05 $m^3$/s (pipes 1 and 4 respectively). The remaining 150 mm diameter pipe (pipe 2) was adjusted to a mass flow rate of 0.15 $m^3$/s and the remaining 250 mm pipe (pipe 3) was adjusted to 0.10 $m^3$/s.

## 4. DATA ANALYSIS

The results presented here are based on 50 weeks of data. There will be no attempt to draw long term conclusions because the data represent conditions which existed during the start-up phase of an experimental system. A more thorough analysis of data will be required after the system has been allowed to operate over a period of time. The purpose of this paper is to recognize and discuss some of the trends which appear to be occurring thus far.

The discussion of the data will occur in four parts. First, the temperature movement through the soil radially outward from the pipe surface, 1.0 m from the inlet end. Next, the temperature movement through the soil, 250 mm from the surface for the length of the pipe. Thirdly, a comparison of outlet temperatures and inlet temperatures will be given. Finally, the discussion will conclude with a short explanation of the warming/cooling effects which occurred in the pipes at various inlet temperatures.

In the interest of brevity, pipe 4 will be considered in detail while pipes 1 and 3 will be referred to only for comparison. The data available for pipe 2 are limited because of a drainage problem. The location of this pipe in relation to the fan housing and thermocouple concentrations make excavation to solve the problem impractical and as of yet a long term solution has not been found.

Soil temperatures radially outward from the pipes were monitored to determine how radial distance affects energy flow. The soil volume which was considered was a cylinder with a radius equal to the pipe radius plus 1.0 m. Data presented are for a point 1.0 m from the inlet end of pipe 4. Figures 1, 2 and 3 show the soil temperatures at 250 mm intervals along the radius, over three separate time periods.

Figure 1 shows the start-up soil temperature and the soil temperature during the first 5 weeks of operation (December 84 - January 85). The greatest temperature change occurs at the pipe surface where the temperature gradient is largest. Over this six week period, soil temperatures at the pipe surface decreased by about 12°C while temperatures 1.0 m from the pipe surface varied by only 4 or 5°C. In general, temperatures in the soil around the pipes behaved as we had expected them to during the start-up period.

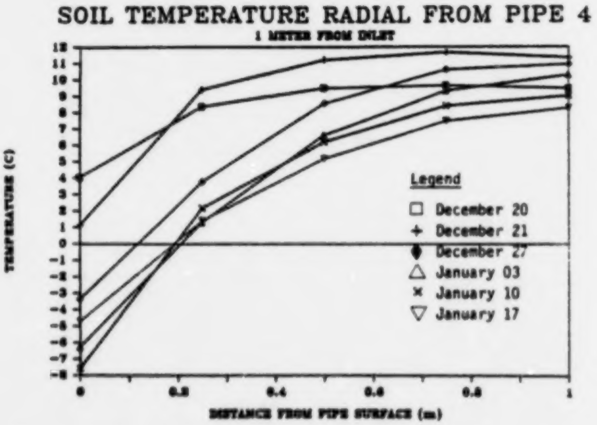

Fig. 1. December 20, 1984 to January 17, 1985.

Figure 2 shows soil temperatures around pipe 4 from February 04, 1985 to March 04, 1985. The ground had frozen to a distance of 500 mm from the pipe surface. Daily ambient air temperatures had begun to increase. This is reflected in the soil temperatures near the pipe surface. The soil temperatures 1.0 m from the pipe surface continued to decrease. This is an indication of the time lag between the temperature changes at the pipe surface and 1.0 m from the pipe surface. Soil temperatures 1.0 m from the pipe surface were now at 2°C, a decrease of about 7°C from the original condition. Therefore, the assumption that the majority of the heat transfer would occur within a 1.0 m radius of the pipe surface, appears to have been inaccurate.

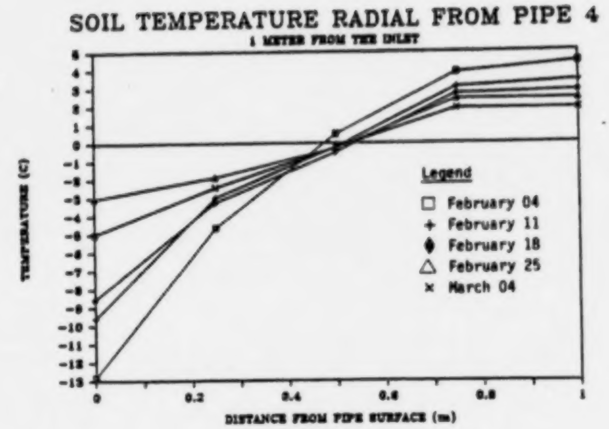

Fig. 2. February 04, 1985 to March 04, 1985.

Figure 3 shows the soil temperatures at the same location from July 2, 1985 to August 8, 1985. This plot of summer data shows the warming which occurred in the soil. By the end of this period, the soil temperature at the pipe surface had risen to 17ºC while the soil temperature 1.0 m from the pipe surface was up to 9ºC. This demonstrates a favourable warming trend and indicates that a substantial capacity for heat storage exists.

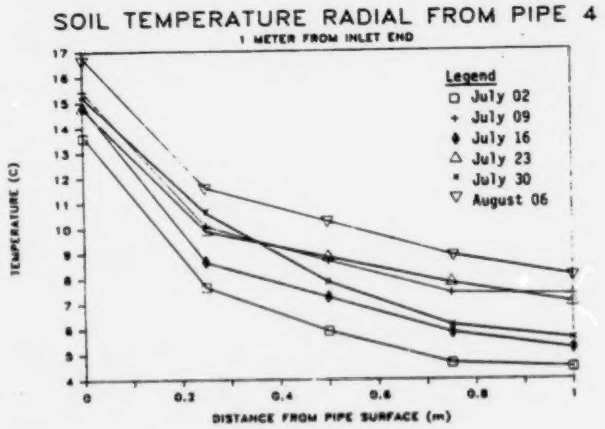

Fig. 3. July 02, 1985 to August 06, 1985

The soil around pipes 1 and 3 behaved in a manner similar to pipe 4. Since pipe 3 has a larger volumetric flow rate, the tempering effect occurs more uniformly along its length than in pipes 1 and 4 where the bulk of tempering occurs near the inlet end. Therefore, the effect on the soil 1.0 m from the inlet and 1.0 m from the surface of pipe 3 is less than the effect on the soil 1.0 m from pipe 1 or pipe 4.

In summary then, the heat flow occurred over a longer radial distance than was originally anticipated, however, the pattern of soil temperatures was as predicted. Significant cooling occurred during the winter and sufficient warming occurred in the summer. The greatest temperature variations occurred near the pipe surface.

Figures 4, 5 and 6 are graphs of soil temperatures as monitored 250 mm from the surface of pipe 4 at 1.0 m, 5.0 m, 10.0 m. 15.0 m, 20.0 m and 29.0 m from the inlet end. Each graph monitors a distinct time period.

Figure 4 illustrates the start-up conditions of pipe 4. During the first weeks of operation, the soil temperatures decreased all along the pipe. The greatest temperature change occurred at the inlet end. This was as expected. During this period, the soil temperature at the inlet dropped an average of 8ºC but the soil had not yet become frozen.

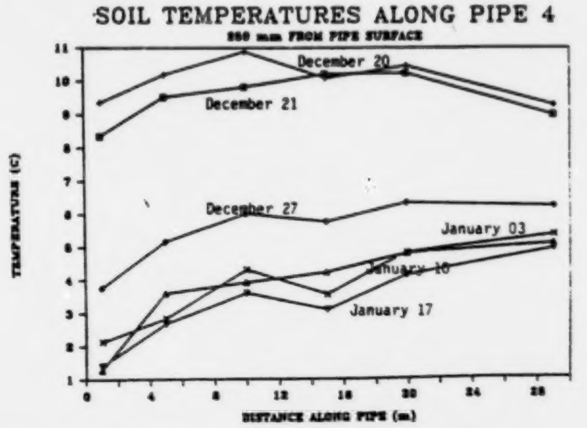

Fig. 4. December 20, 1984 to January 17, 1985.

Figure 5 plots the soil temperatures at the same locations from February 4, 1985 to March 4, 1985. This is after approximately six weeks of operation. At this time, the ground had become frozen for a distance of about 16.0 m along the pipe. The ambient air temperature had begun to increase, an occurrence reflected in the soil temperatures nearest the inlet. At the outlet end of the pipe, there is very little temperature change.

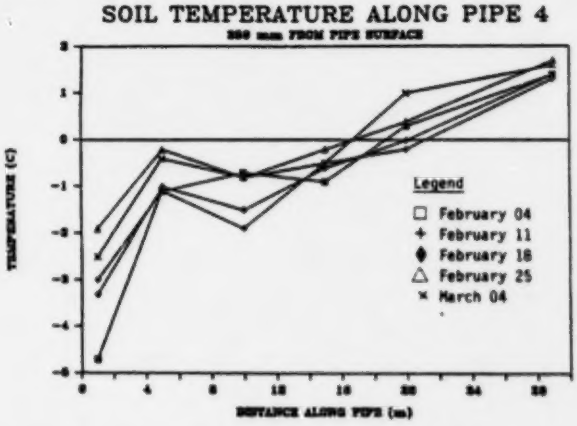

Fig. 5. February 04, 1985 to March 04, 1985.

Soil temperatures, at the same locations, from July 2, 1985 to August 6, 1985 are shown in Figure 6. The soil temperatures are once again above freezing over the length of the pipe. The ambient air temperature increased over this period. This created increased temperature rises in the soil along the pipe. The soil at the inlet end had been warmed to about 12ºC while the soil at the outlet end had been warmed to about 9ºC.

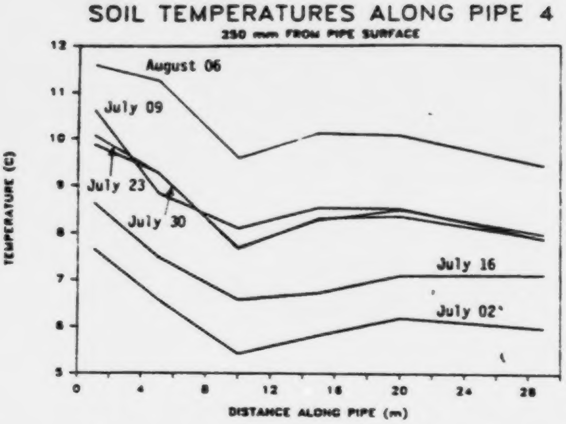

Fig. 6. July 02, 1985 to August 06, 1985.

Once again the behavior of pipes 1 and 3 followed trends similar to those observed in pipe 4. Pipe 1 has a larger area and a lower air velocity than pipe 4 so that more tempering occurred near the inlet end than in pipe 4. Pipe 3 has the highest velocity and a large pipe diameter. Therefore, the temperature effect was more evenly distributed over the length of this pipe than in pipe 4. Less tempering of the ambient air occurred as it moved along the pipe so that the air temperature at the outlet end was quite near ambient temperature. For this reason, during the period from February 4, 1985 to March 4, 1985, the soil was frozen 250 mm from the pipe surface over the length of pipe 3. By August, these locations had been heated to about 11°C. As predicted the greatest temperature changes occurred near the inlet end. However, with a larger flow rate this effect was reduced.

For each of the three pipes being considered, outlet temperatures were plotted with ambient air temperatures, the graphs are intended to show daily temperature peaks as well as the relationship between inlet and outlet temperatures. Figure 7 shows data from January 29, 1985 to February 4, 1985. While Figure 8 shows summer results from July 26, 1985 to August 2, 1985.

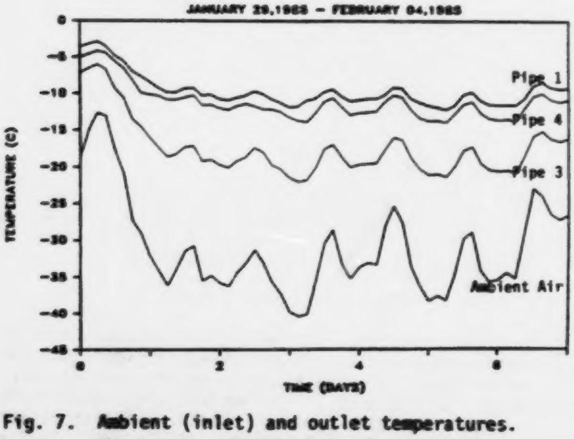

Fig. 7. Ambient (inlet) and outlet temperatures. January 29, 1985 to February 04, 1985.

The winter data show a variation in ambient temperatures from -12°C to -40°C. Under these conditions the outlet temperatures varied from -3°C to -9°C from pipe 4, -4°C to -10°C from pipe 1 and -6°C to -20°C from pipe 3. The outlet temperature responses of pipes 1 and 4 were very similar. This is reasonable since they were designed to have equal volumetric flow rates.

The outlet air temperatures from pipe 3 were more variable and consistently lower than the outlet temperatures from the other two pipes. This follows the argument presented earlier, that the larger airflow rate results in more air moving through the pipe and not being tempered as fully. The peaks and valleys of the ambient air temperature are reflected in the outlet temperatures. Once again, though, these extremes are most visibly reflected in pipe 3.

Figure 8 shows a similar relationship between ambient air temperature and outlet air temperatures under summer conditions. The degree of tempering was similar for pipe 1 and pipe 4 and was less for pipe 3. Ambient air temperatures ranged from 5°C to 32°C. Outlet air temperatures ranged from 9°C to 14°C for pipes 1 and 4, and from 9°C to 18°C for pipe 3. The temperature behavior followed trends similar to those discussed previously.

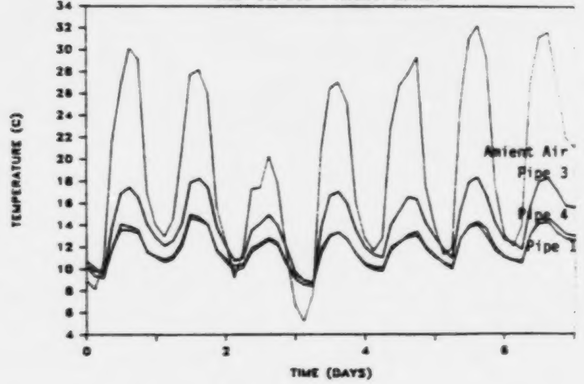

Fig. 8. Ambient (inlet) and outlet temperatures. July 26, 1985 to August 02, 1985.

The tempering effects achieved at various ambient air temperatures are shown in Figures 9 and 10. As expected pipes 1 and 4 create similar tempering effects under similar conditions. Pipe 3 tempers the air to a lesser degree than both pipes 1 and 4. Under winter conditions, pipes 1 and 4 will warm ambient air at -40°C to approximately -13°C while pipe 3 will warm the same air to -22°C. Alternately, under summer conditions, pipe 1 and pipe 4 will cool ambient air at 30°C to approximately 15°C while pipe 3 will cool the same air to 18°C.

## 5. SUMMARY

This report has attempted to identify and discuss some of the trends which are developing during the first year of operation of an experimental air tempering system. A definite difference between data collected from different pipes was illustrated. The relationship between ambient air temperatures and outlet air temperatures was also shown. As these are only preliminary data we do not wish to draw long term conclusions, however, a few observations worth noting are:

a. most of the temperature change occurs at the inlet end of the pipe,

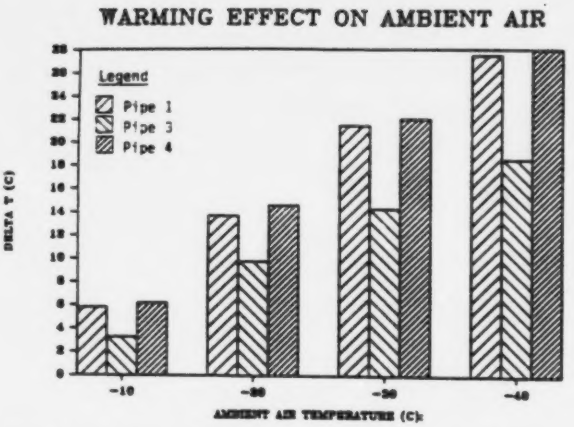

Fig. 9. Degree of warming of ambient air through each pipe.

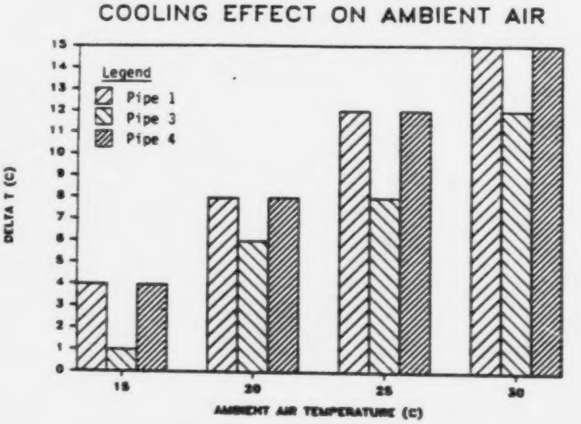

Fig. 10. Degree of cooling of ambient air through each pipe.

b. the lower the airflow rate, the greater the degree of tempering which is accomplished,

c. the temperature change is much greater at the pipe surface than 1.0 meter from the pipe,

d. ambient air temperature has a greater affect on soil near the pipe than on soil 1.0 meter from the pipe surface,

e. the outlet temperatures of all three pipes are affected by the ambient air temperature, and

f. preliminary results would suggest that favourable heating and cooling can be realized.

## 6. ACKNOWLEDGEMENTS

The authors gratefully acknowledge the financial assistance received from Agriculture Canada under the research contract, "Tempering Ventilation Air Using Soil Heat".

## 7. REFERENCES

(1) Braud, H.J., H. Klinkowski and J. Oliver. 1983. Earth-source heat exchanger for heat pumps. TRANSACTIONS of the ASAE 26(6):1818-1822.

(2) Braud, H.J., H. Klinkowski and J. Oliver. 1983. Earth-coupled heat pump research and application in Louisiana. ASAE Paper No. 83-3086.

(3) Braud, H.J., H. Klinkowski, F.E. Baker, J.L. Smilie and T.A. Costello. 1984. Water-source heat exchanger for heating and cooling in agricultural and rural residence use. Louisiana State University Research Report, Project 2061.

(4) Ewen, L.C., J.N. Walker and J.W. Buxton. 1980. Environment in a greenhouse thermally buffered with ground conditioned air. TRANSACTIONS of the ASAE 23(4):485-993.

(5) Goetsch, W.D., W.H. Peterson and A.J. Muehling. 1981. Field study of earth tempered swine ventilation systems. ASAE Paper No. 81-4520.

(6) Goetsch, W.D. and A.J. Muehling. 1983. Evaluation of earth-tube heat exchangers as air tempering systems for swine farrow-nursery housing. ASAE Paper No. 83-4023.

(7) Lei, Q. 1985. Computer aided design for soil-air heat exchangers. Unpublished M.Sc. Thesis, University of Manitoba, Winnipeg, Manitoba.

(8) Scott, N.R., R.A. Parsons and T.A. Koehler. 1965. Analysis and performance of an earth-air heat exchanger. ASAE Paper No. 65-840.

(9) Walker, J.N., W.O. Peterson, G.A. Duncan and D.T. Anastasi. 1976. Temperature and humidity in a greenhouse ventilated with coal mine air. TRANSACTIONS of the ASAE 19(2):311-317.

(10) Walker, J.N. and J.W. Buxton. 1977. Can circulating air through a buried pipe be used to heat and cool greenhouses? J. Amer. Soc. Hort. Sci. 102(5):626-629.

# COMPUTER ANALYSIS OF HEAT EXTRACTION FROM THE GROUND

V.R. Tarnawski - Associate Professor
Division of Engineering
Saint Mary's University
Halifax, N.S.
B3H 3C3 Canada

W. H. Leong - Undergraduate Student
P. K. Yuet - Undergraduate Student

## ABSTRACT

This paper describes a numerical study on the heat and moisture transfer in the ground heat storage using a single or a double layer ground heat exchanger. A double layer system has a higher performance than the single layer configuration and because of that is very promising for smaller free ground surface areas. Moreover this system also provides more protection against the ecological damage caused by heat extraction from the ground. The moisture phase change, at the heat exchanger level only, can provide about 30% of the total amount of heat extracted from the ground during the winter period considered. The remaining 70% is delivered by heat conduction mode. The share of heat flow by convection mode is negligible in comparison with conduction mode and a heat release due to phase change.

## 1. INTRODUCTION

A large energy demand for space heating takes place every winter in Canada. This is about 18.5% of the total secondary energy obtained mainly from nonrenewable energy resources such as e.g., oil, gas and coal, which are not unlimited. However, it is worth pointing that a greater part of a building's total thermal energy requirement could be supplied in the winter period by a heat pump system using solar energy collected in seasonal storage during the summer season. In urban areas, the ground seems to be one of the most appropriate medium for natural seasonal heat storage. The use of the ground, as a heat source for a heat pump, requires an application of earth heat exchangers to extract the harnessed solar energy for heating purposes. Ground heat exchangers are buried in soil mainly in horizontal or vertical configuration. At present, the single horizontal coil system is very popular, but it requires quite a large free ground surface area. As a means of lowering this requirement, attention has recently been directed to a double layer coil system. Experimental results for this system are very scarce, but those available are very promising.

## 2. REVIEW OF LITERATURE

Up to the present time, several mathematical models on ground heat storage have been developed. Comprehensive reviews on this subject have been published by Ball et al (1982), Tarnawski (1982), Swedish Council of Building Research (1983), and Parker et al (1985). Here, the papers related to the double horizontal pipe system in the ground are briefly discussed.

Geeraert and Steffens (1979) developed a two-dimensional mathematical model of heat recovery from the ground with the double layer ground heat exchanger. Authors concluded that the heat pump with a double layer ground heat exchanger had better coefficient of performance (COP) than a single layer one by 14%.

Ahlkrona and Johansson (1983) recommended a double layer ground heat exchanger in order to reduce the area of the free ground surface required. In general their experience was very encouraging. They had also reported on the damage of plants and soil biology caused by single layer ground heat exchangers. the damage of plants and soil biology caused by heat extinction, but in general their experience was very encouraging.

According to Claesson and Dunand (1983) a double layer ground heat exchanger could provide 62% more heat than the single upper pipe alone.

## 3. MATHEMATICAL MODEL

The main objective of this paper was to update the existing one-dimensional model for a ground heat storage with a single layer coil, by including a double layer pipe system. The transient one-dimensional model was based on the following assumptions, namely:

(i) Soil is unsaturated and homogeneous within any volume element.

(ii) Soil mass flow and thermal characteristics are a function of the soil type and water or ice content.

(iii) Moisture flow in soil occurs only by liquid movement according to Darcy's law.

(iv) Heat and moisture flow in the freezing soil are modeled assuming that soil-water system is freezing at constant temperature.

(v) Pipes of a double layer system are represented as two points of heat sink.

A complete description of the mathematical formulation of the model for a single layer coil system as well as the deriviation of finite difference equations was given by Tarnawski (1982). A verification of the mathematical model was carried out by running a computer program for soil and climatological data at Jokioinen (Finland) excluding artificial heat sinks in the ground. Numerical results were compared with experimentally obtained data on temperature distribution in soil over a one year period, i.e., since August 27th, 1969 until August 26th, 1970.

Numerical results (Fig. 1) indicate a good agreement with experimental data.

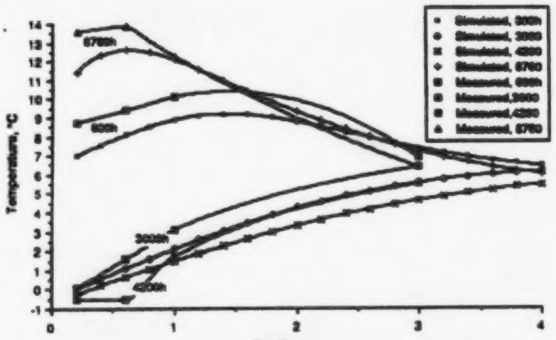

Fig. 1 : Simulated and Measured Temperature of Soil vs. Depth

More data on the mathematical model verification can be found in the paper published by Tarnawski (1982).

## 4. SCOPE OF NUMERICAL CALCULATIONS

Comparative computations were made for a ground heat storage system with a single and a double layer heat exchanger. Identical climatological and soil data, and heat requirement for space heating were used in both cases. Moreover the following data were used for input:

(i) Depth of a single layer coil: d = 0.5m

(ii) Depth of a double layer system: $d_1$= 0.5m; $d_2$=2.0m

(iii) Area of the free ground surface: 150; 300; 450; 600$m^2$

(iv) Maximum heat requirement for space heating: 6kW

(v) Lowest ambient temperature before space heating begins: -10°C

The most important climatological data used in numerical calculations is depicted in Fig. 2.

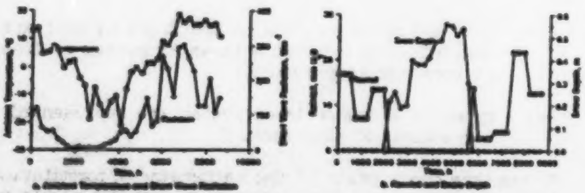

a. Ambient Temperature and Short Wave Radiation

b. Rainfall and Snow Depth

Fig. 2 : Climatological Data (mean five-days values) vs. time

## 5. RESULTS

### 5.1 Temperature and moisture content profiles

A considerable change of soil temperature outlines resulted for a ground heat storage system with buried heat exchangers. Figures 3 and 4 display changes of mean soil temperature and moisture in the ground against time. The mean soil temperature and moisture content were calculated as the arithmetic mean of temperature and moisture values, at all nodals between the soil surface and the depth of the heat exchanger.

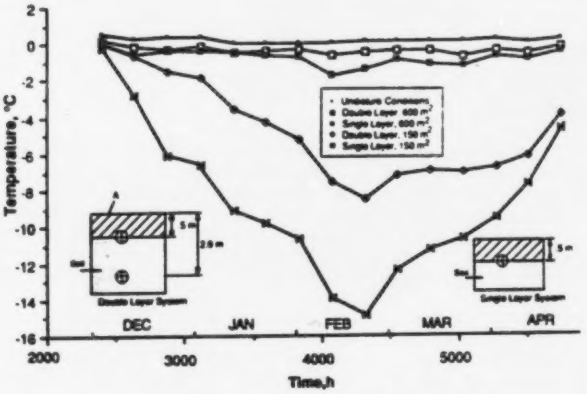

Fig. 3 : Mean Soil Temperature vs. Time

A double layer coil system provides smaller soil temperature changes than a single layer, especially for the smaller free ground surface areas used. A double layer system with a free ground surface area of 600$m^2$ produces temperature profiles that are very close to that obtained for undisturbed conditions. Noticeable changes of mean soil moisture content over winter period, for the same two systems, were also observed.

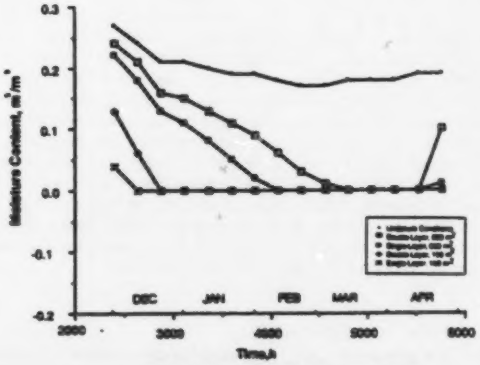

Fig. 4 : Mean Soil Moisture vs. Time

For the refered depth of 0.5 m the entire volume of the ground can be in frozen state; however, the duration of this state is shorter for a double layer system.

### 5.2 Heat flows interaction in the ground

A general heat conduction equation for the case of heat extraction from the ground, at the coil level, can be written as follows:

$$q_{cd}''' + q_{cv}''' + q_{sh}''' = q_{st}''' \qquad (1)$$

where: $q_{cd}'''$, $q_{cv}'''$, $q_{sh}'''$, $q_{st}'''$ are heat flows by conduction, convection, heat sink and storage plus a phase change, respectively. Figures 5 and 6 show heat flow variation against time for a free ground surface area of $600 m^2$, for single and double layer, respectively.

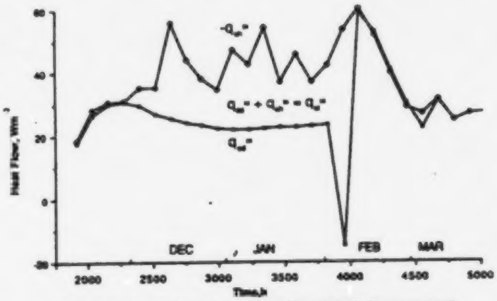

Fig. 5 : Heat Flow Variation Against Time (single layer system)

Three different periods can be distinguished during heat extraction from the ground in winter season. In the first period, the total amount of heat extracted is due primarily to heat conduction flow (90-95%). The remaining 5-10% represents a heat storage. Duration of this period is shorter for a single layer system (2364 hrs) than for a double layer system (2652 hrs). During this period no phase change of soil moisture, at the pipe level, is observed. In the second period, soil moisture in the pipe control volume undergoes a phase change and due to this phenomenon the share of heat flow as a function of the total amount of heat being extracted increases considerably. It can even exceed the heat extraction requirement that was observed for the case of a single layer system.

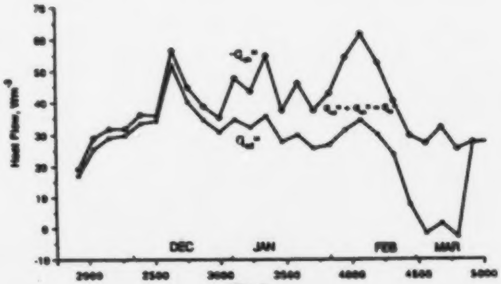

Fig. 6 : Heat Flow Variation Against Time (double layer system)

Duration of this period is again shorter for a single layer system (from 2364 until 3972) than for a double layer one (from 2652 until 4824).

In the third period the soil moisture phase change at the coil level is completed and again almost the entire heat extraction is provided by conduction mode.

It is obvious that a time-lag of the phase change appearance for both systems was caused by the different heat extraction density, which is, for a single layer, 100% and, for a double layer, 50% for each coil.

### 5.3 Coefficient of performance

A comparison of a single and double layer performance with respect to the free ground surface area is displayed in Fig. 7.

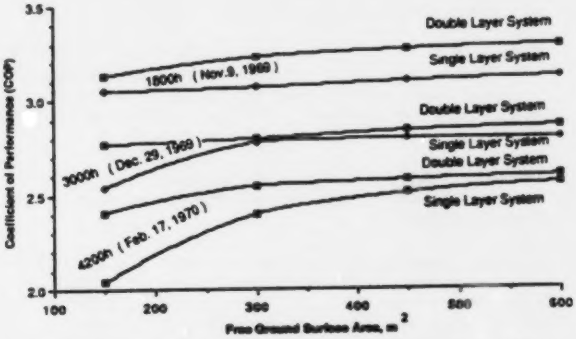

Fig. 7 : Coefficient of Performance vs. Free Ground Surface Area

A double layer system provides a higher COP than a single layer one, for a free ground surface area between 150 and $600 m^2$. Its superiority increases with a decrease in the free ground surface area and the ambient temperature.

## 6. CONCLUSIONS

(i) A double layer system is more efficient than a single layer coil configuration. The performance of this system is very promising for small free ground surface areas.

(ii) A double layer system also provides more protection against the ecological damage caused by heat extraction from the ground.

(iii) The soil moisture phase change, at the heat exchanger level only, provides about 30% of the total amount of heat extracted from the ground, for the winter period considered. The remaining 70% is delivered by heat conduction mode. Total contribution of the phase change phenomenon is much larger than 30%, because it takes place in the entire region between the ground surface and the first coil, in that way releasing a considerable amount of heat transferred to the coil by conduction mode.

(iv) Share of the heat flow by convection mode is negligible in comparison with that obtained in conduction mode and heat release due to phase change.

## 7. REFERENCES

Ahlkrona, D. and Johansson, I. (1983), Experience of shallow pipe grids in soil as heat source for heat pumps. Swedish Council for Building Research, Report D16: 1983, Part 2, Stockholm.

Ball, D.A., et. al., (1982), State of the art survey of existing knowledge for the design of ground-source heat pumps. Battelle Columbus Laboratories. Report to Oak Ridge National Laboratory under Subcontract No. 7800, Contract W-7405-eng-26 to US Dept. of Energy.

Claesson, J. and Dunand, A. (1983), Heat extraction from the ground by horizontal pipes. A mathematical analysis. Swedish Council for Building Research, Report D1: 1983, Stockholm.

Geeraert, B. and Steffens, J.C., (1979), The use of soil with and without heat generation as a heat source for the heat pump. Commission of European Communities, Proc. Int'l Seminar-entitled New Ways to Save Energy, Brussels, pp. 94-101.

Parker, J.D., Bose, J.E. and McQuiston, F.C., (1985), The ASHRAE Design/Data Manual for Ground-Coupled Heat Pumps, ASHRAE.

Swedish Council of Building Research (1983), Proc. of the International Conference on subsurface heat storage, Stockholm, June 6-8, 1983, Part 1 and 2, Swedish Council of Building Research: Report D16, 17: 1983.

Tarnawski, V.R., (1982), An analysis of heat and moisture movement in soils in the vicinity of ground heat collectors for use in heat pump systems. Acta Polytechnica Scandinavica. Mechanical Engineering Series No. 82, Helsinki.

# A STUDY OF BASEMENT HEAT LOSS

W.R. Richmond, R.W. Besant
Department of Mechanical Engineering
University of Saskatchewan
Saskatoon, Saskatchewan
S7N 0W0

## ABSTRACT

It has been found that heat losses from basement floors is very important in low energy homes. In this paper, heat losses from a two-dimensional, steady state, basement model are investigated. It is shown that radiation heat loss is very important in modelling basement heat loss. As well, various parameters such as soil thermal conductivity, basement air temperature, surface convection coefficients, as well as others are examined to investigate their effects on below grade basement surface losses. Also, the importance of basement floor insulation and the elimination of thermal bridges between building components is discussed.

## 1. INTRODUCTION

In many parts of Canada basements are considered to be an essential part of any house for storage, utility, recreation, and living space. Depending on the type of construction basements may account for heat losses in the range of 15-50%. In energy conservation homes in which the basement floor remained uninsulated homeowners have found that, in addition to higher than expected rates of heat loss, basement living areas were uncomfortable and required auxiliary heating.

In recent years, researchers have published several methods of predicting basement heat loss. However, little has been published describing the effects of various parameters such as soil thermal conductivity, basement air temperature, radiation heat transfer, or insulation amounts and their placement. In addition, there has been little discussion as to insulation strategies or basement construction.

This paper will examine these concerns by the use of a two-dimensional, steady state, finite element model. Transient effects are addressed in a previous paper by the authors (Richmond and Besant (1985)).

## 2. DESCRIPTION OF BASE MODEL USED IN PARAMETRIC STUDY

The base model used in the parametric study conducted to examine the above mentioned effects was based on a two-dimensional cross-section of a home discussed in previous work (Richmond and Besant (1985), and Richmond (1986)). (It has been found that axially symmetrical models can be used to predict three-dimensional heat losses in most well insulated basements.) The model was created through the use of a general purpose, commercially available, finite element package, ANSYS, distributed by Swanson Analysis Systems Inc.). The model consisted of 319 nodes and 468 elements. One unique aspect of this model was the inclusion of 155 radiation elements to model radiation exchange among basement surfaces.

The model consisted of four materials: concrete, expanded polystyrene extruded insulation, fibreglass insulation, and soil. Placement of this material is seen in Figure 1. The model boundary conditions are discussed below. References to boundary A,B,C, etc. refer to the boundary lettered in Figure 1. Where applicable, the boundary conditions used were based on average values for January 1984.

The two interior surfaces of the basement, boundaries A and B, are subject to both radiation and convection boundary conditions. Because of the low air velocities along these surfaces a convection coefficient of 1.5 $W/m^2.K$ was used. Based on measurements taken at House 2 the average air temperatures near the floor and ceiling for January 1984 were 18.4°C and 20.3°C respectively. These temperatures were assumed to be uniform over the floor and ceiling. The floor temperature was used with the convection boundary condition along the floor while the ceiling temperature was used with the radiation heat transfer from the ceiling. The temperature distribution of the air along the side of the basement wall was assumed to be linear with air temperatures along the wall interpolated between those of the floor and ceiling based on the distance above the floor. Shape factors for the radiation heat transfer were calculated for each floor and ceiling element for radiation with the ceiling and between the wall and floor using Hottel's method (Sparrow & Cess (1978)) for two dimensional radiation exchange between surfaces. Emissivity of the surfaces were assumed to be 0.9.

Boundary C was assumed to be adiabatic for ease of analysis. Energy added or deleted through that boundary in real life would be negligible. Boundary D had a heat transfer coefficient of 0.47 $W/m^2.K$ imposed on it based on the R-value of the insulation applied externally to the wall and the natural convection coefficient. The ambient outdoor temperature imposed along boundaries D and E was -12.1°C. The heat transfer coefficient imposed along boundary E, based on snow cover and wind speed, was 3.3 $W/m^2$ K. Because of the high reflectivity of the snow cover it was assumed that the difference between the sol-air temperature and ambient air temperature would be negligible. Boundary G had a temperature of 7.1°C imposed on it.

## 3. RESULTS

### 3.1 Results of Base Model

The results from the base model show radiation as the major mode of heat transfer in the basement. In the base case the floor experienced a net heat loss of 34.0 W/m (heat loss is expressed in terms of W/m since the model used was two-dimensional). This was a result of a net gain of 39.6 W/m by radiation heat transfer and a convection loss of 5.6 W/m from the floor surface to the air above the floor. The net effect of the radiation gain and the convection loss was 34.0 W/m heat conduction through the floor. For the basement wall the total heat loss of 32.1 W/m was the result of a radiation and convection heat gain of 24.5 W/m and 7.6 W/m respectively.*

The model showed that an assumption of one-dimensional heat loss through the basement floor was only valid at the interior zone. At the perimeter, however, total heat loss through the floor was 13.2 W/m while the heat lost vertically through the insulation at the perimeter was only 5.8 W/m, a difference of -56.3%. However, at the floor interior the total heat loss was 20.9 W/m while the heat loss vertically through the insulation was 20.6, an error of only -1.3%. This same phenomona was found for the other cases studied except where noted otherwise. This can be best seen in Figure 2a and 2b which illustrate the temperature and the heat loss profiles at the basement floor. The heat flux rates illustrated are the energy loss (or gain) rates for the specific area being examined in the model. They were obtained from the model by dividing the energy rates into the node by the representative area around the node (considered as the length between the midpoints between the node and its neighboring two nodes).

### 3.2 Effect of Soil Thermal Conductivity

The influence of soil thermal conductivity on the heat loss from basements was investigated through the use of several different soil thermal conductivities in the base model described previously. The conductivities used ranged from 0.75 W/m.K to 2.5 W/m.K. For the type of soil sampled this range of thermal conductivity would account for a full range of moisture conditions from dry to saturated, frozen or unfrozen soil, and variations in the concentrations of sand and clay.

The results indicated the following:

1. Below grade heat loss from the walls, for both sections, was found to show a nearly linear variation in heat loss with varying thermal conductivity. Assuming a linear variation in heat loss compared to soil thermal conductivity, correlation coefficients for the upper and lower below grade wall sections were 0.91 and 0.97 respectively. The plot of heat loss versus soil thermal conductivity for the below grade wall surfaces is shown in Figure 3a.
2. Heat loss from the floor was also found to have a linear variation with changing thermal soil conductivity. Correlation coefficients were 0.98 for both the interior and perimeter regions. The plot of heat loss versus soil thermal conductivity for the floor is found in Figure 3b.
3. Increasing the soil conductivity was found to cause the fraction of heat loss at the perimeter to decrease (as expressed as a percentage of the total floor heat loss) while the interior heat loss increased.

### 3.3 Effect of Other Parameters

The effect of changing parameters such as the deep ground temperature, outdoor ambient air temperature, basement convection coefficients, etc. is seen in Table 1. It was found that the relationship between heat loss and the parameter varied could be well represented by a linear relationship.

### 3.4 Effect of Removing the Snow Cover

As previously mentioned, the base model assumes that the average amount of snow on the ground for the month of January 1984 is present. Removing the snow cover, simulated by modifying the ground heat transfer coefficient to include the insulation value of the snow cover, was accomplished by changing the convection coefficient to what it would be without snow cover.

The difference between the base case with a snow cover of approximately 3.3 cm and this case without snow cover was a 6.8% increase in the overall heat loss from the basement. The wall experienced a higher percentage increase of 11.4% as opposed to an increase of 2.4% from the floor.

### 3.5 Effect of Sol-Air Temperature

The base case model, using the average conditions for the month of January 1984, did not incorporate the solar energy received during that month into any of the input parameters for the model. Because of the high reflectivity of snow, absorption of the sun's energy at the surface would be negligible at that time. However, during the months of the year when snowcover is not present absorption of solar energy by the ground is capable of raising its surface temperature by several °C.

To determine the effect of incorporating the solar energy received at the earth's surface the model was run with the average air temperature for August 1983 and compared to the same model which instead used the average sol-air temperature for the month of August 1983 (other model inputs incorporate the other average boundary conditions for the month of August). Sol-air temperature is defined by the ASHRAE Handbook - 1981 Fundamentals as "that temperature of the outdoor air which in the absence of radiation exchanges, would give the same rate of heat entry into the surface as would exist with the actual combination of incident solar radiation, radiant energy from the sky and other outdoor surroundings, and convective heat exchange with the outdoor air." The average air temperature for August 1983 was 20.0°C while the average sol-air temperature for the same month, assuming a surface with an emittance of 0.9, was 24.8°C.

Comparison of the results for August from the two runs showed a 15.5% decrease in total basement heat loss in going from the average air temperature to the average sol-air temperature. The greatest influence was in the wall zones where heat loss became a heat gain for the above ground and the 0-0.6 m below grade wall zones. For the wall zone adjacent to the floor there was a 36.7% decrease in heat loss, a 13.3% decrease in the heat loss from the floor perimeter, and a 1.9% decrease in the heat loss from the interior floor zone in going from average monthly air temperature to monthly average sol-air temperature. Ground vegetation and the effects of shading due to the house, other houses, and trees would significantly reduce these effects.

### 3.6 Effect of Radiation Heat Transfer

To simulate no radiation heat transfer in the model the emissivity of the floor, ceiling, and walls were changed to 0.001. Two cases were investigated. The first case had only the emissivity of the radiation elements changed. The second case was the same as the first with the exception of changing the convection coefficients along the floor and wall to 6.1 and 8.3 W/m$^2$.K respectively. These convection coefficients, obtained from Table 1, page 23.12 of the ASHRAE Handbook - 1981 Fundamentals include the effect of radiation heat transfer based on the assumption included with the Table.

---

* The terms floor interior and floor perimeter are the same as those which Mitalas (1982) used. The floor perimeter is that region of the floor which is within 1 m of the inside edge of the concrete basement wall. The floor interior is that portion of the floor which is not part of the perimeter.

The first case experienced an overall decrease in total basement heat loss of 17.3% from the base case while the second case experienced only a 2.1% decrease from the base case. The differences in the first case were accounted for in a 15.6% decrease in the wall heat loss and an 18.9% decrease in the floor heat loss. In the second case the differences were accounted for in a 8.0% increase in wall heat loss and an 11.7% decrease in the floor heat loss.

While increasing the convection coefficients along the floor and wall, as was done for the second case, is capable of simulating the total amount of heat being lost from the basement it nonetheless fails to account for the nature of the heat transfer processes occurring in the basement. In the base case the ceiling loses energy to the floor and walls by radiation. The floor and walls in turn lose energy to the surrounding air by convection and lose energy by conduction to the surrounding soil. By using only convection and conduction heat transfer processes the air must therefore lose energy to the floor, i.e. the floor temperature must be lower than the air temperature. While the reduction in floor surface temperatures from the base case to the second case is only approximately 1°C, it may be significant in terms of thermal comfort and condensation of moisture on the floor surface. The failure to model basement heat loss without the radiation heat loss could lead to serious errors in the prediction of thermal comfort in the basement, and the failure to anticipate condensation problems.

### 3.7 Effect of Adding Perimeter Insulation At The Footing

Exterior perimeter insulation has been recommended or suggested by a number of design publications. This insulation is intended to prevent freezing of the wall footings. To investigate the effect of adding horizontal perimeter insulation at the footing of the basement model, the mesh of the finite element model was changed so as to permit the addition of a 0.61 m wide by 0.05 m thick piece of extruded polystyrene insulation at the footing, exterior to the wall in the horizontal plane.

The addition of such insulation only decreases the total heat loss from the basement by 0.1%. Losses from the floor perimeter decreased by 0.7% and from the floor interior decreased by 0.3%. On the other hand heat losses from the wall increased by 0.2%. It should be noted that in the base case used the soil freezing front did not approach the footing.

### 3.8 Various Insulation Strategies for Basement Floors

To investigate the effect of the floor insulation on the heat loss through the floor four different strategies were adopted and compared to the base load case. These different load cases used essentially the same model as the base case with exceptions as noted below. Case 1 had the thermal conductivity of the insulation changed to the same value as that of the surrounding soil - i.e. no floor insulation. Case 2 had the last element on the floor surface before the wall changed from the material properties of concrete to those of the floor insulation which in effect provided a thermal break between the concrete floor and footing. Cases 3 and 4 changed the thermal conductivities of the floor insulation to twice and one half, respectively, the value of the insulation used in the base case.

The following observations may be noted from the numerical results from those runs:

1. The case of no floor insulation resulted in a 29.2% increase in total wall and floor heat loss with that increase being accounted for in a 4.3% decrease in heat loss from the wall and a 60.8% increase in heat loss from the floor. Below grade wall losses were found to be less with increasing depth when compared to the base case. This may be accounted for by the increased floor heat loss raising the ground temperatures outside the basement wall. The interior floor region was found to experience a larger percentage increase in heat loss than the perimeter floor region in comparison to the base case.
2. Introducing a thermal gap, i.e. eliminating the thermal bridge, between the floor and the concrete footing caused a reduction in total basement heat loss (walls and floor) of 4.9% with that being accounted for by a 0.9% increase in wall heat loss and a 10.3% decrease in floor heat loss. Through this, and other test cases run it is apparent that any decrease in floor heat loss results in an increase in wall heat loss - albeit small. The perimeter region experienced a 28.9% decrease in floor loss while the interior experienced a nominal 1.4% increase in heat loss. Introducing the thermal gap not only reduces the floor heat loss but improves the thermal comfort of the basement occupant by reducing the thermal gradient horizontally across the floor. Condensation of moisture from the air on the floor would also be reduced by adding the insulation in the gap to prevent thermal bridging.
3. Doubling the thermal conductivity of the floor insulation (i.e. halving the R-value of the insulation) caused an increase in the total basement heat loss of 10.3% with that being accounted for in a 1.4% decrease in heat loss from the walls and a 21.3% increase in heat loss from the floor. The greater percentage increase in the heat loss occurred from the interior floor region with a 26.7% increase as opposed to only 12.8% from the perimeter is due to the fact that the perimeter is less sensitive to the insulation because of the heat being conducted through the floor, into the footing, and out into the ground.
4. Halving the thermal conductivity of the floor insulation (i.e. doubling the R-value of the insulation) caused a decrease in total basement heat loss of 10.8% from that of the base case. The decrease was accounted for in a 1.4% increase in the wall heat loss and a 22.4% decrease in the floor heat loss.

## 4. CONCLUSIONS

The preceding discussion of the various parameters affecting heat loss gives an indication of the effects of these parameters and the relative magnitude of change which may be expected. As well, it is shown that radiation heat loss plays a dominant role in basement heat loss.

For a house with a full basement in a climate such as Saskatoon's, the importance of eliminating thermal bridges between the various components is demonstrated. As well, the importance of floor insulation is also illustrated.

## 5. REFERENCES

ASHRAE. 1981. ASHRAE Handbook--1981 Fundamentals. Atlanta: American Society of Heating, Refrigerating, and Air-Conditioning Engineers, Inc.

Mitalas, G.P. 1982. "Basement Heat Loss Studies At DBR/NRC". National Research Council of Canada, Division of Building Research. DBR Paper No. 1045. Ottawa.

Richmond, W.R.; and Besant R.W. 1985. "A Study of Heat Loss Through Basement Floors." *Proceedings of the ASHRAE/DOE/BTECC Conference Thermal Performance of the Exterior Envelopes of Buildings III.* To be published by the American Society of Heating, Refrigerating and Air-Conditioning Engineers.

Richmond, W.R. 1986. *A Study of Heat Loss Through Basement Floors.* M.Sc. Thesis. Department of Mechanical Engineering. University of Saskatchewan.

Sparrow, E.M.; and Cess, R.D. 1978. *Radiation Heat Transfer.* Washington: Hemisphere Publishing Corporation.

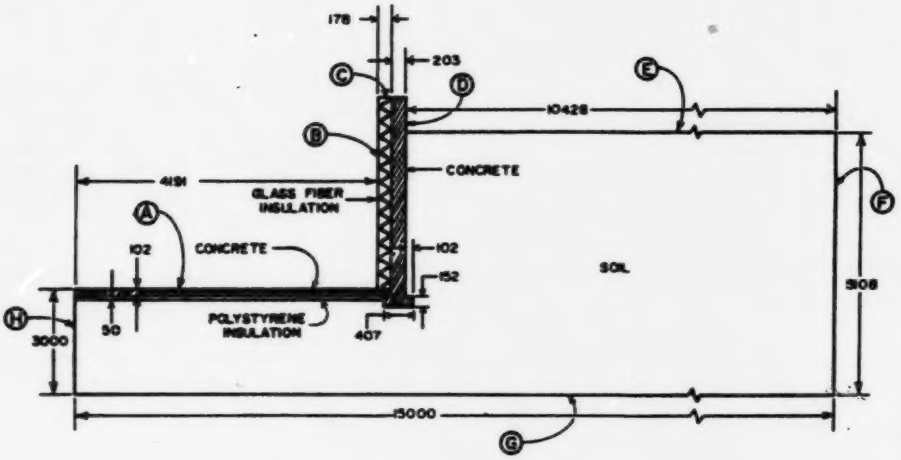
178
203
Ⓒ
Ⓓ
Ⓔ
10428
Ⓑ
CONCRETE
4191
GLASS FIBER INSULATION
Ⓐ
Ⓕ
102
CONCRETE
102
152
SOIL
5108
Ⓗ
50
3000
POLYSTYRENE INSULATION
407
15000
Ⓖ

Fig. 1 Outline of Finite Element Model

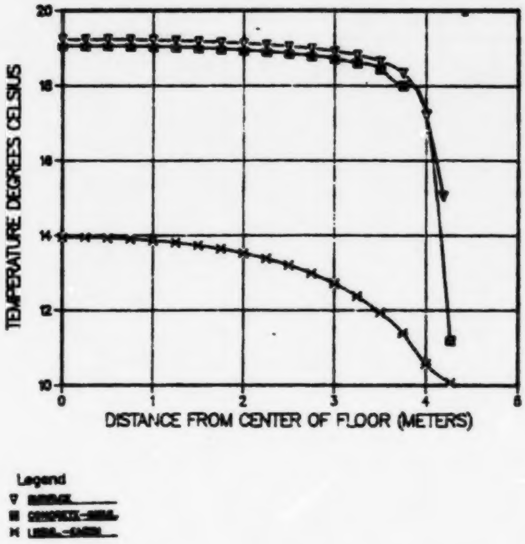

Fig. 2a Basement Floor Temperature Profiles for Base Case

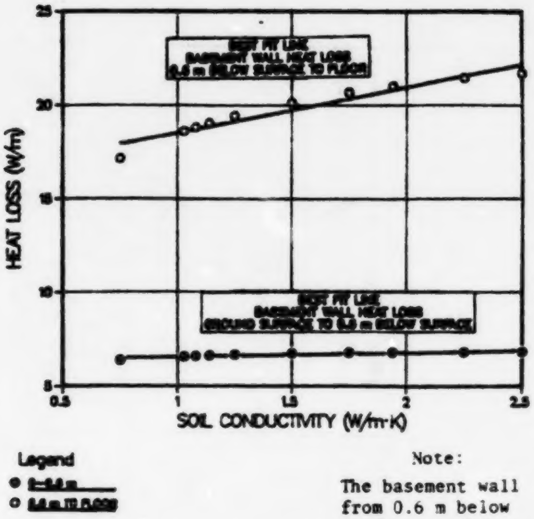

Note:

The basement wall from 0.6 m below surface to the floor has a length of 1.508 m.

Fig. 3a Comparison of Heat Loss Versus Soil Thermal Conductivity for Basement Wall

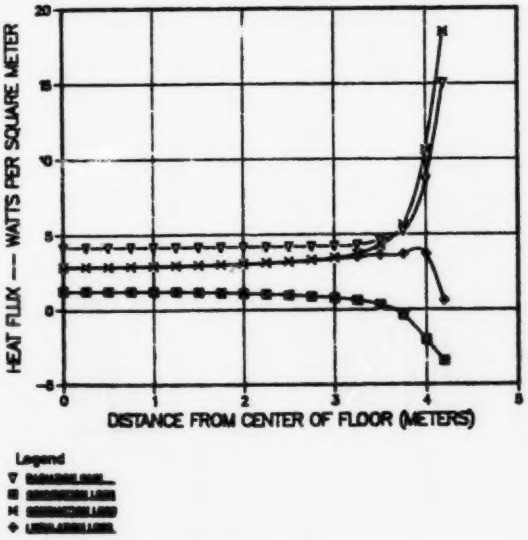

Fig. 2b Basement Heat Loss Profiles for Base Case

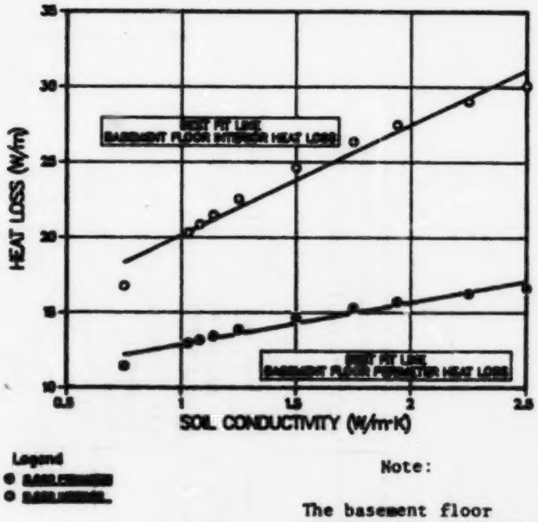

Note:

The basement floor interior has a length of 6.738 m. The basement floor perimeter consists of 2 - 1 m sections.

Fig. 3b Comparison of Heat Loss Versus Soil Thermal Conductivity for Basement Floor

Table 1
Results of Parametric Runs
Using Base Model

| Zone | Parameter Varied | Range | Linear Regression Coefficient | Slope of Line | y-intercept |
|---|---|---|---|---|---|
| Basement Wall From Ground Surface to 0.6 m Beneath Surface | Soil Thermal Conductivity | 0.75 W/m.K to 2.50 W/m.K | 0.9103 | 0.2277 K | 6.342 W/m |
| | Deep Ground Temperature | 1.8°C to 13.0°C | -1.000 | $-2.357 \times 10^{-2}$ W/m.K | 6.770 W/m |
| | Outdoor Ambient Air Temperature | -20.0°C to 0.0°C | -1.000 | -0.1964 W/m.K | 4.227 W/m |
| | Basement Floor and Wall Convection Coefficients | 1.0 to 4.0 $W/m^2.K$ | 0.9281 | $6.379 \times 10^{-3}$ m.K | 6.592 W/m |
| | Air Temperature Adjacent to Basement Floor | 16.0°C to 20.3°C | 0.9999 | $3.579 \times 10^{-2}$ W/m.K | 5.946 W/m |
| | Basement Ceiling Temperature | 18.4°C to 23.0°C | 1.000 | 0.1860 W/m.K | 2.829 W/m |
| Basement Wall From 0.6 m Beneath Surface to Floor Level | Soil Thermal Conductivity | 0.75 W/m.K to 2.50 W/m.K | 0.9656 | 2.433 K | 16.10 W/m |
| | Deep Ground Temperature | 1.8°C to 13.0°C | -1.000 | -0.3575 W/m.K | 21.35 W/m |
| | Outdoor Ambient Air Temperature | -20.0°C to 0.0°C | -1.000 | -0.4534 W/m.K | 13.32 W/m |
| | Basement Floor and Wall Convection Coefficients | 1.0 to 4.0 $W/m^2.K$ | 0.9941 | 0.4877 m.K | 18.06 W/m |
| | Air Temperature Adjacent to Basement Floor | 16.0°C to 20.3°C | 0.9996 | 0.3357 W/m.K | 12.65 W/m |
| | Basement Ceiling Temperature | 18.4°C to 23.0°C | 0.9998 | 0.5067 W/m.K | 8.546 W/m |
| Basement Floor Perimeter | Soil Thermal Conductivity | 0.75 W/m.K to 2.50 W/m.K | 0.9761 | 2.827 K | 10.06 W/m |
| | Deep Ground Temperature | 1.8°C to 13.0°C | -1.000 | -0.4998 W/m.K | 16.73 W/m |
| | Outdoor Ambient Air Temperature | -20.0°C to 0.0°C | -1.000 | -0.2158 W/m.K | 10.57 W/m |
| | Basement Floor and Wall Convection Coefficients | 1.0 to 4.0 $W/m^2.K$ | 0.8430 | $18.79 \times 10^{-3}$ m.K | 13.15 W/m |
| | Air Temperature Adjacent to Basement Floor | 16.0°C to 20.3°C | 0.9999 | 0.2506 W/m.K | 8.566 W/m |
| | Basement Ceiling Temperature | 18.4°C to 23.0°C | 1.000 | 0.4848 W/m.K | 3.341 W/m |
| Basement Floor Interior | Soil Thermal Conductivity | 0.75 W/m.K to 2.50 W/m.K | 0.9837 | 7.321 K | 12.83 W/m |
| | Deep Ground Temperature | 1.8°C to 13.0°C | -1.000 | -1.418 W/m.K | 30.92 W/m |
| | Outdoor Ambient Air Temperature | -20.0°C to 0.0°C | -0.9785 | $-6.667 \times 10^{-2}$ W/m.K | 19.93 W/m |
| | Basement Floor and Wall Convection Coefficients | 1.0 to 4.0 $W/m^2.K$ | 0.9954 | -0.2004 m.K | 21.16 W/m |
| | Air Temperature Adjacent to Basement Floor | 16.0°C to 20.3°C | 1.000 | 0.3754 W/m.K | 13.95 W/m |
| | Basement Ceiling Temperature | 18.4°C to 23.0°C | 1.000 | 1.180 W/m.K | -3.082 W/m |

# EFFECT OF EXTERIOR INSULATION PLACEMENT ON BASEMENT HEAT LOSSES

T. M. Kostyniuk and A. C. Trupp
Department of Mechanical Engineering
University of Manitoba
Winnipeg, Manitoba
R3T 2N2

## ABSTRACT

A finite-difference computer program for transient heat conduction was developed and utilized to investigate the effects of exterior insulation placement on basement heat loss. A comparative study was made of the effectiveness of exterior wall, ground surface, and footing insulation in reducing the below-grade basement heat loss during the heating season. Ground surface insulation was found to be about 80 and 93% as effective in reducing heat loss as wall insulation based on the same insulation lengths of 1.8 and 1.2 m, respectively. Thus, ground surface insulation may be a viable alternative to exterior wall insulation for existing basements. On the other hand, footing insulation was found to actually increase the average heat loss rate from the basement, indicating that it should be installed only if necessary to prevent frost penetration underneath footings.

## 1. INTRODUCTION

Exterior basement insulation is being installed on many homes due to the significant heat loss reductions that can be achieved by using this insulation. In fact, basement walls and floors are responsible for up to 25% of the total heat loss from a house [1], and this can be significantly reduced by suitable placement of insulation [2].

As shown in Fig. 1, there are three main areas where insulation can be installed on the exterior of a house basement. These include exterior wall insulation, ground surface insulation, and footing insulation. At present, footing insulation is primarily used in conjunction with wall insulation to prevent frost penetration and frost heave underneath foundations [3].

Exterior wall basement insulation has several advantages over conventional interior basement insulation. These advantages include a warmer outside concrete wall, no possibility of frost damage on the outside concrete work, and no loss of inside living space is incurred as when interior basement insulation is used [4].

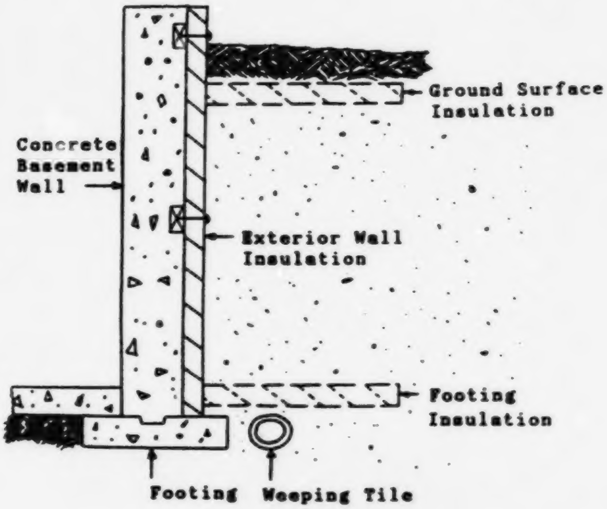

Fig. 1: Areas of Exterior Basement Insulation Placement

## 2. MODEL DESCRIPTION

The soil temperature distribution around a house basement follows a steady periodic pattern from year to year, ie. the soil temperature at a specified soil location is the same on the same day of each year. This steady periodic temperature solution is required in order to determine the time-dependent heat losses from a house basement.

The finite-difference computer model developed to predict the thermal regime and heat loss occurring around an insulated basement is documented in detail in reference [5]. In the finite-difference model, heat transfer through the basement wall and floor and then through the surrounding soil was assumed to occur exclusively by conduction. As well, the house was assumed to be a rectangular building with a length sufficiently greater than its width to allow for two-dimensional modelling (see Fig. 2). Due to the symmetry of the temperature distribution about the centerline of the house, only half of the basement needed to be considered. The width and depth of the basement were chosen as 8.3 and 2.4 m, respectively. These values are typical for houses of deep basement construction.

The grid size was chosen as 20 nodes wide by 15 nodes deep (24.6 meters wide by 21.6 meters deep). This size was large enough to contain the thermal disturbances caused by a basement of 4.15 m half-width and 2.4 m depth. A non-uniform grid was employed in which a fine spatial step-size of 0.6 m was used near the basement for improved resolution, whereas a coarse spatial step-size of 2.4 m was used far from the basement. The grid system and boundary conditions for the model are summarized in Fig. 2.

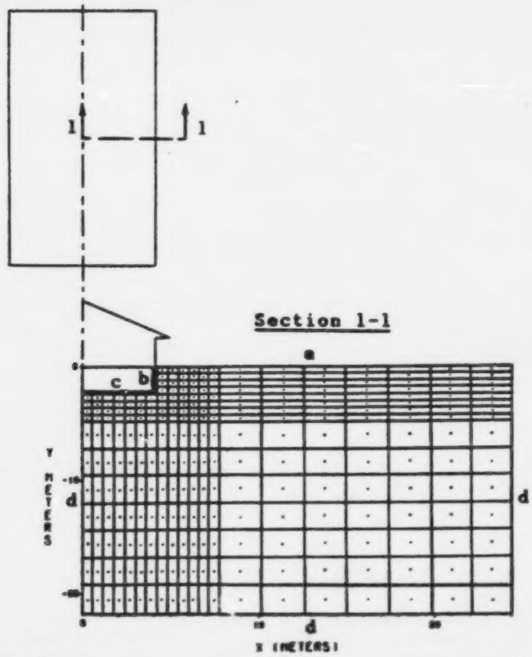

Boundary Conditions:
a)Ground surface: Mean daily air temperature
b)Basement wall: 20°C interior concrete temp.
c)Basement floor: 20°C interior concrete temp.
d)Adiabatic (no net heat flow) boundary

Fig. 2: Finite-Difference Grid Pattern and Boundary Conditions

The location chosen for this study was Winnipeg, Manitoba. Thermal properties for typical silty clay soil of 30% water content were used in the analysis. The mean air temperature and snow cover data for Winnipeg were obtained from the Atmospheric Environment Service Canada [6]. In the model, a seasonal average depth of snow cover was used, while the effects of surface convection, solar flux, and other ground surface cover such as grass were not considered. Phase change of the water contained in the soil was handled using the excess degrees method suggested by Dusinberre [7].

The options of having insulation that extends down the wall or that extends horizontally away from the wall at either the ground surface or the footing were also incorporated into the computer model. The insulation could be applied in varying thicknesses and lengths and any combination of insulation placement could be used.

## 3. RESULTS AND DISCUSSION

### 3.1 General

The purpose of the study was to investigate the effects of exterior insulation placement on the heat loss from a house basement. For a given insulation configuration, the computer program first calculated the steady periodic temperature regime and subsequently the heat loss occurring around the basement for a specified heating season. For this study, a typical heating season from November 30 to April 30 was selected.

The effect of insulation placement on below-grade basement heat loss was investigated for the following cases:

1) wall insulation of variable thickness and depth,
2) ground surface insulation of variable length and 5 cm thickness,
3) footing insulation of variable length and 5 cm thickness.

The type of insulation used for the study was a high-density extruded polystyrene having a thermal conductivity of 0.029 W/m-K (eg. STYROFOAM SM, Trademark of the Dow Chemical Company).

### 3.2 Effect of Wall Insulation on Heat Loss

The effect on heat loss of varying the thickness and depth of exterior wall insulation was first investigated. Table 1 shows the percentage reductions in average heat loss from the basement for the various insulation thicknesses. As can be seen from this table, 5 and 10 cm thicknesses of full-depth wall insulation reduce heat loss by 41.0% and 51.4%, respectively, as compared to an uninsulated basement. Thus, increasing the insulation thickness results in greater heat loss reductions, but it is likely that the added savings do not justify the extra cost of increasing the insulation level from a 5 to 10 cm thickness.

The depth of a constant thickness of wall insulation was then varied. For a constant insulation thickness of 5 cm, the depth of insulation was varied from 0.6 to 2.4 m deep. From Table 1, it can be seen that by increasing the depth of wall insulation from 0 to 2.4 m, the average heat loss rate decreases from 6.65 to 3.92 Watts/square meter of basement surface area. As well, the results in Table 1 indicate that insulating the upper half of the basement wall produces the highest heat loss reductions,

Table 1: Variation of Basement Heat Loss with Insulation Configuration

| Insulation Configuration | Insulation Thickness (cm) | Insulation Length (m) | Average Heat Loss Rate (W/m²) | Reduction (%) |
|---|---|---|---|---|
| Wall insul. only | 0.0 | 0.0 | 6.65 | 0.0 |
| | 5.0 | 2.4 | 3.92 | 41.0 |
| | 10.0 | 2.4 | 3.23 | 51.4 |
| Partial depth wall insul. | 0.0 | 0.0 | 6.65 | 0.0 |
| | 5.0 | 0.6 | 5.84 | 12.2 |
| | 5.0 | 1.2 | 5.06 | 23.9 |
| | 5.0 | 1.8 | 4.48 | 32.7 |
| | 5.0 | 2.4 | 3.92 | 41.0 |
| Ground surface insul. only | 0.0 | 0.0 | 6.65 | 0.0 |
| | 5.0 | 0.6 | 5.67 | 14.8 |
| | 5.0 | 1.2 | 5.18 | 22.1 |
| | 5.0 | 1.8 | 4.90 | 26.2 |
| Footing insul. and 2.4 m wall insul.(5cm thick) | 0.0 | 0.0 | 3.92 | 0.0 |
| | 5.0 | 0.6 | 4.04 | -3.0 |
| | 5.0 | 1.2 | 4.12 | -5.1 |
| | 5.0 | 1.8 | 4.17 | -6.3 |

while insulating the lower half of the wall is about 70% as effective as insulating the upper half of the wall. Thus, the heat loss reductions achieved by insulating the lower half of a basement wall are still significant even though they are not as high as for the upper half of the wall. Again, economic considerations such as energy and insulation costs inevitably influence the actual installed depth of insulation.

## 3.3 Effect of Ground Surface Insulation

The next case considered was the effect of ground surface insulation on heat loss. The heat loss reductions resulting from installing a specified length of 5 cm thick ground surface insulation were compared to installing the same amount of insulation on the wall.

As can be seen from Table 1, ground surface insulation is actually more effective than wall insulation in reducing heat loss for a 0.6 m length. Compared to an uninsulated basement, a 0.6 m depth of 5 cm thick wall insulation reduces heat loss by 12.2%, while the same insulation applied at the ground surface reduces heat loss by 14.8%. Thus, ground surface insulation is about 21% more effective than wall insulation for a 0.6 m length. The reason for this is that a wall insulated to only a 0.6 m depth loses a lot of heat through the uninsulated lower portion of the wall, and the ground surface insulation is more effective in reducing this flow of heat. However, insulating a basement wall to a shallow depth of 0.6 m is not a very practical situation since significant heat losses occur for this depth of insulation.

For the more realistic cases of installing 1.2 and 1.8 m insulation lengths, the wall insulation is more effective than the ground surface insulation in reducing heat loss. As shown in Table 1, the wall insulation reduces heat loss by 23.9% and 32.7% for 1.2 and 1.8 m depths, respectively, as compared to an uninsulated basement, while the ground surface insulation reduces heat loss by only 22.1% and 26.2% for the same respective lengths.

These results indicate that for a newly constructed basement, wall insulation is generally superior to ground surface insulation. However, for an existing basement, ground surface insulation is easier and cheaper to install, and it achieves heat loss reductions of 80 and 93% of that of wall insulation for 1.8 and 1.2 m lengths, respectively.

## 3.4 Effect of Footing Insulation on Heat Loss

The effect of using footing insulation on basement heat loss was the last case to be considered. At the present time, insulation is occasionally installed at the footings in order to prevent possible frost penetration underneath basement footings. If freezing occurs underneath footings, frost heave can occur, resulting in cracking of the concrete basement.

Basement heat loss for full-depth wall insulation of 5 cm thickness was compared to the heat loss for the same level of wall insulation together with varying lengths of footing insulation of 5 cm thickness. As shown in Table 1, the use of footing insulation slightly increases the average heat loss rate from the basement. In fact, as the length of footing insulation increases from 0.6 to 1.8 m, the average heat loss rate for the heating season increases from 3.0% to 6.3% as compared to a basement without footing insulation. The explanation for this is that footing insulation acts as a resistance to heat flow originating from the basement floor. As a result, the soil temperatures adjacent to the basement wall are lower than they would be otherwise, and thus the wall heat loss increases slightly. Thus, it is not recommended that insulation be placed at the base of a foundation unless there is a real danger of frost penetration since protection carries a penalty in the form of slightly higher heating costs.

As a further point concerning footing insulation, the effect of seasonal snow cover on the temperature distribution around an insulated house basement was considered. Fig.

3 compares the significant difference in the temperature distribution around the basement with and without seasonal snow cover present. In particular, the 0°C isotherm extends much deeper and closer to the house when seasonal snow cover is not present. This is significant because it indicates that areas around a house that are cleared of snow such as walkways and driveways freeze much deeper and thus experience higher heat losses than snow covered areas. Thus, footing insulation may be necessary around snow cleared areas due to the greater depth of soil freezing.

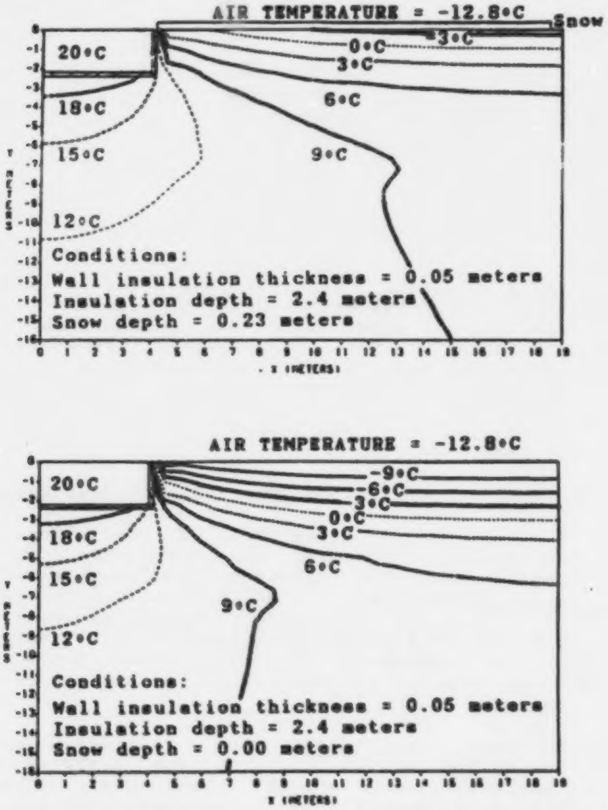

Fig. 3: Comparison of Soil Temperatures Around a Basement With and Without Snow Cover (March 1)

## 4. CONCLUSIONS

In this paper, the effect of exterior insulation placement on basement heat loss was studied. From the results of the study, exterior wall insulation extending to half the depth of a 2.4 m deep basement produced a significant heat loss reduction. However, insulating the lower half of the wall was still about 70% as effective in reducing heat loss as compared to insulating the upper half of the wall.

Comparing an equivalent length of insulation extending down the outside basement wall to placing the same insulation horizontally away from the basement at the ground surface indicated that the wall insulation is generally more effective in reducing heat loss. For the practical cases of using 1.2 and 1.8 m insulation lengths, the wall insulation was 7% and 20% more effective than ground surface insulation, respectively. Thus, for a newly constructed basement, exterior wall insulation is preferable to ground surface insulation. However, for an existing basement, installation of ground surface insulation may be a viable alternative since it is easier and cheaper to install than exterior wall insulation, and it is still about 80% to 93% as effective as wall insulation for the same insulation length.

Footing insulation used in conjunction with wall insulation was found to actually reduce the effectiveness of the wall insulation. In fact, the heat loss increased from 3% to 6.3% as compared to a basement without footing insulation when the length of footing insulation was increased from 0.6 to 1.8 m. Hence, this study indicates that footing insulation should only be used if there is a real danger of frost penetration underneath a foundation.

## 5. ACKNOWLEDGEMENTS

The authors of this paper would like to thank A. R. Morrison, of Manitoba Hydro, for suggesting the topic of this research, and Professor R. E. Chant, Department of Mechanical Engineering at the University of Manitoba, for providing valuable reference material.

## 6. REFERENCES

[1] Titley, G.L., Outside Basement Insulation Using Styrofoam SM, Bulletin No. 64, Dow Chemical of Canada, Limited, Sarnia, Ontario, 1978, p. 2.

[2] Bligh, T.P., Shipp, P., and G. Meixel, Energy Comparisons and Where to Insulate Earth-Sheltered Buildings and Basements, Energy, Vol. 5, 1980, pp. 451-465.

[3] Figley, D.A., and L.J. Snodgrass, The Effect of Basement Insulation on the Depth of Frost Penetration Adjacent to Insulated Foundations, Journal of Thermal Insulation, Vol. 7, April 1984, pp. 266-294.

[4] Middleton Associates, Energy Conservation and House Basements: A Research Report, BETT Publication No. 82.01, Energy Mines and Resources Canada, 1982, pp. 52-53.

[5] Kostyniuk, T. M., Analysis of Exterior Basement Insulation Using the Finite-Difference Method, B. Sc. Thesis, University of Manitoba, Winnipeg,1986.

[6] Canadian Normals 1951-1980, Atmospheric Environment Service, Environment Canada.

[7] Dusinberre,G.M., Heat-Transfer Calculations by Finite Differences, International Textbook Company, Scanton, Pennsylvania, 1961, p. 189-190.

# Building
# Component
# Performance

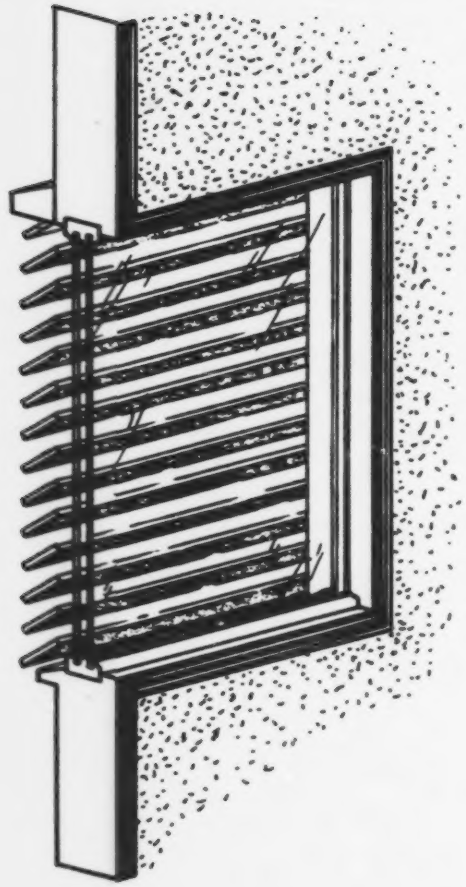

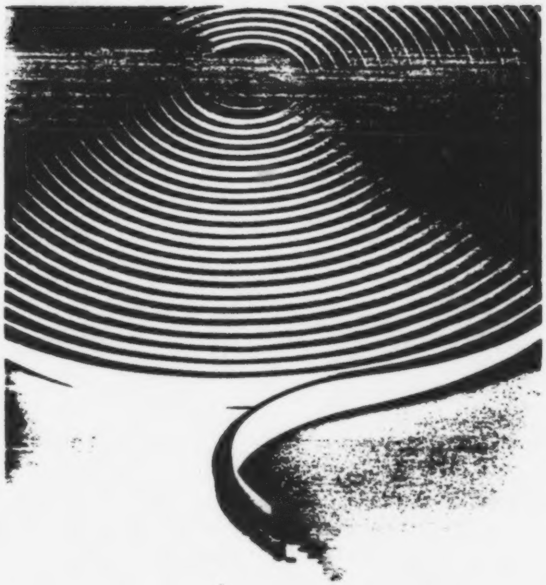

Swiggle Strip® is an extruded butyl based tape of a quality thermoplastic compound which contains a corrugated aluminum spacer and molecular sieve desiccant. The corrugation lends sufficient strength to the spacer to more than withstand forces which the glass lites would receive during fabrication, shipping, glazing and service.

## Swiggle Unit Design

To better understand how Swiggle works, it is helpful to compare the component parts of a Swiggle unit with those of a conventional unit which uses spacer, corner keys and desiccant. When the sketches are examined, it becomes apparent that each system has a metallic spacer separating the two lites of glass. Both systems use molecular sieves for desiccant. They both use sealant, but the Swiggle unit has a controlled quantity, providing improved quality, and performance.

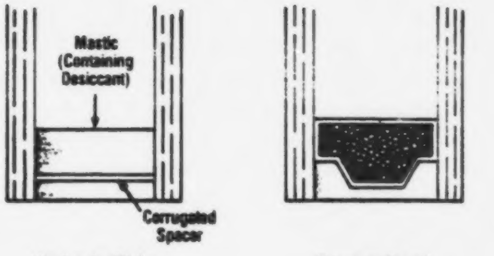

**Swiggle Strip®** **Conventional**

---

## Superior Thermal Efficiency

- *Warmer interior glass temperatures = Reduced Condensation*
- *Reduced heat flow through the unit = Energy savings*

Independent laboratory tests* have shown that Swiggle units demonstrate warmer interior glass surface temperatures and less heat flow than do conventional units under thermal load conditions.

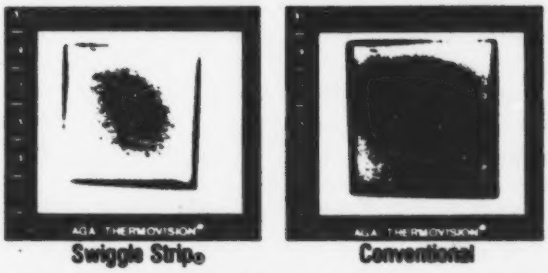

**Swiggle Strip®** **Conventional**

The photos (above) are infrared thermograms comparing heat loss through a Swiggle unit and a conventional spacer bar unit. The test conditions used a 40°C temperature differential between the warm and cold sides of the unit. Viewed here from the warm side, the darker the shading, the colder the glass temperature thus indicating greater heat loss. Note that not only is the glass in the Swiggle unit warmer at the edges, but also over its entire surface area.

## Outstanding Life Expectancy

- *Low moisture vapour transmission compound = Reduced rate of moisture penetration to the air space*
- *Greater moisture vapour path = Increased resistance to moisture travel*
- *Continuous corners = Fewer potential problem areas*
- *Desiccant on all four sides = Lower long term dew points*

## Reduced Stress On The Glass Perimeter

- *100% Solids = No edge stress due to sealant shrinkage*
- *No nitrogen absorption = Reduced glass deflection at low temperatures*
- *No rigid spacer bar = No localized stress build-up*

---

*Tests conducted by Ontario Research Foundation

## SESCI/BIOMASS CONFERENCE '86

# Thermal Scans and Isotherms of Windows and Frames

I.H. (Ike) Warkentin
Box 50, Group 32, R.R. 1B
Winnipeg, Manitoba
R3C 4A3
(204) 474-3744 (Business)
(204) 338-5960 (Residence)

Thermal scans and isotherms (surface temperature measurements) of windows and frames are presented on actual installation on two buildings in Winnipeg, Manitoba. Initially all windows consist of triple glazed sealed units, with conventional metal 1/2" air spaces. The houses' window frames are P.V.C. (DURACO) type and the Commercial building window frames are aluminum with thermal breaks.

Thermal scans were performed on January 6, 1986. Outside temperatures were recorded at -28°C to -29°C and the room temperatures at 21°C to 22°C (approx. 50°C $\Delta T$).

Two of the triple glazed house windows were replaced following the initial thermal scan. One sealed unit was replaced with a triple glazed "swiggle strip (TREMCO) 1/2" air spaces" unit, the other replacement was a double glazed "low E" (suptter-coated glass) and the "swiggle strip 1/2" air space" (see Figure 1). A follow up thermal scan is planned next winter for comparison of the surface temperatures on the three types of windows now installed in the house.

The initial observation of the double glazed "low E" window with the "swiggle strip and 1/2" air space"is that the unit developed considerable condensation on the lower edge of the window pane, whereas no condensation was evident on the triple glazed windows with the "swiggle strip" or the "conventional metal"spacers. All three window types were on the same wall of the house and therefore exposed to the identical indoor and outdoor conditions. The outside temperature at the time was recorded as approximately -8°C, the room temperature 17°C and the inside relative humidity at 55 to 60%. This would suggest that the surface temperature of the "low E glass - double glazed window", has a lower surface temperature and may not be adequate for the cold prairie climate. This was further evidenced by taking thermocouple temperature readings on 86 04 20 and 21 (see Table 1).

To maintain a comfortable level of relative humidity (eg. 40 - 50%) in a house during the winter months, the surface temperature must be maintained above the dew point, or condensation will form on the window potentially resulting in moisture damage to the walls below the windows. Triple glazed windows with 1/2" air spaces are primarily used in the prairie provinces today. "Low E" or so called "super windows" will have to prove themselves more cost effective in the market place, to be accepted.

Figures 2 and 3 show initial thermal scan results of the surface temperatures of walls, window frames, moullian and glazings of triple glazed sealed units with conventional metal spacers.

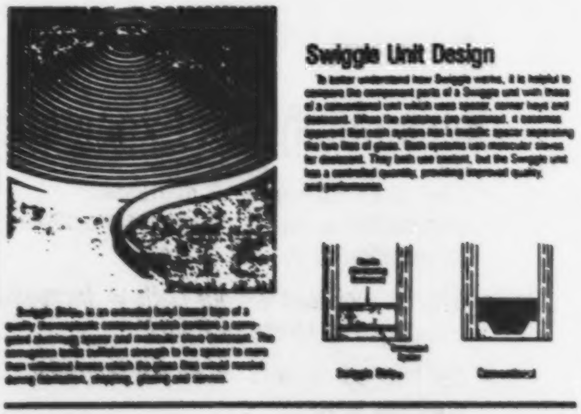

Figure 1

## HOUSE WITH DURACO P.V.C. WINDOW FRAMES

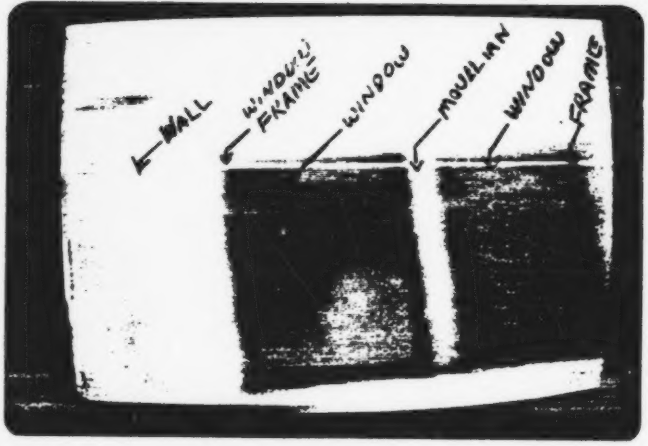

Figure 2a: Thermal scan of south east bedroom wall/window taken 86 01 06, 8:00 p.m.

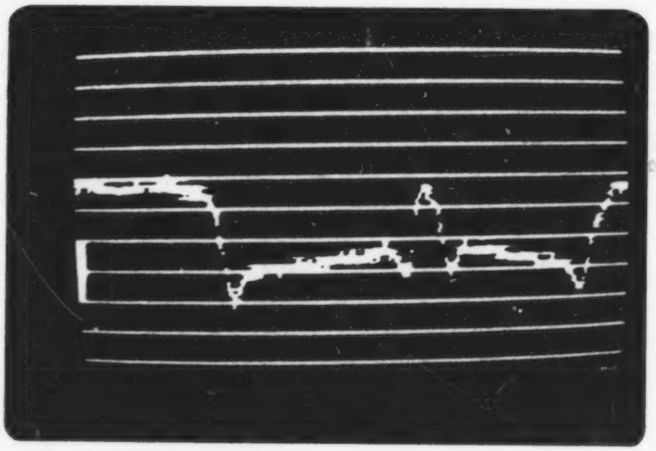

Figure 2b: The temperature line (L to R) represents the wall and window components surface temperatures. The window frame at the conventional metal spacers on the sealed unit is 8°C colder, than the wall surface temperature. The window surface temperature is 6°C colder, and the window moullian is slightly colder than the wall surface temperature. NOTE: Each horizontal line represents 2°C.

## COMMERCIAL BUILDING
## WITH ALUMINUM WINDOW FRAME WITH THERMAL BREAK

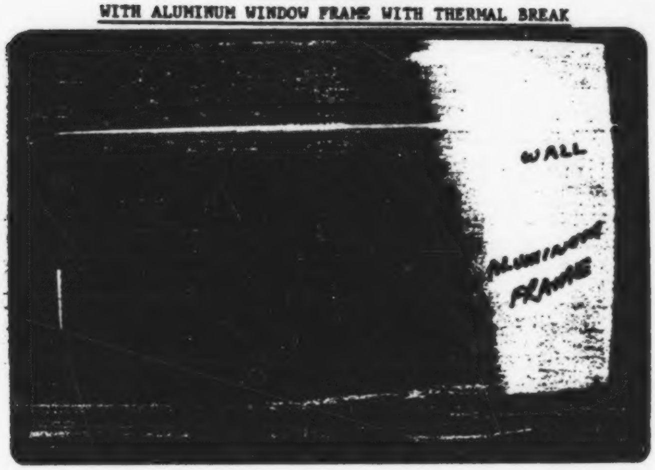

Figure 3a: Thermal scan of North facing wall/window frame/window (L to R).

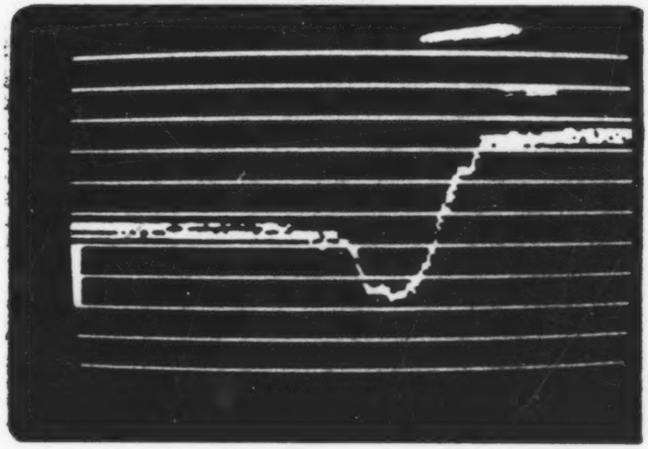

Figure 3b: The left half of the temperature line represents the inside window pane surface temperature recorded at 6°C below the wall temperature. The lowest point of 10°C is the temperature of the aluminum window frame compared to the wall temperature (high line)on the right side of the picture.

Table 1

## THERMOCOUPLE TEMPERATURE READINGS ON SOUTH FACING WINDOWS

| Date | Time | Low "E" Dbl. Glaze | Conventional Triple Glaze | Room Temp. | Out.* Temp. |
|---|---|---|---|---|---|
| 86 04 20 | 8:30 am | 10°C | 14°C | 18°C | -3°C |
| | 9:00 pm | 11°C | 14°C | 18°C | -4°C |
| 86 04 21 | 7:30 am | 11°C | 15°C | 18°C | -6°C |
| | 9:00 am | 12°C | 14°C | 18°C | -4°C |
| | 11:40 am | 13°C | 16°C | 18°C | 18°C |
| | 2:45 pm | 21°C | 27°C | 18°C | 14°C |
| | 4:45 pm | 31°C | 31°C | 22°C | 9°C |
| | 5:30 pm | 28°C | 29°C | 20°C | 8°C |
| | 6:00 pm | 23°C | 24°C | 18°C | 6°C |

* South side of house

# THE USE OF HOTCAN 3.0 TO EVALUATE THE EFFECT OF GLAZING SYSTEMS AND THERMAL CAPACITY ON RESIDENTIAL HEATING

Leon O. Feduniw
Department of Interior Design
Faculty of Architecture
The University of Manitoba
Winnipeg, Manitoba
Canada

## ABSTRACT

This study examines the influences of south-facing window area, glazing systems (without interior or exterior movable nighttime insulation), and thermal storage on the Solar Heating Fraction of the total space heating requirement and the Auxiliary Heating Requirement for wood frame houses located in the Winnipeg Area.

Solar Heating Fraction (in percentages) and Auxiliary Heating Requirement (in KWHRS) values were produced by Hotcan/R-2000, an energy-analysis computer program, through a study model designed to represent a typical two-storey house on the current (1986) speculative market. Graphs and tables developed from these values indicate that increases in the Solar Heating Fraction and reductions in the Auxiliary Heating Requirement can be achieved through increases in window area and thermal storage. Also, triple-glazed systems result in greater Auxiliary Heating Requirement reductions than double-glazed systems.

## 1. INTRODUCTION

Vertical south-facing windows provide a good potential for solar heat gains. During Winnipeg's heating season, which normally begins in September and ends in May, the sun is low on the horizon (altitude at solar noon, Dec. 21, is 16.63°) and deep penetration of sunlight into interior spaces is possible. In addition to providing natural light, the sun's radiant energy is converted into heat energy by absorbant surfaces of the interior, and is disbursed throughout the space.

Because Winnipeg housebuilders and homeowners have found that the new minimum thermal standards effectively reduce space heating requirements to an acceptable cost, they continue to build houses without regard to orientation. There is an attendant need, therefore, to illustrate the importance of south-facing windows and the effect of solar heat gains upon residential space heating.

## 2. OBJECTIVES

The first objective was to use solar heating fraction (SHF) values generated through a study model to develop a series of graphs which would illustrate the relationships of the SHF to south-facing window area, glazing systems, and thermal storage mass.

The second objective was to use Auxiliary Heating Requirement (AHR) values generated through a study model to develop a series of graphs which would illustrate the relationships of the AHR to south-facing window area, glazing systems, and thermal storage mass.

## 3. METHODOLOGY

Hotcan! (1), the key to the nation-wide R-2000 program, allows the user to input various easily available building construction characteristics which it then uses to estimate a monthly space heating load and energy consumption of the entire building.

A weakness in the Hotcan! program is the limitation of thermal storage to four vaguely described, fixed levels identified as thermal mass levels A, B, C, and D. This weakness limits the house designer's flexibility to determine in detail the material, location, and amount of thermal storage mass required. The weakness is not critical to this study however, because only generalized thermal storage mass levels are required to illustrate their effect on the SHF and AHR.

The general approach to this study was to use Hotcan! to produce SHF and AHR values through a suitable study model and to relate these values to south-facing window area, glazing systems, and thermal storage.

A rectangular 144.92 $M^2$ two-storey frame house was selected because the configuration of this house type, as well as representing 25% of the speculative houses on the current market, allows for large window areas to be placed on a street or yard facing elevation that is restricted to narrow (12.19 M to 15.24 M) lot widths (Fig. 1).

### 3.1 Building Parameters

House Volume - 662.61 $M^3$
ACH - 0.5
Main Floor Temp. 21 C
Basement Temp. 18 C
Rise Above 21 C - 5.5 Deg.
Daily Base Elec. Consumption - 14 KWH/D
Daily Hot Water Energy Consumption - 14 KWH/D
Sensible Heat Gains From Occupants - 3.2 KWH/D
Av. Window Height - 0.76 M
Av. Overhang Width - 0.45 M
Av. Header Height - 0.13 M
Htg. Season Starts in September and Ends in May

| Component | Area $M^2$ | RSI |
|---|---|---|
| Ceiling | 72.46 | 6.69 |
| Main Walls | 154.03 | 4.93 |
| Doors | 3.9 | 1.99 |
| Basement Walls Above Grade | 23.23 | 2.43 |
| Upper 0.6 M Basement Walls | 26.01 | 2.43 |
| Lower Basement Walls | 36.42 | 2.43 |
| Floor Perimeter 1 M | 26.2 | 0.32 |
| Floor Center | 38.67 | 0.32 |
| South Windows | 3.62 | 0.35 |
| North Windows | 3.72 | 0.56 |
| East Windows | 0.56 | 0.56 |

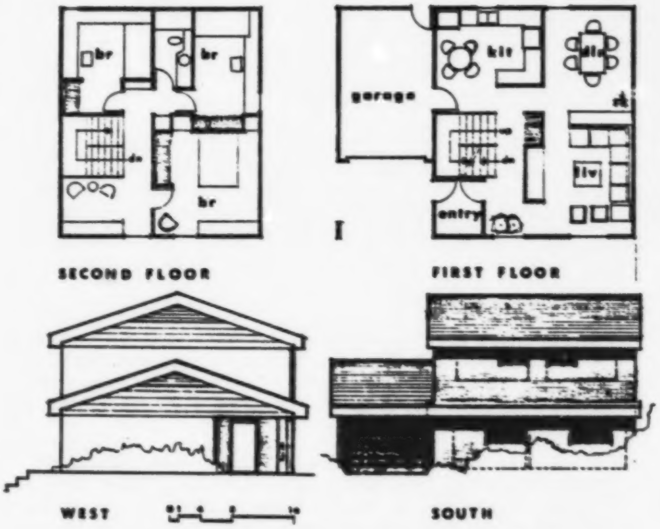

Fig. 1. Modified Version of the Typical Two-Storey House Based on Design 132 Greentree Homes, Winnipeg.

Shading for south-facing windows was designed so that windows received full sun on December 21, but no sun on June 21. R.J. Cole's formulae (2) were used for calculating the overhang projection and its height above the window. The east window was not shaded.

In order to generate comparative SHF and AHR values, the south-facing window area was increased from 3.62 $M^2$ to 5.43, 7.25, 9.06, 12.63, 16.30, and 18.12 respectively. An energy analysis of the model was then made at each increment.

Two sets of SHF values and AHR values at each incremented area of south-facing windows were produced: one for double-glazed systems, the other for triple-glazed systems.

Three of the four levels of thermal storage mass available in the Hotcan/R-2000 Energy Analysis Program were used in the process of generating SHF values and AHF values. Thermal storage mass level D was not used because it is not likely to be used in the building type the study model represents.

The data compiled were then assembled to produce charts which graphically illustrate the following:

- the effect of increasing the area of south-facing double-glazed windows on the SHF;
- the effect of increasing the area of south-facing triple-glazed windows on the SHF;
- a comparison between double-glazed and triple-glazed windows and their influence on the SHF;
- the effect of increasing the area of south-facing double-glazed windows on the AHR;
- the effect of increasing the area of south-facing triple-glazed windows on the AHR;
- a comparison between double-glazed and triple-glazed windows and their effects on the AHR.

In each case the effects are illustrated for thermal storage mass levels A, B, and C.

## 4. DATA ANALYSIS

Data for the graphs were derived from 42 separate Hotcan! analyses and summaries of the study models' thermal performance. Twenty-one of these summaries were made for double-glazed windows and twenty-one for triple-glazed windows. In each case, the summaries were for the seven different areas of south-facing windows and for mass levels A, B, and C. Values for the SHF (%) and AHR (KWHRS) obtained from these summaries were then charted so that a comparative analysis could be made.

An examination of the relationship between south-facing window area and the SHF can be made by comparing SHF values. Fig. 2 indicates that, for the study model, the SHF increases with south-facing window area and that the rate of increase varies with each month.

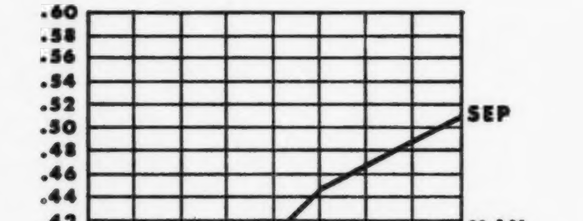

Fig. 2. The Effect of Window Area on the SHF.

SHF values for both window systems were plotted for each month. The results indicate that for all three mass levels, SHF values for double-glazed south-facing window are slightly higher than values for triple-glazed south-facing windows. The difference is greatest in September for a window area of 18.2 $M^2$. In December SHF values for both systems are almost identical (Fig. 3).

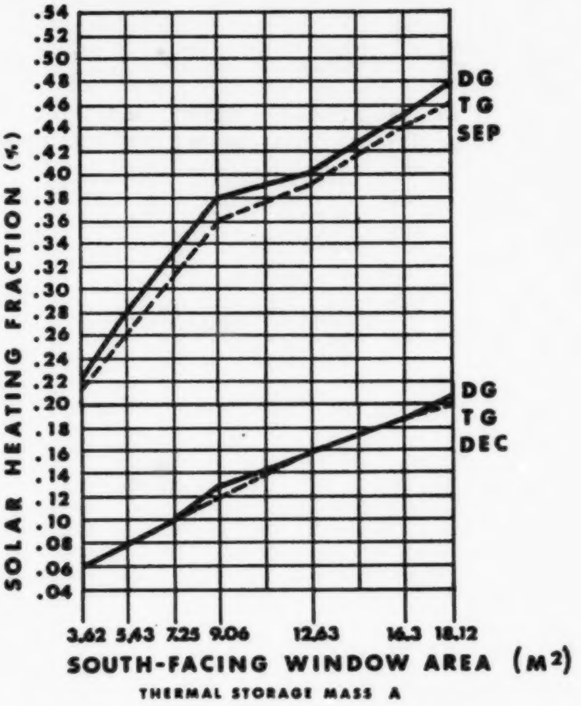

Fig. 3. The Effect of Glazing Systems on the SHF.

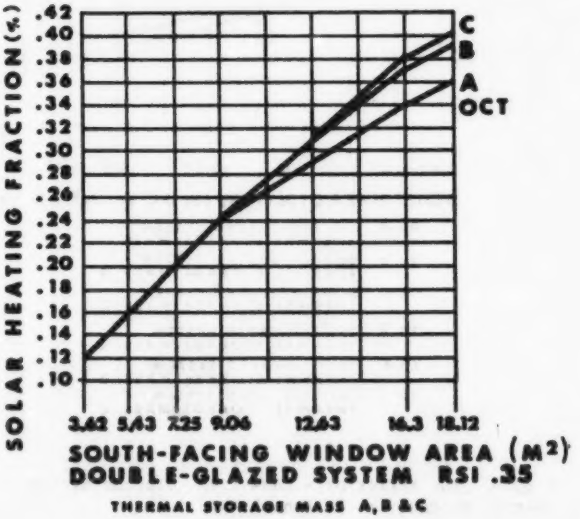

Fig. 4. The Effect of Thermal Storage on the SHF.

SHF values for each mass level were also plotted. Fig. 4 indicates that higher SHF values are obtained when provision is made for thermal storage and that higher SHF values can be obtained with mass C than with masses A or B.

An examination of the influence of south-facing windows upon the study model's AHR was made by comparing monthly values (watts) of the predicted auxiliary heating consumption. Fig. 5 indicates that the AHR decreases with increased areas of south-facing windows and that the rate of decrease varies with each month. The exceptions are December and January for mass levels A and B. There are also slight increases in AHR values with mass level C using double-glazed systems for April and with mass level B using triple-glazed systems for February, March and May (Fig. 6).

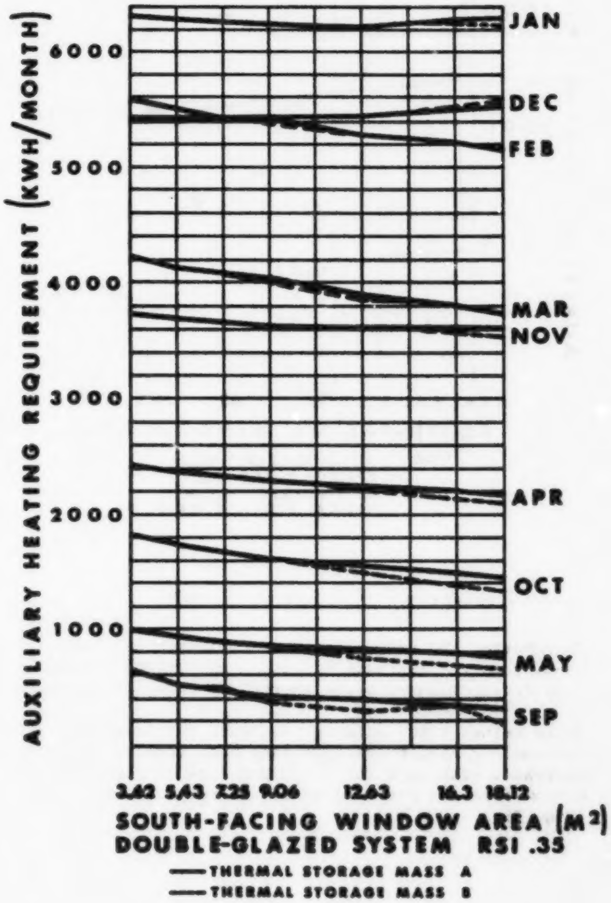

Fig. 5. The Effect of Window Area on the AHR.

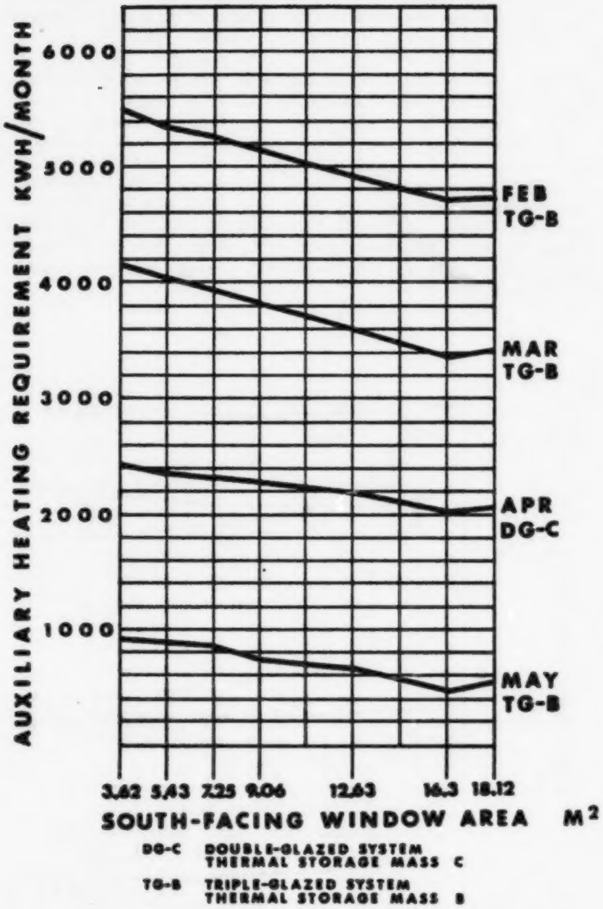

Fig. 6. Exceptions to Reductions in AHR.

The charted AHR values indicate that less auxiliary heating energy is required with high thermal storage mass levels than with low thermal storage mass levels.

These values also indicate that with triple-glazed systems and high thermal storage mass levels, the AHR decreases with each increment increase in south-facing window area for every month of the heating season (Fig. 7).

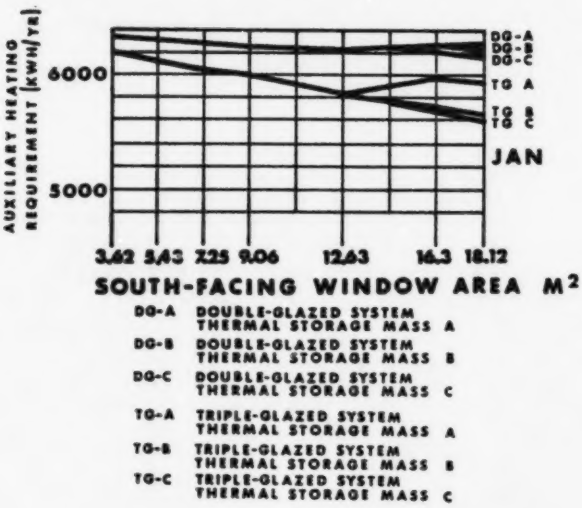

Fig. 7. The Effect of Thermal Storage on the AHR.

An examination of the annual AHR values indicates that for the study model (mass level A), increasing the double-glazed south-facing window area from 3.62 $M^2$ to 18.12 $M^2$ reduced the seasonal AHR by 6.8%. By using triple-glazed windows the AHR was reduced a further 8.6% to 15.4%. A reduction of 19% in the AHR is indicated with 18.12 $M^2$ of triple-glazed south-facing windows using mass level C for the thermal storage (Fig. 8).

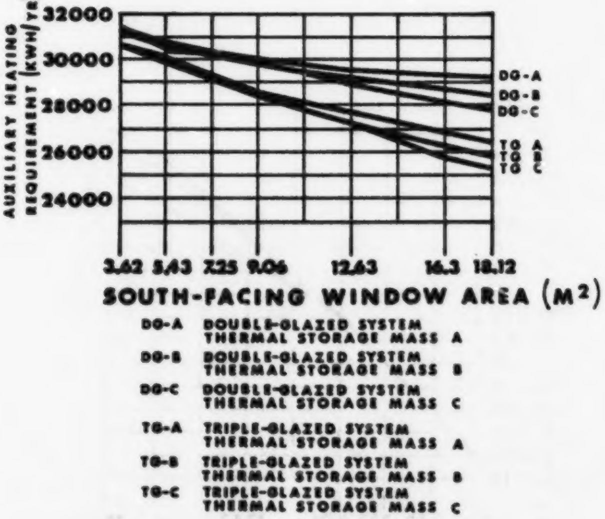

Fig. 8. The Effect of Window Area, Glazing System and Thermal Storage on the Annual AHR.

## 5. CONCLUSIONS

The graphs developed in this study clearly indicate that for the study model, increases in the SHF necessary to reduce the AHR can be achieved with increases in double-glazed (RSI .35) or triple-glazed (RSI .55) south-facing window area.

Triple-glazed south-facing window systems do not produce higher SHF values than double-glazed south-facing window systems, but they do have a major effect on the annual AHR regardless of the thermal storage mass used.

With small areas (less than 9.06 $M^2$) of south-facing windows, thermal storage mass levels B and C (as defined by the Hotcan! program) have little or no effect on either SHF increases or AHR decreases. With large (more than 9.06 $M^2$) window areas, however, the effect of these mass levels becomes important.

## 6. NOMENCLATURE

Auxiliary heating requirement (AHR) - heating supplied by some means other than solar energy (oil, gas, or electricity).

Auxiliary heating requirement values - monthly and annual auxiliary heating in addition to solar and internal heat gains, required to maintain an inside temperature of 21 C. These values, expressed in KWHRS, were derived through the Hotcan Energy Analysis Program.

Hotcan 3.0 - is a computer model for estimating the design heat loss and annual space heating requirement of residences and small buildings that do not require simultaneous heating and cooling. The program uses a month by month calculation technique. Steady-state heat loss calculations for above grade heat losses are used. Improved models for below grade heat losses and utilization of solar and internal gains are included, based on methods developed at the National Research Council of Canada. The input to the program defines the house envelope by such values as the component and sub-component areas and R- values, envelope tightness and air change rates, and window geometry. The program output includes the design heat loss, the thermal load on a daily basis for each month, the corresponding solar and internal gains, and the space heating load.

Solar heating fraction (SHF) - ratio of the useful solar input to the space heating requirement in a given period. In this study, the periods are for each month of the heating system and for the entire heating season.

Solar heating fraction values - monthly and annual solar contribution to the total space heating requirement expressed as a percentage. Values for this study were derived through the Hotcan/R-2000 Energy Analysis program.

Solar heat gain- an increase in the amount of heat contained in a space resulting from direct solar radiation.

Solar noon - that instant of any day at which the sun crosses the meridian of the observer and thus has its maximum altitude.

Study model - in order to generate a data base through Hotcan!, a study model had to be developed. This hypothetical model, a two storey single family house, is based on new house designs offered on the current (1986) Winnipeg market. For this study the building was assumed to be rectangular in shape and of wood frame construction over a poured in place concrete basement. South facing window area, window shading, glazing systems, and thermal storage mass levels were varied.

Thermal mass - the amount of potential heat capacity available in a given assembly or system. Concrete floors, brick walls, extra layers of gyproc, and other containers are examples of thermal mass. Four mass levels are available in the Hotcan/R-2000 Energy Analysis program. These are as follows:

- thermal storage mass level A - wood frame construction, one-half inch gyproc walls and ceilings and carpet over a wood floor.
- thermal storage mass level B - as A, except two-inch gyproc walls and one-inch gyproc ceiling.
- thermal storage mass level C - interior wall finish of four inch brick, one-half inch gyproc ceiling, and carpet over a wood floor.
- thermal storage mass level D - very heavy commercial office building, twelve inch concrete floor. This level is not applicable to the study model.

## 7. REFERENCES

(1) Lux, M. Hotcan 3.0 Guide and User's Manual. Computer Program Mo 54 of the Division of Building Research. Developed by the National Research Council of Canada. Produced under license from Canadian Patents and Development Limited, Ottawa, April, 1985.

(2) Cole, R.J. Solar Heat Gain Through Windows For Selected Locations in Canada. Solar Energy Society of Canada, Inc. 1. Winnipeg: SESCI, 1982.

(3) International Solar Energy Society. "Glossary of Terms Used in Solar Energy". Solar Energy 33.1 (Jan. 1984): 97-114.

# WHAT SHALL WE DO WITH SUPER-WINDOWS ?

Cyril Carter
Trent University
Peterborough, Ontario K9J 7B8

## ABSTRACT

This paper uses simple quantitative arguments and computer simulations to compare the use of super-glazings in various energy-efficient and passive solar building designs. We show that south-facing super-windows would save some energy in standard superinsulated, direct gain and indirect gain designs. North-facing superwindows do not save energy in such standard passive designs, but would do so in innovative super-solar designs which incorporate remote thermal storage and/or a glazed buffer space, like an atrium or sunspace, in which quite large temperature variations are acceptable. Such designs are hardly competitive with superinsulated designs at present, but could become so with a trend towards more efficient appliances, and an accompanying reduction in internal heat gains. Temperature variations in such glazed buffer spaces are large by human comfort standards, but would be much less with super-windows than with standard glazings, and would permit more possible uses for the buffer space.

## 1. INTRODUCTION

Considerable research effort is being invested in the development of super-windows, which might perhaps have the solar transmission properties of double glazing but double the thermal insulation of triple glazing, say a transmittance of .8 and a thermal resistance of 1.0 RSI (1,2,3). Currently, the best commercially available glazing has a transmittance of .7 and a thermal resistance of .7 RSI. The so-called hard-coat low e double-glazed glass unit now commonly available from glass dealers has a transmittance of .7 and a thermal resistance of .5 RSI, or roughly the same properties as a standard triple-glazed unit.

Less thought seems to have been given to the possible uses of superwindows. It is sometimes rather glibly stated that even a north-facing super-window would gain more winter diffuse solar energy than it would lose in heat. The hidden implication here is that we could heat our buildings simply by covering their north and south walls with super-windows. Unfortunately the pressing demand for a balance between mass and glass to maintain an even comfortable interior temperature is not so easily satisfied.

A north-facing super-window could indeed provide considerable net heat in daytime, but it would still lose considerably more heat at night than a well-insulated wall. A south-facing super-window would have a larger net heat gain than an ordinary window, but unless appropriate extra thermal storage is provided, some of this extra gain could not be utilised. We will analyse the possible uses of a .8 transmittance, 1 RSI super-glazing by a series of simple quantitative calculations. First we consider the net energy transmission characteristics of the glazing on its own with an interior temperature of 20°C and ambient temperatures of 0 and -20°C, and varying incident solar radiation, and compare these with other possible components of a building envelope. Secondly we will do some simple network model simulations in which the glazing is considered as a part of a complete building.

## 2. NET ENERGY TRANSMISSION THROUGH GLAZINGS

Table 1 gives the net energy transmitted through standard double, triple glass and super-glass, with bright sunshine of 600 watts/m$^2$, and with diffuse sunshine of 80 watts/m$^2$. Similar net energy losses (with - sign) are given for night conditions for the glazing alone and the glazing with RSI 2 shutters. The final row gives an average 24-hour cloudy-day energy transmission, evaluated as .4 diffuse sunshine + .6 night. All of these values vary linearly with ambient temperature, so values for ambient temperatures other than the two given can be found by linear interpolation.

The values in Table 1 are appropriate for most of Canada except the far north. Much of Eastern and Central Canada and the Prairies has a mean winter ambient temperature between -5 and -10 °C, where super-glazing increases the bright day net solar transmission by about 10 percent. Thus to avoid overheating in a solar-tempered or direct-gain building, other factors being equal, the glazed area needs to be decreased by about 10 percent when super-glazing is used. However, at lower ambient temperatures, and in diffuse sunshine, the super glazing gives a larger net increase, so we can expect a higher net utilisation of solar energy from the smaller glazed area in all climates, with the actual increase depending on the cli-mate. Table 2 gives approximate data for Toronto and Winnipeg.

TABLE 1. Net energy (watts/m$^2$) through glazings with interior temperature, 20°C.

| | Ambient 0°C | | | Ambient -20°C | | |
|---|---|---|---|---|---|---|
| | double glaze | triple glaze | super glaze | double glaze | triple glaze | super glaze |
| Bright sun 600 w/m$^2$ | 540 | 500 | 580 | 480 | 460 | 560 |
| Diffuse sun 80 w/m$^2$ | 20 | 32 | 60 | -40 | -8 | 40 |
| Night: | | | | | | |
| glazing | -60 | -40 | -20 | -120 | -80 | -40 |
| glazing + shutters | -9 | -8 | -7 | -17 | -16 | -13 |
| Average cloudy day | | | | | | |
| glazing | -28 | -11 | -12 | -88 | -51 | -8 |
| glazing + shutters | 3 | 8 | 20 | -26 | -12 | 8 |

TABLE 2. Simplified meteorological data

| | ambient oC | Number of hours during heating season | | |
|---|---|---|---|---|
| | | bright sun | diffuse sun | night |
| Toronto | 0 | 600 | 1080 | 1920 |
| | -20 | 120 | 200 | 400 |
| | (mid October - mid April) | | | |
| Winnipeg | 0 | 600 | 840 | 1680 |
| | -20 | 360 | 720 | 1080 |
| | (October - April) | | | |

The entries in Table 2 are chosen to fit the numbers of daylight hours, bright sunshine hours, and heating degree days. Since the net energy values in Table 1 vary linearly with the ambient temperature, there is no need to use the exact incidences of ambient temperatures and sunshine conditions. When the data from Tables 1 and 2 are combined, we obtain the results given in Table 3 for the total seasonal net energy flows through normal and super-glazings facing south and north.

TABLE 3. Net seasonal energy flows through glazings

Seasonal net energy flow, kwh/m$^2$

| | South-facing | | | North-facing | | |
|---|---|---|---|---|---|---|
| | double glaze | d.glaze +insul. | super-glaze | double glaze | d.glaze +insul. | super-glaze |
| Toronto | 235 | 372 | 437 | -139 | -2 | 62 |
| Winnipeg | 254 | 454 | 552 | -245 | -45 | 53 |

As explained above, provided the super-glazed area is reduced by about 10 percent to prevent overheating, it is likely that most of the net solar energy gain through the glazing can be utilised.

On the basis of the above figures, the use of super-glazing looks promising. There is a significant overall increase in useful solar gain through south-facing windows, and the net loss through north-facing double glazing is turned into a seasonal net gain through north-facing super-glazing. Super-glazing even performs better than double glazing with night insulation. There are several problems however.

North-facing super-glazing does have a net seasonal heat gain, but it loses considerably more heat at night than a RSI 5 wall, and has a lower inside surface temperature. At -20°C ambient, the surface temperatures would be 16°C for super-glazing, 18°C for insulated glazing, and 19° for the wall. So it would be rather uncomfortable to have too much uncovered glazed area in a living space.

A second problem with a north-facing super window is that it has a bright-sunshine net gain about 10 percent of a south-facing window, so that the south-facing glazed area would have to be reduced to prevent overheating. Table 3 shows that the actual seasonal net gain for a north-facing window is about 10 percent of a south-facing window, so a more sophisticated energy calculation is needed to decide whether large north-facing glazed areas are desirable energy-wise in a solar-tempered or direct-gain house.

A third problem requiring further study is the comparison between south-facing super-glazing and double-glazing with night insulation. Table 3 indicates that the super-glazing gives a seasonal net heat gain larger by 15 to 20 percent, but this involves both a larger heat gain by day, and a larger heat loss by night, when ambient temperatures are usually lower. With the same thermal storage, the super-glazing will give rather larger temperature swings, so again a more detailed study is needed to decide which is more energy-efficient. We shall study these problem areas with the aid of some simple computer network simulations.

Currently, a large part of the heat load of a superinsulated house is met by internal gains from appliances and people. With the development of more efficient appliances, internal heat gains will decrease, and there will be an opportunity to utilise more solar gain. Keeping these developments in mind, we have done all our simulations using the rather low value of 500 watts for the average internal gain.

## 3. SIMPLE NETWORK SIMULATIONS

The idea of representing a building by a heat transfer network is well-established in the passive solar simulation field (4,5). Often very large non-linear networks are used with very detailed building and meteorological data, in an attempt to predict accurately the energy performance of a building. The utility of this approach has often been questioned, not least by the present author (6). Here, however, we are interested in a conceptual study of the use of a building material which does not currently exist, but may be available sometime in the future. For this purpose, there is no alternative to a simulation study, but the simulation should be kept as simple as possible. Accordingly, we shall use only small linear networks. Generally the approach will be to use as few nodes in the network as are needed to represent the main macroscopic processes of heat transfer and storage. Thus, for example, a building with a sun-collecting sunspace, an interior space, and thermal storage in the building structure, must be represented by at least three nodes, one for each main component. For detailed simulations, we might use many more nodes, but for conceptual purposes, three nodes will likely be sufficient to show the main differences between such a building and, say, a superinsulated house with no sunspace and minimal glazing.

All simulations have been done using the program NETSPEC, developed by the author (6). NETSPEC computes the temperature variations at the nodes of a linear heat transfer network, using a spectral (modal) expansion (6,7) in terms of the eigenmodes of the heat transfer matrix. The advantage of the modal method is that it enables a very course mesh to be used in time as well as in space, without encountering the stability problems which can occur with finite difference numerical solutions. Thus for crude conceptual calculations, a 24 hour day can often be divided into only two time intervals, day and night, with use of a finer division only where necessary. Simple simulations like this are in fact just one step beyond the basic quantitative analysis of the previous section. They enable the balancing effects of mass and glass to be assessed in a very simple way without complicating the picture with unnecessary detail.

The type of meteorological data to be used in simple simulations depends on the type of building. For standard or superinsulated houses which have little capacity to store heat for much longer than 24 hours, it is adequate to use simple data like that of Table 1, ensuring that total seasonal heating degree-days and sunshine hours are represented correctly. For buildings which can store significant amounts of heat for several days, the statistical distribution of sunshine hours becomes more important. Such a building might be able to manage with virtually zero auxiliary heat if there are no very prolonged sunless periods. This is the reason why many simulations have used representative hour-by-hour meteorological data through a complete year, so that the seasonal distribution of sunshine is input implicitly. Even this approach has its problems, due to the normal variability of meteorological conditions from one year to another, and we consider it too complicated for a simple conceptual study (8).

## 4. STANDARD, DIRECT GAIN & SUPERINSULATED HOUSES

Each house is represented by a 3-node linear network, one node for the interior, and two nodes for the building structure. Simulation is over a 24 hour day, divided into day and night only, with the night temperature 9°C below the day. Four different days are simulated, sunny and dull with average ambient temperatures of 0 and -20 °C. Total solar input is 40 kwh/m$^2$ on a sunny day through South-facing glazing, and 6 kwh/m$^2$ on a dull day though South-facing glazing or on any day through North-facing glazing. Where appropriate, a two day Sunny/Dull sequence is modelled to allow for any carryover of stored solar energy, but this is significant only in one case.

The standard house has a total heat loss of 200 watts/m$^2$, representative of good current building practice, without any special efforts to superinsulate or superseal, and has 10 m$^2$ of windows equally divided between north and south-facing. There is no significant overheating on a sunny day, so total window area is assumed unchanged with the use of superwindows. The direct gain house has a heat loss of 180 watts/m$^2$2, with 20 m$^2$ of South-facing window, reduced by 10 percent when superwindows are used. The superinsulated house has a heat loss of 100 watts/m$^2$, with 10 m$^2$ of South-facing window in the standard case. Two uses of superwindow are considered, 9 m$^2$ south-facing, and a combination of 7 m$^2$ south-facing with 10 m$^2$ north-facing. Both window areas are chosen to limit the maximum interior temperature to 27 °C on a mild sunny day. All input data used in these simulations are given in the Appendix. The total auxiliary heats required on each day are given in Table 4, together with estimated seasonal auxiliary heatloads in Toronto and Winnipeg.

From the results in Table 4, we see that South-facing superwindows reduce seasonal auxiliary heatloads by about 200 kwh/m$^2$ in Toronto, and about 270 kwh/m$^2$ in Winnipeg, and these reductions do not depend strongly on the building type. However, overall, night window shutters save slightly more energy than superglazing. This small advantage of night shutters arises from the balance of better performance on sunny and mild dull days with worse performance on dull cold days.

North-facing superwindows cause a slight deterioration in energy performance of a superinsulated home in both Toronto and Winnipeg. The higher gains through the north-facing windows on a mild dull day are more than counterbalanced by the lower gains on sunny days and the higher losses on cold dull days. We have discussed above other disadvantages of large superglazed areas in a living area. Thus, if and when superwindows do become available, it would appear wise to limit their use on the north-face of living area to what is needed for good daylighting.

Table 4. Auxiliary heat inputs, kwh

| | Heat loss | Daily kwh | | | | Seasonal kwh | |
|---|---|---|---|---|---|---|---|
| | | Sunny | | Dull | | Toronto | |
| | w/$^{\circ}$C | 0 | -20 $^{\circ}$C | 0 | -20 | | Winnipeg |
| Standard home | | | | | | | |
| Doubleglaze | 200 | 63 | 156 | 79 | 173 | 15590 | 22620 |
| Doubleglaze+ nightshutters | 200<br>175 | 54 | 138 | 69 | 156 | 13650 | 19990 |
| Superglaze | 180 | 55 | 139 | 70 | 155 | 13760 | 19990 |
| Direct Gain | | | | | | | |
| Doubleglaze | 180 | 20 | 95 | 63 | 149 | 9860 | 14860 |
| Superglaze | 139 | 0 | 63 | 44 | 110 | 5880 | 9430 |
| Superinsulated | | | | | | | |
| Doubleglaze | 100 | 8 | 50 | 30 | 78 | 4780 | 7470 |
| Doubleglaze+ nightshutters | 100<br>75 | -2 | 32 | 21 | 61 | 2780 | 4760 |
| Superglaze S-facing | 79 | 0 | 35 | 21 | 59 | 2980 | 4960 |
| Superglaze S and N | 85 | 5 | 40 | 19 | 60 | 3280 | 5510 |

## 5. SUNSPACE & ATRIUM DESIGNS

The terms sunspace and atrium are often used interchangeably with no very precise meaning. We shall use the word sunspace to refer to a sun-collecting, extensively glazed, space attached to the south face of a building. We shall use the term atrium for a glazed buffer space attached to any or all exterior walls of the building. More specifically, we have simulated a sunspace with 30 m$^2$ of south-facing glazing, attached to the south face of a superinsulated house. The simulated atrium is a sunspace together with a north-facing buffer space, also with 30 m$^2$ of glazing, and loosely coupled thermally to the south-facing sunspace.

We are using the sunspace and the atrium as simple examples of designs which attempt to increase useful solar gain by storing solar heat outside the main living area of the building. Two different implementations of this design concept are the Harold Hay roof pond and the Norman Saunders sandwich design (8). In the roof pond design, the "sunspace" is actually a pond of water either on the roof in mild climates, or in the attic in colder climates. The Saunders sandwich design has various forms, but it usually includes a physical sunspace, with fans to move the hot air into remote storage in the attic and underfloor. The essential of this design concept is that the building is both superinsulated and superinsolated, and we shall refer to it as a "supersolar" design.

Our simulations of the sunspace and the atrium are intended only as conceptual studies of the possible advantages of using super-glazings in supersolar designs. We make no claims that the particular configurations chosen are in any way the best, but we believe that they do highlight the essential principles involved. The sunspace design has a total heat loss of 99 watts/m$^2$ when standard double glazing is used, dropping to 83 watts/m$^2$ with super-glazing. The atrium design has a heat loss of 82 watts/m$^2$ with superglazing.

The essential of a supersolar design is that solar energy can be stored for use during subsequent cloudy days, so it is necessary to simulate over several-day periods. Table 5 gives simulation results for single cloudy days at ambients of 0$^{\circ}$C and -20$^{\circ}$C, for a 3 day sun/dull/dull period at 0$^{\circ}$C and a 2 day sun/dull period at -20$^{\circ}$C. As discussed above, the conversion of such simulation results into a seasonal heat load requires information about the statistical distribution of sunshine as well as the absolute amount. The last columns in Table 5 give estimates of these seasonal loads for

TABLE 5. Simulation results for sunspace and atrium.

| | Heat loss | Auxiliary heat inputs, kwh | | | | | |
|---|---|---|---|---|---|---|---|
| | | Period kwh | | | | Seasonal kwh | |
| | | Sun/Dull | Sun/Dull | Dull | | Toronto | |
| | w/$^{\circ}$C | /Dull,0 | -20 $^{\circ}$C | 0 | -20 | | Winnipeg |
| Sunspace doubleglaze | 99 | 40 | 137 | 29 | 76 | 3370 | 5570 |
| Sunspace superglaze | 83 | 28 | 65 | 21 | 61 | 2040 | 3240 |
| Atrium superglaze | 82 | 0 | 27 | 13 | 52 | 600 | 1460 |

| | Minimum/maximum sunspace $^{\circ}$C | | | |
|---|---|---|---|---|
| | Sun/Dull/Dull | Sun/Dull | Dull | Dull |
| | 0 | -20 $^{\circ}$C | 0 | -20 |
| Sunspace doubleglaze | 10/36 | 1/23 | 9/13 | -6/-2 |
| Sunspace sauperglaze | 21/45 | 17/40 | 16/19 | 3/6 |
| Atrium, South space superglaze | 20/43 | 19/42 | 16/19 | 3/6 |
| North space | 19/30 | 15/25 | 15/21 | 2/8 |

Toronto and Winnipeg, but we caution that they are less reliable estimates than those given in Table 4.

The simulation results in Table 5 indicate that the super-solar designs can be expected to need smaller auxiliary heat loads than superinsulated houses, and the atrium design comes close to zero auxiliary energy. In contrast to the superinsulated house, the north-facing glazing in the atrium always saves energy. This is the case for all four simulation periods considered in Table 5, so it must be true overall, whatever the seasonal statistical distribution of sunshine might be.

The maximum and minimum temperatures in Table 5 indicate that the north space in the atrium design could be a very pleasant area for various purposes. It is subject to much smaller temperature variations than the south space, and remains above freezing with ambient temperatures of -20°C.

## 6. CONCLUSIONS

South-facing superwindows would reduce auxiliary heat-loads in passive solar houses by upwards of 200 $kwh/m^2$ in eastern, central and mid-Canada. They would provide about the same savings as the use of night insulation shutters on conventional windows, so their use will be decided by economic and other non-technical factors. In spite of the seasonal net energy gains through north-facing super-windows, large areas of north-facing windows are not a good idea in building living spaces. North-facing super-glazing holds great promise for use in innovative super-solar designs which have south and north buffer spaces surrounding the main living areas. North-facing spaces with super-glazing have comparatively small temperature swings, and could be very attractive areas for growing plants, recreational activities, etc.

The actual use of superwindows will depend of course on whether the technical specifications assumed in this study can be achieved or surpassed, and at what cost.

## 6. REFERENCES

(1) J.E,Ferguson and J.L. Wright, Computer Simulation of the Thermal Performance of Super Windows, SESCI'84 Conference Proceedings, 251-4, 1984, SESCI

(2) Jerry Germer, A Revolution in Glazing, Solar Age, August 1985.

(3) Day Chahroudi, The Future of High-Performance Glazings, Solar Age, February 1986.

(4) R.D. McFarland, PASOLE: A general simulation program for passive solar energy, Los Alamos Report UC-59, 1978.

(5) C. Carter, Solving the Heat Transfer Netrwork Equations in Passive Solar Simulations, 5th US National Passive Solar Conference Proceedings, 238-42, 1978, American Section, ISES.

(6) C. Carter, J. DeVilliers, Principles of Passive Solar Building Design, to be published by Pergamon, 1986.

(7) C. Carter, Predicting Passive Performance using modal expansions, 3rd US National Passive Solar Conference Proceedings, 309-13, 1979, American Section ISES.

(8) C. Carter, Some Passive Solar Principles Revisited, SESCI'84 Conference Proceedings, 212-6, 1984, SESCI.

## 7. APPENDIX

Building data used in the simulations

Standard, direct gain and superinsulated houses all are represented by a 3 node network plus ambient node. Node 1 is house interior, nodes 2,3 building structure, node 4 ambient.

Standard house

| | Node | 1 | 2 | 3 | 4 | |
|---|---|---|---|---|---|---|
| Thermal masses | | 1500 | 1000 | 1000 | | wthr/°C |
| Heat transfer | 1 | | 240 | 0 | 120 | |
| coefficients | 2 | | | 240 | 0 | |
| | 3 | | | | 240 | wt/°C |

With night shutters, coefficient(1,2) is 95
With super glazing, coefficient(1,2) is 100

Direct Gain

| | Node | 1 | 2 | 3 | 4 | |
|---|---|---|---|---|---|---|
| Thermal masses | | 4000 | 2000 | 2000 | | wthr/°C |
| Heat transfer | 1 | | 240 | 0 | 120 | |
| coefficients | 2 | | | 240 | 0 | |
| doubleglazing | 3 | | | | 120 | wt/°C |
| Heat transfer | 1 | | 242 | 0 | 78 | |
| coefficients | 2 | | | 242 | 0 | |
| superglazing | 3 | | | | 121 | |

### Superinsulated

|  | Node | 1 | 2 | 3 | 4 |  |
|---|---|---|---|---|---|---|
| Thermal masses |  | 2000 | 1000 | 1000 |  | wthr/°C |
| Heat transfer | 1 |  | 240 | 0 | 60 |  |
| coefficients | 2 |  |  | 240 | 0 |  |
| doubleglazing | 3 |  |  |  | 60 | wt/°C |

With night shutters, coefficient(1,2) is 35

|  | Node | 1 | 2 | 3 | 4 |
|---|---|---|---|---|---|
| Heat transfer | 1 |  | 241 | 0 | 39 |
| coefficients | 2 |  |  | 241 | 0 |
| S.superglazing | 3 |  |  |  | 60 |

|  | Node | 1 | 2 | 3 | 4 |
|---|---|---|---|---|---|
| Heat transfer | 1 |  | 232 | 0 | 47 |
| coefficients | 2 |  |  | 232 | 0 |
| S&N.superglazing | 3 |  |  |  | 57 |

The sunspace house is also represented by 3 nodes. Node 1 is sunspace, node 2 building interior, node 3 structure, node 4 ambient. The atrium house is represented by a similar network, but with node 3 the north-facing buffer space.

### Sunspace design

|  | Node | 1 | 2 | 3 | 4 |  |
|---|---|---|---|---|---|---|
| Thermal masses |  | 4000 | 1000 | 2000 |  | wthr/°C |
| Heat transfer | 1 |  | 40 | 0 | 100 |  |
| coefficients | 2 |  |  | 120 | 40 |  |
|  | 3 |  |  |  | 40 | wt/°C |

With super glazing, coefficient(1,2) is 20
coefficient(1,4) is 40

### Atrium design

|  | Node | 1 | 2 | 3 | 4 |  |
|---|---|---|---|---|---|---|
| Thermal masses |  | 4000 | 2000 | 2000 |  | wthr/°C |
| Heat transfer | 1 |  | 20 | 80 | 40 |  |
| coefficients | 2 |  |  | 20 | 55 |  |
|  | 3 |  |  |  | 40 | wt/°C |

For both sunspace and atrium designs, coefficient(1,2) may be increased upto 500 as needed by a fan.

# EFFECTIVE U-VALUES AND SHADING COEFFICIENTS OF PREHEAT/SUPPLY AIR GLAZING SYSTEMS

John L. Wright

Department of Mechanical Engineering
University of Waterloo
Waterloo, Ontario
N2L 3G1

## ABSTRACT

Research is documented which makes use of a computer program called VISION. This computer program was developed specifically to provide a detailed analysis of heat transfer occuring in glazing systems. VISION was modified to perform an analysis of the energy flows in supply air windows. A model used to quantify heat transfer in the supply air flow is described. Ventilation air is brought in through supply air windows and the energy recovered by the preheat of the air flow is credited to the thermal performance of the window itself. Thus, the net energy flow between the conditioned space and the window was used to calculate an effective U-value and shading coefficient. The use of these "effective" window performance parameters permits the subsequent quantification of energy flows to or from the supply air glazing system without the necessity of modelling the detailed mechanisms of energy transport within the glazing system itself. A variety of glazing system designs are simulated. Indoor glazing temperature is reported for each system. In all cases the presence of preheat ventilation improved the effective shading coefficient moderately and increased the effective thermal resistance appreciably.

## INTRODUCTION

Substantial energy conservation benefits are attainable through the use of "supply air windows". In order to reduce the space heating load the supply air required for ventilation passes into the building by way of a flow path provided within the glazing system instead of through leakage sites or openings located elsewhere in the building envelope. This glazing system arrangement is shown conceptually in Figure 1. Figure 1 also shows the numbering system that is applied to the indoor, outdoor, supply air and individual glazing temperature nodes. As the air passes between the glazings it is preheated by drawing on absorbed solar gains and/or thermal losses from the building interior. The need to restrict supply air flow solely to the window passages indicates that supply air windows should perform well when installed in a very airtight building envelope and used in conjunction with an exhaust air device that holds the building at a slightly negative pressure.

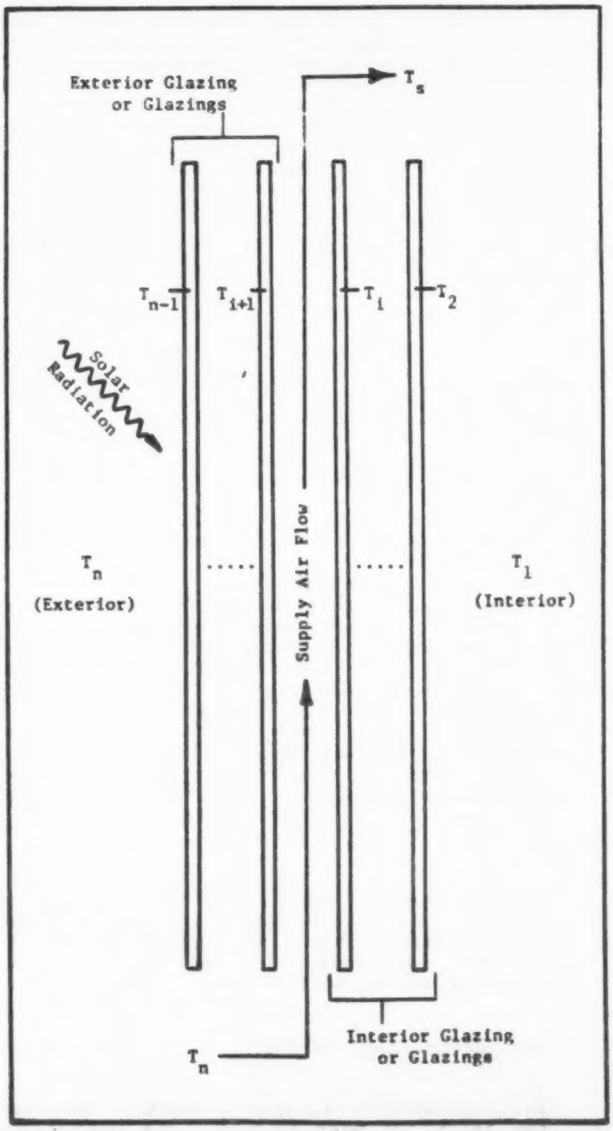

Figure 1: Preheat/Supply Air Flow Concept

Results of the relatively modest amount of research that has been performed on supply air windows are encouraging. Korkala, etal [1] examined some practical aspects of several double glazed configurations showing that useful amounts of supply air could be taken in without serious loss of thermal comfort. Barakat has noted [2] a decrease in required space heating energy of about 25% when one unit of the NRC Passive Solar Facility [3] (located in Ottawa) was fitted with triple glazed supply air windows and compared to a similar unit fitted with conventional double glazed windows. A decrease in required energy was also noted when triple glazed supply air windows were compared to conventional triple glazed windows.

The VISION computer program [4] has been modified in order to simulate the performance of supply air glazing systems. VISION was developed specifically to provide reliable U-value and shading coefficient estimates for innovative glazing systems. Heat transfer within the glazing system is quantified using a detailed one dimensional (1-D) analysis. The capabilities of this analysis have been extended to include the treatment of supply air flow between glazings without resorting to a major rewrite of the VISION source code. Instead, the existing program has been modified to only a limited degree and is tricked to model the internal air flow. The conduction/convection heat transfer rates from the walls adjacent the forced air flow are determined using a two dimensional (2-D) analytical solution [5] of basic equations describing the elemental energy balance in the fluid flow. The two solutions that are applied - one dealing with heat transfer between glazings and the other with the heat transfer to the forced flow of supply air - are well suited to be applied simultaneously since both are based on the assumption that each glazing is isothermal.

The results of this analysis serve not only to support the intuitive and qualitative understanding of preheat/supply air glazing systems. In addition they provide quantitative feedback regarding the merits of various design options, their energy conservation potential and the principles governing their operation. For instance, it is recognized that the flow of supply air between the glazings will lower the temperature of the indoor glazing. Indoor glazing temperature is reported for each system simulated in order to determine the change in allowable indoor humidity.

Glazing system designs range from a simple double glazed system to more complex configurations involving the use of two, three or four glazings, low emissivity (low E) coatings and argon fill gas.

## THE SUPPLY AIR FLOW MODEL

The following paragraphs present an overview of the technique used to model the heat transfer between the glazing system and the supply air flow. This presentation is not complete in every detail. The remaining information can be found in the references provided. The nomenclature needed to understand this analysis is shown in Figure 2.

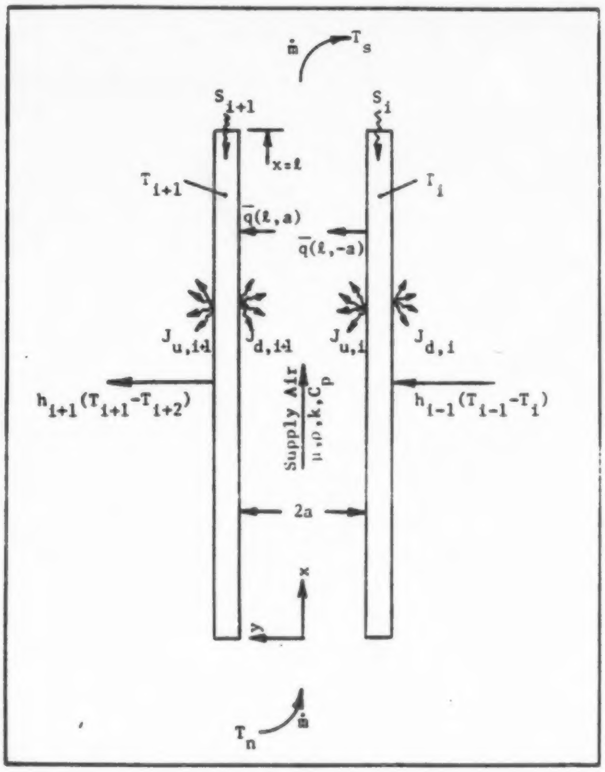

Figure 2: The Supply Air Flow Model

It can be shown that the Reynolds number based on hydraulic diameter and average air speed, $Re_D$, of the supply air flow is given by:

$$Re_D = 2\dot{m}\ell/\mu \tag{1}$$

where $\dot{m}$ is the mass flow rate per unit aperture area, $\mu$ the dynamic viscosity of the air and the length of the flow path is $\ell$. $\ell$ is equal to the height of the window. Note that the hydraulic diameter, D, is equal to four times the half width of the flow gap.

$$D = 4a \tag{2}$$

The value of $\dot{m}$ can be calculated using equation 3.

$$\dot{m} = \rho H(A_f/A_a)ACR \tag{3}$$

where $\rho$ is the air density, H is ceiling height, ACR is the air change rate and $A_f/A_a$ is the ratio of floor area to aperture area. Based on the following assumed values,

$H = 2.44$ m

ACR = 0.5 air changes per hour

and $\Lambda_f/\Lambda_a = 10$

the value of $\dot{m}$ was taken to be 15.6 Kg $m^{-2}$ $hr^{-1}$ for all simulations carried out. Further assuming that $\ell$=1m the Reynolds number was estimated to be $Re_D$=525.

The Reynolds number result shown above indicates that the supply air flow can safely be assumed to be laminar in nature. Referring to equation 1, it can be seen that the height of the window can approach 4m before the critical Reynolds number marking the onset of turbulence (approx. 2000) is approached. The supply air flow in all simulations is treated as laminar, steady and fully developed.

An energy balance applied to an elemental control volume in the supply air flow, while neglecting conduction in the flow direction, yields equation 4:

$$u(\partial T/\partial x) = \alpha(\partial^2 T/\partial y^2) \qquad (4)$$

where $\alpha$ is the thermal diffusivity of the air and u is the velocity component in the x direction. Solutions to equation 4 can be found in references 5 through 10 among others. The particular solution used in this analysis is found in reference 5 where Cess and Shaffer express the 2-D temperature solution in terms of Stieltjes integrals. Application of the Fourier-Biot law to the temperature field yields an expression for the local heat flux in the y direction.

$$q(x,y) = (-k/a)[(1 - 2\theta'(x,y))(T_{i+1}-T_n) + (-1 + 2\theta'(x,-y))(T_i-T_n)]/2 \qquad (5)$$

Once the flow space half width, a, and the Peclet number are fixed the function $\theta'(x,y)$ is a function of x and y only. The Peclet number, Pe, is given by:

$$Pe = Re_D \, Pr \qquad (6)$$

where Pr is the Prandtl number of the air flow. An expression for $\theta(x,y)$ is given in reference 5.

The average heat flux to the supply air at the adjacent glazings can be found by setting y=a or y=-a in equation 5 and integrating with respect to x from x=0 to x=$\ell$.

$$\bar{q}(\ell,a) = (1/\ell)\int_0^{\ell} q(x,a)\,dx \qquad (7)$$

$$\bar{q}(\ell,-a) = (1/\ell)\int_0^{\ell} q(x,-a)\,dx \qquad (8)$$

These average heat transfer rates, $\bar{q}(\ell,a)$ and $\bar{q}(\ell,-a)$ are shown in Figure 2. The net heat flux from the glazings to the supply air is given by:

$$q_s = \bar{q}(\ell,-a) - \bar{q}(\ell,a) \qquad (9)$$

and can be used to calculate the temperature of the supply air as it leaves the glazing system, $T_s$.

$$T_s = T_n + q_s/(\dot{m}C_p) \qquad (10)$$

where $C_p$ is the specific heat of the supply air.

## INCORPORATION OF THE SUPPLY AIR MODEL

The VISION computer program quantifies the various energy flows within a glazing system by simultaneously applying an energy balance to each individual glazing. Reference 4 can be used as a complete source of detailed information. This energy balance applied at the $i^{th}$ glazing is given by equation 11.

$$h_{i-1}(T_{i-1} - T_i) + J_{u,i-1} - J_{d,i} + S_i = h_i(T_i - T_{i+1}) + J_{u,i} - J_{d,i+1} \qquad (11)$$

The heat transfer coefficients, $h_{i-1}$ and $h_i$, are used to quantify convective heat transfer from glazing i-1 to glazing i and from glazing i to glazing i+1, respectively. The quantities $J_u$ and $J_d$ represent radiosities that account for various upward and downward (in this case outdoor and indoor) bound fluxes of thermal radiation. Solar radiation which is absorbed at the $i^{th}$ glazing and appears as an energy source is equal to $S_i$.

Referring to the $i^{th}$ glazing shown in Figure 2 it can be seen that equation 11 cannot be directly applied. The heat transfer coefficient $h_i$ has no apparent meaning in the supply air gap. Instead, the VISION computer code is tricked using a two step procedure. First, the coefficient $h_i$ at the air flow gap is set equal to zero. This eliminates what VISION sees as convective heat transfer across the gap. Second, VISION is supplied with a modified source term, $S_i'$, in the place of $S_i$. $S_i'$ represents the energy source due to absorbed solar radiation minus the energy lost to the supply air flow.

$$S_i' = S_i - \bar{q}(\ell,-a) \qquad (12)$$

Substitution into equation 11 yields a more meaningful energy balance.

$$h_{i-1}(T_{i-1} - T_i) + J_{u,i-1} - J_{d,i} + S_i' = J_{u,i} - J_{d,i+1} \qquad (13)$$

Applying the same procedure at glazing i+1 gives:

$$S'_{i+1} = S_{i+1} + \overline{q}(\ell,a) \qquad (14)$$

and
$$J_{u,i} - J_{d,i+1} + S'_{i+1} = h_{i+1}(T_{i+1} - T_{i+2}) + J_{u,i+1} - J_{d,i+2} \qquad (15)$$

VISION incorporates an iterative procedure where glazing temperatures are determined as a function of the various heat transfer coefficients within the glazing system/-environment array. At each iteration the heat transfer coefficients are updated and iteration continues until the temperature solution converges. In the supply air solution the heat flux to the supply air was also updated at each iteration. When convergence was reached a full solution including all glazing temperatures, heat transfer rates and supply air temperatures had been found.

## CALCULATION OF EFFECTIVE U-VALUE

The U-value is calculated using an indoor temperature of $T_1$=21 C, an outdoor temperature of $T_n$ = -18 C, a fraction cloud cover of 0.5 and zero solar radiation. See reference 4 for more detail. VISION performs this calculation using the total heat flux from the conditioned space to the interior glazing. An effective U-value, $U_e$ , can be calculated by crediting the window with the energy gained by the supply air flow, $q_s$.

$$U_e = [h_1(T_1 - T_2) + J_{u,1} - J_{d,2} - q_s]/(T_1 - T_n) \qquad (16)$$

In the absense of solar radiation the heat flux from the interior to the inside glazing is greater than the heat flux from the outside glazing to the exterior environment by the amount of energy transferred to the supply air, $q_s$. Therefore, a simpler expression for the effective U-value is:

$$U_e = [h_{n-1}(T_{n-1} - T_n) + J_{u,n-1} - J_{d,n}]/(T_1 - T_n) \qquad (17)$$

## CALCULATION OF EFFECTIVE SHADING COEFFICIENT

The shading coefficient is calculated in the absence of indoor/outdoor temperature difference ($T_1$=$T_n$=19 C), 741 W $m^{-2}$ of incident solar radiation and zero cloud cover. Reference 4 provides detailed information. The effective shading coefficient , $SC_e$ , is found when the window is credited with the supply air energy gain, $q_s$, in addition to the customary quantities of absorbed/retransmitted and directly transmitted solar gain. The total energy gain is divided by the energy gain of a conventional single glazed window subjected to the same conditions , $q_{ref}$.

$$SC_e = [h_1(T_2 - T_1) + S_1 + q_s]/q_{ref} \qquad (q_{ref} = 612.3 \text{ W m}^{-2}) \qquad (18)$$

## OPTICAL PROPERTIES

All of the glazing systems simulated consisted of conventional glass with or without one of two types of low E coating. Input data used to characterize the solar properties of glass were index of refraction ($\underline{n}$=1.52) and extinction coefficient (K=0.024 $mm^{-1}$). All glazings were taken to be 3.175 mm thick. The glass/low E glazing element was modelled as having 60% normal solar transmissivity, and normal reflectivities of 25% and 22% with respect to solar radiation incident from the coating or substrate sides, respectively.

The hemispheric/hemispheric long wave ( $\lambda$ >3μm) properties were specified such that all glazings were opaque. The emissivities of the low E coating used in sealed spaces and of plain glass were 0.09 and 0.84, respectively. In cases where a low E coating was used in an air flow gap the emissivity was set at 0.35 in order to model the more durable coating that would be required.

## SIMULATION RESULTS

Computer simulations were carried out for eleven different glazing systems that incorporate a variety of low E coating(s), air flow locations and fill gas options. All pane spacings including the supply air flow gap were set at 15 mm. Each glazing system was simulated with and without supply air flow. Thus, four primary results consisting of two U-values and two shading coefficients were calculated for each system. These simulation results plus a variety of intermediate calculation results are presented in Table 1.

Examining the U-value results shown in the left hand portion of Table 1 a number of observations can be made. In all of the glazing systems simulated the presence of supply air flow reduced the U-value. Although the amount of reduction in U-value might vary widely from one system to another, it is noteworthy that this reduction was always appreciable. The smallest U-value reduction was 31%.

It is also remarkable that the U-value reduction can be greater for systems that are more intricate and that have relatively low U-values without supply air flow. Most of the two and three glazing systems exhibit a 30 to 40% U-value reduction but all of the four glazing systems provide a reduction of more than 50% when supply air is used. This sizeable reduction of an already low U-value results in exceptionally low effective U-values. For instance, system eleven shows a 58% reduction in U-value giving an effective U-

TABLE 1: PREHEAT/SUPPLY AIR SIMULATION RESULTS

Subscript "e" indicates presence of supply air

Marks low E coating

| System No. | | U-VALUE | | | | | SHADING COEFFICIENT | | | |
|---|---|---|---|---|---|---|---|---|---|---|
| | | U $W/m^2C$ | $T_2$ C | $T_{2,e}$ C | $T_s$ C | $U_e$ $W/m^2C$ | $S_1$ $W/m^2$ | SC | $q_s$ $W/m^2$ | $SC_e$ |
| 1 | 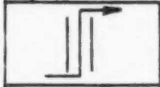 | 2.88 | 6.2 | 4.3 | -6.7 | 1.94 | 501.2 | 0.87 | 10.4 | 0.88 |
| 2 | 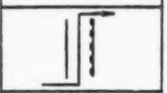 | 2.35 | 9.1 | 7.3 | -5.7 | 1.30 | 358.6 | 0.71 | 21.0 | 0.72 |
| 3 | 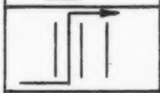 | 1.84 | 11.8 | 10.9 | -11.0 | 1.22 | 425.4 | 0.78 | 19.8 | 0.80 |
| 4 | 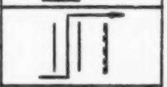 | 1.32 | 14.5 | 13.9 | -13.1 | 0.88 | 307.3 | 0.65 | 26.5 | 0.68 |
| 5 | 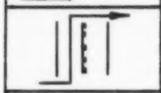 | 1.32 | 14.5 | 13.9 | -13.1 | 0.88 | 306.9 | 0.60 | 41.8 | 0.65 |
| 6 | 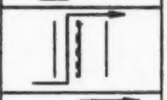 | 1.59 | 13.1 | 12.1 | -9.9 | 0.87 | 306.9 | 0.63 | 36.7 | 0.67 |
| 7 | 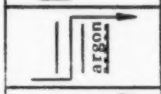 | 1.12 | 15.5 | 14.9 | -13.8 | 0.76 | 307.3 | 0.65 | 26.4 | 0.68 |
| 8 | 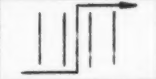 | 1.34 | 14.4 | 11.7 | -7.5 | 0.67 | 362.5 | 0.71 | 40.6 | 0.74 |
| 9 | 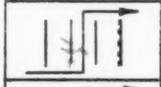 | 1.01 | 16.1 | 14.4 | -10.5 | 0.49 | 263.7 | 0.59 | 53.3 | 0.65 |
| 10 | 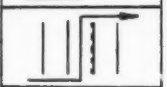 | 1.19 | 15.2 | 12.5 | -7.4 | 0.51 | 263.6 | 0.59 | 58.1 | 0.63 |
| 11 | 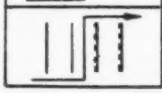 | 0.90 | 16.6 | 14.9 | -10.3 | 0.38 | 194.8 | 0.49 | 77.2 | 0.57 |

value of 0.38 W $m^{-2}$ $C^{-1}$. This is equivalent to a thermal resistance of RSI 2.6 or R 14.9.

The results of the U-value calculations also highlight a relationship between the location of the supply air flow (or the location of thermal resistance) and supply air temperature, $T_s$. As more thermal resistance is added between the supply air flow and the conditioned space the temperature of the supply air flow drops. Compare system one and system three. The addition of one glazing on the interior decreases effective U-value by 37% but at the same time the supply air temperature drops from -6.7 C to -11.0 C. A similar comparison can be made between systems three and four where the only change is the addition of one low E coating. On the other hand the addition of thermal resistance between the supply air gap and the exterior environment not only decreases the effective U-value but an increase in supply air temperature is produced at the same time. This effect can be seen by comparing systems three and eight, four and nine or six and ten.

The inside glazing temperature also varies according to the presence of supply air flow and as a function of the placement of thermal resistance. The presence of supply air always reduces the temperature of the inside glazing. If thermal resistance is added anywhere in the glazing system the temperature of the inner glazing rises and approaches the temperature of the conditioned space. Compare systems three and four, three and six as well as three and eight. However, it is worth noting that only in the case of system one itself was the inside glazing temperature - with supply air present - lower than the inside glazing temperature of a conventional double glazed system (system one) operated without supply air flow. The inside glazing temperature of system three with supply air flow was 10.9 C. This surface temperature corresponds to an allowable relative humidity level in excess of 50%.

The use of a low E coating in the supply air flow gap illustrates an interesting phenomenon. Compare systems five and six. These two configurations provide essentially the same effective U-value but system six delivers supply air at -9.9 C rather than -13.1 C. The same effect can be seen by comparing systems nine and ten. A low E coating placed in the air flow gap suppresses overall heat transfer by reducing radiative exchange across this gap but does not act to reduce the energy transferred directly from the interior to the supply air. In contrast, a low E coating placed in the interior side sealed space does reduce energy flow from the interior to the supply air causing the supply air to enter the room at a lower temperature. As a result of this effect, a low E coating placed in the flow air gap, rather than in the interior side sealed gap, appeared to be of greater benefit. Not only were the resulting supply air temperatures higher but the effective U-values were comparable in spite of the higher emissivity of the durable low E coating used in the flow air gap.

The shading coefficient calculation results shown on the right hand side of Table 1. also show a number of interesting trends. In all systems simulated the presence of supply air flow increased the shading coefficient. Most of these increases are marginal - in the range of from 1 to 5%. Similar to the change in U-value the increase in shading coefficient was greater, as a general trend, for more intricate glazing systems. For example, the shading coefficient of system eleven which has four panes and two low E coatings increased by 16% when supply air was introduced. On the other hand, the more intricate glazing systems have lower shading coefficients and effective shading coefficients as a general rule.

The effective shading coefficient appears to be relatively insensitive to the location of low E coatings that are placed between the supply air flow and the interior. Compare systems four to system five or six. In system four the solar radiation that is absorbed at the low E coating can readily transfer to the conditioned space directly. In systems five and six the solar radiation absorbed at the coating more readily transfers to the supply air and is again supplied to the interior. In the latter case the supply air is given more preheat energy.

## CONCLUDING REMARKS

A calculation method has been presented which makes possible the analysis of a preheat/supply air flow passage within the framework of the VISION computer program. Results are consistent with intuition regarding the mechanisms governing operation of this type of window. Reliable generalizations or "rules of thumb" are difficult to make when dealing with the design of supply air windows. The number of design options is extremely large. Where particular design options are considered a detailed simulation of each system is recommended.

It is noted that the introduction of supply air flow consistently decreased the U-value and increased the shading coefficient of the various glazing systems simulated. These changes were generally larger for more intricate glazing designs. The effective U-values of four glazing systems can be exceptionally small without seriously sacrificing solar gains.

The use of multiple panes and low E coatings can be used to tailor effective U-value and effective shading coefficient in much the same way as is possible with conventional glazing systems. Similar trade-offs exist. In addition, there exists a trade-off between increasing the temperature of the supply air flow and lowering the temperature of the interior glazing. Results from the simulations carried out indicate that interior glazing temperatures are not low enough to aggravate water condensation problems in all but the very simple double glazed system. In light of this finding, it is expected that glazing system design can be more directly determined by the possibility of maximizing the temperature of the supply air. In order to accomplish this goal the use of a durable low E coating in the air flow gap looks promising and warrants further attention.

Effective U-values and effective shading coefficients can be used directly in the place of U-values and shading coefficients as input to building energy analysis programs. However, caution must be exercised because these results are based on a specific rate of ventilation air flow inward (per unit aperture area) at the building envelope. This same inflow rate of unheated air must be included in the building energy analysis. The superior performance of the supply air/preheat window relies on the fact that this ventilation air would be required regardless of its infiltration path.

The work presented in this study raises many questions. It is intended that future work will include prototype testing, the simulation of multiple pass supply air flow passages as well as the sensitivity analysis of performance results with respect to air flow rate and the length and thickness of the air flow gap.

## REFERENCES

[1] Korkala, T., Saarnio, P., Siitonen, V., "Air Intake Arrangements of the Supply Air Window from the View of Comfort and Ventilation Efficiency", Proceedings of the Windows in Buildings Conference, Sweden, June, 1984

[2] Barakat, S.A., Personal communication, December, 1985

[3] Barakat, S.A., "NRCC Passive Solar Test Facility Description and Data Reduction", DBR/NRC Technical note BRN #214, May, 1984.

[4] Ferguson, J.E., Wright, J.L. "VISION: A Computer Program to Evaluate the Thermal Performance of Super Windows", Solar Energy Program, NRC report no. Passive-10.June, 1984.

[5] Cess, R.D., Shaffer, E.C., "Summary of Laminar Heat Transfer Between Parallel Plates With Unsymmetrical Wall Temperatures", Journal of the Aero/Space Sciences, August, 1959, page 538.

[6] Lundberg, R.E., Reynolds, W.C., Kayes, W.M., "Heat Transfer with Laminar Flow in Concentric Annuli with Constant and Variable Wall Temperature with Heat Flux", NASA TN D-1972, Washington, August, 1963.

[7] Yih, C.S., Cermack, J.E., "Laminar Heat Convection in Pipes and Ducts", Civel Engineering Department, Colorado Agricultural and Mechanical College, Fort Collins, Colorado, September, 1951, ONR Contract No. N90nr-82401, NR 063-071/1-19-49.

[8] Prins, J.A., Mulder, J., Schenk, J., "Heat Transfer in Laminary Flow Between Parallel Plates", Applied Scientific Research, Section A Vol 2, pp. 431-438, 1949-51.

[9] Schenk, J., Beckers, H.L., "Heat Transfer in Laminar Flow Between Parallel Plates", Applied Scientific Research, Section A, Vol 4, pp. 405-413, 1953-54.

[10] Sellars, J.R., Tribus, M., Klein, J.S., "Heat Transfer in Laminar Flow in a Round Tube or Flat Conduit - The Graetz Problem Extended, Trans. ASME, Vol. 78, pp. 441-448, 1956.

## ACKNOWLEDGEMENTS

The author acknowledges financial support from The Renewable Energy Branch of The Department of Energy, Mines and Resources.

# A STUDY OF THE THERMAL EFFICIENCY OF SIX NATURAL GAS FUELLED RESIDENTIAL FURNACES

J.D. Dale, Ph.D., P.E.
M.Y. Ackerman, P.E.
J. Kasha
Department of Mechanical Engineering
University of Alberta
Edmonton, Alberta
T6G 2G8

## Abstract

An experimental study of the insitu efficiency of six natural gas fuelled residential furnaces has shown that generally the steady state efficiency is higher than that achieved in an insitu environment. The Canadian Gas Association proposed standard CGA P.1 does however provide a very good estimate of the seasonal insitu efficiency and since it is the rating method used by the manufacturers the rated efficiency is very close to that achieved in a field environment.

Measured air infiltration rates showed that a major reduction in air leakage was produced through the downsizing of the furnace flue as is common when furnace rating and building load are closely matched. Operation of standard and mid efficiency units, those that utilize vertical furnace flues and draft diverters, lead to a measurable increase in test module air infiltration rates while operation of units utilizing blowers to meter combustion air did not.

## Introduction

In response to queries concerning the rated vs insitu thermal efficiency of natural gas fuelled residential furnaces a study involving six furnaces was undertaken in 1984 at the Alberta Home Heating Research Facility. The Alberta Home Heating Research Facility is an experimental facility consisting of six uninhabited test modules, each 49 square meters in plan, located on the University of Alberta farm south of the City of Edmonton, Alberta. The test site is at an altitude of 700m above sea level and as such standard furnaces are normally derated by 10%.

Each of the test modules is unique in one or more ways but all share common features such as full height cast in place concrete basements and elevated roof trusses which will accomodate up to 600mm of insulation without structural modification. Module details pertinent to the present study are shown in Table 1 while complete construction details have been reported previously [1].

Evaluation of the six furnaces took place over a period of two years and utilized two of the test modules; the passive and conservation. The choice of module/furnace combination was based largely on the presence of an existing furnace flue . As indicated in Table 1 the passive module has a flue but the conservation module does not. It was important during the study to modify the module envelopes as little as possible so as not to upset the historic heating energy requirements or alter the building envelope leakage characteristics.

Table 2 lists the furnaces that were evaluated and the module in which they were placed. As indicated in Table 2 three of the furnaces; ICG, Lennox and Amana are condensing models and as such require no vertical flue but may be vented through an exterior wall using a plastic pipe. The Airco furnace is an induced draft model that requires a vertical flue but that reduces off period flue stack flow rates with the use of an orfice plate in the flue. The final two furnaces were a single model, ICG standard, with an atmospheric burner and pilot light that was later upgraded with and electronic ignition and flue damper to control off period losses.

TABLE 1 TEST MODULE DESIGN DETAILS

| Module | Insulation Levels (RSI) Ceiling | Wall | Basement | Flue Diameter (mm) |
|---|---|---|---|---|
| 1) Conservation | 14.08 | 7.04 | 3.52* | none |
| 2) Passive | 7.04 | 3.52 | 1.76* | 100 |
| 3) Standard | 2.11 | 1.76 | 1.76** | 152 |

* insulated externally full height
** insulated externally to 0.61m below grade

TABLE 2 TEST FURNACE DETAILS

| | Input Rating (kW) | Test Module | Description |
|---|---|---|---|
| 1) ICG Standard | 18 | Passive | atmospheric burner |
| 2) ICG Conserver | 18 | Passive | electronic ignition, flue damper |
| 3) Airco Turbo | 18 | Passive | induced draft |
| 4) ICG Ultimate | 16 | Conservation | condensing |
| 5) Lennox Pulse | 12 | Conservation | condensing |
| 6) Amana Energy Command | 13 | Conservation | condensing |

The furnaces were installed in either the Passive or Conservation modules and evaluated over a period of roughly 1700°C days. It should be noted that all of the furnaces tested were new and that the test periods were not long enough to quantify the effects of long term operation on performance.

Each of the furnaces was tested under steady state operation and according to the Canadian Gas Association proposed standard CGA P.1 [2] which provides an estimate of seasonal thermal efficency. To obtain insitu seasonal thermal efficency the furnaces were run on a one week cycle with an electric forced air system providing space heating on alternate weeks. Attempts were also made to determine whether or not efficencies were load dependent.

During the insitu testing natural air infiltration rates were determined on a continous basis using a constant concentration tracer gas ($SF_6$) system.

## Results

### Steady State Thermal Efficiency

Steady state thermal efficiency is a term used to describe the performance of a gaseous fuel appliance after sufficent time has elapsed for exhaust gasses to reach and maintain a stable temperature. During laboratory testing the amount of time required to reach this point may be upwards of 20 minutes. In the past the sizing of furnaces to loads was at best a hit and miss affair with furnace size being determined more often by a simple rule of thumb than any type of detailled calculation. As such, most installed furnaces (especially those in houses which have undergone insulation uprades) are grossly oversized for the load. Testing recently done in one of the authors home in Edmonton showed that the existing furnace operated less than 12% of the time when the ambient temperature was -20°C. During a typical on/off cycle with a period of about 1/2 hour the furnace burners would be on for less than 4 minutes. Under typical winter conditions the furnace would never reach a "steady state" operating point.

The steady state thermal efficiency of each of the furnaces under study was evaluated using methods outlined in the CGA P.1 proposed standard. Measurements of fuel input rate, flue gas composition and temperature were made after sufficent warm up time had elapsed. From these measurements the steady state thermal efficency of each furnace was determined as indicated in Table 3. For the condensing furnaces the procedure was slightly different with condensate collected and weighed over a 30 minute period.

TABLE 3 RESULTS OF LABORATORY TESTING OF NATURAL GAS FURNACES

| Furnace | Rated Efficiency (%) | Steady State Efficiency (%) | Simulated Seasonal (%) |
|---|---|---|---|
| 1. ICG Standard | 77 | 71.6 | 67.3 |
| 2. ICG Conserver | -- | 69.0 | 75.4 |
| 3. Airco Turbo | 83 | 80.6 | 82.9 |
| 4. ICG Ultimate | 92 | 92.4 | 91.6 |
| 5. Lennox Pulse | 98 | 96.4 | 95.3 |
| 6. Amana Energy Command | 98 | 97.2 | 96.3 |

The most striking result during the steady state testing was the unexpectedly high efficencies, 71.6% and 69%, obtained respectivly for the standard and upgraded standard furnaces. Current information and advertizing suggests that the typical thermal efficency of a standard furnace with and atmospheric burner falls in the 50% to 65% range. As indicated in Table 3 the Airco Turbo produced a steady state efficency of 80% while the condensing units tested were all in excess of 90%.

### Simulated Seasonal Efficiency

Simulated seasonal efficencies were also evaluated using the methods outlined in the Canadian Gas Association Standard CGA P.1. As in the steady state test, the seasonal performance test requires that a profile of flue temperature as a function of time be determined while the unit warms up from a cold start and while cooling down from steady state operation. From the information gathered effective flue gas temperatures are calculated and together with factors describing flue and stack flow rates the dynamic system losses may be evaluated. Basically the system losses accounted for are sensible stack heat loss during on and off periods, infiltration losses, and in the case of a condensing model both the latent heat gain from the condensate and the loss associated with disposal of warm condensate. Pilot losses are also included if applicable.

If the furnace is a condensing model a cyclical test is performed in which the furnace is cycled on and off under a simulated loading of 22.5%. Following each cycle the condensate is collected ane weighed to determine the latent heat gain under part load operation.

The calculation of simulated seasonal efficency also requires such as average annual heating degree days, average indoor and outdoor temperature and infiltration parameters. Thus although the method may not give efficencies that may actually be obtained in the field it does ensure that results are repeatable and enables one to make comparisons regarding relative furnace performance.

As indicated in Table 3 the simulated seasonal efficencies obtained using the aformentioned methods were generally in good agreement with both manufacturers ratings and steady state results. It should be noted that the CGA P.1 procedure is the method used by manufacturers to rate their furnaces.

### Measured Insitu Thermal Efficiency

As was mentioned previously the furnaces were installed in either of the Conservation or Passive test modules at the facility and operated on alternate weeks with an electric forced heating system supplying space heat during gas furnace off weeks. Parameters monitored during the testing included natural gas usage, electrical energy usage, appliance operation time, hourly natural air infiltration rates, room and ambient temperature and solar insolation. At first glance the determination of furnace efficency seems straight forward through the direct comparison of total energy usage during weeks of gas and electric heating. Evaluations of this type proved extremely difficult to intepret with individual weekly calculated efficencies ranging from 50% to over 100% due mainly to changes in radiation gains and infiltration rates.

A second method of evaluation examined utilized another test module, the Standard, to provide a basis for comparison during gas or electric heating periods. Past analysis of module performance has shown that in the long term the total energy usage of the Passive or Conservation modules could be normalized with that of the Standard module simply by accounting for differences in indoor temperature as indicated by equation (1).

$$\frac{C \cdot Q_{standard}}{\Sigma(T_i - T_a)_{standard}} = \frac{Q_{test\ module}}{\Sigma(T_i - T_a)_{test\ module}} \qquad (1)$$

The constant, C, being termed the relative normalized energy usage of a test module with respect to the Standard module. Q represents the total electrical energy input to the module while $T_i$ and $T_a$ represent indoor and abmient temperature respectivly. This method, while providing a better indication of efficency could not account for short term variations of module performance primarily due to radiation levels and changing infiltration rates and as such was found unacceptable.

The final method used to evaluate efficency accounted for the various losses and gains such as radiation, infiltration, above grade envelope losses and basement losses. The fundamental assumption used was that the overall conductance area product, UA, of the above grade portion of the structure remains unchanged over successive test periods and that the the various losses can be treated individually as indicated in the equations below. The first equation (2) relates the various parameters during periods where the electric heating system was used to maintain indoor conditions.

$$UA\Sigma\Delta T_1 + Q_{i1} - Q_{r1} = Q_{e1} \qquad (2)$$

Conductive losses, $UA\Sigma\Delta T$, plus infiltration losses, $Q_i$, minus radiation gains through the windows, $Q_r$, are equal to the net auxilliary energy, $Q_e$, added to the conditioned space. Solar gains were quantified using pyranometers placed to measure total horizontal, total vertical, and radiation transmitted through a south facing window. Infiltration rates as mention previously were measured on an hourly basis using a constant concentration tracer gas ($SF_6$) system.

A similar relationship (3) can be written for periods when the module auxiliary space heat was supplied with the natural gas furnace under testing.

$$UA\Sigma\Delta T_2 + Q_{i2} - Q_{r2} = Q_{e2} + \eta Q_{g2} \qquad (3)$$

Where $Q_i$ and $Q_r$ are the same parameters as used in equation (2), $Q_e$ reflects energy used by the fan motor and lights and $Q_g$ is the energy equivalent of the natural gas used. $\eta$ is the conversion efficency of the furnace under testing or the fraction of the total gas energy equivalent used to meet the space heat requirement. The subscripts 1 and 2 denote periods of heating with electricity or natural gas respectivly.

Equations (2) and (3) were combined and solved for efficency, $\eta$, as indicated by equation (4).

$$\eta = \frac{1}{Q_{g2}}\left[\frac{\Sigma\Delta T_2}{\Sigma\Delta T_1}(Q_{e1} - Q_{i1} + Q_{r1}) - Q_{e2} + Q_{i2} - Q_{r2}\right] \qquad (4)$$

Efficencies determined using this method show very small variations between test periods because of the method used to account for gains and losses. The small variations may be partially due to variations in furnace loading but insufficent information is available to verify this.

Table 4 illustrates the results of the analysis for each of the furnaces tested as well as the manufacturers rating.

**TABLE 4 FURNACE EFFICIENCIES DETERMINED THROUGH INSITU TESTING**

| Furnace | Rated Efficency (%) | Insitu Rating (%) |
|---|---|---|
| 1) ICG Standard | 77 | 66 |
| 2) ICG Conserver | -- | 76 |
| 3) Airco Turbo | 83 | -- |
| 4) ICG Ultimate | 92 | 93 |
| 5) Lennox Pulse | 98 | 95 |
| 6) Amana Energy Command | 98 | -- |

Effects of Furnace Operation on Natural Air Infiltration Rates

Since all of the furnaces tested with the exception of the Lennox Pulse draw combustion air from the conditioned space it was expected that some change in the test modules natural air infiltration rates would be evident during furnace operation. As infiltration rates vary significantly throughout the year in response to changing ambient temperature and wind speed it is difficult to quantify small changes caused by furnace operation in an absolute sense. For this reason and based on historical results the natural infiltration rate of each test module was normalized with that of the Standard module. Given that there are no structural changes in a test module, this method results in normalized rates that vary by less than 5% over the long term, say several months. Thus in examining Table 5 it is important to note that changes in relative rates of less than 5% should not be attributed to anything other than data scatter.

With this in mind one may examine Table 5 which shows both the relative infiltration rate during each furnace test period as well as the percentage change in relative rate due to furnace operation. The ICG Standard furnace, installed in the Passive, module produced increased relative infiltration rates during periods of operation of approximately 18% or a change in relative rate from 0.52 to 0.62. The ICG Conserver, equipped with pilotless ignition and flue damper, shows a marked reduction caused primarily by damper operation. Relative infiltration rates decreased from 0.52 to 0.34 during periods of damper operation and increased slightly to 0.39 when the furnace was firing. Similarily the Airco Turbo shows a large reduction due to flue obstruction, 0.52 to 0.36 relative rate, and a slight increase during periods of furnace firing. The condensing furnaces, ICG Ultimate, Lennox Pulse and Amana Energy Command, evaluated in the Conservation module, produced changes in relative infiltration rates at or below the resolution of the infiltration measurement system and can be said to have little or no effect on the test modules natural infiltration rate. This result would not be indicative of the situation where a condensing furnace was installed in a residential structure and a flue was eliminated. The envelope characteristics of the two test modules are such that a 5% change in relative infiltration rate translates to an approximate change in module energy usage of 1%. Thus, in the worst case, that of the standard furnace with pilot ignition the resulting change in module energy usage as a direct result of furnace operation was less than 5%. Significantly greater effects were noted when the original 150mm flue in the Passive module was down sized to 100mm to accomodate the furnaces. In addition, since the furnace flues are major leakage sites in the test modules the changes might be noticably smaller in full sized housing

**TABLE 5 MEASURED NATURAL AIR INFILTRATION RATES RELATIVE TO THE STANDARD MODULE**

| | Heating Mode | | Increase Due to Furnace Operation |
|---|---|---|---|
| | Electric | Natural Gas | (%) |
| 1) ICG Standard | .52 | .62 | 18 |
| 2) ICG Conserver | .34 | .39 | 16 |
| 3) Airco Turbo | .36 | .38 | 7 |
| 4) ICG Condensing | .27 | .28 | 3 |
| 5) Lennox Pulse | .23 | .22 | -4 |
| 6) Amana Energy Command | .26 | .26 | 0 |

## Conclusions

Based on the results of this study the following conclusions may be drawn.

1. The furnace evaluation test procedure, proposed standard CGA P.1 produces results which are in very good agreement with field test results.
2. Field testing of a standard furnace showed that the insitu efficency was lower than the nameplate rating but that CGA P.1 results agreed with field measurements.
3. Field testing of two condensing furnaces showed that both achieved insitu efficencies very close to manufacturers stated seasonal utilization efficencies.
4. The operation of a standard furnace produced a measurable increase in air infiltration rates while a flue damper effectivly reduced off period losses.
5. None of the three condensing furnaces tested produced a measurable increase in long term module infiltration rates.

## Acknowledgement

This research project was funded in part from the Alberta/Canada Energy Resources Research Fund, jointly established by the Government of Canada and Government of Alberta and administered by Alberta Energy and Natural Resources. Their support is gratefully acknowledged. In addition the authors would like to thank the Inter-City Gas Corporation (ICG) and Werners Refrigeration Ltd. of Edmonton for donating furnaces to be used in the study.

## References

1) Gilpin R.R., et al, Construction of the Alberta Home Heating Research Facility and Results for the 1979-1980 Heating Season, Department of Mechanical Engineering Report No.23, University of Alberta.

2) Canadian Gas Association Proposed Standard CGA P.1, Seasonal Gas Utilization Efficencies of Gas Fired Central Furnaces, Fifth Draft, Canadian Gas Association, Don Mills, Ontario.

# CANADIAN FEDERAL BIOENERGY PROGRAMS

Allan J. Dolenko, Ph.D.
Renewable Energy Branch
Energy, Mines and Resources Canada
Ottawa, Ontario, Canada K1A 0E4

## ABSTRACT

### Background

Canadian government involvement in the development of bioenergy as an alternate energy source began in earnest in 1978. In that year the government introduced several program initiatives in conservation and renewable energy. This was a period of great uncertainty and instability with regard to oil price and supply. Canada was a net importer of approximately 300,000 barrels of oil per day. Conventional oil reserves were being rapidly depleted and predictions were that oil prices would rise to $60 a barrel or more by 1990.

It was generally perceived at the time that the potential for increased bioenergy development in Canada was significant. The contribution of bioenergy was already estimated at between 300 to 350 PJ, about 3% of the primary energy demand, and was largely attributed to the combustion of liquors and mill residues in the forest products industries. It was recognized that biomass could be economically attractive as an alternate energy source and could contribute to the national goals of energy self-reliance, job creation and regional development as well.

It was also recognized however, that a number of barriers existed which impeded the widespread introduction of bioenergy as a viable energy alternative. These barriers included the following.

1) A lack of precise knowledge of bioenergy supply, availability and costs. While it was apparent that there was a huge quantity of biomass in Canada, there was a lack of reliable statistical data on its availability and costs.

2) A fragmented and weak supply infrastructure. This of course was part of the chicken and egg situation where the establishment of a viable biomass supply infrastructure was entirely dependent upon the development of an assured market.

3) The high cost associated with the introduction of proven bioenergy technologies. It was recognized that the capital cost of bioenergy equipment can be up to several times greater than the cost of conversion equipment for conventional energy sources such as oil, natural gas or electricity. Even with lower fuel costs, the payback period was often too long to encourage industry to make the necessary capital investment.

4) A lack of awareness of opportunities. There was very little information available for potential bioenergy users as to the technologies and economic opportunities associated with the use of biomass.

5) The high risk and cost of introducing new technology. Canadians are generally conservative in their approach to the introduction of new technologies. We tend to be followers rather than innovators and therefore quite reluctant to take on the risks involved in the introduction of new technologies.

6) Lack of available expertise. There were few individuals who had much knowledge of or first-hand experience with biomass as an energy source.

The initiatives introduced in 1978 and in subsequent years were designed to address the barriers described above and take advantage of the energy and economic opportunities of bioenergy. They were comprised of programs which offered direct incentives to the bioenergy user as well as programs which support research, development and demonstration of bioenergy technologies and applications. The overall objective was to increase the total bioenergy contribution from 3% to 6% of primary energy demand by 1990.

Before giving a description of the programs and their status, it is desirable to first address the biomass supply question.

## BIOMASS AVAILABILITY AND PRICE

Current estimates show that the availability of forest biomass alone is in the order of 100 million dry tonnes annually. This is equivalent to approximately 25% of Canada's total primary energy demand. Figures 1 and 2 show the source and supply/price estimates respectively for forest biomass in Canada.

Forest biomass sources are broadly divided into five categories.

1) Mill residues are comprised of bark, sawdust, shavings, pulping liquors, etc. which are the waste byproducts of forest products processing mills. They represent some of the lowest cost biomass at 0 to $15/dry tonne and represent 14% of the forest biomass available. Much of this residue is used for energy by the mills themselves.

2) Logging residues are composed of the residual material left in the forest after normal harvesting operations i.e., slash (tops, branches, etc.), small trees, non-commercial species as well as deformed and defective trees. These residues represent a large potential source of forest biomass at 23.6% of the total available, but tend to be somewhat difficult and costly to collect ranging from $25 to $90/dry tonne.

3) The salvaging of wood killed by fire, insects, disease, wind or flooding, and

4) the conversion of stands of non-commercial trees and scrub represent another large potential source of biomass (24.9% and 9.6% respectively) which are recoverable at costs ranging from $30 to $60/dry tonne.

5) Finally, there is the surplus material which is over and above the current industry demand for fiber used in the manufacture of conventional forest products. In Canada this is almost 30% of the total forest biomass available at costs between $30 to $60/dry tonne.

The current demand for forest biomass is roughly equivalent to 26 million dry tonnes per annum. This suggests that the utilization of forest biomass could readily be doubled at supply costs not exceeding $45/dry tonne provided suitable markets and applications were available. The utilization of biomass obtained from logging residues, stand conversion and salvaging operations for energy and chemicals can provide the necessary economic return to encourage more intensive forest management and regeneration. This concept is being applied with considerable success in a number of parts of the country.

In addition to the forest biomass, substantial quantities of agriculture biomass are available particularly in eastern Canada as well as municipal solid wastes (MSW) in the densely populated urban areas.

## BIOENERGY INCENTIVE PROGRAMS

Beginning in 1978, the Canadian government introduced a number of direct incentive programs to address the barriers of high capital costs of bioenergy conversion equipment, the underdeveloped supply infrastructure and the general lack of awareness of the potential of bioenergy. These programs were aimed at the industrial, commercial and residential sectors.

The most ambitious bioenergy program initiated in 1978 was the Forest Industry Renewable Energy (FIRE) Program. Its purpose was to promote energy security and self-sufficiency by substituting readily available renewable biomass fuels for fossil fuels in the forest products industry. The original program budget was $103M over five years ending in 1983-84. As part of the National Energy Program, announced in 1980, the program budget was increased to $288M and its duration extended to March 31, 1986. In addition, the program was expanded to include non-forest industrial, commercial and institutional organizations as well as other forms of biomass such as municipal and agricultural wastes and peat. The program budget was later reduced to $96M.

FIRE is a capital cost sharing program which contributes between 10 and 20% towards the capital costs of modifying existing equipment or establishing new facilities to convert biomass into primary energy. Contributions are determined by a cash flow analysis which takes into account all eligible capital and operating costs as well as revenues and avoided costs. Almost all costs associated with purchasing and installing the necessary equipment are eligible capital costs.

The program officially ended March 31, 1986 and is now in a two year wind-down period during which time projects still underway will be completed, a number of selected projects will be carefully monitored to obtain actual benefit/cost data. In addition, a concerted effort will be made to transfer this information to the commercial/industrial and institutional sectors in order to promote as many replications as possible.

Table 1 summarizes the results of the program to date. Approximately $96 million have been contributed to 180 projects having a total cost of about $725 million. This represents exceptionally good leverage in private sector investment in Canadian goods and services for the number of federal dollars spent. Once completed, the projects will displace approximately 9.3M BOE per year. As anticipated, the greatest number of projects were undertaken by the forest products industries. Furthermore, projects in the wood industries, i.e. sawmills, furniture factories, particle-board mills, etc. gave the greatest return in terms of program dollars spent per BOE displaced per year. This result is not unexpected since such projects are characterized by the lowest relative capital and feedstock costs. In contrast, energy from waste projects carried out primarily by municipalities are characterized by high capital costs associated with the safe and efficient handling as well as combustion of solid waste.

In response to the 1979 oil price shocks, the Canadian government introduced the National Energy Program in 1980. A major initiative under this program was the establishment of the Canada Oil Substitution Program (COSP). This program was aimed at the residential sector and provided a one-time taxable grant of up to $800 for homeowners to convert from oil to natural gas, electricity, solar or wood. The program was originally scheduled to run for 10 years to 1990. It was terminated in 1985 as part of a general government effort to cut cost and reduce the deficit.

Residential wood heating in Canada is quite significant with over 2 million (25%) of Canadian homes using wood as a primary (50%) or secondary (10 to 50%) heating source. This does not include open fireplaces. Under COSP, approximately 225,000 grants having a value of $230 million were issued to homeowners to convert off oil to wood representing 23% of all off-oil conversions. The number of installations of wood burning appliances has levelled-off with the market being largely saturated. Installations which have occurred over the past five to ten years are characterized by low technology systems with inadequate attention paid to safety and performance. This has resulted in an increased number of house fires as well as increased levels of pollution in areas having high concentrations of wood-burning appliances. The bioenergy program in the residential sector is focussing on the development of safety standards as well as efficiency and emission standards in cooperation with the Canadian Standards Association and the industry itself; the promotion of public awareness on these issues and on the development of improved technology through R,D&D.

In 1984, a sort of mini-FIRE program known as the Alternate Energy Development Program (AEDP) was initiated in Canada's smallest province of Prince Edward Island. PEI has a small population of less than one hundred and fifty thousand which is largely rural. Energy costs on the Island are considerably higher than the Canadian average as it has no fossil reserves and little hydro. The objective of AEDP is to displace imported fossil fuels with indigenous biomass fuels. A large forest biomass resource exists on the Island which is under-utilized and has little traditional commercial value. Under the program, the commercial/industrial and institutional sectors are eligible for contributions of up to 62.5% of the total cost of the installation of biomass conversion systems, thus guaranteeing a three year pay-back In conjunction with AEDP, a massive forest management and improvement program has been undertaken which provides the biomass fuel in the form of woodchips. The program is scheduled to run through to 1989 and is expected to displace some 50,000 BOE per year.

## BIOENERGY RESEARCH, DEVELOPMENT AND DEMONSTRATION PROGRAMS

In order to address several of the barriers impeding the progress of bioenergy such as the high risk and cost of developing and implementing new technologies, the lack of awareness of bioenergy technologies and the lack of technical expertise, the federal government has initiated a number of programs to support research, development and demonstration of new methods and technologies to substitute biomass for non-renewable fuels and chemicals. Because of the diversity of interest in bioenergy technologies, the Canadian R,D&D program has involved a number of federal departments and agencies.

The first major bioenergy R&D program was the Energy From the Forest Program (ENFOR) initiated in 1978. This was a five year, $30M program to support research and development of new methods and technologies aimed at substituting forest biomass for non-renewable fuels and chemicals.

ENFOR was comprised of two sub-programs: Biomass Production, dealing with forest related topics involving resource assessment and raw material supply; and Biomass Conversion, dealing with the transformation of biomass into energy and chemicals. In 1983/84 the final year of its authorized term, responsibility for the conversion sub-program was transferred from the Canadian Forestry Service (CFS), Environment Canada to the Renewable Energy Branch of Energy, Mines and Resources. This transfer was carried out to permit better integration of biomass conversion R&D with other related R&D activities within EMR and to broaden the program to include all forms of biomass. This integration was carried out in 1984-85 resulting in a new, restructured R&D program called the Bioenergy Development Program (BDP). The CFS is still responsible for the Biomass Production sub-program of ENFOR.

Under NEP announced in 1980, energy R&D funding was greatly expanded. Particular emphasis was given to the development of alternative transportation fuels to displace gasoline and diesel. This included the use of biomass as a feedstock for the production of fuels. Federal departments and agencies involved with R&D included the CFS, Energy, Mines and Resources, Agriculture Canada, Environment Canada and the National Research Council (NRC). The programs managed by these departments were largely contracted-out to the private sector, universities, provincial and other non-profit research organizations and were supported in most instances by a small in-house R&D effort. The various departmental programs were co-ordinated by the Bioenergy Program Office of the NRC. Then in late 1984 the government instituted a number of measures to reduce expenditures in an effort to come to grips with the growing federal deficit. Among those cost-cutting measures was a drastic reduction in the energy R&D budget involving the virtual elimination of all bioenergy R&D activities at the NRC. The Bioenergy Development Program managed by Doug Hayes is attempting to fill the gap left by the NRC and the reduction in bioenergy activities by other departments.

Figure 3 traces the estimated bioenergy R&D expenditures beginning with under $1 million in 1977, reaching a peak of about $20 million in 1984, then dropping back sharply to about $8 million where hopefully it will stabilize. Government reductions in spending and lower oil prices have taken their toll on federal bioenergy R&D spending in Canada as they have in many other countries. Of even greater significance is the fact that these extreme swings in budget allocations make it very difficult to plan or implement an effective R&D program which, of necessity, must be long-term in nature.

In parallel with its efforts in R&D the federal government also initiated the Conservation and Renewable Energy Demonstration Program (CREDA) in 1978 managed by Energy, Mines and Resources.

The objective of this program was to demonstrate promising new technologies and applications which exploit renewable energy sources, conserve energy or make its use more efficient. In effect, the program was designed to defer the technical and commercial risk involved in the deployment of new technologies and, in so doing, gain consumer acceptance. A program budget of $114M was allocated over five years ending in 1983-84. CREDA was a bilateral program which involved cost shared agreements with the provinces. The program has been extended an additional year to wrap-up on-going projects. A new federally delivered demonstration program, ENERDEMO-Canada was announced in 1984. With the change in government that year however, the program never became operational. The current goverment's policy is to return to the joint federal/provincial program mode. As a result EMR has negotiated a number of Memoranda of Understanding (MOU) with the provinces under which bioenergy demonstration activities are being undertaken. These demonstration activities have been incorporated into the BDP.

Well over one hundred bioenergy demonstration projects have been carried out under the programs across the country having a total cost of just under $50 million and a federal contribution of approximately $12 million.

Examples of typical bioenergy demonstration projects supported under the programs include: co-generation from energy-from-waste, wood-fueled district heating, energy from solid-waste, wood-chip furnaces and boilers, anaerobic digestion of hog manure, medium-scale wood chippers, whole-tree chipping and large-scale, fully automated wood heating systems.

As currently structured, the BDP is comprised of R&D as well as demonstration activities and is managed by the Bioenergy Division of EMR. Theoretically, the delivery of an R,D,&D activity by a single group should improve operational efficiency and should also improve the rate at which new technologies achieve commercialization. A wide spectrum of activities are being supported under this program as outlined below:

1) Biofuel Production. activities range from the development of improved harvesting and forest management techniques, to the development of equipment for the harvesting of logging residues, to the development of a sophisticated computer program (FORCYTE) which assess the impact of various forest management systems on the forest ecosystem.

2) Combustion. diverse range of activities including such projects as the development and implemenation of a test program to improve the cost-performance of industrial wood boilers. These boilers had functioned more as incinerators rather than energy producers and required substantial amounts of fuel oil to supplement combustion. A number of tested units have not only reported fuel oil savings, some in the $1 million range annually, but also have reduced emissions as well. At the residential scale, R&D activities have centered on the development of safety, efficiency and emission standards for conventional roundwood burning appliances. A substantial effort is going into the development of central, wood-chip furnaces which are completely automated. Under the auspices of Environment Canada, a number of generic municipal solid waste burning facilities are being tested with regard to optimizing efficiency and reducing emissions under the National Incinerator Test Program.

3) Thermochemical Conversion. in the area of biomass gasification, work is well underway on the operational phase of the world's largest fluidized-bed gasifier (Biosyn) in Quebec. To date this gasifier installation has been used to demonstrate the production of electricity in engine generators using a low-joule value gas (LJV). Biodev, a sister company of Biosyn, is installing a 6.7MWe, $9M unit, in French Guyana on behalf of Eléctricité de France. Work is continuing on the utilization of oxygen as the combustive gas under

pressure for the production of a medium joule value (MJV) gas for use in the production of chemicals or fuels such as methanol. Work is also underway on the development of the two-stage Heuristic gasifier which can operate using wet hog fuel as feedstock.

Research on the direct liquefaction of biomass for the production of fuels and chemicals is proceeding at a fairly high level among several world-reknown Canadian researchers in the field including Dr. Scott's fluidized-bed process at the University of Waterloo and Dr. Roy's Vacuum Pyrolysis process at Laval University. The federal strategy is to wrap-up most of the basic studies in this area within the next couple of years and select one or two processes which have potential commercial interst for scale-up to the pilot level.

4) Biological Conversion. research is focussed on the enzymatic cellulose hydrolysis process being developed at the Iotech/Monenco 1 tonne wood/day pilot plant using steam exploded wood and the hydrogen fluoride (HF) process originally begun by Canertech. Mohawk Oil Company, Canada's only distributer of gasohol, has announced plans for the 9 million l/day expansion of its grain alcohol plant in Minnedosa, Manitoba based on the Iotech process. The recent drop in world oil prices, however, makes the economics for the process more tenuous.

Regarding anaerobic digestion, work is limited to the monitoring of several installations using various digestion techniques. Applications for the advanced concepts for anaerobic digestion (e.g. fixed film) will be promoted in various industrial installations (as opposed to farms).

5) Materials Handling and Pretreatment. The efficient handling and reliable feeding of biomass is crucial to any biomass conversion process. Therefore, this area continues to receive a high priority. Past work has resulted in rapid commercialization of the technique developed. For example, a new bin and silo design developed by B.C. Research for the efficient storing and transfer of biomass eliminates flow stoppages. A moisture metering device developed by Forintek is undergoing field trials to allow better process control for wood-fired boilers. Steam pretreatment processes developed by Iotech and Stake Technology hold considerable promise in cellulose hydrolysis applications.

6) IEA. Canada plans to continue its active involvement in the IEA through participation in the new Bioenergy Implementing Agreememt.

## THE FUTURE OF BIOENERGY PROGRAMS IN CANADA

According to current estimates, bioenergy now contributes approximately 5.6% of Canada's primary energy demand or about 230,000 BOE per day (Table 2). This contribution is mainly in the residential and industrial sectors of the economy where bioenergy contributes approximately 14% and 17% of the primary energy demand respectively (Figure 4). The overall contribution is well on its way to meeting the target of 6% of primary by 1990.

Under the National Conservation and Alternative Energy Initiative (NCAEI) announced by the government last year, bioenergy will continue to receive significant funding in keeping with its role as a significant contribution to the national energy budget. In keeping with fiscal realities however, the trend will be away from large incentive type programs such as the FIRE program toward more selective R,D&D and information transfer. The budget for the various bioenergy activiites under the NCAEI is summarized in Table 3. It is anticipated that the budgets for R,D&D will remain fairly constant into the foreseable future. We shall attempt to gain the maximum leverage on the limited funds available through cost sharing arrangements with the private sector and other levels of government as well as the international community. Our objective is to carry on a viable bioenergy program with particular emphasis on shorter-term applications during the present oil glut while continuing work on promising longer-term opportunities for possible implementation when oil prices rise once again.

This paper was originally presented at the Energy from Biomass and Wastes X Conference held in Washington, D.C. April 1986.

Figure 1

## Forest Biomass and Distribution

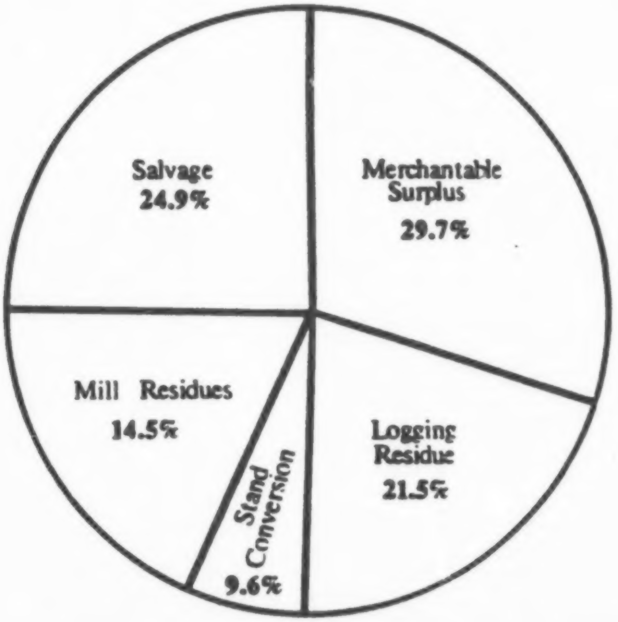

Figure 2

Supply/Price Curve Forest Biomass Availability

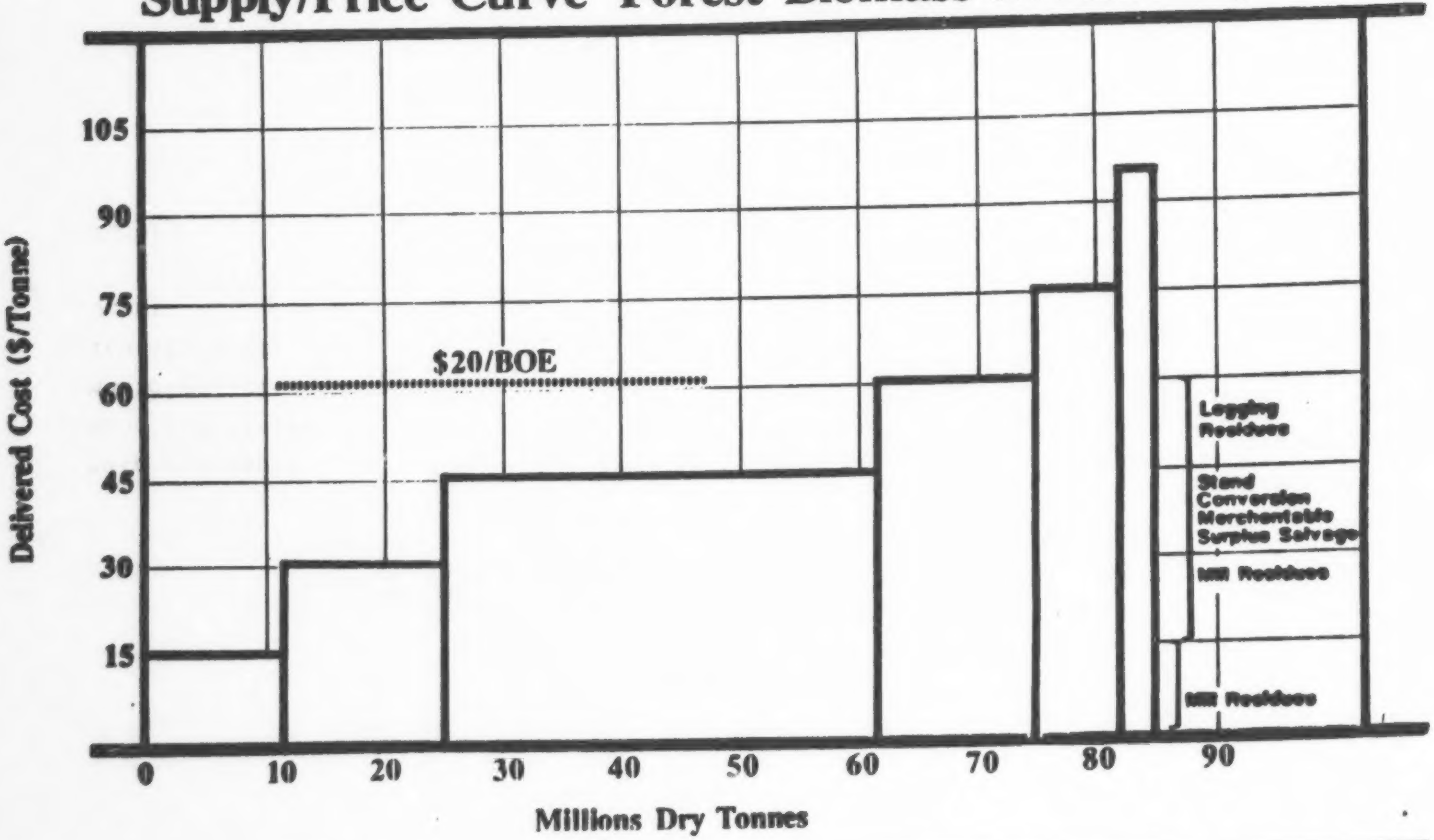

### TABLE 1

### FIRE PROJECTS

| | No. of Projects | Capital Cost ($ x $10^6$) | Fire Contribution ($ x $10^6$) | Calculated BOE Savings/yr. ( x $10^6$) | $/BOE/yr |
|---|---|---|---|---|---|
| Pulp and Paper | 46 | 426.4 | 51.5 | 5.7 | $ 9.03 |
| Wood Industries | 89 | 104.5 | 14.4 | 2.7 | $ 5.33 |
| Municipalities | 7 | 127.2 | 18.3 | 0.4 | $45.75 |
| Institutions | 10 | 43.5 | 7.4 | 0.2 | $37.00 |
| Other | 28 | 25.6 | 4.6 | 0.3 | $15.33 |
| **TOTALS** | 180 | 725.5 | 96.2 | 9.3 | $10.34 |

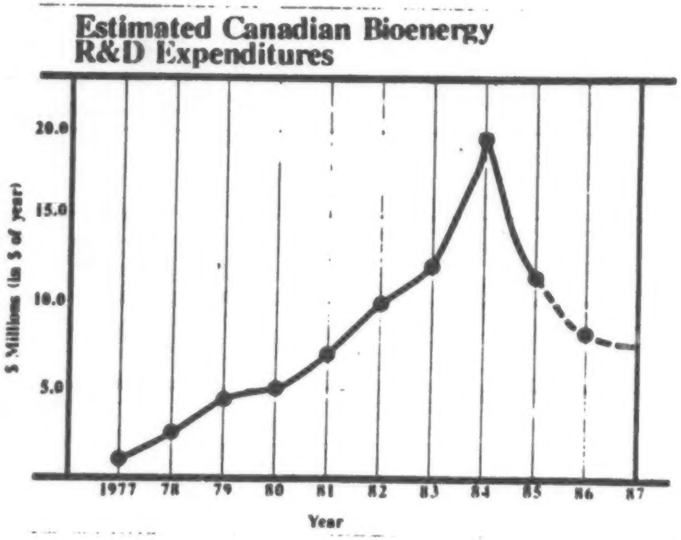
Estimated Canadian Bioenergy
R&D Expenditures
$ Millions (in $ of year)
20.0
15.0
10.0
5.0
1977
78
79
80
81
82
83
84
85
86
87
Year

Figure 3

Figure 4

# Bioenergy Contribution

## Residential Sector

- *14% from Bioenergy*
- *2.1 million households*

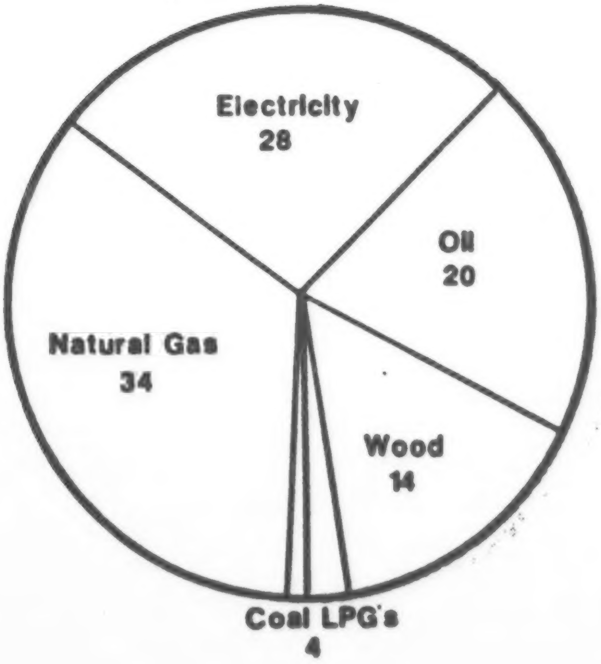

## Industrial Sector

- *17% from Bioenergy*
- *About 550 firms, mainly pulp and paper plants*

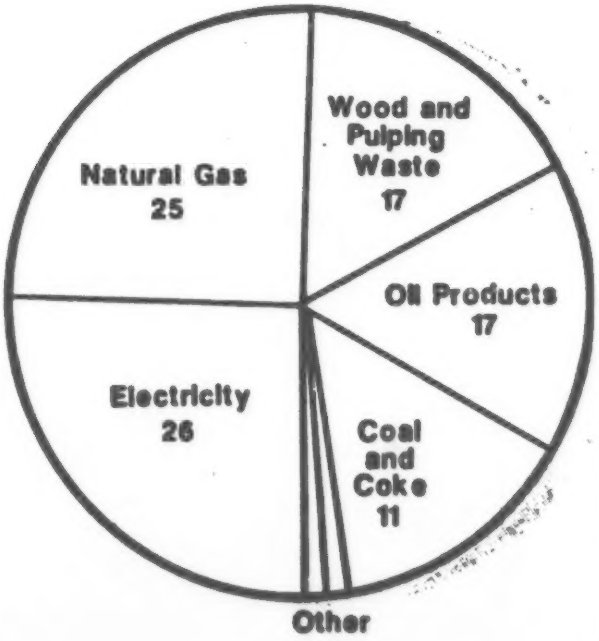

## TABLE 2

### CONTRIBUTION BIOENERGY

(BOE/DAY, PRIMARY ENERGY)

| | CURRENT | NEAR TERM (1995) |
|---|---|---|
| Residential | 76,000 | 85,000 |
| Commercial/Industrial | 153,000 | 200,000 |
| MSW | 1,800 | 4,500 |
| Liquid Fuels | 50 | 2,200 |
| TOTAL | 230,850 | 291,700 |
| % Primary Energy Demand | 5.6% | |

TABLE 3

## SUMMARY OF BIOENERGY ACTIVITIES AND BUDGETS

| | 1985/86 | 1986/87 $ millions | 1987/88 |
|---|---|---|---|
| 1. Forest Industry Renewable Energy (FIRE) | 9.8 | 12.8 | 4.2 |
| 2. Bioenergy Development Program (BDP) | | | |
| Research & Development | 4.5 | 5.9 | 6.0 |
| Demonstrations | .6 | 3.0 | 2.5 |
| 3. Canada/PEI Alternate Energy Development Program | 2.0 | 2.0 | 1.7 |
| 4. Biosyn | 1.0 | 1.0 | 0.2 |
| 5. Liquid Fuels from Biomass (E from C) | 0.1 | 0.7 | 0.1 |
| TOTAL | 18.0 | 25.4 | 14.7 |

# VENTURE CAPITAL AND ENERGY CONSERVATION

Graham Chignall
Market Manager - Modernization & Retrofit
Honeywell Limited
740 Ellesmere Road
Scarborough, Ontario M1P 2V9

## ABSTRACT

The market opportunity of savings financing has become one of a substantial nature in the U.S.A. and has now started to appear more recently in Canada. The cost of energy in the U.S.A. is much higher than that of Canada where we have a low relative cost of energy. It would appear that the different market sectors have an influence on this opportunity because of the way they run their businesses, receive funds or income, and the treatment of taxes.

We must also consider the size of the market to assess its potential and the amount of resources that a company which is actively involved in the energy management field should consider before entering into any form of activity level.

## THE MARKET

Referring to a study by the Department of Energy in the U.S.A. "Characteristics of Commercial Buildings 1983", of approximately 4 million buildings, 93% are of three floors or less. The largest buildings were health care institutions, and educational facilities. Computerized control was used for heating and cooling systems in approximately 105,000 buildings or about 2.9% of all commercial buildings. Those constructed between 1980 and 1983 were likely to have computer controls (9.2%) and those larger than 100,000 square feet equipppped with computerized controls (21.5%).

The report also indicates that of those 4 million buildings, approximately 11% had some form of energy audit.

Those audits that were performed by private companies represented about 50%, by utility companies 37%, and by others 21%.

From all of the audits that had been completed, 47% of the building owners adopted some measure of energy conservation.

So to summarize the market we may say that the actual number of potential agreements that may be signed could be very small compared to the number of audits completed.

It is a well-known fact that the property owner or energy user who is willing to invest in energy management is very hard to find. In addition, regardless of the financial or technical attractiveness of a given energy management improvement proposal, owners are usually unwilling to assume the technical and financial risks associated with those projects.

In a typical commercial or institutional building, there is rarely an effective energy management programme or even a provision for one. Usually the builder or developer has no incentives to install or obtain expensive, high effeciency equipment in the building. High efficiency, energy saving equipment has not yet been recognized as an important building asset. The location, type of building lease and occupancy rates are seen as the most important factors when assessing or purchasing commercial property. Building efficiency is simply not part of the picture.

It would seem to some people that if it takes professional engineers to design and build new buildings then surely it seems logical to have them run the building. The quality of operator knowledge on buildings systems seems to be generally low, and deteriorates even further when a sophisticated building E.M.S. is installed, and in many cases never used properly.

## ENGINEERING ANALYSIS

Once the initial audit has been performed and the client wishes to proceed further, the engineering analysis has to be detailed to accommodate a variety of system changes and upgrades. The report will typically cover the following (dependent on the end user):

1) Historical analysis of energy consumption
2) Base data period of energy use
3) Empirical formula for energy calculations
4) Occupany periods
5) Standard of service and comfort levels
6) R.O.I's for different system implementations

Once the detailed analysis has been developed and the engineering complete the aspect of how to finance the project then becomes a decision for the client.

## SAVINGS FINANCING METHODS

In essence there are many different forms of savings financing for retrofit opportunities. Some of those may be described as follows:

## CHAUFFAGE

With this approach, the ESCO agrees to pay all energy bills and be reimbursed by the user at a prescribed (and guaranteed) percentage of pre-retrofit energy costs as adjusted for degree day differences and energy price inflation. For example, a user might agree to pay 90% of what his bill would have been had no retrofit work been done. The 10% reduction in energy costs (termed "the discount) represents the user's share of savings. The balance of savings (the difference between current actual energy bills and reimbursement from the user) is realised by the ESCO.

## FIRST OUT

This has been the most active approach in Canada in the savings financing field so far. The key feature of this approach is the fact that the ESCO receives 100% of the savings for a period of time that is typically four-five years. The specific period is calculated on the basis of a formula incorporating a variety of factors.

a) Cost of detailed energy audit and retrofit package.
b) Actual realized savings.
c) ESCO's gross profit (project management and administration).
d) A financing chargé for the project.
e) The ESCO agrees that the maximum period in which it has to a claim on project savings is 5 years, even if the formula indicates the ESCO is not paid out.

## Shared Savings

In this arrangement, the calculated savings attributed to the retrofit measure are divided between the ESCO and energy user. For example, the ESCO could receive 75% and user 25% of savings for a 5-7 year period. Whilst these percentages vary so do the number of partners vary also. It is not uncommon to have more than three to four partners all receiving some form of benefit from the retrofit.

Under the shared savings formula, the owner is offered a no-risk, no expenditure opportunity to substantially improve energy management and save very considerable sums of money. Under this formula, the ESCO undertakes all necessary steps to develop, finance, and implement an energy management improvement program.

For the duration of the shared savings contract (normally 4-7 years), the energy user's only obligation is to share a certain portion of the energy being saved by the energy management improvement program with the ESCO. In addition, a buy out clause allows the energy user to purchase the installed system prior to the contract expiry date.

Often refered to as "third party financing", the shared savings formula was invented in the U.S.A. 7-8 years ago. Apart from the other forms of savings financing this has proved to be the most successful and widely used by ESCO's.

In the U.S.A. approximately 35 States and Municipalities are active in the shared savings agreements. However, in Canada some of the outstanding issues which face us are:

1) Title, of the retrofit package "to whom does it belong".
2) Treatment of taxes, whether it be savings or capital costs of equipment.

Income taxes have a profound impact on optimum investment decisions. By changing the effective values to the firm of the revenues and costs associated with an investment, taxes can reverse the relative profitability of alternative projects as evaluated apart from taxes, and they can alter the optimal size of investments. Taxes are therefore an important element in the economic evaluation of investment in the retrofit of builings systems. If, for example, an investment results in increased taxable revenues, the effective value of the traditional revenue to the firm is reduced by taxation. Similarly, if an investment in benefits in the form of cost savings, the after tax value of the benefits will be lessened by the loss of any related income tax deductions, ie. the cost savings are generally not tax free.

On the other hand, investment costs are also reduced somewhat by the value of corresponding tax deductions. Effective after tax costs in present value term can be calculated. An economic analysis of investment in energy recovery systems might involve each of these three tax effects. For instance, system equipment costs may give rise to tax deductions in terms of depreciation allowances and/or investment tax credits; savings in fuel costs will reduce deduction from taxable income of current operating costs; and sale of excess heat or energy to other firms will result in additional taxes on the revenue received.

Even though depreciation is not itself a cash flow, it affects the firm's cash flow through the deduction from taxable income. By its choice of depreciation methods (eg. declining balance methods as opposed to the straight line method of depreciation), an investment firm can affect the timing of the tax deduction and thereby influence the effective amount of income tax payments. The choice of depreciaton method which yields higher depreciation allocation in the early years will increase the present value of depreciation deductions, thereby decreasing the present value of income tax payments and raising the profitability of the investment of the firm.

3) Capital cost allowances, who can claim them, and whether there should be changes in status for future activity.

4) Procurement strategy, how should a customer analyse a proposal.

5) Available amount of financing in the market.

## CONCLUSIONS

Before any company wishes to invest funds into any new venture, the basic question of "is it good business" will always present itself.

a) It is only good business if the activity provides the right kind of I.R.R.'s for the organization.

b) Can the organization control the investment, and what outside influences can affect its investment?

c) Does the activity have a substantial effect on balance sheets and cash flows?

d) How far should we be prepared to go?

It is felt that there will be a future for this type of approach to the market. However, it may be a very small one. Organizations that enter into it must be able to manage all aspects of the business and be prepared to act swiftly to protect their investments.

# BIOENERGY TECHNOLOGY DEVELOPMENTS IN ONTARIO

J.R. Herberman, M.E.S., and P.J. Carrie, B.A.
Technology Development Section
Ontario Ministry of Energy
Queen's Park, Ontario M7A 2B7

## ABSTRACT

This paper presents a summary of experience with several waste wood combustion systems in Ontario. The systems are described with respect to technology, economic performance, and environmental emissions.

Ontario has had mixed experience with the technical and economic performance of the systems. Economics are often marginal, even for large commercial systems where economies of scale are present. Most of the systems in place are quite reliable. Where problems have been present, they usually are related to system utilization factors and/or feed handling systems.

Environmental emissions are generally within provincial guidelines. Analysis of emissions for some projects includes trace metals, PAH's, dioxins, furans and particulates.

## 1. OVERVIEW

Since the late 1970's the federal and provincial governments have funded a variety of programs to encourage the production of energy from biomass. Wood represents an important energy source in Ontario. Wood fuel is used by industries, institutions, farms and homes. The province has substantial forest resources, with processing mills currently burning or dumping over one million metric tonnes of wood residue per year. Wood currently displaces over $100 million (Canadian) worth of conventional fuels in the home heating market.

The use of wood waste by industry, particularly the forest products industry, currently displaces over $400 million (Canadian) worth of fuel annually. Wood and wood wastes could provide 4 percent (167 petajoules) of Ontario's total primary end use requirements (4,174 petajoules) in the year 2000.

## 2. Programs To Encourage The Use Of Biomass In Ontario

The Ontario Ministry of Energy supports wood energy development and utilization as part of the provincial government's committment to improve energy efficiency, increase energy self-reliance and recover resources from waste. The following projects are representative of the Ministry's activities in the Biomass area.

## 3. GRENVILLE - CHRISTIAN COLLEGE

### 3.1. Background/Rationale For Conversion

The Grenville-Christian College Woodburning Project represents the first modern large-scale (1460 KW; 5.25 GJ/hour) commercial/institutional sector installation of a woodburning system in Ontario. The system was commissioned in the fall of 1982 and was monitored from that time until December 1984.

This demonstration project was initiated for the following reasons:

- to demonstrate the significant potential for wood energy in the commercial/institutional sector; and,
- to help overcome barriers to the expansion of markets in this sector. The primary barrier was the lack of knowledge of wood energy technology and the consequent

perception that it represented a high risk investment.

## 3.2. System Description

The Anga Varme woodburning system is made up of three basic components; fuel receiving and storage; woodburning and hot water production; and hot water heating.

### 3.2.1. Fuel Receiving and Storage

Independent contractors gather wood fuel from the surrounding area mills and deliver it to the College in self-dumping trucks. This material is required to conform to specifications that limit particle size and moisture content.

The bunker holds sufficient fuel to run the plant for one week.

A staff member of the College checks the quality of the fuel being delivered. The samples are later analyzed to determine moisture content. Payments to the supplier are based on the weight of dry fuel.

The wood storage bunker is equipped with a "live bottom". From here a system of screw conveyors feeds the furnace.

### 3.2.2. Wood Burning and Hot Water Generation

The wood burning unit consists of an ignition cell, a combustion cell and a fire-tube hot water boiler.

Wood fuel, conveyed by the stoker screw conveyor, enters the combustion cell where it is exposed to hot gases and radiation from the furnace walls. A considerable amount of moisture is thus vapourized from the fuel before it enters the adjacent ignition cell. Once in the ignition cell the fuel is forced upward through an opening where it spreads over a number of sloping grates arranged in a circle. Underfire air is injected under the grates to assist combustion of the fuel and help cool the grates. Overfire air is introduced above the grates mixing with the gases as they depart to the combustion cell. The narrow passageway between the two cells causes the gases to accelerate to the combustion cell. The burning process is completed in the combustion cell. Here the velocity of the gases slows and causes large unburned particles to drop into the stoker screw conveyor which feeds them back to the ignition cell along with fresh fuel.

The spent combustion gases are induced through the boiler into a fly ash collector. The clean gas is then passed out through the chimney.

A system of screw conveyors automatically removes the ash from the ash pits and deposits it in an ash container outside the boiler house.

### 3.2.3. Hot Water Heating

The hot water generated by the boiler is pumped to College buildings through a series of pipes located in underground tunnels. In each of the buildings, unit heaters are used to distribute heat.

The boiler is also used to provide domestic hot water via a water to water heat exchanger.

The temperature of the water leaving the boiler is used to control the boiler output. When the building requires heat, the screw conveyors run more often.

## 3.3. Energy Performance

A detailed performance log was maintained from November 1982 to December 1984 and specific tests of efficiency were carried out. The wood burning system had an availability factor of 96% over the two year period. The thermal efficiency averaged 70% which is high in systems that burn wet fuel.

However, the system output was generally not higher than 1.5 GJ/hr, which is only about 28% of the rated capacity (5.25 GJ/hr).

## 3.4. Emissions Monitoring

Eight separate stack emission tests were conducted during the first year of operation. The tests involved a determination of the following parameters:

- stack gas particulate content and emission rate; and
- sulphur dioxide concentration and emission rate.

Particulate emissions ranged slightly above provincial standards of 100 x $10^{-6}$ g/$m^3$. Further study is required to reliably characterize average particulate emissions. $SO_2$ emissions from the system were measured at levels well below provincial standards.

### 3.5. Economics

The final installed cost of the system was $363,000. The measured savings over the two year period, in terms of oil displaced, was $151,000.

Savings would be much greater if the system was servicing a larger heat demand. Currently, only 28% of the 5.25 GJ/hour capacity is used under full load.

The system will pay for itself in nominal dollars in under 5 years. This is not attractive to industrial investors but could be attractive to commercial and institutional building operators. If the full capacity could be used the simple payback would drop to 1.4 years.

## 5. HILLCREST HIGH SCHOOL

### 5.1 Background/Rationale for Conversion

During 1982, the Ministry of Energy commissioned a study to establish the economic and technical viability of installing a wood-fired boiler system at Hillcrest High School in Thunder Bay, Ontario. The study concluded that the concept was viable and recommended the replacement of one of the three gas-fired boilers at the school with a wood-fired 585 kW boiler. This provided an opportunity to obtain information on system economics and atmospheric emissions. The emissions work done on this system was quite comprehensive and will be discussed in greater detail later.

### 5.2 System Description

The system components are fairly typical, consisting of an underground fuel storage bunker, a feed handling system, an Argusfyr boiler, and a stack with a cyclone. Hot water produced by the boiler is used for space heating during the winter.

#### 5.2.1 Fuel storage

The system utilizes underground storage for the hog fuel. This reduces the requirement for heating the storage area in winter (to prevent the fuel from freezing and agglomerating) and provides easier unloading for the dumptrucks which deliver the fuel. The storage bunker has a capacity of 100 $m^3$, and has loading doors located flush with the ground adjacent to the school parking lot. Fuel is drawn into the boiler room using two large hydraulically-driven rakes.

#### 5.2.3 Feed System

The feed system has proven to be the single most unreliable component of this installation. When using fuel with a high bark content, "bridging" often occurs around feed augers and/or control paddles. At various times, this has resulted in flooding the boiler room with hog fuel, or starving the boiler. As a result, the system requires intermittent operator supervision and it cannot be operated unattended.

Once fuel is drawn into the interior portion of the storage bin by the hydraulic rams, it is "fluffed up" with a rotating breaker bar. A screw conveyer located at the bottom of the storage bin brings the feed to the bottom of a two-stage inclined screw conveyor. The first stage takes the feed to the top of a downcomer shute, where the fuel passes through a star valve. The second stage takes the feed from the bottom of this downcomer directly into the furnace. The system is equipped with photocells and control paddles at various points to control the operation of the augers. Heat sensors in the last feed auger trigger a water quench to prevent fire from backing up through the conveyor system.

Aside from the problem of feed bridging, the feed system has required a lot of maintenance due to wear and tear on the feed augers. This is largely due to the presence of small chunks of wood which bind in the augers and cause premature wear.

### 5.2.4 Boiler

The boiler used for this system was supplied by Argusfyr. It uses 106 46 mm tubes with a total heat exchange area of 45.6 $m^2$. The heat exchange area is somewhat oversized for the application, resulting in good thermal efficiency for the system.

Two fans are used to provide combustion air. The primary (underfire) combustion air is preheated by exhaust gases from the stack using an air to air heat exchanger. A second fan draws secondary (overfire) combustion air directly from the boiler room. Water flow is controlled using an automatic valve.

### 5.2.5 Exhaust Stack and Cyclone Separator

A louvred control valve at the outlet of the boiler maintains a slightly negative pressure in the combustion chamber. After leaving the chamber, exhaust gases pass through an air-to-air heat exchanger to preheat primary combustion air, as mentioned above. Gases are then passed through a cyclone separator equipped with an induced draft (ID) fan. Fly ash collected in the cyclone drops through a star valve onto the ash conveyer from the furnace, and is then transported to an outdoor storage bin.

## 5.3 Energy Performance

Two types of fuel were tested on this system, sawdust and "hogged" bark fuel. The use of bark fuel was discontinued due to bridging problems in the feed system. A number of "Parr Bomb" tests indicated that the heating value for sawdust was 20,280 KJ/Kg. The value for bark fuel was slightly lower at 19,900 KJ/kg.

### 5.3.1 Energy Balance

1. 20% of the total heat input was required to evaporate moisture contained in the fuel (about 50% moisture content when received).

2. 16% of the heat input is lost through the stack.

3. The average thermal efficiency for the unit is 64.8%. It ranged from 57% to 71%.

4. The primary combustion air preheater removed only about 3% of the available heat from the stack gases. The use of this heat exchanger is therefore not economically justified.

### 5.3.2 Utilization factor

Based on the heat load of the building, the wood-fired boiler would be required for 6,300 hours per year. This assumes a 7 day per week, 24 hour per day operation. However, due to the problems mentioned earlier with the feed system and resultant supervision requirements, the boiler operated only 1600 hours during the 1984/85 heating season. Also, the average boiler output during operation was 485 kW, which is somewhat less than the 585 kW rating. This is due to the fact that air and feed flow rates were generally not optimal.

With respect to its potential utilization, this boiler operated at 21% capacity.

In absolute terms, it produced about 2793 GJ, out of a potential 13,300 GJ.

## 5.4 Emissions Monitoring

Extensive emissions monitoring and analysis was done on this system. This can be subdivided into 3 main areas: particulates, metals, and organic compounds.

### 5.4.1 Particulates

Particulate emissions averaged about 0.88 g/kg of dry wood feed for sawdust, and about 1.07 g/kg of dry wood feed for bark fuel. These numbers are at the low end of the scale for similar projects.

### 5.4.2 Metals

Concentrations of lead, mercury, cadmium, arsenic, chromium and nickel were measured. Of these, only lead and nickel were found in significant quantities. However these levels are well below provincial guidelines.

### 5.4.3 Organics

A gas chromatograph (GC) and mass spectrometer were used to ascertain levels of poly-aromatic hydrocarbons (PAH's) and other contaminants. Dioxin levels were also analyzed. The results of these test are quite extensive and are not presented here for the sake of brevity. No PAH or dioxin compounds were present at levels which exceed any existing or likely standards or guidelines.

## 5.5 Economic Performance

The system installed at Hillcrest High School is not an economically attractive proposition for two major reasons:

1. There was a cost overrun on the initial installation due to insolvency on the part of the firm contracted to install the system.

2. The capacity factor is very low due to problems with the fuel feed system.

If the system were able to operate 24 hours per day during the heating season, it would save approximately $27,000 per year worth of natural gas. Since the system cost was $300,000, the simple payback would be about 11 years.

If a 12% discounted rate of return is considered the threshold for economic viability, then the following values would be required for major project variables:

1. wood cost less than $10.60/tonne
2. labour requirement less than one hour per operating day
3. economic lifespan of at least 27 years
4. natural gas cost of at least $\$0.21/m^3$
5. inflation rate of at least 7.3%

# 6. Chapleau Cogeneration Project

## 6.1 Project Background

Although electricity costs in Ontario are generally lower than those in the U.S., the Province recognizes that there are a number of benefits inherent in cogeneration of electricity and steam. Currently, there are 500 MW of cogeneration and parallel generation capacity in Ontario. An additional 500-1000 MW is expected to come on line by the year 2000. The Chapleau cogeneration project (which is being implemented this year) will provide 45 MWh/yr of electricity and about 100 TJ/yr of steam and hot water for the Chapleau Forest Products plant in Chapleau.

## 6.2 System Description

This system is under construction, and is expected to be operational in October, 1986. Three local mills currently produce about 110,000 tonnes of wood waste per year. In addition to its energy benefits, the plant will help to reduce costs associated with disposal of this waste.

The 19.41 MW (70,000 lb/hr) boiler will produce steam at about 6200 kPa (900 psi) and 400°C. This will drive a 7.2 MW steam turbo-gen set, delivering 6.4 MW to the electrical grid. The generator unit produces 60-cycle power at 13,800 volts.

## 6.3 Potential Energy Savings

When operational, the system is expected to produce about 500 TJ (500 M lbs.) worth of steam per year, which will be used to produce over 45 million kWh of electricity. Of the residual steam, 20,000 lbs/hr (at 15 psig) will be provided to Chapleau Forest Products - mostly for space heating during the heating season. The plant availability factor is expected to be about 85%.

## 6.4 Economics

The project has a projected capital cost of $10.6 million. After operating expenses, the earnings are $1,155,000 per year. The economics of the project have been made attractive to the private sector by a total contribution of $2.9 million from the federal and provincial governments. This provides the plant owners with a 15% Return on Investment.

# 7. Other Ontario Wood/Energy Projects

Wood is processed and used in a wide variety of ways in projects throughout Ontario. Following is a synopsis of some of these projects:

7.1 Hybrid poplar plantations are a potentially important future energy source. New varieties have short harvest cycles of two to ten years; one hectare can produce more than 17 green tonnes of wood a year. To develop hybrids with higher energy content, the Ministry of Energy funds research in genetic breeding at the Ministry of Natural Resources Ontario Tree Improvement and Forest Biomass Institute in Maple, Ontario.

7.2 EcoWood Products has established a facility to gather and process waste wood to be sold as fuel. A supply infrastructure for urban wood residues and wastes is now operating successfully and can process up to 10,000 tonnes per year.

7.3 BioShell, a subsidiary of Shell International, turns sawmill residue into compressed wood pellets called Energex fuel pellets. Plants in Iroquois Falls and Hearst can produce 200,000 tonnes of pellets a year. Much of this is used by Abitibi-Price to fuel industrial boilers.

7.4 Kakabeka Timber Limited, a sawmill near Thunder Bay, uses sawdust and wood chips to fuel a drying kiln formerly fired by propane. The system saves about $70,000 a year in fuel costs, giving a simple payback of 2.5 years.

7.5 Foothill Greenhouses Ltd., in Ontario's Holland Marsh area, uses a sawdust-burning system to heat a greenhouse complex producing cucumbers. Since installation in 1982, the $180,000 system has reduced energy costs by about $40,000 to $45,000 a year.

7.6 David Smith, a farmer in Port Ryerse, has a small scale system which burns sawdust, corn cobs, peanut shells, and other agricultural residues to fire a 60-horsepower, restored locomotive boiler. The boiler provides heat to dry grain and heat a small greenhouse for growing tomatoes.

7.7 The Ajax District Heating project is an example of wood waste utilization to cogenerate steam and electricity. Bio-Char Inc. is currently converting the existing district heating system in Ajax to wood burning to displace natural gas. The first phase of the project consists of installing two wood waste combustors; in the second phase, two more combustors and two steam turbo-generator sets will be installed.

7.8 Near Dorset, Ontario, the Leslie M. Frost Natural Resources Centre demonstrates three different wood-fired central heating systems in homes originally heated by oil. Monitoring has provided valuable data on relative performance and cost-effectiveness.

A summary of the projects reviewed in this paper is presented in Table 1, Representative Ontario Wood Energy Projects.

Table 1

REPRESENTATIVE ONTARIO WOOD ENERGY PROJECTS

| PROJECT/START-UP DATE FEEDSTOCK/ ENERGY PRODUCT | CAPACITY TONNES/ YEAR | CAPACITY COST ($/tonne .yr) | CAPITAL COST $1,000's |
|---|---|---|---|
| EXISTING PROJECTS | | | |
| Shell Woodex/1980<br>Wood/Solid Fuel | 225,000 | 20 | 4,500 |
| Grenville College/1982<br>Wood/Hot Water | 1,400 | 259 | 363 |
| Kakabeka Timber/1982<br>Shavings and sawdust/Steam | 1,100 | 163 | 180 |
| Foothill Greenhouses/1982<br>Dry Wood/Steam | 1,000 | 180 | 180 |
| Hillcrest High School/1983<br>Hog fuel/Hot Water | 1,700 | 176 | 300 |
| Kingsway College/1984<br>Dry Wood/Steam | 2,100 | 619 | 1,300 |
| L.M. Frost Centre/1984<br>Wood/Hot Air | 30 | 1,666 | 50 |
| UNDER CONSTRUCTION | | | |
| Chapleau/1986<br>Wood/Steam+Elect. | 108,000 | 92 | 10,000 |
| Ajax/estim. 1986<br>Wood/Steam (Stage 1) | 20,000 | 103 | 2,075 |
| UNDER STUDY | | | |
| Hearst Furnaces<br>Wood Pellets/Hot air | 40 | 1,500 | 60 |

## 8.0 CONCLUSIONS

The adoption of biomass energy technologies in Ontario has been accelerating in recent years due to government incentives and increasing interest from the private sector. These technologies will play an increasingly important role in satisfying the province's energy requirements, both for thermal energy and electricity.

Currently, system operator experience varies significantly concerning reliability and economic viability. Most reliability problems stem from feed handling equipment, rather than boiler packages or other system components. Economic viability is sensitive to conventional fuel costs, feedstock prices, maintenance costs, and the scale of the system. The effect of scale on system economics is fairly consistent for the projects summarized in this report. Graph 1. summarizes the relative capacity costs of these systems.

GRAPH #1

Economies of Scale
Biomass Energy Systems

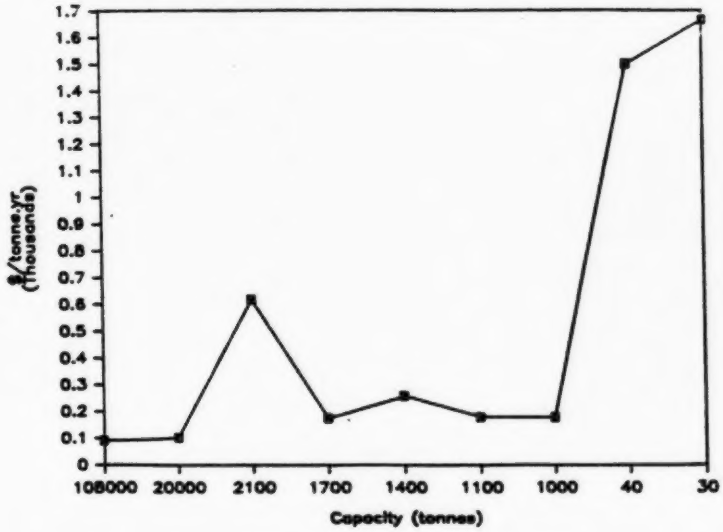

From an environmental emissions standpoint, wood-fired combustion systems are relatively benign with respect to dioxins, PAH's, other organics, and trace metals. The use of cyclones and proper stack heights should ensure the particulate levels are maintained within provincial guidelines.

## 9.0 BIBLIOGRAPHY

Dick Consulting Services Ltd., "Monitoring and Evaluation of Demonstration Wood Burning System at Grenville Christian College," Ontario Ministry of Energy, 1985.

Fels, M. et.al., "Hillcrest High School Wood Burning System Monitoring Study," Ontario Ministry of Energy, 1986.

Jellicoe Resources Associates Ltd, "Kingsway College Monitoring Program," Ontario Ministry of Energy, 1986.

Ontario Ministry of Energy, "Fuelling Ontario's Future," Ontario Ministry of Energy, 1985.

# "A REVIEW OF NRC's SOLAR ENERGY PROGRAM"

Tom LeFeuvre
Division of Energy
National Research Council of Canada
Ottawa, Ontario, K1A 0R6

Jim Rollefson
Industry Development Office
National Research Council of Canada
Ottawa, Ontario, K1A 0R6

## ABSTRACT

The program of solar energy R&D at the National Research Council of Canada is reviewed from the standpoint of technology status at program closure in 1986. The considerable developments in the technology by Canadian performers in industry, government and university are noted. The thermal performance and reliability of active systems manufactured in Canada rank well in the international marketplace. On-going developments focus on significant cost reduction through concepts such as low flow systems. R&D on passive systems has lead to guidelines on appropriate passive design for Canada and to substantial opportunities in the super window area. Significant energy benefits are forseen through the implementation of super window technology in the Canadian construction industry. Photovoltaic systems have a market niche in Canada for remote applications of navigational aids and monitoring equipment. Canadian researchers, developers, and systems manufacturers have specific capabilities and expertise through which they are competing in the domestic and international markets.

## 1. INTRODUCTION

This paper summarizes a state-of-the-art review recently prepared as the program wrap-up document (1) of the Solar Energy Program (SEP) of the National Research Council. At the same time some of the "lessons learned" during the conduct of the SEP activities over the past decade are noted. Major work on solar energy R&D at the National Research Council (NRC) started with a $0.8 M project in 1976 within the Division of Building Research, grew into the Solar Energy Program within the Division of Energy, an $11 M/a program of some 200 contracted projects in 1984, and was discontinued as a result of the Government's Economic Message of November 1984. As of March 1986, some ten years from its start up, the NRC solar energy activity is essentially terminated. However, the federal government, through Energy Mines and Resources, continues to support the research, development and demonstration of solar energy technologies at about 40% of previous funding levels.

In 1978 the Canadian Government decided to encourage the creation of an indigenous solar energy industry. It announced the creation of the Program of Assistance to Solar Equipment Manufacturers (PASEM), the Program for the Purchase and Use of Solar Heating (PUSH) both to be administered by Public Works Canada, and an accelerated R&D program to be managed by the Solar Energy Project of NRC. PASEM was to help ten selected companies to develop the industrial capability to produce active solar products. PUSH was to provide the early market for the products with possible funding of $125M over five years. The policy of government procurement rather than incentives was to have the collectivity assume the high risk of failure associated with the technology. The NRC was mandated to ensure the availability of test methods for standards, and to foster the development of the technology via contracted R&D in industry.

In 1980 the NRC program was realigned onto systems and applications, with activity being focused on passive/hybird systems, domestic hot water and commercial/industrial process heat active systems, and photovoltaic systems.

The government set forth a new plan for active solar energy in 1983 with a principal objective to make the Canadian solar industry self-supporting with cost-effective products in five years. A budget of $79M was ear-marked for this research, development and demonstration program.

As this introduction suggests active solar technology has dominated the funding and priorities of governmental involvement in solar energy to date. Nevertheless, the progress made in the passive solar R&D program has been substantial. Further R&D in the most promising areas identified by the passive program can lead to a significant impact on conventional energy consumption in Canada. The Canadian photovoltaics R&D program has been small in comparison with national programs in the U.S., Japan and Europe. From the modest base of Canadian PV research a limited role in future PV development is envisaged.

The material in the sections which follow is largely synthesized from the reports from the contracts funded by SEP over the past eight years. It is impractical to reference all of these reports. A thorough guide to this literature is contained in the Contract Registries, published by SEP in July '82, July '83, July '84 and March '86. These have been widely distributed within the Canadian renewable energy community and are also available from NRC Publication Sales. All contractor reports, or precis thereof, are available on loan from the Canada Institute for Scientific and Technological Information (CISTI) at NRC.

## 2. ACTIVE SOLAR - STATE OF THE ART

An underestimation of the rigours of the operating conditions under which solar systems must operate led to early problems in reliability and durability in most national accelerated development programs. Especially difficult was ensuring the freeze protection of systems at a reasonable cost.

The simple water based thermosyphon solar DHW system is certainly among the most cost effective options where the climate permits its use. Units which feature close-coupled collection and storage can retail for about $1300 in Australia. In Japan sales of thermosyphon units are presently 500 000/a at a retail price installed of $850. (Prices are in $CAN. unless otherwise noted)

Freeze protection can be achieved by antifreeze collector loops, but the maintenance required for the antifreeze closed-loop DHW system appears to be beyond that to be expected of the average homeowner. With one visit by a qualified tradesperson costing almost as much as the annual savings realized by the system it is clear why this type of DHW unit is waning in popularity. Drainback and freeze tolerant systems based on simple reliable designs appear to present the most promise from today's perspective.

The seasonal variations of solar availability and temperature at latitudes typical of Canada not only affect freeze-protection measures, they impact on the performance and the optimum solar fraction to be sought from a system. A very low-temperature application for preheating industrial water has delivered 3 GJ/(m$^2$.a) output in the Canadian climate, whereas good solar DHW systems give 1.5-2 GJ/(m$^2$.a) when properly sized. A Solar DHW system should be large enough to meet at least about 50% of the load because of the substantial fixed cost component associated with this size of unit. However, beyond about a 65% solar fraction the extra collector area is only being fully used in winter and excess energy will need to be "dumped" in the summer. The diminishing returns are directly reflected in a reduced solar output per unit area. For solar DHW and CIPH systems to achieve good performance they must be properly sized for the load and the load should be year round.

The use of active solar technology for space heating runs into the obvious problem that there is a mismatch between the solar availability and its need for heating. The choice becomes to put in a very low cost system giving a small solar fraction or to use seasonal storage. Research efforts to develop economic methods of storing energy seasonally in order to use the sun's summer energy in the winter have been shown to be economically feasible in only very limited areas like parts of Sweden. Here some district heating networks allow one to consider very large underground storage systems. Very large sizes are more economical because heat losses increases as the dimension squared while heat stored augments as the dimension cubed.

In Canada virtually no active liquid solar energy systems are being installed for residential space heating following the rather conclusive studies of the National Research Council showing it as an uneconomic proposition.

Solar air collectors can be less material intensive than liquid ones so the costs for the collector itself can be kept low. If the distribution system can be kept extremely simple then some case can be made for the use of air based systems. For instance, a simple solar air wall system is well suited to the preheating of ventilation air for large interior spaces.

The Canadian solar energy technology now is in many respects on a par or superior to products available internationally. Some industrial advantages, mainly through export sales to the U.S., can be realistically envisaged. However it is anticipated that active solar will not play any major role in energy displacement in Canada before the year 2000.

### 2.1 Simulation Programs

Simulation programs can indicate how much energy one expects to be delivered and used. Considerable effort has been expended on developing these simulation tools because:

a) simulation forces a quantification of knowledge and ignorance;
b) simulations can indicate performance levels attainable for different applications;
c) simulation permits sensitivity analysis of the effects of different components on overall performance, thus helping to design systems or identify priorities for R&D to improve them.

The principal set of simulation programs for active solar in Canada is WATSUN developed at the University of Waterloo. The applications to which the different programs apply are industrial or commercial process heating, pool heating and solar domestic hot water. A number of subroutines are available to simulate most kinds of systems. For instance, options to simulate tank-in-tank, immersed coil, wrap-around or external heat exchangers all are available. The storage tank model can be chosen to be fully mixed or stratified. Pipe losses and some heat capacity effects can be taken into account. Collector characterization models, especially valuable for evacuated tube or boiling/condensing units, have been incorporated into WATSUN.

A number of experiments to validate WATSUN have shown it to be accurate to 5-15%, eg. Sibbitt (2). Any errors larger than this can almost always be attributed to improper designation of system parameters, system malfunction or observed problems like snow accumulation on collectors.

Syphon, another simulation program available from the WATSUN user service, has been derived particularly for thermosyphon systems. Through comparison with test results it has been shown to give good estimations of thermosyphon performance although as used presently, it tends to overestimate by some 5-15%, see Laporte (3).

### 2.2 Monitoring Techniques

The monitoring and analysis of the performance of solar energy systems have been time consuming, difficult, and expensive. However significant progress has been made in monitoring methodology such that one can currently tailor the monitoring and analysis procedure to meet specific needs. The coupling of simulations and commissioning procedures into one step looks very promising as a cost effective approach to commissioning and system characterization, particularly for engineered systems. Whether one is concerned with laboratory or field experiments, complete or partial control of parameters, long term integrated data or short term time-variant data, the reliability of the monitoring system should be several orders of magnitude superior to that expected from the solar energy system.

One aspect of field monitoring remains important. Load characteristics given in design studies for CIPH applications have far too often proven to be significantly in error. As the system design and performance depend critically on this load data, monitoring of the actual load should precede the solar installation.

### 2.3 Performance Improvements

Significant improvements in the performance of active solar energy systems have been noted over the past seven or eight years. At an NRC workshop on Monitoring (4) in February 1984 the Canadian Solar Industries Association presented an overview of the large gap between predicted and measured performance through 1982. Although the performance of engineered systems had improved by a factor of almost two from '78 to '82, there was still a factor of two discrepancy between design expectation and measured performance. Recent work by Carscallen and Chandrashekar (5) at NRC gives measured performance within 15% of expected (3.2 versus 3.7 $GJ/m^2.a$) under controlled conditions for a boiler feedwater preheat load.

For SDHW systems the expectation versus actual performance differences were largely traced to the poor reliability of early systems and to mismatch to the real load. Through long term monitoring at NRC it was shown that a variety of systems concepts operate within an efficiency range of 30 to 40% (6, 7). Comparisons of simulation and field monitoring by Sibbitt and Basdeo (2) confirmed the impact of load on performance. A paper by Sibbitt and Onno (8) to be presented later in this conference contributes to the understanding of the 10 to 15% performance advantage of many thermosyphon systems. Several studies (7) have shown that systems with annual solar fractions of 0.55 to 0.60 already provide 100% of heating needs in the peak summer months.

### 2.4 Progress in Reliability and Standards

The reliability of active solar systems has improved considerably over the last seven years. In a 1979 evaluation study of the solar DHW technology available in Canada only one supplier was found able to install a reasonably operational system. Other units failed due to a combination of faulty controls, leaking or frozen pipes, pump failures, etc. The conclusion of the evaluation study was that considerable development of the technology was needed. Essentially the same conclusion could have been reached in 1979-1982 experience with commercial and industrial process heating (CIPH) applications of solar (9, 10).

The R&D and field experience over the past seven years enabled the industry to identify the faulty components. New systems were designed to avoid their use (e.g. air vents), use more appropriate products (e.g. pumps), or develop new products ( e.g. controllers, collectors). The techniques for installation became more refined. Courses sponsored by the Canadian Solar Industries Association were held across Canada and good texts were prepared in collaboration with NRC.

Special efforts were made in the area of collector test methods because evacuated tube and boiling/condensing collector designs were not well characterized by the methods adopted to fit the collectors' efficiency curves to the Hottel-Whillier-Bliss (H-W-B) representation. Harrison (11) showed that collector performance was dependent on irradiance levels and that loss factors were not constant. In the ASHRAE 93-77 test, irradiance levels are typically of the order of 900 $W/m^2$. The method thus does not capture essential information at other irradiance levels. Moreover it appears difficult to determine the appropriate characterization from the H-W-B representation with a small number of measurements. Recent work by Harrison (11) and Guisan (12) demonstrate the strength of an input-output power representation of collector efficiency. Linear relationships in this method lead to simplified testing.

The new approach to testing is important to evacuated-tube technology because higher and more accurate estimations of performance under typical conditions can be made. For the boiling/condensing collector it is important for another reason. $F_R\tau\alpha$ and $F_RU_L$ values (the y-axis intercept and the slope of the thermal efficiency curves) obtained from ASHRAE 93-77 lead to overestimates of actual performance. Because the lower real performance has been noted, it often has been assumed that there was something wrong with the collector. The realistic characterization explains the differences between earlier estimates and actual results.

Recent work by Beale (13) comparing the monitored (long-term) performance of SDHW systems with tests (short-term) at the National Solar Test Facility (NSTF) promises to open the door to a whole new area of research on SDHW system characterization via short term tests.

The creation of the National Solar Test Facility constitutes in itself an accomplishment of the Canadian solar program. Tests with its indoor solar simulator have been shown to be in excellent agreement with outdoor results. The indoor facility allows much quicker testing of equipment and the irradiance-adjustable simulator lamp gives new scope to research and to testing. In particular, it greatly facilitates measurements for the new input-output presentation. One important benefit of the testing program of NSTF is the added credibility to Canadian products.

### 2.5 Innovative Technology Development in Canada

One concept that has survived from the very beginning of the accelerated solar development program is the boiling/condensing collector with integral condenser. It is a unique collector using a heat transfer process of which little was known prior to the solar research.

A number of serious problems had to be resolved to convert this concept into the practical one it is today. In the early versions superheating of the liquid was occurring prior to boiling. This decreased the effective heat transfer so that a nucleating site was added to initiate boiling as soon as possible. Contaminants in the form of non-condensible gases were found to be very detrimental to performance and it was concluded that special care was needed in the manufacturing process to avoid this contamination. Optimization studies have determined the proper fluid solution, pressures, riser tube diameter and geometric configuration of the header. Advantages of the boiling/condensing collector include simplified array distribution piping and the potential for simple freeze protection in moderate cldimates.

The advantages of the thermal diode collector are shared by the heat pipe concept (as is used in one of the evacuated tube collectors). Which of these two related heat-transfer concepts will eventually prove more cost effective will depend on the result of further design refinements. The following paragraphs give other examples of product innovations by Canadian industry resulting from support through the SEP program.

Connectors between collectors in arrays have, until recently, been relatively cheap but leak-prone, or effective but expensive. A long search for a cheap and effective solution has led to the development of a short brass tube with one large central O-ring and additional O-rings at each end. It is a new and unknown Canadian product now but soon it should be extensively used because of its obvious advantages.

A selective surface that efficiently absorbs the solar radiation but re-emits very poorly in the infra-red has been shown to be one of the most effective measures to use in improving the performance of solar collectors. Production techniques for the deposition of these surfaces on both copper and aluminum substrates are among the most advanced in Canada. Canadian companies are major suppliers of selective-surface absorber plate to collector manufacturers in the U.S..

Several innovative concepts have evolved in the '80s in the SDHW area. The tank-in-tank thermosyphon system has been shown to have a performance advantage which may translate to a market advantage. The integral-collector-storage (ICS) concepts appears attractive to the market in moderate climates like south western British Columbia. Possibly the most promising new SDHW concept is the "low flow" concept, see Hollands et al (14), which has been shown to offer advantages in terms of performance and cost. The low flow facilitates the creation and maintenance of stratification in the storage tank. Moreover fluid lines can be smaller, less material is required, and installation is less complicated, thus less costly. In fact, the cost savings on installation may be the largest contributor to the overall cost reduction.

To use solar energy for illumination is hardly a new idea but to do so well within a building's interior required the invention of the light pipe. It relies on total internal reflection at high incidence angles to provide low-loss light transmission through it. The key technical feature is a very fine prismatic corrugation on the the outer edge of the plastic pipe surface.

## 3. PASSIVE SOLAR - STATUS

Passive solar technology integrates the collection, distribution and storage of energy into the design of a building itself. As building techniques vary widely from country to country and as the relative needs of heating, cooling and daylighting are strongly affected by climate, appropriate passive design tends to be specific to a given area.

The passive solar program of SEP has quantified possible solar contributions, researched technological solutions to improve window performance, and worked on total energy management within the building. Thus passive solar in Canada is viewed in a very broad sense.

The principal advantage of a passive system is that most components serve a dual purpose, e.g. the windows are both collectors and part of the building envelope, so the costs attributable to solar use can be small. For a new wood-frame house there are no direct incremental costs in construction to attain a solar contribution of about 20% to the space heating needs.

The keys to enhanced direct gain systems in northern climates are windows that provide better thermal resistance, and effective storage systems for the surplus daytime heat. Led by large multinationals, companies are starting to offer the better products that typically provide the equivalent resistance of a triple-glazed window or slightly better. Research in Canada is at the forefront of efforts to provide even higher thermal resistance for the next generation of "super" windows as discussed in more detail in section 3.1. The search for cost-effective storage systems has found no clear winners yet but modest progress has been made in the use of phase change materials.

The analysis of direct-gain systems has led to the development of simple methods for the prediction of energy performance. Solar radiation data and transmission figures for the glazings give the solar gains over the heating season. The fraction of this gain that is useful (the solar utilization factor) is determined as a function of the mass to solar gain ratio, the solar gain to total load ratio and the temperature swing the homeowner is willing to accept. The load minus the product of the solar gain and the utilization factor then gives the purchased heating fraction. These principles are thoroughly treated by Harrison and Barakat (15) and Barakat (16) of NRC's Institute for Research in Construction, formerly, the Division of Building Research.

The implications of this research on present passive solar design is the understanding that for wood-frame construction in Canada the optimum south-facing window area for lowest energy use is modest. The simple passive design in Canada does not have more window area than a normal house. The only difference is that due account is taken of window orientation, with south-facing windows taking preference over west and north windows.

The information already available from the monitoring of sunspaces at NRC (17) is sufficiently compelling for designers to reconsider this approach, at least as a prime means of collecting and using solar energy. Most people acquiring a solarium are looking first of all for a certain aesthetic improvement in quality of living through an open, light sunspace. Secondly they are looking for an energy-efficient design. To respond to the first goal the solarium must have a tempered climate suitable for occupancy over a large part of the year. But the vast window areas associated with sunspaces typically have a very high net energy gain during the day and a high net energy loss in the night that make it very difficult to realize either the tempered climate or the energy efficiency. The goals may be achieved but only with great care taken in the design and construction stages.

The experiments on sunspaces at NRC relied on forced convection by fans to transfer heat from the sunspace to the parent building. This did not appear to be very efficient. With 38% greater solar gain to the sunspace as compared to the reference direct-gain system, the utilized solar gain by the parent building was only 50% of that of the direct-gain system. However, the sunspace reduced by 40% the heat loss from the building so that auxiliary heating of the parent building with sunspace was 75% of that required by the direct-gain unit. In this case the heat loss reduction was more important than the solar gain. If the sunspace were maintained above a minimum temperature at night the heating requirements would far outweigh these heat loss reductions.

Again the overall conclusion in residential construction is that with present technology only modest passive solar contributions should be sought when economic energy efficiency is the objective. For the sunspace this means that only the window area necessary to produce the desired lighting levels should be used. To avoid overheating in summer and reduce costs, the windows are best left vertical and oriented to the south. A retrofit of a sunspace on to a patio door may make good sense as this will limit the heat loss from the door through a buffering effect.

In the same line of thinking, glazing between the solarium and the main home gives clarity and solar energy to the main residence area with lesser losses than with the glazing directly exposed to outside conditions.

The Solar Energy Program has had success in the use of a Level-B Monitoring Procedure to evaluate some alternative approaches to passive solar design (18). The cost incurred per project ($25 000) and recent advances in data acquisition equipment suggest a modified approach for the future. The new equipment allows much faster analysis through ready link-up of the data to versatile programming systems. The new monitoring methodology would use this capability to define the principal characteristics of the building over a period of about one month and then rely on energy integrating meters and feedback from the occupants to verify the anticipated performance of the house.

### 3.1 The Super Window Program

One of the major challenges to better energy efficient housing is in the improvement of the thermal performance of windows. Current double-pane windows have a thermal resistance of about 0.35 $m^2 \cdot {}^\circ C/W$ while walls about them are six to fifteen times more effective in impeding heat loss. Current windows also make it necessary to have good heat distribution systems to compensate for their uncomfortable cooling effects. In new super-insulated houses window losses can account for 30% of total heat losses. The research into high-performance super windows has been one of the main focuses of the Canadian passive solar program.

One of the first concerns is identifying what factors can have an important effect on a window's performance. A computer simulation program, VISION, has been developed that permits the assessment of almost any glazing configuration of interest, see Ferguson (19) and Wright (20). It uses accurate equations to calculate the heat transfer and optical transmission for the glazing area.

The ultimate window unit would be a double-glazed unit with a very low emissivity coating to suppress infrared radiative transfer and a vacuum or other means to eliminate heat conduction and convection. A Canadian project shows that it is at least technically feasible to produce such a window today. One design feature, a superior edge seal, has already attracted serious attention from industry.

A number of projects have been undertaken to overcome the practical problems associated with super window design. Low emissivity coatings are available on the market but tend to be overly expensive and questions have been raised concerning their durability. One group has developed a very promising chemical vapour deposition (CVD) technique for low emissivity coating of glass (21). Other CVD techniques have not been successful because the uniformity of the thickness could not be maintained. An electrostatically charged spray solved this problem as charge repulsion keeps the spray droplets from coalescing. Another approach for low emissivity coating, this time on thin-film polymers, has been demonstrated as promising for full scale-up to commercial production.

To assess the potential of advanced window concepts the energy performances of a number of options have been combined with a threshold price for energy to calculate an acceptable cost premium over a double glazed unit. On this basis many options appear feasible. This is all the more interesting when one realizes that the present cost for the sealed double glazings represents only 15-20% of the total cost of the conventional window. With the major expenditures now being on the sash and frame it also appears eminently feasible to improve the performance on these components cost-effectively. In brief, the super window area is a very promising field of development.

Super windows will be popular with the individual homeowner because it allows new flexibility in house design with attractive, light areas added and no energy penalties. The windows will allow new, more healthy levels of humidity to be maintained in winter with no condensation build-up on the windows. For commercial buildings, a key advantage of super-windows is that expensive perimeter heating systems are not needed and that buildings can be designed with the popular "all-glass look" without incurring an energy penalty.

## 4. PHOTOVOLTAICS

Photovoltaic technology directly converts solar radiation into electricity. Because the energy output is high grade and versatile it is the most attractive of the solar energy options as a long term replacement for the fossil fuels. Present applications include powering communication relays, monitoring equipment, navigational aids and other remote-site equipment where the solar cost effectiveness is gained not through direct competition with the cost of conventional fuels but with the cost of transport of the fuel to the site. Another large market area now is in powering calculators, wrist watches and the like. Other markets such as cathodic protection, remote lighting, and water pumping are expected to emerge as module prices drop from the current 8$/Wp to the projected 3 to 4$/Wp around 1990 (Wp = peak watts).

In pumping applications and even more so for village power, direct competition with diesel power units becomes increasingly important. The competitiveness of photovoltaic systems will depend not only on the reduced price of PV cells but on cost reductions in batteries, inverters and regulators as well as the evolution of world oil prices.

Photovoltaic research is costly and risky and the high level of government support in the U.S., Japan and Europe is critical to maintaining the momentum. Many paths to success (and to failure) are still open. The Japanese government budget for photovoltaics (heavily concentrated on amorphous silicon research) was about $44 000 000 in 1984 while that of the U.S. was some $55 000 000. The current U.S. research plan of 1984-88 strongly emphasizes the high-risk, longer-term research as opposed to the earlier strategy that had a larger component of very substantial demonstration projects.

### 4.1 Canadian Accomplishments in Photovoltaics

Through contracts with NRC some of the small Canadian companies were able to make contributions to the international efforts in increasing the efficiency and reducing the costs of the solar cells. Norman (22) reported progress in using a method of fabricating low-cost solar-cell grade substrates directly from metallurgical grade silicon. A fast three-step leaching process was used to upgrade this silicon. The refined powder was then spread on a reusable graphite substrate and subjected to two scans with an electron beam to produce a smooth flat polycrystalline substrate. The same group has had some success in assembling photovoltaic modules using techniques requiring a fair level of manpower but small capital investment. In countries with low wages this is an attractive combination and sales of complete assembly lines have been made to India and China.

Research is on-going at a number of universities to solve some of the problems associated with the degradation of amorphous silicon. There have been no major breakthroughs yet but the quality of the work already performed indicates that Canada can make significant scientific contributions in the field.

One example of a successful project to develop a total system that would work well with photovoltaic power was that using a special reverse osmosis desalination process perfected in Canada (23). The energy recovery pumps of the system maintain very high efficiency over a wide range of input power as opposed to conventional units that work much better at fixed voltage and current. The Canadian unit is thus particularly well suited to operation with solar cells. The results from experiments with the prototype confirmed the very high efficiency possible with this system configuration. Analysis also showed that the combination of energy recovery features and photovoltaic power was superior from an economic viewpoint to more conventional PV-powered desalination units.

The recent focus of NRC in-house research was aimed at providing much better information to designers and installers on how to optimize PV systems for performance in the Canadian climate. Some work had already begun in 1984 on simulation of PV systems. The TRNSYS package was taken as a starting point for detailed hour-by-hour simulation work.

The National Solar Test Facility has recently acquired new capabilities in testing photovoltaic modules. With only a few minor exceptions the NSTF can test modules to a) the Canadian Coast Guard Specification MA 2055, b) the Canadian Standards Association standard on PV modules F380, and c) the JPL Test Specification 5101-161. As part of a total program to develop and evaluate photovoltaic-powered pumping systems new facilities to test these systems have been built at NSTF. Equipment includes a 60-m borehole, a power supply, a test control and data acquisition system and a computer modelling program.

Solar cells are finding cost effective applications and the first was in the displacement of primary battery power supply at remote sites. The power, generally in the 50 to 200 Wp range, can be for navigational aids, monitoring and sensing devices or VHF repeater stations. The PV system can reduce the number of helicopter visits from once every two weeks to once a year (a helicopter rents for about 400 $/h) or it can reduce the necessary battery storage from one year to 10-20 days. The Canadian Coast Guard and Environment Canada among others are making large scale conversions of primary battery to photovoltaic systems.

Photovoltaic systems can also be competitive in remote applications where external combustion generators coupled to thermo-electric or heat-cycle systems are now used. The latter are reliable but inefficient in heat to electricity conversion. Photovoltaic market penetration in this sector is more dependent on having optimized and very reliable PV systems (including batteries) than on further substantial reductions in module costs. One of the first applications that could become cost effective in specific areas for photovoltaic cells displacing gasoline units is water pumping but even for this it will require 3 $/$W_p$ PV modules and optimized systems. Third-world countries offer the best prospects for significant medium-term market for solar cells to displace gasoline internal combustion units because the potential low maintenance requirement for the PV system will be a major advantage there.

## 5. OUTLOOK

Over the next twenty to thirty years it is the passive element of the solar R/D program that will have the largest impact on energy demand in Canada. This is passive solar in the broad context defined in section 4. above. It involves having the same window area as typically used now but orienting a majority of it towards the south, and using superior technology to reduce heat loss from the windows. Depending on the rate of penetration of the new concepts the effect by the year 2000 could be an annual energy saving of up to 30 PJ, and a 100 to 200 PJ cumulative saving by that date.

Canada's active solar industry has made great progress over the last ten years and now is in a position to compete internationally with its products. The industry will need to maintain its R&D activities to remain competitive and develop more fully its export trade. Active solar technology should not be expected to contribute substantially to Canada's energy supply through the medium term but it can realistically be expected to generate industrial benefits.

To encourage a more economic and rational exploitation of the PV technology the focus should be on developing an expertise in systems' optimization. The communication and power companies and government agencies like the Canadian Coast Guard are exploiting photovoltaic technology in appropriate applications. A coordinated program for the development, analysis and testing of systems still appears as one of the most logical contributions the government can make to promoting PV development and keeping Canada in a position to profit from this attractive long-term energy option.

The degree of success achieved to date in the development of innovative window technology owes much to the SEP/NRC project management process which provided coordination, information transfer and evaluation. This infrastructure has allowed expertise in universities, research centres and small innovative companies to collectively direct research efforts to the areas with most potential for industrial and economic benefits. With much remaining to be done it is important to continue a directed program of coordination and evaluation if the economic and energy potential of super window and other solar technology, is to be realized in Canada.

## 6. REFERENCES

( 1) Rollefson, J.P., "Canadian Solar Energy Review - March 1986" Solar Energy Program, Division of Energy, NRC, NRC # 25713, Available from Publication Sales, NRC.

( 2) Sibbitt, B.E., and Basdeo, A., "Measured and Simulated Performance of SDHW Systems in Eastern Canada", Proceedings ASES Conference, Anaheim, Ca., U.S.A., June 1984.

( 3) Laporte, F., et al, "Surveillance et analyse de systèmes solaires saisonniers d'eau chaude", INTERSOL '85, ISES, Montreal, June 1985.

( 4) Rollefson, J.P. and Hill, J.E., "Commercial and Industrial Process Heating Solar Systems - Information Feedback and Monitoring" - a report on SEP Workshop 23 Feb. 1984, SEP/NRC.

( 5) Carscallen, W.E., and Chandrashekar, M., "M-48 Solar Systems Test Facility", SEP, August 1985, in draft.

( 6) Shewen, E.C. et al; "Examination of S.D.H.W. System Performance" Proceedings of the 9th SESCI Annual Conference, Windsor, Ont., August 1983.

( 7) Beale, S.B., and Sibbitt, B.E., "Monitoring of Solar Domestic Hot Water Systems at the National Research Council of Canada", INTERSOL '85, ISES, Montreal, June 1985.

( 8) Sibbitt, B.E., and Onno, T., "Detailed Performance Comparisons Between Thermosyphon and Drainback Solar Domestic Hot Water Systems," Proceedings of the SESCI '86/Biomass Energy Institute Conference, Winnipeg, June 1986.

( 9) Wardrop, W.L. and Associates; "Monitoring of Solar Heating Systems in Multi-Unit Residential Building and Commercial Hot-Water Systems - Phase I", Final Report to SEP/NRC on DSS Contract #02SX.31155-9-2604, July 1981, Available on Loan from CISTI.

(10) Wardrop, W.L. and Associates, "Commissioning, Upgrading, Maintenance, and Recalibration of Solar Energy Systems", Final Report to SEP/NRC on DSS Contract #04SX.31155-0-2663, July 1983, Available on loan from CISTI.

(11) Harrison, S.J., "The Effects of Irradiance Levels on the Thermal Performance Tests of Solar Collectors," INTERSOL '85, ISES, Montreal, June 1985.

(12) Guisan, O., "Evacuated Collector Systems Characterization," IEA/SHAC TASK VI, Report TV1-3, University of Geneva, Switzerland, December 1985.

(13) Beale, S.B., "Comparison of Short-Term Testing and Long-Term Monitoring of Solar Domestic Hot Water Systems", Presented at 8th Annual ASME Solar Energy Division Conference, Anaheim, Ca., U.S.A., April 1986.

(14) Hollands, K.G.T., et al, "Re-engineering Domestic Hot Water Systems for Low flow", INTERSOL '85, ISES, Montreal, June 1985.

(15) Harrison, S.J., and Barakat, S.A., "A Method for Comparing the Thermal Performance of Windows", ASHRAE Transactions, 1983, Vol. 89, Part 1A.

(16) Barakat, S.A., Comparison of the Thermal Performance of Glazing Systems", INTERSOL '85, ISES, Montreal, June 1985.

(17) Ruberg, K., "NRCC's Sunspace and Direct Gain Test Facility: Thermal Performance During 1982-83 Heating Season", Proceedings of the 10th Annual SESCI Conference, Calgary, August 1984, and available as DBR #1320, August 1984, NRCC #24950, available from Publication Sales, NRC.

(18) Project Summaries - Passive Solar Performance, Division of Energy, NRC, Available from SEDP/REB/Energy Mines and Resources.

(19) Ferguson, J.E., and Wright, J.L., "Computer Simulation of the Thermal Performance of Super Windows", Proceedings of the 10th Annual SESCI Conference, Calgary, August 1984.

(20) Wright, J.L., "The Computer Simulation of Super Window Glazing Systems which Incorporate TEFLON (FEP) Inner Glazings", INTERSOL '85, ISES, Montreal, 1985.

(21) Morrison, S.R., (Simon Fraser Univ.), "Preparation of Low Emissivity Coating on Glass Using Electrostatic Spray Deposition - Phase 2" - Final Report to SEP/NRC on DSS Contract #03ST.31926-3-5039, January 1985.

(22) Norman, C.E. (TPK Solar) "Development of Low Cost Large Area Silicon Substrates for Solar Cells", Final Report to SEP/NRC on DSS Contract 02SX.31155-2-2720, April 1984, available on loan from CISTI.

(23) Bowie Keefer & Associates, "Photovoltaic Powered Desalination", Final Report to SEP/NRC on DSS Contract #01SX.31926-3-3024, May '85, available on loan from CISTI.

# DEVELOPMENT OF A NEW THERMOSIPHON PACKAGE

Robert K. Swartman
Solcan Ltd
London, Ontario

## ABSTRACT:

The objective of this work was to improve a residential thermosiphon hot water system. Some aspects required analysis using computer simulation with SYPHON as well as experimental verification. The package has been redesigned resulting in a thermosiphon system which has been optimized to achieve maximum energy delivery for the minimum cost. This product is significant in our efforts to reduce the cost of solar domestic hot water systems.

## INTRODUCTION:

Solar systems must be durable, efficient, simple to operate and less expensive. A thermosiphon solar system is very simple; a density difference causes the warm water to rise by natural convection from the collectors into the tank so there is no need for a pump or control. Baughn and Dougherty (1) found that a higher elevation of the tank above the collectors results in a higher thermosiphon flowrate and a higher system efficiency, whereas a lower flowrate, induced by lower tank elevations, improves thermal stratification in the storage tank.

Braun and Fanney (2) evaluated the performance of thermosiphon hot water heating systems using TRNSYS. They determined that one of the most important factors governing the performance of a thermosiphon system is the collector flowrate. The two factors which were found to have a profound effect on the system flowrate are system pressure drop and the tank elevation. The tank elevation which yields the optimum performance depends very much on the system pressure drop; if the system pressure drop is negligible a tank elevation of 0.5 m is sufficient.

Braun and Fanney also compared the solar fraction to the ratio of collector flow-to-load flow on a daily basis. The optimum occurs when the collector flowrate is equal to the load flow. No improvement in performance was observed for a collector flow greater than the load flow. This can be achieved by ensuring t the load flowrate is always equal to or greater than the collector flowrate.

Carpenter and Chamberlain (3) developed SYPHON to predict the seasonal performance of thermosiphon solar hot water systems. SYPHON can be used to determine the effect of varying the load, storage factor and the collector characteristics. System thermal performance (specifically average tank temperature) and mass flowrate were used as the basis of comparison between experimental and predicted results in order to evaluate the accuracy of SYPHON. When comparing the model estimates to experimental work conducted by Young and Berguam (4), Carpenter and Chamberlain found the final tank temperature underpredicted by 7% and the maximum flowrate overpredicted by 13%. This comparison was considered to be the best indication of the accuracy of the SYPHON program because the experimental results were the most complete of all work surveyed.

Carpenter and Chamberlain (3) used SYPHON to investigate the design of thermosiphon DHW systems for the Canadian climate. Their study examined only those design parameters unique to thermosiphon systems (none of which affect mass flowrate). Their general conclusion was that standard thermosiphon systems are relatively insensitive to most thermosiphon design parameters including collector pressure drop, height of tank above the collector, location of the collector return connection on the storage tank and the diameter of collector piping. They found that variations in system performance due to an increase in tank height are negligible. Although the maximum collector flowrate decreases with lower tank height, even at minimum tank height the maximum flowrate was greater than the required optimum value. The optimum collector return pipe connection was found to be at the mid point of the tank although little penalty is incurred if other locations are used. The incoming water tends to rise or fall to the location in the tank closest in temperature regardless of the inlet position. With regards to collector piping 12 mm (1/2") piping was found to be sufficient. Piping larger than this size had little effect on the system performance.

Further correlation between small thermosiphon systems and SYPHON was undertaken in a study by INRS (5). Energy collected and flowrate values were monitored and simulated for a number of small thermosiphon systems, one of which was the Solcan TS 40-40 which is comprised of 3.5 $m^2$ of collector area and a 180 L storage tank. The system was monitored from 20 July to 4 September 1984 while being subjected to a 225 L/day load according to the CSA draw schedule. The results revealed a 24% overprediction of the energy delivered. The discrepancy was attributed to a number of factors including: i) the general tendency of SYPHON to overpredict collector efficiency; ii) under performing collectors; iii) experimental error; iv) load line losses not accounted for by SYPHON.

It was also reported by INRS that during withdrawals the thermosiphon flow increased markedly regardless of the presence of incident radiation. This indicates that during draws a portion of the incoming cold water enters the storage through the collectors. This is evident as both collector inlet and outlet temperatures drop rapidly during the draw period. This situation will obviously degrade system performance as energy stored within the solar storage is not being transferred efficiently to the load. Such occurences have not been detected in testing of the TS 40-40 system.

## METHOD:

SYPHON has been used to analyse various design parameters in a residential thermosiphon system including: storage volume-to-collector area ratio, hot water load with respect to collector area and storage factor, collector pressure drop, storage elevation, piping size and collector performance characteristics. The flowrate was known to significantly affect efficiency and performance. Therefore, each parameter was varied independently to determine its relationship to system performance as well as to flowrate.

The SYPHON results were verified by comparison to experimental results. Two small thermosiphon systems were tested, each with the same storage volume but one with half the collector area of the other. The experimental and simulated results were evaluated in terms of net energy produced and flowrates. The various parameters were optimized and incorporated into an improved thermosiphon system.

## RESULTS:

Two small thermosiphon systems were tested and the results compared to SYPHON: System A with a collector area of 3.5 $m^2$ and storage volume of 182 L, and System B with the same storage volume but half (1.75 $m^2$) the collector area. A detailed record of meteorological conditions, system operating temperature, fluid flowrates, collector performance characteristics and piping configuration was made. The tests with the most complete information were selected for comparison. The experimental and simulated results were evaluated in terms of net energy produced and operating flowrate.

The comparison of actual and estimated energy collected is illustrated in Figure 1 for the two systems. Net energy collection values agree within 3% for System A and 14% for System B. In System A the maximum flowrate was overpredicted by 5% and in System B by 24% which is consistent with other studies.

The relationship between collector area, storage volume and daily hot water load for a thermosiphon system was investigated using SYPHON. The systems selected were simulated from 10 April to 1 November using TMY Ottawa weather data and CSA load profiles. It was found that larger storage improves system performance until the storage factor reaches a maximum of 100 L/$m^2$.

Optimum Pipe Diameter:

The effect of pipe diameter on the performance of a thermosiphon system was investigated experimentally using two small systems; one with serpentine copper tube collectors (2005) and the second using collectors with parallel copper risers connected to copper headers (3001). The performance of the system with serpentine

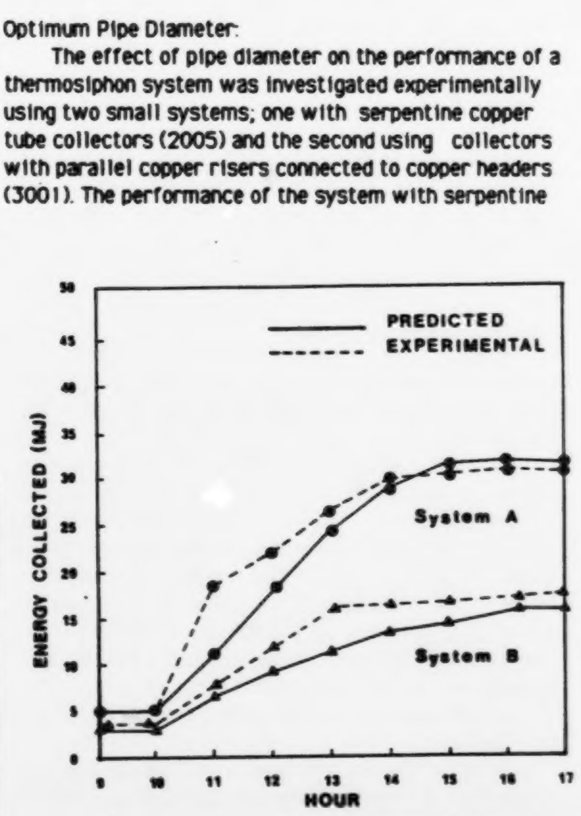

Figure 1- Comparison of Energy Collected.

collectors was significantly reduced by the smaller pipe size while the performance of the system with parallel risers was essentially unchanged. The latter observation supports work by Carpenter and Chamberlain (4) who found that pipe diameters of 12 mm or greater had little effect on system performance.

The poor performance of the serpentine collectors system can be attributed to the high pressure drop in the long flow path (18 m of 12 mm tubing). With a 18 mm diameter interconnecting pipe, the average flowrate in the two collectors was 0.6 L/min, only 15% of the recommended value. A 12 mm interconnecting pipe reduced the average flowrate to 6% of the recommended value. With these less favourable operating conditions, the heat removal factor is greatly reduced, resulting in significantly degraded performance characteristics. By comparison the average flowrates in the system with parallel 12 mm risers were 30% and 15% of the recommended value for the 18 mm and 12 mm diameter piping respectively. Thus, the performance penalty is substantially less than that experienced in the serpentine collector system.

Increasing the pipe diameter will increase the maximum flowrate 30 to 45% and improve performance from 5 to 9%. The lower pressure drop collectors allow for greater performance and flowrate but systems with greater collector friction can have the losses compensated by larger pipe diameters. The pipe size was assumed to be 12 mm and then increased to 18 mm and 25 mm. Increasing the pipe diameter to 25 mm increased the flowrate by a significant amount while improving performance less than 1.5 percent over the 18 mm diameter.

The relationship between system performance and storage tank elevation was investigated experimentally. Three similar thermosiphon systems, varying only in the difference in elevation between the collector outlet and the tank bottom were simultaneously monitored. The distance between the collector outlet and tank bottom for System A was 622 mm (24.5"), 292 mm (11.5") for System B and -127 mm (-5.0") for System C.

Optimum Tank Elevation:

A comparison of system efficiencies for various tank elevations is shown in Figure 3. Efficiency is defined as the total energy collected in the storage tank divided by the total incident radiation (or cumulative daily efficiency). There was no significant pattern in the plot.

When examining the effect of storage tank elevation one must consider the effect of nocturnal reverse siphoning. Reverse siphoning occurs on clear nights when the solar panels can radiate energy to cold space. When the radiative loss is sufficient, the fluid in the collector plate cools, increasing the fluid density and causing it to move down. The dependence of reverse siphoning on the tank elevation was investigated experimentally on the three systems above. The reverse flowrate was not measured directly, but the collector inlet and outlet temperatures, as well as the ambient temperature, were monitored throughout a clear night following a day of good sunshine. The trend indicates that nocturnal reverse flow losses increase with decreasing tank elevation.

The collector operating characteristics are critical to the performance of any solar thermal system but are even more significant in the operation of a thermosiphon system. The degree of stratification in a thermosiphon tank is generally superior to all other designs. A thermosiphon system has the collector inlet temperature operating as cool as possible for the majority of the day. During the seasonal operating period of May to October a cool collector inlet will allow the collector to operate at a higher efficiency. Therefore, a collector with a high $F_R$t.a will enhance the performance of a thermosiphon system. Also, a collector with a high heat loss coefficient ($F_RU_L$) may not degrade collector performance too severely under thermosiphon conditions.

The final aspect of the collector in a thermosiphon system to be considered was the effect of changing the collector flowrate. In a forced convection system the optimum flow is 1.2 L/min.m$^2$ which is the optimum balance between the heat removal and the pumping power required to circulate fluid through the panel. In a thermosiphon system fluid moves by natural convection at a much slower rate. The collector performance consequently decreases as the flowrate falls below the recommended value.

Optimum Location of Ports:

The location of the inlet and outlet ports on the storage vessel can significantly affect the overall performance of the thermosiphon solar system. This aspect of the system design becomes even more critical as the storage volume is decreased to improve the cost/performance ratio. It is important to maximize stratification during solar collection and minimize mixing or fluid short circuiting during draw conditions.

Three different port location configurations were investigated and are shown in Figure 2. The solar supply and return positions were kept the same in all cases but the locations for the cold water supply and hot water delivery were varied. Using transparent acrylic models and die injections into the cold and hot water streams, the thermosiphon system operation was demonstrated in a qualitative way and the flow patterns for the various port designs were observed and photographed.

Configuration #1 showed excellent thermal stratification initially, then a disruption in stratification as the system was placed under a draw, and finally that the stratification recovers quickly after the draw. The behaviour of flow during a draw indicates this is not the most appropriate placement for the cold water supply port.

Configuration #2 was similar to #1 except in the position of the cold water supply, on the end of the tank rather than on the bottom, allowing the fluid movement to carry the length of the tank. The flow pattern showed excellent stratification of warm water returning from the collector, with little mixing of the cold water during draw conditions. This is definitely an efficient port location design for the thermosiphon tank.

In configuration #3 the collector return and hot water delivery ports are at the one end of the tank while the cold water supply and the collector supply are at the other. It showed good thermal stratification with thermosiphoning, but mixing is quite severe during a draw as the cold and warm streams create turbulent mixing in the middle of the tank. This is definitely not an appropriate placement for the cold water supply port.

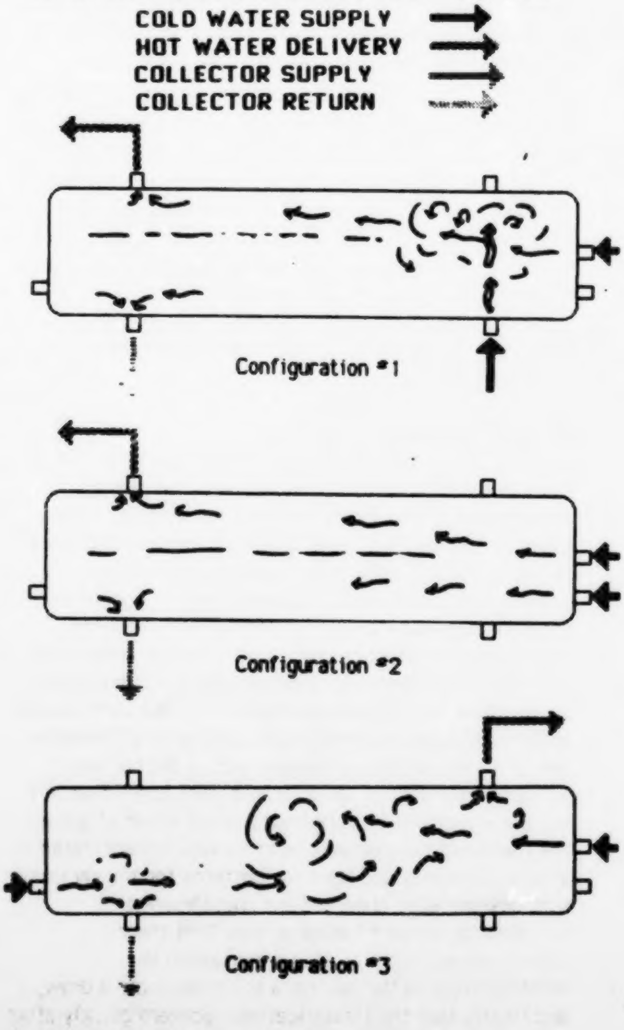

Figure 2 - Stratification Results

The most favourable arrangement is undoubtedly configuration #2. This design allows the cold and warm streams to flow in the same direction through the tank. This results in minimal mixing under draw conditions, while maintaining good thermal stratification and efficient use of the storage volume.

Optimum Flowrate:

The effect of flowrate and thermosiphon system performance was investigated using SYPHON. A TS 4.5-200 was used as the base system for evaluation of collector pressure drop and tank elevation parameters. The effects of collector area, storage volume and system load were also examined for a complete range of systems.

The pipe length between the collector and storage, representing the pressure drop, was initially held constant but then varied to accommodate changes in elevation. The increase in performance generally obtained with a higher elevation is offset by the increased piping runs.

Design and Construction of the Prototype:

The appearance of the thermosiphon package should be "high tech" while utilizing the basic elements of the system. The collectors must be located below the tank, and the tank should be insulated. The package must be inclined at an angle appropriate for the latitude. Generally, use in Canada will be seasonal, so mounting on a conventional roof of slope between 3/12 and 5/12 is ideal. There may be situations such as flat roofs where legs must be provided to tilt the package. The structure of the package must be able to withstand wind forces on

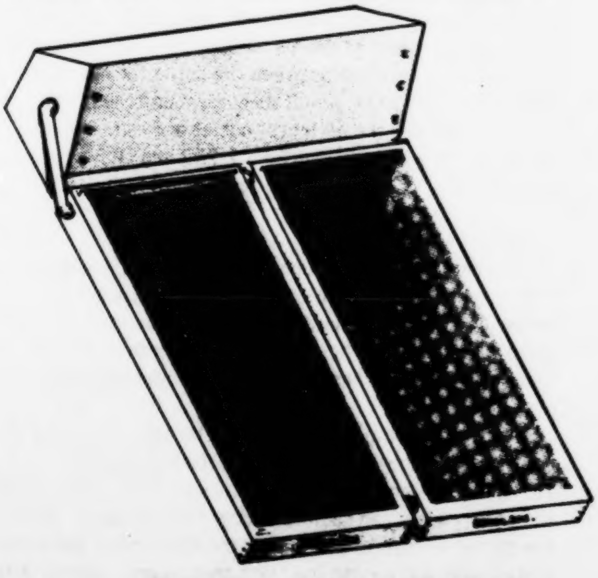

Figure 3 - Prototype TS 4.5-200

the outside as well as the static load of the filled water tank. Steel saddles supporting the tank are designed to transfer the load to the roof. The combination of tank, tank enclosure and collectors must be structurally adequate and able to be installed readily. Figure 3 shows the TS 4.5-200 package comprising two Solcan 3001L collectors and a 200 L tank.

The design of a thermosiphon solar hot water system suitable for the residential market requires a thorough understanding of the relationship between system size, performance and the cost to the consumer. We have considered material and installation costs with ,ective of determining which system design is cost-effective and attractive to the residential consumer. Fifteen systems were evaluated as shown in Table 8, assuming a 300 litre load and the appropriate CSA draw schedule.

TABLE 8: Evaluation of Thermosiphon Systems

| Model | Areas $m^2$ | Storage L | Energy GJ/Yr | Installed System Cost $ | Energy Cost $/GJ |
|---|---|---|---|---|---|
| TS 2.2-40 | 2.2 | 40 | 4.4 | 820 | 186 |
| TS 2.2-100 | 2.2 | 100 | 4.6 | 940 | 204 |
| TS 3.0-40 | 3.0 | 40 | 5.0 | 900 | 155 |
| TS 3.0-100 | 3.0 | 100 | 6.1 | 1020 | 167 |
| TS 3.0-200 | 3.0 | 200 | 6.3 | 1120 | 178 |
| TS 3.0-300 | 3.0 | 300 | 6.4 | 1170 | 183 |
| TS 3.7-40 | 3.7 | 40 | 6.8 | 1040 | 153 |
| TS 3.7-100 | 3.7 | 100 | 7.1 | 1160 | 163 |
| TS 3.7-200 | 3.7 | 200 | 7.3 | 1260 | 173 |
| TS 3.7-300 | 3.7 | 300 | 7.5 | 1310 | 175 |
| TS 4.5-40 | 4.4 | 40 | 7.4 | 1250 | 169 |
| TS 4.5-100 | 4.4 | 100 | 7.8 | 1370 | 176 |
| TS 4.5-200 | 4.4 | 200 | 8.1 | 1470 | 182 |
| TS 4.5-300 | 4.4 | 300 | 8.3 | 1520 | 183 |
| TS 4.5-450 | 4.4 | 450 | 8.4 | 1610 | 192 |

Some significant trends are obvious. The TS systems with a larger storage factor produce more energy but are not as cost effective as similar systems with smaller storage. The larger area systems produce more energy but are not as cost effective. Due to optimized piping and collector pressure drop, the sensitivity of performance to storage volume is reduced down to about 40L, and thereafter drops rapidly.

The cost of thermosiphon systems is significantly affected by storage costs. A minimal storage is desirable for applications where daytime load is intermittent. By minimizing the storage volume the system is simplified and opens the potential for cost reduction; zero storage systems eliminate the cost of storage and are the most cost effective. However, they are better suited for applications where the load demand is continuous. In residential applications approximately 50% of the hot water load can be expected after the sunlight hours. In these and similar applications with intermittent loads some storage is necessary. Thus, for a residential load of 300 L/day a storage of approximately 150 litres should be appropriate. Yet from the relationship determined between thermosiphon system design and performance, even low storage systems are cost effective for residential applications. A consequence of using a smaller storage is that the maximum temperature in the storage is increased which would be in the order of 80°C to 100°C.

Of all the systems examined for a typical residential application the TS 2.2-40 is the most efficient and cost effective system. The load-to-collector area ratio is high and so the collectors operate at their optimum efficiency. The storage volume is reduced to a minimum, cutting significantly the total system cost. The pressure drop is minimized which allows higher system flowrates which results in faster recovery. The solar fraction for these systems is in the 35 to 40 percent range whereas for a TS 4.5-200 the solar fraction would be 60 to 65 percent. In each case auxiliary heating would be required for dependability. It is evident that the storage volume and hot water load are significant in determining solar energy delivered. System performance improves markedly with increases in storage factor and load although the performance does not improve significantly as the storage volume approaches the load volume.

To optimize the performance of a residential-sized thermosyphon system the following design parameters should be employed:

1) Maximize load to collector area
2) Size storage equal to daily load
3) Maximize storage tank elevation i.e. up to 1.0 m
4) Minimize collector pressure drop.
5) Use piping of 12 mm diameter or greater
6) Minimize piping runs
7) Use a collector with a high $F_R$t.a and low $F_RU_L$

These optimum parameters were entered into the SYPHON program. The thermal performance for a thermosiphon system with 4.5 $m^2$ of collector area is 8.4 GJ of energy per annum with a solar fraction of 54%. However, using more realistic design parameters (tank height = 0.3 m, 19 mm piping, collector $F_RU_L$ = 5.07, 200 liter storage and a constant load profile from 8 am to 4 pm) the system performance according to SYPHON was just as high.

The sensitivity of system cost performance to collector area and to storage volume was analysed and the following trends observed.

1. As storage volume decreases the cost/performance ratio and the cost per unit area decrease and become more favourable.
2. As the collector size increases the cost per unit area decreases i.e. a 4'x10' is more cost effective than a 4'x8'

which is better than a 3'x8' collector.

3. The cost/performance decreases as collector area decreases to a minimum between 3.0 and 4.0 $m^2$, but increases thereafter.

The total cost of the system to the consumer is used in assessing marketing potential. The TS 4.5 models have yearly energy outputs in the 7 to 8.8 GJ range and, thus, qualify for an EMR subsidy of $900. The net costs for the systems examined range from $340 to $620 installed. This system cost is significantly lower than a typical active residential solar domestic hot water system installation which costs from $1200 to $1800 installed. This should definitely improve the market potential for thermosiphon residential solar systems.

The result is a thermosiphon package which has been optimized to achieve maximum energy delivery for the minimum cost. This product is significant in our efforts to reduce solar system costs.

## CONCLUSIONS:

There is increasing consumer demand for solar domestic hot water systems at lower costs. This project has enabled Solcan to develop a thermosiphon system with a significant improvement in cost/performance.

## ACKNOWLEDGMENT:

This is to acknowledge the financial support of the National Research Council of Canada and Energy, Mines and Resources Canada in aspects of this work.

## REFERENCES

1. Baughn & Dougherty, "Effect of Storage Height on the Performance of a Natural Circulation (thermosiphon) Hot Water System", Proc. 2nd Nat. Passive Conf., Philadelphia, PA, 16-18 March 1978, Vol. 2, pp 637-641.
2. Braun, James E., & Hunter A. Fanney; "Design and Evaluation of Thermosiphon Solar Hot Water Heating Systems; Proceedings of American Solar Energy Society; Annual Conference, Minneapolis, MN, 1983.
3. Carpenter, S.C. & M.J. Chamberlain; :Design of Thermosiphon Solar D.H.W. Systems for the Canadian Climate"; NRC Contract # 0SX83-0028, October 1983, 52 pp.
4. Young, M.F. and T.B. Beryquom; "Performance Characteristics of a Thermosiphon Solar Domestic Hot Water System". Solar Energy; Volume 103, pp 193-200.
5. Laporte F., M. Maranda, F. Rheault. (INRS) Institute National de la Recherche Scientifique " Monitoring of Seasonal SDHW Systems", NRC Contract #OSR 84-00011, May 1985, 19pp.

# THE THERMAL PERFORMANCE EVALUATION OF A PASSIVE SOLAR LOW-RISE OFFICE BUILDING

Dr. Gren Yuill and Michael Zahn
G.K. Yuill and Associates Ltd.
Winnipeg, Manitoba

## ABSTRACT

Monitored data and a sophisticated building energy loads computer simulation program were used to evaluate the thermal performance of a low-rise office building. Significant thermal parameters, including outdoor temperature and solar radiation, selected operating temperatures within the building and its systems, and electrical energy input to the building and its various systems, were monitored using a microprocessor-based data acquisition system. Over periods during which data was collected, the thermal operation of the building was simulated using the BLAST (Building Loads and System Thermodynamics) computer program. The BLAST model of the building was then improved by the calibrated modelling technique. Discrepancies between monitored parameter values and those predicted by BLAST were analysed, and characteristics of the building which may have been in error in the computer model were adjusted or calibrated to yield a better prediction of building performance. since the BLAST program utilizes an hour-by-hour calculation scheme, modelling the transient performance of the building during cool-down or heat-up periods was possible, and was used to calibrate the thermal mass of the structure.

The structure which was evaluated using this modelling technique is a 1500 square metre energy conserving office building which has a significant amount of glazing incorporated into its design. there is a white fibreglass skylight system atop a two-storey atrium in the centre of the building, as well as a large amount of glazing on the north and south faces. Heating and cooling loads are met by a ground water heat pump system serving a variable air volume fan system. the primary objective of the project was to determine the solar contribution to heating load, and the paper emphasizes this particular application of the calibrated modelling technique. In passive solar systems, direct measurement of the solar contribution is extremely difficult because the passive solar heating systems are integrated into the construction of the building. Directly monitoring such systems is expensive, time consuming, and depending on the particular building, may often be unfeasible. However a detailed BLAST computer model developed using the calibrated modelling technique can be readily utilized in determining the solar fraction. Basically this involves simulating the actual building over a given weather period with and without the presence of solar radiation and comparing the heating and/or cooling loads in the two cases. Although the main interest in the present project was solar contribution, an accurate thermal computer model of the building could also be used to evaluate other performance characteristics and design alternatives. Therefore, this paper also discusses the flexibility and applicability of the calibrated modelling technique to building performance evaluating in general.

# AUTHORS INDEX

| AUTHOR | PAGE |
|---|---|
| ACKERMAN, M. | 225 |
| ALLEN, G. | 153 |
| ASHLEY, K.I. | 41 |
| ATHIENITIS, A.K. | 107 |
| BASU, R.N. | 53 |
| BESANT, R.W. | 99<br>113<br>125<br>195 |
| BOLTON, J.R. | 1 |
| BRITTON, M.G. | 186 |
| BRUDRETT, E. | 87 |
| BRUNGER, A.P. | 22 |
| BUELNA, G. | 5 |
| BURNETT, E. | 159 |
| CARD, D.C. | 46 |
| CARPENTER, S. | 153<br>159 |
| CARRIE, P.J. | 244 |
| CARTER, C. | 213 |
| CHAPIN, F.W. | 93 |
| CHAPIN, H.D. | 93 |
| CHIGNALL, G. | 241 |
| COGGER, L.L. | 53 |
| COLLICUT, J.A. | 183 |

D'ANDREA, L. 5
142

DALE, J.F. 225

DOLENKO, A. 229

DUNFORD, W.G. 41

ELIAS, E.M. 146

FEDUNIW, L.O. 208

FRASER, D.W.H. 46

GEAST, M.S. 26

GESSER, H.D. 64

GLOVER, M. 153

GRAY, B.F. 113

GREEN, G.H. 113

HAMLIN, T.L. 99

HAMPTON, D. 137

HAWTHORNE, S. 10

HASSANI, V. 87

HERBERMAN, J.R. 244

HOLLANDS, K.G.T. 107
142
170

IVES, C. 131

KASHA, J. 225

KIERKUS, W.T. 32

KOSTYNIUK, T.M. 201

KRAWI, A.A. 33

LAFEUVRE, T. 251

LAWAND, T.A. 131

LEE, T. 145

LEONG, W.H. 191

LIGHTSTONE, M.F. 170

LOVE, J.A. 76

LUX, M.E. 125

MA, H.F. 32

MAGRO, J. 16

MAHI, I.M. 33

MCINTYRE, E.D. 66

MOLCZAN, T.J. 16

MORRIS, R.J. 26

MORRISON, I.D. 142

MURRAY, T.V. 186

ONNO, T. 119

POULOIT, V. 5

RICHMOND, W.R. 195

ROLLEFSON, J. 251

RUSH, C.K. 177

SAMOILOFF, M. 82

SEARS, R. 10

SCHOENAU, G. 99, 113

SCRIVEN, A.P. 16

SIBBETT, B.E. 119

SORDI, R. 145

SPAULDING, W.J. 177

STERLING, E.M. 66

SULLIVAN, H.F. 107

SWARTMAN, R.K. 260

TARNAWSKI, V.R. 191

| | |
|---|---|
| TOWNSEND, J. | 84 |
| TRUPP, A.C. | 201 |
| WARD, P.R.B. | 41 |
| WALKINSHAW, D.S. | 54 |
| WARKENTIN, I.H. | 205 |
| WORMAN, JAMES. | 10 |
| WORMAN, JOSEPH. | 10 |
| WRAY, C. | 164 |
| WRIGHT, J.L. | 219 |
| WRIGHT, W. | 131 |
| YOUNG, O'C. J.C. | 183 |
| YUET, P.K. | 191 |
| YUILL, G.K. | 70<br>100<br>164<br>259 |
| ZAHN, M. | 259 |